Using aerosol Bacille Calmette-Guérin in non-human primates to model the immune response to *Mycobacterium Tuberculosis*: A translational bridge between preclinical models and clinical trials

Emily Hoogkamer
Thesis submitted for Doctor of Philosophy in Clinical Medicine
Linacre College
Hilary Term 2022

Jenner Institute, University of Oxford
Supervisors: Professor Helen McShane and Dr Iman Satti

UK Health Security Agency (UK-HSA), Porton Down
Supervisors: Dr Sally Sharpe and Dr Andrew White

Abstract

Tuberculosis (TB) is a major cause of death worldwide. We have a limited understanding of how the human immune system responds to *Mycobacterium tuberculosis* (*M.tb*), the main infectious agent that causes TB. In this project, non-human primates (NHPs) were exposed by aerosol to $1x10^7$ colony forming units (CFU) of Bacille Calmette-Guérin (aeBCG). BCG is a live attenuated strain of *Mycobacterium bovis,* which can be used as a model of *M.tb* infection, and was safe to deliver to NHPs in a controlled manner.

The immune response to aeBCG was characterised across different tissue compartments: blood, broncho-alveolar lavage (BAL), lymph nodes (LNs) and lung. There was little overall change in the immune parameters measured in either rhesus or cynomolgus macaques (RM or CM) at Day 2 (D2), D7 or D14 after aeBCG. Expression of cluster of differentiation-161 (CD161) on lymphocyte subsets was an early marker of this response at Week 2 (Wk2).

Purified Protein Derivative (PPD)-specific interferon-gamma (IFNγ)-producing spot forming unit (SFU) frequency increased from Wk4 to Wk16 after aeBCG. The peak immune response, measured by flow cytometry was at Wk12. PPD-specific immunoglobulin-G (IgG) titre increased at Wk9 in serum. The kinetic of the immune response to aeBCG measured was similar, but delayed, compared to the previously published immune response to intradermal (ID) BCG[7, 8]. The aeBCG delivery method (mask or mouthpiece) had no effect on the observed changes in immune parameters. Data from animals in both delivery groups were combined (n=16).

A parallel experimental clinical medicine study showed the peak immune response to $1x10^7$ CFU aeBCG in humans was at D7 (McShane group, Oxford – ClinicalTrials.gov ID: NCT03912207). The differences in immune response kinetic detected

between NHPs and humans shown in this project have not been previously described and merit further study.

Acknowledgements

Thank you to my funders, UK-HSA, for making this DPhil possible.

I would like to express my sincerest gratitude to my supervisors: Helen McShane, Sally Sharpe, Iman Satti and Andrew White. I am very lucky to have had four people to count on for advice and support throughout my PhD. Andrew and Iman, thank you for helping me in the lab, and for coming to rescue me whenever I got stuck with something. Helen and Sally, the way you work together between lab groups is inspiring and I have really enjoyed being part of two lab groups led and filled with confident women. Thank you for showing me how science should be, and what good leadership looks like.

Thank you to all the other hardworking scientists I have been privileged to work alongside. The lab team at UK-HSA taught me how to be efficient and prepare for large experiments, and treated me like one of their own, even though I spent half my time in Oxford. Thank you, Charlotte and Laura, for all your guidance, and thank you Alex, Adam and Dinos for your help and enthusiasm. Without the NHP team at UK-HSA, this project would not have been possible – so a huge thank you to Mike and his team.

In Oxford, thank you Rachel for going above and beyond in helping me to think through ideas and get work published – your work ethic is incredible. Thank you, Steph, for always knowing what is going on, and helping me with lab work. Thank you, Marco, for teaching me how to run ELISAs. Well done to Julia for finishing your PhD and balancing such a huge workload over the last few years. I have really enjoyed having a friend to work in parallel with and share this experience with. There are lots of others who have helped me out or kept me smiling when I was at work, thank you – Julie, Maria, Rhiannon, Drew, Rachel W, Isabel, Hazel, Salem, and Danny.

Outside of the lab, thank you to my friends and family, who have kept my life relatively normal throughout this process. You all know how much you mean to me and how important keeping a life/work balance has been. Thank you for your support and for helping me to keep perspective.

Table of contents

USING AEROSOL BACILLE CALMETTE-GUÉRIN IN NON-HUMAN PRIMATES TO MODEL THE IMMUNE RESPONSE TO *MYCOBACTERIUM TUBERCULOSIS*: 1

ABSTRACT 2

ACKNOWLEDGEMENTS 4

TABLE OF CONTENTS 6

List of figures 8
List of tables 11

CHAPTER 1: INTRODUCTION 13

1.1 The problem of TB 14
1.2 BCG vaccination against TB 17
1.3 Bettering BCG – vaccines 22
1.4 Bettering BCG – BCG delivery routes 26
1.5 Use of animal models in TB research 30
1.6 The pathogen that causes TB – M.tb 33
1.7 Immune response to *M.tb* – innate 36
1.8 Immune response to *M.tb* - adaptive 43
1.9 Immune response to *M.tb* - humoral 53
1.10 Immune response to *M.tb* - other players 58
1.11 Studying the immune response to *M.tb* 60
1.12 This project 65

CHAPTER 2: MATERIALS AND METHODS 68

2.1 Materials 68
2.2 Samples 72
2.3 Methods 76

CHAPTER 3: EARLY IMMUNE RESPONSE TO AEBCG 97

3.1 Statement of authorship 97
3.2 Background 97
3.3 Objectives & hypotheses 98
3.4 Results 99
3.5 Discussion 160
3.6 Summary and conclusions 174

CHAPTER 4: LATE IMMUNE RESPONSE TO AEBCG – DELIVERED BY MASK OR MOUTHPIECE 179

4.1 Statement of authorship 179
4.2 Background 179
4.3 Objectives & hypotheses 181
4.4 Results 183
4.5 Discussion 240
4.6 Summary and conclusions 254

CHAPTER 5: NHP VS HUMAN RESPONSES TO AEBCG 259

5.1 Statement of authorship 259
5.2 Background 259
5.3 Objectives & hypotheses 260
5.4 Results 261
5.5 Discussion 279
5.6 Summary and conclusions 286

CHAPTER 6: CONCLUSIONS AND FUTURE DIRECTIONS 288

6.1 Summary 288
6.2 Key findings 290
6.3 Future directions 294
6.4 Concluding remarks 300
APPENDICES 302
7.1 Additional tables 302
7.2 Supplementary figures 335
7.3 Publications 339
7.4 References 340

List of figures

Chapter 1

Figure 1.1 TB vaccine candidate pipeline 24

Figure 1.2 Frequency of PPD-specific IFNγ spot forming cells after mucosal BCG (reproduced) 29

Figure 1.3 Mycobacterium tuberculosis mechanism of infection 35

Figure 1.4 T-cell responses in broncho-alveolar lavage (BAL) cells after mucosal BCG (reproduced, left) 49

Figure 1.5 T-cell responses in PBMC after mucosal or intradermal (ID) BCG (reproduced) 51

Figure 1.6 Antibody responses in broncho-alveolar lavage (BAL) and serum after mucosal BCG (reproduced) 57

Figure 1.7 The Gut-lung axis in TB 59

Figure 1.8 BCG as a model of M.tb infection 64

Chapter 2

Figure 2.1 BCG dosing across aeBCG studies in non-human primates 77

Figure 2.2 Example gating strategies to identify cell populations 89

Figure 2.3 Example gating to identify MerTK- or CD163-positive cells 91

Chapter 3

Figure 3.1 Study design (early time points) 100

Figure 3.2 Clinical data 102

Figure 3.3 Frequency of PPD-specific IFNγ spot forming cells after aeBCG 103

Figure 3.4 CD4+/CD8+ frequency on T-cells characterised among peripheral blood mononuclear cells (PBMCs) 108

Figure 3.5 γδ cell frequency among T-cells characterised among peripheral blood mononuclear cells (PBMCs) 110

Figure 3.6 MAIT cell frequency among CD8+ T-cells characterised among Peripheral blood mononuclear cells (PBMCs) 112

Figure 3.7 NK cell frequency among CD8+ T-cells characterised among Peripheral blood mononuclear cells (PBMCs) 114

Figure 3.8 Non-lymphocyte populations characterised among PBMCs 116

Figure 3.9 MAIT cell frequency among CD8+ T-cells characterised among broncho-alveolar lavage (BAL) cells 120

Figure 3.10 Non-lymphocyte populations characterised among broncho-alveolar lavage (BAL) cells 122

Figure 3.11 Cell populations of interest, characterised among lung mononuclear cells 125

Figure 3.12 CD56+CD4+ T-cells, characterised among lymph node mononuclear cells 128

Figure 3.13 NKT-like cells, characterised among lymph node mononuclear cells 129

Figure 3.14 NK and NKT-like (NKT-L) cell frequency among lymphocytes characterised among whole blood (WB) samples (below) 132

Figure 3.15 CD161 expression among lymphocytes characterised among broncho-alveolar lavage (BAL) cells 137

Figure 3.16 Human leukocyte antigen-DR (HLA-DR) expression on lymphocytes characterised among peripheral blood mononuclear cells (PBMCs) 140

Figure 3.17 Human leukocyte antigen-DR (HLA-DR) expression among lymphocytes characterised among broncho-alveolar lavage (BAL) cells 142

Figure 3.18 Human leukocyte antigen-DR (HLA-DR) expression on lymphocytes characterised among lymph node mononuclear cells 144

Figure 3.19 Human leukocyte antigen-DR (HLA-DR) frequency among lymphocytes characterised among whole blood (WB) samples 146
Figure 3.20 MerTK/CD163 expression among non-lymphocyte cells populations 148
Figure 3.21 Monocyte:lymphocyte (M:L) and neutrophil:lymphocyte (N:L) ratios 154
Figure 3.22 PPD-specific IgG in sera 155
Figure 3.23 Phospholipid concentration in broncho-alveolar lavage fluid (BALf) 157
Figure 3.24 PPD-specific IgG in broncho-alveolar lavage fluid (BALf) 159

Chapter 4

Figure 4.1 BCG aerosolisation methods 180
Figure 4.2 Study design (late time points) 184
Figure 4.3 Clinical readouts throughout early time point studies. 185
Figure 4.4 Frequency of PPD-specific IFNγ spot forming units (SFU) later after aerosol BCG 188
Figure 4.5 Cell populations among CD3+ lymphocytes characterised among peripheral blood mononuclear cells (PBMCs) 191
Figure 4.6 CD16+ and related cell populations characterised among peripheral blood mononuclear cells (PBMCs) 194
Figure 4.7 CD4+ and CD8+ T-cells characterised among broncho-alveolar lavage (BAL) cells 196
Figure 4.8 CD4+/CD8+ frequency among T-cells characterised among peripheral blood mononuclear cells (PBMCs) and broncho-alveolar lavage (BAL) cells 198
Figure 4.9 MAIT-cell markers frequency among broncho-alveolar lavage (BAL) cells 199
Figure 4.10 CD14+/CD16+ marker frequency among broncho-alveolar lavage (BAL) non-lymphocyte cells 201
Figure 4.11 Cell populations characterised in whole blood 204
Figure 4.12 Cell populations measured by haematology analyser 205
Figure 4.13 CD161 expression among peripheral blood mononuclear cell (PBMC) lymphocytes 209
Figure 4.14 CD161 expression among broncho-alveolar lavage (BAL) lymphocytes 210
Figure 4.15 Human leukocyte antigen-DR (HLA-DR) expression on peripheral blood mononuclear cell (PBMC) lymphocytes 213
Figure 4.16 Human leukocyte antigen-DR (HLA-DR) expression on broncho-alveolar lavage (BAL) lymphocytes 214
Figure 4.17 Human leukocyte antigen-DR (HLA-DR) expression on whole blood lymphocytes 215
Figure 4.18 MerTK or CD163 expression on whole blood lymphocytes 217
Figure 4.19 CD95 expression on whole blood lymphocytes 218
Figure 4.20 Cytokine expression on peripheral blood mononuclear cell (PBMC) populations 222
Figure 4.21 Cytokine expression on broncho-alveolar lavage (BAL) cell populations 224
Figure 4.22 Polyfunctional cytokine expression on peripheral blood mononuclear cell (PBMC) populations 225
Figure 4.23 Polyfunctional cytokine expression on broncho-alveolar lavage (BAL) cell populations 226
Figure 4.24 PPD-specific antibody standard curves 227
Figure 4.25 PPD-specific IgG antibody production 229
Figure 4.26 PPD-specific IgM antibody production 230
Figure 4.27 Principal component analysis (PCA) of bronchoalveolar lavage (BAL) cytokine expression among cell populations 239

Chapter 5

Figure 5.1 Study design (human study TB043) 262

Figure 5.2 PPD-specific IFNg SFU in humans and NHPs 264
Figure 5.3 CD4+/CD8+ T-cell frequency in humans and non-human primates 267
Figure 5.4 Antigen-specific IFNγ production after aerosol BCG (aeBCG) 269
Figure 5.5 IgG titre in humans and non-human primate serum 271
Figure 5.6 Example gating to identify proliferating cells 276
Figure 5.7 Comparison of proliferation detected by Ki67 vs cell trace violet (CTV). 277
Figure 5.8 PPD-specific proliferation in baseline human and NHP samples. 278

Appendices

Supplementary Figure 1 CD161 gating strategy for flow cytometry 335
Supplementary Figure 2 Example gating for cytokine and HLA-DR frequency 336
Supplementary Figure 3 (i-iv) Cell population ratios, measured by IDEXX Lasercyte Haematology analyser 339

List of tables

Chapter 1

Table 1.1 Objectives 66

Chapter 2

Table 2.1 List of consumables used in this project 68
Table 2.2 List of reagents used in this project 70
Table 2.3 List of solutions used in this project 71
Table 2.4 Non-human primate (NHP) studies 74
Table 2.5 Human clinical trial details 75
Table 2.6 Antibody panels used for flow cytometry 83

Chapter 3

Table 3.1 Peripheral blood mononuclear cell (PBMC) populations 105
Table 3.2 Broncho-alveolar lavage (BAL) cell populations 117
Table 3.3 Lung mononuclear cell (MC) populations 124
Table 3.4 Lymph node mononuclear cell (MC) populations 126
Table 3.5 Whole blood (WB) cell populations 131
Table 3.6 CD161 expression across tissue compartments 135
Table 3.7 Human leukocyte antigen-DR (HLA-DR) expression across tissue compartments 139
Table 3.8 Activation marker expression among whole blood (WB) samples 145
Table 3.9 PPD-specific+ cell cytokine frequency 152

Chapter 4

Table 4.1 Changes in frequency of PPD-specific IFNγ producing cells later after aerosol BCG (aeBCG) 187
Table 4.2 Peripheral blood mononuclear cell (PBMC) populations 190
Table 4.3 Broncho-alveolar lavage (BAL) cell populations 195
Table 4.4 Whole blood cell populations 203
Table 4.5 CD161 expression across tissue compartments 207
Table 4.6 Human leukocyte antigen-DR (HLA-DR) frequency across tissue compartments 212
Table 4.7 Activation markers on whole blood samples 216
Table 4.8 Cytokine expressing cell frequency across tissue compartments 221
Table 4.9 Changes in antibody titre later after aerosol BCG (aeBCG) 228
Table 4.10 Correlations between the frequency of PPD-specific IFNγ SFU measured by ELISpot and cell population frequencies among peripheral blood mononuclear cells (PBMCs) 232
Table 4.11 Correlations between the frequency of PPD-specific IFNγ SFU measured by ELISpot and cell population frequencies among broncho-alveolar lavage (BAL) cells 233
Table 4.12 Correlations between the frequency of PPD-specific IFNγ SFU measured by ELISpot and cytokine-positive cells (peripheral blood mononuclear cells - PBMC) 236

Table 4.13 Correlations between the frequency of PPD-specific IFNγ SFU measured by ELISpot and cytokine-positive broncho-alveolar lavage (BAL) cells 237
Table 4.14 Correlations between the frequency of PPD-specific IFNγ SFU measured by ELISpot and antibody titre 238
Table 4.15 Mucosal BCG studies 245

Appendices

Supplementary Table 1 Wordcount 302
Supplementary Table 2 BCG dosing across studies 303
Supplementary Table 3 Abbreviations & acronyms 303
Supplementary Table 4 Median cell population counts, characterised by flow cytometry 304
Supplementary Table 5 Correlations between IFNγ SFU+ and PBMC cell populations 309
Supplementary Table 6 Correlations between IFNγ+ SFU and BAL cell populations 314
Supplementary Table 7 Correlations between IFNγ+ SFU and IFNγ-positive cells among PBMCs 317
Supplementary Table 8 Correlations between IFNγ+ SFU and IL-2-positive cells among PBMCs 320
Supplementary Table 9 Correlations between IFNγ+ SFU and IL-17-positive cells among PBMCs 323
Supplementary Table 10 Correlations between IFNγ + SFU and IFNγ-positive cells among BAL 326
Supplementary Table 11 Correlations between IFNγ + SFU and IL-2-positive cells among BAL 329
Supplementary Table 12 Correlations between IFNγ + SFU and IL-17-positive cells among BAL 332
Supplementary Table 13 Correlations between IFNγ SFU frequency and IgG antibody titre 333
Supplementary Table 14 Correlations between IFNγ+ SFU frequency and IgM antibody titre 334

Chapter 1: Introduction

1.1 The problem of TB

1.1.1 TB burden today

Until the onset of the COVID-19 pandemic, Tuberculosis (TB) was the leading infectious killer worldwide, ranking above HIV/AIDS (human immunodeficiency virus/acquired immunodeficiency syndrome). TB disease is associated with poverty and in 2020, 86% of new cases were accounted for by the 30 highest burden countries[11]. In high burden areas, rates of TB disease are highest among working-age young adults. In higher income countries incidence is much lower and usually among the elderly, immigrants, and those of low socio-economic background. In 2020, an estimated 10 million new cases of TB disease were diagnosed, 1.5 million deaths were attributed to TB, and it was estimated that one quarter of the world's population were latently infected with *Mycobacterium tuberculosis (M.tb)* - LTBI[11].

Of those with presumed LTBI, 5 to 10% of immunocompetent individuals will develop disease in their lifetime[12]. The number of deaths due to TB increased from 2019 to 2020, and has been attributed reduced diagnosis/treatment caused by COVID-19[11]. Predictions for 2021/2022 demonstrate further impact of COVID-19 on TB, alongside under-funding and continued emergence of drug-resistant strains of *M.tb*[11]. The risk of progression of LTBI, and the high burden of LTBI and TB disease worldwide makes TB a research priority. An effective vaccine would be the most effective preventative measure.

1.1.2 Prevention and treatment of TB

To minimise the impact of TB disease, effective treatment and vaccination are necessary. The antibiotic course required to treat TB disease is long and costly, with toxic side effects, and the added complication of antibiotic resistance[13,14, 15]. Currently, BCG is the

only licenced preventative vaccine against TB. BCG provides protection against infant TB and disseminated disease, but limited protection against adult pulmonary TB (the most common form of disease), particularly in high burden countries[16]. Increased access to treatment and reduction in overcrowding/poverty can also help to prevent the spread of TB disease.

1.1.3 Outcomes of M.tb infection

Outcomes of infection with *M.tb* include: complete clearance, control of infection (no disease), sustained asymptomatic low-level infection (LTBI), latent infection that quickly progresses to disease, and active disease (TB). Over 50% of individuals do not develop active TB after *M.tb* infection[17]. Active disease occurs when infection leads to bacterial spread. Symptoms include: fever, night sweats, persistent cough, and weight loss. If un-treated, TB disease can be fatal. Current treatment regimens involve a long course of antibiotics, and drug-resistant strains of *M.tb* are increasing in prevalence[15].

M.tb affects the lungs in more than 85% of cases[18], hence the respiratory symptoms. In about 20% of cases, extrapulmonary TB disease can develop when bacteria spread[19]. Extrapulmonary TB is most common in immunocompromised individuals and secondary sites of infection include: the LNs, pleural cavity, gastrointestinal tract, bone and nervous system[19]. In up to 20% of extrapulmonary cases, infection becomes widespread via transport in the bloodstream[20]. This is known as disseminated or miliary TB, and was mainly seen in infants until the advent of TB treatment[20].

LTBI is a clinically asymptomatic, contained state of infection, which can be viewed as a balance between the immune system and *M.tb*. LTBI has recently been calculated as 24.8% globally[21], and a large portion of the *M.tb* genome is dedicated to establishing latent infection by resisting bacterial clearance[22]. People with LTBI act as a reservoir for

M.tb and are at risk of disease re-activation. HIV infection, certain treatments (e.g. anti-tumour necrosis factor – anti-TNF) and organ transplantation are risk factors for LTBI re-activation [23].

1.1.4 TB disease diagnosis

Study of natural *M.tb* infection is limited by infection rates, and difficulties associated with working out the point of infection. It takes time for symptoms to develop and bring patients into the clinic, prompting TB disease diagnosis. TB disease diagnosis is usually through a combination of: symptom recognition, sputum testing (for presence of mycobacteria), chest X-ray, interferon-gamma (IFNγ)-release assay (IGRA) and Tuberculin skin testing. The combination used depends on the country or area, and some tests may be more applicable (e.g. IGRA is more applicable to LTBI, in non-endemic countries).

IGRAs are a group of *in vitro* blood tests, which measure the release of IFNγ from T-cells, after *M.tb* antigen stimulation. Early secretory antigen target-6 (ESAT-6) and culture filtrate protein-10 (CFP-10) are commonly used *M.tb* antigens. Conversion from IGRA- to IGRA+ status may be associated with development of active TB. Two commercially available IGRA are the QuantiFERON-TB Gold In Tube assay and the T.SPOT TB assay. These assays are limited by their focus on an IFNγ, T-cell specific response, which is not sufficient to protect against disease[24].

1.1.5 Natural controllers of TB

Exposure to *M.tb* may not lead to active or latent disease (no viable pathogen)[25]. QFT reversion from QFT+ to QFT- may represent bacterial clearance and subsequent dampening of the measurable immune response, or may result from limited sensitivity. A recent meta-analysis of serial QFT testing compared QFT reversion with or without prophylactic treatment and showed that the reversion rate for treated patients was

24.9%, compared to 25.3% for untreated pateients[26]. This suggests that regardless of treatment, about one quarter of patients undergo QFT reversion. Why a proportion of individuals undergo reversion is unknown, and is difficult to study[27].

1.1.6 TB in cattle

Animal TB is also a major problem, particularly affecting livestock (cows), but also causing deaths in other species[28]. Bovine TB affects livestock worldwide, which puts a huge burden on farming communities and associated wealth, and is exacerbated by spread from other wildlife alongside spread between cattle[29]. Bovine TB is mostly caused by *M.bovis*, and may account for up to 10% of human TB cases, through zoonotic transfer[30]. BCG vaccination is not widely used in cattle, because it interferes with diagnostic testing for bovine TB and protection is limited; work is ongoing to develop strategies to boost BCG in cattle - their size means that facilities for this work are limited [31]. Vordermeier *et al.*, showed that boosting BCG with either modified vaccinia virus Ankara-(MVA) 85A or Ad85A significantly reduced pathology after *M.bovis* challenge, improved the induction of T-cell memory and interleukin-17 (IL-17) production, compared to BCG alone[32].

1.2 BCG vaccination against TB

1.2.1 BCG

BCG is a live attenuated strain of *M.bovis*, and offers variable protection against TB, depending on the setting[33]. In 1900, Albert Calmette and Camille Guérin started developing the initial BCG vaccine by growing tubercule bacilli on a medium made of potato and glycerol[34]. By 1921, a non-virulent mycobacterial stain (BCG) that could be tested in humans had been developed by repeat passaging[34]. BCG vaccination is still

routine in many countries, but has been discontinued elsewhere. Discontinuation of routine BCG vaccination in Sweden in 1975 showed an increase in cases of atypical TB[35].

Although BCG has shown up to 80% efficacy in some studies, in other studies efficacy is (closer to) zero[33]. Possible factors affecting this variability include: geographical location[36], vitamin D_3 levels[37, 38], poor nutrition, prior exposure to mycobacteria[39], prior immune status including effects of viral/helminth co-infection[39, 40], vaccination age[41], circadian rhythm influence[42], BCG strain[43], BCG dose[7, 44, 45] and immunisation route[46]. Unfortunately, current understanding of which factors are most important is limited and therefore cannot be included in the rational design of new treatments or vaccinations.

1.2.2 BCG delivery

Vaccine efficacy can vary widely depending on the chosen age group, delivery route and dose. BCG is given by the intradermal (ID) route at a dose of 1-10x10^5 colony forming units (CFU), as close to birth as possible (World Health Organisation recommendation), as it is particularly effective against infant forms TB[33]. Delaying vaccination from birth to 10 weeks old resulted in enhanced T-cell cytokine production capacity at one year of age, but did not correlate with protection in the first two years of life[41]. Modelling suggests that if vaccine coverage at birth could be increased to 92%, 2.8% of TB-related deaths by age 15 could be prevented[47].

Alongside age, time-of-day may also influence vaccine efficacy, because immune cells vary in their numbers and functions during the day. A small study showed that morning vaccination elicited a stronger immune response to BCG vaccination[42]. BCG-induced protection also varies with time elapsed since vaccination. A recent meta-analysis showed that BCG vaccine efficacy declined with time, but that vaccinated

individuals were still less likely to have LTBI, more than 20 years after vaccination[48]. This suggests that BCG offers at least partial long-term protection against disease.

1.2.3 BCG strain

BCG sub-culture and distribution throughout the world has led to divergence into genetically distinct strains of BCG. Strains obtained from the Pasteur Institute pre-1927 can be classified as 'early' strains and strains isolated post-1927 are classified as 'late'[43], but further gene losses since the 1920s mean this classification is imperfect. In mice, BCG Phipps, Pasteur and Tice ('late') showed high virulence, associated with better vaccine efficacy, whilst BCG Sweden and Birkhaug ('early') showed low virulence[49]. Classification of *M.tb* strains into Beijing or non-Beijing lineage showed that infections with multiple strains at once are common[50]. Multiple-strain infections may alter induced immunity, and have implications for treatment and drug resistance[15].

1.2.4 BCG and latitude

Geographical location has been identified as factor affecting the immune response to BCG[36, 51], but may be a simplification of a number of other factors including: prior mycobacterial exposure, prior immune and nutritional status, and vitamin D_3 status. Generally distance from the equator is associated with improved BCG efficacy, as shown in an analysis of 80 studies (overall rho of 0.3853, p=0.0004), which estimated that 15% of the variance in BCG efficacy can be accounted for by latitude[51].

Vitamin D_3 is a natural metabolite with immunomodulatory functions. In a meta-analysis of longitudinal studies, Vitamin D_3 status had a concentration-dependant association with reduced TB disease risk[38]. Upon *in vitro* stimulation with bacterial ligands, peripheral blood mononuclear cells (PBMCs) from vitamin D_3-sufficient adults had a more anti-inflammatory phenotype, and increased cluster of differentiation-14

(CD14)+ monocyte frequency[52]. One-off vitamin D_3 supplementation significantly enhanced the ability of human whole blood to restrict mycobacterial growth *in vitro*[53]. Despite successful mechanistic *in vitro* studies and promising early results, weekly oral vitamin D_3 supplements showed no protection against the TB disease in a phase 3 trial[54].

Other nutrients also modulate immune function[55]. Malnutrition is particularly prevalent in sub-Saharan Africa and Southeast Asia[56], both regions with a high TB burden. Measuring malnutrition is complex, ranging from gross measures of body mass index and deviation from normal growth rates, to measures of specific nutrients and their effects. Further study of the effect of nutritional deficiency on immunity, may help to explain some of the variation in immune responses to mycobacterial pathogens across the globe.

1.2.5 Non-tuberculous Mycobacteria (NTM)

Another factor that varies with latitude is exposure to NTM. NTM are often isolated from water sources or soil, vary in distribution worldwide and are usually non-pathogenic (in immunocompetent individuals)[57]. In humans, mycobacterial antibody levels increase with age, perhaps due to increased NTM exposure[73]. Studies of NTM exposure show contrasting effects[39], and are inhibited by a lack of reliable research tools (e.g. lack of reliable immunological assay to confirm/exclude prior NTM exposure). In mice, BCG efficacy increased after systemic exposure to heat-killed NTM (*Mycobacterium avium*), but efficacy reduced after oral, live exposure[58]. These contrasting results demonstrate that altering the route and viability of NTM can induce different effects.

Prior immune exposure may have a 'masking' or 'blocking' effect[59, 60]. Previous exposure may trigger a small immune response, which is enough to be activated upon second exposure, and to hide (mask) or block any further immune response being mounted. BCG vaccination was compared across two cities in Brazil with similar ethic and

socio-economic status (Manaus and Salvador)[61]. Manaus is closer to the equator, and a more rural city than Salvador, so exposure to NTM is likely to be higher. At birth, vaccine efficacy was similar across geographical locations (40% vs 36%). At school age, first time vaccination with BCG had better efficacy in Salvador (34% vs. 8% in Manaus), as did revaccination (19% vs. 1%, respectively)[61]. Worse BCG efficacy in Manaus at school age may demonstrate masking or blocking due to NTM exposure during childhood.

1.2.6 Viral infections and M.tb

TB disease is the most common cause of AIDS-related death[62], and HIV and TB share high-burden areas[63]. Antiretroviral therapy controls viral load and allows some immune recovery, but this only reduces the increased risk of TB when infected with HIV by 67%[64]. Possible mechanisms by which HIV infection exacerbates *M.tb* infection include: CD4+ T-cell depletion, CD8+ T-cell dysfunction, *M.tb* entry receptor up-regulation, chemotaxis de-regulation, granuloma manipulation, altered Th1/Th2 balance and interference with bactericidal pathways[62]. CD4+ deficient mice are more likely to develop TB, CD4+ depletion in mice increases the chance of LTBI re-activation, and TB pathology is worsened in CD4+ depleted non-human primates (NHPs)[65, 66, 67]. Similarly, SIV (simian immunodeficiency virus), exacerbates TB in NHPs by specific depletion of lung interstitial CD4+ T-cells[68].

Cytomegalovirus (CMV) infection causes immune cell dysregulation and immune senescence[69], and there is emerging evidence that positive CMV status increases the risk of developing TB. TB patients have more CMV-specific immunoglobulin-G (IgG) than controls[70], and there is a dose-response effect between CMV-specific antibody and risk of development of TB[71]. In a retrospective case-control comparison CMV-positive infants

had a higher risk of developing TB[72]. In a cross-sectional study in rural Uganda, higher CMV-specific IgG titre was associated with lower *M.tb*-specific Ig, but not with total IgG[73].

1.3 Bettering BCG – vaccines

A biomarker is a measurable characteristic of the immune system that can be assessed as an indicator of normal immune function, disease process, or response to a therapeutic intervention[74, 75]. Where a biomarker is known to correspond to an immunological response that prevents infection or to reduced disease severity, this is known as a correlate of protection. Progress beyond BCG has been hampered by the lack of a defined immunological correlate of protection[76]. Such a marker could be used in (pre-)clinical testing to show efficacy early on, and down-select candidates for efficacy trials.

1.3.1 Immune correlates of protection

To validate a correlate of protection, clinical trials with an effective vaccine are necessary. A good example of the consequences of finding an immune correlate comes from the development of pneumococcal vaccines. An immune correlate of protection was established for the 7-valent vaccine used pre-2010: 0.35 μg/mL concentration of aggregated anti-capsular polysaccharide antibody. A vaccine against 13 serotypes could then be approved for use, based on the immune correlate data (and safety data), rather than on lengthy efficacy comparisons[77]. Recent data suggests that the efficacy prediction based on correlates was an oversimplification, but this method allowed faster vaccine implementation and licensing, and is therefore a relevant and pragmatic approach[78].

There is no defined immunological correlate of protection against TB, as recently reviewed[79]. Human leukocyte antigen-DR (HLA-DR)+ CD4+ T-cell frequency correlated with increased risk of TB, but not with protection[80]. IFNγ is used as the closest thing to an

immune correlate for TB, and is the primary readout in clinical trials. It seems clear that IFNγ plays a key role, but that this is timing dependant[81], and although IFNγ is necessary for protective immunity, the level of IFNγ induced by vaccination does not correlate with protection[82]. Other possible correlates include: polyfunctional T-cells, Th17 cells, natural killer (NK) cells, γδ cells and CD4-CD8- T-cells[83].

Mycobacteria have co-evolved alongside humans and animals over thousands of years, making it unlikely that one single correlate exists for TB. A combination of markers or genes can be used to split a cohort into those more or less likely to have gained protection against TB from vaccination. Zak *et al.,* identified a 16-gene signature that predicted progression from *M.tb* infection to TB disease with 66.1% sensitivity and 80.6% specificity[84]. Further large cohort genetic studies, studies of vaccines/natural infection that lead to a range of responses, and comparison of immune responses and baseline status may be useful in the search for an immune correlate[85].

1.3.2 TB vaccine candidates

Despite the lack of defined correlate of protection, there are a number of promising BCG alternatives in clinical trials (Figure 1.1). Some target specific stages (e.g. re-activation of LTBI), while others aim to improve on the efficacy of BCG broadly.

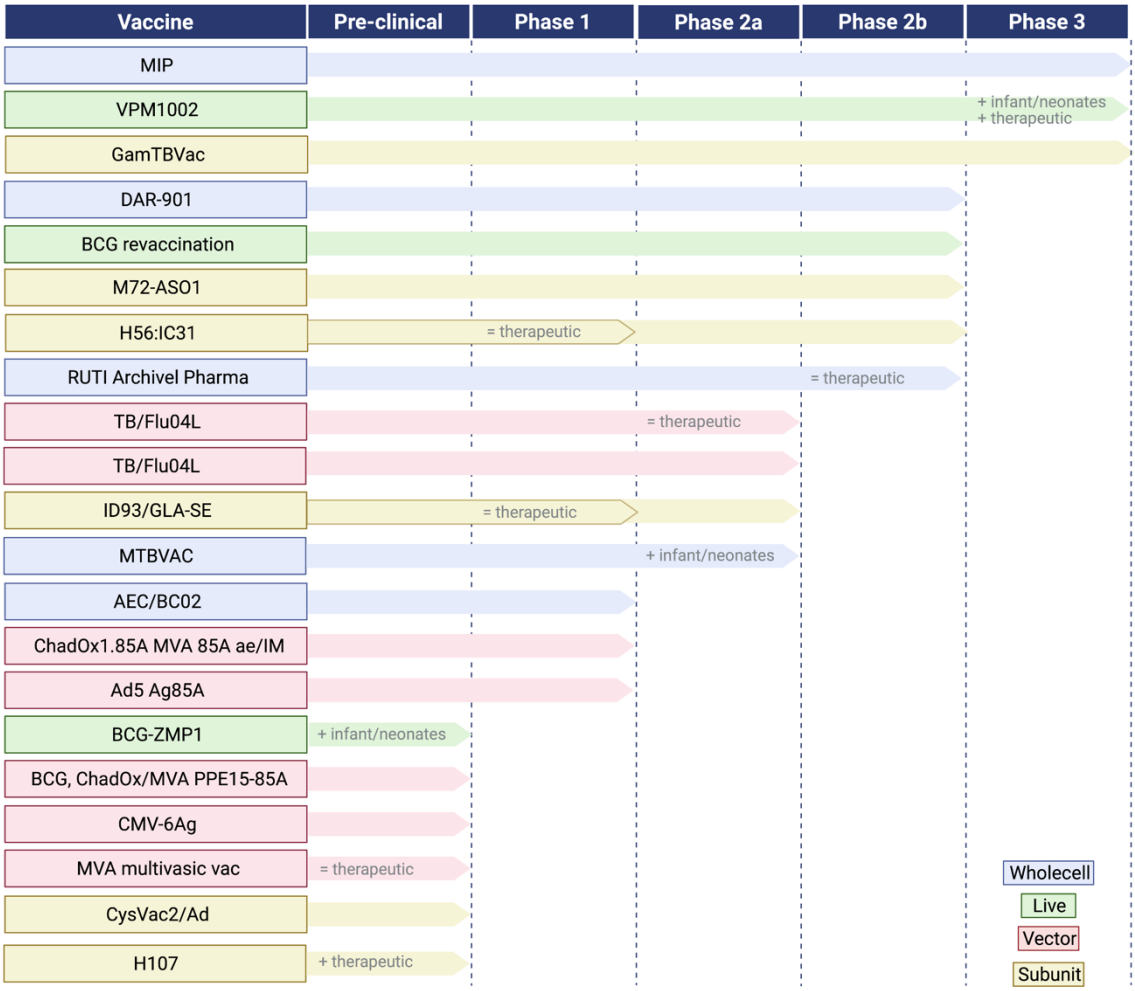


Figure 1.1 TB vaccine candidate pipeline

Adapted from TBVI pipeline (October 2021). Blue = whole cell, green = live, red = vector, yellow = subunit. Trials are for preventative vaccines targeting adolescents and adults, unless otherwise marked on the arrow. Where multiple trials are ongoing for the same candidate and vector combination, this is marked by additional outlined arrows. Created with BioRender.com

Whole cell vaccination has the advantage of a comprehensive antigen repertoire, but may suffer from the same lack of efficacy as the immune response to natural *M.tb* infection[86]. Another strategy is to create recombinant BCG, with overexpression of immunodominant antigens (e.g. overexpression of Ag85B in rBCG30) or with modifications to improve antigen presentation and T-cell memory induction (e.g. return

of lost virulence factors in BCG:ESX-1)[86]. VPM1002 is the most clinically advanced recombinant BCG strain (urease C gene replaced with the pore-forming listeriolysin O protein), and has shown safety in phase IIa clinical trials[87]. Another candidate is MTBVAC, which is an attenuated form of *M.tb* itself (deletion of phoP transcription factor). A recent phase IIa clinical trial has demonstrated the safety of MTBVAC in humans[88] and NHP studies have shown evidence for efficacy of MTBVAC[89, 90, 91].

Many TB vaccine candidates aim to build on the protection provided by BCG, through a heterologous subunit vaccination boost. A phase IIb trial of the fusion protein M72 (*M.tb* antigens 32A and 39A) has shown 50% efficacy against progression to TB disease from LTBI[92]. Further exploration will show whether this vaccine confers protection in those who are BCG-vaccinated[92, 93]. Other subunit vaccine candidates include H56:IC31 and ID93:GLA-SE, both based on a fusion of antigens[94, 95, 96]. Viral vectors allow more specific targeting of subunit vaccines. MVA85A (attenuated Vaccinia virus strain expressing Antigen 85A) was the first TB vaccine to undergo clinical trials since the 1960s, but despite the induction of T-helper 1 (Th1) CD4+ T-cells in phase I/IIa clinical trials, this vaccine did not provide protection in a phase IIb trial of BCG vaccinated infants pre-exposure[97].

1.3.3 BCG re-vaccination

Recently, Nemes *et al.*, showed that re-vaccination of QuantiFERON TB-GOLD (QFT) negative adolescents with BCG itself showed an efficacy of 45.4% against sustained QuantiFERON TB-GOLD conversion (a measure of *M.tb* infection)[98]. This contrasts with previous data by Rodrigues *et al.*, which showed no effect of re-vaccination[99]. Unlike the trial by Nemes *et al.*, Rodrigues *et al.,* did not exclude participants based on previous sensitisation to *M.tb* and looked at children between age 7 and 14 years.

1.4 Bettering BCG – BCG delivery routes

Inhalation of aerosolised droplets into the lung is the primary infection route for *M.tb*. Mucosal delivery to mimic this may offer a physiological or immunological advantage over standard ID delivery.

1.4.1 Alternatives to ID BCG

Aerosol (AE) delivery is equally or more immunogenic than traditional subcutaneous vaccination against measles, and has been licensed for seasonal influenza vaccination[46, 100]. Intranasal (IN) vaccination is used in influenza vaccination. Early reports of Bell's Palsy (facial nerve paralysis) have dampened interest in IN vaccines with potent adjuvants[101], despite these finding not being replicated in a recent analysis[102,103]. Endobronchial (EB) and intratracheal (IT) installation also provide methods of mucosal delivery, but are not feasible vaccination routes[104]. Intravenous (IV) delivery has been explored in animal models, but is also inaccessible in a clinical context[5, 8].

1.4.2 Mucosal BCG

Mucosal BCG was first explored in the 1970s, in a comparison of AE and IV BCG delivery[105]. More recently, EB installation of BCG has shown superior protection to ID BCG in two studies of rhesus macaques (RM)[2, 10]. However, a recent delivery method comparison showed that only IV BCG provided superior protection (AE and ID + AE delivery did not)[5].

1.4.3 Mucosal vaccination by AE

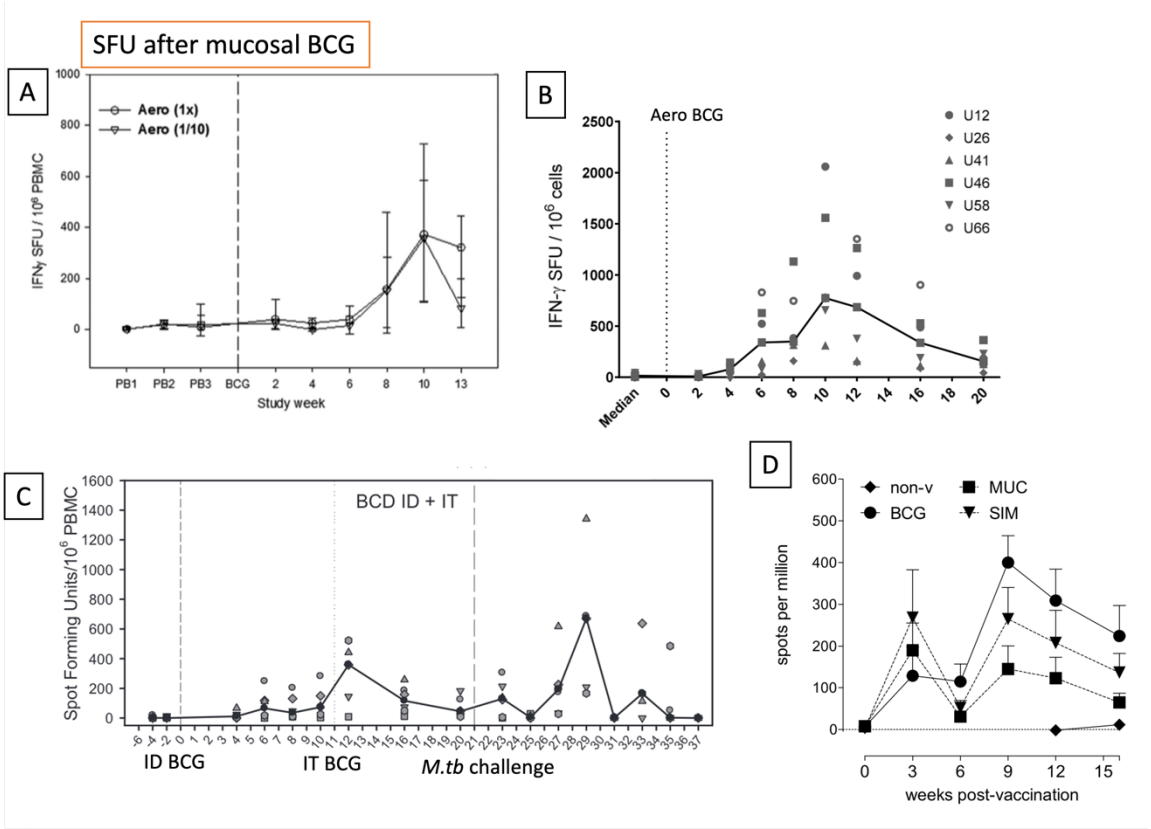
White *et al.*, showed that a standard dose of BCG delivered by AE induced comparable protection against *M.tb* challenge to ID delivery[3]. The increase in Purified Protein Derivative (PPD)-specific IFNγ+ SFU frequency was comparable to ID, but delayed and CD4+ and CD8+ T-cell cytokine production was also delayed in the AE group[7]. EB

installation of BCG also induced comparable IFNγ+ SFU frequency to ID BCG[2]. Published data showing the frequency of IFNγ+ SFU (measured by ELISpot) induced by BCG/*M.tb* challenge are reproduced in Figure 1.2.

In the process of nebulisation to produce AE, approximately 1-3 log CFU is lost[3]. Ari *et al*., showed that a mesh nebuliser delivered 2-4 times more vaccine at the level of the bronchi than a jet nebuliser[106]. Mouthpiece delivery was the most efficient of those tested, and facemask delivery was second[106]. Preliminary data (*White et al., unpublished*), show that AE droplet deposition varies with delivery method, as shown by computerised tomography of RM after aerosolization of gold particles (estimated to be similar in size to *M.tb* bacilli), and delivery with either a mask or mouthpiece. Breathing rate and co-morbidities associated with the lungs also affect deposition of delivered aerosolised substances[107].

1.4.4 IV vaccinations

IV BCG delivery or ID BCG with an IT boost provided improved protection compared to ID BCG (better survival and disease pathology in NHPs)[8]. Protection induced by IV vaccination was strongest, and induction of IFNγ+ and TNFα+ CD4+ T-cells correlated with protection[8]. Darrah *et al.* repeated the finding that IV BCG vaccination provided superior protection against *M.tb* challenge, and that IV delivery induced more antigen-specific T-cells in the blood post-vaccination than other routes[5].


SFU after mucosal BCG
A
Aero (1x)
Aero (1/10)
IFNγ SFU / 10^6 PBMC
PB1 PB2 PB3 BCG 2 4 6 8 10 13
Study week
B
Aero BCG
IFN-γ SFU / 10^6 cells
U12
U26
U41
U46
U58
U66
Median
C
BCD ID + IT
Spot Forming Units/10^6 PBMC
ID BCG
IT BCG
M.tb challenge
D
non-v
BCG
MUC
SIM
spots per million
weeks post-vaccination

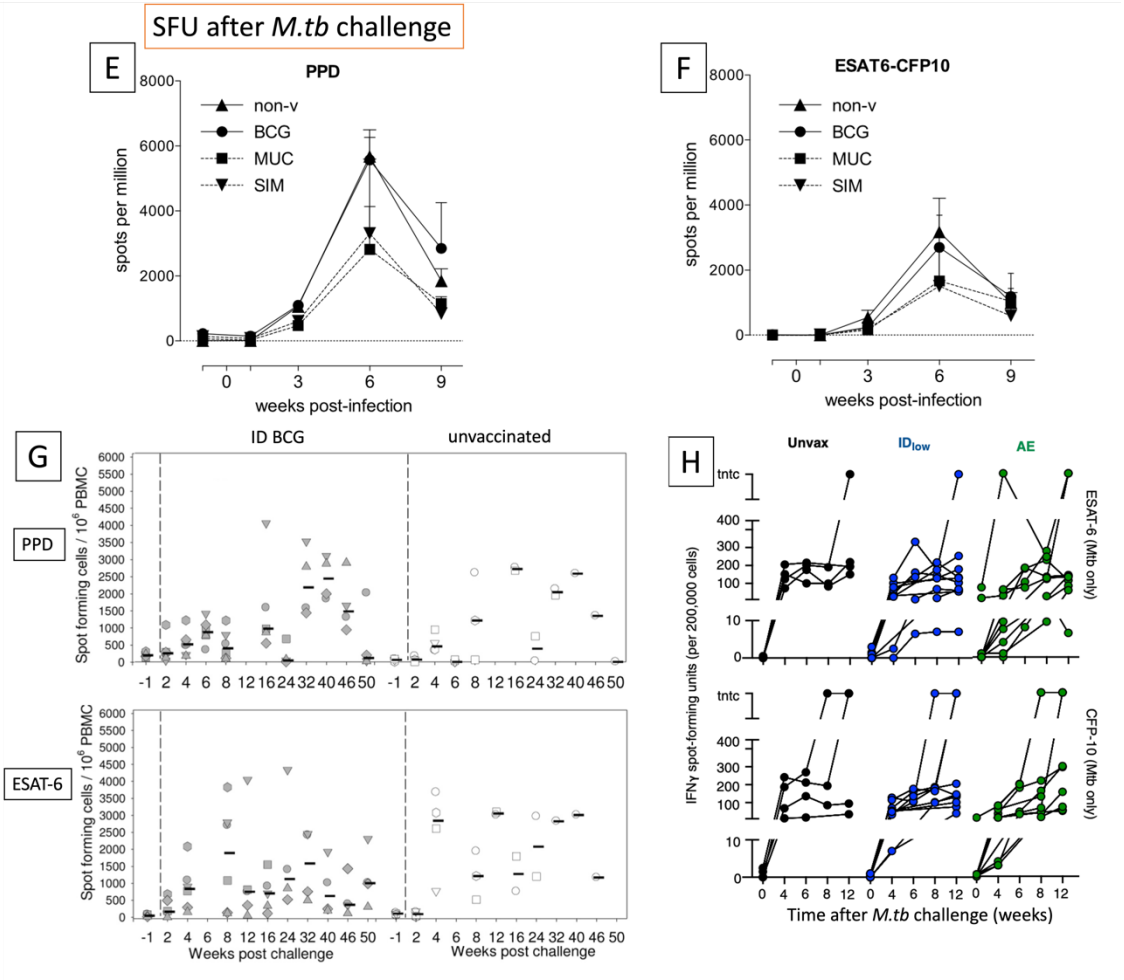

SFU after M.tb challenge
E
PPD
non-v
BCG
MUC
SIM
spots per million
weeks post-infection
F
ESAT6-CFP10
non-v
BCG
MUC
SIM
spots per million
weeks post-infection
G
ID BCG
unvaccinated
PPD
ESAT-6
Spot forming cells / 10^6 PBMC
Weeks post challenge
H
Unvax
ID low
AE
tntc
ESAT-6 (Mtb only)
CFP-10 (Mtb only)
IFNγ spot-forming units (per 200,000 cells)
Time after M.tb challenge (weeks)

Figure 1.2 Frequency of PPD-specific IFNγ spot forming cells after mucosal BCG (reproduced)

*These graphs are reproduced and show antigen-specific interferon-gamma spot forming units (SFU)/million cells (**A**-**F**) or SFU/200,000 cells in rhesus macaques (**H**). **A** shows a standard human dose (2-8x10^6 CFU) of aeBCG compared to 1/10th dose, published by White et al., in 2015[3]. **B** shows a standard human dose (2-8x10^6 CFU) of aeBCG, published by White et al., in 2020[7]. **C** shows a standard dose of ID BCG at time point Week 0, followed by a 10X dose of BCG delivered IT at Wk11. BCG and M.tb challenge are indicated by dashed lines, as published by Sharpe et al., in 2016[8]. **D** shows the response of unvaccinated animals ('non-v'), animals exposed to ID BCG ('BCG'), EB BCG ('MUC') or both ID and EB BCG simultaneously ('SIM') – all doses 2–8×10^6 CFU, published by Verreck et al., in 2017[10].*

*The frequency of PPD-specific (**E**) and early secretory antigen target-6/culture filtrate protein-10 (ESAT-6/CFP10)-specific (**F**) SFU of unvaccinated animals (non-v), for animals exposed to intradermal BCG (BCG), endobronchial BCG (MUC) or intradermal + endobronchial BCG simultaneously (SIM) after endobronchial challenge with 500 CFU M.tb are shown – all doses 2–8×10^6 colony forming units (CFU), as published by Verreck et al., in 2017[10]. **G** shows the PPD-specific (above) and ESAT6-specific (below) SFU for intradermal BCG vaccinated animals (left, grey) and unvaccinated animals (right, clear) after 40-60 CFU aerosol M.tb challenge, as published in 2010 by Sharpe et al[8]. **H** shows the frequency of ESAT6-specific (above) and CFP10-specific (below) SFU for unvaccinated (black), intradermal BCG (blue) or aerosol BCG (green, 5x10^7 CFU) vaccinated animals, after endobronchial M.tb challenge with 4-36 CFU as published by Darrah et al., in 2020[5].*

1.5 Use of animal models in TB research

Animal studies extend the range of tissues available to study TB, combining ongoing sampling of blood and lung mucosa (BAL), with deeper tissue exploration post-mortem (PM). Animal studies can also include *M.tb* challenge, which is not ethical in humans. Parallel studies between humans and animal models will help determine the true relevance and utility of these models.

1.5.1 Small animal models of TB

Guinea pigs, rabbits and marmosets are used to evaluate candidate TB vaccines, study drug kinetics, and antibiotic resistance[108, 109]. Their size and availability makes them particularly applicable for iterative work, but reagents available for these models are limited compared to those available for mice. Mouse models are used across a range of diseases and many tools for genetic manipulation and in-depth study are available: knock-out/knock-in mice, adoptive transfer of cells/proteins/other components (from mice or other species) and alternative strains (e.g. immunodeficient mice).

Although mice are readily available, relatively inexpensive and have many tools associated, there are limits to how comparable mouse and human TB are[110]. Vaccine efficacy is less variable in mice due to genetic homogeneity[111]. Humanised mouse models and outbred mice may produce more representative testing platforms, but have limited application to human TB[111, 112]. Mice do not have CD56 NK cells (no CD56), CD1-restricted T-cells, or Vγ2Vδ2+ subset of γδ T-cells. Toll-like receptors are different in mice, and common strains (Balb.c and C57BL/6) do not develop caseating granulomas[113,114]. Guinea pigs, rabbits and marmosets do develop caseating granulomas, and progress is being made to extend the reagents available to study these small mammals[108]. Small animal models are also limited by sample volume, and difficulty of collecting serial samples.

1.5.2 NHP model of TB

Robust and predictive preclinical data is important to support the advancement of candidate vaccines or treatments into costly clinical trials. NHPs are considered to be the most relevant and reliable animal model for the final stage of preclinical testing as they are naturally susceptible to *M.tb* infection, and develop the same spectrum of human-like disease, with similar pathology including granulomas[115]. NHPs and humans share much of their genetic material and complex double circulatory, immune, and central nervous systems.

Some studies suggest that different species of macaque differ in their susceptibility to disease[4, 116, 117, 118, 119,120]. Asian cynomolgus macaques (CM) control *M.tb* infection better than Mauritian CM[119, 121]. Mauritian CM originate from the island of Mauritius and have a limited MHC diversity after an extreme population bottleneck. Genetic and phenotypic differences between Mauritian and Asian CM, and the increase in genetic homogeneity in the Mauritian CM population through geographical isolation, mean that this species has the potential to contribute to the portfolio of macaque models of TB.

In comparison to Mauritian CM/RM, Asian CM tend towards latent or well controlled disease, where RM infected with the same dose of *M.tb* are more likely to develop active TB, with increased dissemination to LNs[116,122]. Following a very low dose *M.tb* challenge (less than 10 CFU), disease is also more progressive in RM than CM[121]. CM may provide a more representative model of LTBI, given that up to 50% of animals do not develop active disease, whereas more susceptible RM provide a model better able to show a protective vaccination effect. NHP models of TB display features characteristic of both infant TB disease presentation, and adult pulmonary TB. Macaque models have recently been developed to replicate neonatal BCG vaccination in humans[123].

Sibley *et al.*, recently showed that the CD4+:CD8+ T-cell ratio is significantly higher in RM than CM, and that myeloid dendritic cell populations differed between the species[120]. Dijkman *et al.,* have also explored innate immunity between species, to try and determine which mechanisms account for the different disease development identified. After *M.tb* challenge, Dijkman *et al.* could not detect differences between antibody or T-cell responses, but showed that monocytes from RM have a more anti-inflammatory phenotype at baseline and early on in response to mycobacterial infection than CM[4].

Reagents used to study *M.tb* and the corresponding immune response are often cross-reactive between humans and NHPs, which allows for direct species comparison and production of translatable data. For example, IFNγ is produced by immune cells in response to PPD, and to *M.tb*-specific antigens ESAT-6 and CFP-10, in both species. PPD is a culture filtrate from *M.tb*, which contains secreted antigens that are also present in BCG. PPD can be used to characterise antigen-specific immune responses after BCG (e.g. vaccination) in either species, or after *M.tb* challenge (NHPs), which makes this a useful reagent for parallel studies.

Elhmouzi-Younes *et al.*, used parallel experiments to directly compare human and CM innate immune responses by mass cytometry[243]. Overall, macaques showed stronger staining for markers associated with inflammation and activation, including high expression of CD16 on myeloid dendritic cells, and CD11b on neutrophils and monocytes[243]. Silver *et al.,* examined BAL cell composition in CM and humans, before and after *M.tb* infection[124]. BAL T-cell and phagocytic cell populations were identified in both species, with similar differential cell counts[124]. Phagocytic cells co-expressing HLA-DR, CD11b/c and CD206 were the most common phagocytic cell population in both species[124]. The two species differed - CM with LTBI displayed BAL lymphocytosis, whereas humans

with LTBI did not[124]. These studies demonstrate the additional insights that can be gained by running studies in parallel.

In addition to immunological similarity, serial samples can be collected from NHPs, which provides a direct advantage compared to small animal models. In addition to blood and BAL samples (which can be collected in humans), tissue samples can be collected at necropsy, which allows comparison between the immune response in different compartments. NHPs can be exposed to virulent *M.tb* (challenge). *M.tb* challenge of NHPs usually represents the final level of pre-clinical testing of candidate TB vaccines. The timing of the challenge can be tightly controlled, which allows exploration of very early time points[115].

Infections with *M.tb* or BCG to 'challenge' an NHP usually consist of a single dose, sufficient to ensure infection in all animals; this is required for robust comparison between groups, and to determine whether the intervention given reduces disease burden. More recently, single[7, 121], and repeated challenges with a low dose of *M.tb* have been used in NHPs[2], to give a more representative infectious challenge to that experienced by humans during natural infection.

1.6 The pathogen that causes TB – M.tb

Human TB is caused by infection with a member of the *M.tb* complex - usually *M.tb* (also *M.bovis*). *M.tb* has a unique structure, with a thick waxy coating surrounding its membrane: a layer of peptidoglycan, a layer of arabinogalactan and a thick mycolic acid layer interspersed with glycoproteins and glycolipids. This coating helps provide resistance against immunity, and to establish niches, in which they replicate slowly[43].

1.6.1 M.tb mechanism of infection

An understanding of the host immune response to *M.tb* is important. The mechanisms and timings of *M.tb* infection have been elucidated in small animal models[125], supported by study of active human TB and *in vitro* work[126] (current model: Figure 1.3).

Once in the lungs, *M.tb* evades phagocytosis by alveolar macrophages, which are important innate cells that present antigen to T-cells. *M.tb* attenuates the immune response by metabolic adaptations, defence mechanisms against reactive oxygen/nitrogen species and survival at low pH[127]. Infected macrophages are unable to efficiently present *M.tb* antigens via the endogenous pathway, because lipoarabinomannan expressed on *M.tb* inhibits phagolysosome fusion, and inhibits antigen release into the cytoplasm[128]. Upon death of an infected macrophage, or phagolysosomal rupture, *M.tb* antigen is released and presented to T-cells, a few days before antigen-specific T-cells can be identified[129]. Antigen presenting cells (mostly dendritic cells) migrate to local draining LNs[130], where antigen can interact with several host receptors including: toll-like receptors, nod-like receptors and C-type lectins[131].

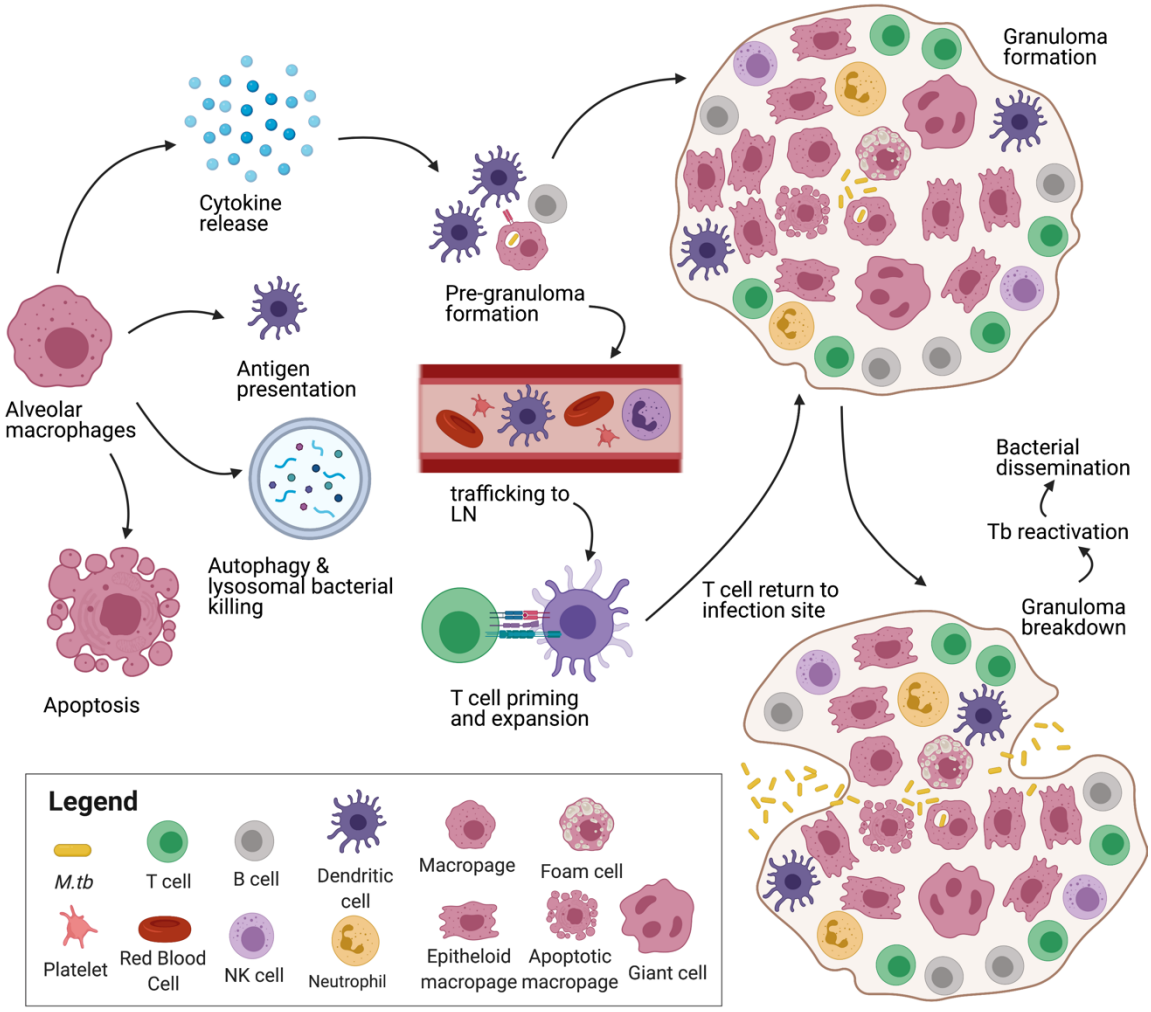


Figure 1.3 Mycobacterium tuberculosis mechanism of infection

Mycobacterium tuberculosis infection of alveolar macrophages in the lung results in several outcomes, and may lead to granuloma formation, driven by immune cell recruitment. Over time, granuloma breakdown can lead to bacterial dissemination and tuberculosis disease reactivation. Created with BioRender.com

In the lymphatic system, naïve T-cells are activated by antigen presenting cells and begin the process of T-cell maturation[131]. Cytotoxic CD8+ T-cells can be stimulated via antigen cross-presentation, and innate-like cells can also be activated[132]. Innate-like cells are activated by a more limited antigen repertoire and include: NK, mucosal associated invariant T cells (MAIT) and gamma-delta ($\gamma\delta$) T-cells. Activated T-cells return to the lungs

to perform effector functions, including: cytokine production, killing of infected cells and B-cell activation and help[132]. Accumulating macrophages, dendritic cells, T and B-cells at the infection site initially form a pre-granuloma, then a granuloma, which encloses bacteria to stop spread[114].

1.6.2 M.tb within the granuloma

Granulomas are a major defining feature of TB and bacteria that survive can lie dormant in granulomas for a lifetime[114]. The granuloma structure starts with infected macrophages, which are surrounded by uninfected macrophages. Cell recruitment results in a layer of dendritic cells, NK cells and neutrophils, which are followed by T and B-cells (require activation/maturation), and a layer of epithelial cells[133]. Granulomas can be an effective control mechanism over decades, but when they fail, bacterial escape and spread can cause disease[134]. This can cause pathogenesis and disseminated TB, where disease spread to organs other than the lungs.

1.7 Immune response to *M.tb* – innate

TB research has focused on the cellular branch of the adaptive immune system because the CD4+ T-cell response appears to be crucial[67]. More recently, humoral, and innate immunity have gained interest as adaptive T-cell immunity has failed to complete the story. Recent advances also question the innate vs adaptive paradigm overall, as cross-over between functions and capabilities of the two systems become increasingly clear[135].

1.7.1 Early immune response

Before the adaptive response has time to develop, the innate immune system interacts with pathogens to limit infection. The innate system developed before vertebrates and invertebrates became distinct, and is the only system used by most multicellular organisms, with recognition capabilities for long-standing pathogens such as

mycobacteria. Cells of this system include: macrophages, neutrophils, NK cells, dendritic cells, and other innate-like cells (e.g. γδs and MAITs). Conventional teaching is that the innate response is short-lived, with no memory component. More recently, this has been challenged by the identification of mechanisms able to prime innate cellular immune components in a process termed 'trained immunity' (discussed below)[135].

As discussed, *M.tb* infection can result in different outcomes[17], most likely depending on the immune response. Early clearance of infection could be mediated by a fast and effective adaptive T-cell response, or this could be attributed to the innate immune system[25]. Possible mechanisms for an early innate response to *M.tb* include clearance in the airways, or infection of the lung parenchyma followed by effective innate immunity[136, 137]. Airways epithelial cells may play an important role in antigen presentation and secretion of chemokines, cytokines and inducible nitric oxide synthase[138]. Neutrophil and NK cell recruitment can alter the inflammatory profile and subsequent cellular milieu[139, 140]. Cells that are classified as 'innate-like' (e.g. MAIT, γδ, induced NK T-cells – iNKT) can respond to non-protein cell wall derivatives and act alongside/before conventional T-cells[141]. Epigenetic changes to these subsets may confer a longer-lasting, more memory-like effect to act upon second infection (below)[142].

1.7.2 Monocytes

At the start of infection, lung resident macrophages are an important first line of defence as fast-acting phagocytic cells, complicated by their role as a bacterial reservoir[143]. Neutrophils, endothelial cells, and circulating monocytes can also be infected with *M.tb.* Macrophages accumulate early after *M.tb* infection before accumulation of some other cell types. Seven days after *M.tb* infection, alveolar macrophages (AMs) were the only infected immune cell type visible in mice, but by week 3 (Wk3) a large number of

recruited neutrophils and monocyte-derived cells were also infected[144]. Pro-inflammatory genes are not expressed in AMs until ten days post-infection with *M.tb,* so there is some question as to AM function[145]. Macrophage activation has several downstream functions, such as recruitment of neutrophils and other cell types. Bacterial clearance is improved in macrophage-depleted mice, mediated by increased cytotoxic and phagocytic cells recruitment, but granuloma formation is perturbed in this model[146].

Monocytes circulate in the bloodstream for one-three days before migrating into tissue and differentiating into macrophages or dendritic cells. Human monocytes can be defined as classical, non-classical and intermediate, according to the combination of CD14 and CD16 expression[147]. Classical monocytes (CD14++CD16-) are the major population of monocytes in human blood (80-90%), and are highly phagocytic. Non-classical monocytes expressing CD14+CD16++ are the most mature monocyte subset (10% of monocytes) and are highly pro-inflammatory. $CD14^{high}$CD16+ intermediate monocytes secrete a range of cytokines and chemokines (5% of monocytes). Intermediate monocytes are a pre-cursor to anti-inflammatory M2 macrophages, which promote tissue repair and proliferation (M1 macrophages are pro-inflammatory and able to kill pathogens)[143].

CD14+CD16+ monocyte expansion has been associated with increased TB disease severity, and in a follow up study, an anti-inflammatory (M2-like) subset of monocytes was identified and defined as CD16+CD163+MerTK+pSTAT3+[148]. Abundance of this subset correlated with disease progression in NHPs, soluble CD163 concentration could distinguish between TB patients and healthy controls[148]. Higher frequency of CD16+CD163+MerTK+ cells was recently detected in RM compared to CM, and this subset correlated with higher disease pathology in the RM[4].

Increased monocyte:lymphocyte ratio (M:L) in peripheral blood is associated with worse outcome of a number of infectious diseases including: TB and HIV[149, 150], mood-related disorders[151], coronary heart disease[152], and some cancers[153]. After successful HIV treatment, M:L is reduced and correlates with patient improvement [149]. High M:L can distinguish between active TB, LTBI and uninfected individuals[149]. In NHPs, progressive TB was associated with increased M:L, and more susceptible macaque species (RM and Mauritian-origin CM) had higher M:L ratios than less susceptible Chinese-origin CM[117].

1.7.3 Dendritic cells

Dendritic cells are primary antigen presenting cells and act as a bridge between the innate and adaptive response. Dendritic cells have also been proposed as a replication niche for *M.tb*, partly because intracellular killing capacity is worse than macrophages[154]. Like macrophages, dendritic cells express mannose and complement receptors, that allow *M.tb* uptake. Infected dendritic cells migrate to draining LNs, where they present antigen to T-cells. *M.tb* attempts to block initiation of the adaptive response by inhibiting acidification of the phagosome in which it resides, and other methods[128].

If dendritic cell trafficking is delayed and antigen reaches the LNs too late, bacteria have more time to spread. Less susceptible mouse strains show earlier antigen dissemination to the LNs than more susceptible strains[129]. Dendritic cell depletion in a transgenic mouse model caused delayed T-cell induction and reduced *M.tb* control[155]. In a comparison of human computational models and data from NHPs, delayed dendritic cell trafficking resulted in a reduced adaptive immune response and increased TB risk[131].

1.7.4 Neutrophils

Macrophage activation stimulates neutrophil recruitment from their reserves in the bone marrow[156]. Neutrophils and macrophages share precursor cells, and therefore express

similar antigens and release similar antimicrobial proteins (e.g. granzyme)[156]. In a typical infection, neutrophils are recruited more quickly than macrophages, and are more microbicidal. Neutrophils are responsible for some of the pathogenesis of TB, and studies of their function are often contradictory[139]. In granulomas, neutrophils produce large quantities of cytokines alongside T-cells. After *ex vivo* stimulation with mycobacterial antigens, peripheral blood neutrophils produced Th1 cytokines IFNγ and TNFα, Th2 cytokine IL-4, and regulatory cytokine IL-10 in a similar manner to T-cells[157].

1.7.5 NK cells

NK cells are recruited to the lungs after AE *M.tb* infection in mice, and can produce IFNγ and perforin[158]. However, *in vivo* antibody depletion of NK cells had no effect on bacterial load in these mice[158]. In T-cell depleted mice, NK cells produce more IFNγ[159]. Together, these studies suggest overlap and redundancy between NK and T-cells. In humans, NKp46 (an NK receptor) was significantly down-regulated on NK cells from QFT+ individuals with LTBI in Kenya, compared to QFT- individuals[160]. A $CD56^{dim}$ NK cell subset correlated with reduced NK cell activity in response to tumour cells *in vitro*, and differed to the phenotype of a healthy US control cohort[160]. Taken together, these phenotypic differences support a role for NK cells in the immune response to TB.

1.7.6 Unconventional T-cells

The dissection of immune cells into innate or adaptive has been challenged by the discovery of unconventional T-cells. These cells do not fit into either classical category: induced NKT-cells (iNKTs), MAITs and γδ T-cells. Despite only making up a fraction of the overall T-cell response, faster action of these subsets gives them critical functions that are non-redundant in some settings[161]. Conventional T-cells are delayed in response by their need for activation and somatic hypermutation of T-cell receptors. Alongside

activity within hours rather than days, unconventional T-cells express memory markers despite no previous encounter with antigen, and can respond to non-peptide antigens.

1.7.7 Unconventional T-cells: iNKT

The term 'NKT-like' (NKT-L) can be used to describe unconventional, innate-like T-cells which express conventional T-cell markers (e.g. CD4+/CD8+) and NK cell markers (e.g. CD56/CD16/CD161). iNKTs are more specifically a functionally distinct lineage of T-cells that express the semi-invariant T-cell receptor Vα24, which recognises glycolipids presented on CD1d[162]. CD1d is a non-polymorphic major histocompatibility (MHC) I-like molecule, which allows presentation of alternative antigens[163]. iNKTs contribute to the immune response against *M.tb* through production of granulocyte-macrophage colony-stimulating factor and IFNγ, and can limit *in vivo* replication in mice[164,165].

iNKT-cell frequency is higher in subjects with LTBI, compared to those with active TB or healthy controls, but there is no difference in iNKT phenotype (measured by HLA-DR, programmed cell death protein-1, chemokine receptor-6 and IFNγ production)[166]. HIV-1 infected individuals on anti-retroviral therapy (without TB) have a reduced frequency of iNKT-cells, with increased PD-1 expression, which suggests T-cell exhaustion[166]. In theory, HIV-induced exhaustion of iNKTs could contribute to the increased susceptibility of HIV-infected individuals to TB.

1.7.8 Unconventional T-cells: MAITs

Mucosal-associated invariant T-cells (MAITs) are donor unrestricted T-cells, that use MR1 to present antigen instead of MHC. MAIT-cells can produce Th1 cytokines, and kill infected cells through cytotoxic granule release[167]. Like other unconventional T-cells, MAIT-cells respond to a limited antigen repertoire; in TB, MAIT-cells recognise metabolites from the riboflavin biosynthesis pathway[168]. MAIT-cells can be characterised

by a combination of antibodies (CD161, CD26, Vα7.2)[169], but are perhaps best studied using MAIT-specific tetramers, which recognise MR1 antigen, and may help to reduce inclusion of iNKTs and other cells with similar lineage markers[170].

In NHPs, tetramer-positive MAIT-cells with minimal proliferative and cytotoxic capacity accumulate in the airways after *M.tb* infection[171, 172]. MR1-deficient mice are more susceptible to *M.tb* infection[173], and MAIT-cells show *in vitro* activity against BCG-infected macrophages[174]. During chronic murine *M.tb* infection, artificial MAIT-cell expansion using MR-1 antigen treatment reduced bacterial load[175]. In contrast, MR-1 knockout mice are not more susceptible to TB and MAIT-cell expansion pre-infection (using 5-OP-RU) delayed the CD4+ T-cell response[175]. This conflicting evidence may indicate a time-dependant role of MAIT-cells in the control of *M.tb*. Further evidence is necessary to elucidate MAIT-cell function in human mycobacterial infection.

1.7.9 Unconventional T-cells: γδ T-cells

Another unconventional T-cell subset of interest are γδ T-cells, which have γδ T-cell receptors (TCRs) in place of αβ TCRs[176] - γδ TCRs recognise an isoprenoid biosynthesis pathway intermediate. γδ T-cells are upregulated and activated upon infection with *M.tb*[177]. γδ cells produce IL-17 and IFNγ, and have cytotoxic capacity through secretion of perforin and granulysin[178, 179]. IL-17+ γδ T-cells are upregulated in TB patients compared to healthy controls, and γδ cells from peripheral human blood respond to *M.tb in vitro*[180, 181]. Mice lacking the γδ receptor have increased bacterial burden early in low dose *M.tb* infection, but go on to control bacterial growth at later time points.

The Vγ9Vδ2+ subset of γδ T-cells is upregulated after BCG in NHPs and humans[182, 183]. In NHPs, BCG-activated Vγ9Vδ2 T-cells show protection against challenge[183]. The

Vγ9Vδ2+ subset does not exist in mice. A recent study of lung resections and blood from TB patients showed that the TCR-δ repertoire in the lungs was highly skewed towards Vδ1 compared with the blood[184]. This suggests that the Vδ1 subset may have a role in mucosal immunity, despite its lower frequency in blood. Ogongo *et al.*, did not show a TCR repertoire difference between the lungs and blood (MAITs and NKTs).

1.7.10 Crossover and crosstalk

Partially shared lineages, functional overlap and genetic similarities blur the lines between innate cell subsets, and suggest some flexibility in their purpose[185]. Functional overlap may account for some difficulties in elucidating the role of individual subsets, and partially explain why *in vivo* interactions can be so complicated to study. T-cell subsets also exhibit plasticity, further demonstrating how complexity spans the innate and adaptive arms of the immune system, and those in between[186].

1.8 Immune response to *M.tb* - adaptive

1.8.1 Adaptive T-cells

The adaptive immune response is pathogen-specific, and develops slower than innate immunity. To mount an adaptive response, antigen must be processed and presented by antigen presenting cells. Once presented (usually on MHC class I/II molecules), naïve T and B-cells can recognise this antigen. Antigen recognition and cytokine production stimulates these naïve cells to differentiate and become activated into effector cells. A proportion of these antigen-specific effector cells differentiate into memory T-cells, which mount a faster response to a second infection with the same pathogen.

1.8.2 Type 1 and type 2 T-cell response

The type of T-cell induced depends on which cytokines stimulate naïve T-cells, and includes: T-helper cells, cytotoxic and regulatory T-cells. The T-cell response can be split into type 1 Th1 cells, which are important for cellular immunity against intracellular pathogens and type 2 Th2 cells, which respond to helminth infection. Type 1 responses are characterised by inflammatory cytokine production and phagocytosis, where type 2 immunity is associated with antibody production and resolution of pathology[187].

These two systems overlap, but comparing Th1 and Th2 responses can be useful as an indication of how a response is progressing[188]. Immune responses often consist of a balance between fighting infection and excessive inflammation which can cause pathology. In TB, a strong initial Th1 response to *M.tb* involves IFNγ production and can help clear infection, before a switch to IL-4/IL-10 production which limits pathology once the infection is under control[187]. A large study in Africa showed that Th2 markers were higher in infected *M.tb* individuals than controls[189]. Uninfected household controls had lower Th2 markers than community controls, which suggests that a low Th2 profile (and higher Th1 profile) might confer some protection amongst highly exposed individuals.

Although a Th1 response has been shown to be protective against TB, a Th1 response is not sufficient alone[97]. It is likely that some combination of unconventional T-cells, innate cells, antibody production and other relevant cell types (e.g. epithelial cells) are necessary for protection against disease, alongside Th1 cells. Working out which aspects of the immune response are crucial at what time points pre- and post-infection will help to guide rational and targeted design of treatments and vaccination.

1.8.3 IFNγ

Th1 cells are stimulated by Interleukin (IL)-12 secretion from dendritic cells, and are characterised by production of IFNγ, TNFα and IL-2. IFNγ activates macrophages to kill intracellular bacteria via production of reactive oxygen species, enzymes, and vitamin D, and through induction of autophagy. IFNγ production from Th1 cells peaks in mice at Wk3/Wk4 after *M.tb* infection[190]. CD4+ T-cell deficient mice are very susceptible to TB, but have little reduction in IFNγ production, suggesting that production may be compensated for by other cells[65].

In humans, IFNγ-related gene deficiencies have been linked to TB susceptibility[191]. Timing of cytokine production seems to be crucial in TB. Higher serum IFNγ levels indicate worse outcome for TB patients, rather than protection[192]. PPD-specific IFNγ production does not correlate with reduced bacterial load during *M.tb* infection in mice, and BCG vaccine-induced IFNγ also does not correlate with reduced load[82, 193]. Among others, these studies show that IFNγ is a major player in the immune response to TB, but that its effects may be time dependant, and that it is not a sufficient correlate of protection against disease.

1.8.4 TNFα

TNFα is also bactericidal, and often correlates well with IFNγ frequency[24], but is crucial in its own right for protection against TB. Individuals using TNFα blocking drugs to block chronic autoimmune diseases like rheumatoid arthritis and Crohn's disease are susceptible to re-activation of LTBI, and worse histopathology[194]. A meta-analysis of randomised controlled trials gave an odds ratio of 1.94 for patients on anti-TNF therapy developing TB compared to controls (CI 1.1-3.44, p=0.02)[195]. Across 29 trials, 45 of 7912 patients given anti-TNF therapy developed TB, compared to 3 out of 3967 allocated

controls (0.57% vs 0.08%)[195]. Data on the effect of other therapies for arthritis (e.g. disease-modifying anti-rheumatic drugs) are limited, but may even lower the risk of TB[196].

TNFα is produced as a stable homodimer transmembrane protein, that can be cleaved into its soluble form to bind TNFα receptor 1 or 2 (TNFR1/2)[194]. Downstream effects of TNF-receptor binding include: chemokine secretion, IFNγ disruption, adhesion molecule upregulation and induction of macrophage apoptosis (and possibly other immune cells). TNFα can either promote cell survival (via NF-κβ) or induce apoptosis (via a caspase cascade). Apoptosis of *M.tb* infected cells helps to remove the replication niche for *M.tb* and exposes antigens to adaptive immune cells. Anti-TNF has pleotropic effects on T-cells, including reduction of CD8+ memory T-cell frequency[197,198].

1.8.5 IL-2

IL-2 plays a role in T-cell expansion and survival, particularly of CD8+ T-cells. In IL-2-receptor knockout mice, cytotoxic CD8+ T-cells exhibit poor killing capacity and produce less granzyme B during chronic viral infection[199]. Strong IL-2 signals promote an effector response, where lower-level persistent IL-2 promotes formation of CD8+ memory cells[199]. A mouse model of T-cell dysfunction demonstrated that persistent *M.tb* exposure (ten/more exposures compared to two) caused a reduction in IFNγ and IL-2 production, accompanied by reduced CD8+ memory T-cell frequency and up-regulation of immune checkpoint PD-1[200]. CD8+ T-cell function was restored after application of therapeutic IL-2[200]. Therapeutic IL-2 was tested alongside multi-drug therapies in the 1990s, and shown to be safe when injected[201], but IL-2 has since shown limited efficacy as a therapy[202].

1.8.6 IL-17

Recently, a hypervirulent strain of *M.tb* (HN878) was used to demonstrate that IL-17 may have an essential role in TB immunity[203]. Whilst protection against less virulent strains

did not require IL-17, IL-17 knockout mice were unprotected against the hypervirulent strain[203]. IL-6, IL-21 and transforming growth factor-β stimulate the production of Th17 cells, which themselves produce IL-17, TNFα, IL-21 and IL-22[204]. IL-17 is a pro-inflammatory cytokine, which induces chemokine production to recruit T-cells and aid granuloma formation. IL-17 receptors are expressed on several cell types and stimulate a range of responses including neutrophil recruitment. Excessive IL-17 can cause immunopathology via over-recruitment of neutrophils, so a balance between IFNγ and IL-17 is necessary[205, 206].

1.8.7 Polyfunctional T-cells

Cells producing multiple cytokines (polyfunctional) may also be important in TB. CD4+ polyfunctional cytokine production is a correlate of protection against *Leishmania* (intracellular pathogen)[207]. Some mouse studies have shown that polyfunctional CD4+ T-cells correlate with protection against *M.tb*, but other studies showed no correlation[208, 209]. A recent review concluded that polyfunctional CD4+ T-cells are not a valid correlate of protection against *M.tb*, despite sometimes being induced by vaccination[208].

1.8.8 Cytokines induced by mucosal BCG

After mucosal BCG vaccination of RMs, cytokine-positive CD4+/CD8+ T-cells increase in the BAL. Published data showing cytokine production after mucosal BCG response are reproduced in Figure 1.4 (BAL) and Figure 1.5 (PBMC). Verreck *et al.,* showed that the frequency of cytokine-positive CD4+ BAL T-cells increased at Wk8 after EB BCG[4]. IFNγ+ CD8+ BAL T-cell frequency also increased[4]. Darrah *et al.*, showed increased cytokine-positive CD4+ memory cell frequency in BAL at Wk8 and Wk16 (trend at Wk4) after $5x10^7$ CFU aerosol BCG (aeBCG)[5]. White *et al*., showed that cytokine-positive BAL T-cell frequency peaked at Wk13 (latest time point studied) after 2-$8x10^6$ CFU aeBCG[3].

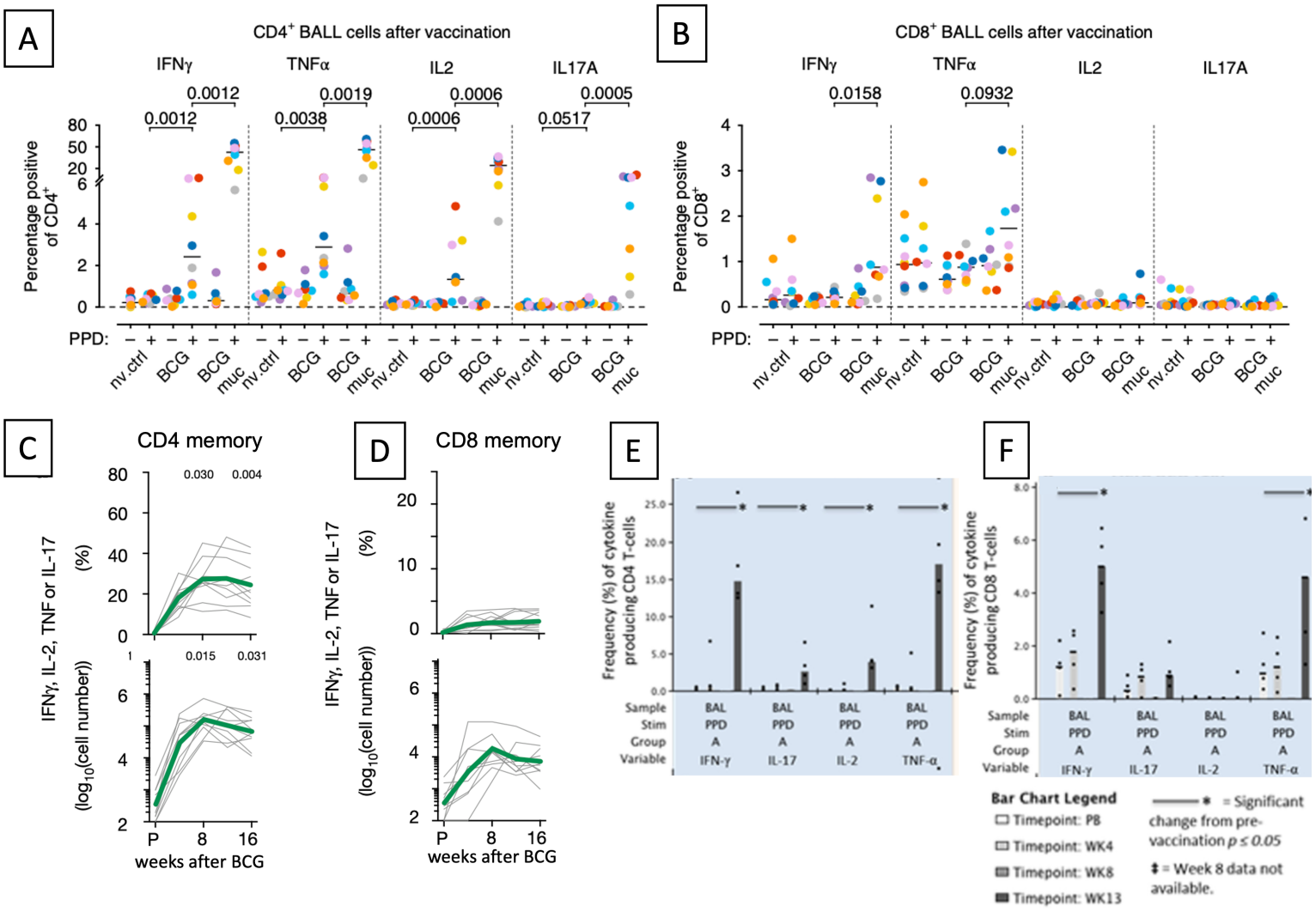
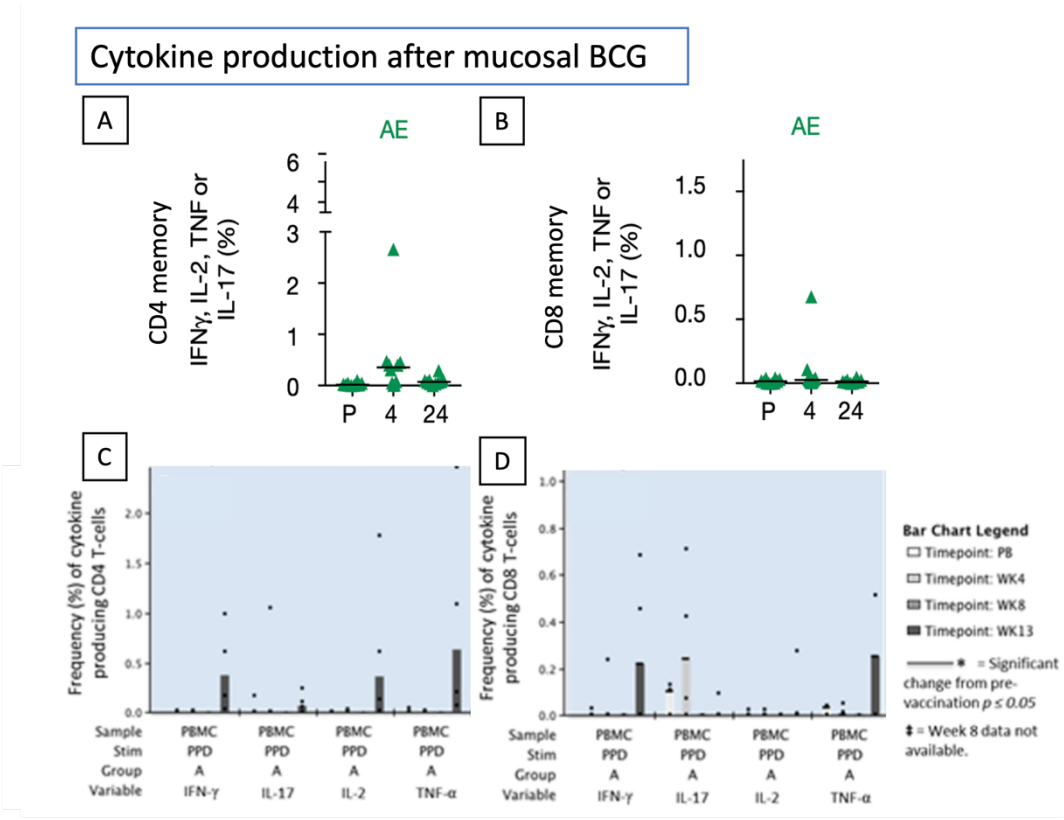

A
CD4+ BALL cells after vaccination
IFNγ
TNFα
IL2
IL17A
0.0012
0.0012
0.0019
0.0038
0.0006
0.0006
0.0005
0.0517
Percentage positive of CD4+
PPD:
nv.ctrl
BCG
muc
B
CD8+ BALL cells after vaccination
0.0158
0.0932
Percentage positive of CD8+
C
CD4 memory
0.030
0.004
0.015
0.031
IFNγ, IL-2, TNF or IL-17 (%)
(log10(cell number))
P
8
16
weeks after BCG
D
CD8 memory
E
Frequency (%) of cytokine producing CD4 T-cells
Sample
Stim
Group
Variable
BAL
PPD
A
IFN-γ
IL-17
IL-2
TNF-α
F
Frequency (%) of cytokine producing CD8 T-cells
Bar Chart Legend
Timepoint: PB
Timepoint: WK4
Timepoint: WK8
Timepoint: WK13
* = Significant change from pre-vaccination p ≤ 0.05
‡ = Week 8 data not available.

Figure 1.4 T-cell responses in broncho-alveolar lavage (BAL) cells after mucosal BCG (reproduced, left)

These graphs are reproduced from published work, and show the percentage of PPD-specific cytokine (IFNγ/IL-2/TNFα/IL-17) producing CD4+ or CD8+ T-cells, characterised among BAL cells. ***A*** *&* ***B*** *show the frequency of cytokine-producing cells eight weeks after endobronchial BCG (1.5–6.0×10^5 colony forming units - CFU), as published by Verreck et al., in 2019[4]. Horizontal lines represent group medians, '+' indicates PPD-stimulated, '-' indicates culture medium only, and groups were compared using Mann-Whitney U-testing, adjusted for multiple comparisons.* ***C*** *&* ***D*** *show the percentage of cytokine-producing CD4+/CD8+ T-cells (above) and the number of cells (below), after aerosol BCG (5×10^7 CFU), as published by Darrah et al., in 2020[5]. A green line shows the median values and individuals are in grey.* ***E*** *&* ***F*** *show the frequency of cytokine-producing CD4+/CD8+ cell after aerosol BCG (2–8×10^6 CFU), as published by White et al., in 2015[3].*


Cytokine production after mucosal BCG
A
AE
CD4 memory IFNγ, IL-2, TNF or IL-17 (%)
P 4 24
B
AE
CD8 memory IFNγ, IL-2, TNF or IL-17 (%)
P 4 24
C
Frequency (%) of cytokine producing CD4 T-cells
Sample PBMC PBMC PBMC PBMC
Stim PPD PPD PPD PPD
Group A A A A
Variable IFN-γ IL-17 IL-2 TNF-α
D
Frequency (%) of cytokine producing CD8 T-cells
Sample PBMC PBMC PBMC PBMC
Stim PPD PPD PPD PPD
Group A A A A
Variable IFN-γ IL-17 IL-2 TNF-α
Bar Chart Legend
Timepoint: PB
Timepoint: WK4
Timepoint: WK8
Timepoint: WK13
* = Significant change from pre-vaccination p ≤ 0.05
‡ = Week 8 data not available.

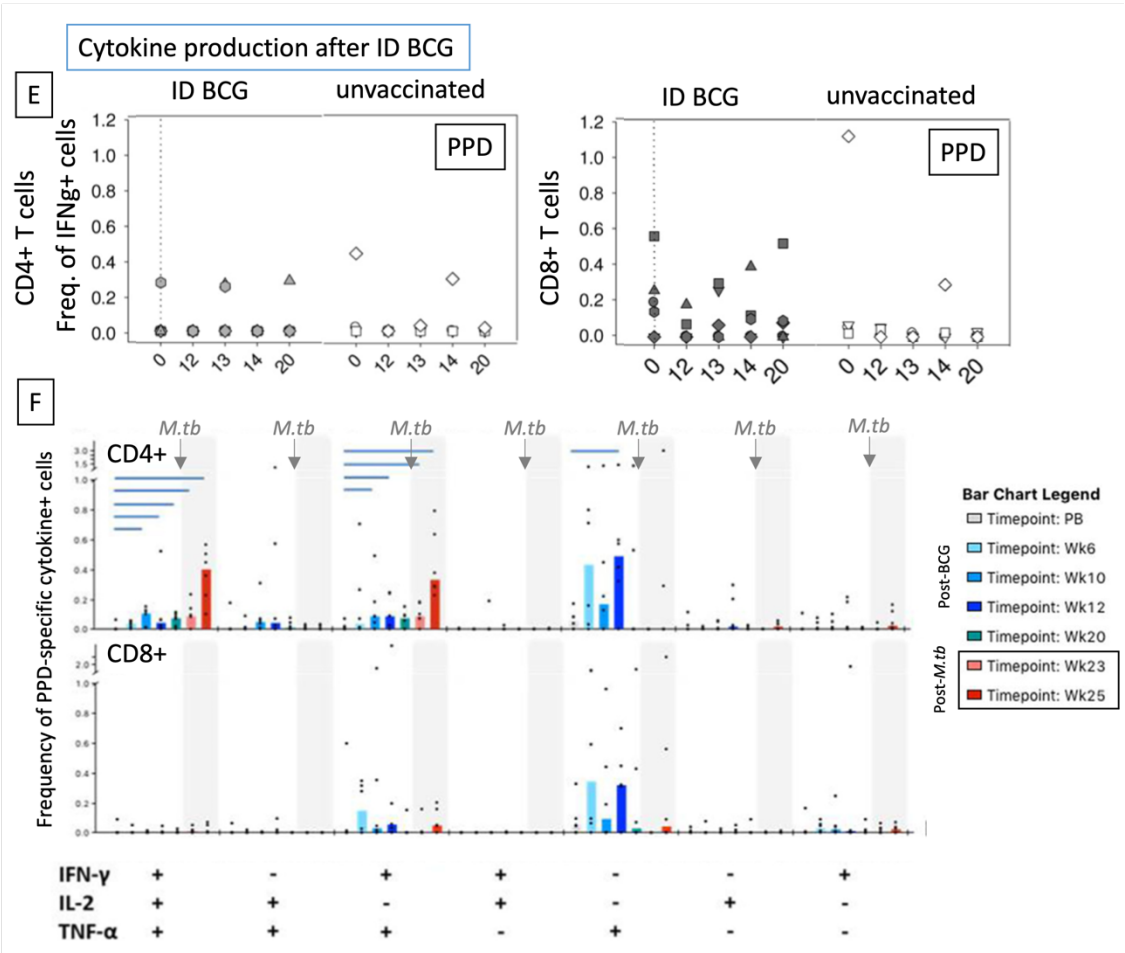

Cytokine production after ID BCG
E
ID BCG
unvaccinated
PPD
CD4+ T cells Freq. of IFNg+ cells
CD8+ T cells
F
M.tb
CD4+
CD8+
Frequency of PPD-specific cytokine+ cells
Bar Chart Legend
Timepoint: PB
Timepoint: Wk6
Timepoint: Wk10
Timepoint: Wk12
Timepoint: Wk20
Timepoint: Wk23
Timepoint: Wk25
Post-BCG
Post-M.tb
IFN-γ + - + + - - +
IL-2 + + - + - + -
TNF-α + + + - + - -

Figure 1.5 T-cell responses in PBMC after mucosal or intradermal (ID) BCG (reproduced)

These graphs are reproduced from published work, and all show the percentage of PPD-specific cytokine (IFNγ/IL-2/TNFα/IL-17) producing CD4+ or CD8+ T-cells, characterised among PBMCs. ***A/B*** *show the percentage of CD4+/CD8+ T-cells producing any of the four cytokines explored and the number of cells (below), at baseline (P), Wk8/16 (Wk4/12 also plotted), after 5×10^7 CFU aeBCG, as published by Darrah et al., 2020[5].* ***C/D*** *show CD4+/CD8+ specific cytokine responses at baseline/Wk4/8/13 after 2–8×10^6 CFU aeBCG, as published by White et al., 2015[3].* ***E*** *shows the frequency of PPD-specific IFNg+ CD4+ (left) and CD8+ (right) T-cells after ID BCG (grey) or in unvaccinated animals (clear), as published by McShane et al., in 2010[9].* ***F*** *shows the frequency of PPD-specific polyfunctional CD4+ (above) and CD8+ (below) T-cells up to twenty weeks after ID BCG, then after M.tb challenge at Wk21 (orange and red), as published by Sharpe et al., 2016[8]. Blue horizontal lines mark significant changes from baseline, measured by Wilcoxon-Rank testing ($p \leq 0.05$).*

1.8.9 Non-Th1 response

Protective immunity against helminth infection is mediated by a Th2 response, and helminth co-infection has been associated with worse BCG efficacy[210]. A Th2 response may be harmful in *M.tb* infection, counteracting Th1 responses and directing alternative immune activation. Studies of LTBI reactivation show a shift from Th1 to Th2 in humans and mice[189, 211]. IL-4 is a key Th2 cytokine (alongside IL-5 and IL-13), and impairs antimicrobial activity through a reduction in TNFα-mediated apoptosis and inducible nitric oxide synthase (produces reactive nitric oxide) activity, and by up-regulation of regulatory T-cells (T-regs)[212]. IL-4 also drives TNFα-mediated pathology[212].

T-regs express transcription factor Forkhead box P3 and are important in regulating immunopathology. Early after *M.tb* infection, T-reg expansion may delay

efficient responses and increase pathogenesis, whereas in chronic infection T-regs can limit pathology[213]. T-reg frequency is higher in TB patients than healthy controls, and *ex vivo* depletion of T-regs causes re-expansion of *M.tb*-specific IFNγ+ T-cells[214].

1.8.10 CD8+ T-cells

CD8+ T-cells are activated by antigen presentation on MHC class I or CD1 proteins[215], and their importance in TB immunity is unclear. Cross-presentation of antigen is required for suitable presentation to CD8+ T-cells because *M.tb* is an intracellular pathogen. Infected macrophage apoptosis allows uninfected antigen presenting cells to engulf and cross-present extracellular antigen to CD8+ T-cells. Experimental inhibition of apoptosis reduced antigen presentation and subsequently CD8+ T-cell activation[215]. Activated CD8+ T-cells can be cytotoxic, killing infected cells via release of enzyme-containing granules, or through Fas-Fas ligand interaction to induce apoptosis. Mice only naturally express the CD1d isotype, which limits the use of mice in studying CD8+ T-cell responses. In NHPs, CD8+ T-cell depletion reduced BCG-induced immunity to *M.tb* challenge, and CD8+ T-cell depletion caused TB re-activation in successfully treated NHPs[216].

1.8.11 T-cell memory

Immunity to TB disease involves an acute and efficient response to clear infection, as well as immunological memory to prevent disease re-activation, or re-infection. Immunological memory forms after clonal expansion of T and B-cells. Around 10% of cells gain a memory phenotype and are distributed away from the infection site. Upon re-infection, memory cells can become 'secondary' effector cells[217]. Memory can be divided according to preferred cell niche: periphery for T effector memory and central immune tissues for T central memory, depending on their favoured niche[218]. T effector memory cells respond first, and are found in the lungs, gut, and skin. T central memory niches

include LNs and the bone marrow, and are a secondary defence system, should T effector memory cells fail to clear an infection[217]. Phenotypic homing markers distinguish between subsets[217].

1.9 Immune response to *M.tb* - humoral

1.9.1 Humoral immune response

As discussed above, cell mediated immunity is crucial for protection against TB. Evidence suggests that humoral immunity may be more important than anticipated[219, 220]. In mice, antibodies against the carbohydrate component of lipoarabinomannan showed a dose-dependent protective effect against IV *M.tb* challenge[221]. In humans, post-hoc analysis of the MVA85A vaccine efficacy trial found that BCG-vaccinated infants with higher Ag85A-specific IgG antibody levels had a reduced risk of TB disease[80]. In some cases, healthcare workers regularly exposed to *M.tb* develop antibodies without succumbing to TB disease, and these antibodies are protective in mice[222].

Antibodies have several function and possible mechanisms of action in TB include: opsonisation for enhanced phagocytosis, neutralisation of bacteria, and immune cell activation[219]. Antibodies are produced by B-cells. Studies of B-cell knockout mice and B-cell restoration have come to conflicting conclusions about the importance of B-cells in protection[223, 224]. In humans, B-cell function is impaired in individuals with active TB or LTBI, compared with healthy controls or successfully treated patients[225]. In these experiments, T-cell activity was dependant on a functional B-cell compartment[225].

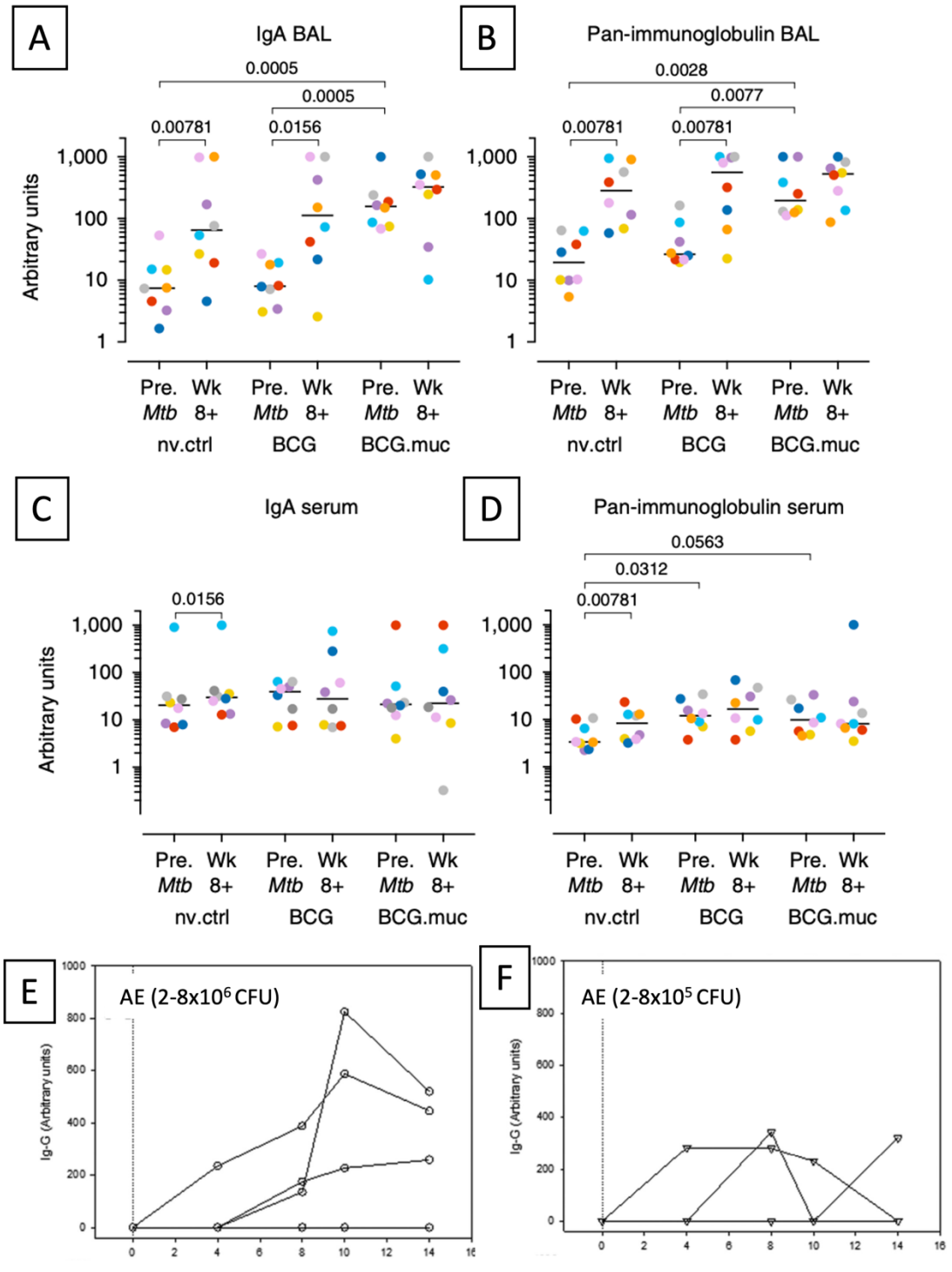
As mature B (and T)-cells become activated, Fas (CD95) expression increases. Fas is linked to an intracellular death domain and signals apoptosis when it binds to

complementary Fas-ligand. B and T-cells express Fas after activation and become more susceptible to Fas-mediated apoptosis over time.

1.9.2 Humoral immune response to mucosal BCG

Antibodies are produced after mucosal BCG administration (published data reproduced in Figure 1.6). After EB installation of 1.5-5x10^5 CFU BCG in RM, PPD-specific antibody titre was increased in BALf at Wk8 compared to naïve controls or NHPs exposed to ID BCG[2]. This antibody increase was only detected in BAL (not in serum). PPD-specific antibody production increased at Wk10 after 2-8x10^6 CFU aeBCG at a standard dose[3].

Darrah *et al*., did not detect a difference in antibody production after 5x10^5 CFU aeBCG did not induce a significant change in antibody response[5]. Darrah *et al*., looked at *M.tb* whole cell lysate-specific responses, rather than PPD-specific responses, which may alter the amount of antibody detectable after BCG only. The strongest antibody responses to BCG measured by Darrah *et al*., were after IV BCG delivery. Antibody binding and correlations with genetic changes were further explored by the authors in a follow-on paper[226].


A
IgA BAL
0.0005
0.0005
0.00781
0.0156
Arbitrary units
1,000
100
10
1
Pre. Mtb
Wk 8+
nv.ctrl
BCG
BCG.muc
B
Pan-immunoglobulin BAL
0.0028
0.0077
0.00781
0.00781
C
IgA serum
0.0156
D
Pan-immunoglobulin serum
0.0563
0.0312
0.00781
E
AE (2-8x10⁶ CFU)
Ig-G (Arbitrary units)
F
AE (2-8x10⁵ CFU)

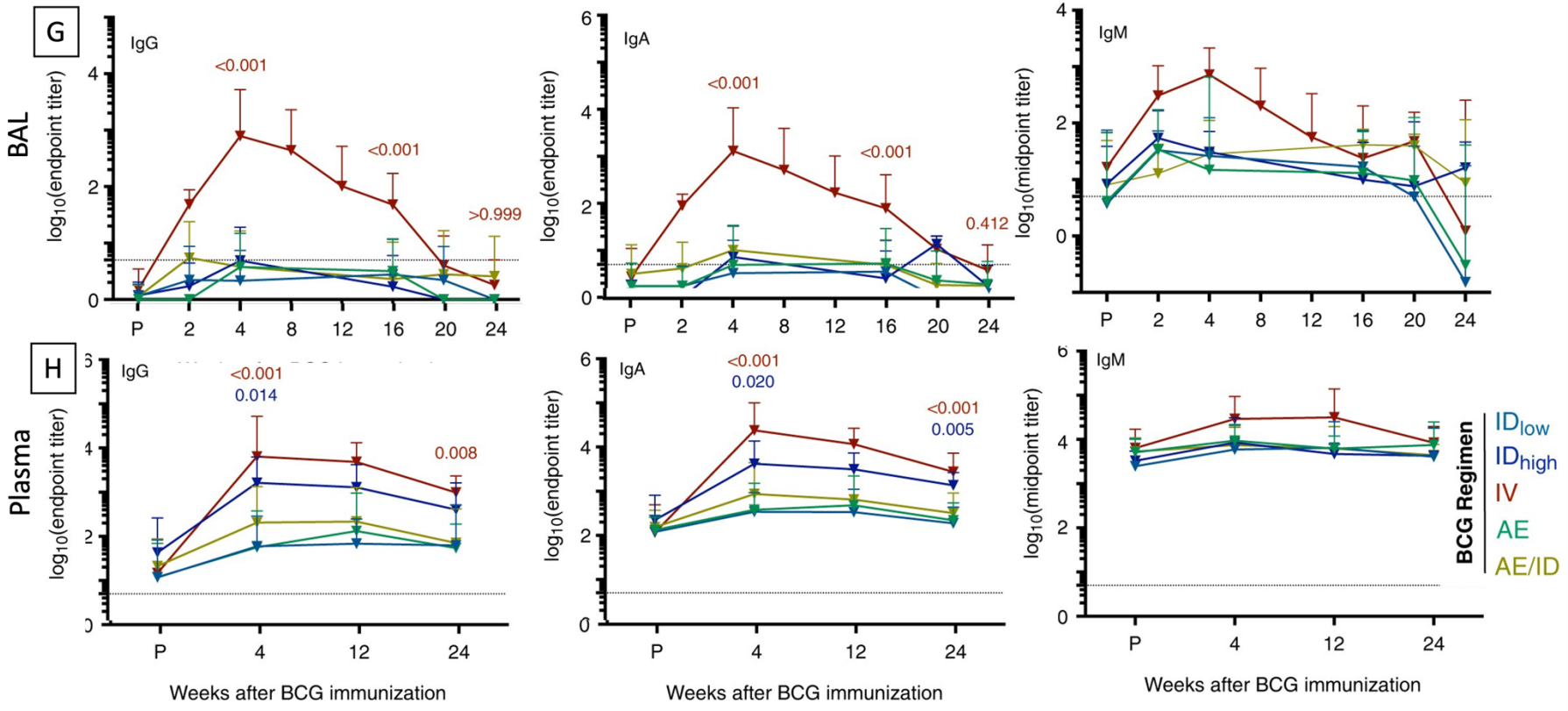

G
H
BAL
Plasma
IgG
IgA
IgM
log10(endpoint titer)
log10(midpoint titer)
<0.001
>0.999
0.412
0.014
0.020
0.008
0.005
P
2
4
8
12
16
20
24
Weeks after BCG immunization
BCG Regimen
IDlow
IDhigh
IV
AE
AE/ID

Figure 1.6 Antibody responses in broncho-alveolar lavage (BAL) and serum after mucosal BCG (reproduced)

A-D *are reproduced from work published by Verreck et al., in 2019[2], and all show the percentage production of antibody 8 weeks after saline control ('nv.ctrl'), standard ID BCG (BCG) or 1.5–6.0×10^5 CFU BCG delivery EB ('BCG.muc'). This time point is marked as 'Pre-M.tb', and is shown in comparison to antibody level post-M.tb challenge (Wk8 onwards). Antibody concentration was measured in both the BAL (**A/B**) and serum (**C/D**). IgA (**A/C**) and pan-IgG (**B/D**) were explored. Horizontal lines represent group medians, and group differences were compared using Mann-Whitney U-test adjusted for multiple comparisons. Within group comparisons were made with a Wilcoxon-Rank test. Animals are colour coded throughout. PPD-specific IgG titre in serum following aeBCG delivery is shown in comparison to the mean baseline level (arbitrary units), at a standard dose of 2-8x10^6 CFU (**E**), or 1/10th dose of 2-8x10^5 CFU (**F**), as published by White et al., in 2015[3]. **G** & **H** show the fold change in antibody response after BCG delivery by ID (light blue), high dose ID (dark blue), IV (red), AE (green, 5x10^7 CFU), AE/ID (mustard), as published by Darrah et al., 2021[5]. Responses in BAL (10x concentrated) are shown in **G** (baseline/Wk2/4/8/12/16/20/24), and serum in **H** (baseline – 'P'/Wk4/12/24). Lines represent geometric mean with standard deviation, and a Kruskal-Wallis with Dunn's multiple comparisons was used to compare fold change at each time point to the standard ID group (P-values shown colour coded to delivery method). The dashed grey line represents the threshold for detection.*

1.10 Immune response to *M.tb* - other players

1.10.1 Trained innate immunity

Recently, the concept innate immune memory has been applied to TB. Innate immune memory results in a more substantial innate response to subsequent, often heterologous insults[227]. Netea *et al*., showed that monocytes undergo epigenetic changes in response to BCG[137], so that secondary mycobacterial challenge stimulates a more rapid response. This increase in innate cell activity may alter the overall status of immune system, and contribute to the non-specific effects of BCG vaccination. Local BCG injection has long been used as a treatment for bladder cancer, but the success of BCG as a treatment for bladder cancer is not well understood[228]. It is possible that non-specific long-term epigenetic changes to innate cells are partially responsible.

1.10.2 Microbiome & epithelium

Alongside interplay between innate and adaptive cells, immune cells are also influenced by host microbiota and epithelial cells at the site infection[138]. The respiratory tract epithelium offers a physical barrier against TB. Epithelial cells can be infected with *M.tb* and release cytokines that contribute to the local inflammatory milieu[229].

Microbiota in the airway may also influence immunity. Our current understanding of the gut-lung axis in TB is summarised in Figure 1.7, adapted from Cervantes *et al.,* [1] and Sekyere *et al.*[6]. 16S rRNA sequencing revealed increased abundance of Actinobacteria and Firmicutes in TB patients compared to healthy controls, and a general increase in opportunistic bacteria colonisation[230]. Antibiotic-induced gut microbiota dysbiosis in mice significantly increases susceptibility to *M.tb* infection, and is associated with an increased in T-reg frequency and decrease in Th1 cytokines IFNγ and TNFα[231]. *M.tb* infection itself causes a short-term loss in microbial diversity in mice, suggesting two-way

interactions between the pathogen and host bacteria[232]. In mice, two independent groups have shown that *Helicobacter hepaticus* infection early in life increases susceptibility to TB when challenged, possibly driven by increased IL-10[1].

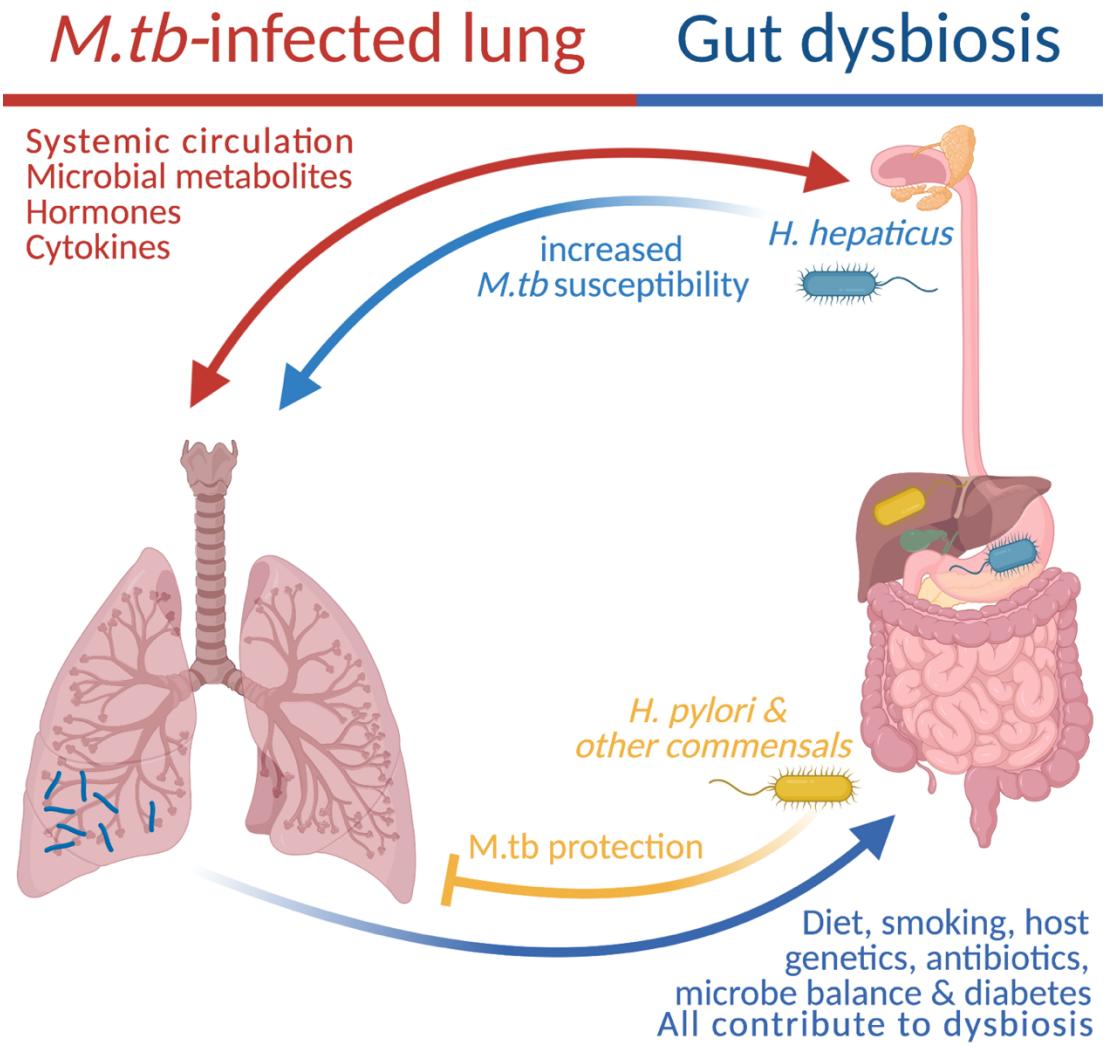


Figure 1.7 The gut-lung axis in TB

Diagram summarising gut-lung interactions and how they affect M.tb infection (adapted from Cervantes et al.[1], and Sekyere et al.[6]). Some pathogenic bacterial species (e.g. H. hepaticus) increase susceptibility to TB, where others provide protection. Other factors that contribute to gut dysbiosis and therefore to increases TB susceptibility include: diet, smoking, host genetics, antibiotic use, microbe balance and diabetes.

1.11 Studying the immune response to *M.tb*

1.11.1 BAL to study mucosal immunity

In humans, PBMCs are commonly studied in TB research, because they are easy to access. Recent interest in mucosal immunity has increased the study of BALf, especially in the context of respiratory pathogen such as *M.tb*. The lung has its own unique, relatively anti-inflammatory microenvironment. Several studies have shown differences between systemic and local responses in TB patients and animal models[5, 209, 233]. Where facilities are accessible, BALf can be used to sample the respiratory mucosa and characterise local immune cells, activation markers and genetics. BAL collection is invasive and is therefore not always possible.

Another option is to study cells collected from induced sputum. Sputum samples have previously been used for immunoassays in TB patients, but are difficult to work with because of the presence of microorganisms[46, 234]. A recent paper has also shown the safety and feasibility of isolating a small number of cells (median $6x10^5$ cells) using EB ultrasound guided transbronchial needle aspiration to sample human mediastinal LNs[235]. Davids *et al.*, described the application of this technique to study cellular composition, and this could be an interesting method of human study going forward. Although lung biopsies in healthy or *M.tb* infected humans are feasible, it is hard to obtain sufficient cell numbers for immune profiling.

1.11.2 In vitro measures of M.tb growth inhibition

Another way to explore the response to mycobacterial infection is to consider how well infected cells can control mycobacterial growth *ex vivo*. Individuals who can better control mycobacterial growth *ex vivo* usually control disease better *in vivo*[236]. In animals and humans, mycobacterial growth inhibition correlates well with better long-term

prognosis (measured by IGRA conversion in humans, and long-term survival after *M.tb* challenge in NHPs)[237]. The mycobacterial growth inhibition assay (MGIA) is reproducible between users, within sites and between sites[238]. Mycobacterial growth inhibition measured may be more representative than studying cell types in isolation, and correlates with: inflammatory monocytes, atypical B-cells, IgG and serum cytokines[239].

The direct MGIA has been developed for use in humans and mice, and more recently for NHPs[238, 240]. Rather than exposing animals to *M.tb* challenge, which is classified as 'Moderate' severity by the United Kingdom (UK) home office, multiple samples can be tested from frozen PBMCs, using BCG as the challenge agent. This method can be used to detect the presence and magnitude of a BCG-induced vaccination response. An equivalent method for the diagnosis of bovine TB is under development[241]. Having an assay that can act as a surrogate for efficacy trials to demonstrate protection against *M.tb* is useful for comparative studies, and the minimisation of animals use.

1.11.3 Controlled infection models

To study TB disease in a non-endemic areas and look at the early immune response, animal models or a controlled human infection models can be used. Models that allow serial mucosal and systemic sampling can also help to define the interaction between innate and adaptive immune responses.

'Controlled infection', and 'challenge models' have shown their use in humans and animals across several diseases. Controlled human infection models (CHIMs) have been applied to test vaccination strategies and study infection at distinct time points for pathogens including: malaria[242], dengue fever (being developed)[243], influenza[244], typhoid[245], and COVID-19 (being developed). Challenge models are designed to give a specific dose of an infectious agent, at a specific (known) time, in a controlled setting. The

controlled setting means that other variables can be accounted for, and that symptoms can be monitored and treated immediately where necessary. For some diseases it is possible to give the infectious agent that causes disease in a CHIM, because treatment is effective and readily available.

Study of TB disease through a CHIM using *M.tb* would be unethical, as the treatment regime is lengthy and has side-effects. Additionally, there is a possibility that individuals continue to have a lifelong, latent, low level of infection after TB treatment, that could be re-activated later in life[23]. Controlled infection with *M.tb* is possible in animal models, under strict regulation, and using specialist facilities[2, 5, 7]. *M.tb* challenge of small animal models and NHPs are used as a final testing platform for vaccination, but development of a human challenge model might produce more translatable results[110].

1.11.4 BCG as a surrogate for M.tb

Although a CHIM using *M.tb* is not possible, BCG can be used as an alternative infectious agent[246, 247]. BCG is licensed for use as a vaccination and does not require containment level three facilities. Compared to *M.tb*, BCG does not induce granuloma formation or disseminate, and prognosis is good. Despite these differences, the major advantage of using BCG as a model infectious agent is that can be used safely in humans and animals.

BCG and non-virulent mycobacterial strains have deletions of some genes that allow *M.tb* to continue as a successful pathogen. ESAT-6 and CFP-10 have been deleted from the region of deletion-1 locus of BCG. ESAT-6 and CFP-10 form a secretory complex responsible for the release of *M.tb* from the phagosome into the cytosol, which can cause cell death. The pathogenicity of BCG is greatly reduced by the deletion of these genes. ESAT-6 and CFP-10 have been linked to virulence by studies of their presence/absence, and may function by modulation of TNFα production from macrophages[248].

In an immunocompetent individual, BCG infection is well controlled and can be safely given. BCG challenge studies can therefore be performed in parallel in humans and animals (Figure 1.8). Parallel studies allow cross-species comparison, and additional data gathering that is not possible in humans (e.g. in-depth study of animal tissues). In some limited circumstances, BCG itself can cause disease. In particular, HIV-positive and immunosuppressed infants are at risk of local or disseminated disease[249]. Treatment options are limited as all strains of *M.bovis* are resistant to pyrazinamide (a first line anti-TB drug), and infections can be fatal.

A phase 1 trial has recently shown the safety of a human lung BCG challenge model using EB delivery[104]. Adverse events were low, and immune responses were highly compartmentalised according to the location of installation. This supports further exploration into localised responses induced by mycobacterial infection using a CHIM.

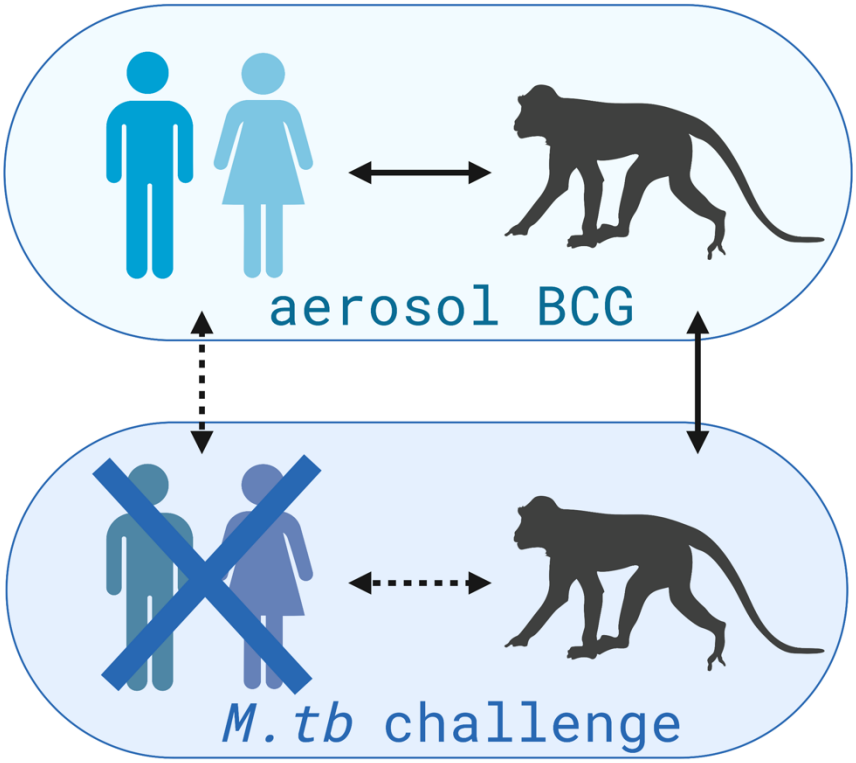


Figure 1.8 BCG as a model of M.tb infection

BCG can be safely used as a model of infection in both humans and NHPs. TB challenge studies are only possible in animal models, under tightly regulated conditions, due to the ethical implications of experimenting with potentially lethal disease. By performing studies in parallel, human, and animal models of BCG (and M.tb in animals) can be used to bridge between results.

1.11.5 Parallel human and NHP studies

In general, parallel study of humans and NHPs is well supported by cross-over between reagents and techniques. Designing a parallel experiment across species is logistically complicated, but important for providing direct comparisons. Elhmouzi-Younes *et al.*, used 30 antibodies to stain and compare samples from humans and CM by mass cytometry, revealing similarities and differences between the species, using 15 shared clustering markers[250]. Direct comparisons like this provides strong evidence for species similarity and supports further parallel studies.

Where studies are planned independently across species, methodology differences can further complicate comparison. For example, human TB studies use a mouthpiece fitted to a nebuliser to deliver AE, whereas similarly designed NHP studies use a nebuliser fitted to a mask attachment[7, 9]. In addition, independent studies often explore different combinations of time points and samples at each time point, whether due to logistical limitations, or the focus of a particular study. For these reasons, it can be hard to compare data from across studies of different species.

1.12 This project

1.12.1 aeBCG in NHPs

As discussed, TB disease is a major burden globally. As treatment resistant strains become more prevalent, improved vaccines and treatments remain urgently required. Thus far, in depth immunological analysis of how the immune system responds to mycobacterial infection in the lungs after exposure by AE is limited. In this project local and peripheral immune responses to aeBCG are explored in NHPs, and compared to responses measured in humans in parallel work (McShane group, Oxford – ClinicalTrials.gov ID: NCT03912207/NCT02709278).

Two species of macaques were chosen for analysis of the early immune response to aeBCG, at time points where innate cell activity could be expected. RM and CM show differing susceptibilities to TB, which means that in-depth, direct comparison of the immune responses of these species may give some indication of which components of the immune response are beneficial. Two AE delivery methods (mouthpiece and mask) were compared, to examine the response to aeBCG at later time points. Both methods have been used in previously published studies, but have not yet been directly compared to each other (to our knowledge). The final part of this project was to compare the NHP immune response to aeBCG to the human immune response and consider similarities and differences that were detected. Improved understanding of the immune response to mycobacteria will aid development of preventative and treatment measures.

1.12.2 Project aims

This project addresses several objectives (Table 1.1). The outlined objectives will be explored throughout this thesis under the following chapter headings: Chapter 2 - Materials and methods, Chapter 3 - Early response to aeBCG, Chapter 4 – Late immune response to aeBCG, Chapter 5: NHP vs human responses to aeBCG.

	Objectives
1	study the early immune response to aeBCG in NHPs
2	compare immune responses across different species of macaque
3	compare the immune response to aeBCG delivered by mask or mouthpiece
4	study the kinetic of the immune response to aeBCG in NHPs
5	compare results to parallel human study

Table 1.1 Objectives

Overall objectives of this project are summarised in this table.

Chapter 2: Materials and Methods

Chapter 2: Materials and methods

2.1 Materials

Consumables (Table 2.1), reagents (Table 2.2) and solutions (Table 2.3) used in this project are listed alphabetically.

2.1.1 Consumables

Consumables		
Consumable	**Supplier**	**Catalogue number**
Filters (0.22 uM)	N/A	N/A
Tubes (0.5 mL, 2 mL 15 mL, 50 mL)	N/A	N/A
Syringes (1 mL, 10 mL)	N/A	N/A
CASY tubes (10 mL)	N/A	N/A
Pipette tips (10 uL, 200 uL and 1 mL)	N/A	N/A
Pipette tips (as above, filter)	N/A	N/A
Needle (21 gauge)	N/A	N/A
Plates (96 well U/V-bottom, 48 well)	N/A	N/A
ELISpot plates	Sigma/Merck	MSIPS4510
Accuspin tubes	Sigma/Merck	A2055
Amicon Ultra-15 Centrifugal filter devices	Millipore	UFC900324
C-tubes	Miltenyibiotec	130-096-334
Cryovials	N/A	N/A
ESR capillary tubes	Guest Medical	D5534
gamma-radiated petri dishes	N/A	N/A
Pastettes	N/A	N/A
Stripettes (2 mL, 10 mL, 25 mL)	N/A	N/A
Troughs	N/A	N/A

Table 2.1 List of consumables used in this project

Reagents used in this project are listed alphabetically, with suppliers and catalogue numbers shown where reagents are not standard.

2.1.2 Reagents

Reagents		
Reagent	**Supplier**	**Catalogue no.**
10X facs lysing solution	BD Biosciences	349202
2-mercaptoethanol	Gibco	21985023
7H11 Agar powder	Sigma/Merck	M0428-500G
Ammonium-Chloride-Potassium buffer	Sigma/Merck	11814389001
AF700 Isotype control	BD Biosciences	557882
anti-CD28	BD bioscience	MA1-20792
anti-CD49d	BD bioscience	16-0492-82
BCG Danish	AJ Vaccines	N/A
BCIP/NBT (plus) solution	Europa bioproducts	MO711A
Benzonase (10 kU)	Sigma/Merck	70664-3
Brefeldin A	Sigma/Merck	B7651-5MG
Brilliant Stain buffer	BD Biosciences	566349
Carbonate-bicarbonate buffer	Sigma/Merck	C3041-50CAP
CASYclean	Open life science	3402 2090
Casein	Life technologies limited	6945695
CASYton	Open life science	3822 0000
CD14 PE	Beckman Coulter	A07764
CD16 BV785	BioLegend	302046
CD161 PeCy7	BioLegend	339918
CD3 AF700	BD Biosciences	557917
CD4 PerCP Cy5.5	BD Biosciences	552838
CD56 BV605	BioLegend	318334
CD8 APC FIRE 750	BioLegend	344746
Cell trace violet	ThermoFisher Scientific	C34571
Collagenase	Sigma/Merck	COLLD-RO
Compensation Beads	BD Biosciences	552843
Compensation Beads (amine)	Invitrogen	A10628
Cytofix/cytoperm, Perm/Wash	BD Biosciences	554714
5X Diethanolamine substrate buffer	ThermoFisher Scientific	34064
Deoxyribose-nucleic acid-se	Sigma/Merck	D5025-15KU
Earles Media	Sigma/Merck	M5650
Ethylenediaminetetraacetic acid	G Biosciences	R013

Reagents (continued)		
Reagent	**Supplier**	**Catalogue no.**
Ficoll paque plus	Fisher	11768538
Foetal calf serum	Labtech/Biosera	FB-1001
gd TCRBV421	BioLegend	331218
gd TCR PeCy7	Biolegend	331221
Goat anti-NHP γ-chain IgG alkaline phosphatase	Rockland antibodies	617-105-012
Goat anti-NHP μ-chain IgG alkaline phosphatase	Rockland antibodies	617-105-006
Hanks balanced salt solution	Sigma/Merck	H6648
Hepes buffer	Sigma/Merck	83264
HLA-DR BUV395	BD Biosciences	564040
IFNg FITC	BD Biosciences	552882
IL-17 BV711	BioLegend	512327
IL-2 APC	Macs Miltenyi	130-091-644
Ionomycin (Calcium ionophore)	Cambridge bioscience	CAY11932
Ki67 FITC	BioLegend	151211
L-Glutamine	Sigma/Merck	G7513
Live/Dead aqua	ThermoFisher Scientific	L34957
Live/Dear red	ThermoFisher Scientific	L23102
MGIT supplement	BD Biosciences	245124
Monkey IFNg ELISpot kit	Mabtech	3421M-2A
Paraformaldehyde	Sigma/Merck	P6148
PBS	Sigma/Merck	D8537
Penicillin/streptomycin	Sigma/Merck	P4333
Percoll	Sigma/Merck	P1644
Phospholipid assay kit	Sigma/Merck	MAK122-1KT
PMA (phorpol 12-myristate)	Sigma/Merck	P1585
pNPP (tablets)	Sigma/Merck	N2765
PPD	Statens serum institute	N/A
RPMI 1640	Sigma/Merck	R8758
SEB	Sigma/Merck	S4881
Trypan blue	ThermoFisher Scientific	15250061
Tween-20	Sigma/Merck	P9416
Va7.2 PeDazzle594	BioLegend	351730

Table 2.2 List of reagents used in this project

Reagents used in this project are listed alphabetically, with suppliers and catalogue numbers shown.

2.1.3 Solutions

Solutions	
Name	**Method**
Facs lyse solution (1x)	1:10 diilution of 10X facs lyse solution in sterile water
PFA (4%)	Sterile PBS is added to PFA powder, and the solution is heated until the powder dissolves
BCG for vaccination	Reconstitute 2 vials of BCG in 0.55 mL diluent each, combine vials in mixing vial (no bubbles), use 1 mL
Carbonate-bicarbonate	Add 1 tablet/100 mL pure water, then autoclave
Cryopreservation media	10% DMSO in filtered FCS
FACS buffer	1% FCS in sterile PBS
Live/dead aqua antibody	1:50 dilution of powder in DMSO to make original solution, then 1:50 dilution in sterile water on use
R10-Human	Add 50 mL filtered FCS, 5 mL P/S and 5 mL L-Glutamine to 500 mL bottle of RPMI (no Hepes)
R10-NHP	Add 50 mL filtered FCS, 5 mL P/S and 5 mL L-Glutamine to 500 mL bottle of RPMI + Hepes
PBS + 0.01% tween	Add 0.01% Tween-20 to sterile PBS
PBS + 0.05% tween	Add 0.05% Tween-20 to sterile PBS
Percoll	Combine 225 mL Percoll, 154.5 mL DPBS, 24 mL 10X PBS, 1.5 mL HCl
R0-PHE	Add 5 mL P/S, 5 mL L-Glutamine, 15 mL Hepes and 0.5 mL BME to 500 mL bottle of RPMI
R2-PHE	Add 10 mL filtered FCS, 5 mL P/S, 5 mL L-Glutamine, 15 mL Hepes and 0.5 mL BME to 500 mL bottle of RPMI
R5-PHE	Combine 1 part R10 PHE with 1 part R0 PHE (1:2 dilution of FCS in the R10)
R10-PHE	Add 50 mL filtered FCS, 5 mL P/S, 5 mL L-Glutamine, 15 mL Hepes and 0.5 mL BME to 500 mL bottle of RPMI
Tissue digestion media	715 collagenase units/mL + 350 DNase units/mL, diluted in Earle's media, supplemented with 200 mg/L Calcium Chloride
pNPP	Dilute 5X DEA substrate buffer in sterile-filtered water 1:5. Add one 20 mg pNPP tablet per 20 mL and shake. Keep under foil.

Table 2.3 List of solutions used in this project

Solutions used in this project are listed alphabetically, with details of what components were used to make up that solution.

2.2 Samples

2.2.1 NHP samples

The study design and all procedures were approved by the Animal Welfare and Ethical Review Body of UK-HSA and authorised under an appropriate UK Home Office project license, according to the ARRIVE guidelines. Animals were housed in socially compatible groups according to the Code of Practice for Housing and Care of Animals Bred, Supplied or Used for Scientific Purposes - 2014 (updated from Home Office Code of Practice for Housing and Care of Animals used in Scientific Procedures - 1989), and the National Centre for Refinement, Reduction and Replacement of animals in research (NC3Rs) Guidelines on Primate Accommodation, Care and Use - 2006.

46 RM (*Macaca mulatta*, Indian origin) between four and twelve years of age, and nine CM (*Macaca fascicularis*, Indonesian origin) between four and five years of age were sourced from an established, closed UK breeding colony (Table 2.4). Absence of previous mycobacterial antigen exposure was confirmed by tuberculin skin testing as part of colony management. Cages were approximately 2.5 m high, with high-level balconies and a floor of deep litter to allow foraging, alongside additional enrichment through provision of: toys, swings, DVDs (visual stimulation) and feeding puzzles. Standard old-world primate pellets were supplemented with a selection of fresh fruit and vegetables. For each procedure, sedation was applied by intramuscular injection with ketamine hydrochloride (10 mg/kg) (Ketaset, Fort Dodge Animal Health Ltd, Southampton, UK). None of the animals had been used previously for experimental procedures, and animals were randomly assigned to study groups.

Non-human primate study details					
Study Number	**Details of Timepoints**	**Demographic**	**Animals/group**	**Animal ID**	**Timepoints for samples/clinical data**
6114	PBa: clinical data, blood	rhesus (Indian origin) female 5 years old	n=6 at D2 n=6 at D7	6W 22W 36W	Group 1: PBa, PBb, C1, D2A
	PBb: clinical data, blood and BAL				
	C1/2: clinical data, aeBCG			68W 82W 84W	Group 2: PBa, PBb, C2, D2B
	D2: clinical data, blood, BAL, lung, hilar and axillary lymph nodes			76V 77V 9W	Group 3: PBa, PBb, C1, D7A
	D7: clinical data, blood, BAL, lung, hilar and axillary lymph nodes			20W 71W 76W	Group 4: PBa, PBb, C2, D7B
6143	As in 6114 (above)	rhesus female 5 years old	n=3 at D7	U8 U44 U76	Group 1: PBa, C1, D7
6282	PBa: clinical data, blood	rhesus female 5 years old	n=7 at D14 (8th animal R68 culled before aeBCG)	R7 R10 R31	Group 1: PBa, PBb, C1, D14A
	PBb: clinical data, blood and BAL				
	C1/2: clinical data, aeBCG			R4 R36 R51 R64	Group 2: PBa, PBb, C1, D14B
	D14: clinical data, blood, BAL, lung, hilar and axillary lymph nodes				
6181	PBa/b: clinical data, blood, BAL	rhesus 8x male 8x female 5-6 years old	n=8 (mask) n=8 (mouthpiece)	5X (Ma) 38X 40X 48X (Ma) 58X (Ma) 59X * 64X (Ma) 67X	Group 1 (males): PBa, PBb, C1, Wk2a, Wk4a, Wk9a, Wk12a, Wk16a
	C1/2: clinical data, aeBCG (mouthpiece or mask, Ma)			3X (Ma) 8X 20X (Ma) 29X (Ma) 37X 43X 66 (Ma) 70X	Group 2 (females): PBa, PBb, C2, Wk2b, Wk4b, Wk9b, Wk12b, Wk16b
	Wk2/4/9/12/16: clinical data, blood, BAL				
6266	PBa: clinical data, blood	rhesus 3x female 1x male 12 years old	n=2 at D2 n=2 at D7	N50 N66	Group 1: PBa, C1, D2
	C1: clinical data, aeSaline				
	D2 or D7: clinical data, blood, BAL, lung, hilar and axillary lymph nodes			M102 (male) N91	Group 2: PBa, C1, D7
6282	PBa: clinical data, blood	rhesus female 12 years old	n=3 at D7	32Z 46Z 54Z	Group 1: PBa, C1, D14
	C1: clinical data, aeSaline				
	D14: as D2 or D7 in 6266				

Non-human primate study details (continued)					
Study Number	**Details of Timepoints**	**Demographic**	**Animals/group**	**Animal ID**	**Timepoints for samples/clinical data**
6165	PBa: clinical data, blood, BAL	cynomolgus (Indonesian origin) male 4-5 years old	n=3 at D2 n=6 at D7	67E O53	Group 1: PBa, C1, D2a
	C1/2/3: clinical data, aeBCG			958	Group 2: PBa, C3, D2b
	D2a/b, D7a/b/c: clinical data, blood, Bal, lung, hilar and axillary lymph nodes			67F 109	Group 3: PBa, C1, D7a
				633 768	Group 4: PBa, C2, D7b
				558 962	Group 5: PBa, C3, D7c

Table 2.4 Non-human primate (NHP) studies

Breakdown of study details, including: species (Indonesian origin cynomolgus macaques or Indian origin rhesus macaques), age, sex, and groupings. Studies are colour coded as they are in figures throughout this thesis (e.g. turquoise refers to cynomolgus macaques of Study 6165). Unless marked (e.g. Study 6181 mask – 'Ma'), all animals were exposed to aerosol BCG (aeBCG) or aerosol saline (aeSaline) by mouthpiece delivery. Samples were taken at baseline time points (pre-BCG A/B – PBa/PBb), Day 2/7/14 (D2/D7/D14) or at Week 2-16 (Wk2-Wk16) after aeBCG or aeSaline. 59X was temporarily housed separately after weight loss, until this animal had regained weight (*).

2.2.2 Human samples

Human samples were used to compare baseline proliferation, as described Chapter 5. Samples were from clinical trials TB041/TB043, conducted in Oxford (UK) by the McShane group, according to the principals of the Declaration of Helsinki and in accordance with Good Clinical Practice (Table 2.5). Results from experiments with human samples not done by the author are also discussed in Chapter 5 (Marshall, Satti, Harris *et al*., unpublished). Full written consent was obtained from each volunteer prior to enrolment in the trials, and sample storage for exploratory immunological analysis was ethically

approved. All trials were registered on the clinical trials database and were fully approved by the relevant ethical and regulatory agencies: Oxfordshire Research Ethics Committee, the UK Medicines and Healthcare Products Regulatory Agency and Oxford University Tropical Research Ethics Committee. Participants were 67/73% female (TB041/TB043, respectivley), aged 18 to 46, and predominantly white British

Human studies including aerosol BCG (aeBCG)							
Study	**Study title**	**Trial ID**	**BCG strain**	**Group**	**Participants**	**BCG dose**	**Time points**
TB041	Aerosol BCG Challenge Trial in Healthy UK Adults	NCT02709278	Bulgaria	2A	n=3 aeBCG	1x10^4 CFU	PBa, D7, Wk2, Wk4, Wk12, Wk24
				2B	n=3 aeBCG	1x10^5 CFU	PBa, D7, Wk2, Wk4, Wk12, Wk24
				2C	n=3 aeBCG	1x10^6 CFU	PBa, D7, Wk2, Wk4, Wk12, Wk24
				2D/E	n=12 aeBCG	1x10^7 CFU	PBa, D7, Wk2, Wk4, Wk12, Wk24
				2F	n=12 ID BCG	1x10^6 CFU	PBa, D7, Wk2, Wk4, Wk12, Wk24
TB043	Investigating Immune Responses to Aerosol BCG Challenge in Healthy UK Adults	NCT03912207	Danish	1	n=10 aeBCG, n=3 aeSaline	1x10^7 CFU	PBa, D2 (**BAL**), D7, Wk2, Wk4, Wk8, Wk12, Wk24
				2	n=10 aeBCG, n=3 aeSaline	1x10^7 CFU	PBa, D2, D7 (**BAL**), Wk2, Wk4, Wk8, Wk12, Wk24

Table 2.5 Human clinical trial details

In TB041/TB043, individuals were exposed to aerosol BCG (aeBCG), aerosol saline (aeSaline) or intradermal BCG (ID, green). Blood samples were taken at baseline (pre-BCG A – PBa), and at days or weeks (e.g. Week 2 = Wk2) after aeBCG/aeSaline. TB041 was a dose escalation trial, to determine the safety of $1x10^4$-$1x10^7$ colony forming units (CFU) of aeBCG, compared to ID BCG. In TB043, broncho-alveolar lavage (BAL) samples were taken at Day 2/7 (D2/D7) after aeBCG to explore the early immune response, depending on participant group.

2.3 Methods

2.3.1 NHP procedures

2.3.1.1 NHP clinical assessment and care

Animal behaviour was observed daily for contra-indicators such as depression, withdrawal from the group, aggression, reduced food/water intake, changes in respiration rate or cough. Animals undergoing sedation for procedures had their body weight and body temperature recorded. Erythrocyte sedimentation rate (ESR) was measured using the Sediplast system (Guest Medical, Eden- bridge, United Kingdom).

2.3.1.2 BCG preparation

BCG Danish strain 1331 (AJ Vaccines, Copenhagen) is supplied at 2-8x10^6 CFU/vial. Each vial was treated as if it contained 5.5x10^6 CFU/vial. To obtain a dose of 1x10^7 CFU/mL for exposure to one animal, 0.55 mL of sterile saline was added to two vials of BCG to make a total of 1.1x10^7 CFU/1.1 mL of solution. A 'limited volume insulin syringe' was used to reconstitute the BCG, before 1 mL of this solution was added to an Omron MicroAir Mesh Nebuliser (Omron Healthcare UK Ltd., Milton Keynes, UK). The contents of multiple vials were pooled before administration to animals exposed within an hour of reconstitution, to ensure dose consistency. Residual solution was used to confirm vaccine titre. BCG was prepared immediately before use and kept on ice, excluded from light. aeBCG was delivered to sedated animals via the supplied mouthpiece with the nares occluded, or via a modified paediatric anaesthesia mask. Control animals were exposed to 1 mL of aerosol saline (aeSaline) solution by the same method.

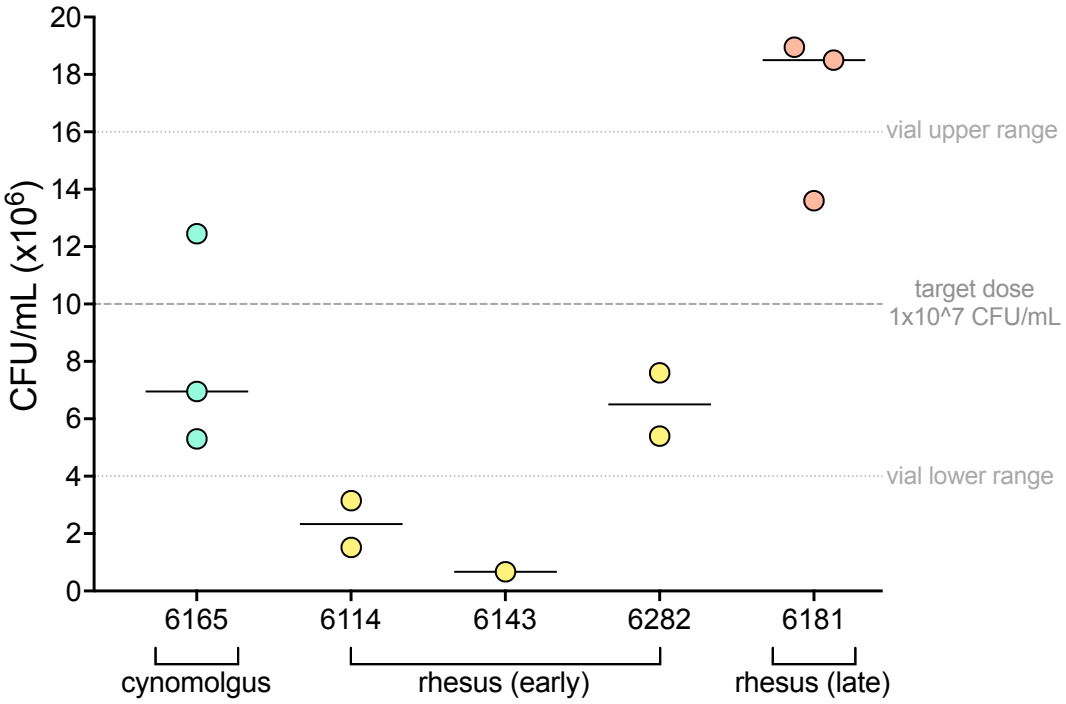


Figure 2.1 Bacille Calmette-Guérin (BCG) dosing across studies in non-human primates

Delivered BCG dose for each Study was calculated from colony counts of plate cultures of left-over BCG on 7H11 Agar plates. CFU/mL were calculated and plotted. The target dose of 1x10^{7}CFU/mL the theoretical range according to values on the vial are shown by grey dotted lines.

2.3.1.3 BCG dosing and quantification

Sterile phosphate-buffered saline (PBS) was used to serially dilute left-over BCG solution (10^{-1}-10^{-4}). Dilutions were spread onto 7H11 agar (duplicate) and incubated for 3-4 weeks or until 20-200 colonies were visible. Colonies were counted and used to back-calculate CFU/vial (Figure 2.1).

2.3.1.4 Necropsy/PM

At the allocated time points after aeBCG, clinical data and blood samples were taken prior to intracardiac injection of a lethal dose of anaesthetic (Dole lethal, Vetoquinol UK Ltd, 140mg/kg). Samples of lung, hilar and axillary LNs were obtained.

2.3.2 Sample processing

2.3.2.1 PBMC isolation from blood

PBMCs were isolated from heparin anti-coagulated blood. For RM, whole blood was added to Accuspin tubes (with fret) containing Ficoll-Histopaque Plus and centrifuged at 800 gravitational force (g) for 15 minutes (maximum brake). The PBMC 'buffy coat' layer was collected and diluted in R10 (25-30 mL R10 per Accuspin tube). Diluted cells were centrifuged at 400 g for 10 minutes, then the supernatant was discarded, and the remaining cell pellet was gently re-suspended (pastette) in 5 mL Ammonium Chloride Potassium buffer to lyse red blood cells. After 5 minutes with gentle agitation, Ammonium Chloride Potassium-treated samples were diluted in R10-NHP (25-30 mL R10), then centrifuged at 400 g for 5 minute (step repeated where necessary). Supernatant was discarded before gently re-suspending the cell pellet in 10 mL R10, ready to count. A Percoll gradient (no fret) was used in place of the Ficoll-Histopaque Plus for CM samples.

2.3.2.2 MC isolation from tissues

Tissue samples were cut into pieces (less than 1 cm^3), then homogenised for one minute in an appropriate volume of Tissue digestion media in GentleMacs C-tubes, on a GentleMacs Dissociator (Miltenyi Biotec). Lung samples were homogenised for one additional hour at a low rotation speed. Homogenised solutions were filtered through a 70 μm cell filter, layered over a Ficoll-Histopaque Plus and centrifuged at 400 g for 30 minutes (no brake). The mononuclear cell (MC) layer was collected, diluted in R2-PHE, and centrifuged at 400 g for 10 minutes. After discarding the supernatant, the cell pellet was gently re-suspended in 2-10 mL of R2, ready for counting.

2.3.2.3 BAL cell isolation and BALf isolation/cryopreservation

BAL samples were collected using an All-Scope XE30 4 mm flexible bronchoscope (VES, Southend on Sea, Essex, SS2 5BZ). Three consecutive washes were performed; 20 mL of Hanks balanced salts solution was instilled into the lungs, then collected. Samples were kept on ice after collection. Sample volume was recorded before spinning samples at 400 g for 10 minutes. Supernatant (BALf) was collected and immediately frozen at -80 °C. The remaining cell pellet was re-suspended in 10 mL R10, filtered through a 70 μm filter to remove mucus or debris, then centrifuged for 10 minute at 400 g. Where necessary, Ammonium Chloride Potassium buffer was added at this stage to remove red blood cell contamination, before an additional 5-minute spin at 400 g. Supernatant was discarded and the cell pellet was gently re-suspended in 1-2 mL R10-NHP, using a pastette, ready for counting.

2.3.2.4 Serum isolation

Specialised BD Vacutainer SST™ tubes pre-loaded with blood were received. Tubes were centrifuged at 800 g for 10 minutes, before serum collection from the top of the tube. Serum was filtered through a 0.2 μM filter into 1 mL aliquots, then stored at -20 °C, before transfer to -80 °C for long-term storage.

2.3.2.5 Cell counting, cryopreservation, transport & thawing

Cells were counted by one of two methods. Cell suspensions were counted on the day of collection (at UK-HSA) using the COUNTESS/EVE cell counter (ThermoFisher Scientific). 10 μL of cell suspension was added to 90 μL of Trypan blue and mixed. 10 μL of this mixture was added to a counting slide and live cells were counted using the COUNTESS/EVE. Samples counted from frozen (at University of Oxford) were counted on a CASY cell counter (Cambridge Bioscience). 5 μL of cell suspension was added to 10 mL of CASYTON

solution, and live cells were counted using the CASY. Where necessary, duplicates or repeats were performed.

Cells were cryopreserved ($1.2x10^7$ cells/vial). Cells that were not needed for on-the-day assays were centrifuged at 400 g for 5 minutes and the supernatant was discarded. Cells were resuspended in the appropriate volume of cryomedia, aliquoted into cryovials (1 mL cell suspension/vial), and transferred to Mr Frosty containers. Mr Frosty containers were immediately frozen at -80°C, before transfer to liquid nitrogen for longer term storage (at least 24 hours later). Cryopreserved samples were transferred from UK-HSA to the Jenner Institute at appropriate shipping temperatures.

For experiments on cryopreserved samples, vials were removed from liquid nitrogen and placed on dry ice. Cells were thawed in a water bath (37°C) until a small amount of ice remained. The cell solution was gently pipetted up and down, transferred to a 15 ml falcon tube containing 2 mL R10 (NHP or human) and centrifuged at 400 g for 5 minutes. Supernatant was removed, and cells were resuspended in 2 mL of R10 with 2 µL/mL of Benzonase and rested for 2 hours before counting (37°C). Cells were re-suspended in fresh media at the relevant concentration, ready for use.

2.3.2.4 BALf concentration

BALf was thawed and phospholipid concentration was measured using the Sigma Phospholipid Assay Kit, as specified. Samples/standards were loaded into a 96-well flat-bottomed plate, then incubated with an enzyme reaction mix for 30 minutes (room temperature, dark). Sample optical density (OD) was measured using a plate reader at 570 nm, and converted into concentration using the standard curve. Phospholipid concentration was calculated using the molecular weight of phosphatidyl choline.

A concentration factor to obtain a concentration of 1 mg/mL was calculated using the measured phospholipoid concentration. 1 mg/mL represents the approximate phospholipid concentration in the human lung (Jordi Torrelles, personal communication). Samples were concentrated by centrifugation in Amicon Ultra-15 Centrifugal filter tubes, according to the Millipore protocol. Samples were centrifuged at 3000 g, until the desired concentrated volume in the upper part of the Amicon tube was obtained. Each tube was limited to 15 mL of sample/run, and each sample was concentrated across two tubes, with one tube used for two rounds of concentration. Concentrated BAL fluid (BALf) was pooled from all tubes for each sample, before aliquoting into 1-2 mL volumes. Concentrated samples were stored at -80 °C, alongside samples of un-concentrated BALf. Phospholipid concentration was re-measured, after concentration by centrifugation.

2.3.3 Flow cytometry methods

2.3.3.1 Flow cytometry on samples stained on the day of acquisition

Samples were plated out at a concentration of 1 million cells/well, and stimulated with co-stimulatory antibodies only (anti-CD29 and anti-CD49d – 'Nil'), or with the addition of PPD or SEB for 2 hours at 37 °C, 5% CO_2 in a 96-well V-bottomed plate. After 2 hours, Brefeldin-A was added to block cytokine secretion, and samples were incubated for 16 hours. Samples were detached from the plate using ethylenediaminetetraacetic acid, before staining with extracellular (Live-dead, CD4, CD8, CD14, CD16, CD56, pan-$\gamma\delta$, Vα7.2, CD161, HLA-DR) and intracellular (CD3, IFNγ, IL-2, IL-17) antibody cocktails for 30 minutes in the dark each, with intermediate washing steps using FACS buffer (antibody panel 1). After staining, samples were fixed using Cytofix/cytoperm, washed using Perm/wash and re-suspended in 4% PFA, to be read immediately.

Antibody panel 1 (14-colour, Table 2.6) was used to characterise cell population dynamics after aeBCG and was designed to: minimise fluorochrome cross-over, balance markers for different cell types without losing clarity and to allow one panel to interrogate responses over time. Compensation was performed for each experiment, using stained compensation beads, processed alongside samples. Samples were acquired in plates, using a five-laser LSRII Fortessa instrument.

A) Antibody panel 1 (fresh samples)				
Marker	**Flurochrome**	**Clone**	**Catalogue no.**	**Manufacturer**
CD3	AF700	SP32.4	557917	BD biosciences
CD4	PerCP Cy5.5	L200	552838	BD biosciences
CD8	APC FIRE 750	SK1	344746	Biolegend
gd	TCR-BV421	B1	331218	Biolegend
Va7.2	PeDazzle594	3C10	351730	Biolegend
CD161	PeCy7	HP-3G10	339918	Biolegend
CD56	BV605	HCD56	318334	Biolegend
CD16	BV785	3G8	302046	Biolegend
CD14	PE	RMO52	quote	Beckman Coulter
IFNg	FITC	4S.B3	552882	BD biosciences
IL-17	BV711	BL168	512328	Biolegend
IL-2	APC	N7.48	130-091-644	Miltenyi Biotec
Live/dead	Live dead aqua	L/D	L34957	Thermofisher
HLA-DR	BUV395	G46-6	564040	BD biosciences

B) Antibody panel 2 (whole blood intracellular cytokine staining)				
Marker	**Flurochrome**	**Clone**	**Catalogue no.**	**Manufacturer**
CD3	AF700	SP32.4	557917	BD biosciences
CD4	PerCP Cy5.5	L200	552838	BD biosciences
CD8	APC FIRE 750	SK1	344746	Biolegend
gd	TCR-BV421	B1	331218	Biolegend
CD20	PeDaz594	BH7	302251	Biolegend
CD161	PeCy7	HP-3G10	339918	Biolegend
CD56	BV605	HCD56	318334	Biolegend
CD16	BV785	3G8	302046	Biolegend
CD14	PE	RMO52	quote	Beckman Coulter
IFNg	FITC	4S.B3	552882	BD biosciences
IL-17	BV711	BL168	512328	Biolegend
IL-2	APC	N7.48	130-091-644	Miltenyi Biotec
CD95	BV510	DX2	305639	Biolegend
HLA-DR	BUV395	G46-6	564040	BD biosciences
merTK	BV650	125518	748104	BD biosciences
CD163	BV650	GHI/61	563888	BD biosciences

C) Antibody panel 3 (proliferation - cell trace violet)				
Marker	**Flurochrome**	**Clone**	**Catalogue no.**	**Manufacturer**
CD3	AF700	SP32.4	557917	BD biosciences
CD4	PerCP Cy5.5	L200	552838	BD biosciences
CD8	APC FIRE 750	SK1	344746	Biolegend
gd	PeCy7	B1	331221/2	Biolegend
CD14	PE	RMO52	quote	Beckman Coulter
CD20	PE	BH7	302251	Biolegend
cell trace violet			C34571	Thermofisher
Live/dead red (amine beads)			L23102	Thermofisher

D) Antibody panel 4 (proliferation - Ki67)				
Marker	**Flurochrome**	**Clone**	**Catalogue no.**	**Manufacturer**
CD3	AF700	SP32.4	557917	BD biosciences
CD4	PerCP Cy5.5	L200	552838	BD biosciences
CD8	APC FIRE 750	SK1	344746	Biolegend
gd	PeCy7	B1	331221/2	Biolegend
CD14	PE	RMO52	quote	Beckman Coulter
CD20	PE	BH7	302251	Biolegend
Ki67	FITC		151211/2	Biolegend
Live/dead red (amine beads)			L23102	Thermofisher

Table 2.6 Antibody panels used for flow cytometry

*Flow cytometry panels were designed to characterise: cells isolated and stained on the same day as sample collection (panel 1, **A**), for whole blood cells (panel 2, **B**) and proliferative response (panel 3 & 4, **C** & **D**).*

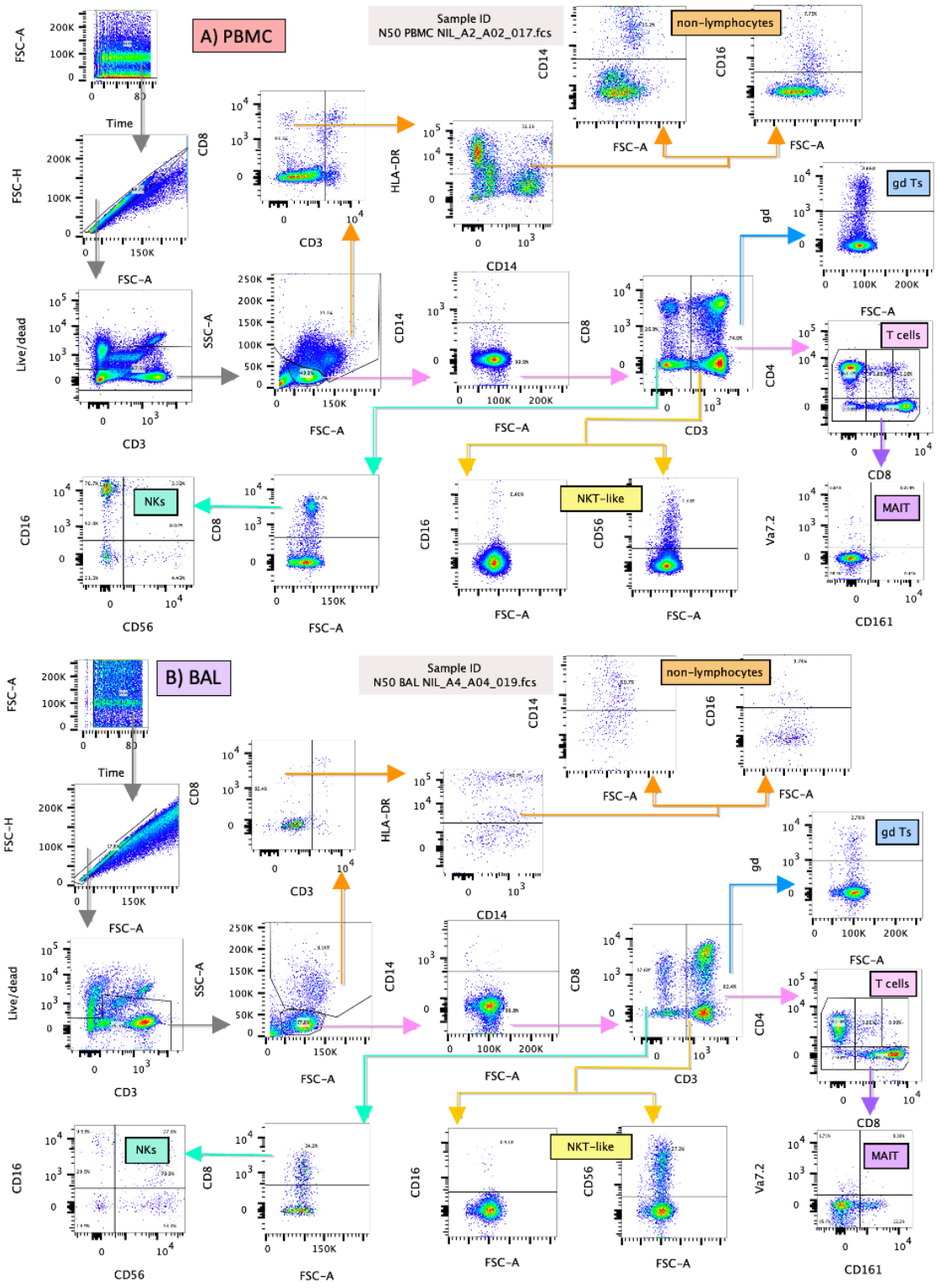
Data were analysed using FlowJo (version 10.6.1, Beckton Dickinson & Company 2006-2011). Non-viable cells and doublets were excluded, before gating for lymphocytes and using a wide gate to capture 'non-lymphocyte' cells (Figure 2.2). After excluding CD14+/CD20+ cells, sequential gating was applied to identify CD3+ T-cells, CD4+/CD8+/$\gamma\delta$+ T-cells and CD16+/CD56+ NKT cells (among CD3+ T-cells), and Vα7.2+CD161+ MAIT cells (among CD8+ T-cells). CD8+CD56+ and CD8+CD16+ NKT-L cells were identified among CD3- T-cells. CD14+/CD16+ cell frequency were explored among non-lymphocyte cells, as the majority of these cells were hypothesised to be monocytes. Fluorescence minus one (FMO) controls were

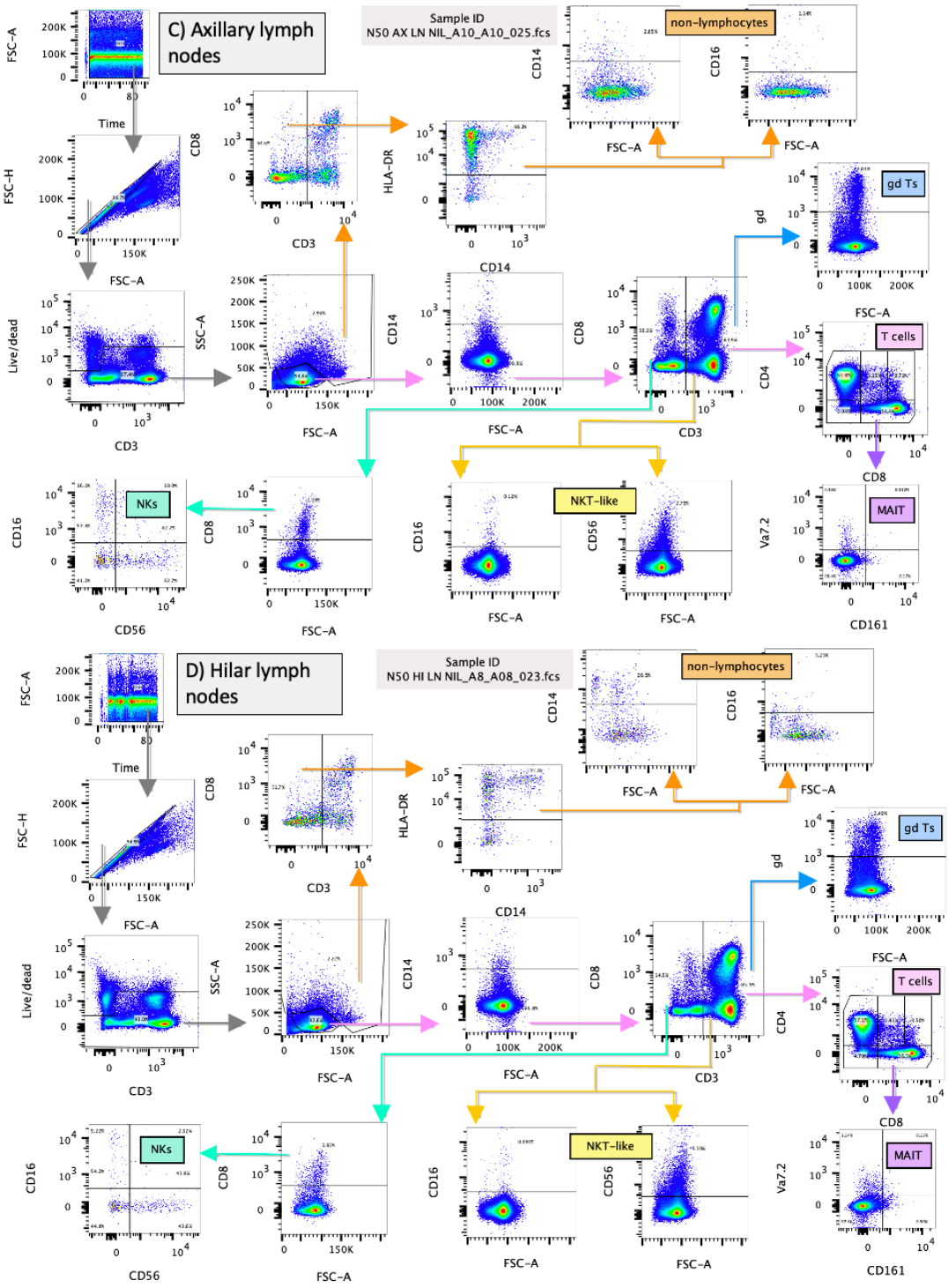
used to determine gate positions and gating was applied across groups to minimise manual gate adjustments.

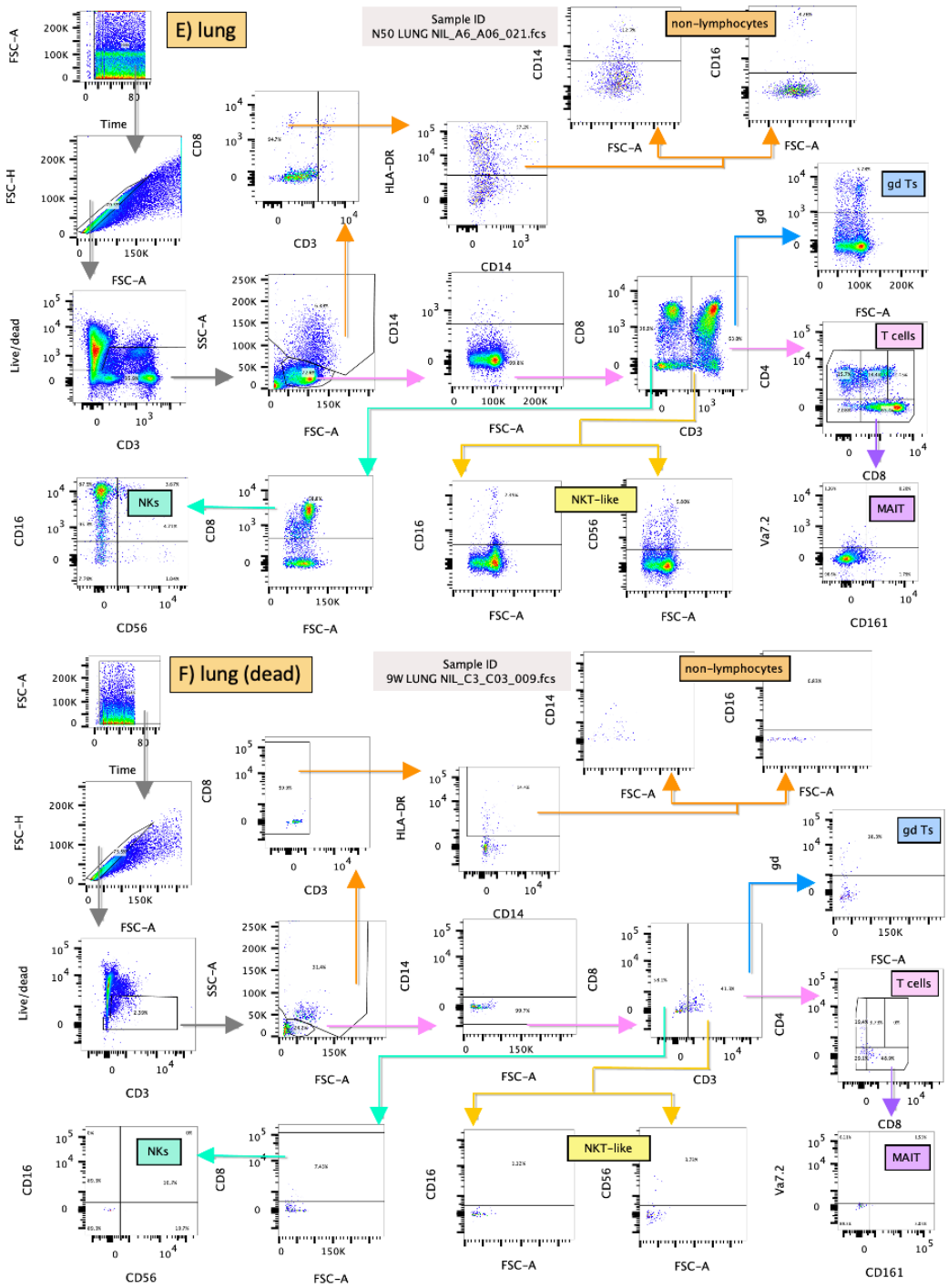
Further gating was applied to identify IFNγ-, IL-2-, and IL-17-producing cells among lymphocyte/non-lymphocyte populations. Antigen-specific cytokine responses were determined by subtracting background cytokine responses (unstimulated samples) from PPD-stimulated sample (negative values were adjusted to zero). Polyfunctional cells were identified using Boolean gating combinations of cytokine-producing CD4+ or CD8+ T-cells.

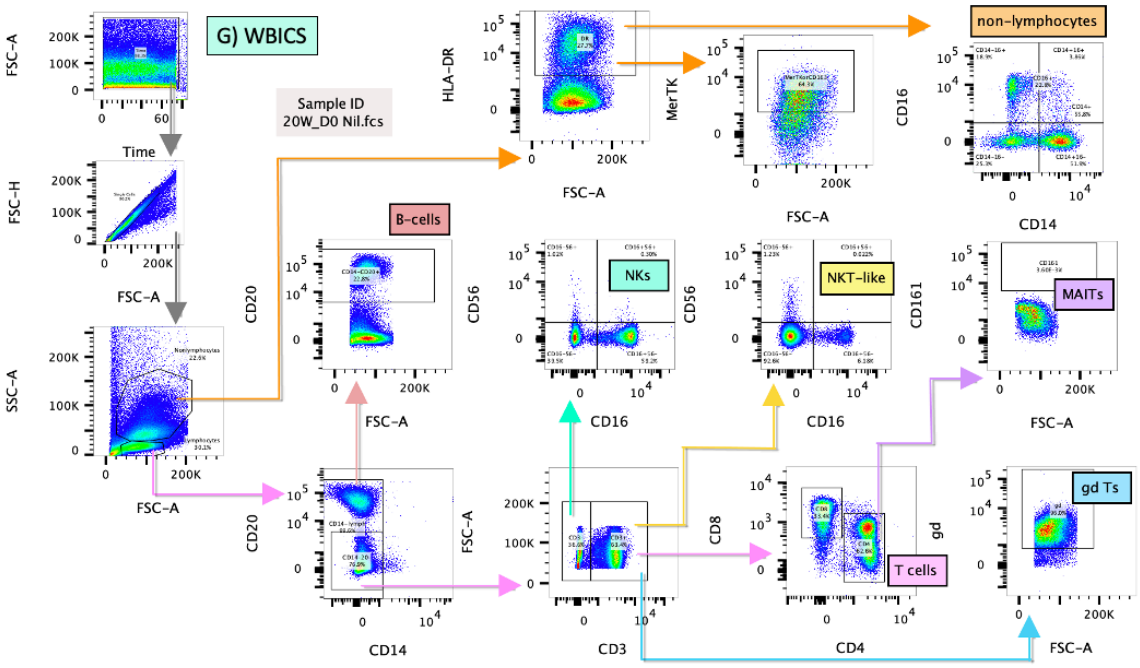
2.3.3.2 WB intracellular staining (WBICS) assay

The WBICS assay was based on the method developed by Hanekom *et al*[251]. 500 μL of whole blood was stimulated with 20 μg/mL PPD. Unstimulated (Nil) and samples stimulated with 5 μg/mL SEB were used as negative and positive controls. Co-stimulatory antibodies were added to all samples (anti-CD49d and anti-CD28: 0.25 μg/mL each). Cells were incubated for 5 hours at 37°C in a water bath. After 5 hours, Brefeldin-A solution was added at a final concentration of 10 μg/mL, before vortexing and a further 5-hour incubation at 37°C (water bath turned off by timer). After 11 hours, samples were incubated with 2 mM ethylenediaminetetraacetic acid/tube for 15 minutes, to detach monocytes. Samples were diluted 1:10 in 1x Facs lysing solution and incubated for 10 minutes. Cells were washed in PBS, then frozen across two cryotubes at -80°C in cryopreservation media (foetal calf serum + 10% dimethyl sulphoxide), before transfer to liquid nitrogen. Samples were thawed in bulk at 37°C, washed and plated out in 100 μL FACS buffer/sample, before staining with antibody panel 2 and acquisition using a five laser LSRII Fortessa.

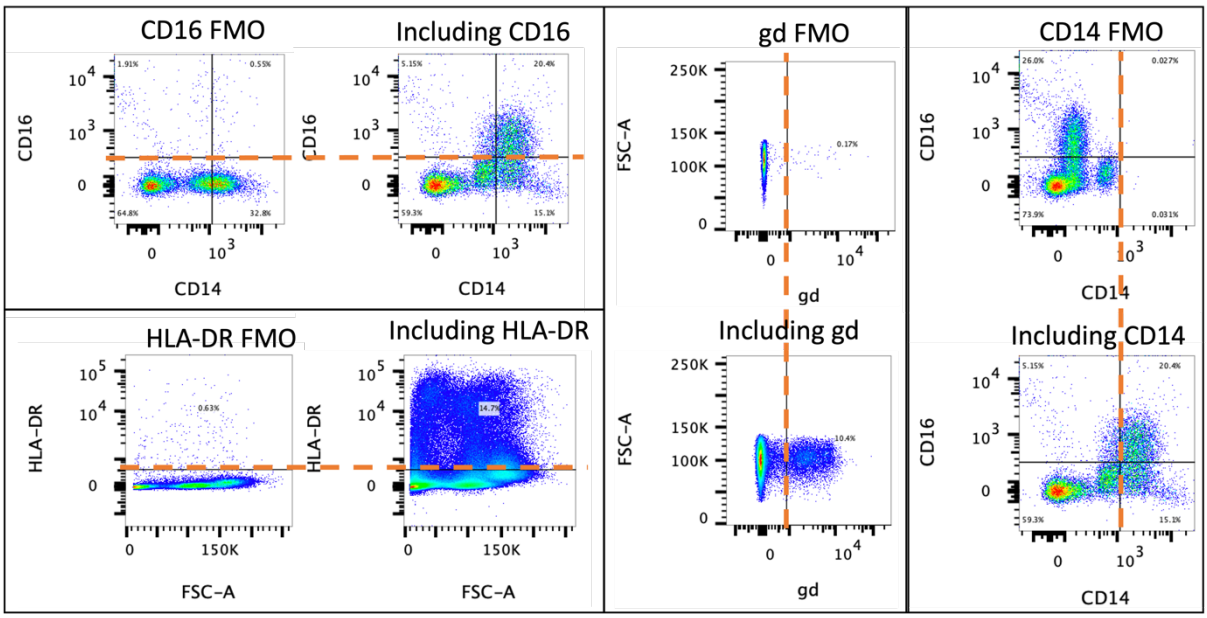

A) PBMC
Sample ID
N50 PBMC NIL_A2_A02_017.fcs
non-lymphocytes
gd Ts
T cells
NKs
NKT-like
MAIT
B) BAL
Sample ID
N50 BAL NIL_A4_A04_019.fcs
non-lymphocytes
gd Ts
T cells
NKs
NKT-like
MAIT


C) Axillary lymph nodes
Sample ID
N50 AX LN NIL_A10_A10_025.fcs
non-lymphocytes
gd Ts
T cells
NKs
NKT-like
MAIT
D) Hilar lymph nodes
Sample ID
N50 HI LN NIL_A8_A08_023.fcs
non-lymphocytes
gd Ts
T cells
NKs
NKT-like
MAIT


E) lung
Sample ID
N50 LUNG NIL_A6_A06_021.fcs
non-lymphocytes
gd Ts
T cells
NKs
NKT-like
MAIT
F) lung (dead)
Sample ID
9W LUNG NIL_C3_C03_009.fcs
non-lymphocytes
gd Ts
T cells
NKs
NKT-like
MAIT



H) FMO examples



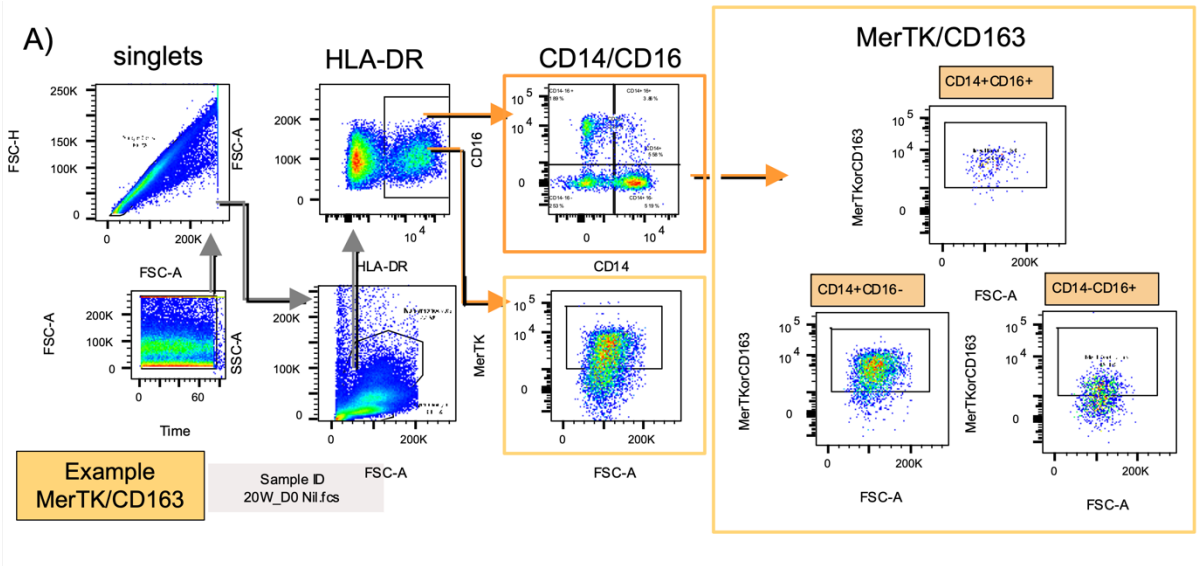
I)

Initial gating	Population-specific gating	Population name
time gate, singlets, live cells, lymphocytes based on FSC-A/SSC-A	CD14-CD3+	T-cells
	CD14-CD3+CD4+CD8-	CD4+ T-cells
	CD14-CD3+CD4-CD8+	CD8+ T-cells
	CD14-CD3+CD4+CD8+(+)	CD4+CD8+(+) T-cells
	CD14-CD3+CD4+CD8-CD56+	CD56+ CD4+ T-cells
	CD14-CD3+gd+	gamma-delta T-cells
	CD14-CD3+CD4-CD8+Va7.2+	Va7.2+ CD8+ T-cells
	CD14-CD3+CD4-CD8+CD161+Va7.2+	MAIT cells
	CD14-CD3+CD4-CD8+CD161+Va7.2-	CD161+Va7.2- CD8+ T-cells
	CD14-CD3+CD4-CD8+CD161-Va7.2+	CD161-Va7.2+ CD8+ T-cells
	CD14-CD3+CD16+	CD16+ NKT-like cells
	CD14-CD3+CD56+	CD56+ NKT-like cells
	CD14-CD3+CD16+CD56+	CD16+CD56+ NKT-like cells
	CD14-CD3-CD8+CD16+CD56+	CD16+CD56+ NK cell
	CD14-CD3-CD8+CD16-CD56+	CD16-CD56+ NK cell
	CD14-CD3-CD8+CD16+CD56-	CD16+CD56- NK cell
time gate, singlets, live cells, non-lymphocytes based on FSC-A/SSC-A	CD3-HLA-DR+CD14+	CD14+ non-lymphocyte
	CD3-HLA-DR+CD16+	CD16+ non-lymphocyte
	CD3-HLA-DR+CD14+CD16+	CD14+CD16+ non-lymphocyte
	CD3-HLA-DR+CD14+CD16-	CD14+CD16- non-lymphocyte
	CD3-HLA-DR+CD14-CD16+	CD14-CD16+ non-lymphocyte

Figure 2.2 Example gating strategies to identify cell populations

*Representative plots for unstimulated samples from a rhesus macaque (baseline) are shown to demonstrate the gating strategy to isolate cell populations of interest among: peripheral blood mononuclear cells (PBMCs - **A**), broncho-alveolar lavage (BAL - **B**), axillary lymph node (LN) mononuclear cells (MCs - **C**), hilar LN MCs (**D**) and lung MCs (**E**). **F** shows an example gating strategy from a lung sample that was excluded from analysis because cells were largely dead. **G** shows the gating strategy applied to flow panel 2, used to analyse whole blood samples. **H** shows example unstimulated PBMC plots for gates identified using an FMO, within the population of interest (FMO bounds marked in orange). **I** shows the gating strategy used in a written format.*

WBICS samples were dead and fixed before staining, so no Live/Dead stain was included in panel 2. The Vα7.2 marker taken out in panel 2, as this marker showed minimal staining when used in panel 1. Panel 2 was otherwise unchanged compared to panel 1, to make results more comparable. In place of Live/Dead and Vα7.2, anti-CD95 and anti-CD20 were added, to allow identification of B-cells (CD20) and activated T-cells (CD95). Sequential gating was used to characterise cell populations (Figure 2.2). In addition to the gating described above, B-cells were identified as CD14-CD20+ lymphocytes. Anti-MerTK and anti-CD163 antibodies were also included in panel 2 to characterise activated monocytes (antibodies conjugated to the same fluorochrome). In 2019, Dijkman *et al.,* identified a subset of HLA-DR+CD14+CD16+ monocytes expressing CD163 and MerTK, that were more common in RM than CM[4]. Live, HLA-DR+ non-lymphocyte cells were identified sequential gating, after exclusion of doublets. MerTK+/CD163+ cell frequency was determined among combinations of CD14+/CD16+ non-lymphocyte cells (compared to the original paper in Figure 2.3).



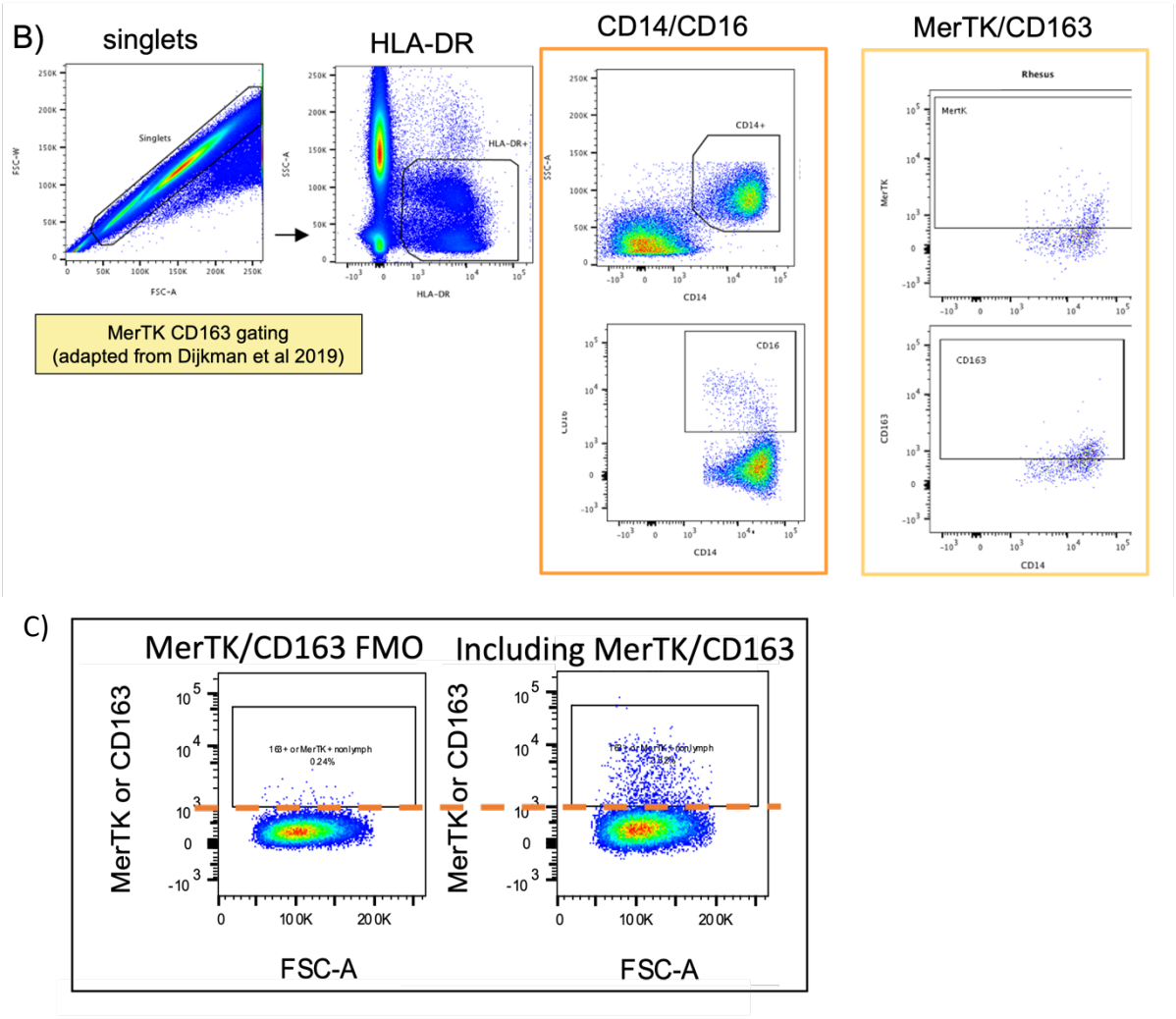


Figure 2.3 Example gating to identify MerTK- or CD163-positive cells

*Representative plots for unstimulated samples from a rhesus macaque (baseline) are shown to demonstrate the gating strategy to determine the frequency of human leukocyte antigen-DR (HLA-DR+ non-lymphocyte cells expressing CD163 or MerTK (**A**). This is shown alongside a reproduced gating strategy previously published by Dijkman et al (**B**)[4]. **C** shows example unstimulated plots for gates identified using an FMO, within the population of interest (FMO bounds marked in orange).*

2.3.3.3 PBMC proliferation assay

Two methods to measure proliferation were compared. For method 1, thawed PBMC cells were counted and plated out in a U-bottomed 96-well plate with R10 (NHP/human), at 250,000 cells/well; outer wells were filled with PBS. Each sample had duplicate wells for Nil (no stimulation), PPD (1 mg/mL) or phorbol 12-myristate 13-acetate (PMA) + Ionomycin (0.025 μg/mL + 0.25 μg/mL, 'PMA+I'). Plates were incubated at 37°C, 5% CO_2 for 4 days. Plates were centrifuged at (500 g, three minutes), and the top 100 μL of media was carefully removed and replaced with fresh R10 media. After two more days of incubation, plates were centrifuged, and duplicate wells were combined into a new plate. Samples were stained with antibody panel 3, and sequential gating was applied to identify Ki67+ cells. In brief, samples were gated for live lymphocytes, and to exclude doublets, CD14+ and CD20+ cells. The percentage of Ki67+ cells was determined among CD3+ and CD3- lymphocytes, with additional gating to determine Ki67+ CD4+/CD8+ T-cell frequency, within the CD3+ subset.

Method 2 used Cell Trace Violet (CTV) as a proliferation marker. Thawed samples were resuspended in R10 (NHP/human) at 1.65 million cells/sample. This allowed for 6 conditions of 0.25 million cells, plus extra for cells lost in the staining process. After 2 washes in PBS, 1 mL of 0.5 μL/mL CTV dye was added (in PBS), and incubated for 10 minutes at room temperature, in the dark. To quench the CTV dye, 4 mL of ice-cold PBS was added for 5 minutes (4°C). Samples were centrifuged and re-suspended in 1 mL of R10, then transferred to a new tube and incubated for 5 minutes at 37°C. Then, samples were centrifuged, re-suspended in 1140 μL R10 and loaded into a U-bottomed 96-well plate (duplicate wells for Nil/PPD/PMA+I). From here, six-day culture and staining were the same as in method 1, but

used antibody panel 4. CTV-unstained samples were cultured to act as FMOs. Sequential gating was applied as in method 1, but to identify CTV- cells, rather than Ki67+ cells.

2.3.3.4 IDEXX

500 μL of heparin anti-coagulated whole blood was analysed using the IDEXX Lasercyte analyser (IDEXX, USA) following the manufacturer's instructions.

2.3.5 Immunology

2.3.5.1 Ex vivo IFNγ ELISpot

An IFNγ ELISpot assay was used to estimate the numbers of cells producing PPD-specific IFNγ, as previously described[252]. PBMCs were stimulated with 10 μg/mL PPD, left unstimulated (negative control) or stimulated with 100 ng/mL PMA and 1 μg/mL ionomycin (positive control). Plates were developed using a human/monkey IFNγ kit, according to manufacturer's instructions (Mabtech, Nacka, Sweden), then spots were counted. Data were analysed by subtracting the mean spot count from control wells from the mean spot count in PPD-stimulated wells; this is presented as spot-forming units per million cells (SFU).

2.3.5.2 Enzyme-linked immunosorbent assay (ELISA)

Serum/BALf samples were thawed and diluted in Casein blocking buffer, alongside positive (pooled antibody-positive serum from NHPs exposed to *M.tb* challenge) and negative controls (casein-only). Samples were initially diluted to 1:100 (serum), 1:2 (concentrated BALf), or used without dilution (neat BALf).

96-well flat-bottom microtiter plates were coated overnight with 50 μL of 5 μg/mL PPD. The next day, excess coating solution was flicked off and plates were washed six times with PBS 0.05% Tween-20. Plates were blocked with 100 μL Casein per well for one hour (20°C), before the blocking solution was flicked off and plates were blotted. Samples/controls

were thoroughly vortexed, 50 µL was added per well (duplicates), and plates were incubated for two hours (20°C). Unbound sample was flicked off plates, before six washes with PBS 0.05% Tween 20. 50 µL of secondary antibody was added per well and plates were incubated for one hour at 20°C (IgG diluted 1:1000 or IgM diluted 1:2000 in Casein). Excess secondary antibody was flicked off and plates were washed 6 times with PBS 0.05% Tween 20. 100 µL of pNPP was added per well and plates were covered in foil and incubated for 30 minutes (20°C).

OD405 was read using a Model 550 Microplate Reader (Bio-Rad, UK). Mean OD405 values were converted to arbitrary units (AU) according to the standard curve. Where samples generated OD values below the lower limit (OD < 0.2), these were designated as antibody-negative. Where the OD value was too high (OD > 3.0), samples were diluted further and re-run, until the OD was within range. Plates failed and were repeated if the standard curve did not fall within the pre-determined range.

2.3.6 Statistical analysis

Graphs were plotted in GraphPad Prism (version 9.2.0 - GraphPad Software Inc, La Jolla, California, USA). Statistical comparisons were made in GraphPad Prism, with the exception of correlation analysis, which was made using SPSS (version 27 – IBM SPSS Statistics).

2.3.7.1 Comparison between limited time points (Chapter 3)

Pairwise comparisons were made using Wilcoxon-Rank testing, and comparisons between different groups of animals were made using Mann-Whitney U-testing.

2.3.7.2 Comparison between multiple time points (Chapter 4)

A Shapiro-Wilk test was applied to determine data normality, where serial time points were available. Parametric data were analysed using a repeated measures analysis of variance (ANOVA) or a Mixed Effects model (to account for randomly missing data), and corrected for

multiple comparisons using Dunnett's test. Non-parametric data with no randomly missing data were analysed using a Friedman test and corrected for multiple comparisons using Dunnett's test. Non-parametric data with randomly missing data were analysed using a Wilcoxon-Rank test. The PBMC flow cytometry dataset was only analysed using a Wilcoxon-Rank test, because of missing samples. Corrected P-values are presented for data analysed using a repeated measures ANOVA/Mixed Effects model/Friedman test, and uncorrected values are presented for data analysed using a Wilcoxon-Rank test. Comparisons between aeBCG delivery groups over time were made using Area Under the Curve analysis (AUC), and at each time point, using a Mann-Whitney U-test. Outliers were excluded after identification using a Grubb's test (α=0.05).

2.3.7.3 Correlation analysis

When exploring correlations, data were compared using a Spearman's correlation. Statistically significant correlations are presented, where significant at two consecutive time points.

2.3.7.4 Principal component analysis (PCA)

PCA was applied to distinguish trends between different time points for all measurements of cytokine in BAL cell subsets. Components with an Eigenvector of one or more were selected. PCA and data visualisation were performed in Prism.

Chapter 3: Early immune response to aeBCG

Chapter 3: early immune response to aeBCG

3.1 Statement of authorship

The author processed NHP samples from UK-HSA (Porton Down), with help from the NHP team where necessary to process a large number of samples. Andrew White and members of the Biological Investigations group exposed animals to aeBCG or aeSaline, and BCG titres were calculated by the bacteriology team, led by Simon Clark at UK-HSA. All assays described were performed and analysed by the author. Flow cytometry panel 1 was based on previous panels designed by Andrew White, and panel 2 was adapted from this, with help from Andrew White and Iman Satti.

3.2 Background

Experimental aeBCG was chosen as a biologically relevant model for *M.tb*, that is feasible in humans and NHPs[3, 46]. The work described in this chapter is focused on the evaluation of responses to early time points after exposure, given the growing interest in the innate immune system's role in TB. Compared to human studies, the more invasive sampling possible in animal models allows specific study of tissue compartments. Recent evidence points to a 'local' response in the lungs that is hard to study in humans, due to restrictions with repeat sampling. Tissue samples can be obtained from lung and selected LNs in NHPs, alongside BAL (possible in humans). The response to mycobacterial infection differs depending NHP species[122]. CM (Asian genotype) control *M.tb* better, more often resulting in a latent or controlled phenotype than active disease[253]. RM with the same level of infection are more likely to develop active TB[121]. In this project, the same experimental design was applied to CM and RM, to allow direct comparison.

3.3 Objectives & hypotheses

Experiments in this chapter were designed to:

1. Study the early response to aeBCG, across tissue compartments:
    - PBMCs, whole blood (WB) and serum
    - BALf and cells from the lung mucosa
    - MCs from LNs and lung tissue
2. Compare immune responses across two macaque species:
    - RM
    - CM
3. Explore the following hypotheses:
    a) An immune response to $1x10^7$ CFU aeBCG in RM and CM will be detected within the first 14 days after delivery, and be detectable by a difference in PPD-specific ELISpot assay
    b) $\gamma\delta$ T-cell frequency will increase in the first seven days after aeBCG, particularly in BAL
    c) MAIT cell frequency will increase in BAL in the first seven days after aeBCG
    d) RM and CM will show different levels of cellular activation as part of the immune response to aeBCG. MerTK/CD163 expression on monocytes will be higher in RM than CM, as previously demonstrated[148]
    e) These early time points will be too early for detection of an antigen-specific antibody response by PPD-specific ELISA

3.4 Results

3.4.1 aeBCG study design

RM and CM with no prior exposure to BCG were exposed to a single dose of aeBCG or aeSaline, across a number of experiments (Figure 3.1). Clinical data, blood and BAL samples were taken two weeks before exposure, at pre-BCG A (PBa). An additional baseline blood sample was taken where possible (PBb). An estimated dose of $1x10^7$ CFU was obtained from multiple vials of BCG, and delivered by AE at Day 0 (D0). Animals were allocated into groups to be euthanised at different early time points. At D2/D7/D14, clinical data, blood, and BAL samples were collected before intracardiac injection of a lethal dose of anaesthetic. Lung lobes, hilar and axillary LNs were also collected at these PM time points. Remaining cells (after performing assays on the day of isolation), serum and BALf were cryopreserved.

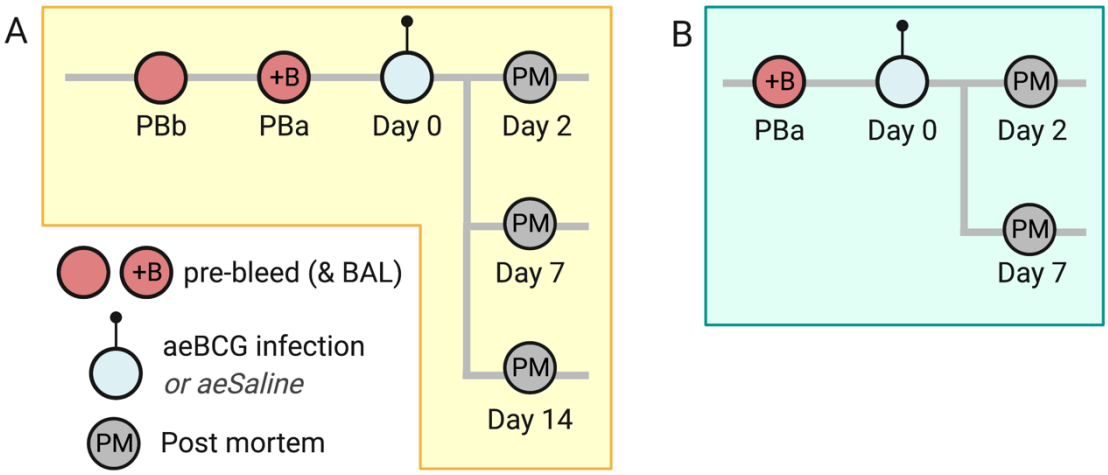


Figure 3.1 Study design (early time points)

*Experimental design for comparison of early responses to aeBCG delivery. Samples were collected from rhesus (RM, **A**) and cynomolgus macaques (CM, **B**). Before aerosol BCG (aeBCG) or aerosol saline (aeSaline), clinical data, blood and broncho-alveolar lavage (BAL) samples were taken at pre-BCG A (PBa) and pre-BCG B (PBb, only RM). 1x10^7 CFU of aeBCG (target dose) or aeSaline was delivered via Omron nebuliser at Day 0. Animals were euthanised, and clinical data, blood, BAL, and tissue samples were taken post-mortem (PM). Different groups of animals were allocated to Day 2/7/14 post-mortems. Image created with Biorender.com.*

3.4.2 Clinical measures of health after aeBCG

Clinical and laboratory parameters monitored throughout this project included: body weight, rectal temperature, red blood cell haemoglobin level, size of LNs (measured and scored at left and right, axillary, and inguinal LNs) and other observable signs of change (e.g. skin damage, behaviour). Erythrocyte sedimentation rate was unchanged after aeBCG. One animal was excluded from this project, due to excessive weight loss between PBb and D0 (Study 6282, animal not shown in graphs). Neither body weight nor temperature changed after aeBCG or aeSaline (Figure 3.2).

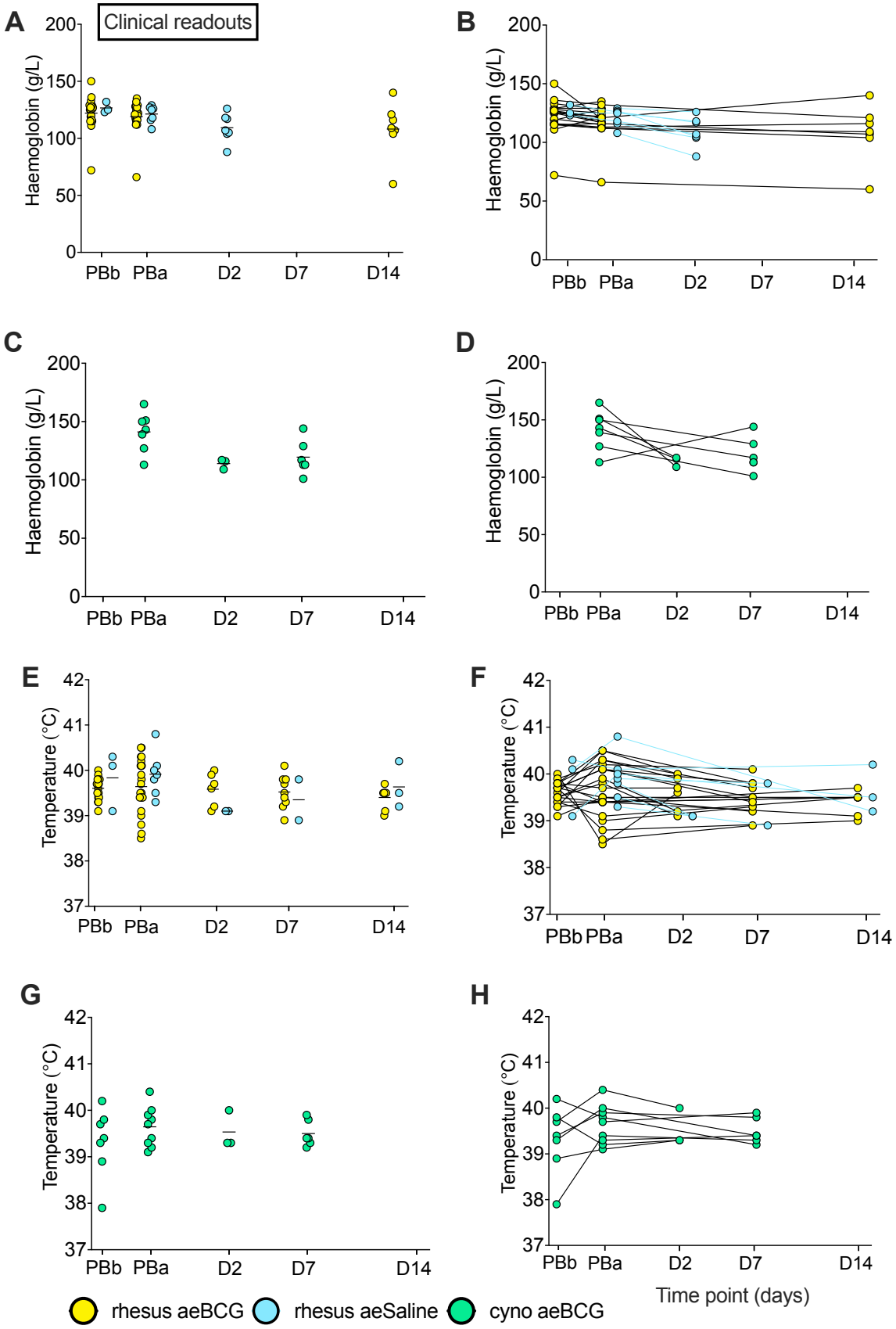

A
Clinical readouts
Haemoglobin (g/L)
200
150
100
50
0
PBb
PBa
D2
D7
D14
B
C
D
E
Temperature (°C)
42
41
40
39
38
37
F
G
H
rhesus aeBCG
rhesus aeSaline
cyno aeBCG
Time point (days)

Figure 3.2 Clinical data

*Body weight (**A-D**) and rectal temperature (**E-H**) for rhesus macaques (RM) exposed to aeBCG are shown in yellow (**A, B, E & F**) and cynomolgus macaques in green (**C, D, G & H**). RM exposed to aeSaline are shown in blue (**A, B, E & F**). Individual animals and group medians (**A, C, E & G**) are compared to animals tracked over time (**B, D, F & H**). Baseline values are shown at pre-BCG A and B (PBa and PBb) before aeBCG or aeSaline at day 0. Paired data were compared using Wilcoxon-Rank Testing, and unpaired using Mann-Whitney U-testing. All comparisons were not significant.*

3.4.2 Frequency of PPD-specific IFNγ spot forming units

The systemic immune response to aeBCG was profiled using an *ex vivo* ELISpot assay. There was no difference in the number PPD-specific IFNγ spot forming units (SFU) measured at early time points post-exposure (Figure 3.3). There was a trend towards an increased SFU at D7 in RM compared to PBa (not significant), but no trend was apparent at D7 compared to PBb. Variation within time points was observed for RM and CM.

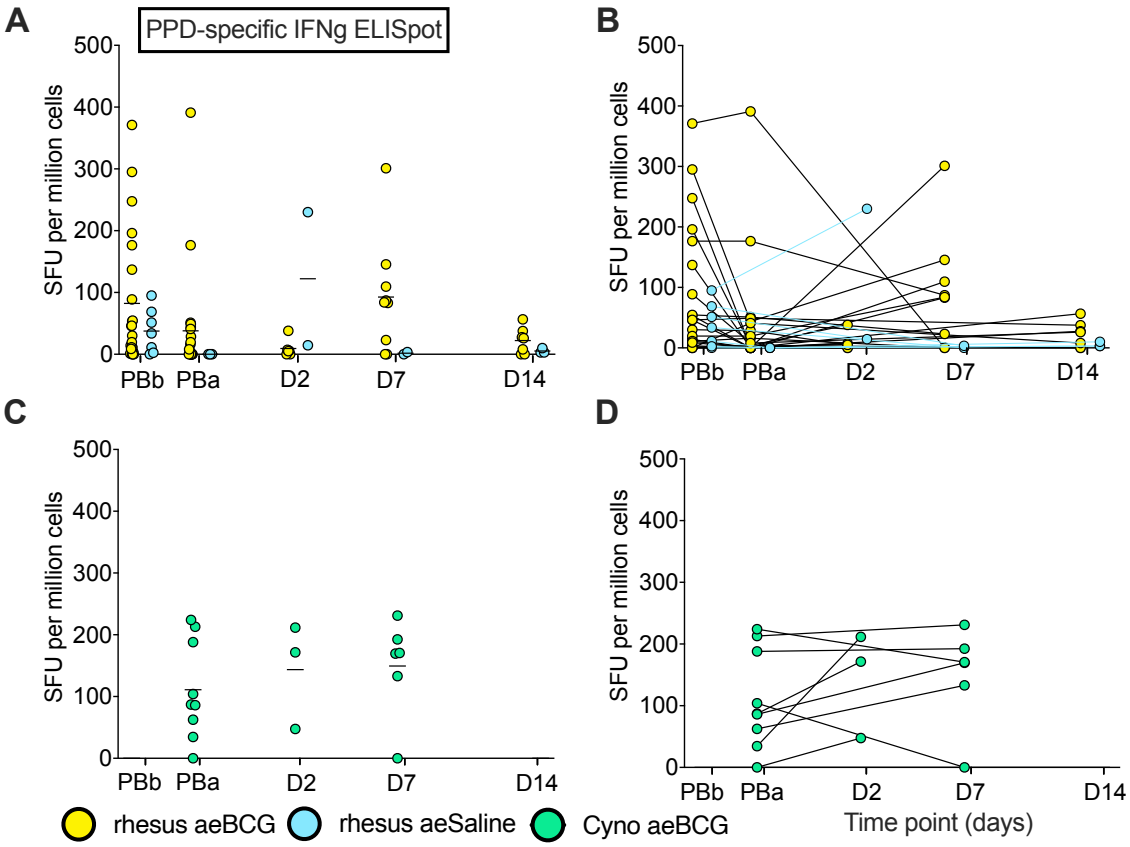


Figure 3.3 Frequency of PPD-specific IFNγ spot forming cells after aerosol BCG (aeBCG)

*Systemic PPD-specific IFNγ spot forming units (SFU) are shown per million cells, for rhesus macaques (RM) in yellow (**A** & **B**) and cynomolgus macaques (CM) in green (**C** & **D**). RM exposed to aeSaline are shown in blue (**A** & **B**). Individual animals and group medians (**A** & **C**) are compared to animals tracked over time (**B** & **D**). Baseline values are shown at pre-BCG A and B (PBa and PBb) before aeBCG or aeSaline (grey dashed line). Paired data were compared using Wilcoxon-Rank Testing, and unpaired using Mann-Whitney U-testing. All comparisons were not significant.*

3.4.3 PBMC cell populations

Groups of animals were allocated for euthanasia at D2/D7/D14 after exposure to aeBCG. Table 3.1-Table 3.4 show the results of statistical comparison between time points for PBMC, BAL cells and MC isolated from lung and LNs. Median cell counts for each population characterised are shown in Supplementary Table 4.

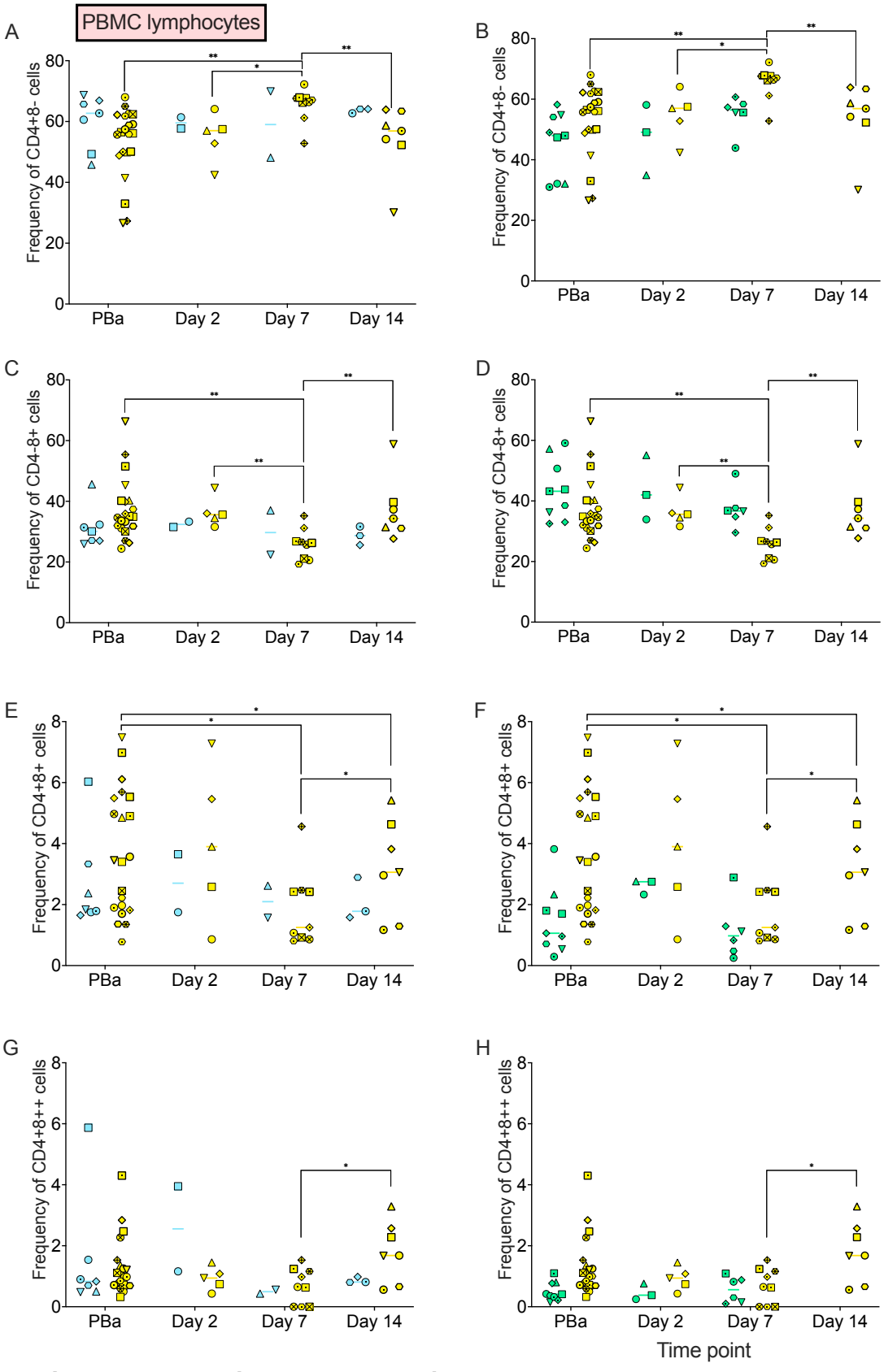
In PBMC samples, the frequency of CD3+ T-cells (CD14-lymphocytes) from RM was lower at D7 and D14 after aeBCG, compared to D2. CD3+ T-cell frequency at D7/D14 did not differ from baseline levels, but there was a trend towards increased frequency at D2 compared to baseline (p=0.0625). Groups of animals euthanised at D2/D7/D14 were comprised of different individual animals. Ongoing analysis and commentary will focus on results where there is a significant change compared to baseline, or a difference between PM time points and a significant change compared to baseline.

Among CD3+ T-cells, the following subsets were defined by CD4 and CD8 expression: CD4+CD8- (CD4+ T-cells), CD4-8+ (CD8+ T-cells), CD4+CD8+, CD4+CD8++, and CD4-8-. The CD4+CD8+ and CD4+CD8++ subsets were clearly defined within this NHP dataset. CD4+ T-cell frequency increased at D7 compared to baseline in RM (p=0.0039) and CM (not significant - p=0.0938). CD4+ T-cell frequency was lower at D14 than at D7 (p=0.0079, Figure 3.4 - RM). The reverse of this pattern was observed for CD8+ T-cell frequency, causing an increase in the CD4+:CD8+ T-cell ratio from baseline to D7 in RM. The median CD4+:CD8+ ratio increased from baseline to D7 from 1.63-2.66 in RM, and from 1.38-1.51 in CM. CD4+CD8+ and CD4+CD8++ frequency followed the same pattern as the CD8+ T-cells (RM).

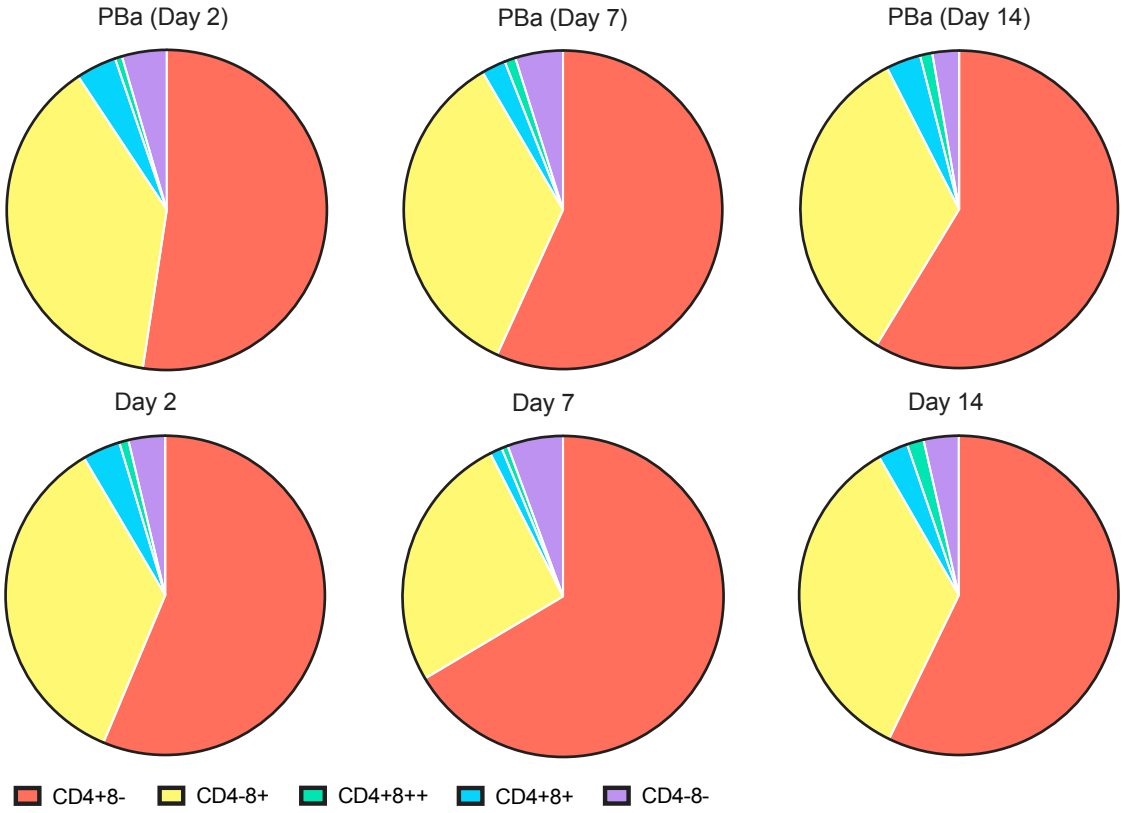
PBMC									
species	cynomolgus			rhesus					
time point comparison	PBa D2	PBa D7	D2 D7	PBa D2	PBa D7	PBa D14	D2 D7	D2 D14	D7 D14
T cells (CD14-3+)	ns	ns	ns	ns	ns	ns	*	**	ns
CD4 T cell	ns	ns	ns	ns	**	ns	*	ns	**
CD8 T cell	ns	ns	ns	ns	**	ns	**	ns	**
CD4+8+ T cell	ns	ns	ns	ns	*	*	ns	ns	*
CD4+8++ T cell	ns	ns	ns	ns	ns	ns	ns	ns	*
CD4-8- T cell	ns	*	ns	ns	ns	ns	ns	ns	ns
CD56+ CD4+ T cell	ns	*	ns	ns	ns	ns	ns	ns	ns
gamma-delta T cell	ns	*	ns	ns	ns	*	ns	ns	ns
Va7.2+ CD8+ T cell	ns	ns	ns	ns	**	ns	ns	ns	ns
CD161+Va7.2+ CD8+ T cell	ns	*	ns	ns	ns	*	ns	ns	ns
CD161+Va7.2- CD8+ T cell	ns	*	ns	ns	**	ns	ns	ns	*
CD161-Va7.2+ T cell	ns	ns	ns	ns	**	ns	ns	ns	ns
CD16+ T cell (NKT-like)	ns	ns	ns	ns	*	ns	ns	ns	ns
CD56+ T cell (NKT-like)	ns	*	ns	ns	ns	ns	ns	ns	ns
CD16+CD56+ T cell (NKT-like)	ns	ns	ns	ns	ns	ns	ns	ns	ns
CD16+56+ CD3- (NK cell)	ns	*	ns	ns	ns	ns	ns	ns	ns
CD16-56+ CD3- (NK)	ns	ns	ns	ns	**	ns	*	ns	ns
CD16+56- CD3- (NK)	ns	ns	ns	ns	**	ns	*	ns	ns
CD14+ non-lymphocyte	ns	*	ns	ns	*	ns	ns	ns	ns
CD16+ non-lymphocyte	ns	*	*	ns	ns	ns	ns	ns	ns
CD14+CD16+ non-lymphocyte	ns	ns	ns	ns	ns	ns	ns	ns	ns
CD14+CD16- non-lymphocyte	ns	*	ns	ns	*	ns	ns	ns	ns
CD14-CD16+ non-lymphocyte	ns	*	*	ns	ns	ns	ns	ns	*

Table 3.1 Peripheral blood mononuclear cell (PBMC) populations

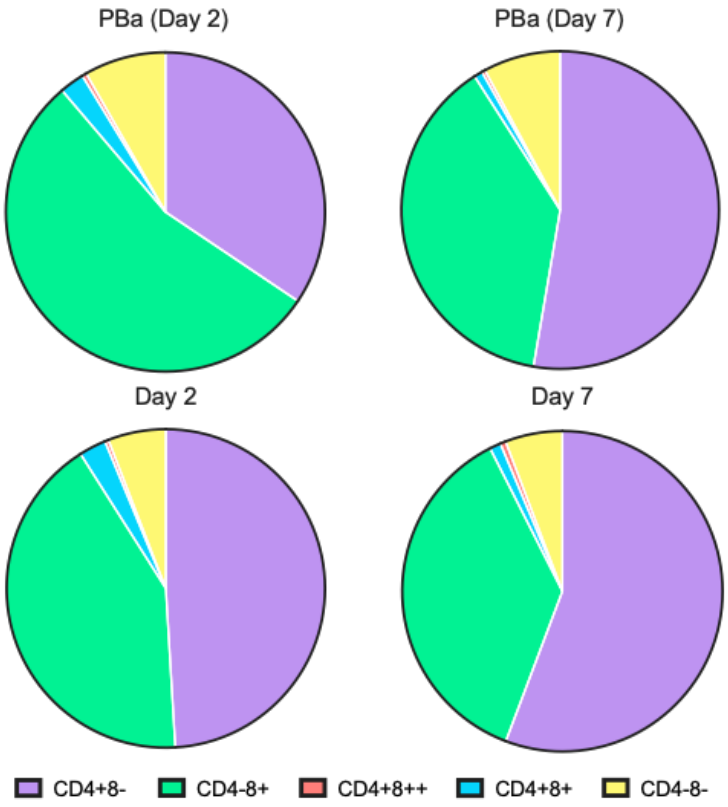
The frequency of different cell populations among PBMCs from rhesus macaques were compared between groups of animals euthanised at Day 2/7/14 (D2/D7/D14). Statistical comparisons between paired samples at baseline (PBa) and their post-mortem time point were made using Wilcoxon-Rank testing. Mann-Whitney U-testing was used to compare unpaired data (e.g. D2 compared to D7). Comparisons are marked as not significant (ns), P < 0.05 (*) or P < 0.005 (**), with increases shown in yellow, and decreases in blue.


A
PBMC lymphocytes
Frequency of CD4+8- cells
B
Frequency of CD4+8- cells
C
Frequency of CD4-8+ cells
D
Frequency of CD4-8+ cells
E
Frequency of CD4+8+ cells
F
Frequency of CD4+8+ cells
G
Frequency of CD4+8++ cells
H
Frequency of CD4+8++ cells
PBa
Day 2
Day 7
Day 14
Time point
Rhesus aeBCG
Rhesus aeSaline
Cyno aeBCG

I CD4/CD8 expression (RM - PBMC)



J CD4/CD8 expression (CM - PBMC)



K

CD4+:CD8+ ratio		
Timepoint	RM	CM
PBa (D2)	1.37	0.63
D2	1.62	1.17
PBa (D7)	1.61	1.46
D7	2.58	1.53
PBa (D14)	1.63	-
D14	1.66	-

Figure 3.4 CD4+/CD8+ frequency on T-cells characterised among peripheral blood mononuclear cells (PBMCs)

*The frequency of CD4+ T-cells (**A** & **B**), CD8+ T-cells (**C** & **D**), CD4+CD8+ (**E** & **F**) and CD4+CD8++ (**G** & **H**) among CD3+ lymphocytes from PBMCs are shown. Animals exposed to aerosol BCG (aeBCG) are shown in yellow (rhesus macaques) and green (cynomolgus macaques), and rhesus macaques exposed to aerosol Saline (aeSaline) are shown in blue. Each symbol represents a different animal and group medians are shown. Statistical comparisons between paired samples at baseline (PBa) and their post-mortem time point were made using Wilcoxon-Rank testing. Mann-Whitney U-testing was used to compare unpaired data (e.g. D2 compared to D7). Significant comparisons are marked as P < 0.05 (*) or P < 0.005 (**).*

*The same data is presented in pie charts, using the median value for each cell population (rhesus macaques in **I**, cynomolgus macaques in **J**). The median ratio of CD4+:CD8+ T-cells is shown in **K**.*

γδ cell frequency among T-cells decreased at D7 compared to baseline (*p*=0.0312), for all CM (Figure 3.5). In contrast, γδ cell frequency increased at D14 compared to baseline in RM (*p*=0.0312). This increase was small, and control animals (exposed to aeSaline) showed a similar trend towards increase. There were too few (n=3) control animals to analyse this trend statistically.

Vα7.2+CD161+ CD8+ T-cells frequency (MAIT) increased at D14 compared to baseline in RM (*p*=0.0312) and at D7 compared to baseline in CM (*p*=0.0312 – Figure 3.6). Other combinations of Vα7.2 and CD161 were also analysed. In CM, Vα7.2-CD161+ cell frequency also increased at D7 compared to baseline. In contrast, Vα7.2-CD161+ cell frequency decreased in RM at D7 compared to baseline (returned to baseline at D14).

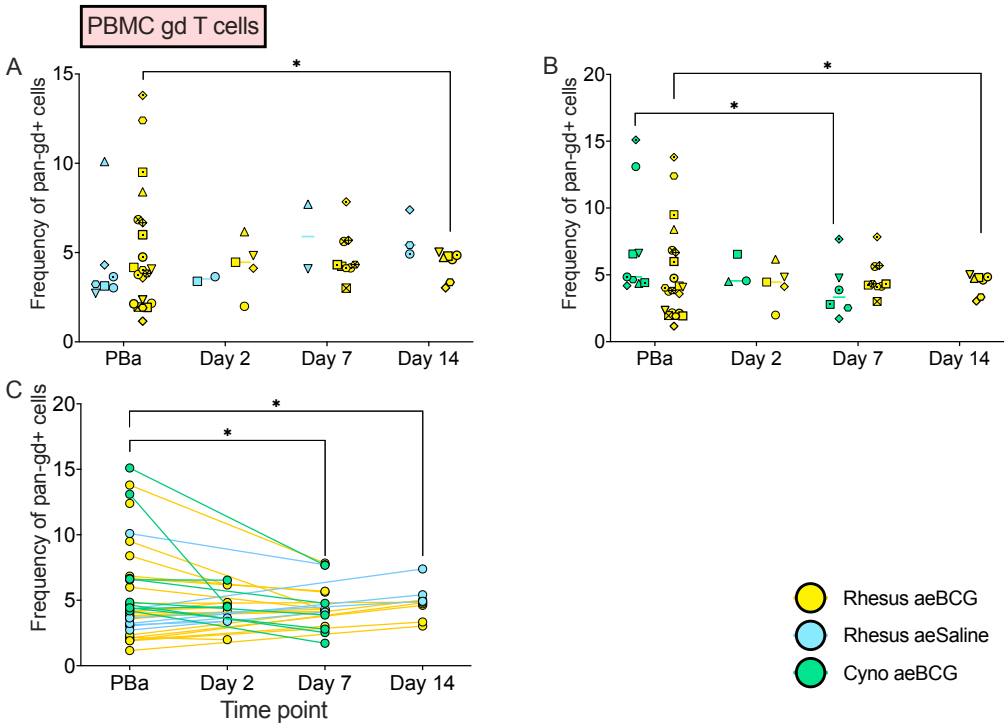


Figure 3.5 γδ cell frequency among T-cells characterised among peripheral blood mononuclear cells (PBMCs)

The frequency of pan-γδ+ among CD3+ lymphocytes from PBMCs are shown. Animals exposed to aerosol BCG (aeBCG) are shown in yellow (rhesus macaques, left hand side) and green (cynomolgus macaques, right hand side), and rhesus macaques exposed to aerosol saline (aeSaline) are shown in blue. Each symbol represents a different animal and group medians are shown. Statistical comparisons between paired samples at baseline (PBa) and their post-mortem time point were made using Wilcoxon-Rank testing. Mann-Whitney U-testing was used to compare unpaired data (e.g. D2 compared to D7). Significant comparisons are marked as P < 0.05 (*) or P < 0.005 (**).

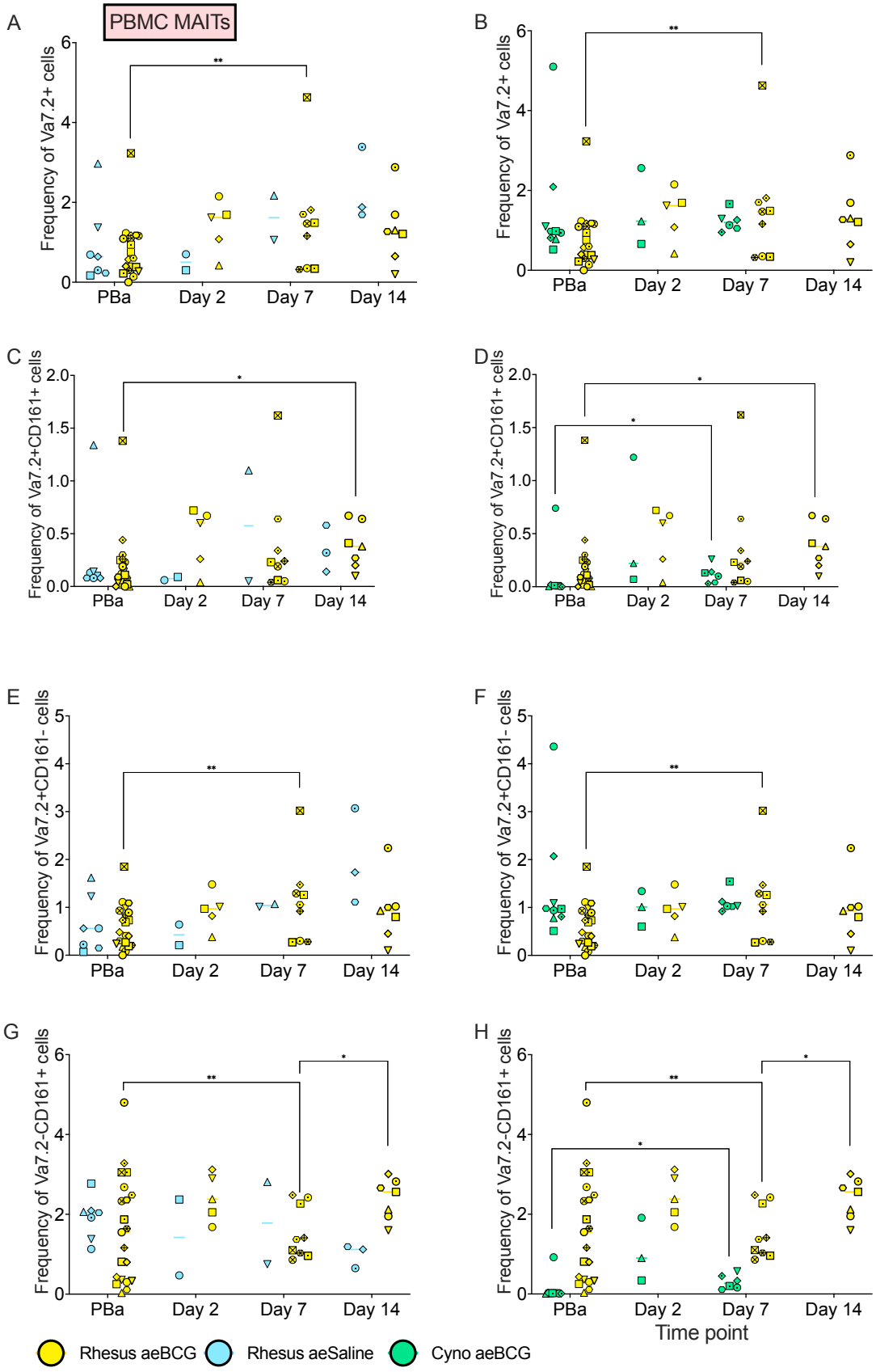

A
PBMC MAITs
Frequency of Va7.2+ cells
B
Frequency of Va7.2+ cells
C
Frequency of Va7.2+CD161+ cells
D
Frequency of Va7.2+CD161+ cells
E
Frequency of Va7.2+CD161- cells
F
Frequency of Va7.2+CD161- cells
G
Frequency of Va7.2-CD161+ cells
H
Frequency of Va7.2-CD161+ cells
PBa
Day 2
Day 7
Day 14
Time point
Rhesus aeBCG
Rhesus aeSaline
Cyno aeBCG

Figure 3.6 MAIT cell frequency among CD8+ T-cells characterised among peripheral blood mononuclear cells (PBMCs)

*The frequency of CD161 and Vα7.2 cell subsets (MAITs), among CD8+ T-cells from PBMCs are shown: total Vα7.2 (**A** & **B**), Vα7.2+CD161+ (**C** & **D**), Vα7.2-CD161+ (**E** & **F**) and Vα7.2+CD161- (**G** & **H**). Animals exposed to aerosol BCG (aeBCG) are shown in yellow (rhesus macaques, left hand side) and green (cynomolgus macaques, right hand side), and rhesus macaques exposed to aerosol Saline (aeSaline) are shown in blue. Each symbol represents a different animal and group medians are shown. Statistical comparisons between paired samples at baseline (PBa) and their post-mortem time point were made using Wilcoxon-Rank testing. Mann-Whitney U-testing was used to compare unpaired data (e.g. D2 compared to D7). Significant comparisons are marked as P < 0.05 (*) or P < 0.005 (**).*

CD56+ and CD16+ cell frequency was explored in CD3+ and CD3-CD8+ lymphocytes, to identify NKT-L and NK cells (PBMC). CD16+ CD3+ lymphocytes (NKT-L) frequency decreased at D7 compared to baseline in RM (p=0.0117), and CD56+ CD3+ lymphocyte frequency increased at D7 compared to baseline in CM (p=0.0312). Both changes in NKT-L markers were transient and only at one time point, compared to baseline. There was no change in CD16+CD56+ T-cell frequency. In humans, NK cells are defined as CD56+, with a proportion of cells also expressing CD16. In NHPs, NK cells are CD8+ and express CD56 or CD16[254]. NK cell frequency changes at D7 compared to baseline in RM (ns compared to D2, Figure 3.7). CD16+CD56- NK cell frequency decreased at D7 compared to baseline, and CD16-CD56+ NK cell frequency increased at D7 compared to baseline (p < 0.005 for both subsets). A similar pattern was seen in RM exposed to aeSaline.

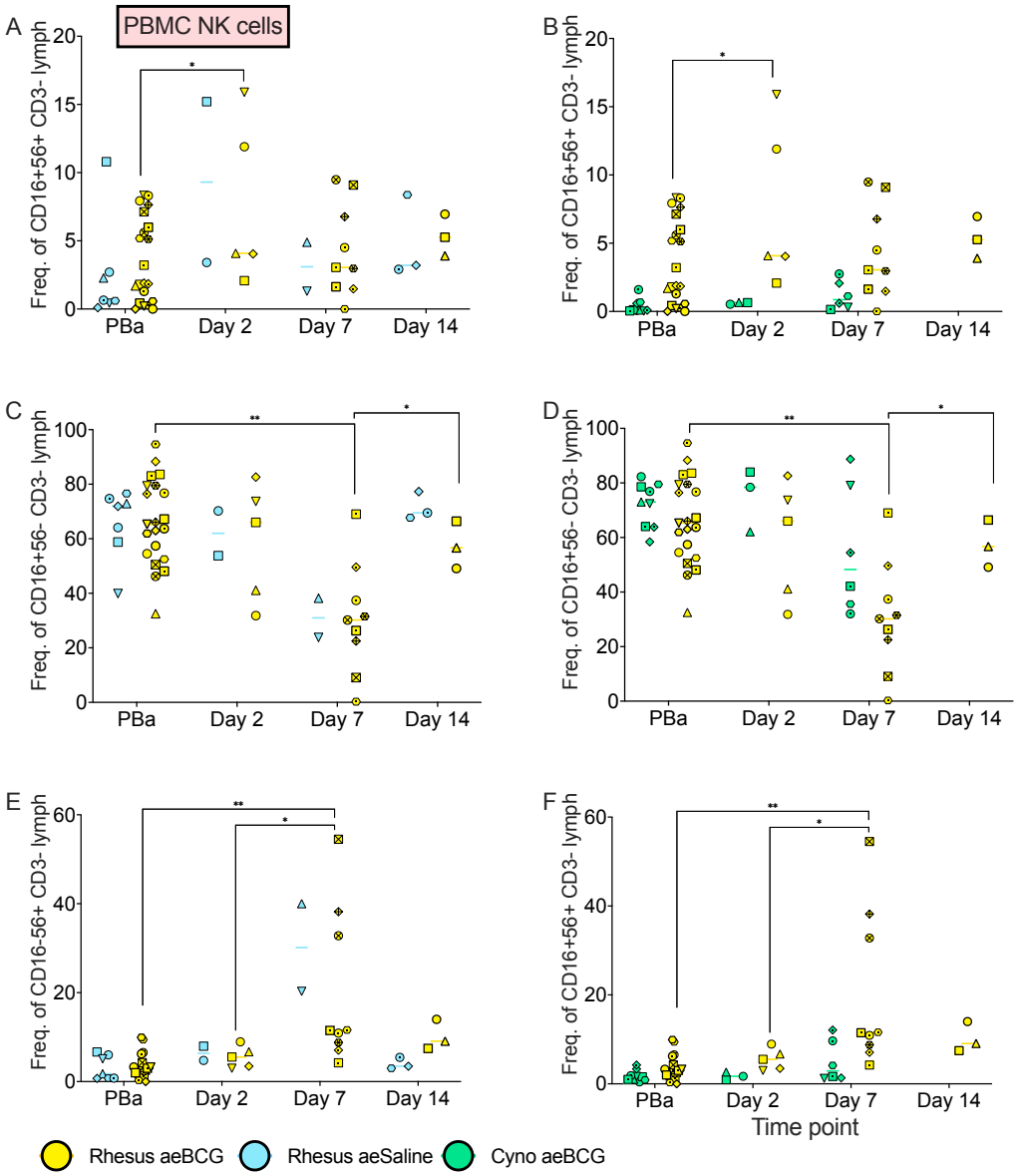

A
PBMC NK cells
Freq. of CD16+56+ CD3- lymph
B
Freq. of CD16+56+ CD3- lymph
C
Freq. of CD16+56- CD3- lymph
D
Freq. of CD16+56- CD3- lymph
E
Freq. of CD16-56+ CD3- lymph
F
Freq. of CD16+56+ CD3- lymph
PBa
Day 2
Day 7
Day 14
Time point
Rhesus aeBCG
Rhesus aeSaline
Cyno aeBCG

Figure 3.7 NK cell frequency among CD8+ T-cells characterised among peripheral blood mononuclear cells (PBMCs)

*The frequency of CD16+/CD56+ cell populations, among CD3-CD8+ T-cells from PBMCs are shown: CD16+CD56+ (**A** & **B**), CD16+CD56- (**C** & **D**), CD16-CD56+ (**E** & **F**). Animals exposed to aerosol BCG (aeBCG) are shown in yellow (rhesus macaques, left hand side) and green (cynomolgus macaques, right hand side), and rhesus macaques exposed to aerosol saline (aeSaline) are shown in blue. Each symbol represents a different animal and group medians are shown. Statistical comparisons between paired samples at baseline (PBa) and their post-mortem time point were made using Wilcoxon-Rank testing. Mann-Whitney U-testing was used to compare unpaired data (e.g. D2 compared to D7). Significant comparisons are marked as P < 0.05 (*) or P < 0.005 (**).*

In RM, CD14+CD16- and total CD14+ cell frequency decreased at D7 compared to baseline (both p = 0.0312, Figure 3.8). In contrast, total CD14+ and CD16+ non-lymphocyte frequency, and CD14+CD16- and CD14-CD16+ non-lymphocyte frequency increased at D7 compared to baseline in CM. CD14+CD16+ non-lymphocyte frequency did not increase in CM.

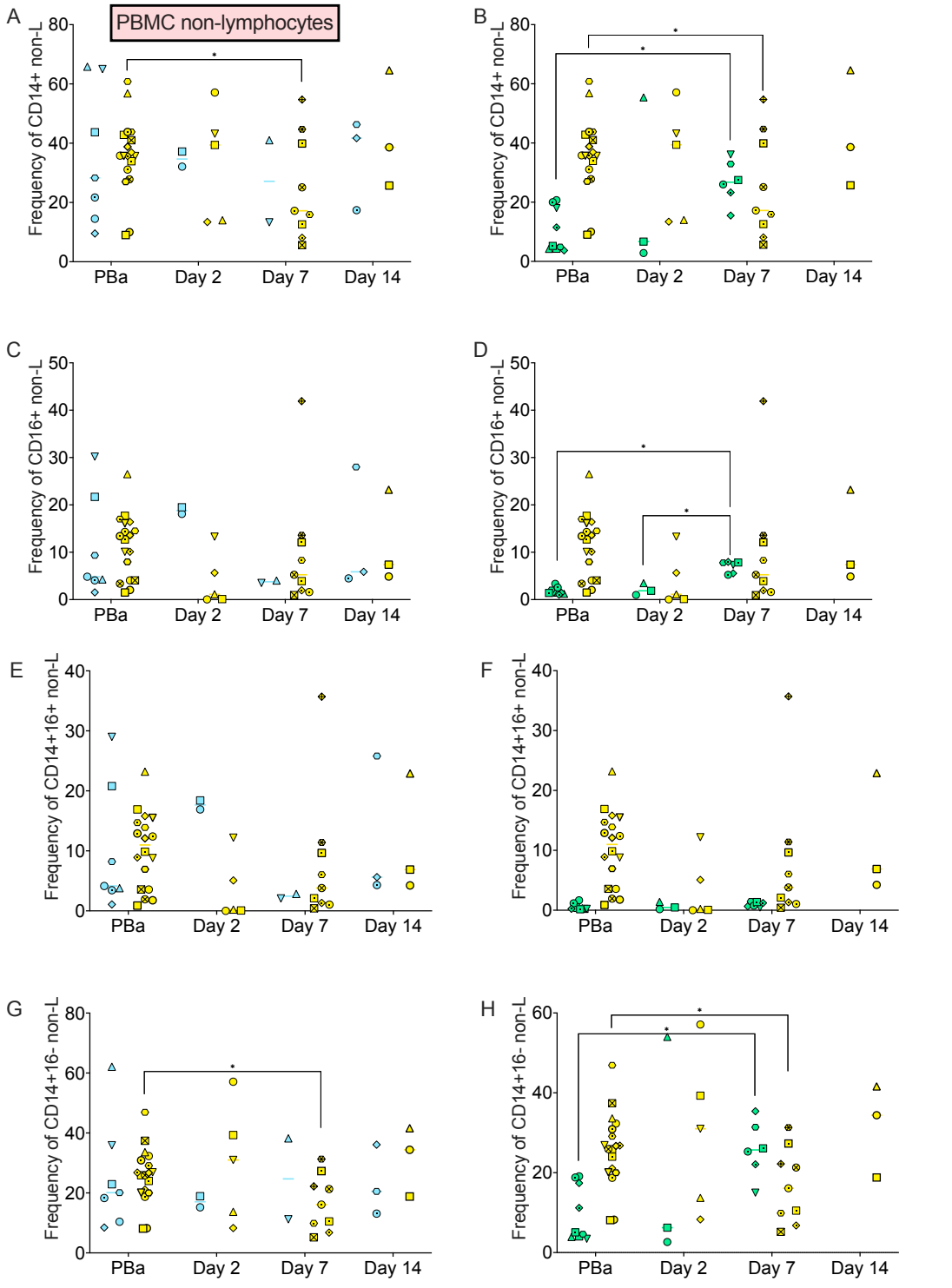


Figure 3.8 continued on next page

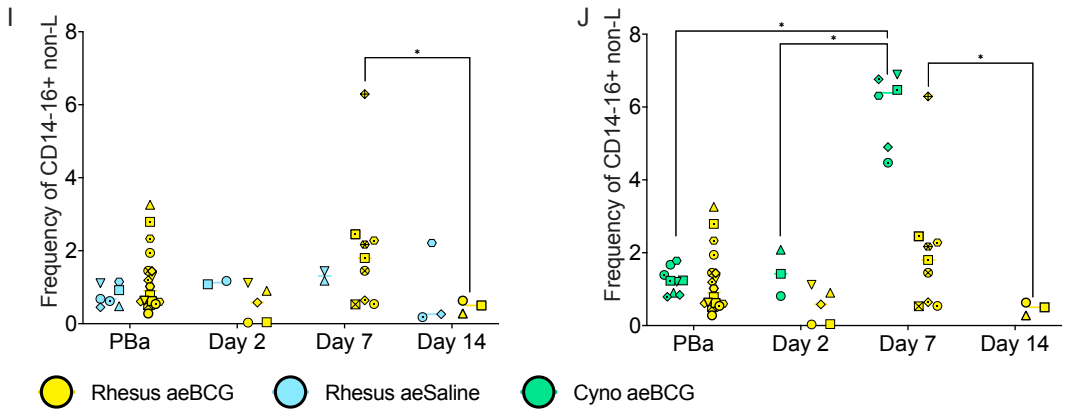


Figure 3.8 Non-lymphocyte populations characterised among PBMCs

*The frequency of CD14+/CD16+ cell populations, among CD3- human leukocyte antigen-DR (HLA-DR)+ non-lymphocyte cells from PBMCs are shown: total CD14+ (**A** & **B**), total CD16+ (**C** & **D**), CD14+CD16+ (**E** & **F**), CD14+CD16- (**G** & **H**), CD14-CD16+ (**I** & **J**). Animals exposed to aerosol BCG (aeBCG) are shown in yellow (rhesus macaques, left hand side) and green (cynomolgus macaques, right hand side), and rhesus macaques exposed to aerosol saline (aeSaline) are shown in blue. Each symbol represents a different animal and group medians are shown. Statistical comparisons between paired samples at baseline (PBa) and their post-mortem time point were made using Wilcoxon-Rank testing. Mann-Whitney U-testing was used to compare unpaired data (e.g. D2 compared to D7). Significant comparisons are marked as $P < 0.05$ (*) or $P < 0.005$ (**).*

BAL									
species	cynomolgus			rhesus					
timepoint	D0vD2	D0vD7	D2vD7	D0vD2	D0vD7	D0vD14	D2vD7	D7vD14	D2vD14
CD14-3+	ns	*	ns	*	ns	ns	ns	ns	ns
CD4+8-	ns	ns	ns	ns	ns	ns	ns	ns	ns
CD8+4-	ns	ns	ns	ns	ns	ns	ns	ns	ns
CD4+8+	ns	ns	ns	ns	ns	*	ns	ns	ns
CD4+8++	ns	ns	ns	ns	ns	ns	ns	ns	ns
CD4-8-	ns	ns	ns	ns	ns	*	ns	ns	ns
CD4+56+	ns	ns	ns	ns	*	*	ns	ns	**
gd	ns	ns	ns	ns	ns	ns	ns	ns	*
MAIT 7.2+	ns	ns	ns	*	ns	*	ns	ns	ns
MAIT 161+7.2+	ns	*	ns	*	ns	*	ns	ns	ns
MAIT 161+7.2-	ns	ns	ns	ns	ns	*	ns	ns	ns
MAIT 161-7.2+	ns	ns	ns	*	ns	ns	ns	ns	ns
NKT 16+	ns	*	ns	ns	ns	ns	ns	ns	*
NKT 56+	ns	*	ns	ns	ns	ns	ns	ns	ns
NKT 16+56+	ns	ns	ns	ns	ns	ns	ns	ns	ns
NK 16+56+	ns	*	ns	ns	ns	ns	ns	**	ns
NK 16-56+	ns	ns	ns	*	ns	ns	ns	ns	ns
NK 16+56-	ns	*	ns	ns	*	ns	ns	ns	ns
non 14+	ns	*	ns	ns	*	ns	ns	*	ns
non 16+	ns	*	*	ns	ns	ns	ns	ns	ns
non 14+16+	ns	ns	*	ns	ns	ns	ns	ns	ns
non 14+16-	ns	*	ns	*	*	ns	ns	ns	ns
non 14-16+	ns	*	*	*	ns	ns	ns	ns	ns

Table 3.2 Broncho-alveolar lavage (BAL) cell populations

The frequency of different cell populations among BAL cells from rhesus macaques were compared between groups of animals euthanised at Day 2/7/14 (D2/D7/D14). Statistical comparisons between paired samples at baseline (PBa) and their post-mortem time point were made using Wilcoxon-Rank testing. Mann-Whitney U-testing was used to compare unpaired data (e.g. D2 compared to D7). Comparisons are marked as not significant (ns), P < 0.05 (*) or P < 0.005 (**), with increases shown in yellow, and decreases in blue.

3.4.4 BAL cell populations

BAL cells were isolated, simulated and stained in parallel with PBMCs, to allow comparison across these compartments (Table 3.2). CD3+ lymphocyte frequency

increased at D7 in CM (p=0.0312) and at D2 in RM (p=0.0312), both compared to baseline. There was no change in CD4+:CD8+ T-cell ratio in the BAL (CM or RM). In RM, CD4-CD8- and CD4+CD8+ T-cell frequency increased at D14 compared to baseline. CD56+CD4+ T-cell frequency increased at D7 and D14 compared to baseline (p=0.0195, p=0.0156, respectively), and at D14 compared to D2 (p=0.0082) in RM.

$\gamma\delta$ T-cell frequency did not change compared to baseline in BAL (CM or RM). Total Vα7.2+CD8+ cell frequency increased at D2 and D14 compared to baseline, but not at D7 in RM (Figure 3.9). Vα7.2+CD161+CD8+ cell frequency also increased at D2 and D14 compared to baseline for RM (p=0.0312 and p=0.0156, respectively), and at D7 for CM compared to baseline (p=0.00312). Total CD161+CD8+ cell frequency increased at D14 compared to baseline, and Vα7.2+CD161-CD8+ cell frequency increased at D2 compared to baseline, both in RM.

CD16+ T-cell frequency in CM decreased at D7 compared to baseline (p=0.0312), and CD56+ cell frequency increased (p=0.0312). Similar patterns for NKT-L cells were seen in RM, and CD16+ T-cell frequency increased at D14 compared to D2 (p=0.0476). Due to a technical error, populations that relied on gating for CD16+ or HLA-DR were excluded for four animals at D14, leaving n=3. Among CD3-CD8+ cells, CD16+CD56+ and CD16+CD56- cell frequency (NK cells) increased at D7 compared to baseline in CM (p=0.0312 for both). CD16+CD56+ NK cell frequency also increased at D14 compared to D2 in RM, but D14 was limited to n=3. In RM, CD16-CD56+ cell frequency increased at D2 and CD16+CD56- cell frequency increased at D7.

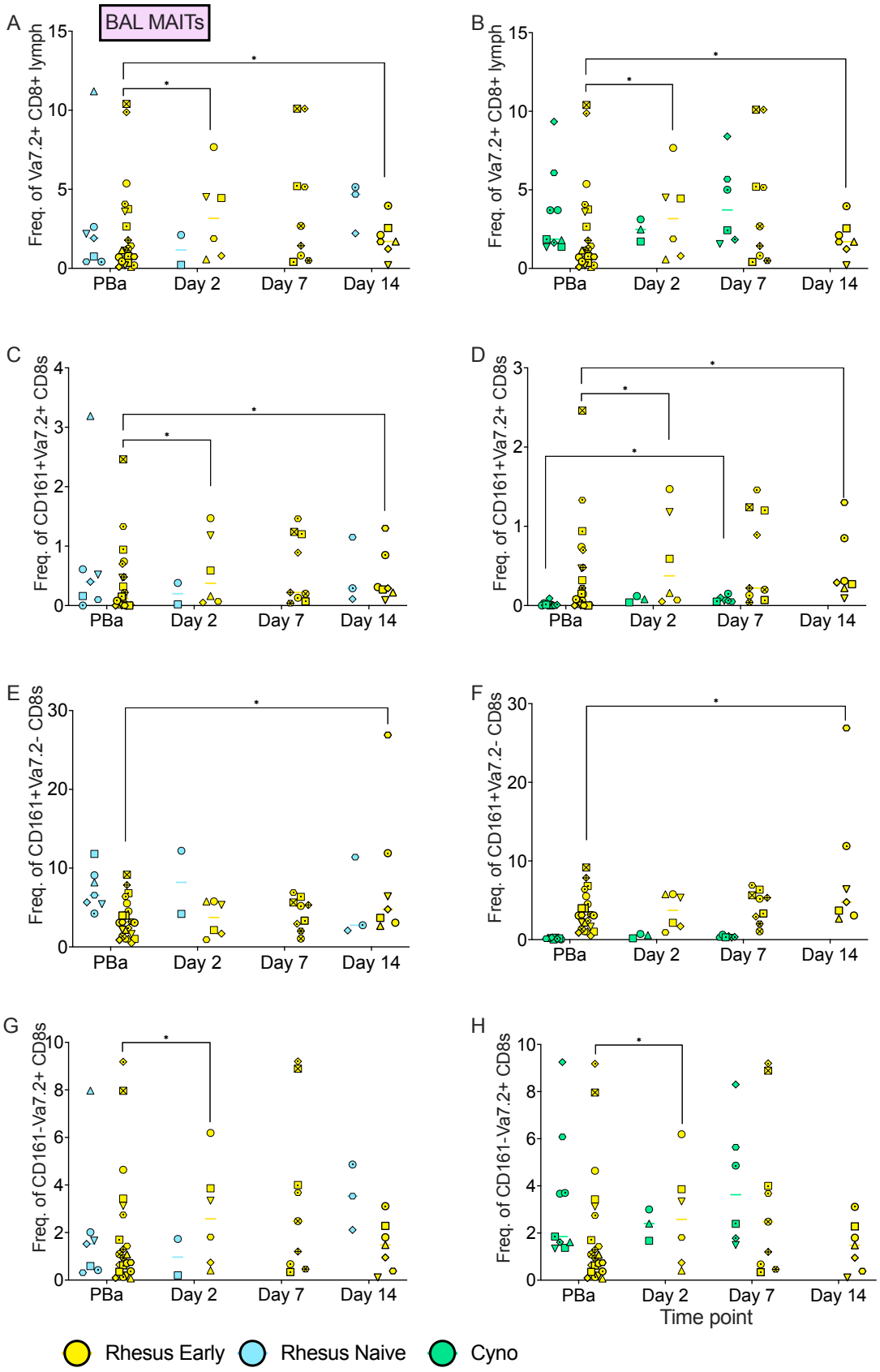

A
BAL MAITs
Freq. of Va7.2+ CD8+ lymph
B
Freq. of Va7.2+ CD8+ lymph
C
Freq. of CD161+Va7.2+ CD8s
D
Freq. of CD161+Va7.2+ CD8s
E
Freq. of CD161+Va7.2- CD8s
F
Freq. of CD161+Va7.2- CD8s
G
Freq. of CD161-Va7.2+ CD8s
H
Freq. of CD161-Va7.2+ CD8s
PBa
Day 2
Day 7
Day 14
Time point
Rhesus Early
Rhesus Naive
Cyno

Figure 3.9 Mucosal associated invariant T-cell (MAIT) frequency among CD8+ T-cells characterised among broncho-alveolar lavage (BAL) cells

*The frequency of CD161+ and Vα7.2+ cell subsets (MAITs), among CD8+ T-cells from BAL cells are shown: total Vα7.2+ (**A** & **B**), Vα7.2+CD161+ (**C** & **D**), Vα7.2-CD161+ (**E** & **F**) and Vα7.2+CD161- (**G** & **H**). Animals exposed to aerosol BCG (aeBCG) are shown in yellow (rhesus macaques, left hand side) and green (cynomolgus macaques, right hand side), and rhesus macaques exposed to aerosol saline (aeSaline) are shown in blue. Each symbol represents a different animal and group medians are shown. Statistical comparisons between paired samples at baseline (PBa) and their post-mortem time point were made using Wilcoxon-Rank testing. Mann-Whitney U-testing was used to compare unpaired data (e.g. D2 compared to D7). Significant comparisons are marked as P < 0.05 (*) or P < 0.005 (**).*

Total CD14+ non-lymphocyte cell frequency decreased at D7 compared to baseline, but was comparable to baseline at D14 in RM (Figure 3.10). In contrast, total CD14+ non-lymphocyte cell frequency increased at D7 in CM. Total CD16+ non-lymphocyte cell frequency decreased at D2, and D7 in CM compared to baseline (p=0.0238 and p=0.0312, respectively). There was no difference in total CD16+ non-lymphocyte cell frequency in RM. CD14+CD16- non-lymphocyte cell frequency increased at D2 and D7 compared to baseline in RM (both p=0.0312), and at D7 compared to baseline in CM (p=0.0312). CD14-16+ non-lymphocyte cell frequency decreased at D2 compared to baseline (RM).

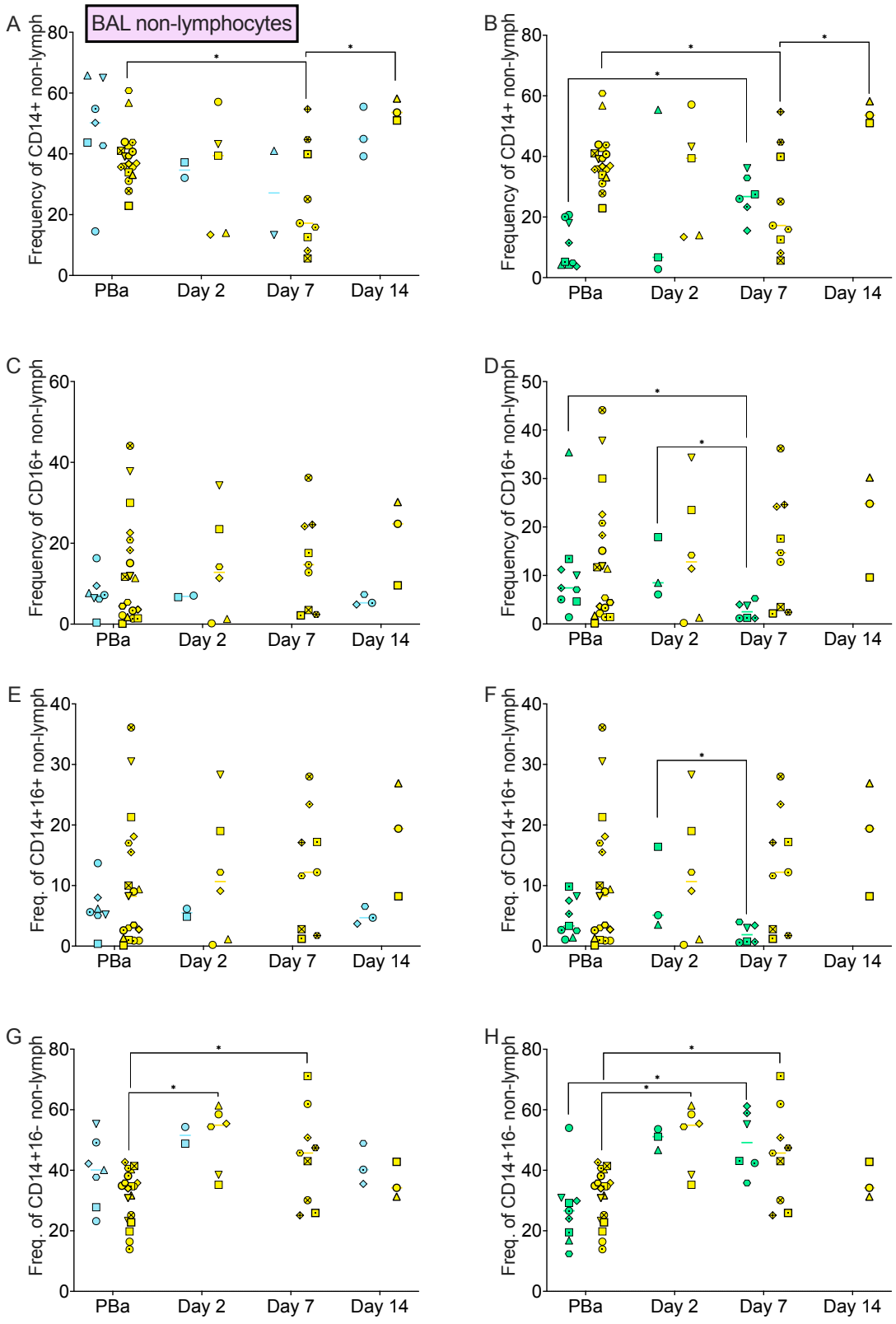


Figure 3.10 on next page

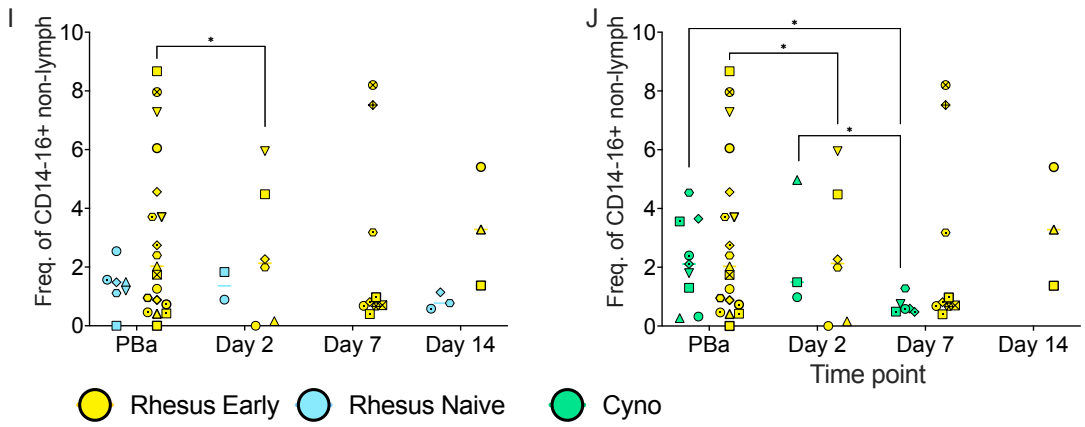


Figure 3.10 Non-lymphocyte populations characterised among broncho-alveolar lavage (BAL) cells

*The frequency of CD14+/CD16+ cell populations, among CD3- human leukocyte antigen-DR (HLA-DR)+ non-lymphocyte cells from BAL cells are shown: total CD14+ (**A** & **B**), total CD16+ (**C** & **D**), CD14+CD16+ (**E** & **F**), CD14+CD16- (**G** & **H**), CD14-CD16+ (**I** & **J**). Animals exposed to aerosol BCG (aeBCG) are shown in yellow (rhesus macaques, left hand side) and green (cynomolgus macaques, right hand side), and rhesus macaques exposed to aerosol saline (aeSaline) are shown in blue. Each symbol represents a different animal and group medians are shown. Statistical comparisons between paired samples at baseline (PBa) and their post-mortem time point were made using Wilcoxon-Rank testing. Mann-Whitney U-testing was used to compare unpaired data (e.g. D2 compared to D7). Significant comparisons are marked as P < 0.05 (*) or P < 0.005 (**).*

3.4.5 Lung cell populations

PM (post-mortem) examinations were conducted at specific time points. Lung MCs were isolated in parallel with BAL/PBMC, and were stimulated and stained with the same set of antibody markers. A proportion of the lung samples had to be excluded due to low viability, which resulted in abnormal staining patterns and forward scatter/side scatter-

area (FSC-A/SSC-A) distribution. Tissue samples can only be collected PM, so all comparisons are between groups of different animals.

Among CD4+ T-cells characterised among lung MCs, there was a significant increase in CD56+ cell frequency at D14 compared to D2 (p=0.0047) for RM (Figure 3.11). There were no further changes in NKT-L marker (CD16+ and CD56+) cell frequency. CD161+Vα7.2- cell frequency increased at D14 compared to D2 or D7 for RM (p=0.0082 and p=0.0221, respectively) and at D7 compared to D2 for CM (p=0.0476). CD14+CD16- non-lymphocyte cell frequency decreased at D14 compared to either D2 or D7 in RM (Table 3.3).

Lung				
species	cyno	rhesus		
timepoint comparison	D2 D7	D2 D7	D2 D14	D7 D14
CD14-3+ (T cell)	ns	ns	ns	ns
CD4 T cell	ns	ns	ns	ns
CD8 T cell	ns	ns	ns	ns
CD4+8+ T cell	ns	ns	ns	ns
CD4+8++ T cell	ns	ns	ns	ns
CD4-8- T cell	ns	ns	*	ns
CD56+ CD4+ T cell	ns	ns	**	ns
gamma-delta T cell	ns	ns	ns	ns
Va7.2+ CD8+ T cell	ns	ns	ns	ns
CD161+Va7.2+ CD8+ T cell	ns	ns	ns	ns
CD161+Va7.2- CD8+ T cell	*	ns	**	*
CD161-Va7.2+ T cell	ns	ns	ns	ns
CD16+ T cell (NKT-like)	ns	ns	ns	ns
CD56+ T cell (NKT-like)	ns	ns	ns	ns
CD16+CD56+ T cell (NKT-like)	ns	ns	ns	ns
CD16+56+ CD3- (NK cell)	ns	ns	ns	ns
CD16-56+ CD3- (NK)	ns	ns	ns	ns
CD16+56- CD3- (NK)	ns	ns	ns	ns
CD14+ non-lymphocyte	ns	ns	ns	ns
CD16+ non-lymphocyte	ns	ns	ns	ns
CD14+CD16+ non-lymphocyte	ns	ns	ns	ns
CD14+CD16- non-lymphocyte	ns	ns	*	*
CD14-CD16+ non-lymphocyte	ns	ns	ns	ns

Table 3.3 Lung mononuclear cell (MC) populations

The frequency of different cell populations among lung MCs from rhesus macaques were compared between groups of animals euthanised at Day 2/7/14 (D2/D7/D14). Mann-Whitney U-testing was used to statistically compare unpaired data (e.g. D2 compared to D7). Comparisons are marked as not significant (ns), P < 0.05 (*) or P < 0.005 (**), with increases shown in yellow, and decreases in blue.

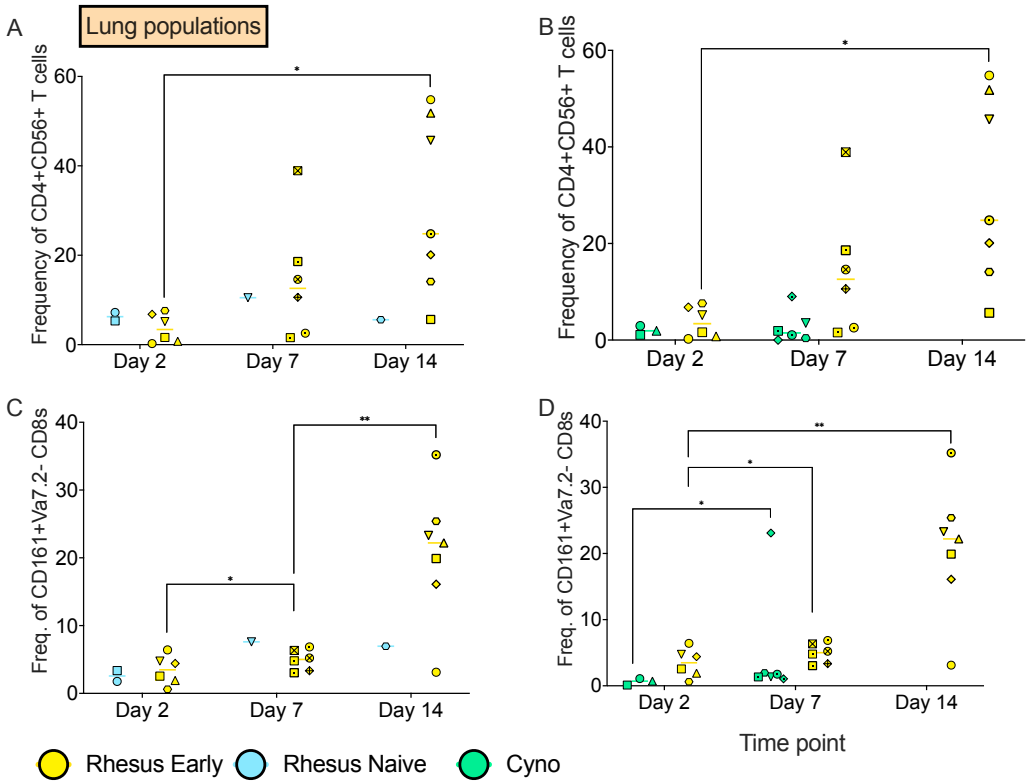


Figure 3.11 Cell populations of interest, characterised among lung mononuclear cells

*The frequency of lung mononuclear cells of interest are shown: CD4+CD56+ T-cells (**A** & **B**) and CD161+Vα7.2- CD8+ T-cells (**C** & **D**). Animals exposed to aerosol BCG (aeBCG) are shown in yellow (rhesus macaques, left hand side) and green (cynomolgus macaques, right hand side), and rhesus macaques exposed to aerosol saline (aeSaline) are shown in blue. Each symbol represents a different animal and group medians are shown. Mann-Whitney U-testing was used to statistically compare unpaired data (e.g. D2 compared to D7).*

Lymph nodes	Hilar				Axillary			
species	cyno	rhesus			cyno	rhesus		
time point comparison	D2	D2	D2	D7	D2	D2	D2	D7
	D7	D7	D14	D14	D7	D7	D14	D14
CD14-3+ (T cell)	ns	ns	ns	ns	ns	ns	ns	ns
CD4 T cell	ns	ns	ns	ns	ns	ns	ns	ns
CD8 T cell	ns	ns	ns	ns	ns	ns	ns	ns
CD4+8+ T cell	ns	ns	ns	ns	ns	ns	ns	ns
CD4+8++ T cell	ns	ns	**	**	ns	ns	*	*
CD4-8- T cell	ns	ns	ns	ns	ns	ns	ns	ns
CD56+ CD4+ T cell	ns	*	**	**	ns	*	**	ns
gamma-delta T cell	ns	ns	*	ns	ns	ns	ns	ns
Va7.2+ CD8+ T cell	ns	ns	ns	ns	ns	ns	ns	ns
CD161+Va7.2+ CD8+ T cell	ns	ns	ns	ns	ns	ns	ns	**
CD161+Va7.2- CD8+ T cell	ns	ns	**	**	ns	ns	**	**
CD161-Va7.2+ T cell	ns	ns	ns	ns	ns	ns	ns	ns
CD16+ T cell (NKT-like)	ns	ns	ns	ns	ns	ns	ns	ns
CD56+ T cell (NKT-like)	ns	**	**	ns	ns	**	*	ns
CD16+CD56+ T cell (NKT-like)	ns	*	ns	*	ns	**	*	ns
CD16+56+ CD3- (NK cell)	ns	ns	ns	ns	ns	ns	ns	ns
CD16-56+ CD3- (NK)	ns	ns	ns	ns	ns	ns	ns	ns
CD16+56- CD3- (NK)	ns	ns	ns	ns	ns	ns	ns	ns
CD14+ non-lymphocyte	ns	*	*	ns	ns	ns	ns	ns
CD16+ non-lymphocyte	ns	*	*	ns	ns	ns	ns	ns
CD14+CD16+ non-lymphocyte	ns	ns	*	*	ns	ns	ns	ns
CD14+CD16- non-lymphocyte	ns	*	ns	ns	ns	ns	ns	ns
CD14-CD16+ non-lymphocyte	ns	*	ns	ns	ns	**	*	ns

Table 3.4 Lymph node mononuclear cell (MC) populations

The frequency of different cell populations among lung MCs from rhesus macaques were compared between groups of animals euthanised at Day 2/7/14 (D2/D7/D14). Mann-Whitney U-testing was used to statistically compare unpaired data (e.g. D2 compared to D7). Comparisons are marked as not significant (ns), P < 0.05 (*) or P < 0.005 (**), with increases shown in yellow, and decreases in blue.

3.4.6 LN cell populations

MCs were also isolated from axillary and hilar LNs at PM time points. Axillary LNs drain lymph vessels from the upper region of the chest and hilar LNs are located at the point where the bronchus joins the lungs. Both LNs were explored to determine whether there was a difference between the more local hilar LNs and the more lateral draining axillary LNs.

Among MCs characterised among LNs, CD4+:CD8+ T-cell ratio, and CD4+/CD8+ T-cell frequencies remained the same (Table 3.4). CD4+CD8++ T-cell frequency increased at D14 compared to D2 (p=0.0076 hilar & p=0.0276 axillary) and D7 in RM (p=0.0087 hilar & p=0.0260 axillary). CD4+CD8++ cells represented up to 1.5% of the total CD3+ lymphocyte population. CD56+CD4+ T-cell frequency increased at D7 compared to D2 in the hilar LNs, and at D14 compared to D2/D7 (RM only). A similar trend was observed for axillary LNs (not significant – Figure 3.12). γδ+ T-cell frequency increased at D14 compared to D2 in hilar LNs of RM (p=0.0152), and there was a small increase at D7 compared to D2 (not significant). CD161+Vα7.2-CD8+ T-cell frequency increased at D14 compared to D2 (p=0.0022 hilar & p=0.0022 axillary) and D7 (p=0.0014 hilar & p=0.0028 axillary) in RM. CD161+Vα7.2+CD8+ T-cell frequency increased at D14 compared to D7 in axillary LNs (RM).

Compared to D2, CD56+CD16- T-cell frequency increased at D7 (p=0.0076 hilar and p=0.0176 axillary, respectively) and D14 in LNs of RM (p=0.0022 hilar and p=0.0022 axillary, respectively – Figure 3.13). In RM, CD16+CD56+ T-cell frequency increased at D7 compared to D2 in hilar and axillary LNs (p=0.0224 and p=0.0018, respectively), and at D14 compared to D7 in axillary LNs alone (p=0.0238). Although a similar pattern was

observed for CD16+CD56- T-cell frequency, use of CD16+ to identify cell populations at D14 was limited to n=3 at D14, as described previously. There were no clear patterns for these NKT-L markers in CM, or when these markers were explored in CD3-CD8+ lymphocytes (NK cells).

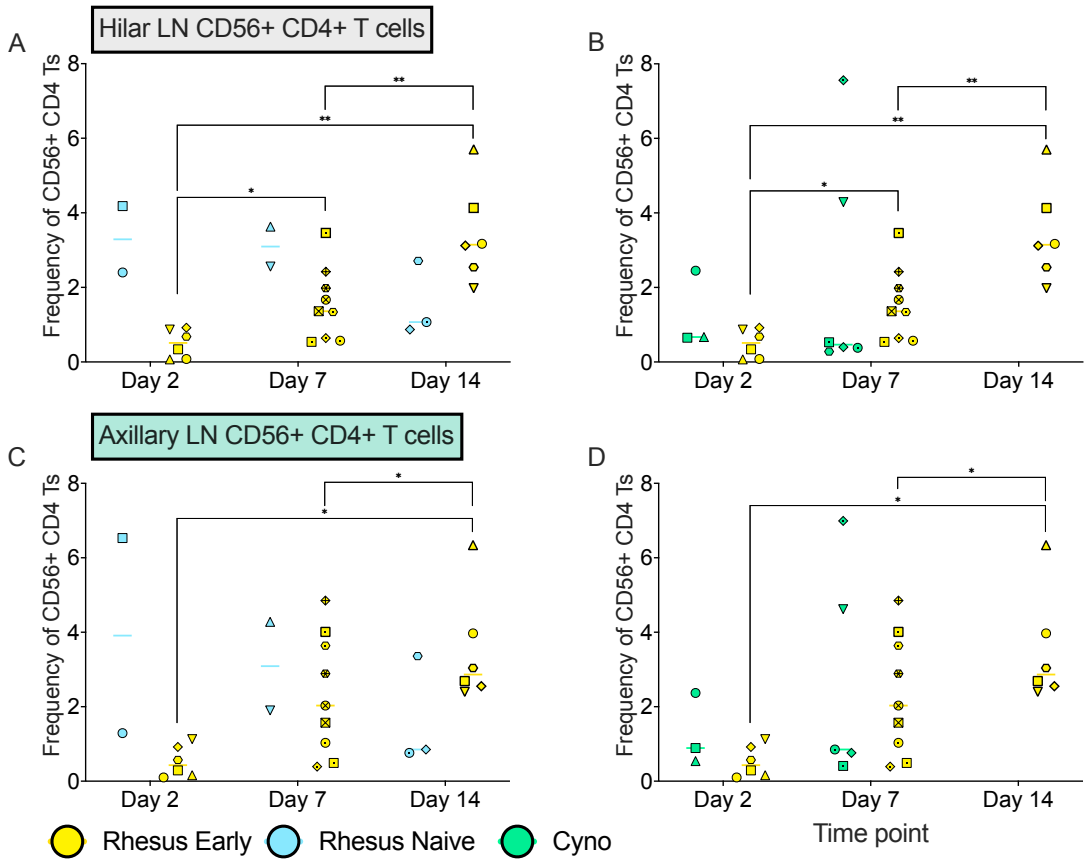


Figure 3.12 CD56+CD4+ T-cells, characterised among lymph node mononuclear cells

*The frequency of CD56+CD4+ T-cells identified among mononuclear cells characterised among hilar (**A** & **B**) and axillary (**C** & **D**) lymph nodes are shown. Animals exposed to aerosol BCG (aeBCG) are shown in yellow (rhesus macaques, left hand side) and green (cynomolgus macaques, right hand side), and rhesus macaques exposed to aerosol saline (aeSaline) are shown in blue. Each symbol represents a different animal and group medians are shown. Mann-Whitney U-testing was used to statistically compare unpaired data (e.g. D2 compared to D7).*

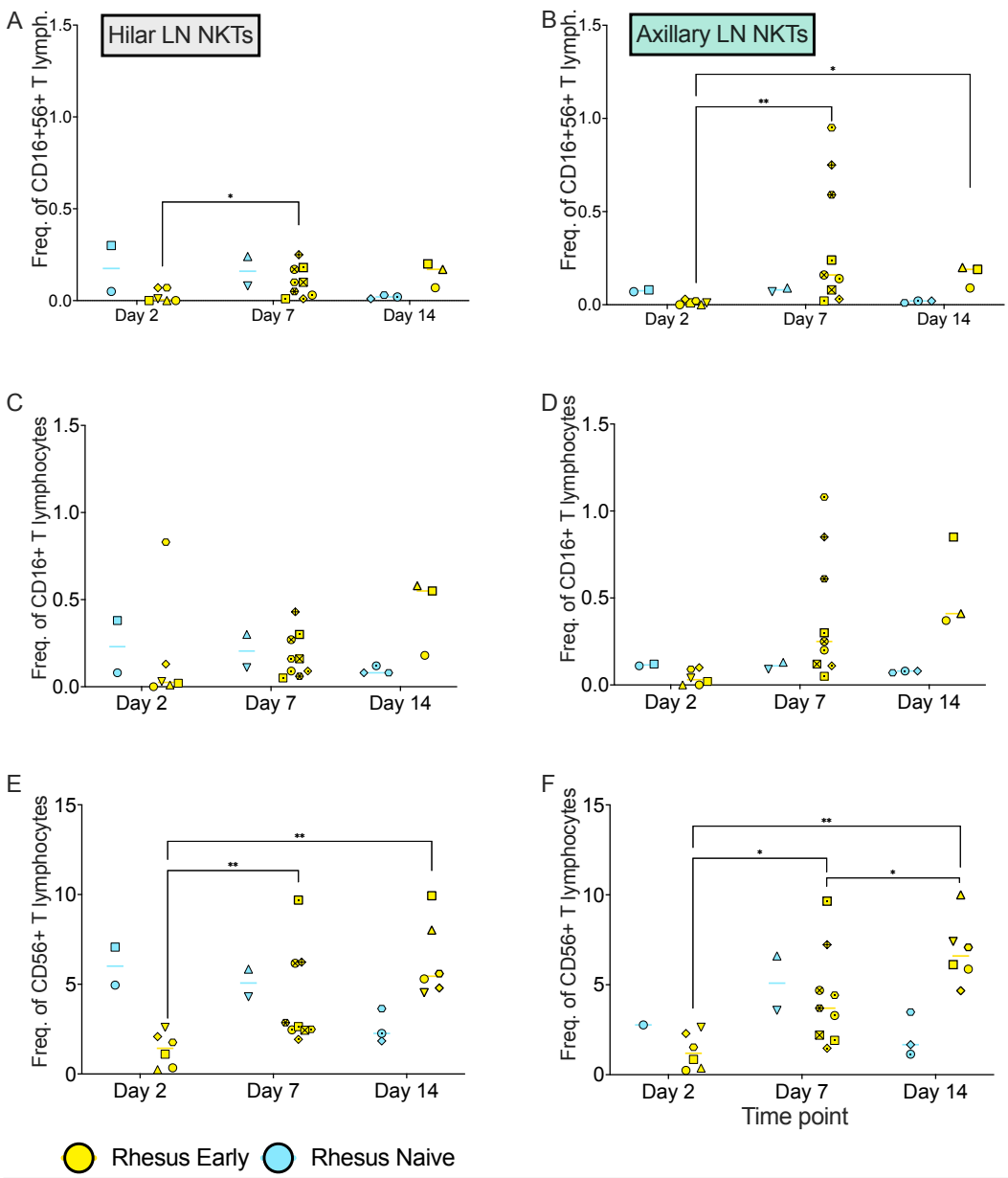


Figure 3.13 NKT-like cells, characterised among lymph node mononuclear cells

*The frequency of CD16+ and CD56+ T-cells subsets identified among mononuclear cells characterised among hilar (left hand side) and axillary (right hand side) lymph nodes are shown: CD16+CD56+ (**A** & **B**), CD16+ (**C** & **D**) and CD56+ (**E** & **F**). Rhesus macaques exposed to aerosol BCG (aeBCG) are shown in yellow and rhesus macaques exposed to aerosol saline (aeSaline) are shown in blue. Each symbol represents a different animal and group medians are shown. Mann-Whitney U-testing was used to statistically compare unpaired data (e.g. D2 compared to D7).*

CD14+ non-lymphocyte frequency increased at D7 compared to D2 (p=0.0496), and D14 compared to D2 (p=0.0238) among hilar LN MCs. The same pattern was observed for CD16+ non-lymphocyte cells (p=0.0265 D7 vs D2, p=0.0238 D14 vs D2). CD14+CD16+ non-lymphocyte cell frequency increased at D14 compared to D2 and D7 (p=0.0238, p=0.0364, respectively), whereas CD14+CD16- and CD14-16+ non-lymphocyte cell frequency increased at D7 compared to D2 (p=0.0468, p=0.0360, respectively). Two animals had high CD14+CD16- and CD14-CD16+ non-lymphocyte cell frequency at D7, and changes were no longer significant if these animals were excluded. There were no changes in the non-lymphocyte population frequencies of CM.

3.4.7 WB cell populations

A previously published method for WBICS[255] was used and compared to PBMC results, because granulocytes are excluded from PBMCs (Table 3.5).

WBICS						
species	**cynomolgus**			**rhesus**		
time point comparison	PBa D2	PBa D7	D2 D7	PBa D2	PBa D7	D2 D7
CD14-3+ (T cell)	ns	*	ns	ns	ns	ns
CD4 T cell	ns	*	ns	*	**	ns
CD8 T cell	ns	ns	ns	*	**	ns
CD16+ T cell (NKT-like)	ns	ns	ns	*	**	ns
CD56+ T cell (NKT-like)	ns	ns	ns	*	ns	ns
CD16+CD56+ T cell (NKT-like)	ns	ns	ns	ns	ns	ns
CD16+56+ CD3- (NK cell)	ns	ns	ns	*	ns	ns
CD16-56+ CD3- (NK)	ns	ns	ns	ns	*	ns
CD16+56- CD3- (NK)	ns	ns	ns	*	**	ns
CD14+ non-lymphocyte	ns	ns	ns	*	ns	ns
CD16+ non-lymphocyte	ns	*	ns	*	*	ns
CD14+CD16+ non-lymphocyte	ns	ns	ns	*	ns	ns
CD14+CD16- non-lymphocyte	ns	ns	ns	*	ns	*
CD14-CD16+ non-lymphocyte	ns	ns	ns	*	ns	ns
CD14-20+ (B cell)	ns	*	ns	*	ns	ns

Table 3.5 Whole blood (WB) cell populations

The frequency of different cell populations in WB from rhesus macaques were compared between groups of animals euthanised at Day 2/7/14 (D2/D7/D14). Statistical comparisons between paired samples at baseline (PBa) and their post-mortem time point were made using Wilcoxon-Rank testing. Mann-Whitney U-testing was used to compare unpaired data (e.g. D2 compared to D7). Comparisons are marked as not significant (ns), P < 0.05 (*) or P < 0.005 (**), with increases shown in yellow, and decreases in blue.

Upon thawing and staining, 6266 study samples (animals exposed to aeSaline) showed abnormal staining patterns and FSC-A/SSC-A compared to other WB samples evaluated at the same time, consistent with dead cells (see gating examples in chapter 2). Therefore, 6266 samples were excluded. WB samples from study 6282 were not available at the time of batch WB thawing, staining and analysis. Three baseline samples from study 6282 (e.g. before aeSaline) were included in analysis and were comparable to other baseline samples, but for simplicity, these are not shown in graphs.

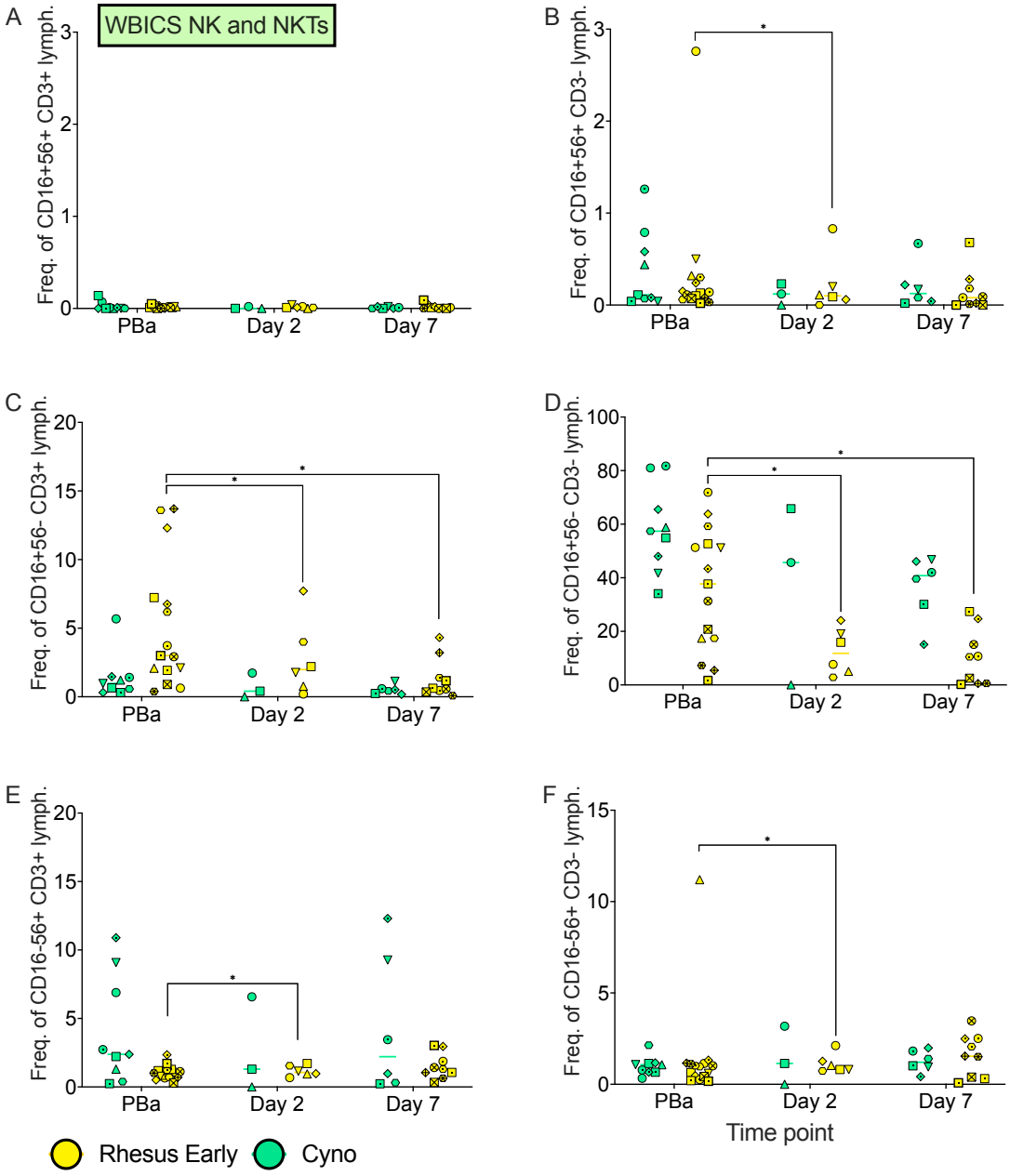
CD3+ lymphocyte frequency increased at D7 compared to baseline in CM (p=0.0312), but not in RM. The increase in CD3+ lymphocytes observed here is comparable to the increase in the same population seen in RM and CM in BAL, but opposite to the decrease in CD3+ lymphocytes seen in RM PBMCs. In RM WB, the CD4+:CD8+ T-cell increases (similar to PBMCs), due to increase CD4+ T-cell frequency and decreased CD8+ T-cell frequency at D2 and D7 (p=0.0312 and p=0.0390, respectively). The CD4+:CD8+ T-cell ratio in RM increased from a median of 1.07 at D0 to 1.72 at D2, and 1.53 at D0 to 2.43 at D7. The same pattern was detected in CM: increased CD4+ T-cell frequency at D2 (p=0.0312), and a ratio change of 1.15 at D0 to 1.33 at D2 and 1.56

at D0 to 1.63 at D7. B-cell frequency increased at D7 in CM, and at D2 in RM (both *p*=0.0312).

In RM, CD16+CD56- CD3+ lymphocyte (NKT-L) frequency decreased at D2 and D7 compared to baseline (*p*=0.0312 and *p*=0.0039, respectively – Figure 3.14). Among CD3-CD8+ lymphocytes (NK), CD16+CD56- frequency also decreased at D2 and D7 in RM (*p*=0.0312 and *p*=0.0312, respectively). CD16+CD56+ NK cell frequency also decreased at D2 compared to baseline (RM). CD16-CD16-CD56+ NKT-L cell frequency increased at D2 compared to baseline (*p*=0.0312) and CD16-CD56+ NK cell frequency increased at D7 compared to baseline (*p*=0.0195, RM). Total CD16+ cell frequency decreased among non-lymphocyte cells at D7 compared to baseline, in RM and CM (*p*=0.0117, *p*=0.0312, respectively). CD14-CD16+ non-lymphocyte cell frequency increased at D2 compared to baseline (*p*=0.0312), which means that total CD16+ non-lymphocyte cell frequency did not determine the changes for all subsets.

Figure 3.14 NK and NKT-like (NKT-L) cell frequency among lymphocytes characterised among whole blood (WB) samples (below)

*The frequency of CD16+ and CD56+ cell subsets, among CD3+ (NKT-L) and CD3-CD8+ (NK) lymphocytes from WB are shown: CD16+CD56+ (**A** & **B**), CD16+CD56- (**C** & **D**) and CD16-56+ (**E** & **F**). Animals exposed to aerosol BCG (aeBCG) are shown in yellow (rhesus macaques, left hand side) and green (cynomolgus macaques, right hand side), and rhesus macaques exposed to aerosol saline (aeSaline) are shown in blue. Each symbol represents a different animal and group medians are shown. Statistical comparisons between paired samples at baseline (PBa) and their post-mortem time point were made using Wilcoxon-Rank testing. Mann-Whitney U-testing was used to compare unpaired data (e.g. D2 compared to D7). Significant comparisons are marked as P < 0.05 (*) or P < 0.005 (**).*



3.4.8 CD161 expression among lymphocytes

To further explore the changes in CD161 expression on CD8+ T-cells, I developed a second, modified gating strategy (Supplementary Figure 1). This strategy eliminated the 'lymphocyte' gate based on size and granularity (FSC-A/SSC-A), to avoid uncessarily excluding cells at this stage. CD161 expression was analysed among the following cell

populations: CD4+, CD8+ and γδ T-cells, NKT-L and NK cells. Increased CD161 expression is summarised in Table 3.6 for PBMC (A), BAL cells (B), lung MCs (C) and LN MCs (D).

A) PBMC CD161 expression									
species	**cynomolgus**			**rhesus**					
time point comparison	PBa D2	PBa D7	D2 D7	PBa D2	PBa D7	PBa D14	D2 D7	D2 D14	D7 D14
CD14- cell	ns	ns	ns	*	ns	*	*	**	ns
CD4+ T cell	ns	*	ns	ns	*	*	ns	**	**
CD8+ T cell	ns	ns	ns	*	*	*	ns	**	*
gamma-delta T cell	ns	ns	ns	ns	ns	*	ns	***	**
CD16+ T cell (NKT-like)	ns	ns	*	*	ns	*	ns	ns	ns
CD56+ T cell (NKT-like)	ns	ns	ns	ns	ns	*	ns	***	**
CD16-56+ CD3- (NK)	ns	ns	ns	*	ns	*	ns	ns	ns
CD16+56- CD3- (NK)	ns	ns	ns	*	ns	*	*	***	ns

B) BAL CD161 expression									
species	**cynomolgus**			**rhesus**					
time point comparison	PBa D2	PBa D7	D2 D7	PBa D2	PBa D7	PBa D14	D2 D7	D2 D14	D7 D14
CD14- cell	ns	*	ns	*	ns	*	ns	ns	ns
CD4+ T cell	ns	*	ns	*	ns	*	ns	ns	ns
CD8+ T cell	ns	*	ns	*	ns	*	ns	*	*
gamma-delta T cell	ns	*	ns	*	ns	*	ns	***	**
CD16+ T cell (NKT-like)	ns	*	*	ns	ns	ns	ns	ns	ns
CD56+ T cell (NKT-like)	ns	*	ns	*	ns	*	ns	***	**
CD16-56+ CD3- (NK)	ns	*	ns	ns	ns	*	ns	ns	ns
CD16+56- CD3- (NK)	ns	*	ns	ns	ns	*	ns	ns	ns

C) Lung CD161 expression				
species	**cyno**	**rhesus**		
time point comparison	D2 D7	D2 D7	D2 D14	D7 D14
CD14- cell	ns	ns	ns	ns
CD4+ T cell	ns	ns	*	ns
CD8+ T cell	ns	ns	*	*
gamma-delta T cell	ns	ns	*	*
CD16+ T cell (NKT-like)	ns	ns	*	*
CD56+ T cell (NKT-like)	ns	ns	ns	ns
CD16-56+ CD3- (NK)	ns	ns	ns	ns
CD16+56- CD3- (NK)	ns	ns	ns	ns

D) Lymph nodes	Hilar				Axillary			
species	cyno	rhesus			cyno	rhesus		
time point comparison	D2	D2	D2	D7	D2	D2	D2	D7
	D7	D7	D14	D14	D7	D7	D14	D14
CD14- cell	ns	ns	**	***	ns	ns	**	***
CD4+ T cell	ns	ns	**	*	ns	ns	**	***
CD8+ T cell	ns	ns	**	***	ns	ns	*	ns
gamma-delta T cell	ns	ns	**	***	*	ns	**	***
CD16+ T cell (NKT-like)	*	ns	ns	ns	ns	ns	**	*
CD56+ T cell (NKT-like)	ns	ns	*	***	ns	ns	ns	**
CD16-56+ CD3- (NK)	ns	ns	ns	ns	ns	ns	**	***
CD16+56- CD3- (NK)	ns	ns	*	*	ns	ns	ns	**

Table 3.6 CD161 expression across tissue compartments

CD161 expression on different lymphocyte populations were compared between groups of animals euthanised at Day 2/7/14 (D2/D7/D14). Statistical comparisons between paired samples at baseline (PBa) and their post-mortem time point were made using Wilcoxon-Rank testing. Mann-Whitney U-testing was used to compare unpaired data (e.g. D2 compared to D7). Comparisons are marked as not significant (ns), P < 0.05 (*) or P < 0.005 (**), with increases shown in yellow, and decreases in blue.

The increase in CD161 expression is least clear in the lungs (Table 3.6C). The sample size for lung MCs was limited after exclusion of samples (previously described). The increase in CD161 expression is more pronounced in BAL, than PBMC. In RM, increased CD161 expression was observed as early as D2 compared to baseline (PBMCs and BAL). Within these early time points, the most striking increase in CD161 expression is at D14 after aeBCG (note that n=6 at D2, n=9 at D7 and n=7 at D14). Figure 3.15 shows the changes in CD161 expression for BAL cells, with animals exposed to aeSaline shown in Figure 3.15B as an example of how CD161 expression remained consistent control samples. Other graphs show RM and CM exposed to aeBCG only (to conserve space).

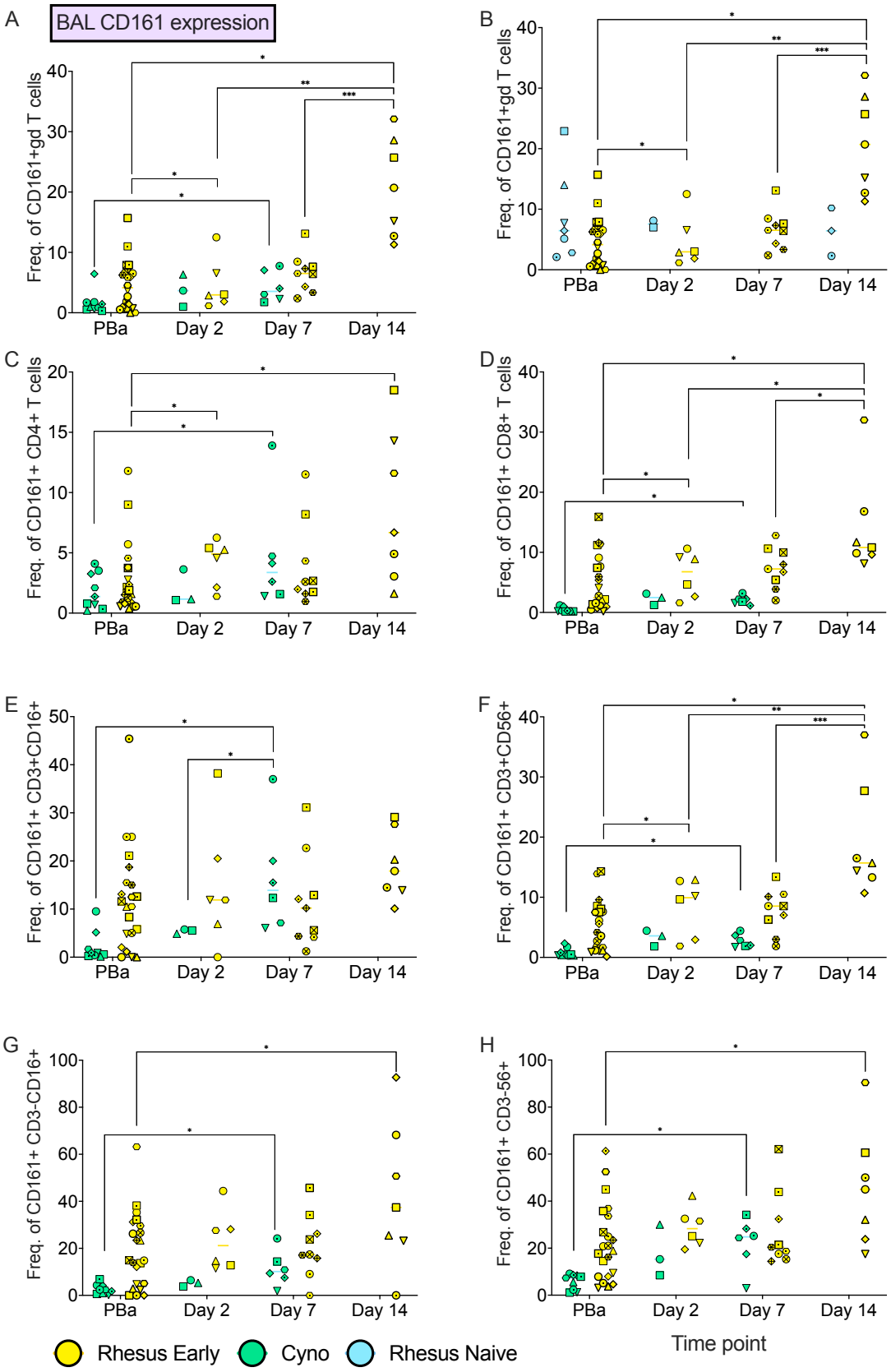

A
BAL CD161 expression
Freq. of CD161+gd T cells
B
Freq. of CD161+gd T cells
C
Freq. of CD161+ CD4+ T cells
D
Freq. of CD161+ CD8+ T cells
E
Freq. of CD161+ CD3+CD16+
F
Freq. of CD161+ CD3+CD56+
G
Freq. of CD161+ CD3-CD16+
H
Freq. of CD161+ CD3-56+
PBa
Day 2
Day 7
Day 14
Time point
Rhesus Early
Cyno
Rhesus Naive

Figure 3.15 CD161 expression among lymphocytes characterised among broncho-alveolar lavage (BAL) cells

*CD161 expression on γδ T-cells (**A** & **B**), CD4+ and CD8+ T-cells (**C** & **D**), CD3+ CD16+ and CD56+ NKT (**E** & **F**), CD3-CD8+ CD16+ and CD56+ NK (**G** & **H**). Animals exposed to aerosol BCG (aeBCG) are shown in yellow (rhesus macaques, left hand side) and green (cynomolgus macaques, right hand side), and rhesus macaques exposed to aerosol saline (aeSaline) are shown in blue (**B**). Each symbol represents a different animal and group medians are shown. Statistical comparisons between paired samples at baseline (PBa) and their post-mortem time point were made using Wilcoxon-Rank testing. Mann-Whitney U-testing was used to compare unpaired data (e.g. D2 compared to D7). Significant comparisons are marked as P < 0.05 (*) or P < 0.005 (**).*

3.4.9 HLA-DR expression among lymphocytes

HLA-DR is up-regulated on activated T-cells, and therefore can be used to measure activation status within different cell populations[80] (Table 3.7). No changes were detected for CM in any tissue compartment, except for an increased HLA-DR expression on B-cells detected at D7 compared to D0 in WB (*p*=0.0312).

Among RM PBMCs, the HLA-DR expression increased at D14 compared to D7 among CD8+ T-cells and CD161+ CD8+ T-cells, and at D14 compared to D2 in Vα7.2+ CD8+ T-cells (MAIT subset) and in CD16+CD56+ NKT-L cells (Figure 3.16). There were no significant differences between D14 and baseline, but D14 samples were limited to n=3. The increase in HLA-DR expression on CD16+CD56+ NKT-L cells from D2 to D7/D14 is due to a decreased expression at D2 compared to baseline, rather than to a change at D7/D14 compared to baseline. HLA-DR expression among Vα7.2+ CD8+ T-cells also increased at D7 compared to baseline (*p*=0.0078, Figure 3.16C/D).

A) PBMC HLA-DR expression									
species	cynomolgus			rhesus					
time point comparison	PBa D2	PBa D7	D2 D7	PBa D2	PBa D7	PBa D14	D2 D7	D2 D14	D7 D14
CD4+ T cell	ns	ns	ns	ns	ns	ns	ns	ns	ns
CD8+ T cell	ns	ns	ns	ns	ns	ns	ns	ns	*
gamma-delta T cell	ns	ns	ns	ns	ns	ns	ns	ns	ns
Va7.2+ CD8+ T cell	ns	ns	ns	ns	**	ns	ns	*	*
CD16+ T cell (NKT-like)	ns	ns	ns	*	ns	x	*	x	x
CD56+ T cell (NKT-like)	ns	ns	ns	ns	ns	x	ns	x	x
CD16+CD56+ T (NKT-like)	ns	ns	ns	*	ns	x	**	x	x

B) BAL HLA-DR expression									
species	cynomolgus			rhesus					
time point comparison	PBa D2	PBa D7	D2 D7	PBa D2	PBa D7	PBa D14	D2 D7	D2 D14	D7 D14
CD4+ T cell	ns	ns	ns	*	*	ns	ns	*	**
CD8+ T cell	ns	ns	ns	*	*	ns	ns	*	**
gamma-delta T cell	ns	ns	ns	*	ns	ns	*	*	*
Va7.2+ CD8+ T cell	ns	ns	ns	ns	**	ns	ns	*	*
CD16+ T cell (NKT-like)	ns	ns	ns	*	ns	x	ns	ns	*
CD56+ T cell (NKT-like)	ns	ns	ns	*	*	x	ns	*	**
CD16+CD56+ T (NKT-like)	ns	ns	ns	*	ns	x	*	*	**

C) Tissues	Lung		Hilar lymph nodes				Axillary lymph nodes			
species	cyno	rhesus	cyno	rhesus			cyno	rhesus		
time point comparison	D2 D7	D2 D7	D2 D7	D2 D7	D2 D14	D7 D14	D2 D7	D2 D7	D2 D14	D7 D14
CD4+ T cell	ns	ns	ns	ns	*	*	ns	ns	ns	*
CD8+ T cell	ns	ns	ns	ns	*	**	ns	ns	*	*
gamma-delta T cell	ns	ns	ns	ns	*	ns	ns	ns	*	ns
Va7.2+ CD8+ T cell	ns	ns	ns	ns	*	**	ns	ns	ns	ns
CD16+ T cell (NKT-like)	ns	ns	ns	ns	ns	ns	ns	ns	ns	ns
CD56+ T cell (NKT-like)	ns	ns	ns	ns	*	*	ns	ns	ns	ns
CD16+CD56+ T (NKT-like)	ns	ns	ns	*	ns	ns	ns	ns	ns	ns

D) WBICS HLA-DR expression						
species	cynomolgus			rhesus		
time point comparison	PBa D2	PBa D7	D2 D7	PBa D2	PBa D7	D2 D7
CD4+ T cell	ns	ns	ns	*	**	ns
CD8+ T cell	ns	ns	ns	*	**	ns
gamma-delta T cell	ns	ns	ns	*	**	ns
Va7.2+ CD8+ T cell	ns	ns	ns	ns	ns	ns
CD16+ T cell (NKT-like)	ns	ns	ns	ns	ns	ns
CD56+ T cell (NKT-like)	ns	ns	ns	*	**	ns
CD16+CD56+ T (NKT-like)	ns	ns	ns	ns	ns	ns
CD20	ns	*	ns	ns	ns	ns

Table 3.7 Human leukocyte antigen-DR (HLA-DR) expression across tissue compartments

*Peripheral blood mononuclear cells (PBMCs - **A**), broncho-alveolar lavage (BAL - **B**), lung (**C**), hilar and axillary lymph nodes (**D**) were stained using a 14-colour antibody panel, after overnight stimulation with co-stimulatory antibody only. HLA-DR expression was examined on different lymphocyte populations. Groups of animals euthanised at Day 2/7/14 (D2/D7/D14). Statistical comparisons between paired samples at baseline (PBa) and their post-mortem time point were made using Wilcoxon-Rank testing. Mann-Whitney U-testing was used to compare unpaired data (e.g. D2 compared to D7). Comparisons are marked as not significant (ns), P < 0.05 (*) or P < 0.005 (**), with increases shown in yellow, and decreases in blue.*

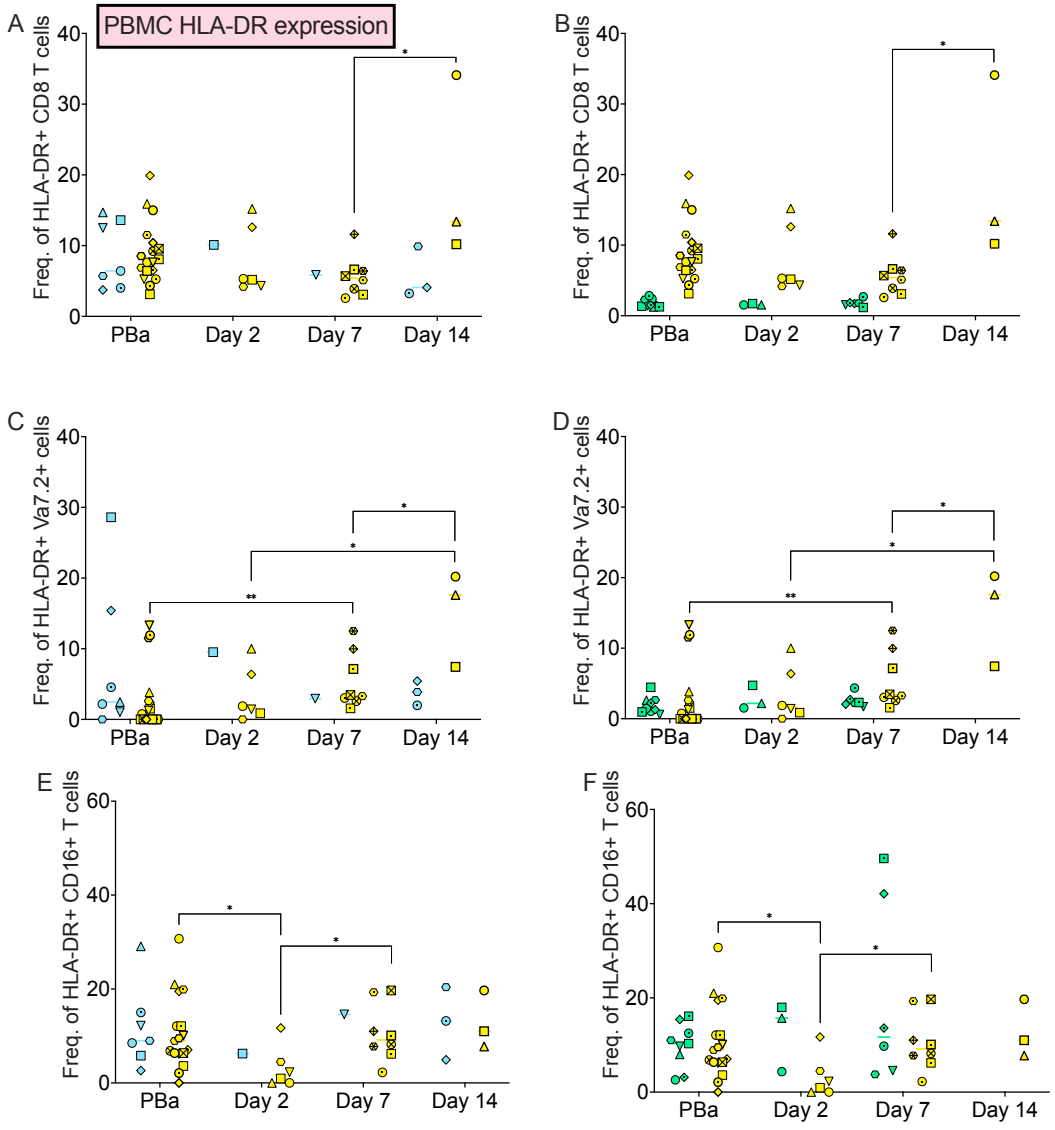


Figure 3.16 continued on next page

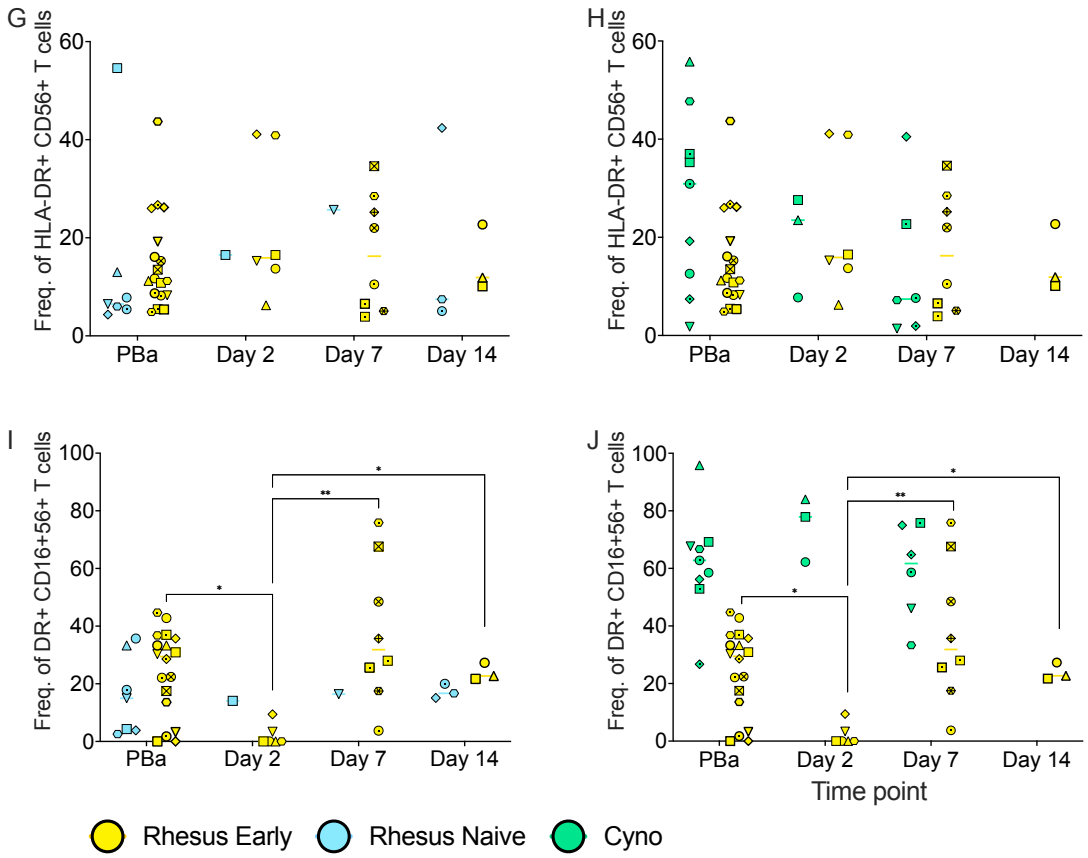


Figure 3.16 Human leukocyte antigen-DR (HLA-DR) expression on lymphocytes characterised among peripheral blood mononuclear cells (PBMCs)

*HLA-DR expression on CD8+4- T-cells (**A** & **B**), Vα7.2+ CD8+ T-cells (**C** & **D**), and NKT cell populations (**E-I**) from PBMCs are shown. Animals exposed to aerosol BCG (aeBCG) are shown in yellow (rhesus macaques, left hand side) and green (cynomolgus macaques, right hand side), and rhesus macaques exposed to aerosol saline (aeSaline) are shown in blue (**B**). Each symbol represents a different animal and group medians are shown. Statistical comparisons between paired samples at baseline (PBa) and their post-mortem time point were made using Wilcoxon-Rank testing. Mann-Whitney U-testing was used to compare unpaired data (e.g. D2 compared to D7). Significant comparisons are marked as P < 0.05 (*) or P < 0.005 (**).*

HLA-DR expression in BAL lymphocyte subsets decreased at D2/D7 in RM, before returning to baseline levels at D7/D14. HLA-DR expression was lower at D2 and D7 compared to baseline for CD4+ and CD8+ T-cells, and for CD56+ NKT-L cells. For all BAL subsets measured, the HLA-DR expression increased at D14 compared to D7 and D2, except for D14 compared to D2 for CD16+ NKT-L cells (Table 3.7B and Figure 3.17). A similar pattern was observed for RM exposed to aeSaline, and for CM exposed to aeBCG.

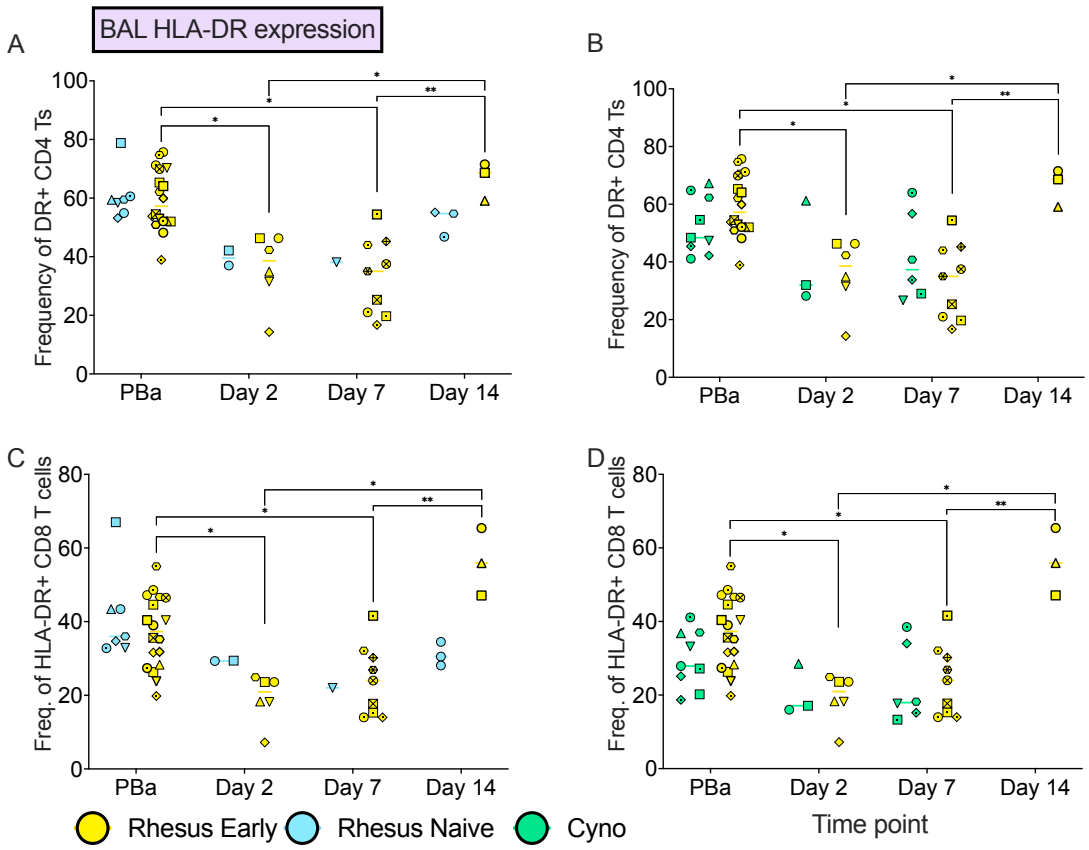


Figure 3.17 Human leukocyte antigen-DR (HLA-DR) expression among lymphocytes characterised among broncho-alveolar lavage (BAL) cells

*HLA-DR expression on CD4+CD8- T-cells (**A** & **B**) and CD4-8+ T-cells (**C** & **D**) from BAL cells are shown. Animals exposed to aerosol BCG (aeBCG) are shown in yellow (rhesus macaques, left hand side) and green (cynomolgus macaques, right hand side), and rhesus macaques exposed to aerosol saline (aeSaline) are shown in blue (**B**). Each symbol represents a different animal and group medians are shown. Statistical comparisons between paired samples at baseline (PBa) and their post-mortem time point were made using Wilcoxon-Rank testing. Mann-Whitney U-testing was used to compare unpaired data (e.g. D2 compared to D7). Significant comparisons are marked as P < 0.05 (*) or P < 0.005 (**).*

HLA-DR expression increased on several lymphocyte populations among RM LNs (hilar and axillary, Table 3.7 and Figure 3.18). For example, HLA-DR expression on CD4+ T-cells increased at D14 compared to D2 (0.0182 hilar vs *p*=0.0364/ns axillary) and at D14 compared to D2 (*p*=0.0238 hilar vs *p*=0.0952/ns axillary). There were no changes in HLA-DR expression in lung MCs (RM or CM). It was not possible to compare HLA-DR expression on cells at D14 to other time points (n=3).

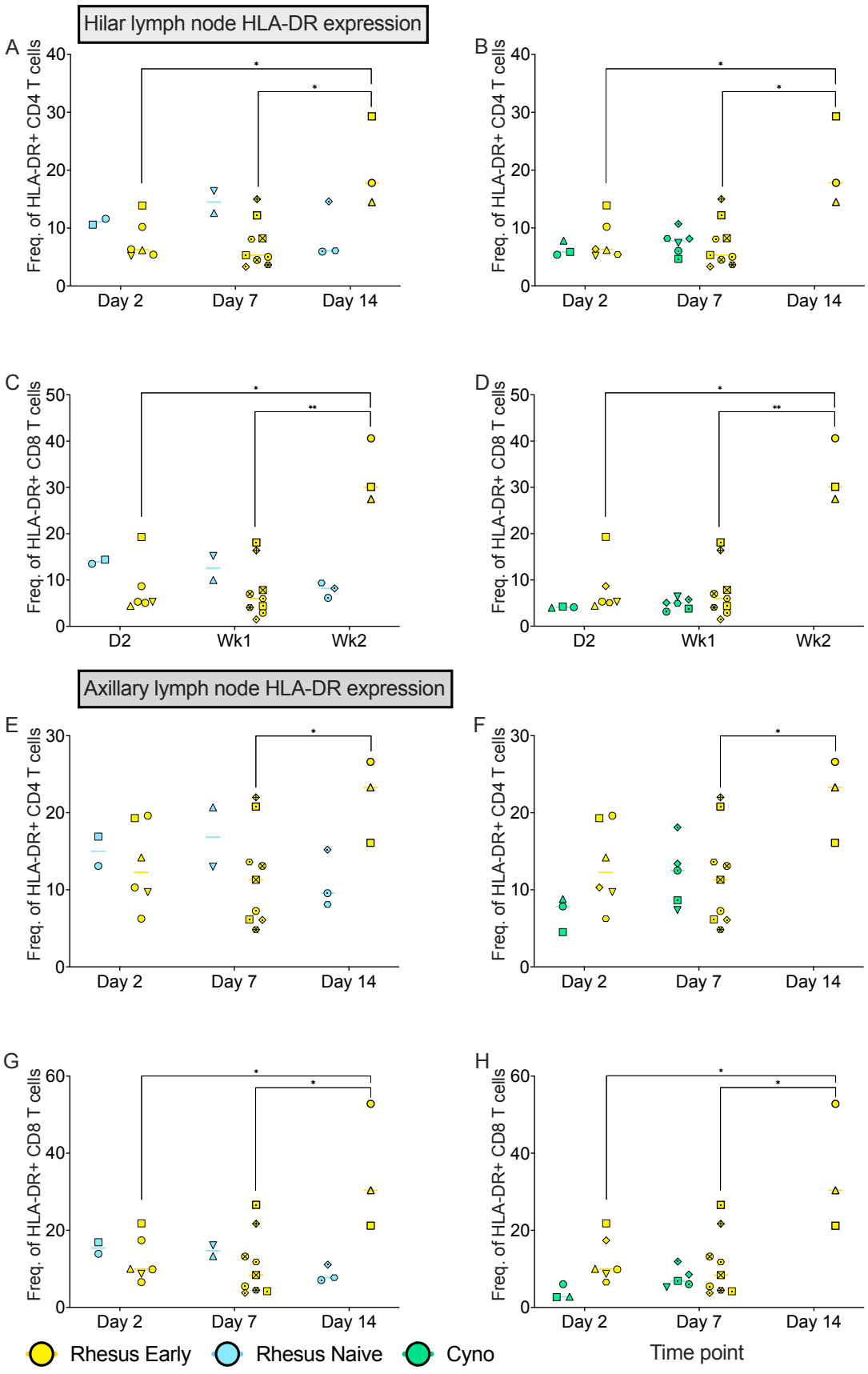

Hilar lymph node HLA-DR expression
A
Freq. of HLA-DR+ CD4 T cells
0
10
20
30
40
Day 2
Day 7
Day 14
*
*
B
Freq. of HLA-DR+ CD4 T cells
0
10
20
30
40
Day 2
Day 7
Day 14
*
*
C
Freq. of HLA-DR+ CD8 T cells
0
10
20
30
40
50
D2
Wk1
Wk2
*
**
D
Freq. of HLA-DR+ CD8 T cells
0
10
20
30
40
50
D2
Wk1
Wk2
*
**
Axillary lymph node HLA-DR expression
E
Freq. of HLA-DR+ CD4 T cells
0
10
20
30
Day 2
Day 7
Day 14
*
F
Freq. of HLA-DR+ CD4 T cells
0
10
20
30
Day 2
Day 7
Day 14
*
G
Freq. of HLA-DR+ CD8 T cells
0
20
40
60
Day 2
Day 7
Day 14
*
*
H
Freq. of HLA-DR+ CD8 T cells
0
20
40
60
Day 2
Day 7
Day 14
*
*
Rhesus Early
Rhesus Naive
Cyno
Time point

Figure 3.18 Human leukocyte antigen-DR (HLA-DR) expression on lymphocytes characterised among lymph node mononuclear cells

*The frequency of HLA-DR+ cells among CD4+CD8- T-cells (**A** & **B**) and CD4-8+ T-cells (**C** & **D**) from hilar (**A-D**) and axillary (**E-H**) lymph node mononuclear cells are shown. Animals exposed to aerosol BCG (aeBCG) are shown in yellow (rhesus macaques, left hand side) and green (cynomolgus macaques, right hand side), and rhesus macaques exposed to aerosol saline (aeSaline) are shown in blue (**B**). Each symbol represents a different animal and group medians are shown. Statistical comparisons between paired samples at baseline (PBa) and their post-mortem time point were made using Wilcoxon-Rank testing. Mann-Whitney U-testing was used to compare unpaired data (e.g. D2 compared to D7). Significant comparisons are marked as P < 0.05 (*) or P < 0.005 (**).*

3.4.10 Activation markers in WB, measured by flow-cytometry

In RM WB, HLA-DR expression was reduced at D2 and D7 compared to baseline for CD4+, CD8+, γδ, and CD56+ T-cells. There are no differences in HLA-DR expression between D2 and D7 in RM (Figure 3.19). Antibody panel 2 included antibodies for MerTK and CD163, typically considered markers of activation in non-lymphocyte monocyte cell populations. Both markers were conjugated to the same fluorochrome and MerTK+/CD163+ CD14+CD16+ non-lymphocyte cell frequency was between 80-100% (Figure 3.20).

MerTK+/CD163+ cell frequency varied depending on the non-lymphocyte cell subset, with lowest expression on the CD14-CD16- non-lymphocyte cells, and highest expression on CD14+CD16+ non-lymphocyte cells. In CM, MerTK+/CD163+ non-lymphocyte cell frequency was higher at D2 than baseline (n=3, *p*=0.0312). In RM,

MerTK+/CD163+ CD14-CD16- and CD14-CD16+ non-lymphocyte cell frequency decreased at D2 compared to baseline (both *p*=0.0312, n=6, Table 3.8).

A) WBICS: MerTK expression						
species	**cynomolgus**			**rhesus**		
time point comparison	PBa D2	PBa D7	D2 D7	PBa D2	PBa D7	D2 D7
total non-lymphocytes	ns	*	ns	*	ns	ns
CD14+CD16+ non-lymphocytes	ns	ns	ns	*	ns	ns
CD14+CD16- non-lymphocytes	ns	ns	ns	ns	ns	ns
CD14-CD16+ non-lymphocytes	ns	ns	ns	*	ns	ns
CD14-CD16- non-lymphocytes	ns	ns	ns	*	ns	ns

B) WBICS: CD95 expression						
species	**cynomolgus**			**rhesus**		
time point comparison	PBa D2	PBa D7	D2 D7	PBa D2	PBa D7	D2 D7
CD4+ T cell	ns	ns	ns	ns	ns	ns
CD8+ T cell	ns	ns	ns	*	*	ns
CD8+161+ (MAIT)	ns	ns	ns	ns	ns	ns
CD14-CD20+ (B cell)	ns	ns	ns	ns	ns	ns

Table 3.8 Activation marker expression among whole blood (WB) samples

To identify different cell populations, thawed WB samples were stained with a 14-colour antibody panel, after overnight stimulation with co-stimulatory antibody only. The table shows comparisons between the expression of MerTK+/CD163+ (A) and CD95 (B) measured at different time points among non-lymphocyte and lymphocyte populations. Groups of animals euthanised at Day 2/7/14 (D2/D7/D14). Statistical comparisons between paired samples at baseline (PBa) and their post-mortem time point were made using Wilcoxon-Rank testing. Mann-Whitney U-testing was used to compare unpaired data (e.g. D2 compared to D7). Comparisons are marked as not significant (ns), P < 0.05 (*) or P < 0.005 (**), with increases shown in yellow, and decreases in blue.

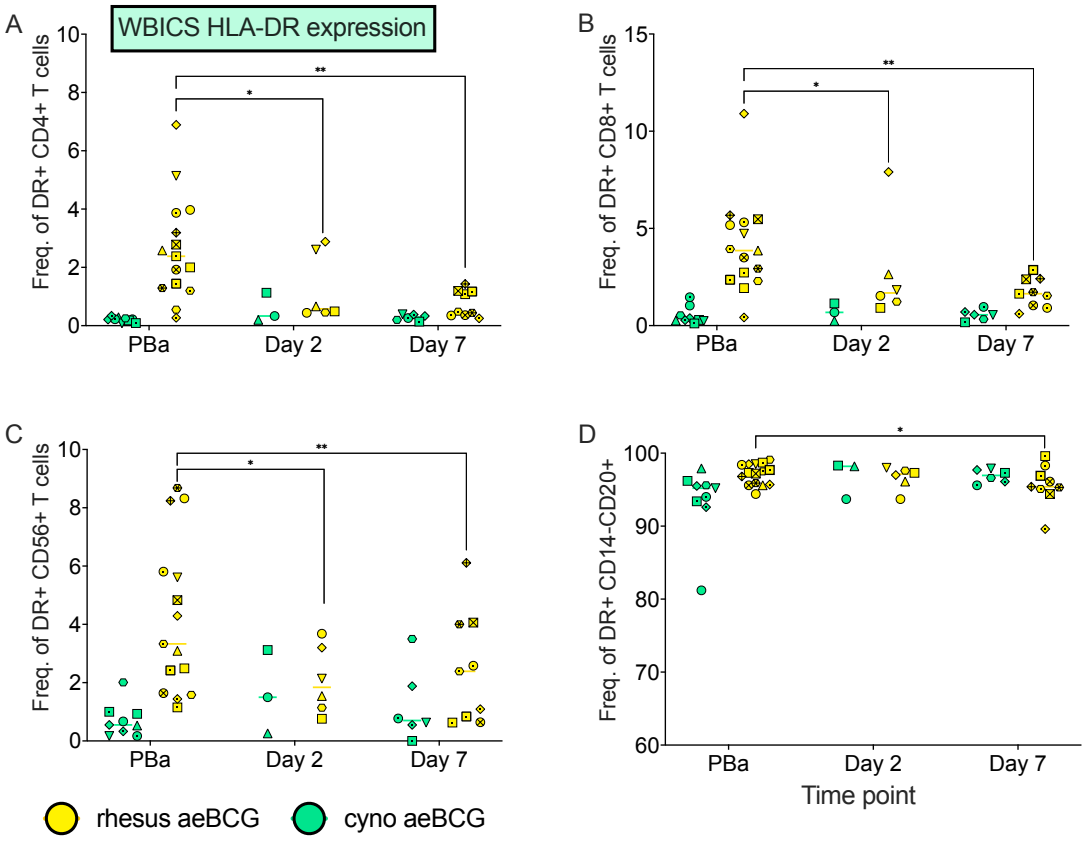


Figure 3.19 Human leukocyte antigen-DR (HLA-DR) frequency among lymphocytes characterised among whole blood (WB) samples

*The frequency of HLA-DR+ cells among CD4+ (**A**), CD8+ (**B**), and CD56+ (**C**) T-cells, and CD20+ B-cells (**D**) from WB are shown. Animals exposed to aerosol BCG (aeBCG) are shown in yellow (rhesus macaques, left hand side) and green (cynomolgus macaques, right hand side). Each symbol represents a different animal and group medians are shown. Statistical comparisons between paired samples at baseline (PBa) and their post-mortem time point were made using Wilcoxon-Rank testing. Mann-Whitney U-testing was used to compare unpaired data (e.g. D2 compared to D7). Significant comparisons are marked as $P < 0.05$ (*) or $P < 0.005$ (**).*

In addition to these monocyte markers, CD95 expression was evaluated in WB. Fas is up-regulated on activated T/B cells, and can be used to identify activated cells. Fas+ B-cell and CD4+ T-cell frequency remained the same (Table 3.8B). In RM, Fas+CD8+ T-cell frequency increased from a median of 3.72 at baseline to 6.41 at D2 (p=0.0312) and from 4.21 at baseline to 6.02 at D7 (p=0.0391, not shown). No change was observed for Fas expression on CD8+CD161+ T-cells, which is a small population, and has low baseline expression of Fas. No change was observed for any sub-population in CM.

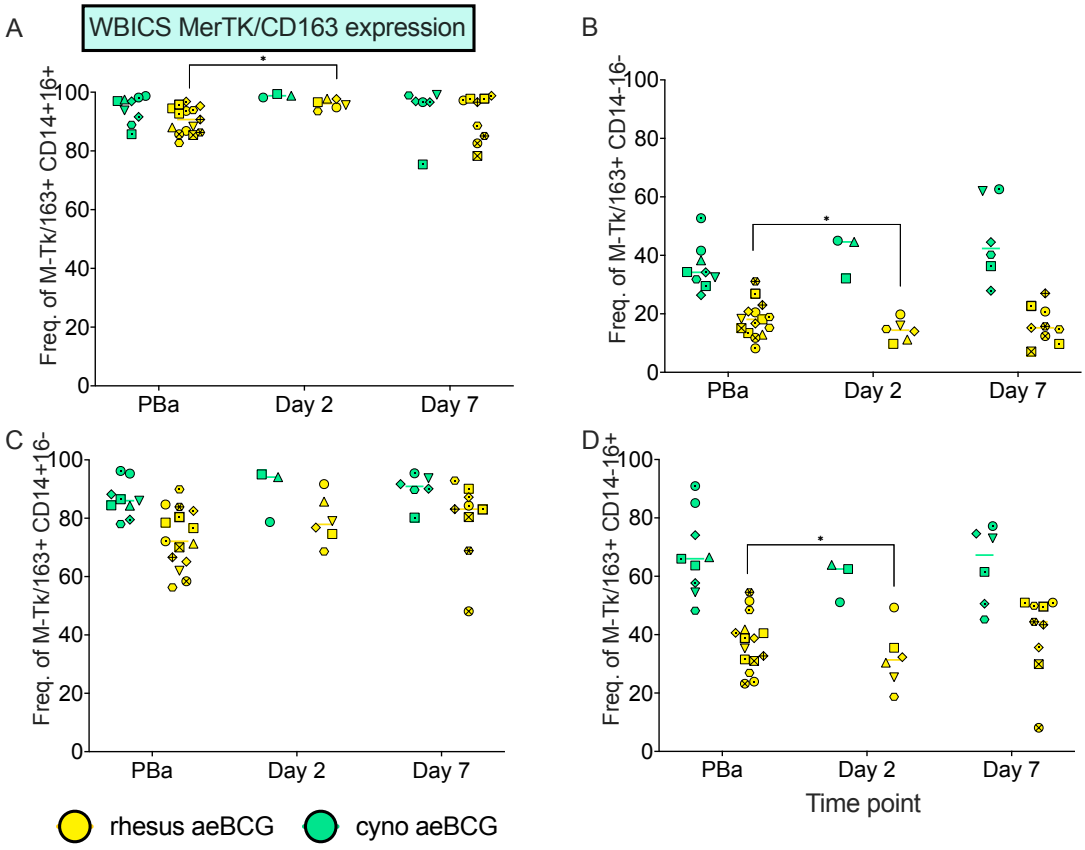


Figure 3.20 MerTK/CD163 expression among non-lymphocyte cells populations

*The frequency of MerTK+/CD163+ cells among CD14+CD16+ (**A**), CD14+CD16- (**B**), CD14-16+ (**C**) and CD14-CD16- (**D**) non-lymphocyte cells from whole blood intracellular cytokine staining samples are shown. Animals exposed to aerosol BCG (aeBCG) are shown in yellow (rhesus macaques, left hand side) and green (cynomolgus macaques, right hand side). Each symbol represents a different animal and group medians are shown. Statistical comparisons between paired samples at baseline (PBa) and their post-mortem time point were made using Wilcoxon-Rank testing. Mann-Whitney U-testing was used to compare unpaired data (e.g. D2 compared to D7). Significant comparisons are marked as P < 0.05 (*) or P < 0.005 (**).*

3.4.11 Intracellular cytokine staining

There were very few significant changes in PPD-specific IFNγ+ or IL-2+ cell frequency for PBMCs in RM or CM (Table 3.9, Supplementary Figure 2). In CM, IL-17+ CD3+ lymphocyte frequency decreased from D2 to D7, but there were no differences compared to baseline. In RM PBMCs, IL-17+ CD56+ T-cells (NKT-L) frequency increased at D14 compared to baseline (p=0.0312) and compared to D7 (p=0.0186). IL-17+ CD8+ and γδ T-cell frequency decreased at D7 compared to baseline (RM), and returned to baseline levels at D14. There were no clear changes in cytokine production among BAL or lung MCs.

In MCs characterised among hilar LNs of RM, IFNγ+ CD16+ and CD16+CD56+ NKT-L cell frequency increased at D14 compared to baseline. IFNγ+ cell frequency among D14 samples (n=3) was less than 0.9%, compared to 0% IFNγ+ cells at D2/D7. There was no change in IL-2+ cell frequency from hilar LNs. IL-17+ CD8+/CD4+/γδ T-cell frequency increased at D7 compared to D2 in hilar LNs (p=0.0198/0.0028/0.0146). In axillary LN

samples, IL-2+ CD56+ NK cell frequency increased at D14, compared to D2 and D7 (both p=0.0119).

A) PBMC cytokines									
IFNg									
species	**cynomolgus**			**rhesus**					
time point comparison	PBa D2	PBa D7	D2 D7	PBa D2	PBa D7	PBa D14	D2 D7	D2 D14	D7 D14
CD4 T cell	ns	ns	ns	ns	ns	ns	ns	ns	ns
CD8 T cell	ns	ns	ns	ns	ns	ns	ns	*	ns
gamma-delta T cell	ns	ns	ns	ns	*	ns	ns	ns	ns
Va7.2+ CD8+ T cell	ns	ns	ns	ns	ns	ns	ns	ns	ns
CD16+ T cell (NKT-like)	ns	ns	ns	ns	ns	ns	ns	ns	ns
CD56+ T cell (NKT-like)	ns	ns	ns	ns	ns	ns	ns	ns	ns
CD16+CD56+ T cell (NKT-like)	ns	ns	ns	ns	ns	ns	ns	ns	ns
CD16-56+ CD3- (NK)	ns	ns	ns	ns	ns	ns	ns	ns	ns
CD16+56- CD3- (NK)	ns	ns	ns	ns	ns	ns	ns	ns	ns
CD14+CD16+ non-lymphocyte	ns	ns	ns	ns	ns	ns	ns	ns	ns
CD14+CD16- non-lymphocyte	ns	ns	ns	ns	ns	ns	ns	ns	ns
CD14-CD16+ non-lymphocyte	ns	ns	ns	ns	ns	ns	ns	ns	ns
IL-2									
species	**cynomolgus**			**rhesus**					
time point comparison	PBa D2	PBa D7	D2 D7	PBa D2	PBa D7	PBa D14	D2 D7	D2 D14	D7 D14
CD4 T cell	ns	ns	ns	ns	ns	ns	ns	ns	ns
CD8 T cell	ns	ns	*	ns	ns	ns	ns	ns	ns
gamma-delta T cell	ns	ns	ns	ns	ns	ns	ns	ns	ns
Va7.2+ CD8+ T cell	ns	ns	ns	ns	ns	ns	ns	ns	ns
CD16+ T cell (NKT-like)	ns	ns	ns	ns	ns	ns	ns	ns	ns
CD56+ T cell (NKT-like)	ns	ns	ns	ns	ns	ns	ns	ns	ns
CD16+CD56+ T cell (NKT-like)	ns	ns	ns	ns	ns	ns	ns	ns	ns
CD16-56+ CD3- (NK)	ns	ns	ns	ns	ns	ns	ns	ns	ns
CD16+56- CD3- (NK)	ns	ns	ns	ns	ns	ns	ns	ns	ns
CD14+CD16+ non-lymphocyte	ns	ns	ns	ns	ns	ns	ns	ns	ns
CD14+CD16- non-lymphocyte	ns	ns	ns	ns	ns	ns	ns	ns	ns
CD14-CD16+ non-lymphocyte	ns	ns	ns	ns	ns	ns	ns	ns	ns
IL-17									
species	**cynomolgus**			**rhesus**					
time point comparison	PBa D2	PBa D7	D2 D7	PBa D2	PBa D7	PBa D14	D2 D7	D2 D14	D7 D14
CD4 T cell	ns	ns	ns	ns	ns	ns	ns	ns	ns
CD8 T cell	ns	ns	*	ns	*	ns	ns	*	*
gamma-delta T cell	ns	ns	*	ns	*	ns	ns	*	*
Va7.2+ CD8+ T cell	ns	ns	ns	ns	ns	ns	ns	ns	ns
CD16+ T cell (NKT-like)	ns	ns	ns	ns	ns	ns	ns	ns	*
CD56+ T cell (NKT-like)	ns	ns	ns	ns	ns	*	ns	*	ns
CD16+CD56+ T cell (NKT-like)	ns	ns	ns	ns	ns	ns	ns	*	ns
CD16-56+ CD3- (NK)	ns	ns	*	ns	ns	ns	*	ns	*
CD16+56- CD3- (NK)	ns	ns	*	ns	ns	ns	ns	ns	*
CD14+CD16+ non-lymphocyte	ns	ns	ns	ns	ns	ns	ns	ns	*
CD14+CD16- non-lymphocyte	ns	ns	ns	ns	ns	ns	ns	ns	ns
CD14-CD16+ non-lymphocyte	ns	ns	ns	ns	ns	ns	ns	ns	ns

B) BAL cytokines									
IFNg									
species	**cynomolgus**			**rhesus**					
time point comparison	PBa D2	PBa D7	D2 D7	PBa D2	PBa D7	PBa D14	D2 D7	D2 D14	D7 D14
CD4 T cell	ns	ns	ns	ns	ns	ns	ns	ns	ns
CD8 T cell	ns	ns	ns	ns	ns	ns	ns	ns	ns
gamma-delta T cell	ns	ns	ns	ns	ns	ns	ns	ns	ns
Va7.2+ CD8+ T cell	ns	ns	ns	ns	ns	ns	ns	ns	ns
CD16+ T cell (NKT-like)	ns	ns	ns	ns	ns	ns	ns	ns	ns
CD56+ T cell (NKT-like)	ns	ns	ns	ns	ns	ns	ns	ns	ns
CD16+CD56+ T cell (NKT-like)	ns	ns	ns	ns	ns	ns	ns	ns	ns
CD16-56+ CD3- (NK)	ns	ns	ns	ns	*	ns	ns	ns	ns
CD16+56- CD3- (NK)	ns	ns	ns	ns	ns	ns	ns	ns	ns
CD14+CD16+ non-lymphocyte	ns	ns	ns	ns	ns	ns	ns	ns	ns
CD14+CD16- non-lymphocyte	ns	ns	ns	ns	ns	ns	ns	ns	ns
CD14-CD16+ non-lymphocyte	ns	ns	ns	ns	ns	ns	ns	ns	ns
IL-2									
species	**cynomolgus**			**rhesus**					
time point comparison	PBa D2	PBa D7	D2 D7	PBa D2	PBa D7	PBa D14	D2 D7	D2 D14	D7 D14
CD4 T cell	ns	ns	*	ns	ns	ns	ns	ns	ns
CD8 T cell	ns	ns	ns	ns	ns	ns	ns	ns	ns
gamma-delta T cell	ns	ns	ns	ns	ns	ns	ns	ns	ns
Va7.2+ CD8+ T cell	ns	ns	ns	ns	ns	ns	ns	ns	ns
CD16+ T cell (NKT-like)	ns	ns	ns	ns	ns	ns	ns	ns	ns
CD56+ T cell (NKT-like)	ns	ns	*	ns	ns	ns	ns	ns	ns
CD16+CD56+ T cell (NKT-like)	ns	ns	ns	ns	ns	ns	ns	ns	ns
CD16-56+ CD3- (NK)	ns	ns	ns	ns	ns	ns	ns	*	ns
CD16+56- CD3- (NK)	ns	ns	ns	ns	ns	ns	ns	ns	ns
CD14+CD16+ non-lymphocyte	ns	ns	ns	ns	ns	ns	ns	ns	ns
CD14+CD16- non-lymphocyte	ns	ns	ns	ns	ns	ns	ns	ns	ns
CD14-CD16+ non-lymphocyte	ns	ns	ns	ns	ns	ns	ns	ns	ns
IL-17									
species	**cynomolgus**			**rhesus**					
time point comparison	PBa D2	PBa D7	D2 D7	PBa D2	PBa D7	PBa D14	D2 D7	D2 D14	D7 D14
CD4 T cell	ns	ns	ns	ns	ns	ns	ns	ns	ns
CD8 T cell	ns	ns	ns	ns	ns	*	ns	ns	ns
gamma-delta T cell	ns	ns	ns	ns	ns	ns	ns	ns	ns
Va7.2+ CD8+ T cell	ns	ns	ns	ns	ns	ns	ns	ns	ns
CD16+ T cell (NKT-like)	ns	ns	ns	ns	ns	ns	ns	ns	ns
CD56+ T cell (NKT-like)	ns	ns	ns	ns	ns	ns	ns	ns	*
CD16+CD56+ T cell (NKT-like)	ns	ns	ns	ns	ns	ns	ns	ns	ns
CD16-56+ CD3- (NK)	ns	ns	ns	ns	ns	ns	ns	ns	ns
CD16+56- CD3- (NK)	ns	ns	ns	ns	ns	ns	ns	ns	ns
CD14+CD16+ non-lymphocyte	ns	ns	ns	ns	ns	ns	ns	ns	ns
CD14+CD16- non-lymphocyte	ns	ns	ns	ns	ns	ns	ns	ns	ns
CD14-CD16+ non-lymphocyte	ns	ns	ns	ns	ns	ns	ns	ns	ns

C) Lung cytokines												
cytokine	IFNg				IL-2				IL-17			
species	**cyno**	**rhesus**			**cyno**	**rhesus**			**cyno**	**rhesus**		
time point comparison	D2	D2	D2	D7	D2	D2	D2	D7	D2	D2	D2	D7
	D7	D7	D14	D14	D7	D7	D14	D14	D7	D7	D14	D14
CD4 T cell	ns	ns	ns	ns	ns	ns	ns	ns	ns	ns	ns	ns
CD8 T cell	ns	ns	ns	ns	ns	ns	ns	ns	ns	ns	ns	ns
gamma-delta T cell	ns	ns	ns	ns	ns	ns	ns	ns	ns	ns	ns	ns
Va7.2+ CD8+ T cell	ns	ns	ns	ns	ns	ns	ns	ns	ns	ns	ns	ns
CD16+ T cell (NKT-like)	ns	ns	ns	ns	ns	ns	ns	ns	ns	ns	ns	ns
CD56+ T cell (NKT-like)	ns	*	ns	ns	ns	ns	ns	ns	ns	ns	ns	ns
CD16+CD56+ T cell (NKT-like)	ns	*	ns	ns	ns	ns	ns	ns	ns	ns	ns	ns
CD16-56+ CD3- (NK)	ns	ns	ns	ns	ns	ns	ns	ns	*	ns	ns	ns
CD16+56- CD3- (NK)	ns	ns	ns	ns	ns	ns	ns	ns	ns	ns	ns	ns
CD14+CD16+ non-lymphocyte	ns	ns	ns	ns	ns	ns	ns	ns	ns	ns	ns	ns
CD14+CD16- non-lymphocyte	*	ns	ns	ns	ns	ns	ns	ns	ns	ns	ns	ns
CD14-CD16+ non-lymphocyte	ns	ns	ns	ns	ns	ns	ns	ns	ns	ns	ns	ns

D) Hilar lymph node cytokines												
cytokine	IFNg				IL-2				IL-17			
species	**cyno**	**rhesus**			**cyno**	**rhesus**			**cyno**	**rhesus**		
time point comparison	D2	D2	D2	D7	D2	D2	D2	D7	D2	D2	D2	D7
	D7	D7	D14	D14	D7	D7	D14	D14	D7	D7	D14	D14
CD4 T cell	ns	ns	ns	ns	ns	ns	ns	ns	ns	ns	ns	*
CD8 T cell	ns	ns	ns	ns	ns	ns	ns	ns	ns	ns	ns	**
gamma-delta T cell	ns	ns	ns	ns	ns	ns	ns	ns	ns	ns	ns	*
Va7.2+ CD8+ T cell	ns	ns	ns	ns	ns	ns	ns	ns	ns	ns	ns	ns
CD16+ T cell (NKT-like)	ns	ns	ns	*	ns	ns	ns	ns	ns	ns	*	ns
CD56+ T cell (NKT-like)	ns	ns	ns	ns	ns	ns	ns	ns	ns	ns	ns	ns
CD16+CD56+ T cell (NKT-like)	ns	ns	*	*	ns	ns	ns	ns	ns	ns	ns	ns
CD16-56+ CD3- (NK)	ns	ns	ns	ns	ns	ns	ns	ns	ns	ns	ns	ns
CD16+56- CD3- (NK)	ns	ns	ns	ns	ns	ns	ns	ns	ns	ns	ns	ns
CD14+CD16+ non-lymphocyte	ns	ns	ns	ns	ns	ns	ns	ns	ns	ns	ns	ns
CD14+CD16- non-lymphocyte	ns	ns	ns	ns	ns	ns	ns	ns	ns	ns	ns	ns
CD14-CD16+ non-lymphocyte	ns	ns	ns	ns	ns	ns	ns	ns	ns	ns	ns	ns

E) Axillary lymph node cytokines												
cytokine	IFNg				IL-2				IL-17			
species	**cyno**	**rhesus**			**cyno**	**rhesus**			**cyno**	**rhesus**		
time point comparison	D2	D2	D2	D7	D2	D2	D2	D7	D2	D2	D2	D7
	D7	D7	D14	D14	D7	D7	D14	D14	D7	D7	D14	D14
CD4 T cell	ns	ns	ns	ns	ns	ns	ns	ns	ns	*	ns	ns
CD8 T cell	ns	ns	ns	ns	*	ns	ns	ns	ns	**	ns	ns
gamma-delta T cell	ns	ns	ns	ns	ns	ns	ns	ns	ns	*	ns	ns
Va7.2+ CD8+ T cell	ns	ns	ns	*	ns	ns	ns	*	*	ns	ns	ns
CD16+ T cell (NKT-like)	ns	ns	ns	ns	ns	ns	ns	*	ns	**	ns	ns
CD56+ T cell (NKT-like)	ns	ns	ns	ns	ns	ns	ns	ns	ns	*	ns	ns
CD16+CD56+ T cell (NKT-like)	ns	ns	ns	ns	*	ns	ns	ns	ns	ns	ns	ns
CD16-56+ CD3- (NK)	ns	**	ns	ns	ns	ns	*	*	ns	ns	ns	ns
CD16+56- CD3- (NK)	ns	ns	ns	ns	ns	ns	ns	ns	ns	ns	ns	ns
CD14+CD16+ non-lymphocyte	ns	ns	ns	ns	ns	ns	ns	ns	ns	ns	ns	ns
CD14+CD16- non-lymphocyte	ns	ns	ns	ns	ns	ns	ns	ns	ns	ns	ns	ns
CD14-CD16+ non-lymphocyte	ns	ns	ns	ns	ns	ns	ns	ns	ns	ns	ns	ns

Table 3.9 PPD-specific+ cell cytokine frequency

*To identify different cell populations, peripheral blood mononuclear cells (PBMCs - **A**), broncho-alveolar lavage (BAL - **B**), lung (**C**), hilar and axillary lymph nodes (**D** & **E**) samples were stained with a 14-colour antibody panel, after overnight stimulation with co-stimulatory antibody only (Nil), or with the addition of PPD. Cytokine production from unstimulated samples was subtracted from PPD samples to account for background levels. Groups of animals euthanised at Day 2/7/14 (D2/D7/D14). Statistical comparisons between paired samples at baseline (PBa) and their post-mortem time point were made using Wilcoxon-Rank testing. Mann-Whitney U-testing was used to compare unpaired data (e.g. D2 compared to D7). Comparisons are marked as not significant (ns), P < 0.05 (*) or P < 0.005 (**), with increases shown in yellow, and decreases in blue.*

3.4.12 Populations measured using haematology analyser

Using a haematology analyser, cell populations of neutrophils, monocytes, lymphocytes, eosinophils, and basophils were measured in WB samples. In RM, fewer lymphocytes were detected at D2/D7 compared to baseline. In CM, monocytes and neutrophil counts decreased at D7 compared to baseline (Supplementary Figure 3). The reduction in lymphocyte count in RM was detectable as an increase in the monocyte:lymphocyte (M:L, not significant) and neutrophil:lymphocyte ratio (N:L - p=0.0312 at D2 vs. baseline, p=0.0312/0.0156 at D7 vs baseline, Figure 3.21). In CM, there were no changes in ratio. Consistent with previously published data[117], the M:L and N:L were lower in CM than RM.

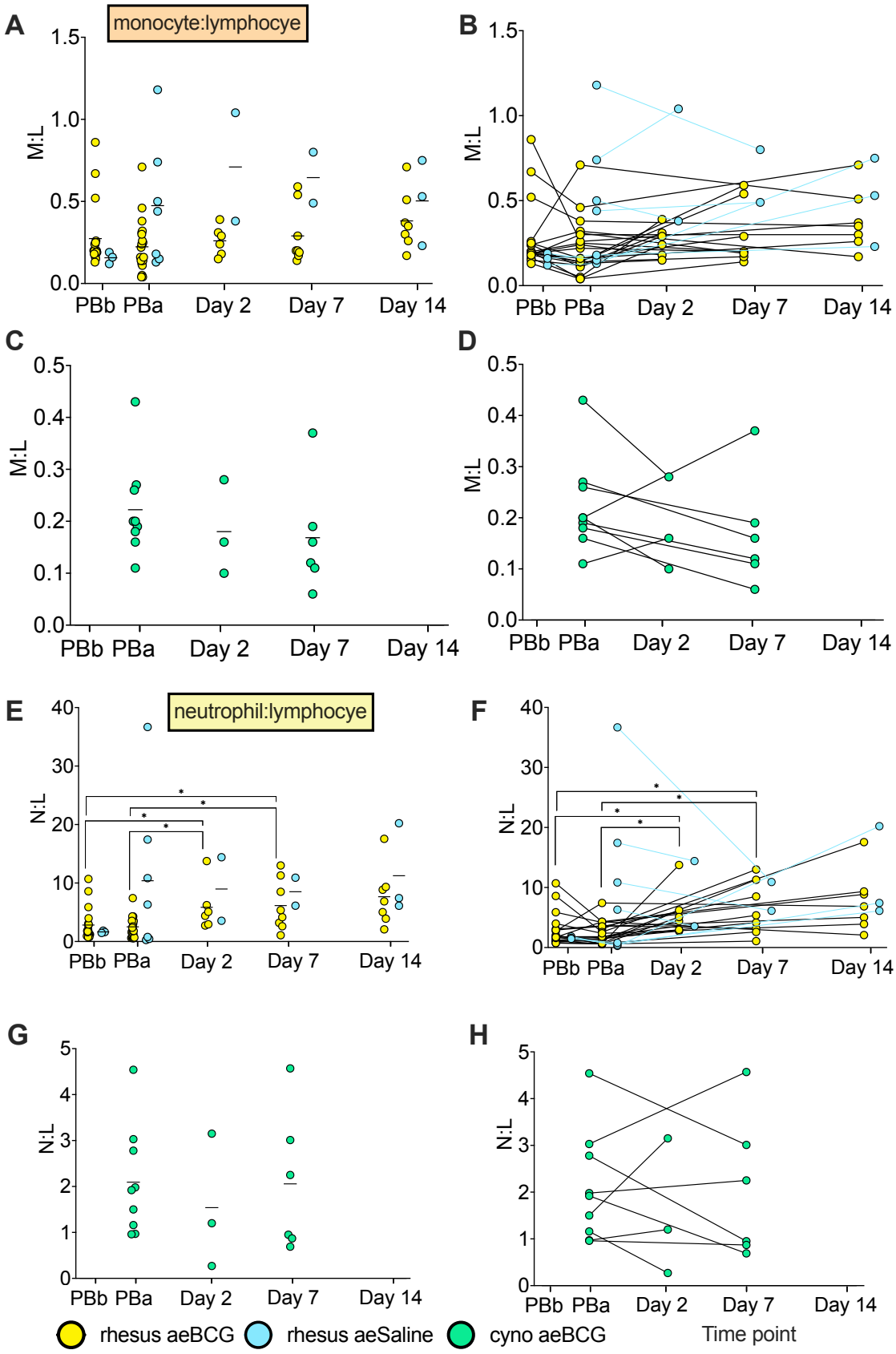

A
monocyte:lymphocye
M:L
1.5
1.0
0.5
0.0
PBb PBa
Day 2
Day 7
Day 14
B
C
D
E
neutrophil:lymphocye
N:L
40
30
20
10
0
F
G
5
4
3
2
1
H
rhesus aeBCG
rhesus aeSaline
cyno aeBCG
Time point

Figure 3.21 Monocyte:lymphocyte (M:L) and neutrophil:lymphocyte (N:L) ratios

*Counts of neutrophils, monocytes, lymphocytes, eosinophils, and basophils were measured in blood samples using IDEXX Lasercyte Haematology analyser. The ratio of M:L (**A-D**) and N:L (**E-G**) are shown. Animals exposed to aerosol BCG (aeBCG) are shown in yellow (rhesus macaques, **A, B, E, F**) and green (cynomolgus macaques, **C, D, G, H**). Rhesus macaques exposed to aerosol saline (aeSaline) are shown in blue (**A, B, E, F**). Individual animals and group medians are shown on the left, and animals are tracked over time on the right. Statistical comparisons between paired samples at baseline (PBa) and their post-mortem time point were made using Wilcoxon-Rank testing. Mann-Whitney U-testing was used to compare unpaired data (e.g. D2 compared to D7). Significant comparisons are marked as P < 0.05 (*).*

3.4.13 Antibody response at early time points

PPD-specific ELISAs were performed at early time points, using sera and BALf. BALf was only collected at PBa, so this time point was used as the baseline. Additional samples taken at PBb and Wk17 were included to expand the sera dataset where available. In serum, three RM had a baseline PPD-specific IgG titre of over 1000 arbitrary units (Figure 3.22). PPD-specific IgG in serum was decreased at D2 (p=0.0312) and D14 (p=0.0156) compared to baseline in RM. There was no change in IgG titre in sera for CM.

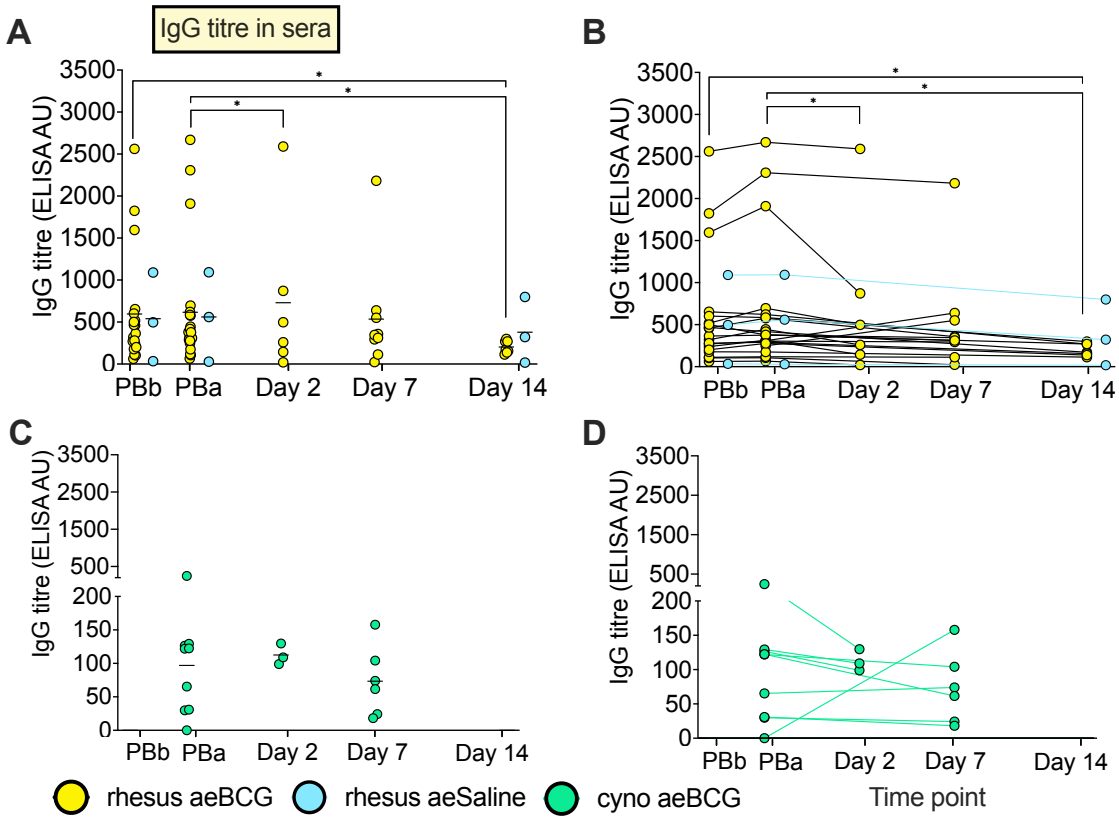


Figure 3.22 PPD-specific IgG in sera

*PPD-specific IgG titre in serum samples. Animals exposed to aerosol BCG (aeBCG) are shown in yellow (rhesus macaques, **A** & **B**) and green (cynomolgus macaques, **C** & **D**). Rhesus macaques exposed to aerosol saline (aeSaline) are shown in blue (**A** & **B**). Individual animals and group medians are shown on the left, and animals are tracked over time on the right. Statistical comparisons between paired samples at baseline (PBa) and their post-mortem time point were made using Wilcoxon-Rank testing. Mann-Whitney U-testing was used to compare unpaired data (e.g. D2 compared to D7). Significant comparisons are marked as P < 0.05 (*) or P < 0.005 (**).*

The same PPD-specific IgG ELISA was also applied to BALf. This fluid was retrieved by suction, after installation of 60 mL of saline into the lungs. The volume of fluid retrieved is variable and much more dilute than the fluid in the lungs. Phospholipid concentration is estimated to be 1 mg/mL in human lungs (Jordi Torrelles, personal communication). To standardise the BALf concentration, phospholipid concentration was measured using a colorimetric assay, and used to calculate the concentration factor needed to obtain a target concentration of 1 mg/mL. BALf was concentrated using Amicon-Ultra 15 centrifuge tubes, before re-measuring phospholipid concentration by the same method. This process is referred to as 'concentration by centrifuging' to avoid confusion with phospholipid concentration. Samples were concentrated by centrifuging, from 42-45 mL of neat BALf to 3-8 mL of concentrated BALf (5-15x concentration in terms of volume – Figure 3.23).

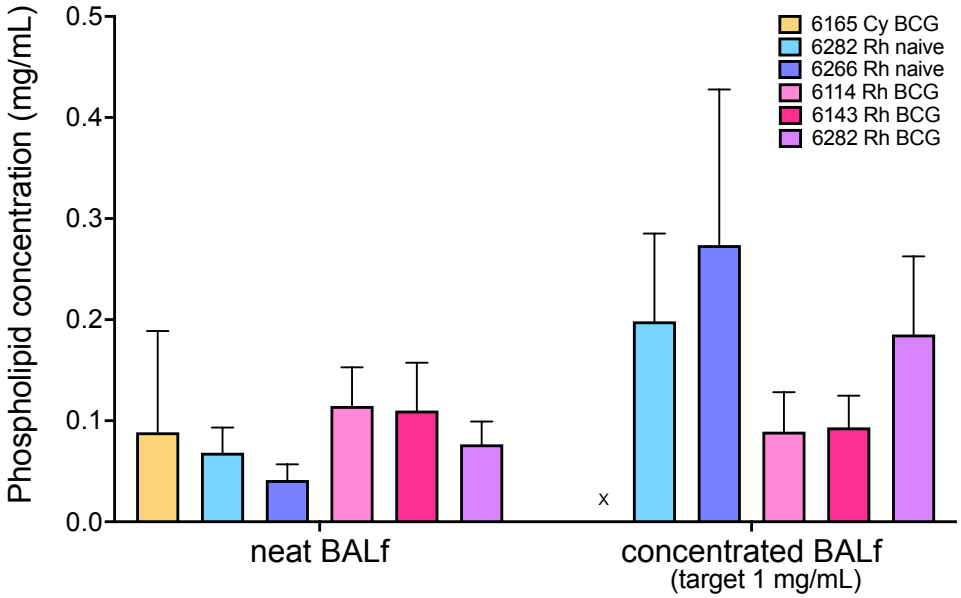


Figure 3.23 Phospholipid concentration in broncho-alveolar lavage fluid (BALf)

Phospholipid concentration was measured in BALf by colorimetric detection of hydrolysed choline. The phospholipid concentration in neat BALf was used to calculate the concentration factor needed for a target concentration of 1 mg/mL phospholipid. Phospholipid concentration was re-measured after concentration using the same process.

PPD-specific IgG titre was measured in neat and concentrated BALf. Although the original aim had been to normalise samples according to phospholipid concentration, samples were analysed and are presented without this mathematical correction. This was to avoid further artificial variation, given that the phospholipid concentration measured after concentration by centrifugation did not reflect the increased concentration of antibody detected after this process. In a proportion of samples, the phospholipid concentration measured after concentration by centrifugation was lower in the concentrated BALf than in the neat BALf. After concentration by centrifugation, the PPD-specific IgG titre detected in BALf increased from a maximum of 2-34 arbitrary units (neat BALf-concentrated BALf), so it is not biologically plausible that the concentration had decreased.

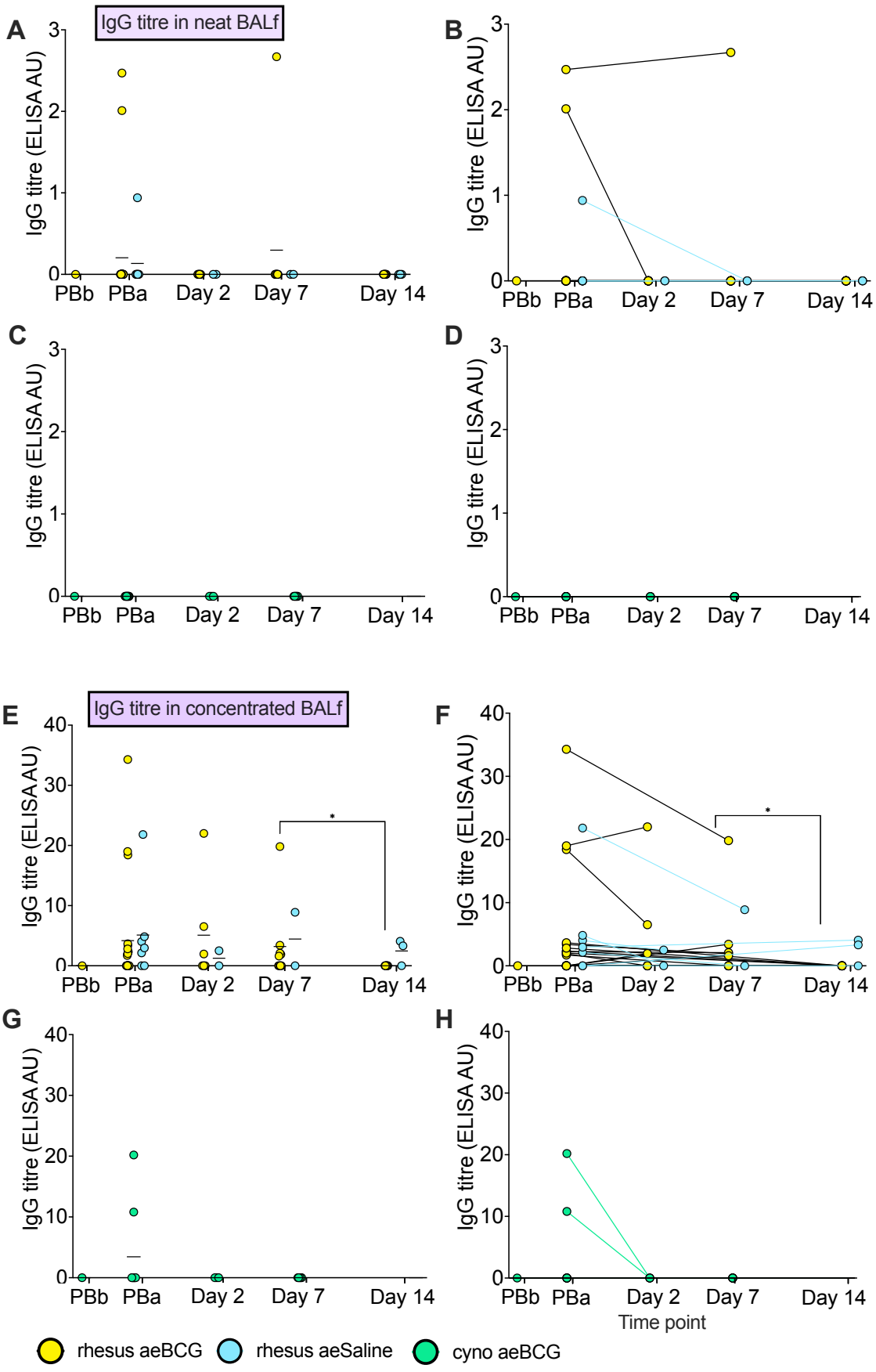

A
IgG titre in neat BALf
IgG titre (ELISA AU)
PBb
PBa
Day 2
Day 7
Day 14
B
C
D
E
IgG titre in concentrated BALf
F
G
H
*
Time point
rhesus aeBCG
rhesus aeSaline
cyno aeBCG

Figure 3.24 PPD-specific IgG in broncho-alveolar lavage fluid (BALf)

*PPD-specific IgG titre in neat (**A-D**) and concentrated (**E-H**) BALf. Animals exposed to aerosol BCG (aeBCG) are shown in yellow (rhesus macaques, **A**, **B**, **E** & **F**) and green (cynomolgus macaques, **C**, **D**, **G** & **H**). Rhesus macaques exposed to aerosol saline (aeSaline) are shown in blue (**A**, **B**, **E** & **F**). Individual animals and group medians are shown on the left, and animals are tracked over time on the right. Statistical comparisons between paired samples at baseline (PBa) and their post-mortem time point were made using Wilcoxon-Rank testing. Mann-Whitney U-testing was used to compare unpaired data (e.g. D2 compared to D7). Significant comparisons are marked as P < 0.05 (*) or P < 0.005 (**).*

Figure 3.24 shows the PPD-specific IgG titres measured in neat BALf (A-D) compared to concentrated BALf (E-H). IgG titre was very low in all BAL samples. In RM, there was no detectable IgG measured at D14, which meant that IgG titre at D14 was lower than at D7 (different animals). There was no decreased between matched baseline and D14 samples.

3.5 Discussion

3.5.1 Study design and safety of aeBCG

Exposure to aeBCG did not impact the overall health of macaques, consistent with published studies using aeBCG as a vaccination method[3, 7]. The study design allowed in depth comparison of different tissue compartments at early time points post aeBCG. Animals exposed to aeSaline only were included as controls, but could not be compared statistically as the sample sizes were small (n=2 at D2, n=2 at D7, n=3 at D14). However, these animals provided a useful reference point for within group variation and variation caused by evaluation of samples on different days. For logistical reasons, animals across studies were not always of the same age or sex. To minimise inter-assay variation, samples that were not evaluated immediately after isolation were evaluated in batches. Samples from different animals were evaluated in the same batch, and a samples from each study were spread across different batches.

3.5.2 Frequency of systemic PPD-specific IFNγ-secreting cells

The *ex vivo* IFNγ ELISpot assay is widely used within the field of TB research to evaluate the mycobacterium-specific cellular immune response. PPD-specific IFNγ responses are often used to indicate vaccine-induced responses or to exclude mycobacterium-exposed participants from vaccine trials[256]. *M.tb*-specific antigens (e.g. ESAT-6 and CFP-10) are used to distinguish between BCG-specific and *M.tb*-specific responses, and can therefore be used to distinguish *M.tb* infection from vaccination status[90].

After aeBCG, the systemic immune response measured by PPD-specific *ex vivo* IFNγ ELISpot did not change up to D14 after aeBCG. In a proportion of RM, more IFNγ SFU were detected at D7 than at baseline (PBa), but this did not reach significance, and there

was no increase at D14 compared to baseline. There was a lot of variation between animals, including one control animal showing an increased response at PBb/D2 compared to PBa. A limitation of using outbred populations is increased variation between individuals. In humans, larger sample sizes can be used to gain a better representation of the population as a whole. This is not possible in NHPs (cost and ethics). It is likely that the time points measured here were too early to detect a response to aeBCG by ELISpot (adaptive), and any innate cell production of IFNγ was too small to be detected using this assay.

The majority of NHP studies looking at BCG as a vaccine use time points from at least D14 post-vaccination, and the peak response is at Wk6-Wk9. After ID BCG, the frequency of PPD-specific IFNγ SFU measured by ELISpot in the peripheral blood increases at Wk9 in Indian and Chinese RM[10]. White *et al.,* found that after exposure to aeBCG (standard ID dose) the SFU frequency increased from Wk8, but only reached significance at Wk10[3] (see Chapter 1 for figures). In these published studies of mucosal BCG, the earliest time point explored is Wk3 (after EB installation of BCG[10]).

3.5.3 Conventional T-cell response

The role of antigen-specific T-cells is well-acknowledged as an essential, if not sufficient component of the immune response to mycobacteria[65, 67, 132]. In human infants, the initial T-cell response peaks between Wk6-Wk10 after vaccination, with CD4+ T-cell production of IFNγ/TNFα/IL-2[257]. The role of CD8+ T-cells in TB disease is less clear, and harder to study because this subset is smaller[258]. In NHPs, CD8+ T-cell depletion compromised the protection against *M.tb* that is afforded by BCG vaccination[216]. Studies of mycobacterial infection usually focus on D14 onwards, so there is limited data to show how CD4+ and

CD8+ T-cells interact in the early stages of infection. The studies reported in this chapter focused on early time points to address this knowledge gap.

Low CD4+:CD8+ T-cell ratio is associated with a higher risk of developing TB, as demonstrated in a long-term follow up of HIV patients with successful viral repression[259]. In this project, the CD4+:CD8+ T-cell ratio in PBMCs showed a transient increase towards D7, which may represent early induction of the adaptive immune response (RM and CM). In NHPs, Sibley *et al.,* found that the CD4+:CD8+ ratio was higher in RM compared to CM (Mauritian, Asian or Chinese)[120]. In accordance with this published work, the CD4+:CD8+ ratio was higher in RM than CM in this study.

There was also a decrease in CD3+ frequency in RM PBMCs at D14 compared to D2 and D7. However, where differences in frequencies observed between D2/D7/D14 were not accompanied by a change in frequency measured at those PM time points compared to baseline (e.g. in this case), it is hard to be sure of biological relevance. There was evidence of an increase in CD3+ T-cells in the BAL, which could reflect movement of T-cells from the periphery into the lungs. This was not reflected in the MCs characterised among lung tissue, where a small reduction in the CD4-CD8- fraction of CD3+ lymphocytes was the only significant change in CD4+ or CD8+ cell frequency.

T cells simultaneously expressing CD4 and CD8 have been identified in other NHP studies[260, 261]. The exact function of this double positive subset is unknown. After aeBCG, CD4+CD8+ and CD4+CD8++ T-cell subsets were identified and decreased in frequency at D7 after aeBCG, following the same pattern as CD8+ T-cells. This early change in CD4+ and CD8+ T-cell frequency suggests that aeBCG is recognised by these cells by D7, preceding any detectable change in antigen-specific functional responses. CD4+CD8++ T-

cell frequency increased at D14 compared to either D2 or D7 in MCs from LNs. Double positive cells may come into being when terminally differentiated CD4+ effector T-cells acquire an additional CD8 chain, or when CD8+ T-cells are activated and express a low level of CD4[261]. Given the possibility that double positive cells represent a form of activation, increased CD4+CD8++ in the LNs local to the lung at D14 may demonstrate activation at the site of antigen presentation and T-cell activation[131].

3.5.4 Unconventional T-cell response

Across all tissue compartments, CD56+CD4+ T-cell frequency increased from D7 after aeBCG. This increase was strongest at D14 in the LNs, and also detected in CM at D7 (compared to baseline) in PBMCs. The data set available from CM was limited as D14 was not evaluated, and the sample size at D2 was limited (n=3). These CD4+56+ T-cells may represent NKT-L cells being activated in the LNs.

CD56 is a good marker of both NK and NKT-L cells in humans, but is limited in NHPs[254, 262, 263]. In NHPs, CD16 is also used to identify NK cells among CD3-CD8+ lymphocytes, and NKT-L cells among CD3+ lymphocytes[162]. Both markers were included in the antibody panels used in this project, and a general pattern of increased CD56+ and decreased CD16+ expression was identified among NK and NKT-L cells. Functionally, CD56+ cells are capable of cytokine production, which can help to control mycobacterial infection. At Wk10 after BCG immunisation, CD56+ NK cells are the major IFNγ-producing subset in children and infants[182].

$\gamma\delta$ cell frequency remained relatively unchanged across the early time points measured. $\gamma\delta$ T-cells are usually classified by frequency of Vδ1 or Vδ2, with the Vδ2 subset dominating in the circulatory system, where they can expand in response to non-MHC

presented unprocessed antigen, including antigens found in BCG[264]. Up-regulation of the Vδ2 subset after BCG has been shown in TB patients compared to healthy controls[182, 183]. In NHPs, upregulation of the Vδ2 subset was detected at Wk3-Wk5 after exposure to BCG, and at D4 after a second exposure to BCG[183]. The use of a pan-γδ antibody may mask more subtle changes within specific γδ cell subsets.

Despite good performance in testing of the antibody panel 2 on PBMC and WB, γδ staining in WB was un-expectedly high (up to 80%) and did not reflect the frequency of 0.5-5% of CD3+ T-cells as previously published[176, 264]. Given that the γδ cell population could not be clearly identified from this abnormal expression, γδ cell frequency was not analysed within these samples. Compared to PBMC samples processed on the day of isolation, the WBICS samples were isolated from 500 μL of WB, rather than a standardised $1x10^6$ cells/sample, but this should not have affected the proportions of any particular cell subtype.

MAIT cells are localised to mucosal sites, and can expand and produce cytokines in response to *M.tb* infection[199,175]. Evidence for the role and necessity of MAIT cells in TB disease is conflicting; one study showed that MAIT knockout mice are not more susceptible to *M.tb* and that expansion of MAIT cells fails to protect against *M.tb* challenge[175], where another showed that MR1-deficient mice are more susceptible[173]. Previously, MAIT cells identified using an MR1 5-OP-RU MAIT tetramer were found to be comparable in frequency to CD8+CD26+CD161+ T-cells[169]. In this project, Vα7.2 and CD161 expression were used to distinguish MAIT cells within the CD8+ T-cell population, as this is the major NHP MAIT population[258]. MAIT cells are expected to be a small PBMC population[167], but the Vα7.2+CD161+CD8+ population identified in this project was also

minimal in BAL. Use of a MAIT-specific MR1 tetramer might have increased the size of the MAIT population identified, and would confirm the identity of this population more precisely. In this project, the CD161+Vα7.2+ MAIT cell population was not changed after aeBCG exposure.

Total CD161+CD8+ T-cell frequency increased across all tissue compartments after aeBCG. For example, in LNs and lung, Vα7.2-CD161+ cell frequency increased from D2 to D14 in RM, and from D2 to D7 for CM. This effect was robust across experiments and species and was independent of Vα7.2 expression. CD161 is a C-type lectin (also known as KLRB1 or killer cell lectin-like receptor subfamily B) that was initially defined as an NK cell marker. Co-expression of CD161 and other lymphocyte markers was further explored in a secondary analysis of flow cytometry data. In this analysis, CD161 expression increased up to D7 in PBMC in RM (D14 not available). In RM, CD161 expression increased by D2 (compared to baseline), and strongly up to D14. The increase in CD161 expression at D14 was observed across all compartments and lymphocyte subsets explored (CD4+, CD8+ and $\gamma\delta$ T-cells, NK and NKT cells).

It is likely that the increase across compartments is partly due to subset heterogeneity. For example CD4+CD56+ cells would be identified in CD4+ T-cell and CD3+CD56+ NKT-L subsets. The exact function of CD161 across lymphocyte subsets is still being actively explored, making this novel identification of CD161 up-regulation after mycobacterial exposure particularly interesting. CD4+CD161+ T-cells have previously been identified as 'fast-acting' unconventional T-cells that are capable of cytokine and perforin production in response to mycobacterial infection and are present in healthy un-infected humans[265, 266]. Adoptive transfer of this subset provided protection against *M.tb*

challenge in SCID mice[265]. CD4+CD161+ cells have been linked with IL-17 production and are enriched in chronic hepatitis, specifically depleted in HIV (and SIV in NHPs) and accumulate locally in the gut in Crohn's disease[267, 268]. In the gut, CD161+ cells show tissue homing properties[269].

3.5.5 Non-lymphocyte response

The majority of granulocytes are removed in the process of isolating PBMCs or MCs (tissues). To allow for cross-comparison with the total non-lymphocyte population measured in WB, and to include a larger number of the cells characterised among BAL, a wide gate was used to identify all 'non-lymphocyte cells' by FSC-A and SSC-A. The majority of this population is likely to be monocytes, and the non-lymphocyte gate used included a population proximal to lymphocytes (by FSC-A/SSC-A) where it would be expected to find the monocyte population (see gating examples in chapter 2). CD3+ or CD20+ cells were excluded, and the HLA-DR+ cells were selected. CD14+/- and CD16+/- non-lymphocyte cell frequency was measured and analysed alone or in combination. Similar gating strategies have been used in a number of studies to identify different monocyte subsets (usually with a less inclusive FSC-A/SSC-A gate) as classical (CD14++16-), intermediate (CD14+CD16+) or non-classical ($CD14^{dim}16++$)[147, 148].

Bone-marrow derived monocytes are heterogenous and have high levels of plasticity, and can differentiate into monocyte-derived macrophages or dendritic cells[147]. Increased CD16+ monocyte frequency in TB is associated with poorer differentiation in macrophages/dendritic cells and monocyte cell death[270]. In NHPs, classical monocytes (CD14+CD16-) correlate positively with lung pathology after *M.tb* challenge, where non-classical monocytes (CD14-CD16+) correlate negatively[253]. Dijkman *et al.,* showed that

RM monocytes have a more anti-inflammatory phenotype at baseline and early on in response to mycobacterial infection than CM[4]. CD14+/- and CD16+/- cell frequency measured at early time points after aeBCG do not form a clear picture. There was evidence of increased CD14+ and CD16+ cell frequency in RM LNs, but changes in the PBMCs and BAL non-lymphocyte cells were transient and inconsistent in CM and RM.

3.5.6 Activation markers

HLA-DR is an MHC-II cell surface receptor, that is used for antigen presentation, and up-regulated on activated T-cells. CD4+ T-cell activation measured by HLA-DR expression has previously been identified as an immune correlate of risk for the development of TB disease (in BCG-vaccinated South African babies that were studied as part of the MVA85A vaccine trial)[80]. Recent *M.tb* infection (QFT+ <6 months) can be distinguished from persistent or chronic infection (QFT+ for >1 year) by median fluorescence of HLA-DR on antigen-specific T-cells, measured by flow cytometry[271]. After recent *M.tb* infection, HLA-DR expression is up-regulated on CD3+ T-cells compared to chronic infection[271].

In the dataset presented here, HLA-DR expression in RM transiently decreased at D2 in the periphery (PBMCs and WB) and in BAL. However, HLA-DR+ cell frequency was unchanged at D7/D14 compared to baseline, and a similar drop in HLA-DR expression was observed in RM exposed to aeSaline. This could suggest that the difference was caused by the sampling process (e.g. caused by repeat blood or BAL samples within two days), rather than by aeBCG. Changes in HLA-DR expression were not identified in CM. Although published data describes an increase in HLA-DR expression, the time points evaluated in the experiments detailed here are much earlier (D2 rather than weeks-years after infection).

During *M.tb* infection, inflammatory markers are up-regulated as the immune system recognises and tries to kill the pathogen[132, 272]. After anti-TB drug therapy in humans, inflammatory markers in serum are reduced (e.g. IL-6, IFNγ, TNFα)[273]. In this project, T-cell activation was measured in WB using the marker CD95 (Fas), which is up-regulated upon T-cell activation and causes apoptosis in mature T-cells. Fas expression was unchanged in CM, but up-regulated at D2 and 7 in CD8+ RM T-cells. The ratio of CD4:CD8 T-cells increased during this time, so it is possible that CD8-specific Fas up-regulation reflects activation of CD8+ T-cells to the point of apoptosis. It is also possible that CD8+ T-cells are activated after infection, but not increased as a proportion of T-cells compared to CD4+ T-cells.

Lastrucci *et al.,* identified an anti-inflammatory (M2-like) subset of human monocytes, defined as CD16+CD163+MerTK+pSTAT3+[148]. CD16+CD163+MerTK+pSTAT3+ cells correlated with disease progression in NHPs, and soluble CD163 alone could distinguish between healthy humans or those with moderate/advanced TB disease[148]. RM had a higher baseline frequency of CD16+CD163+MerTK+ than CM, and this subset correlated with higher disease pathology in the RM[148]. MerTK (tyrosine-protein kinase Mer) has a number of signalling roles, including in macrophage clearance of apoptotic cells and CD163 is a scavenger receptor that is considered a phenotypic marker of anti-inflammatory monocytes and is involved in bacterial recognition. In contrast to the findings of Dijkman *et al.*,[4] the frequency of CD16+ non-lymphocyte cells expressing CD163/MerTK was lower in RM than CM in this project. Whether MerTK and CD163 are co-expressed or expressed independently cannot be determined here as the same fluorochrome was used for both antibodies.

3.5.7 Intracellular cytokine response

Although the PPD-specific IFNγ ELISpot assay is a reproducible method to profile the overall immune response to a mycobacterial infection, it is limited to one cytokine, and cannot detect which cell type(s) are the source of the IFNγ. In this project, levels of IFNγ, IL-2 and IL-17 were explored across compartments using flow cytometry. In TB, IFNγ activated macrophages release enzymes and reactive oxygen species that can kill intracellular bacteria alongside IL-17, which is another potent, pro-inflammatory cytokine[204, 274]. IL-2 was included to examine the development of the T-cell response, because this cytokine stimulates T-cell expansion[200]. TNFα is often included in studies of TB disease but tends to follow the same pattern for production as IFNγ (Satti *et al.*, personal communication), so was excluded from this analysis (restricted panel size).

At the early time points after aeBCG, PPD-specific cytokine secreting cell frequency was minimal. Changes in IL-17+ cell frequency were the most notable, but were still minimal. In the BAL, there was little change in cytokine-producing cell frequency. IL-17 expression increased in CD4+ T-cells, CD8+ T-cells and γδs cells from RM in hilar (from D7 to D14) and axillary LNs (from D2 to D7). IFNγ and IL-17 are induced in primary *M.tb* infection, and are strong pro-inflammatory cytokines. A balance between Th1 and Th17 responses is necessary during chronic infection, because prolonged production of IL-17 can lead to excessive neutrophil production and infiltration into tissues[204]. Up-regulation of IL-17 in LNs early after mycobacterial infection may indicate that antigen presenting cells have already migrated to the LNs.

3.5.8 WB cell populations measured by haematology analyser

M:L and N:L ratio in peripheral blood are associated with outcome of a number of infectious diseases including: TB and HIV[149, 150], mood-related disorders[151], coronary heart disease[152], and some cancers[153]. After successful HIV treatment in adults, M:L is reduced and correlates with patient improvement[149]. In human TB, high M:L has recently been used to distinguish between active TB, LTBI and uninfected individuals[149]. A recent study of NHPs showed that progressive disease was associated with an increase in M:L, and that two more susceptible species of macaques (RM and Mauritian-origin CM) had higher M:L ratios that the least susceptible Chinese-origin CM species[117]. High N:L ratio has been identified as a possible risk factor for TB disease development, and can be used to distinguish between active TB cases and other diseases such as sarcoidosis[275].

An IDEXX haematology analyser was used to determine population ratios on the day of sample collection, in WB. A reduction in lymphocyte count was observed in RM blood at D7 (not in CM). This caused an increase in the M:L and the N:L. Increased M:L has been associated with TB progression in NHPs, but increased M:L is usually attributed to an increase in monocyte numbers. This early reduction in lymphocytes may pre-date expansion of neutrophils and macrophages in the periphery or could coincide with localised expansion of these cell populations in the lungs, but not in the peripheral blood.

3.5.9 Humoral responses to aeBCG infection

A small (significant) decrease in PPD-specific IgG was observed in serum at D2/D14 after aeBCG in RM. Three RM had a high baseline IgG response to PPD (over 1000 arbitrary units). A higher baseline response to PPD could indicate previous mycobacterial exposure, and therefore alter a specific animal's response to a new exposure. Changes in

antibody production were not observed for CM. A small amount of IgG was detectable at PBb in two CM, but otherwise all CM samples were negative for PPD-specific IgG.

Published data on the role of the humoral responses in TB is conflicting[219]. Across five different studies in plasma and serum (human and NHPs), IgG and IgA were increased at D28 and D56 after ID BCG[276]. In another study by Darrah *et al.*, IV BCG administration showed a significant induction of IgG and IgA in response to *M.tb* whole cell lysate, but peaking at D28, rather than D56[5]. The earliest time point explored in plasma by Darrah *et al.*, was D14, at which time point there was no change in IgG, IgA, or IgM titre after aeBCG, compared to baseline[5]. Darrah *et al.*, also explored responses in BALf (10x concentrated) and showed particularly strong responses at Wk4 post IV BCG exposure. At D14, there was a small increase in IgM titre in the BALf, but no difference in IgG or IgA after aeBCG group (dose of $5x10^7$ CFU)[5].

In this project, changes in IgG titre was not detected in either neat or concentrated (5-15 times) BALf. Discrepancies between the results of the experiments detailed here and published data could be partly influenced by BCG dose at the point of exposure. Although the target dose in these experiments was $1x10^7$ CFU per animal, actual doses ranged from $2.34x10^6$ - $6.50x10^6$ CFU.

3.5.10 Macaque species comparison

After *M.tb* challenge, RM are more likely to succumb to active disease than CM (exception of Mauritian CM)[125]. The resistance of CM to TB has recently been demonstrated using a high dose *M.tb* challenge; all six BCG-vaccinated animals controlled infection until the study endpoint (Wk26), whereas unvaccinated animals had significant disease by Wk10[253]. IFNγ production after high dose *M.tb* challenge in CM was low, and the peak

response after *M.tb* challenge was at Wk2, compared to Wk4 in comparable RM studies[45]. Lower levels of anti-inflammatory monocytes (CD163+MerTK+) were identified in CM compared to RM[4]. Together, this suggest that a fast response to control infection initially, coupled with a bias towards rapid-acting, pro-inflammatory effector memory T-cells, contribute to better mycobacterial control in CM.

Alongside functional differences, the ratio of M:L is different between macaque species. Chinese CM have lower M:L than more susceptible species (RM and Mauritian CM), and this ratio remains stable after *M.tb* infection, where the M:L ratio increases by Wk12 of infection in RM/Mauritian CM[117]. Increased M:L in RM is echoed by the fact that increased M:L ratio is a risk factor for disease in humans[149]. In this project, the M:L ratio for CM remained unchanged, but the ratio increased early after aeBCG for RM. Previously published data showed an increase in M:L weeks after *M.tb* infection in RM driven by increased monocytes, which may represent a different effect to the early (D7) reduction in lymphocytes observed here.

Increased CD4+:CD8+ T-cell ratio at D7 was observed in this project in both species (PBMCs), suggesting an early response to aeBCG. The CD4+:CD8+ ratio was higher in RM than CM, in line with published data[120]. CD161 expression increased across T-cell subsets in both species after aeBCG and $\gamma\delta$ T-cell frequency did not change in either species. CD56+ cell frequency among T-cells increased across compartments (D7), but only in the RM. In RM, HLA-DR expression was temporarily reduced at D2 (BAL and WB), but was no different to baseline at D14 (no change in CM). It is possible that the reduction in HLA-DR expression detected here early after aeBCG represents a slower/less inflammatory initial response in RM, that could hinder their ability to control mycobacteria. This dataset was

limited by the lack of a D14 time point for CM. The actual dose (target dose was the same) given was also higher for animals in the CM study and D14 PM study in RM than in the D2 and D7 RM PM groups.

3.5.11 Selection of early time points

The time points selected as 'early' for this project were D2/D7 and D14 to act as a bridge to late time point studies. These time points were selected to be comparable to span the early days of infection, and D2 was selected as the earliest time point to allow for the slower replication of mycobacteria compared to other bacterial species[17]. Little response was detected at the time points selected for innate cells (e.g. γδ/MAIT/NK cells) or antigen-specific cytokine production. This could be because the D2 time point was not early enough after aeBCG. For example, it is widely accepted that neutrophil infiltration after mycobacterial infection peaks at D1 in mice[139]. After infection with *Mycobacterium kansasaii*, IFNγ is produced at D1 in mice, and bacterial load increases from D1 in NK cell knockout mice[298]. The increase in bacterial load in knockout mice could be rescued by adoptive transfer of IFNγ or NK cells at D1, but not at Wk2, suggesting a crucial response at D1[298].

Studies of other pathogens have also shown immune responses as early as D1. After infection with COVID-19, the peak of viral inflammation is as early as D1, at which time point cytokine production is significantly increase[299]. IFNα/β production from stromal cells peaks at eight hours after CMV infection and NK cell cytotoxicity is detectable from 12 hours after infection[300].

3.6 Summary and conclusions

3.6.1 Summary

- AeBCG delivery in macaques was feasible and safe at a target dose of $1x10^7$ CFU.

In response to aeBCG:

- PPD-specific IFNγ SFU frequency (ELISpot) remained unchanged in the periphery at D2/D7/D14 after aeBCG. This was mirrored by a lack of antigen specific IFNγ production measured by flow cytometry. These time points are early compared to previously published work, and may be before a response to BCG can be detected[3, 8]. This disproves hypothesis a), which postulated that an immune response would be detectable by ELISpot at these time points after aeBCG at this dose.
- CD4+:CD8+ T-cell ratio (PBMC and BAL), increased at D7 (significant in RM, not significant in CM), suggesting T-cell activation. This ratio was higher in RM from baseline.
- CD4+CD8+ T-cell population, as previously identified[261], was present in both species.
- CD4+CD56+ cell frequency was higher at D7 compared to baseline in PBMCs for CM, and at D14 compared to baseline in BAL cells and MCs from tissues for RM. This may represent induction of an NKT-L cell subset[162]. NK cells and NKT cell frequency varied between tissues. In the RM LNs, CD56+ frequency among T-cells (NKT-L) was higher at D7 and D14 compared to baseline.
- γδ T-cell frequency did not change in either species, despite previous reports of γδ T-cell expansion after BCG[183], disproving hypothesis b).
- In RM, CD161 expression was strongly increased at D14 compared to baseline, across tissue compartments for RM, but not necessarily in combination with Vα7.2,

suggesting a non-MAIT population, contrary to hypothesis c). In CM, CD161 expression increased at D7 in the periphery, but otherwise remained constant. CD161 in this context, may be a marker of transcriptionally similar, innate-like lymphocytes[277, 278].

- Non-lymphocyte frequency of CD14+ and CD16+ cells increased in PBMC for CM, but decreased in BAL. In RM, changes in non-lymphocyte cell frequency across PBMCs, BAL cells and WB were transient and in both directions. In hilar LNs (RM), CD14+ and CD16+ non-lymphocyte cell frequency increased across the time points, which could support hypothesis d), that monocyte frequency and activation would be increased in RM but not in CM. Increased monocyte frequency has previously been associated with *M.tb* infection[270].
- In RM BAL cells and WB, HLA-DR expression was reduced at D2 compared to baseline, across T-cell subsets. In BAL, HLA-DR expression increased at D14 compared to baseline (data not available for WB HLA-DR expression at D14). PBMC and tissue frequency of HLA-DR on T-cells increased from at D14 compared to D2/D7. Changes in HLA-DR expression were not observed for CM.
- Frequency of the anti-inflammatory MerTK+ and CD163+ monocyte population in WB was lower in RM than CM, contrary to previously published data and hypothesis d)[4].
- Changes in antigen-specific cytokine production were minimal. The tissue compartment with the most altered cytokine production was the LNs, which is where antigen presenting cells migrate to, to activate T-cells[130]. In other compartments, changes in IL-17 production were more pronounced than changes in IL-2 or IFNγ.
- In WB (measured by haematology analyser), total lymphocytes count decreased at D2 and D7 in RM and caused an increase in the M:L and N:L ratios. Changes in ratio were

not seen for CM. Increased M:L ratio is associated with active TB, but this has previously been attributed to increased monocyte count[117].

- In WB, expression of the B-cell marker CD20 increased slightly at D7 (CM) and D2 (RM). These increases were not accompanied by increased antibody titre. In serum, RM showed low level PPD-specific IgG antibody responses from before aeBCG. IgG titre decreased at D2 and 14 post aeBCG compared to baseline. Almost no IgG antibody was detected in CM at any time point.
- Concentration of 42-45 mL of BALf to 3-8 mL was successful in increasing the measurable PPD-specific IgG titre, but could not be reliably quantified using a phospholipid quantification assay.
- The small quantity of IgG measured in neat or concentrated BALf decreased at D14 (none detected) compared to D7, but was unchanged at D14 compared to baseline. Limited detection of a PPD-specific antibody response early after aeBCG is in alignment with hypothesis e).

3.6.2 Conclusions

- After aeBCG, there was little change in the immune parameters measured here, up until D14 after aeBCG, despite a renewed interest in innate immunity in the context of TB[272]. $\gamma\delta$ T-cell frequency and cytokine production did not substantially change.
- In the early response to aeBCG, RM and CM show a transient ratio change in conventional T-cells (CD4+:CD8+ increase), an increase in CD56+CD4+ T-cells, and an increase in CD161 expression. These subtle changes may represent activation of innate-like T-cells.

- CM and RM differed in that there was: a more pronounced increase in CD161 expression (and across all tissues, not just PBMC) in RM, a detectable loss of lymphocytes at Day2/7 in RM only (haematology analyser and PBMC flow), a decrease in the low level of antibody detected at D2 and 14 compared to baseline in RM only, an increase in Fas expression only on CD8+ T-cells, an increase in monocyte markers in the periphery in CM only and lower frequency of MerTK+/CD163+ monocytes in RM than CM.

Chapter 4: Late immune response to aeBCG - delivered by mask or mouthpiece

Chapter 4: late immune response to aeBCG – delivered by mask or mouthpiece

4.1 Statement of authorship

The author processed NHP samples from UK-HSA (Porton Down), with help from the NHP team at UK-HSA where necessary to process a large number of samples. Andrew White and members of the Biological Investigations group exposed animals to aeBCG or aeSaline, and BCG titres were calculated by the bacteriology team, led by Simon Clark at UK-HSA. All assays described were performed and analysed by the author. Flow cytometry panel 1 was based on previous panels designed by Andrew White, and panel 2 was adapted from this, with the help of Andrew White and Iman Satti.

4.2 Background

To deliver aeBCG to NHPs or humans, an Omron Jet mesh nebuliser can be used in combination with a modified paediatric mask, or with a mouthpiece attachment (Figure 4.1). In pilot studies, mask delivery of $1x10^6$ CFU aeBCG resulted in higher frequency of PPD-specific IFNγ SFU measured by ELISpot, than mouthpiece delivery (White *et al.,* unpublished). aeBCG delivered by mouthpiece resulted in a delayed immune response compared to ID BCG[3, 7]. After $1x10^7$ CFU aeBCG, BCG could be recovered from the BAL immediately after delivery (D1) until Wk4, with significantly higher recovery after mask delivery than mouthpiece (White *et al.*, unpublished).

Preliminary data from another experiment showed that droplet deposition (measured by computed tomography) following AE exposure varied depending on the attachment used to deliver gold particles - estimated to be similar size to *M.tb* bacilli

(White *et al.,* unpublished). After mask delivery, deposition of gold nanoparticles could be identified in the nasopharynx and higher in the trachea, compared to delivery further into the lungs after mouthpiece delivery. After mouthpiece delivery, droplets were also detected in the stomach and oesophagus, which suggests that more BCG might be swallowed using this delivery method. In theory, altered droplet deposition could change the timing and focus of the immune response to aeBCG. BCG location in the lung has previously been explored in studies of the effect of blood flow due to gravity in rabbits and bats[301].

This chapter presents the results of a head-to-head comparison of mask and mouthpiece aeBCG delivery. Evaluation time points included were designed to parallel an ongoing study of aeBCG in humans, using a mouthpiece attachment (TB043: McShane group, Oxford – ClinicalTrials.gov ID: NCT03912207), and to allow characterisation of the immune response to aeBCG.

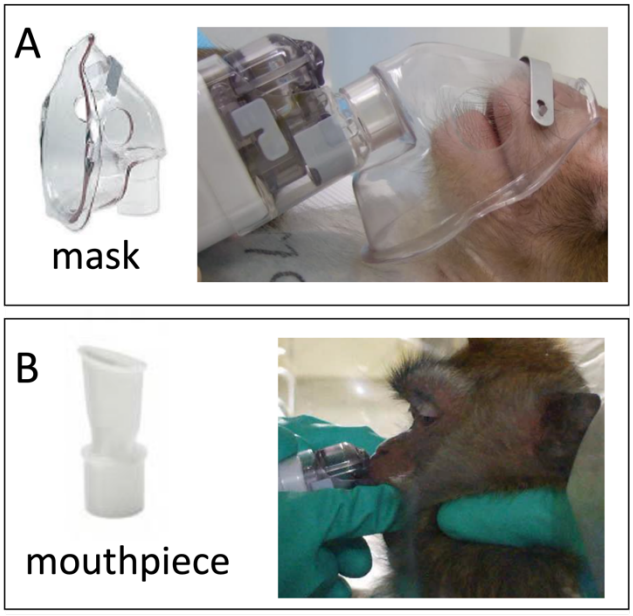


Figure 4.1 BCG aerosolisation methods

*BCG can be aerosolised using an Omron Jet nebuliser and delivered using either a modified paediatric mask (**A**), or a mouthpiece attachment (**B**). This setup can be used in humans or NHPs. Animal images are reproduced from with permission from Andrew White at UK-HSA.*

4.3 Objectives & hypotheses

Experiments in this chapter were designed to:

1. Study the late response to aeBCG, across different tissue compartments:
    - PBMCs, WB and serum
    - BALf and BAL cells from the lung mucosa
    - MCs from LNs and lung tissue
2. Compare immune responses elicited by different aeBCG delivery methods:
    - mask
    - mouthpiece
3. Look for correlations between components of the immune response at different time points
4. Explore the following hypotheses:
    a) The immune response to aeBCG will be faster and stronger after mask delivery than mouthpiece delivery, because BCG will not be delivered to the nasopharynx and more of the BCG will be swallowed and delivered lower into the lungs after mouthpiece delivery.
    b) The immune response induced by aeBCG will be detectable using PBMC ELISpot assay, by increased frequency of CD4+ T-cells and by increased production of antigen-specific cytokines from week 4-6 onwards.
    c) Innate T-cell populations including $\gamma\delta$ T-cells and MAIT cells will increase in frequency earlier after aeBCG than CD4+ and CD8+ T-cells.
    d) The frequency of CD161+ lymphocytes will increase at Wk2 after aeBCG, as identified in the previous chapter.

e) Antigen-specific cytokine production will be stronger in BAL than in PBMCs.

f) Antigen-specific antibodies will be produced after aeBCG and be detectable by ELISA at around eight weeks.

4.4 Results

4.4.1 Clinical responses to aeBCG

RM with no prior exposure to BCG were exposed to aeBCG using a mask or mouthpiece attachment (two groups of eight, four male and four female per group). Serial blood and BAL samples were collected up to Wk16 (Figure 4.2). All animals received a single aerosolised exposure to BCG Danish strain 1331 (AJ Vaccines, Copenhagen). Two/three weeks prior aeBCG, clinical data, blood and BAL samples were taken at pre-BCG A (PBa), and assays were performed to give baseline values. An additional pre-BCG blood sample was taken one week before aeBCG (PBb).

At Wk0, an estimated dose of $1x10^7$ CFU of BCG was obtained from multiple vials, as detailed in the methods section (Chapter 2). The target dose was the same as in the 'early' studies (Chapter 3), so that the mouthpiece group would be comparable. After 16 weeks, a lethal dose of anaesthetic was injected and tissues were collected, processed, and cryopreserved alongside any unused PBMCs/MCs, serum, or BALf (Wk17).

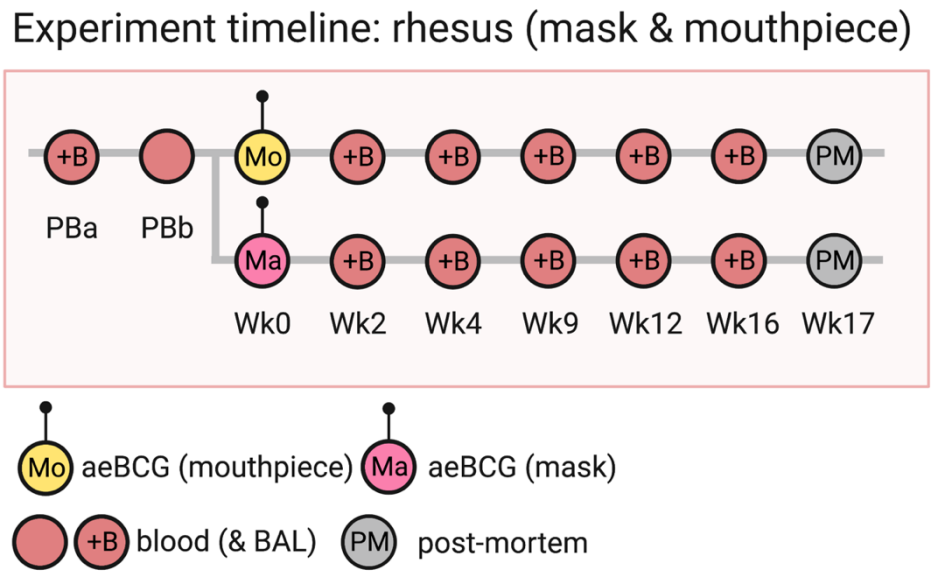


Figure 4.2 Study design (late time points)

Experimental design for comparison of aerosol BCG (aeBCG) delivery methods and to explore the late response to aeBCG delivery. $1x10^7$ CFU of aeBCG (target dose) was delivered to rhesus macaques via Omron nebuliser with either a mask or mouthpiece attachment at Week 0 (Wk0). Clinical data, blood, and broncho-alveolar lavage (BAL) samples were taken at pre-BCG A (PBa), pre-BCG B (PBa), and Wk2-Wk16. Animals were euthanised at Wk17, and clinical data, blood, BAL, and tissue samples were taken post-mortem (PM). Image created with Biorender.com.

4.4.2 Clinical measures of health after aeBCG

Clinical parameters monitored in animals in this project included: body weight, rectal temperature, and red blood cell haemoglobin level (Figure 4.3) and LN size and other observable signs of change. Erythrocyte sedimentation rate was unchanged after aeBCG. Animal 59X was segregated from the group at Wk9 after weight loss, but the animal was returned to the group for the remainder of the study after its weight re-stabilised. After aeBCG, haemoglobin levels dropped from a median of 131 at baseline to 125 at Wk2/ Wk4, before returning to baseline levels by Wk9 (median 131). This reduction in haemoglobin did not bring haemoglobin levels out of the normal range (over 100), and may be due to repeated venesection in a short period of time (4 bleeds within 7 weeks), or aeBCG itself.

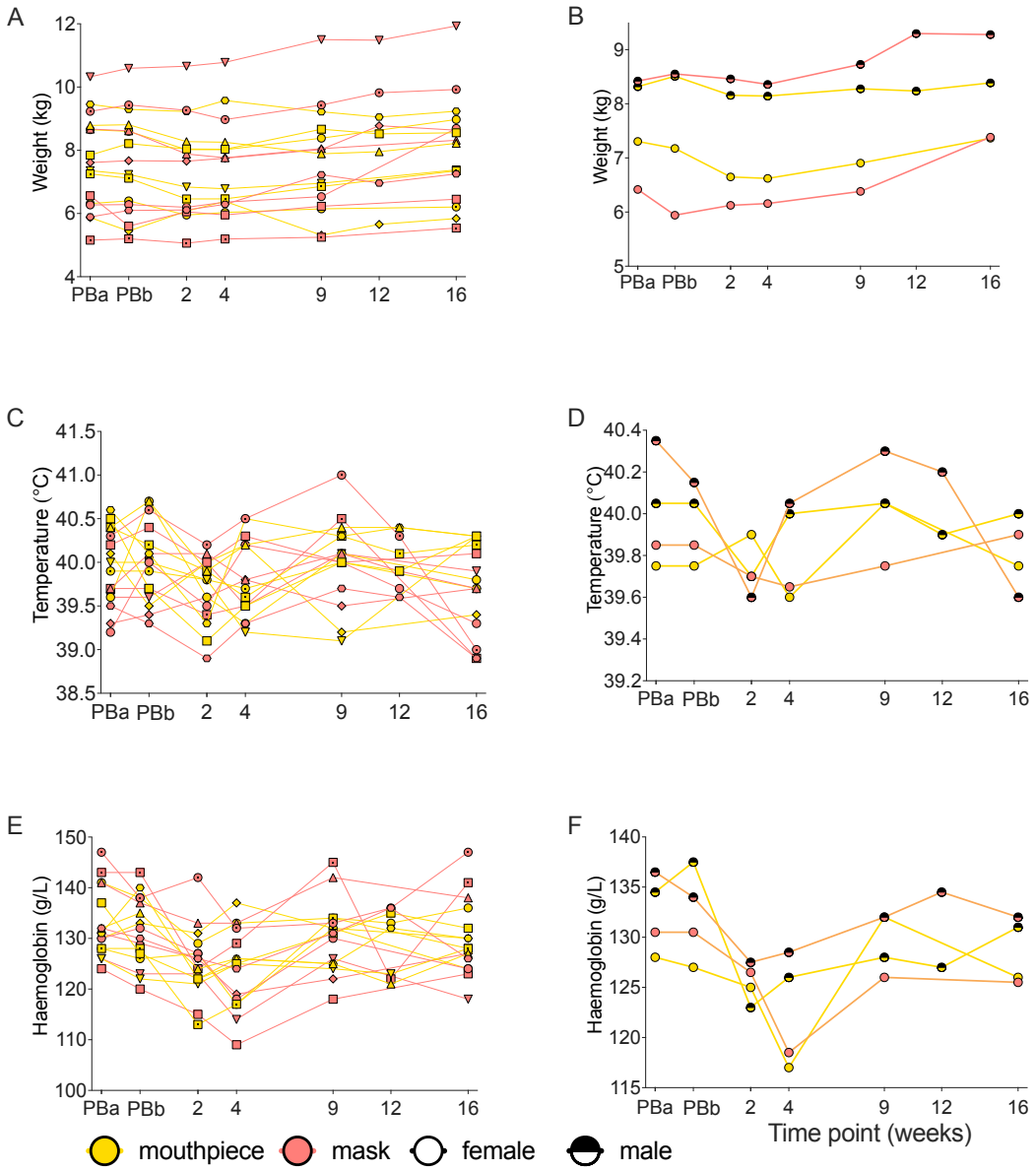


Figure 4.3 Clinical readouts throughout early time point studies.

*Individual body weights were plotted (**A** & **B**), alongside rectal temperature (**C** & **D**), and haemoglobin level (**E** & **F**). Rhesus macaques exposed to aerosol BCG (aeBCG) via a mask attachment are shown in pink, and mouthpiece in yellow. Individual animals are indicated by different symbols (**A**, **C** & **E**) and group medians are shown for female (open circles) and male (half black circles) animals, grouped by delivery method (**B**, **D** & **F**). Samples were taken at pre-BCG A (PBa) and pre-BCG B (PBa), and at different time points after aeBCG (Week 2-16, Wk2-Wk16).*

4.4.3 Frequency of PPD-specific IFNγ SFU

The systemic immune response to aeBCG between Wk2 and Wk16 was profiled using an *ex vivo* ELISpot assay. There was no difference between mask and mouthpiece delivery groups at any time point, by Mann-Whitney U-test between delivery groups at each time point, or by comparison of the area under the curve (AUC) for different animals within each delivery group. For this reason, data from both delivery groups were analysed together to enable more robust evaluation of the immune response to aeBCG.

Two sets of statistical analysis were applied to compare PPD-specific IFNγ SFU frequency after aeBCG to baseline frequency (Table 4.1). Shapiro Wilk's normality test showed that samples were not normally distributed. Therefore, non-parametric Friedman test with Dunnett's correction for multiple comparisons was used to compare each time point after aeBCG to either PBa or PBb. PBa is referred to as 'baseline' for all assays because baseline BAL samples were taken at PBa. Wilcoxon-Rank test between each time point and baseline was also performed (uncorrected), to allow comparison to flow cytometric analysis of PBMC (described later in this chapter).

Spearman's rank correlation coefficient (r_s) was calculated to determine whether SFU frequency at two time points correlated. The only significant correlation was found between Wk2 and Wk4 (r_s=0.605, p=0.0103).

ELISpot: mask and mouthpiece											
analysis		Friedman test & Dunnett's multiple comparisons					Wilcoxon-Rank testing				
time point		Wk2	Wk4	Wk9	Wk12	Wk16	Wk2	Wk4	Wk9	Wk12	Wk16
all data	compared to PBa	ns	*	*	ns	***	ns	**	***	**	****
mask		ns	ns	ns	ns	*	ns	*	*	**	**
mouthpiece		ns	ns	ns	ns	*	ns	ns	*	ns	ns
all data	compared to PBb	ns	ns	*	ns	**	ns	ns	*	ns	**
mask		ns	ns	ns	ns	ns	ns	ns	ns	ns	**
mouthpiece		ns	ns	ns	ns	*	ns	ns	ns	ns	ns

Table 4.1 Changes in frequency of PPD-specific IFNγ producing cells later after aerosol BCG (aeBCG)

PPD-specific IFNγ producing cells in peripheral blood mononuclear cells (PBMC) were measured using ELISpot, and statistical comparisons of this data are shown for all animals or mask/mouthpiece delivery group animals alone (rows). Statistical comparisons between paired samples at baseline (PBa/PBb) and time points after aeBCG were made using either a Friedman test with Dunnett's correction for multiple comparisons (left), or using separate Wilcoxon-Rank tests (right). Adjusted P-values are shown for the Friedman test, and un-corrected values for Wilcoxon-Rank testing. Comparisons are marked as not significant (ns), P < 0.05 (*), P < 0.005 (**), P < 0.001 (***) or P < 0.0001 (****) – increases are shown in yellow.

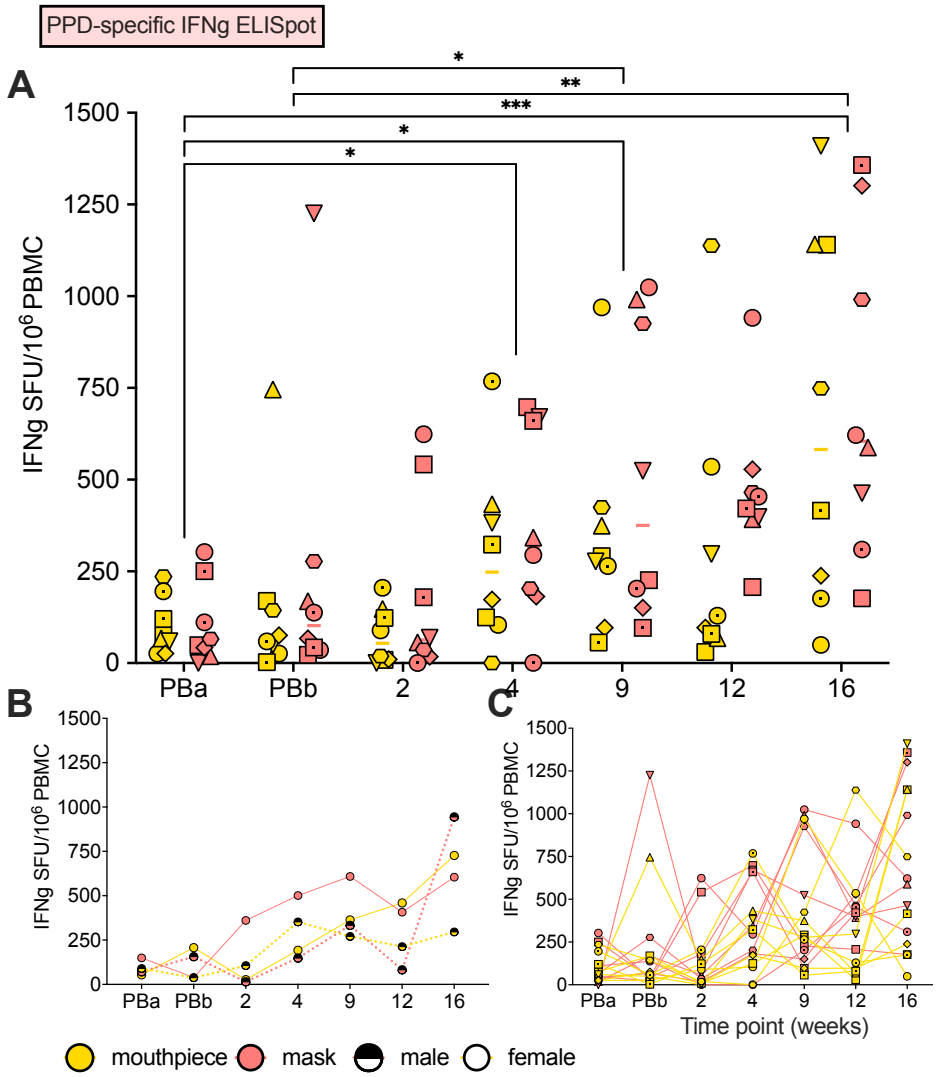


Figure 4.4 Frequency of PPD-specific IFNγ spot forming units (SFU) later after aerosol BCG

*Systemic PPD-specific IFNγ spot SFU are shown per million cells, for rhesus macaques exposed to aerosol BCG delivered by mask (pink) or mouthpiece (yellow). Individual animals and group medians (**A**), animals grouped by sex and delivery method (**B**, males - half black circles, females – open circles), and animals tracked over time (**C**) are shown. Baseline values are shown at pre-BCG A and B (PBa and PBb) before aerosol BCG. Data from all animals were analysed together using a Mixed Effects model with Dunnett's correction for multiple comparisons. Where comparisons remain significant, adjusted P-values are marked (**A** only for simplicity): P < 0.05 (*), P < 0.005 (**) or P < 0.001 (***).*

4.4.4 PBMC cell populations

There was also no difference between the AUC of mask and mouthpiece delivery groups when comparing cell populations profiled in PBMC samples using flow cytometry (antibody Panel 1, as in Chapter 3). Technical issues at PBa (female samples affected) and Wk16 (male samples affected) limited sample size at these time points. AUC analysis of the responses of animals grouped by gender revealed the frequency of CD3+ lymphocytes to be higher in females than males. However, baseline values for female samples could not be included in this AUC analysis, which means that a difference in CD3+ lymphocyte frequency between the sexes cannot be ruled out.

Of 138 Mann-Whitney U-tests conducted to compare PBMC cell populations at each of the time points measured, three significant differences were identified between delivery groups: Vα7.2+ CD8+ T-cell (baseline), CD14+CD16- non-lymphocyte (Wk2) and CD14-CD16+ non-lymphocyte (Wk16) frequency. This exploratory analysis did not include correction for multiple comparisons, and the difference in Vα7.2+ CD8+ T-cell frequency at baseline is not relevant to aeBCG delivery method. The differences in non-lymphocyte populations were transient and were treated as biologically insignificant (Figure 4.5).

To increase sample size, results from both delivery groups were combined to explore aeBCG effect on PBMC cell populations (Table 4.2). It was not possible to use the Freidman test or Mixed Effects model to analyse cell populations characterised by PBMC flow cytometry (technical error at PBa/Wk16). Instead, multiple Wilcoxon-Rank tests were used to compare paired data at each time point to baseline (comparison between baseline and Wk16 was not possible). No significant differences were detected when samples were split by delivery group.

PBMC: mask and mouthpiece					
analysis	Wilcoxon-Rank testing				
time point	Wk2	Wk4	Wk9	Wk12	Wk16
CD14-3+(T cell)	*	ns	ns	ns	x
CD4 T cell	ns	ns	ns	ns	x
CD8 T cell	ns	ns	**	ns	x
CD4+8+ T cell	ns	ns	ns	ns	x
CD4+8++ T cell	**	*	**	*	x
CD4-8- T cell	ns	ns	**	ns	x
CD56+ CD4+ T cell	ns	ns	**	ns	x
gamma-delta T cell	*	*	ns	ns	x
Va7.2+ CD8+ T cell	ns	ns	*	ns	x
CD161+Va7.2+ CD8+ T cell	*	*	*	ns	x
CD161+Va7.2- CD8+ T cell	**	ns	*	ns	x
CD161-Va7.2+ T cell	**	ns	ns	ns	x
CD16+ T cell (NKT-like)	ns	**	**	*	x
CD56+ T cell (NKT-like)	ns	ns	ns	ns	x
CD16+CD56+ T cell (NKT-like)	ns	ns	ns	ns	x
CD16+56+ CD3- (NK cell)	ns	*	ns	ns	x
CD16-56+ CD3- (NK)	*	ns	ns	ns	x
CD16+56- CD3- (NK)	ns	*	**	ns	x
CD14+ non-lymphocyte	ns	ns	ns	ns	x
CD16+ non-lymphocyte	ns	ns	ns	ns	x
CD14+CD16+ non-lymphocyte	ns	ns	ns	ns	x
CD14+CD16- non-lymphocyte	ns	ns	ns	ns	x
CD14-CD16+ non-lymphocyte	*	*	ns	**	x

Table 4.2 Peripheral blood mononuclear cell (PBMC) populations

Changes in cell population frequencies were analysed among PBMCs from rhesus macaques exposed to aerosol BCG. Statistical comparisons between paired samples at baseline and time points after aerosol BCG (aeBCG) were made using Wilcoxon-Rank testing. Significant P-values are marked: P < 0.05 (*), P < 0.005 (**) or P < 0.001 (***), with increases shown in yellow, and decreases in blue.

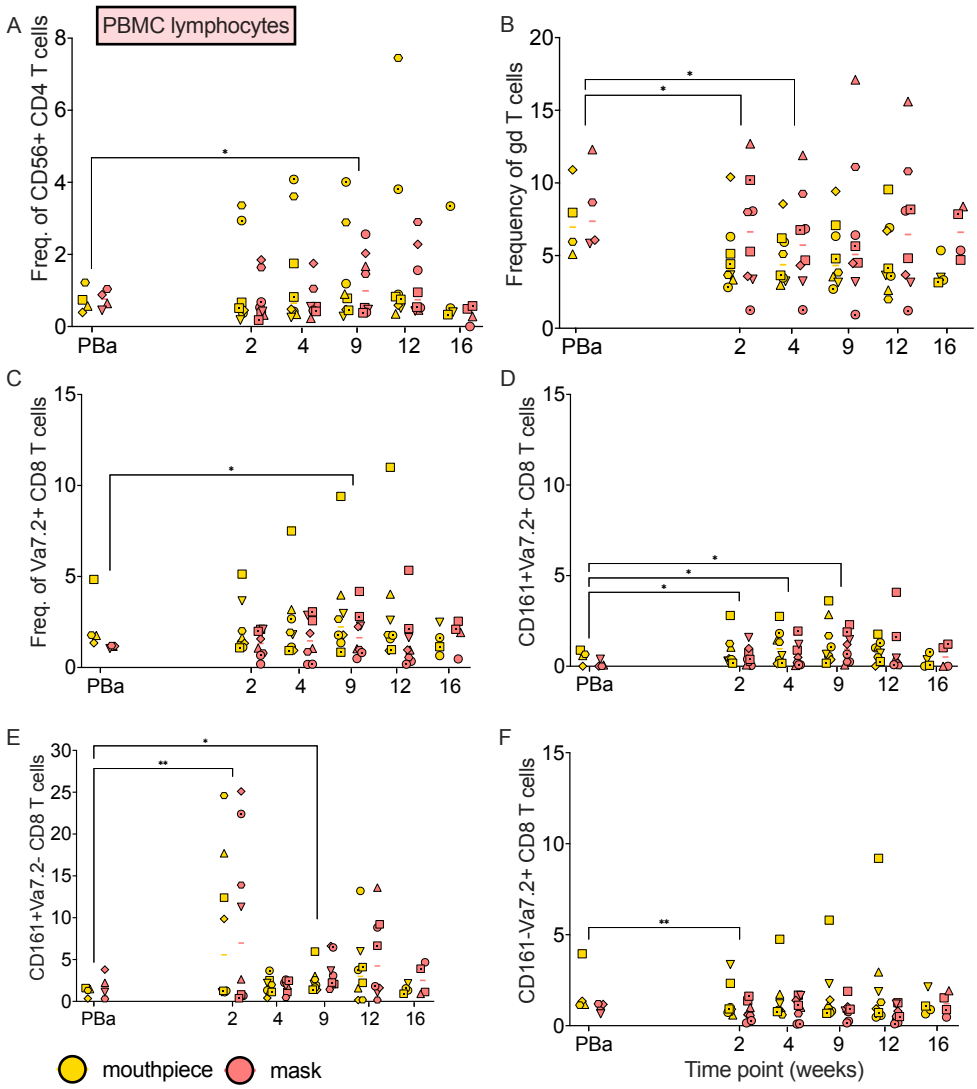


Figure 4.5 Cell populations among CD3+ lymphocytes characterised among peripheral blood mononuclear cells (PBMCs)

*The frequency of CD3+ lymphocytes (**A**), $\gamma\delta$ T-cells (**B**) and MAIT-cell subsets (**C**-**F**) are shown in comparison to pre-BCG A (PBa). Rhesus macaques exposed to aerosol BCG (aeBCG) by mouthpiece (yellow) and mask (pink) delivery are shown at time points after aeBCG (weeks) and at baseline (PBa). Each symbol represents a different animal and group medians are shown. Data from all animals were analysed together. Wilcoxon-Rank Testing was used to analyse changes compared to paired baseline values. Where significant, comparisons are marked: $P < 0.05$ (*) or $P < 0.005$ (**).*

CD3+ lymphocytes (T-cell) frequency among PBMCs transiently decreased at Wk2 compared to baseline (*p*=0.0259 – Figure 4.5). CD4+CD8+ T-cell frequency was increased at Wk2-Wk12 compared to baseline, particularly at Wk9 (*p*=0.0078), when CD8+ T-cell frequency was also increased (*p*=0.0078). At Wk9, CD4-CD8- T-cell frequency was significantly decreased (*p*=0.0078). CD4+ T-cell frequency did not change among PBMCs, but CD56+CD4+ T-cell frequency was also increased at Wk9 (*p*=0.0078). CD56+ and CD4+ co-expression may represent an NKT-L subset among CD4+ T-cells. At Wk2/Wk4, $\gamma\delta$ T-cell frequency was reduced compared to baseline (*p*=0.0156/0.0234).

The frequency of cells expressing CD161 and Vα7.2 among CD8+ T-cells (MAIT markers[171]) increased in line with the kinetic identified by ELISpot/other cell populations. Increased CD161 expression at Wk2 (Chapter 3) was also identified in this dataset. CD161+Vα7.2- CD8+ T-cell frequency (*p*=0.0078). A proportion of animals showed a particularly strong increase at Wk2, where others expressed a similar level to baseline.

CD16+ (NKT-L) cell frequency increased at Wk4/Wk9/Wk12 compared to baseline (*p*=0.0078/0.0078/0.0234, respectively). CD56+ cells T-cell frequency remained unchanged. CD16+ CD3-CD8+ (NK) cell frequency increased at Wk4/Wk9 compared to baseline (*p*=0.0156/0.0078, respectively), and CD56+ CD3-CD8+ cell frequency increased at Wk2 (*p*=0.0312). Among non-lymphocyte cells, CD14-CD16+ cell frequency decreased at Wk2/Wk4/ Wk12 compared to baseline (*p*=0.0391/0.0156/0.0078, respectively). Total CD16+ non-lymphocyte frequency remained unchanged (Figure 4.6).

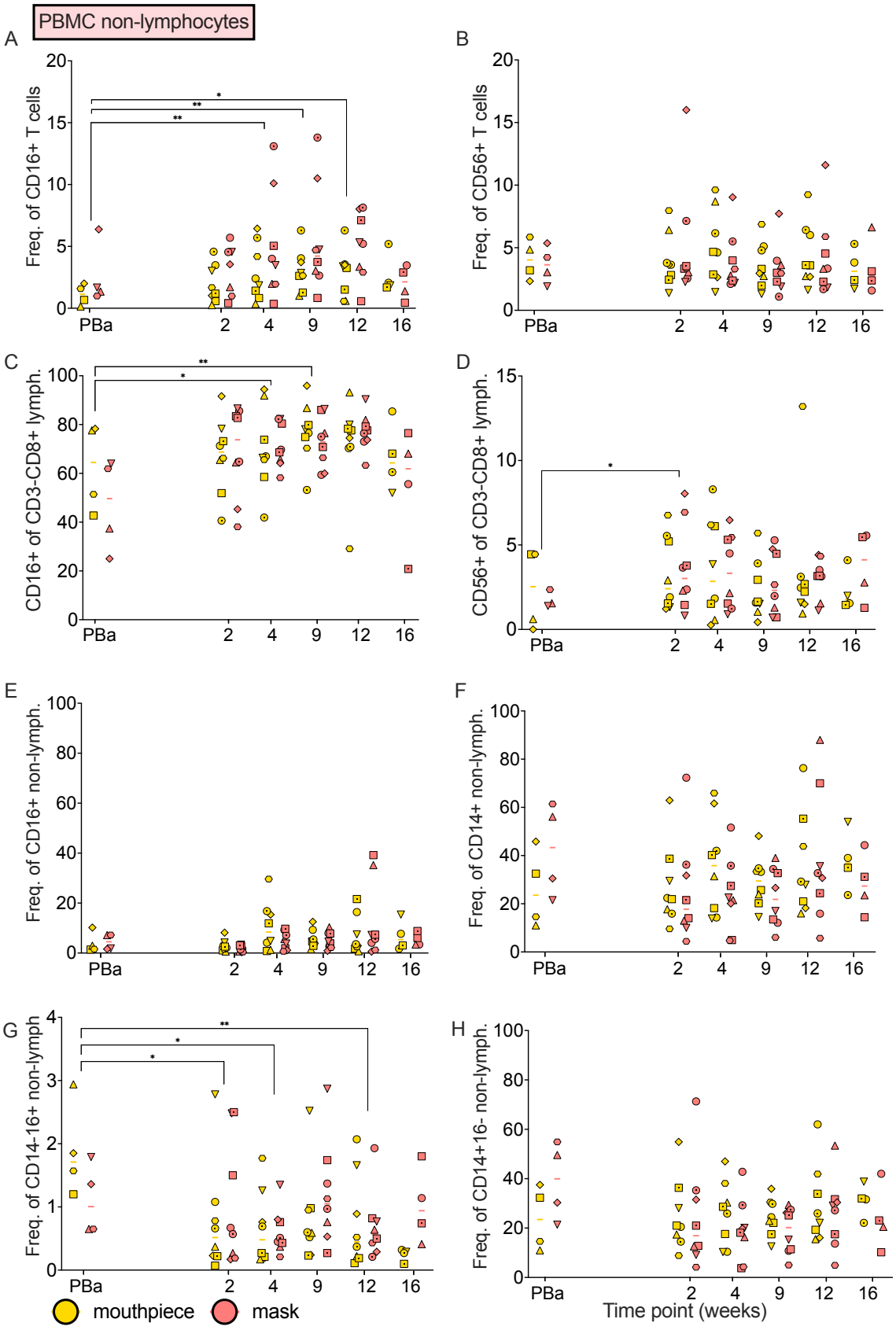

PBMC non-lymphocytes
A
Freq. of CD16+ T cells
B
Freq. of CD56+ T cells
C
CD16+ of CD3-CD8+ lymph.
D
CD56+ of CD3-CD8+ lymph.
E
Freq. of CD16+ non-lymph.
F
Freq. of CD14+ non-lymph.
G
Freq. of CD14-16+ non-lymph
H
Freq. of CD14+16- non-lymph.
PBa
2
4
9
12
16
Time point (weeks)
mouthpiece
mask

Figure 4.6 CD16+ and related cell populations characterised among peripheral blood mononuclear cells (PBMCs)

*The frequency of CD16+ cells within CD3+ lymphocytes (**A**), CD3-CD8+ lymphocytes (**C**), total non-lymphocyte cells (**E**), and CD14- non-lymphocyte cells (**G**) are shown in comparison to pre-BCG A (PBa) on the left-hand side. Other cell populations are shown on the right: CD56+ cells within CD3+ lymphocytes (**B**) and CD3-CD8+ lymphocytes (**D**), CD14+ total non-lymphocyte cells (**F**), and CD14+CD16- non-lymphocyte cells (**H**). Rhesus macaques exposed to aerosol BCG (aeBCG) by mouthpiece (yellow) and mask (pink) delivery are shown at time points after aeBCG (weeks) and at baseline (PBa). Each symbol represents a different animal and group medians are shown. Data from all animals were analysed together and statistical comparisons between paired data were performed using Wilcoxon-Rank Testing. Where significant, comparisons are marked: P < 0.05 (*) or P < 0.005 (**).*

4.4.5 BAL cell populations

No differences were identified between AUC values for BAL cell populations in samples from the different delivery groups or between male/female animals. Mann-Whitney U-test showed differences between delivery groups in frequencies of: CD3+ lymphocytes (Wk16), CD8+ T-cells at Wk9/Wk12 (difference detected at baseline, but not significant), CD4+CD8+ T-cells (from baseline). These differences were not considered biologically relevant, and data from all animals were grouped together to examine the immune response to aeBCG. Shapiro-Wilk normality test was performed followed by the Mixed Effects model with Dunnett's correction for multiple comparisons (parametric data). Non-parametric data were examined using multiple Wilcoxon-Rank tests (Table 4.3). Not all

significant differences identified by Wilcoxon-Rank test (not corrected) persist using the Mixed Effects model with correction for multiple comparisons.

BAL: mask and mouthpiece										
analysis	Mixed Effects (Dunnett's)					Wilcoxon-Rank testing				
time point	Wk2	Wk4	Wk9	Wk12	Wk16	Wk2	Wk4	Wk9	Wk12	Wk16
CD14-3+ (T cell)	ns	ns	ns	ns	ns	ns	ns	ns	*	ns
CD4 T cell	ns	*	*	ns	ns	ns	**	*	*	*
CD8 T cell	ns	ns	**	*	*	ns	ns	**	**	**
CD4+8+ T cell	ns	ns	**	**	**	ns	ns	**	***	**
CD4+8++ T cell	x	x	x	x	x	*	ns	ns	ns	ns
CD4-8- T cell	x	x	x	x	x	**	ns	*	**	ns
CD56+ CD4+ T cell	x	x	x	x	x	*	*	**	**	***
gamma-delta T cell	x	x	x	x	x	ns	*	ns	ns	ns
Va7.2+ CD8+ T cell	x	x	x	x	x	*	**	***	ns	ns
CD161+Va7.2+ CD8+ T cell	x	x	x	x	x	***	***	***	ns	***
CD161+Va7.2- CD8+ T cell	x	x	x	x	x	***	ns	***	ns	*
CD161-Va7.2+ T cell	x	x	x	x	x	ns	ns	ns	**	ns
CD16+ T cell (NKT-like)	x	x	x	x	x	ns	ns	ns	ns	ns
CD56+ T cell (NKT-like)	x	x	x	x	x	ns	ns	ns	ns	ns
CD16+CD56+ T cell (NKT-like)	x	x	x	x	x	ns	ns	ns	ns	ns
CD16+56+ CD3- (NK cell)	ns	ns	ns	ns	ns	ns	*	ns	ns	ns
CD16-56+ CD3- (NK)	ns	ns	ns	ns	ns	ns	ns	ns	ns	ns
CD16+56- CD3- (NK)	x	x	x	x	x	*	**	*	ns	ns
CD14+ non-lymphocyte	x	x	x	x	x	***	**	**	***	*
CD16+ non-lymphocyte	x	x	x	x	x	***	ns	ns	**	ns
CD14+CD16+ non-lymphocyte	x	x	x	x	x	***	ns	ns	**	ns
CD14+CD16- non-lymphocyte	****	**	ns	**	*	***	***	*	***	*
CD14-CD16+ non-lymphocyte	x	x	x	x	x	ns	ns	ns	ns	ns

Table 4.3 Broncho-alveolar lavage (BAL) cell populations

Changes in cell population frequencies were analysed among BAL cells from rhesus macaques exposed to aerosol BCG. Statistical comparisons between paired samples at baseline and time points after aerosol BCG (aeBCG) were made using a Mixed Effects model with Dunnett's correction for multiple comparisons (left – parametric data only) and Wilcoxon-Rank testing (right). Significant P-values are marked: P < 0.05 (*), P < 0.005 (**) or P < 0.001 (***), with increases in yellow, and decreases in blue.

In BAL, CD4+ T-cell frequency increased at Wk4/Wk9, CD4+CD8+ T-cell frequency increased at Wk9/Wk12/Wk16 and CD8+ T-cell frequency decreased at Wk9/Wk12/Wk16 (p=0.0275/0.0289, p=0.0086/0.0079/0.0059 and p=0.0060/0.0459/0.0476, respectively – Figure 4.7).

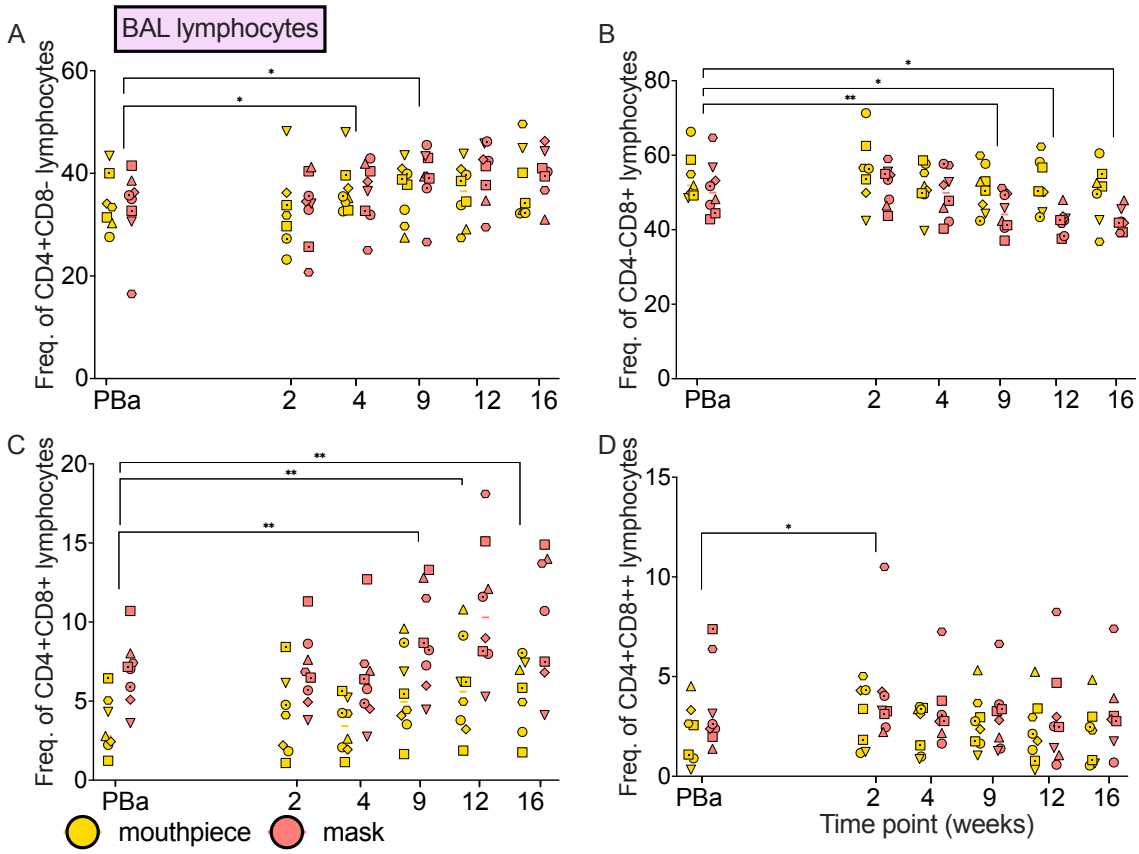
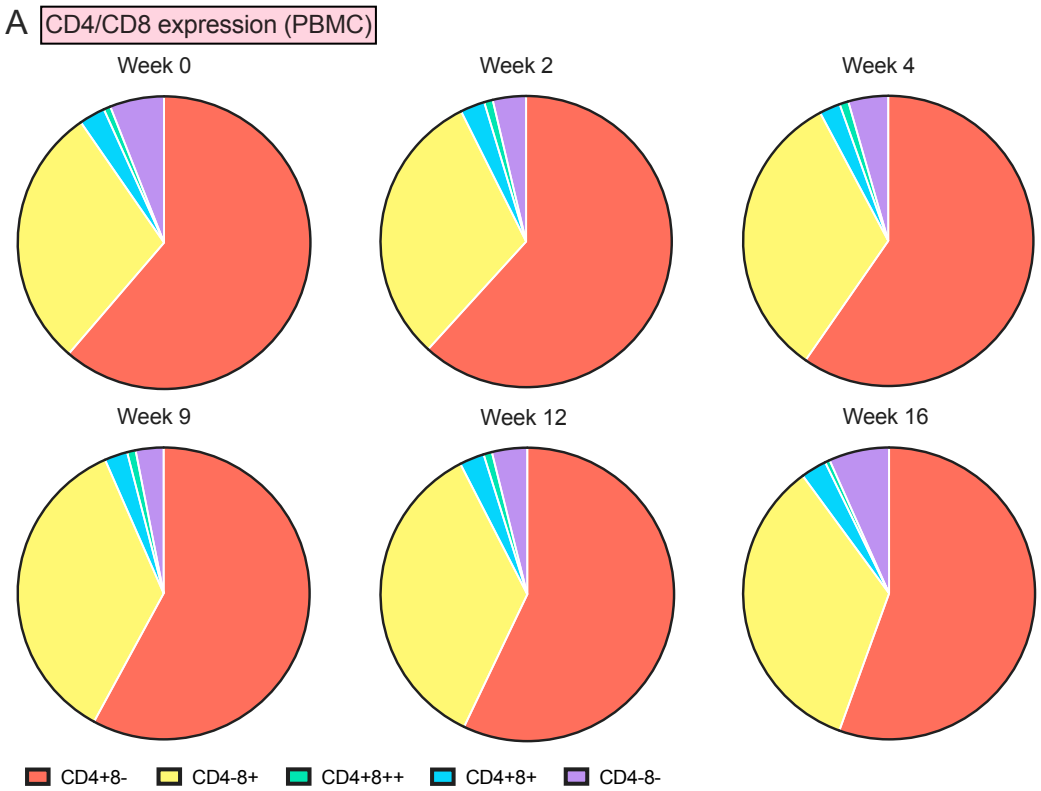


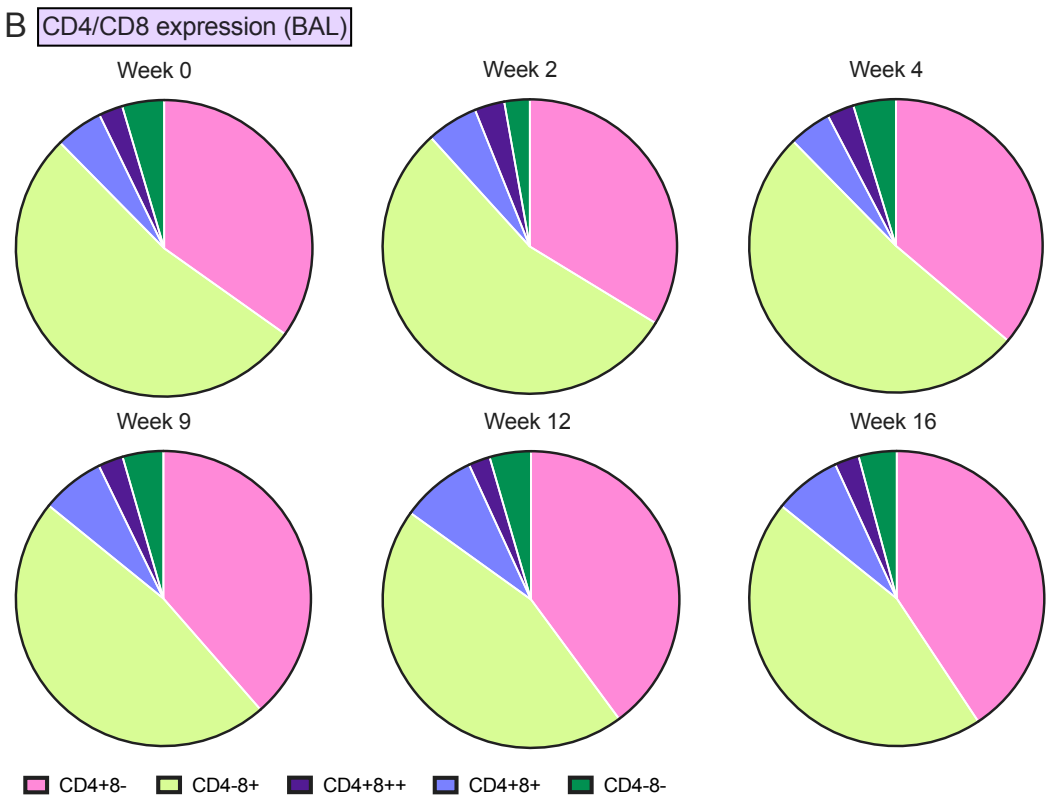
Figure 4.7 CD4+ and CD8+ T-cells characterised among broncho-alveolar lavage (BAL) cells

*The frequency of CD4+/CD8+ subsets within CD3+ BAL lymphocytes are shown in comparison to pre-BCG A (PBa): CD4+CD8- (**A**), CD4-8+ (**B**), CD4+CD8+ (**C**), and CD4+CD8++ (**D**).Rhesus macaques exposed to aerosol BCG (aeBCG) by mouthpiece (yellow) and mask (pink) delivery are shown at time points after aeBCG (weeks) and at baseline (PBa). Each symbol represents a different animal and group medians are shown. Data from all animals were analysed together using a Mixed Effects model with Dunnett's correction for multiple comparisons (parametric), or using multiple Wilcoxon-Rank tests (non-parametric). Where comparisons remain significant, P-values are marked: P < 0.05 (*), P < 0.005 (**) or P < 0.001 (***).*

The CD4+:CD8+ T-cell ratio was higher in PBMCs than BAL at all time points, and increased across time points in the BAL, where it decreased in the PBMC (Figure 4.8). CD4+CD8++ T-cell frequency remained unchanged, and CD4-CD8- frequency was decreased at Wk2 compared to baseline, but not at other time points. CD56+ CD4+ T-cells decreased at Wk2-Wk16 compared to baseline in BAL. This is in contrast to PBMCs, where CD56+ CD4+ T-cell frequency increased at Wk9 compared to baseline.

In BAL, γδ T-cell frequency was unchanged after aeBCG. CD161+Vα7.2+ CD8+ T-cell frequency increased at Wk2/Wk4/Wk9/Wk16 compared to baseline (p=0.0007/<0.0001/<0.0001/0.0005, respectively – Figure 4.9). CD161+Vα7.2+ CD8+ T-cell frequency was higher in BAL cells than in PBMCs (e.g. median 19% CD8+ T-cells at Wk2 in BAL vs 11% in PBMC). CD161-Vα7.2+ CD8+ T-cell frequency was only increased at Wk12 compared to baseline (p=0.0045), which makes it likely that the increased CD8+ T-cell subsets were driven by increased CD161 expression.





CD4+:CD8+ T cell ratio						
Time point	**PBa**	**Wk2**	**Wk4**	**Wk9**	**Wk12**	**Wk16**
PBMC	2.13	2.03	1.81	1.67	1.58	1.72
BAL	0.68	0.63	0.70	0.83	0.85	0.94

Figure 4.8 CD4+/CD8+ frequency among T-cells characterised among peripheral blood mononuclear cells (PBMCs) and broncho-alveolar lavage (BAL) cells

*The frequency of different CD4+/CD8+ T-cell subsets are presented in pie charts, using the median value for each cell population among PBMCs (**A**) and BAL (**B**). The median ratio of CD4+:CD8+ T-cells is shown in **C**.*

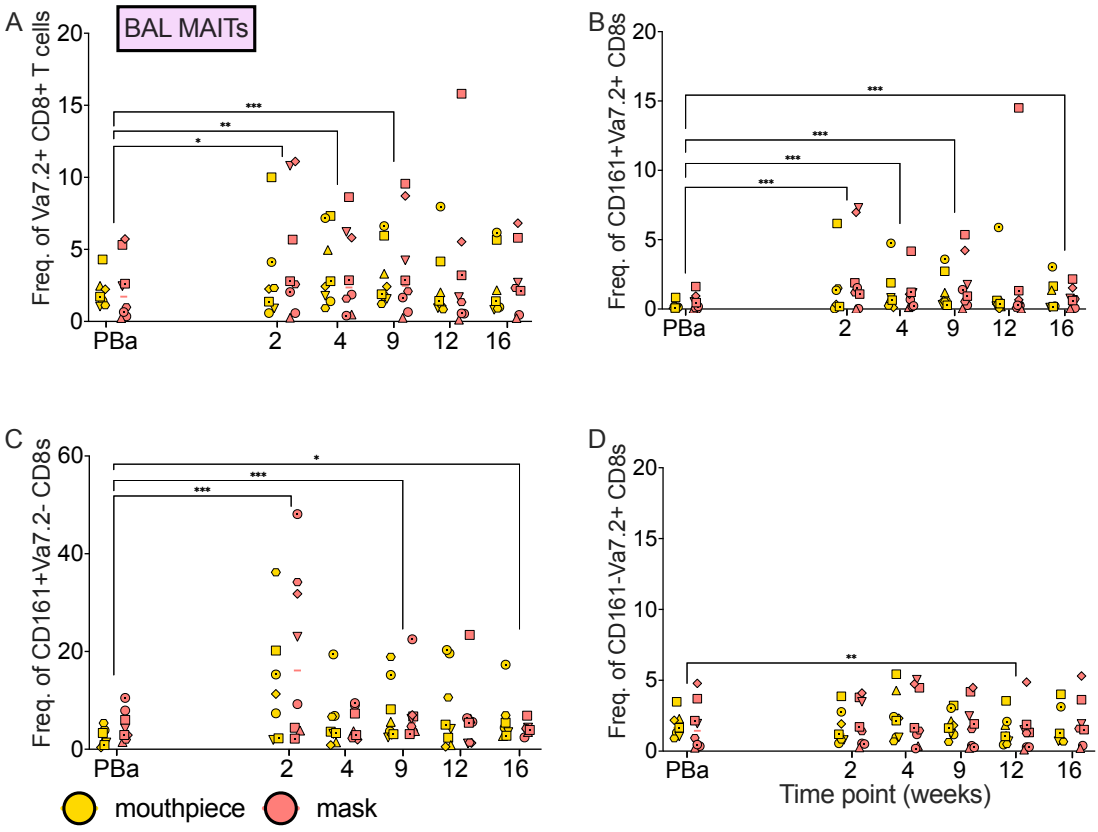


Figure 4.9 MAIT-cell markers frequency among broncho-alveolar lavage (BAL) cells

*The frequency of different CD161/Vα7.2 subsets within CD8+ BAL T-cells are shown: total Vα7.2+ (**A**), CD161+Vα7.2+ (**B**), CD161+Vα7.2- (**C**), and CD161-Vα7.2+ (**D**). Rhesus macaques exposed to aerosol BCG (aeBCG) by mouthpiece (yellow) and mask (pink) delivery are shown at time points after aeBCG (weeks) and at baseline (PBa). Each symbol represents a different animal and group medians are shown. Data from all animals were analysed together using multiple Wilcoxon-Rank tests (non-parametric). Where comparisons remain significant, adjusted P-values are marked: P < 0.05 (*) or P < 0.005 (**).*

CD16+ and CD56+ frequency among T-cells and CD3-CD8+ lymphocytes (NK and NKT-L, respectively) remained largely unchanged in BAL. Total CD14+ and CD16+ non-lymphocyte cell frequency were increased after aeBCG, peaking at Wk2 (Figure 4.10). CD14+ non-lymphocyte frequency increased at Wk2/Wk4/Wk9/Wk12/Wk16 compared to baseline (p=0.0001/0.0014/0.0034/0.0002/0.0266). Total CD16+ non-lymphocyte frequency was increased at Wk2/Wk12 (p=0.0006/0.0034, respectively). Frequency of the CD14+CD16- non-lymphocyte sub-population followed the same pattern as the total CD14+ non-lymphocyte population (significantly increased at all time points except Wk9).

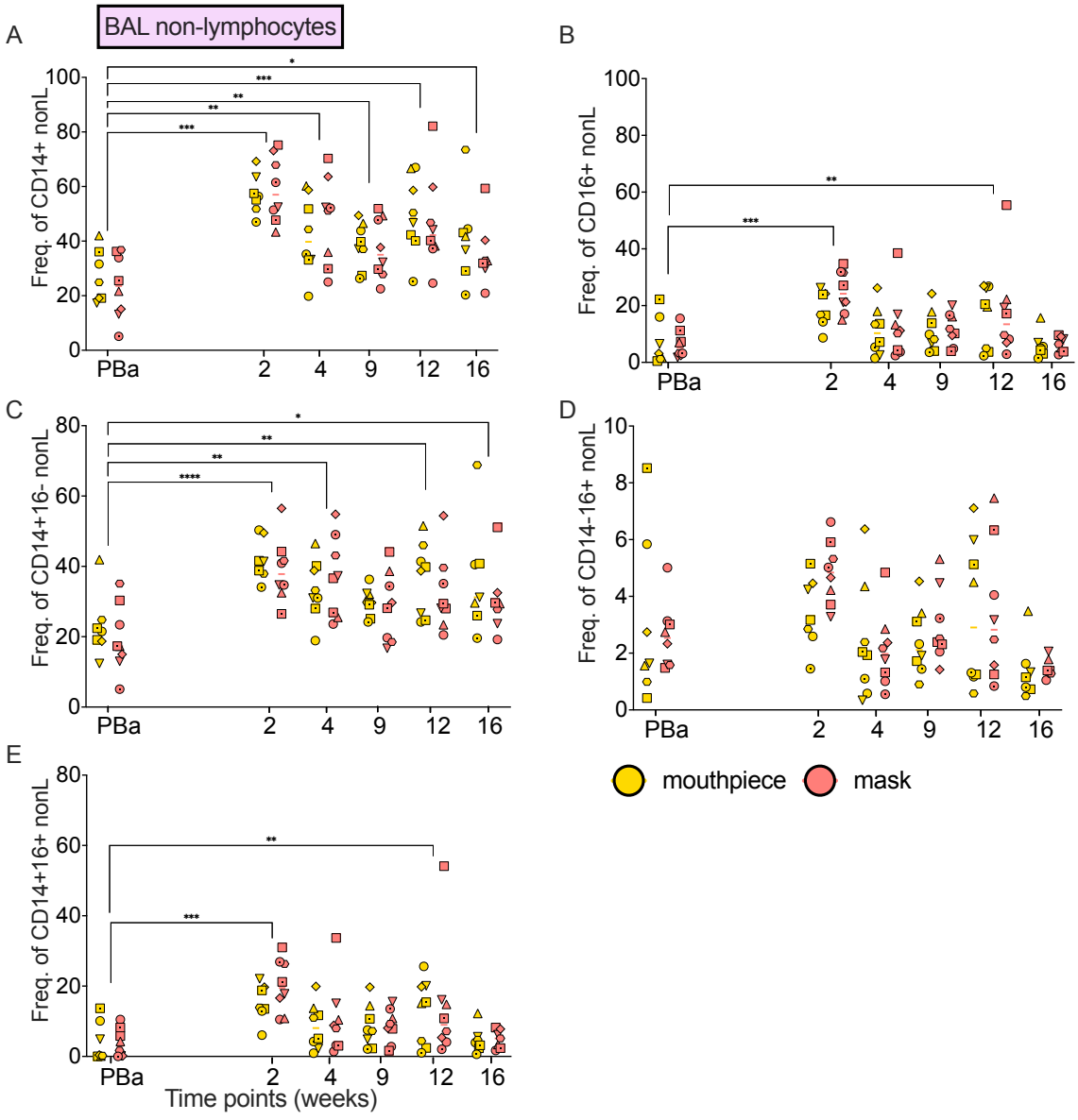


Figure 4.10 CD14+/CD16+ marker frequency among broncho-alveolar lavage (BAL) non-lymphocyte cells

*The frequency of different CD14+/CD16+ subsets within BAL non-lymphocyte cells are shown: total CD14+ (**A**), total CD16+ (**B**), CD14+CD16- (**C**), CD14-CD16+ (**D**) and CD14+CD16+ (**E**). Rhesus macaques exposed to aerosol BCG (aeBCG) by mouthpiece (yellow) and mask (pink) delivery are shown at time points after aeBCG (weeks) and at baseline (PBa). Each symbol represents a different animal and group medians are shown. Data from all animals were analysed together using a Mixed Effects model with Dunnett's correction for multiple comparisons or multiple Wilcoxon-Rank tests (non-parametric). Where comparisons remain significant, P-values are marked: P < 0.05 (*), P < 0.005 (**), P < 0.001 (***) or P < 0.0001 (****).*

A biphasic pattern can be identified in these graphs: one peak of cell population frequency is detected at Wk2, and another more gradual peak at around Wk12. CD14-CD16+ non-lymphocyte frequency followed a similar pattern of increase at Wk2 and Wk12, but this was not significant. The CD14-CD16+ non-lymphocyte subpopulation represents a much smaller part of the BAL non-lymphocyte compartment. 20 to 60% of non-lymphocyte cells measured in BAL cells were CD14+CD16-, 5 to 30% were CD14+CD16+, and 2 to 8% were CD14-CD16+.

4.4.6 WB populations

WB samples were stained with antibody panel 2. Data from all animals were grouped together for statistical analysis (Table 4.4). The sample set was complete, which meant that a repeated measured ANOVA with Dunnett's correction for multiple comparisons was used in place of the Mixed Effects model. Wilcoxon-Rank test between each time point and baseline was included in the results table for comparison to PBMC analysis.

Populations reliant on CD14+ staining were excluded for samples with a staining problem (n=6). Poor CD161 and γδ (described in Chapter 3) staining meant that these markers could not be analysed. AUC analysis revealed a difference between the frequency of CD16+CD56+ NKTs (*p*=0.0011) and CD16+CD56- NKs (*p*=0.0148) between male and female animals. There were no differences between mask and mouthpiece delivery groups by AUC analysis. Mann-Whitney U-test demonstrated that CD3+ lymphocyte frequency was higher at Wk4/Wk12/Wk16 (*p*=0.0190/0.0148/0.0379) for animals in the mask delivery group. CD3+ lymphocytes frequency was higher in the mask group between at baseline, but this was not significant. After aeBCG, WB cell populations remained mostly constant. The double positive CD4+CD8+/CD4+CD8++ populations identified in PBMC/BAL samples were not distinguishable in WB, and were therefore not included in this analysis.

WBICS: mask and mouthpiece										
analysis	ANOVA (Dunnett's)					Wilcoxon-Rank testing				
time point	Wk2	Wk4	Wk9	Wk12	Wk16	Wk2	Wk4	Wk9	Wk12	Wk16
CD14-3+ (T cell)	ns	ns	ns	ns	ns	ns	ns	ns	ns	*
CD4 T cell	ns	ns	ns	ns	ns	ns	ns	ns	ns	ns
CD8 T cell	ns	ns	ns	ns	ns	ns	ns	ns	ns	ns
CD16+CD56+ T cell (NKT-like)	x	x	x	x	x	ns	ns	ns	ns	ns
CD16+ T cell (NKT-like)	x	x	x	x	x	*	ns	ns	ns	ns
CD56+ T cell (NKT-like)	x	x	x	x	x	*	ns	ns	ns	ns
CD16+56+ CD3- (NK cell)	x	x	x	x	x	ns	ns	ns	ns	ns
CD16-56+ CD3- (NK)	x	x	x	x	x	ns	ns	ns	ns	ns
CD16+56- CD3- (NK)	x	x	x	x	x	ns	ns	ns	ns	**
CD14+ non-lymphocyte	x	x	x	x	x	ns	**	ns	ns	ns
CD16+ non-lymphocyte	x	x	x	x	x	ns	ns	ns	ns	ns
CD14+CD16+ non-lymphocyte	x	x	x	x	x	ns	ns	ns	ns	ns
CD14+CD16- non-lymphocyte	ns	*	ns	ns	ns	ns	**	ns	ns	ns
CD14-CD16+ non-lymphocyte	ns	ns	ns	ns	ns	ns	ns	ns	ns	ns
CD14-CD20+ (B cell)	ns	ns	ns	**	**	ns	ns	*	**	**

Table 4.4 Whole blood cell populations

Changes in cell population frequencies were analysed among whole blood samples from rhesus macaques exposed to aerosol BCG. Statistical comparisons between paired samples at baseline and time points after aerosol BCG (aeBCG) were made using a multiple ANOVA with Dunnett's correction for multiple comparisons (left – parametric data only) and Wilcoxon-Rank testing (right). Significant P-values are marked: P < 0.05 (*), P < 0.005 (**) or P < 0.001 (***), with increases in yellow, and decreases in blue.

B-cell frequency decreased at Wk12/Wk16 compared to baseline (p=0.0015/0.0047, respectively). The reduction in B-cell frequency can be seen as a trend from Wk4, but is only significant at Wk12/Wk16. CD14+CD16- non-lymphocyte frequency decreased only transiently at Wk4, (p=0.0464, no change at Wk2/Wk9), and there was considerable variation in frequency of non-lymphocyte markers (Figure 4.11).

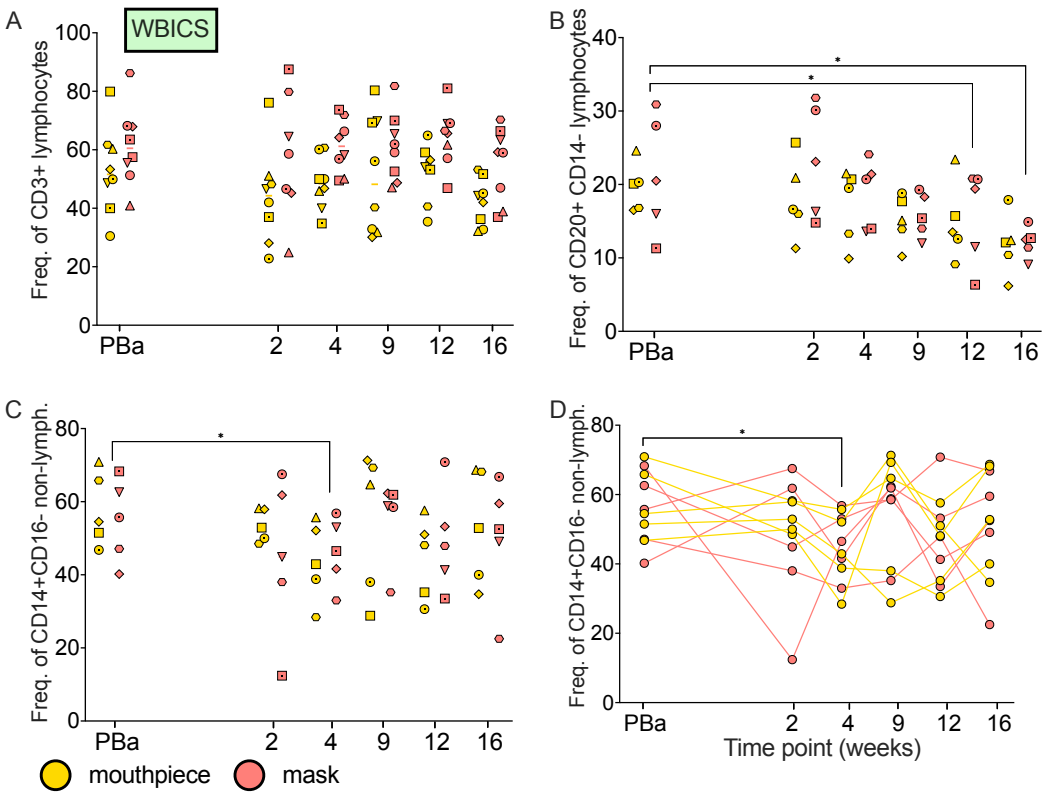


Figure 4.11 Cell populations characterised in whole blood

*The frequency of different cell populations among unstimulated whole blood are shown: CD3+ lymphocytes (**A**), CD14-CD20+ (B cells, **B**), CD14+CD16- non-lymphocyte cells (**C**-**D**). Rhesus macaques exposed to aerosol BCG (aeBCG) by mouthpiece (yellow) and mask (pink) delivery are shown at time points after aeBCG (weeks) and at baseline (PBa). Each symbol represents a different animal and group medians are shown. Data from all animals were analysed together using a multiple ANOVA with Dunnett's correction for multiple comparisons. Where comparisons remain significant, adjusted P-values are marked: P < 0.05 (*).*

4.4.7 Populations measured using haematology analyser

Using a haematology analyser, cell populations of neutrophils, monocytes, lymphocytes, eosinophils, and basophils were measured in recently collected blood samples (Figure 4.12). The number of lymphocytes detected at Wk2 per litre was lower than at PBa/PBb (p=0.0244/p=0.0019, respectively). Lymphocyte number was also lower at Wk4/Wk16 compared to PBb (p=0.0069/p=0.0120, respectively). The detected decrease in number of lymphocytes measured did not result in a change in M:L or N:L ratio.

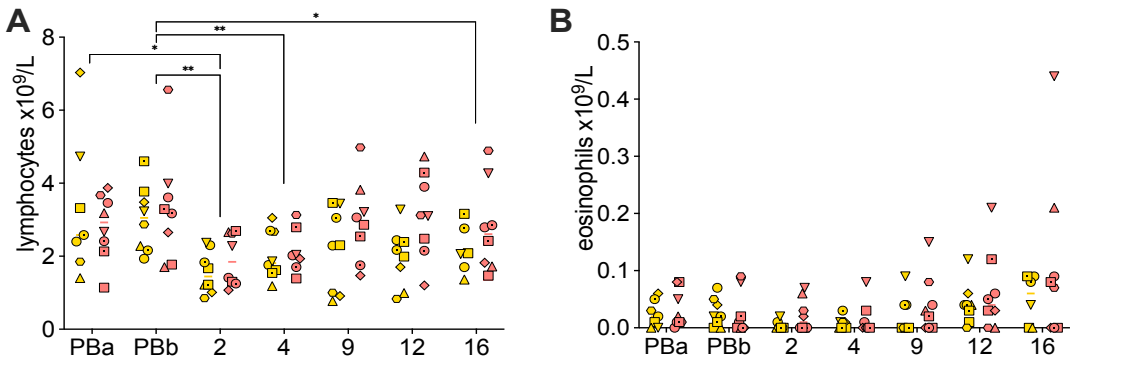


Figure 4.12 *continued on next page*

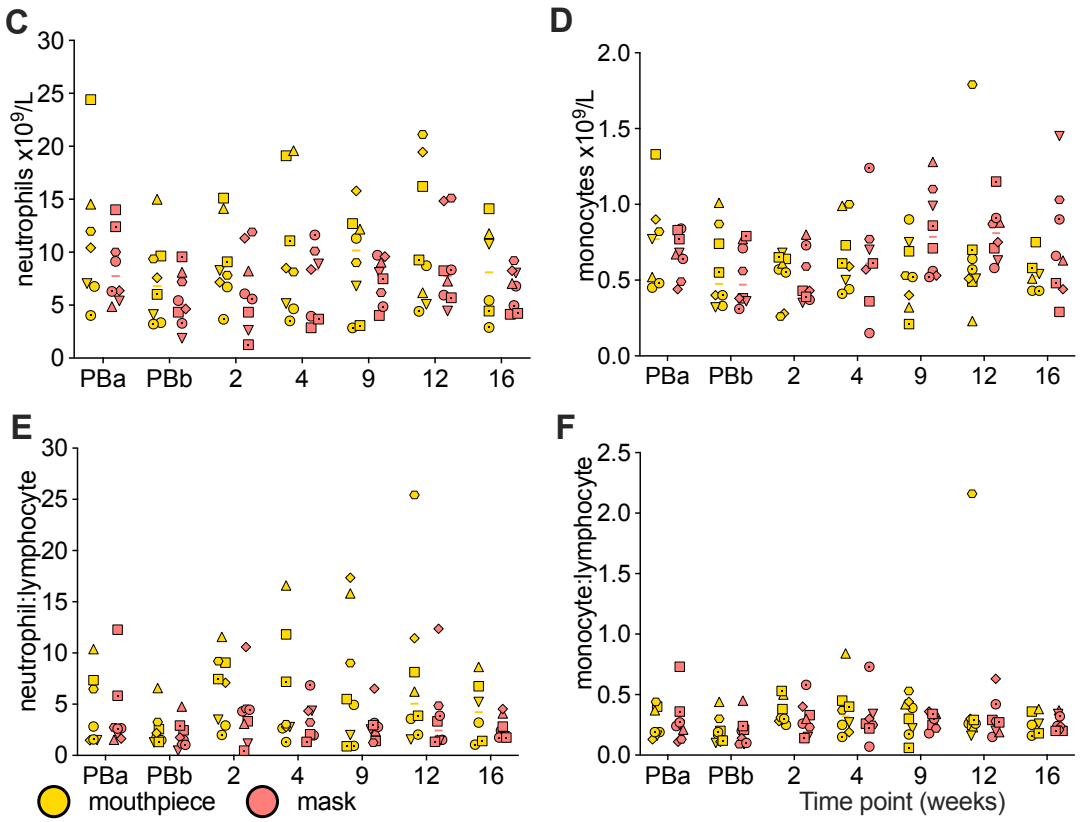


Figure 4.12 Cell populations measured by haematology analyser

*Cell counts of neutrophils, monocytes, lymphocytes, and eosinophils were measured in anti-coagulated blood samples. Counts (x10^9/L) are shown for lymphocytes (**A**), eosinophils (**B**), neutrophils (**C**) and monocytes (**D**). The neutrophil:lymphocyte and monocyte:lymphocyte ratios were calculated and plotted (**E** & **F**). Each symbol represents a different animal and group medians are shown. Data from all animals were analysed together using a Mixed Effects model with Dunnett's correction for multiple comparisons. Where comparisons remain significant, adjusted P-values are marked: P < 0.05 (*) or P < 0.005 (**).*

4.4.8 CD161 expression

After identifying CD161 as a marker of interest among CD8+ T-cells, CD161 expression was analysed across lymphocyte subsets: CD4+, CD8+ and γδ T-cells, CD16+/CD56+ subsets of CD3+ T lymphocytes and CD3-CD8+ lymphocytes (Table 4.5). Use of a Mixed Effects model with Dunnett's correction for multiple comparisons was not possible for PBMC (missing data points). The overall trend for CD161 expression was a strong increase at Wk2, and a second, wider peak at Wk9/Wk12/Wk16, depending on the population.

CD161 expression increased in most PBMC subsets studies at Wk2 and Wk9 (Figure 4.13). CD161 expression varied widely between PBMC cell populations, with fewer than 2% of CD4+ T-cells expressing CD161, compared with more than 30% among CD8+ T-cells in a proportion of animals. In PBMCs, CD161 expression on CD8+ T-cells increased at Wk2/Wk9 (p=0.0078/p=0.0156). Among γδ T-cells, CD161 expression increased at Wk2/Wk4/Wk9 (p=0.0078/0.0078/0.0156, respectively). CD161 expression cells increased at Wk2/Wk9 on CD4+ T-cells (p=0.0391/0.0078, respectively), CD56+ T-cells (p=0.0078/0.039, respectively), CD16+ T-cells (p=0.0078/0.0078, respectively) and CD16+ NK cells (p=0.0078/0.0078, respectively).

In BAL, CD161 expression CD4+ and CD8+ T-cells increased at all time points (with the exception of Wk12 for CD8+ T-cells – Figure 4.14). CD161 expression was particularly strong at Wk9 (CD4+ p=0.0001, CD8+ p=0.0020). Peak CD161 expression among CD8+ T-cells and NKT-L subsets was at Wk2, whereas a more gradual increase in frequency was observed for CD4+ T-cells.

A) PBMC CD161 expression					
analysis	Wilcoxon-Rank testing				
time point	Wk2	Wk4	Wk9	Wk12	Wk16
CD14- lymphocytes	*	ns	**	ns	ns
CD4 T cell	*	ns	**	ns	ns
CD8 T cell	**	ns	*	ns	ns
gamma-delta T cell	**	**	*	ns	ns
CD16+ T cell (NKT-like)	**	ns	**	ns	ns
CD56+ T cell (NKT-like)	**	ns	*	ns	*
CD16+56- CD3- (NK)	**	ns	**	ns	ns
CD16-56+ CD3- (NK)	ns	ns	ns	ns	ns

B) BAL CD161 expression										
analysis	Mixed Effects (Dunnett's)					Wilcoxon-Rank testing				
time point	Wk2	Wk4	Wk9	Wk12	Wk16	Wk2	Wk4	Wk9	Wk12	Wk16
CD14- lymphocytes	x	x	x	x	x	***	**	***	*	**
CD4 T cell	x	x	x	x	x	**	*	****	****	*
CD8 T cell	x	x	x	x	x	**	*	**	ns	*
gamma-delta T cell	x	x	x	x	x	*	ns	*	ns	ns
CD16+ T cell (NKT-like)	**	ns	ns	ns	ns	***	ns	ns	ns	*
CD56+ T cell (NKT-like)	x	x	x	x	x	**	ns	*	ns	*
CD16+56- CD3- (NK)	ns	ns	ns	ns	ns	ns	ns	*	ns	ns
CD16-56+ CD3- (NK)	*	ns	**	ns	*	*	*	**	ns	**

Table 4.5 CD161 expression across tissue compartments

*The frequency of CD161+ cells for different lymphocyte populations in peripheral blood mononuclear cell (PBMC, **A**) and broncho-alveolar lavage (BAL, **B**) samples. Statistical comparisons between paired samples at baseline and time points ('Wk'=week) after aerosol BCG (aeBCG) were made using a Mixed Effects model with Dunnett's correction for multiple comparisons (left – parametric only) and Wilcoxon-Rank testing (right). Significant P-values are marked: P < 0.05 (*), P < 0.005 (**), P < 0.001 (***), P < 0.0001 (****), with increases in yellow/orange.*

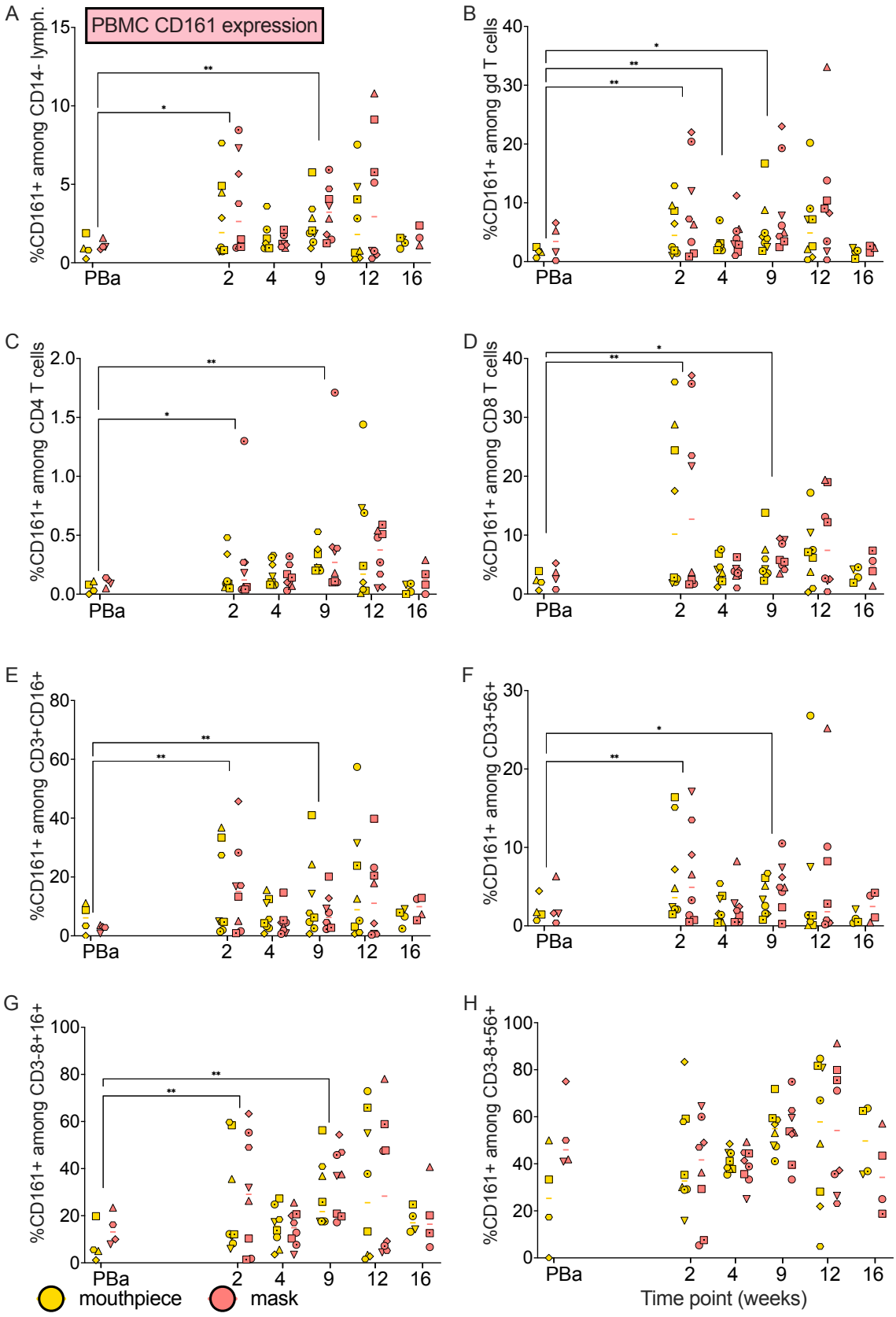

A
PBMC CD161 expression
%CD161+ among CD14- lymph.
B
%CD161+ among gd T cells
C
%CD161+ among CD4 T cells
D
%CD161+ among CD8 T cells
E
%CD161+ among CD3+CD16+
F
%CD161+ among CD3+56+
G
%CD161+ among CD3-8+16+
H
%CD161+ among CD3-8+56+
PBa
2
4
9
12
16
Time point (weeks)
mouthpiece
mask

Figure 4.13 CD161 expression among peripheral blood mononuclear cell (PBMC) lymphocytes

*CD161 expression on different cell populations among PBMC sample are shown for: CD14- lymphocytes (**A**), γδ, CD4+ and CD8+ T-cells (**B**-**D**), NKT and NK cells (**E**-**H**). Rhesus macaques exposed to aerosol BCG (aeBCG) by mouthpiece (yellow) and mask (pink) delivery are shown at time points after aeBCG (weeks) and at baseline (PBa). Each symbol represents a different animal and group medians are shown. Statistical comparisons between paired data (all animals) was performed using Wilcoxon-Rank testing. Where significant, comparisons are marked: P < 0.05 (*) or P < 0.005 (**).*

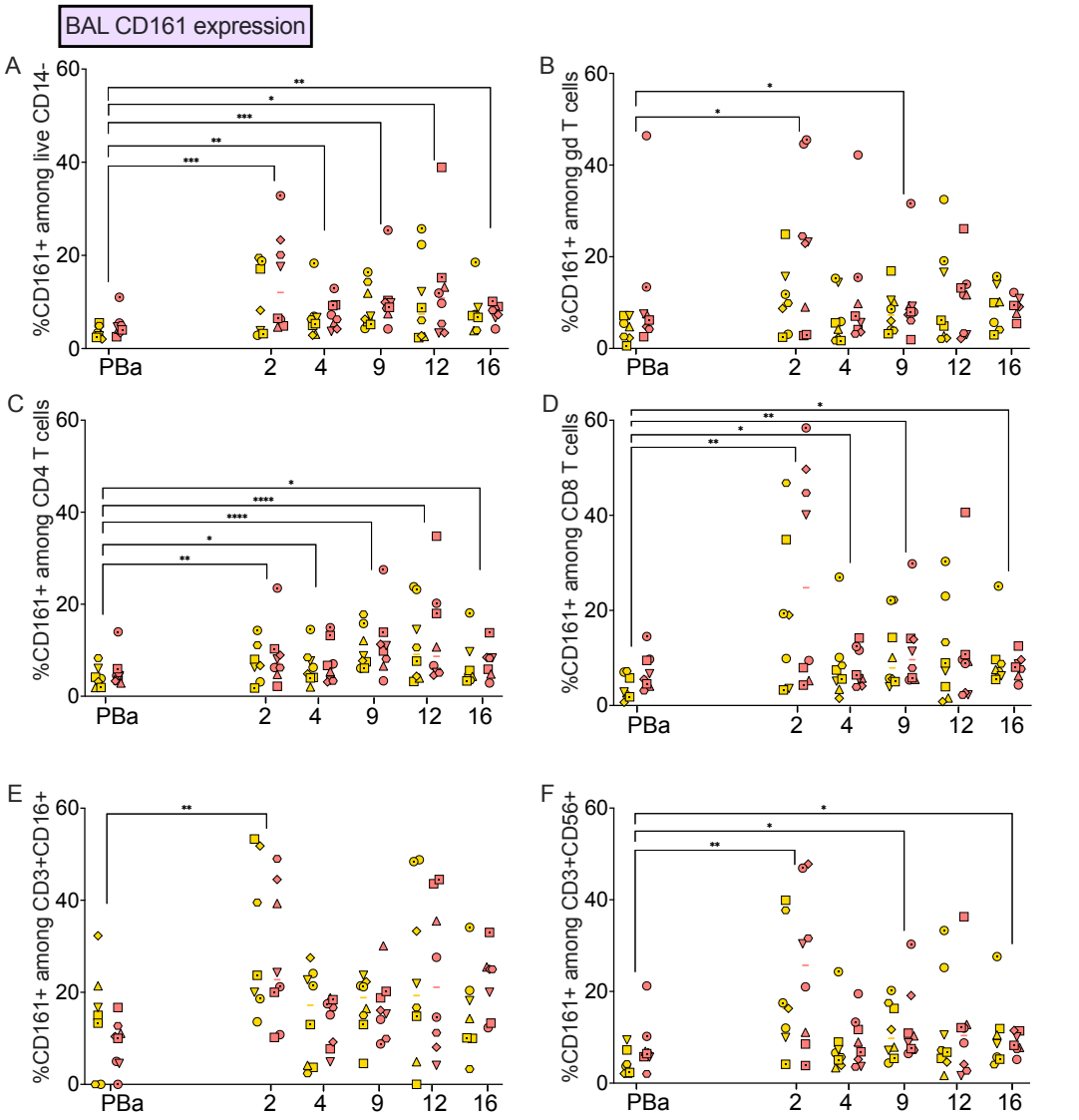


Figure 4.14 continued on next page

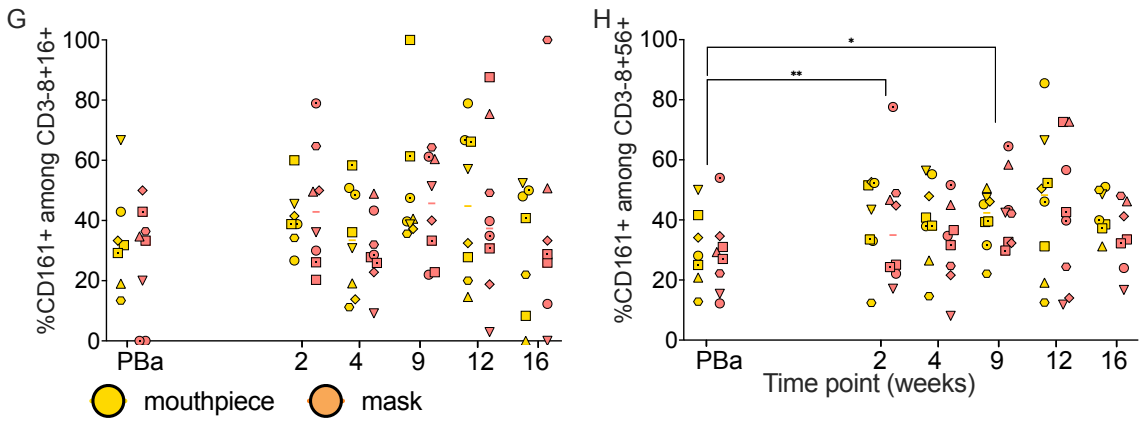


Figure 4.14 CD161 expression among broncho-alveolar lavage (BAL) lymphocytes

*CD161 expression on different cell populations among BAL samples are shown for: CD14- lymphocytes (**A**), γδ, CD4+ and CD8+ T-cells (**B**-**D**), NKT and NK cells (**E**-**H**). Rhesus macaques exposed to aerosol BCG (aeBCG) by mouthpiece (yellow) and mask (pink) delivery are shown at time points after aeBCG (weeks) and at baseline (PBa). Each symbol represents a different animal and group medians are shown. Data from all animals were analysed together using a Mixed Effects model with Dunnett's correction for multiple comparisons or using Wilcoxon-Rank testing (parametric/non-parametric, respectively). Where comparisons remain significant, adjusted P-values are marked: P < 0.05 (*), P < 0.005 (**) or P < 0.001 (***).*

4.4.9.1 Activation marker expression, measured by flow-cytometry

The only change in HLA-DR expression identified among PBMCs was increased HLA-DR expression on γδ T-cells at Wk12 (p=0.0156, Figure 4.15 – Table 4.6). HLA-DR expression on CD4+ and total CD8+ T-cells remained unchanged among PBMCs, but there was a trend for increased HLA-DR expression on CD8+ T-cells at Wk12/Wk16 (not significant). There were few data points for Vα7.2+ CD8+ T-cells at PBa because samples fewer than 50 Vα7.2+ CD8+ T-cells were excluded, and there were missing samples.

A) PBMC HLA-DR expression					
analysis	Wilcoxon-Rank testing				
time point	Wk2	Wk4	Wk9	Wk12	Wk16
CD4 T cell	ns	ns	ns	ns	ns
CD8 T cell	ns	ns	ns	ns	ns
gamma-delta T cell	ns	ns	ns	*	ns
CD8+Va7.2+ T cell (MAIT)	-	-	-	-	-
CD16+ T cell (NKT-like)	ns	ns	ns	ns	ns
CD56+ T cell (NKT-like)	ns	ns	ns	ns	ns
CD16+CD56+ T cell (NKT-like)	ns	ns	ns	ns	ns

B) BAL HLA-DR expression										
analysis	Mixed Effects (Dunnett's)					Wilcoxon-Rank testing				
time point	Wk2	Wk4	Wk9	Wk12	Wk16	Wk2	Wk4	Wk9	Wk12	Wk16
CD4 T cell	ns	ns	ns	ns	ns	ns	ns	ns	ns	ns
CD8 T cell	ns	ns	ns	ns	ns	ns	*	ns	ns	ns
gamma-delta T cell	ns	ns	*	ns	ns	*	ns	*	ns	ns
CD8+Va7.2+ T cell (MAIT)	ns	ns	ns	ns	ns	ns	ns	ns	ns	ns
CD16+ T cell (NKT-like)	ns	ns	ns	*	ns	ns	ns	ns	**	ns
CD56+ T cell (NKT-like)	ns	ns	ns	ns	ns	ns	ns	ns	ns	ns
CD16+CD56+ T cell (NKT-like)	ns	ns	ns	*	ns	ns	ns	ns	**	ns

C) WBICS HLA-DR expression										
analysis	ANOVA (Dunnett's)					Wilcoxon-Rank testing				
time point	Wk2	Wk4	Wk9	Wk12	Wk16	Wk2	Wk4	Wk9	Wk12	Wk16
CD4 T cell	ns	ns	ns	ns	***	ns	ns	ns	ns	***
CD8 T cell	ns	ns	ns	ns	**	ns	ns	ns	ns	**
gamma-delta T cell	ns	ns	ns	ns	ns	ns	ns	ns	ns	ns
CD8+Va7.2+ T cell (MAIT)	ns	ns	ns	ns	ns	ns	ns	ns	ns	ns
CD16+ T cell (NKT-like)	ns	ns	ns	ns	ns	ns	ns	ns	ns	ns
CD56+ T cell (NKT-like)	ns	ns	ns	ns	ns	ns	ns	ns	ns	ns
CD16+CD56- NK cell	*	ns	ns	ns	ns	**	ns	ns	*	ns
CD16-CD56+ NK cell	ns	ns	ns	ns	*	ns	ns	ns	ns	**
CD14-20+ (B cell)	ns	ns	ns	ns	**	ns	ns	ns	ns	**

Table 4.6 Human leukocyte antigen-DR (HLA-DR) frequency across tissue compartments

*HLA-DR expression across lymphocyte populations in peripheral blood mononuclear cell (PBMC, **A**), broncho-alveolar lavage (BAL, **B**) and whole blood samples is shown. There were too few Vα7.2+CD8+ T-cells at baseline to allow valid statistical comparison. Statistical comparisons between paired samples at baseline and time points ('Wk'=week) after aerosol BCG (aeBCG) were made using a Mixed Effects model (multiple ANOVA for whole blood) with Dunnett's correction for multiple comparisons/Wilcoxon-Rank testing (left – parametric/non-parametric, respectively) and Wilcoxon-Rank testing (right). Significant P-values are marked: P < 0.05 (*), P < 0.005 (**), P < 0.001 (***), P < 0.0001 (****), with increases in yellow and decreases in blue.*

HLA-DR expression on BAL $\gamma\delta$ T-cells was lower at Wk4 (not significant) and Wk9 (p=0.0401), then returned to baseline level at Wk12 (Figure 4.16). HLA-DR expression on CD16+ NKT-L and CD16+CD56+ NKT-L increased at Wk12 (p=0.0017 and p=0.0126, respectively). HLA-DR expression did not increase for CD56+ CD3+ T lymphocytes, which suggests that increased CD16+CD56+ NKT-L HLA-DR expression is due to increased expression on CD16+ cells.

HLA-DR expression on B-cells, CD4+ and CD8+ T-cells was decreased at Wk16 compared to baseline in WB (p=0.0002 and p=0.0013, respectively, Figure 4.17). In contrast, HLA-DR expression increased on CD56+ CD3-CD8+ lymphocytes (NK cells) at Wk16 compared to baseline (p=0.0248). HLA-DR expression increased on CD16+ CD3-CD8+ lymphocytes at Wk2/Wk12 (p=0.0052/0.0182, respectively).

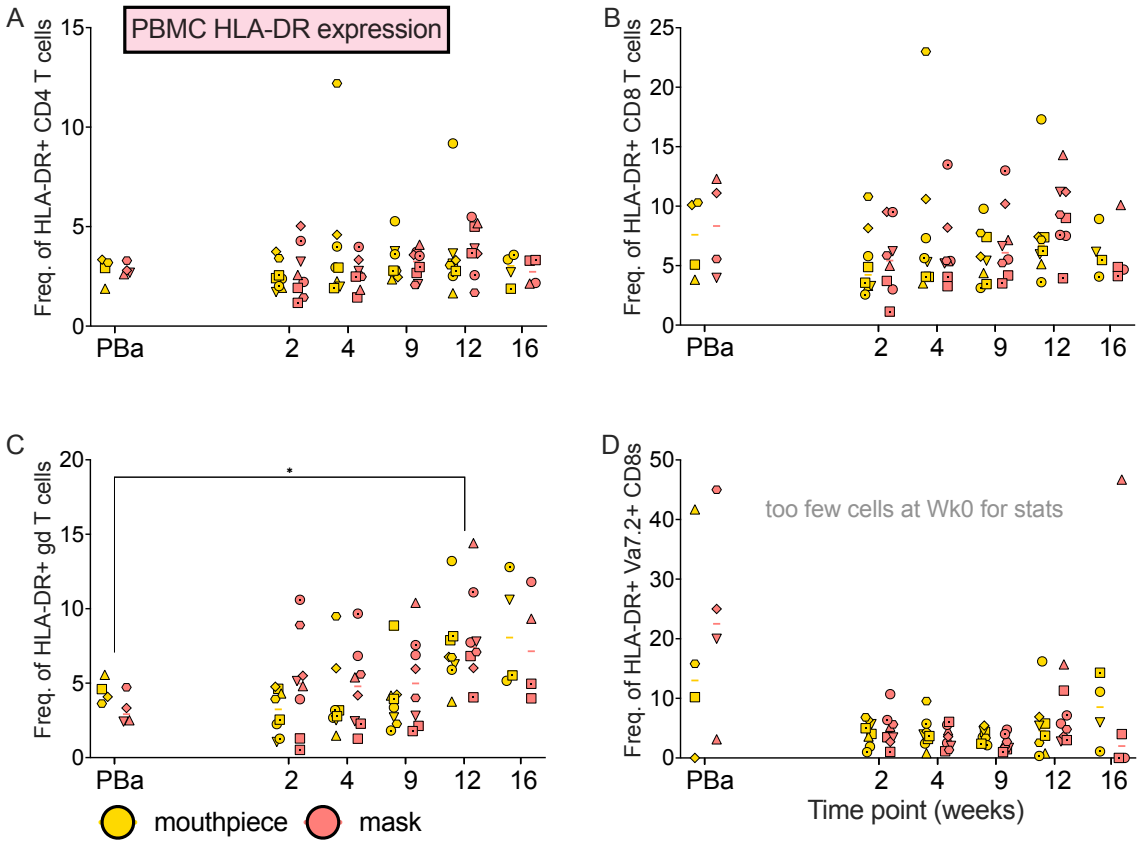


Figure 4.15 Human leukocyte antigen-DR (HLA-DR) expression on peripheral blood mononuclear cell (PBMC) lymphocytes

*HLA-DR expression on different populations of PBMCs are shown for: CD4+, CD8+ and γs (**A**, **B** & **C**), and Vα7.2+CD8+ T-cells (**D**). Rhesus macaques exposed to aerosol BCG (aeBCG) by mouthpiece (yellow) and mask (pink) delivery are shown at time points after aeBCG (weeks) and at baseline (PBa). Each symbol represents a different animal and group medians are shown. Statistical comparisons between paired data (all animals) was performed using Wilcoxon-Rank testing. Where significant, comparisons are marked: P < 0.05 (*).*

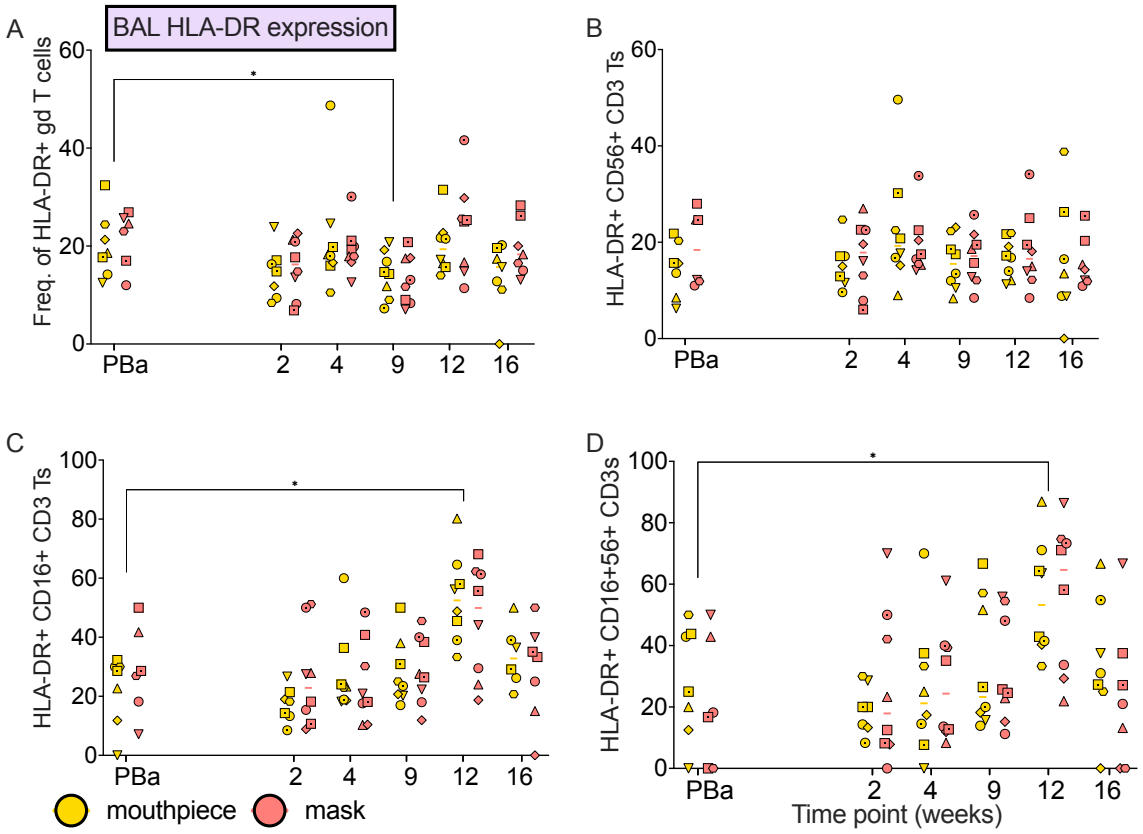


Figure 4.16 Human leukocyte antigen-DR (HLA-DR) expression on broncho-alveolar lavage (BAL) lymphocytes

*HLA-DR expression on different populations of BAL lymphocytes are shown for: γs (**A**), CD56+, CD16+ and CD16+CD56+ T-cells (**B**, **C** & **D**). Rhesus macaques exposed to aerosol BCG (aeBCG) by mouthpiece (yellow) and mask (pink) delivery are shown at time points after aeBCG (weeks) and at baseline (PBa). Each symbol represents a different animal and group medians are shown. Data from all animals were analysed together using a Mixed Effects model with Dunnett's correction for multiple comparisons/using Wilcoxon-Rank Testing (parametric/non-parametric, respectively). Where comparisons remain significant, adjusted P-values are marked: P < 0.05 (*).*

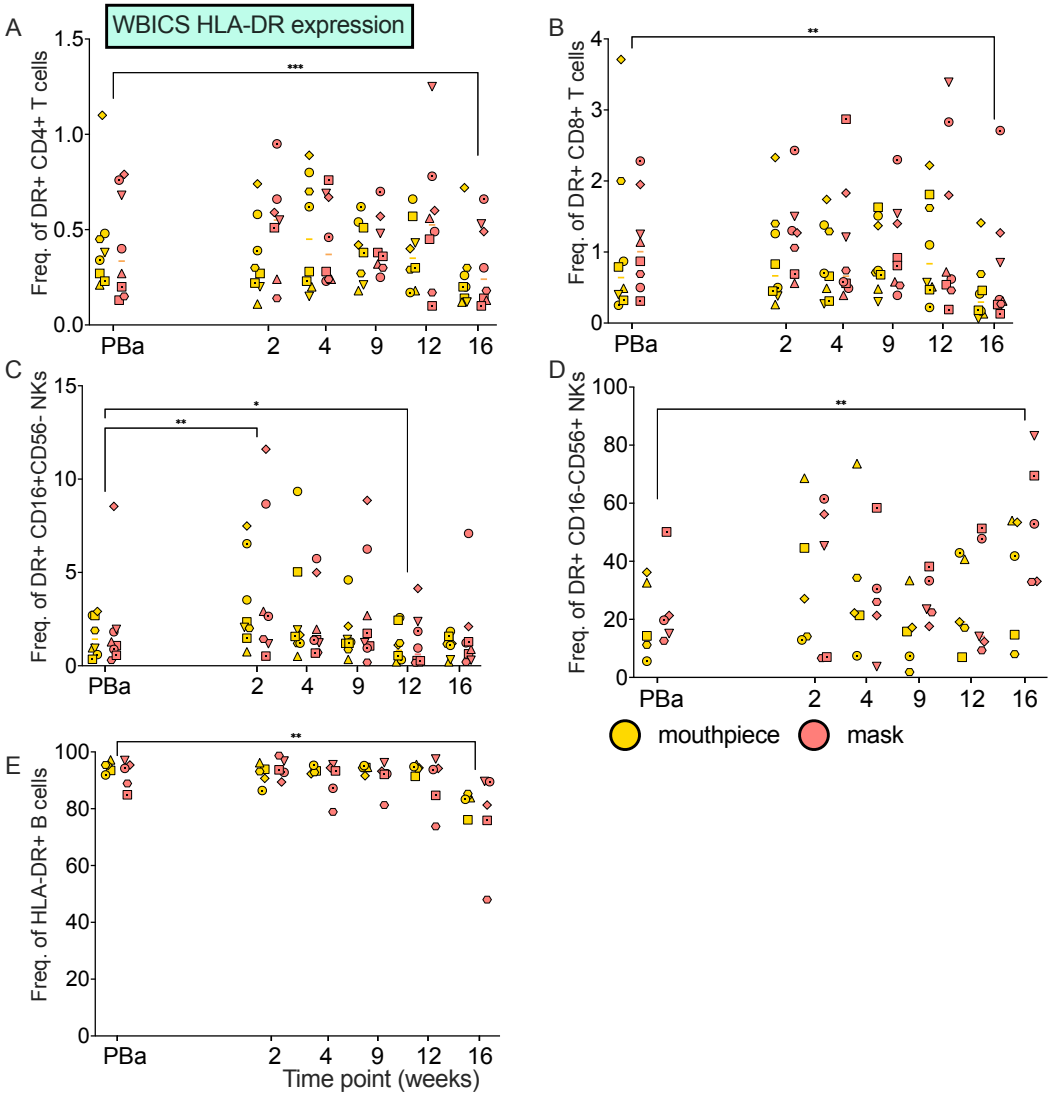


Figure 4.17 Human leukocyte antigen-DR (HLA-DR) expression on whole blood lymphocytes

*HLA-DR expression on different populations of whole blood lymphocytes are shown for: CD4+ and CD8+ T-cells (**A** & **B**), CD16+ and CD56+ CD3-CD8+ lymphocytes (NK cells, **C** & **D**) and B-cells (**E**). Rhesus macaques exposed to aerosol BCG (aeBCG) by mouthpiece (yellow) and mask (pink) delivery are shown at time points after aeBCG (weeks) and at baseline (PBa). Each symbol represents a different animal and group medians are shown. Data from all animals were analysed together using a Mixed Effects model with Dunnett's correction for multiple comparisons/using Wilcoxon-Rank Testing (parametric/non-parametric, respectively). Where comparisons remain significant, adjusted P-values are marked: P < 0.05 (*) or P < 0.005 (**).*

4.4.9.2 Cell-associated activation markers measured by flow-cytometry in whole blood

In WB, CD95 and CD163/MerTK expression were also explored (Table 4.7). Non-lymphocyte cell expression of CD163/MerTK decreased at Wk4 compared to baseline for: total non-lymphocyte cells, CD14+CD16+, CD14+CD16- and CD14-CD16+ non-lymphocyte cells (Figure 4.18). Median CD163/MerTK expression varied over time from: 33.7% to 51.4% in total non-lymphocyte cells, 91.8% to 97.5% in CD14+CD16+ non-lymphocyte cells, 74.7% to 84.1% in CD14+CD16- non-lymphocyte cells, 30.1-47.5 in CD14-CD16+ non-lymphocyte cells and 11.1% to 13.8% in CD14-CD16- non-lymphocyte cells.

A) WBICS: CD163 or MerTK frequency										
analysis	ANOVA (Dunnett's)					Wilcoxon-Rank testing				
time point	Wk2	Wk4	Wk9	Wk12	Wk16	Wk2	Wk4	Wk9	Wk12	Wk16
non-lymphocyte	x	x	x	x	x	ns	***	ns	ns	*
non-lymphocyte CD14+CD16+	x	x	x	x	x	ns	**	ns	ns	ns
non-lymphocyte CD14+CD16-	ns	*	ns	ns	ns	ns	**	ns	ns	ns
non-lymphocyte CD14-CD16+	ns	*	ns	ns	ns	ns	**	*	ns	*
non-lymphocyte CD14-CD16-	x	x	x	x	x	ns	ns	ns	ns	ns

B) WBICS: CD95 frequency										
analysis	ANOVA (Dunnett's)					Wilcoxon-Rank testing				
time point	Wk2	Wk4	Wk9	Wk12	Wk16	Wk2	Wk4	Wk9	Wk12	Wk16
CD4 T cell	x	x	x	x	x	ns	*	ns	*	ns
CD8 T cell	x	x	x	x	x	ns	***	ns	**	ns
CD8+CD161+ T cell (MAIT)	x	x	x	x	x	ns	ns	ns	ns	ns
CD14-20+ (B cell)	ns	ns	ns	ns	**	ns	ns	ns	ns	**

Table 4.7 Activation markers on whole blood samples

*CD613/MerTK (**A**) and CD95 (**B**) expression was compared across lymphocyte populations from whole blood. Statistical comparisons between paired samples at baseline and time points ('Wk'=week) after aerosol BCG (aeBCG) were made using a Mixed Effects model (multiple ANOVA for whole blood) with Dunnett's correction for multiple comparisons (left – parametric only) and Wilcoxon-Rank testing (right). Significant P-values are marked: P < 0.05 (*), P < 0.005 (**) or P < 0.001 (***), with increases in yellow and decreases in blue.*

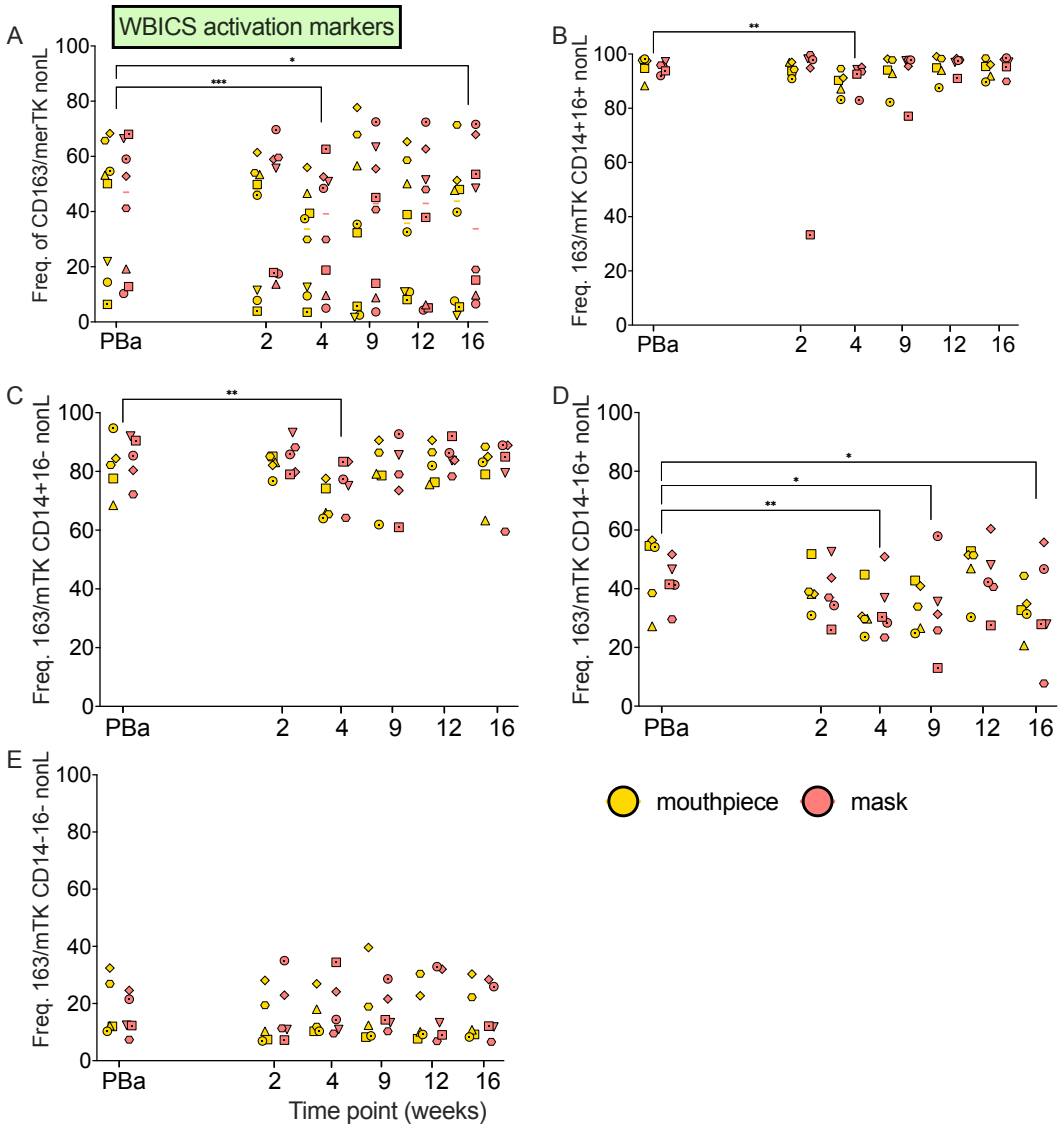


Figure 4.18 MerTK or CD163 expression on whole blood lymphocytes

*MerTK/CD163 expression on different populations of whole blood lymphocytes are shown for: total non-lymphocyte cells (**A**), CD14+CD16+ (**B**), CD14+CD16- (**C**), CD14-CD16+ (**D**) and CD14-CD16- non-lymphocyte subsets (**E**). Rhesus macaques exposed to aerosol BCG (aeBCG) by mouthpiece (yellow) and mask (pink) delivery are shown at time points after aeBCG (weeks) and at baseline (PBa). Each symbol represents a different animal and group medians are shown. Data from all animals were analysed together using Wilcoxon-Rank Testing. Where comparisons remain significant, adjusted P-values are marked: P < 0.05 (*) or P < 0.005 (**).*

CD95 expression on CD8+ T-cells decreased at Wk4/Wk12 compared to baseline (p=0.0001/p=0.0092, respectivley – Figure 4.19). CD95 expression on B-cells increased at Wk16 compared to baseline (p=0.0093). WB P-values are corrected for multiple comparisons (Dunnett's).

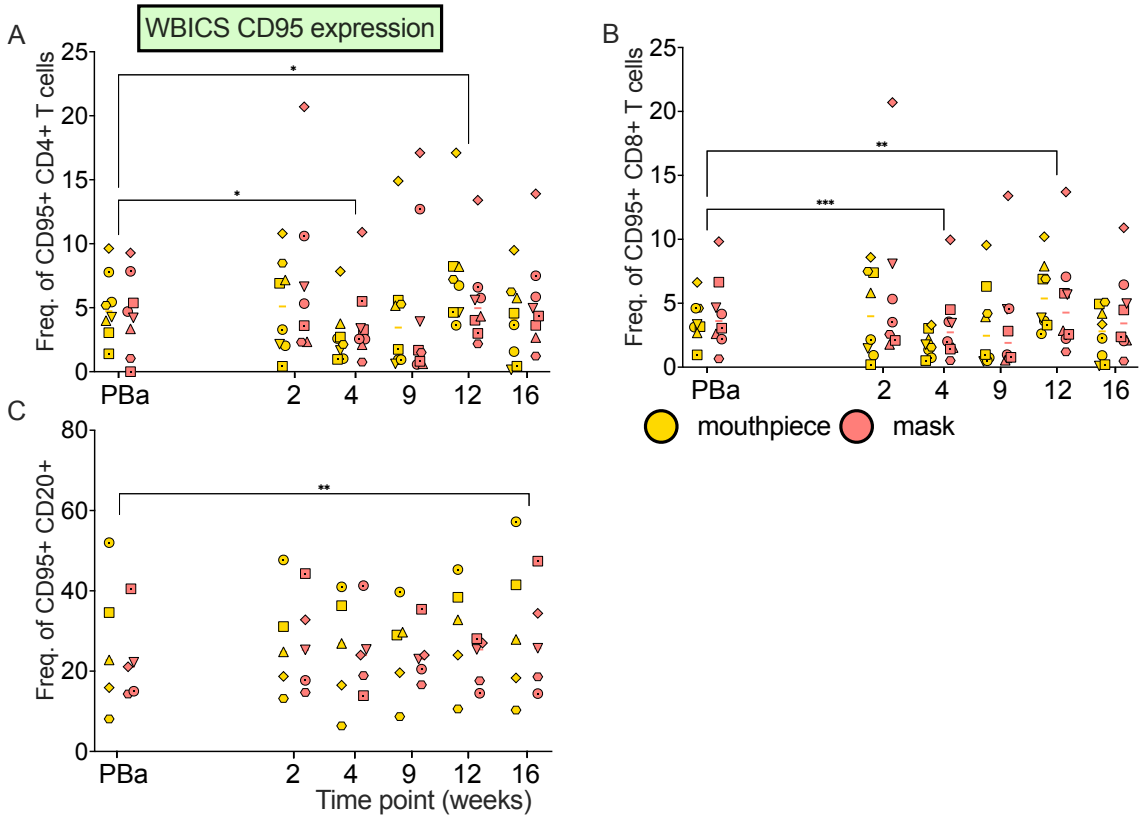


Figure 4.19 CD95 expression on whole blood lymphocytes

*CD95 expression on different populations of whole blood lymphocytes are shown for: CD4+ and CD8+ T-cells (**A** & **B**) and B-cells (**C**). Rhesus macaques exposed to aerosol BCG (aeBCG) by mouthpiece (yellow) and mask (pink) delivery are shown at time points after aeBCG (weeks) and at baseline (PBa). Each symbol represents a different animal and group medians are shown. Data from all animals were analysed together using a Mixed Effects model with Dunnett's correction for multiple comparisons. Where comparisons remain significant, adjusted P-values are marked: P < 0.05 (*) or P < 0.005 (**).*

4.4.10 Intracellular cytokine staining

The frequency of PPD-specific cytokine positive cells was explored in PBMC, BAL and samples from the WBICS assay (Table 4.8). Among PBMCs, IFNγ CD4+ T-cell frequency increased at Wk9/Wk12 (p=0.0156/0.0234, respectively), and a similar trend was observed for CD8+ T-cells (not significant, Figure 4.20). The frequency of IL-2+ and IL-17+ CD4+ T-cells showed a similar, but not significant increase.

A) PBMC cytokines															
cytokine	IFNg					IL-2					IL-17				
analysis	Wilcoxon-Rank testing					Wilcoxon-Rank testing					Wilcoxon-Rank testing				
time point	Wk2	Wk4	Wk9	Wk12	Wk16	Wk2	Wk4	Wk9	Wk12	Wk16	Wk2	Wk4	Wk9	Wk12	Wk16
CD4 T cell	ns	ns	*	*	ns	ns	ns	*	ns	ns	ns	ns	ns	ns	ns
CD8 T cell	ns	ns	ns	ns	ns	ns	ns	ns	ns	ns	ns	ns	ns	ns	ns
gamma-delta T cell	ns	ns	ns	*	ns	ns	ns	ns	ns	ns	ns	ns	ns	ns	ns
Va7.2+ CD8+ T cell	ns	ns	ns	ns	ns	ns	ns	ns	ns	ns	ns	ns	ns	ns	ns
CD16+ T cell (NKT-like)	ns	ns	ns	ns	ns	ns	ns	ns	ns	ns	ns	ns	ns	ns	ns
CD56+ T cell (NKT-like)	ns	ns	ns	ns	ns	ns	ns	ns	ns	ns	ns	ns	ns	ns	ns
CD16+CD56+ T cell (NKT-like)	ns	ns	ns	ns	ns	ns	ns	ns	ns	ns	ns	ns	ns	ns	ns
CD16-56+ CD3- (NK)	ns	ns	ns	ns	ns	ns	ns	ns	ns	ns	ns	ns	ns	ns	ns
CD16+56- CD3- (NK)	ns	ns	ns	ns	ns	ns	ns	ns	ns	ns	ns	ns	ns	ns	ns
CD14+CD16+ non-lymphocyte	ns	ns	ns	ns	ns	ns	ns	ns	ns	ns	ns	ns	ns	ns	ns
CD14+CD16- non-lymphocyte	ns	ns	ns	ns	ns	ns	ns	ns	ns	ns	ns	ns	ns	ns	ns
CD14-CD16+ non-lymphocyte	ns	ns	ns	ns	ns	ns	ns	ns	ns	ns	ns	*	ns	ns	ns

B) BAL cytokines															
cytokine	IFNg					IL-2					IL-17				
analysis	Wilcoxon-Rank testing					Wilcoxon-Rank testing					Wilcoxon-Rank testing				
time point	Wk2	Wk4	Wk9	Wk12	Wk16	Wk2	Wk4	Wk9	Wk12	Wk16	Wk2	Wk4	Wk9	Wk12	Wk16
CD4 T cell	ns	*	****	****	****	ns	*	ns	****	***	*	***	***	****	***
CD8 T cell	ns	ns	*	**	ns	ns	ns	ns	ns	ns	ns	ns	*	***	ns
gamma-delta T cell	ns	ns	ns	**	ns	ns	ns	ns	*	ns	*	ns	ns	*	ns
Va7.2+ CD8+ T cell	ns	*	*	***	ns	ns	ns	ns	ns	ns	ns	ns	*	**	ns
CD16+ T cell (NKT-like)	ns	ns	***	**	*	ns	*	***	***	**	ns	ns	**	ns	*
CD56+ T cell (NKT-like)	ns	ns	ns	**	ns	ns	ns	ns	*	ns	ns	ns	*	*	ns
CD16+CD56+ T cell (NKT-like)	ns	ns	**	**	*	ns	ns	**	**	*	*	ns	*	ns	ns
CD16-56+ CD3- (NK)	ns	ns	ns	ns	ns	ns	ns	ns	*	ns	ns	ns	ns	ns	ns
CD16+56- CD3- (NK)	ns	ns	ns	ns	ns	ns	ns	ns	ns	ns	ns	ns	*	ns	ns
CD14+CD16+ non-lymphocyte	ns	*	ns	ns	ns	ns	ns	ns	ns	ns	ns	ns	ns	ns	ns
CD14+CD16- non-lymphocyte	ns	ns	ns	ns	ns	ns	ns	*	ns	ns	ns	ns	ns	ns	ns
CD14-CD16+ non-lymphocyte	ns	ns	**	***	ns	ns	ns	ns	ns	ns	ns	*	ns	ns	ns

Table 4.8 Cytokine expressing cell frequency across tissue compartments

*The frequency PPD-specific cytokine producing cells (IFNγ, IL-2 and IL-17) was measured among peripheral blood mononuclear cells (PBMCs, **A**) and broncho-alveolar lavage (BAL) cells (**B**). Statistical comparisons between paired samples at baseline and time points ('Wk'=week) after aerosol BCG (aeBCG) were made using Wilcoxon-Rank testing. Significant P-values are marked: P < 0.05 (*), P < 0.005 (**), P < 0.001 (***), P < 0.0001 (****), with increases in yellow and decreases in blue.*

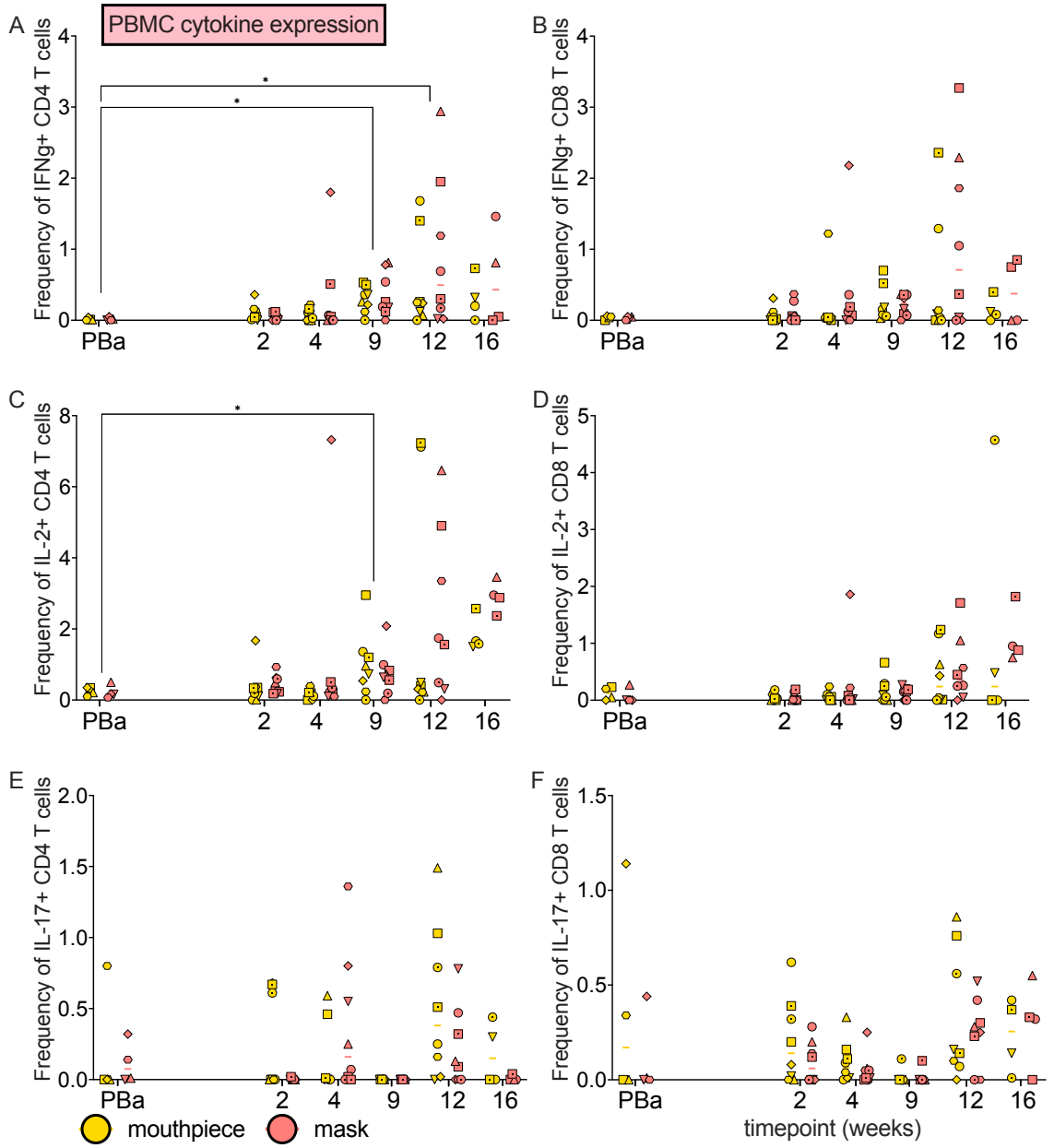


Figure 4.20 Cytokine expression on peripheral blood mononuclear cell (PBMC) populations

*The frequency of PPD-specific cytokine producing cells were measured among CD4+ and CD8+ T-cells among PBMCs: IFNγ (**A** & **B**), IL-2 (**C** & **D**), and IL-17 (**E** & **F**). Rhesus macaques exposed to aerosol BCG (aeBCG) by mouthpiece (yellow) and mask (pink) delivery are shown at time points after aeBCG (weeks) and at baseline (PBa). Each symbol represents a different animal and group medians are shown. Statistical comparisons between paired data (all animals) was performed using Wilcoxon-Rank Testing. Where significant, comparisons are marked: P < 0.05 (*).*

There was a higher frequency of cytokine-positive cells in BAL than PBMCs, with more significant changes after aeBCG compared to baseline (Figure 4.21). For example, the median IFNγ+ CD4+ T-cell frequency went from 0.1% to 0.26% in PBMCs (baseline to Wk9), compared 0.33% to 25.85% in BAL (baseline to Wk12). The peak time point for BAL cell cytokine expression was at Wk12. Cytokine-positive CD4+ T-cell frequency increased at Wk12/Wk16 for all three cytokines, and IFNγ+ and IL-17+ CD4+ T-cell frequency were also increased at Wk4/Wk9, compared to baseline. CD4+ T-cells showed the highest frequency of cytokine-positive cells of any subset measured in the BAL. P-values for BAL cells are adjusted after Dunnett's correction for multiple comparisons.

IFN+ $\gamma\delta$ T-cell frequency increased at Wk12 (p=0.0012). IFNγ+ CD16+ and CD16+CD56+ NKT-L cell frequency increased at Wk9/Wk12/Wk16 (p=0.0002/0.0034/ 0.0391 and p=0.0039/0.0039/0.0312, respectively). IFNγ+ CD14-CD16+ non-lymphocyte frequency increased at Wk9/Wk12 (p=0.0078/0.0010). IL-2+ cell frequency increased in $\gamma\delta$ T-cells at Wk12 (p=0.0043) and in CD16+/CD16+CD56+ NKT-L cells at Wk12 (p=0.0001/ p=0.0020, respectively). IL-17+ cell frequency increased in $\gamma\delta$ and Vα7.2+ CD8+ T-cells at

Wk12 (p=0.0340, p=0.0061, respectively) and NKT-L cells (CD16+ Wk9/Wk16 p=0.0020/0.0391, CD56+ Wk9/Wk12 p=0.0398/0.0101, CD16+CD56+ Wk16 p=0.0156).

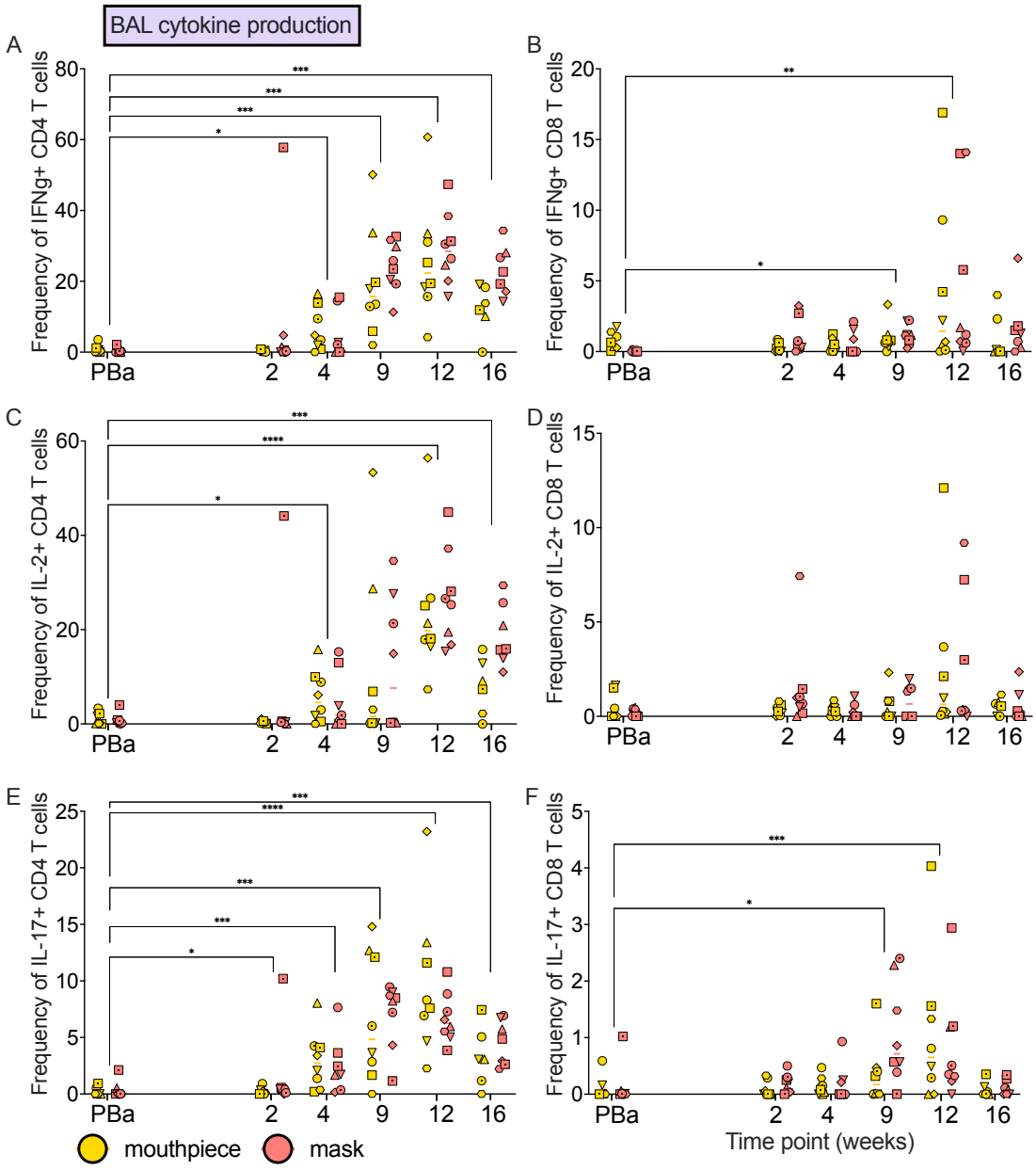


Figure 4.21 Cytokine expression on broncho-alveolar lavage (BAL) cell populations

*The frequency of PPD-specific cytokine producing cells was measured among CD4+ and CD8+ T-cells in BAL fluid: IFNγ (**A** & **B**), IL-2 (**C** & **D**), and IL-17 (**E** & **F**). Rhesus macaques exposed to aerosol BCG (aeBCG) by mouthpiece (yellow) and mask (pink) delivery are shown at time points after aeBCG (weeks) and at baseline (PBa). Each symbol represents a different animal and group medians are shown. Statistical comparisons between paired data (all animals) was performed using Wilcoxon-Rank Testing. Where significant, comparisons are marked: P < 0.05 (*), P <0.005 (**), P < 0.001 (***), or P < 0.0001 (****).*

Co-expression of multiple cytokines was detected on CD4+ and CD8+ T-cells in PBMCs and BAL. In PBMCs, the most common multi-functional subset was the IL-2+IL-17+ cells (Figure 4.22). IFNγ+IL-17+ CD4+ T-cells frequency increased at Wk9/Wk12 compared to baseline (p=0.0156/0.0078).

The percentage of cytokine producing cells was much higher in BAL cell subsets than PBMCs, and there were also more polyfunctional T-cells in BAL compared to PBMC (Figure 4.23). In the BAL, polyfunctional T-cell frequency increased more among CD4+ than CD8+ T-cells. Triple and double cytokine-positive CD4+ BAL T-cells were all increased at Wk12. Single cytokine-positive IFNγ+IL-2-IL-17- and IFNγ-IL-2-IL-17+ CD4+ T-cell frequency increased from Wk2-Wk12, but IFNγ-IL-2+IL-17- CD4+ T-cell frequency remained unchanged.

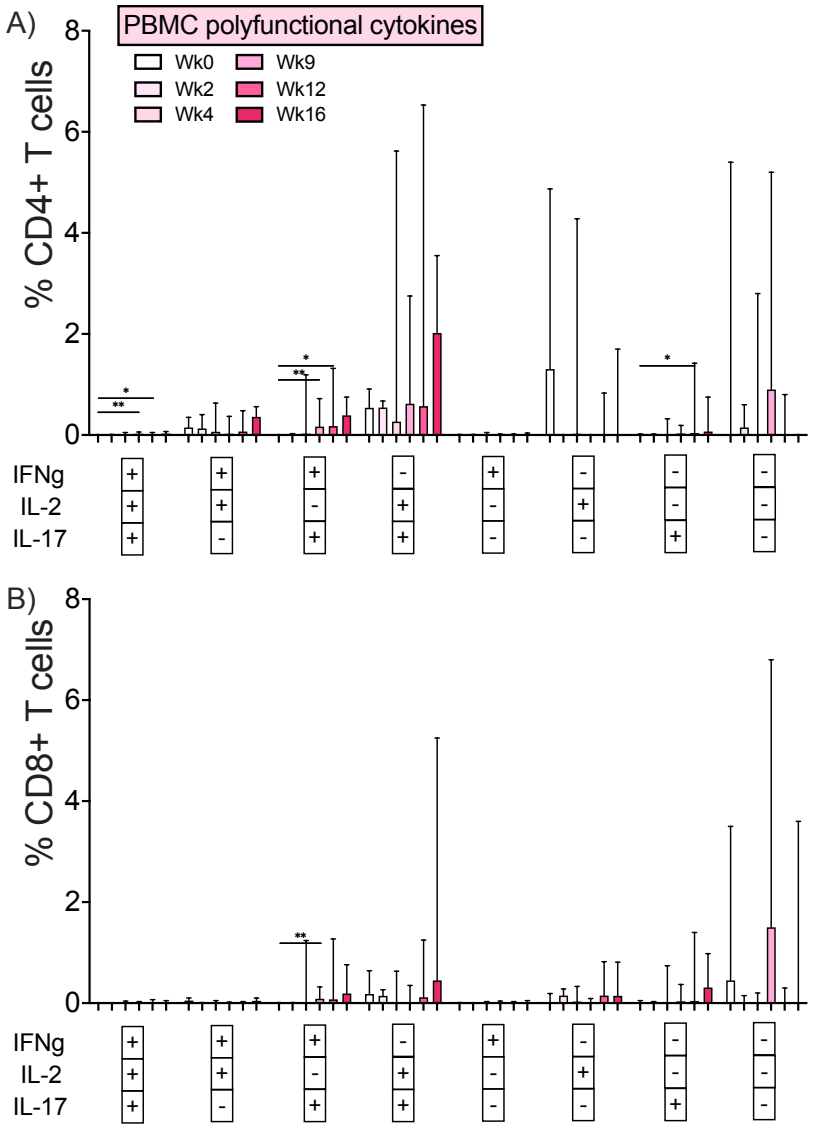


Figure 4.22 Polyfunctional cytokine expression on peripheral blood mononuclear cell (PBMC) populations

*The frequency of polyfunctional PPD-specific cytokine producing cells were measured among CD4+ (**A**) and CD8+ (**B**) PBMC T-cells. Rhesus macaques exposed to aerosol BCG (aeBCG) by mouthpiece (yellow) and mask (pink) delivery are shown at time points after aeBCG (weeks) and at baseline (PBa). Each symbol represents a different animal and group medians are shown. Statistical comparisons between paired data (all animals) was performed using Wilcoxon-Rank Testing. Where significant, comparisons are marked: P < 0.05 (*) or P < 0.005 (**).*

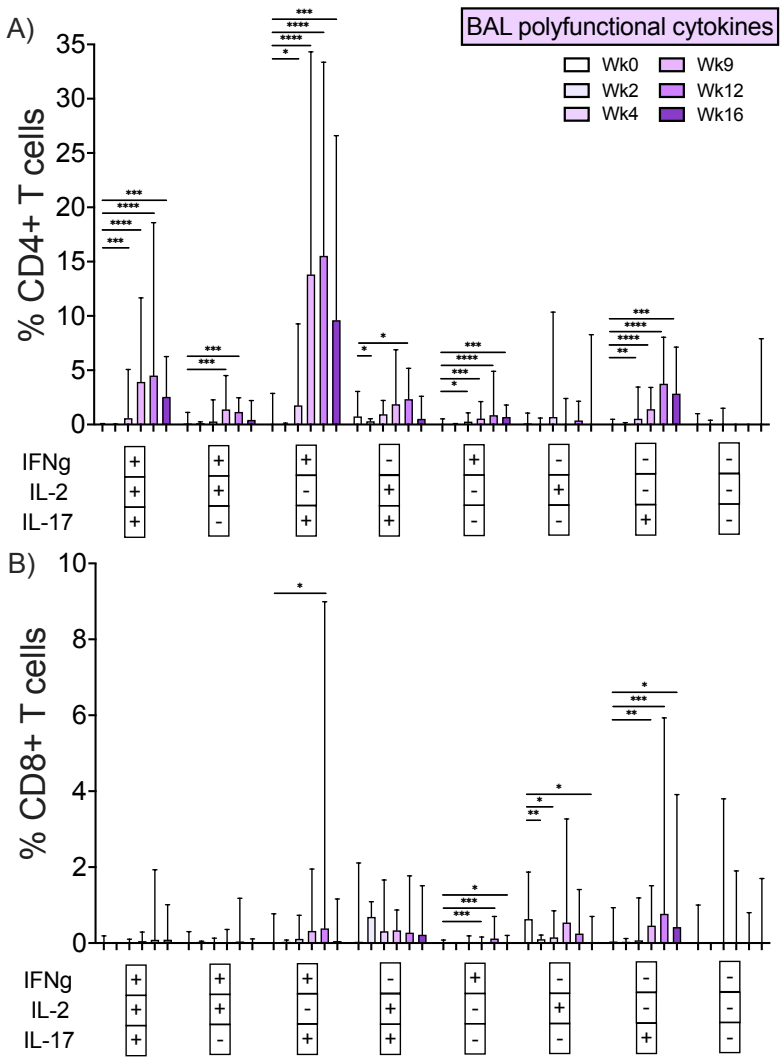


Figure 4.23 Polyfunctional cytokine expression on broncho-alveolar lavage (BAL) cell populations

*The frequency of polyfunctional PPD-specific cytokine producing cells were measured among CD4+ (**A**) and CD8+ (**B**) BAL T-cells. Rhesus macaques exposed to aerosol BCG (aeBCG) by mouthpiece (yellow) and mask (pink) delivery are shown at time points after aeBCG (weeks) and at baseline (PBa). Each symbol represents a different animal and group medians are shown. Each symbol represents a different animal and group medians are shown. Statistical comparisons between paired data (all animals) was performed using Wilcoxon-Rank Testing. Where significant, comparisons are marked: P < 0.05 (*), P <0.005 (**), P < 0.001 (***), or P < 0.0001 (****).*

4.4.11 Antibody response

Wk17 and PBb serum samples were available and included in the comparison of PPD-specific IgG titre after aeBCG. There was no difference between delivery groups when comparing AUC values for IgG titre, or when comparing groups at specific time points. The AUC was only just significantly different between male/female animals (p=0.0499). Mask and mouthpiece animals had significantly different IgM titres by Mann-Whitney U-test at three time points: Wk4/Wk12 in IgM sera (p=0.0281/0.0379, respectively), and at PBa in neat BALf (p=0.0391). Differences between delivery groups were minimal, therefore data from all animals were analysed together. Example standard curves from both IgG and IgM PPD-specific ELISAs are shown in Figure 4.24.

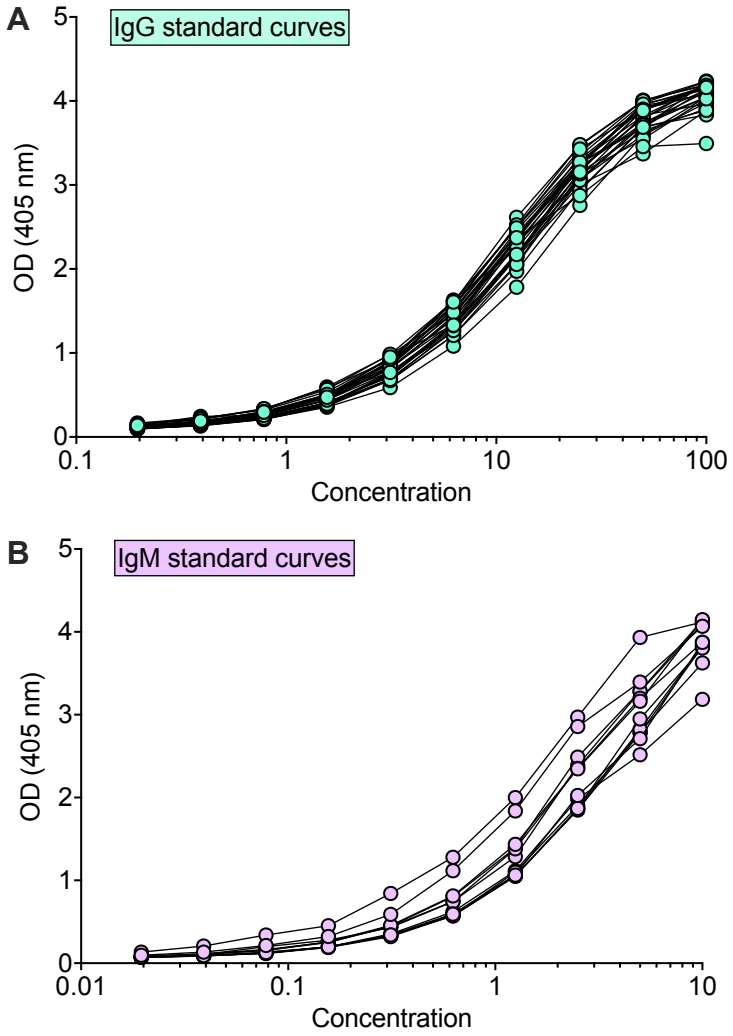


Figure 4.24 PPD-specific antibody standard curves

*Standard curves for PPD-specific IgG (**A**) and IgM (**B**) are plotted from different experiments. Antibody titres were taken when standard curve values reached their endpoint, based on a pre-defined set of parameters.*

Three animals had high baseline PPD-specific IgG titres: 38X (mouthpiece), 64X and 48X (mask). IgG titre for animal 64X and 48X followed the overall trend for increased IgG titre at Wk9 (Figure 4.25). 38X was identified as an outlier by Grubb's test at all time points (Alpha=0.05) and excluded. After excluding 38X, serum IgG titre was significantly increased compared to baseline from Wk4-Wk16 (Table 4.9). In neat BALf, IgG titre was increased at Wk9/Wk12 (p=0.0068/0.0322), and at all time points measured in BALf after concentration by centrifugation.

PPD-specific IgM titre was measured in serum and BALf (Figure 4.26). In serum, IgM was decreased at Wk2 compared to baseline, and increased at Wk16 (p=0.0076 and p=0.0386, respectively). In neat BALf, IgM was increased at Wk2/Wk4 compared to baseline (p=0.00234/0.0234, respectively and in concentrated BALf, IgM was increased at Wk9/Wk16 (p=0.0078 and p=0.0312, respectively).

Antibody titre: mask and mouthpiece								
antibody	sample	baseline	Wk2	Wk4	Wk9	Wk12	Wk16	Wk17
IgG	serum	PBa	ns	ns	***	***	**	ns
		PBb	ns	**	****	****	**	ns
	neat BAL	PBa	ns	ns	*	**	ns	
	conc. BAL	PBa	*	**	***	*	**	
IgM	serum	PBa	**	ns	ns	ns	*	
	neat BAL	PBa	*	*	ns	ns	ns	
	conc. BAL	PBa	ns	ns	**	ns	*	

Table 4.9 Changes in antibody titre later after aerosol BCG (aeBCG)

PPD-specific IgG and IgM titre were measured, and statistical comparisons of this data are shown. Statistical comparisons between paired samples at baseline (PBa/PBb) and time points after aeBCG were made using separate Wilcoxon-Rank tests. Comparisons are marked as not significant (ns), P < 0.05 (*), P < 0.005 (**), P < 0.001 (***) or P < 0.0001 (****), with increases shown in yellow, and decreases in blue.

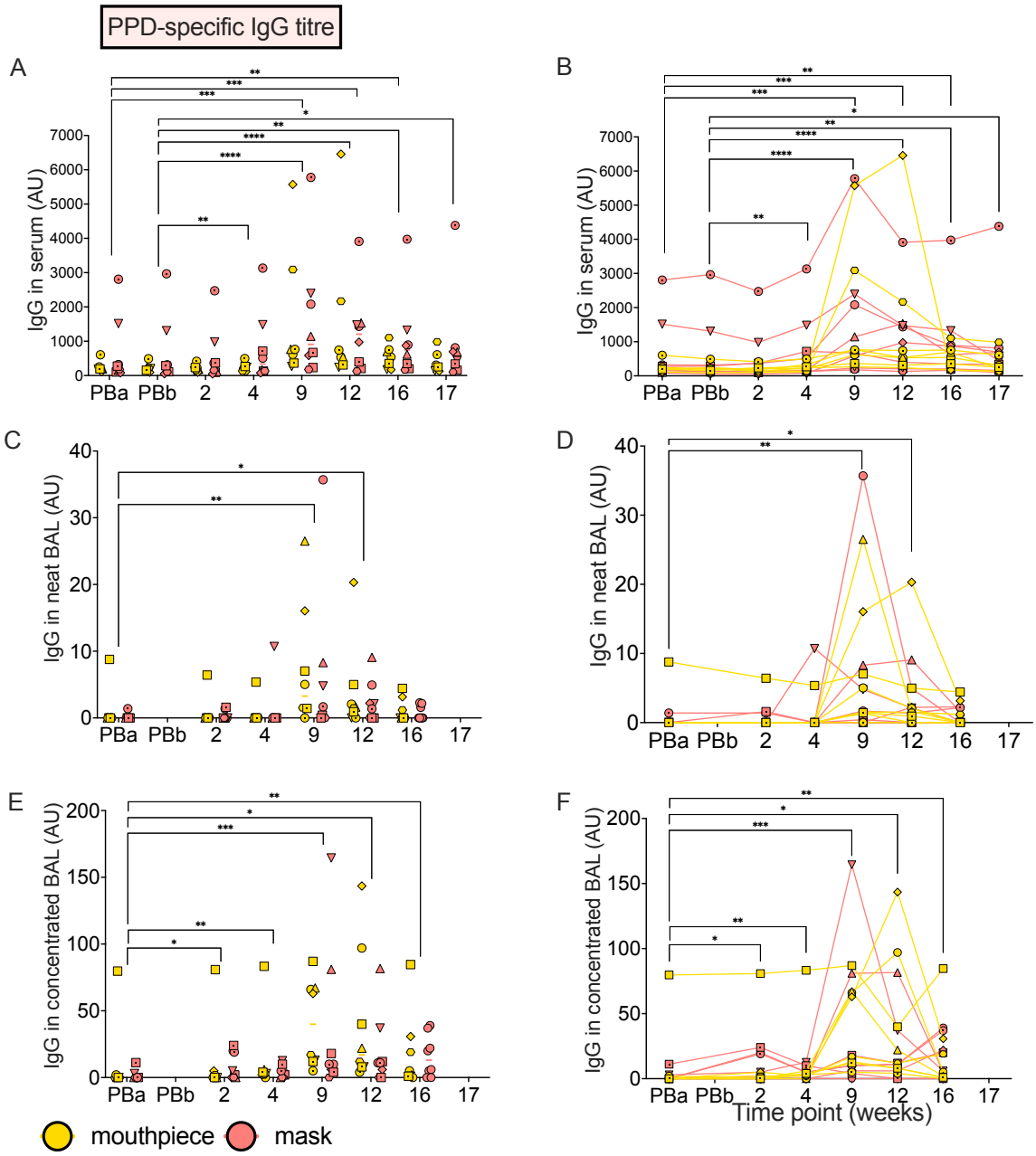


Figure 4.25 PPD-specific IgG antibody production

*PPD-specific IgG titres in response to aerosol BCG are shown in serum (**A-B**), broncho-alveolar lavage (BAL) fluid (**C-D**) and concentrated BAL fluid (**E-F**), in RM exposed via mask (pink) or mouthpiece (yellow) delivery. Values for individual animals are marked by a specific symbol and can be followed using the tracked responses shown on the right. Statistical comparisons between paired data (all animals) was performed using Wilcoxon-Rank Testing. Significant comparisons are marked: P < 0.05 (*) or P < 0.005 (**).*

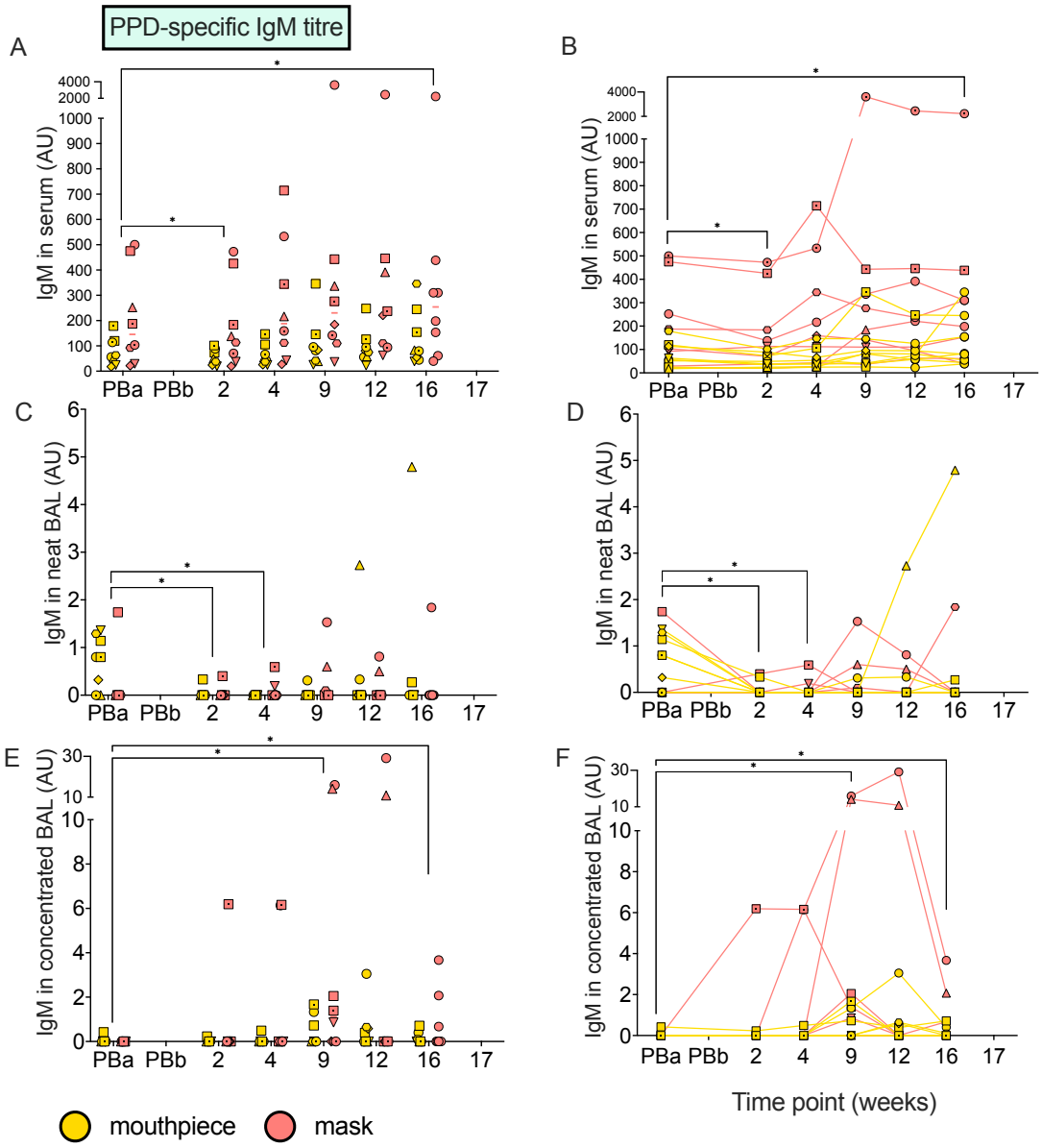


Figure 4.26 PPD-specific IgM antibody production

*PPD-specific IgM titres in response to infection with aerosol BCG (aeBCG) are shown in serum (**A-B**), neat broncho-alveolar lavage fluid (BALf) (**C-D**) and concentrated BALf (**E-F**), in RM exposed via mask (pink) or mouthpiece (yellow) delivery. Values for individual animals are marked by a specific symbol and can be followed using the tracked responses shown on the right. Statistical comparisons between paired data (all animals) was performed using Wilcoxon-Rank Testing. Significant comparisons are marked: P < 0.05 (*) or P < 0.005 (**).*

4.4.12 Correlations between immune readouts

r_s was calculated to compare the frequency of PPD-specific IFNγ+ SFU (ELISpot) to PBMC and BAL cell population frequency (Supplementary Table 5 and Supplementary Table 6, respectively). Correlations that were significant and in the same direction at two time points are summarised Table 4.10 (PBMC) and Table 4.11 (BAL), and highlighted as negative (blue) or positive (yellow).

Missing data (PBMC flow) meant that a proportion of comparisons were limited to n=8. IFNγ SFU frequency at Wk2/Wk4 negatively correlated with PBMC CD4-CD8- T-cell frequency and CD161+ CD8+ T-cell frequency at Wk2. When IFNγ SFU frequency was greatest (Wk12/Wk16), this correlated with the frequency of PBMC cell populations at Wk2/Wk4: T-cell frequency (Wk4), CD16+CD56 NKT-L cell frequency (Wk2/Wk4) and CD16+ NKT-L cell frequency (Wk2), and CD14+CD16+ non-lymphocyte frequency (Wk12). Baseline IFNγ SFU frequency correlated positively with a proportion of PBMC populations at baseline.

Basline IFNγ SFU frequency correlated negatively with a number of CD16+ non-lymphocyte BAL populations at later time points: CD14+CD16+ (Wk4/Wk9/Wk12), CD14-CD16+ (Wk9/Wk16) and total CD16+ (Wk9/Wk12/Wk16). Wk2 SFU frequency positively correlated with BAL γδ T-cell frequency at Wk4/Wk9/Wk12.

IFNg ELISpot correlations with cell populations (PBMC)				
Readout 1	**Readout 2**	**r(s)**	**Significance**	**n=**
ELISpot PBa	PBMC CD3 Wk4	0.567	0.022	16
ELISpot Wk12	PBMC CD3 Wk4	0.565	0.023	16
ELISpot Wk2	PBMC CD4-8- Wk2	-0.695	0.003	16
ELISpot Wk4	PBMC CD4-8- Wk2	-0.526	0.036	16
ELISpot Wk2	PBMC MAIT CD161+Va7.2- Wk2	-0.570	0.021	16
ELSpot Wk4	PBMC MAIT CD161+Va7.2- Wk2	-0.508	0.045	16
ELISpot Wk12	PBMC NKT CD16+CD56+ Wk2	0.562	0.024	16
ELISpot Wk12	PBMC NKT CD16+CD56+ Wk4	0.541	0.030	16
ELISpot PBa	PBMC NK CD16-CD56+ Wk9	-0.559	0.024	16
ELISpot Wk12	PBMC NK CD16-CD56+ Wk9	-0.527	0.036	16
ELISpot PBb	PBMC nonL CD14+ Wk2	-0.515	0.041	16
ELISpot PBb	PBMC nonL CD14+CD16+ Wk2	-0.591	0.016	16
ELISpot Wk16	PBMC nonL CD14+CD16+ Wk2	-0.612	0.012	16
ELISpot PBb	PBMC nonL CD14+CD16+ Wk12	-0.529	0.035	16
ELISpot Wk12	PBMC NKT CD16+ Wk2	0.536	0.040	15
ELISpot Wk12	PBMC NK CD16+CD56+ Wk16	0.536	0.040	15
ELISpot Wk9	PBMC CD4+8+ Wk16	-0.762	0.028	8
ELISpot Wk12	PBMC CD4+8+ Wk16	-0.881	0.004	8
ELISpot PBa	PBMC CD8+ PBa	-0.719	0.045	8
ELISpot PBa	PBMC MAIT 7.2+ PBa	0.905	0.002	8
ELISpot PBb	PBMC NKT CD16+CD56+ PBa	-0.910	0.002	8
ELISpot Wk2	PBMC NKT CD16+CD56+ PBa	-0.850	0.007	8
ELISpot Wk4	PBMC NKT CD16+CD56+ PBa	-0.778	0.023	8
ELISpot PBb	PBMC NKT CD16+CD56+ Wk16	0.738	0.037	8
ELISpot Wk9	PBMC NKT CD16+CD56+ Wk16	0.714	0.047	8
ELISpot PBa	PBMC NK CD16+CD56- Wk9	0.714	0.047	8
ELISpot PBa	PBMC NK CD16+CD56- Wk12	0.762	0.028	8
ELISpot Wk16	PBMC NK CD16+CD56- Wk12	0.714	0.047	8
ELISpot PBa	PBMC NKT 56+ PBa	0.762	0.028	8
ELISpot Wk16	PBMC NKT 56+ PBa	0.714	0.047	8

Table 4.10 Correlations between the frequency of PPD-specific IFNγ SFU measured by ELISpot and cell population frequencies among peripheral blood mononuclear cells (PBMCs)

Spearman's rank correlation coefficient ('r(s)') was calculated to compare the frequency of PPD-specific IFNγ spot forming units and population frequencies among PBMCs. Negative correlations are highlighted in blue and positive correlations are highlighted in yellow. The number of data points compared ('n=') and significance of each correlation ('significance') are also shown.

IFNg ELISpot correlations with cell populations (BAL)				
Readout 1	**Readout 2**	**r(s)**	**Significance**	**n=**
ELISpot Wk4	BAL CD8 PBa	-0.546	0.0350	15
ELISpot Wk4	BAL CD8 Wk4	-0.664	0.0050	16
ELISpot Wk4	BAL CD8 Wk9	-0.680	0.0040	16
ELISpot Wk2	BAL gd Wk4	0.636	0.0081	16
ELISpot Wk2	BAL gd Wk9	0.558	0.0248	16
ELISpot Wk2	BAL gd Wk12	0.518	0.0398	16
ELISpot Wk9	BAL MAIT CD161-Va7.2+ PBa	-0.543	0.0365	15
ELISpot Wk9	BAL MAIT CD161-Va7.2+ Wk16	-0.569	0.0336	14
ELISpot PBa	BAL NKT CD16+ WK2	-0.539	0.0312	16
ELISpot PBa	BAL NKT CD16+ WK12	-0.571	0.0208	16
ELISpot PBb	BAL NKT CD56+ Wk4	-0.512	0.0427	16
ELISpot PBb	BAL NKT CD56+ Wk9	-0.541	0.0304	16
ELISpot PBb	BAL NKT CD56+ Wk12	-0.562	0.0366	14
ELISpot Wk9	BAL NK CD16+CD56+ PBa	-0.543	0.0365	15
ELISpot Wk9	BAL NK CD16+CD56+ Wk9	-0.569	0.0336	14
ELISpot PBa	BAL NK CD16-CD56+ Wk4	-0.522	0.0379	16
ELISpot PBa	BAL NK CD16-CD56+ Wk12	-0.649	0.0065	16
ELISpot PBa	BAL nonL CD14+CD16+ Wk9	-0.614	0.0115	16
ELISpot PBa	BAL nonL CD14+CD16+ Wk12	-0.609	0.0122	16
ELISpot PBa	BAL nonL CD14+CD16+ Wk16	-0.578	0.0304	14
ELISpot PBa	BAL nonL CD14-CD16+ Wk9	-0.517	0.0405	16
ELISpot PBa	BAL nonL CD14-CD16+ Wk16	-0.631	0.0156	14
ELISpot PBa	BAL nonL CD16+ Wk9	-0.609	0.0122	16
ELISpot PBa	BAL nonL CD16+ Wk12	-0.572	0.0205	16
ELISpot PBa	BAL nonL CD16+ Wk16	-0.618	0.0186	14

Table 4.11 Correlations between the frequency of PPD-specific IFNγ SFU measured by ELISpot and cell population frequencies among broncho-alveolar lavage (BAL) cells

Spearman's rank correlation coefficient ('r(s)') was calculated to compare the frequency of PPD-specific IFNγ spot forming units and population frequencies BAL cells. Negative correlations are highlighted in blue and positive correlations are highlighted in yellow. The number of data points compared ('n=') and significance of each correlation ('significance') are also shown.

The same analysis was also applied to compare IFNγ SFU frequency at each time point with cytokine-positive cell frequency at each time point (Supplementary Table 7 to Supplementary Table 12). Correlations that were significant and in the same direction at two time points are summarised Table 4.12 (PBMC) and Table 4.13 (BAL).

IFNγ+ CD4+ T-cell frequency was detected by flow cytometry (PBMCs), but this did not correlate with IFNγ SFU frequency. Wk2 IFNγ SFU frequency positively correlated with IFNγ+ CD16+CD56- NK cell (Wk2/Wk9) and CD14-CD16+ non-lymphocyte (Wk9/Wk12) frequency. Wk12 IFNγ SFU frequency positively correlated with IL-2+ CD16+ NKT-L cell (Wk2/Wk9) and CD14+CD16+ non-lymphocyte (Wk9) frequency. Baseline (PBb) ELISpot SFU frequency correlated with IL-17+ cell frequency among a number of PBMC populations, but these correlations were not detected compared to PBa.

PBa/Wk2 IFNγ SFU frequency positively correlated with IFNγ+ Vα7.2+ CD8+ BAL T-cell frequency at Wk4, but there other significant correlations between IFNγ+ cell subsets in BAL and IFNγ SFU frequency were not identified. Wk9 IFNγ SFU frequency positively correlated with IL-2+ CD4+ T-cell (Wk2), IL-2+ CD16+CD56- NK cell (Wk4/Wk12), and IL-17+ CD14+CD16+ non-lymphocyte (PBa/Wk2) frequency.

IFNγ SFU frequency was also compared with IgG and IgM titre (Supplementary Table 13 and Supplementary Table 14, respectively). Correlations that were significant and in the same direction at two time points are summarised in Table 4.14 (A is IgG, B is IgM). ELISpot SFU frequency at Wk2 correlated negatively with neat BALf IgG titre (PBa/Wk16), serum IgM (PBa/Wk2/Wk4/Wk16) and concentrated BALf IgM titre (Wk9).

IFNg ELISpot correlations with cytokine+ PBMCs					
	Readout 1	**Readout 2**	**r(s)**	**Significance**	**n=**
IFNg	ELISpot PBb	PBMC IFNg gd Wk4	-0.513	0.0423	16
	ELISpot PBb	PBMC IFNg gd Wk9	-0.559	0.0245	16
	ELISpot Wk2	PBMC IFNg NK CD16+CD56- Wk2	0.551	0.0269	16
	ELISpot Wk2	PBMC IFNg NK CD16+CD56- Wk9	0.627	0.0094	16
	ELISpot Wk9	PBMC IFNg NK CD16+CD56- Wk12	-0.553	0.0264	16
	ELISpot Wk9	PBMC IFNg NK CD16+CD56- Wk16	-0.826	0.0114	8
	ELISpot Wk4	PBMC IFNg NKT CD16+CD56+ WK2	-0.656	0.0079	15
	ELISpot Wk4	PBMC IFNg NKT CD16+CD56+ WK9	-0.521	0.0385	16
	ELISpot PBb	PBMC IFNg NKT CD16+CD56+ WK9	0.549	0.0276	16
	ELISpot Wk9	PBMC IFNg nonL CD14+CD16- Wk4	0.684	-0.0035	16
	ELISpot Wk12	PBMC IFNg nonL CD14+CD16- Wk4	0.620	0.0104	16
	ELISpot Wk2	PBMC IFNg nonL CD14-CD16+ Wk9	0.571	0.0210	16
	ELISpot WK2	PBMC IFNg nonL CD14-CD16+ Wk12	0.635	0.0083	16

	Readout 1	**Readout 2**	**r(s)**	**Significance**	**n=**
IL-2	ELISpot Wk12	PBMC IL-2 NKT CD16+ Wk2	-0.591	0.0159	16
	ELISpot Wk12	PBMC IL-2 NKT CD16+ Wk9	-0.509	0.0443	16
	ELISpot Wk2	PBMC IL-2 NKT CD16+CD56+ Wk9	0.555	0.0258	16
	ELISpot Wk4	PBMC IL-2 NKT CD16+CD56+ Wk9	0.661	0.0053	16
	ELISpot PBb	PBMC NKT CD56+ IL-2 PBa	-0.732	0.0390	8
	ELISpot PBb	PBMC NKT CD56+ IL-2 Wk12	-0.541	0.0372	15
	ELISpot Wk9	PBMC IL-2 nonL CD14+CD16+ Wk9	0.605	0.0131	16
	ELISpot Wk12	PBMC IL-2 nonL CD14+CD16+ Wk9	0.588	0.0166	16

	Readout 1	**Readout 2**	**r(s)**	**Significance**	**n=**
IL-17	ELISpot Wk2	PBMC IL-17 gd Wk4	0.606	0.0128	16
	ELISpot Wk4	PBMC IL-17 gd Wk4	0.523	0.0377	16
	ELISpot Wk4	PBMC IL-17 CD8 Wk9	0.499	0.0494	16
	ELISpot Wk4	PBMC IL-17 CD8 Wk12	0.581	0.0182	16
	ELISpot PBb	PBMC IL-17 NK CD16-CD56+ Wk12	0.500	0.0487	16
	ELISpot Wk9	PBMC IL-17 NK CD16-CD56+ Wk12	0.515	0.0413	16
	ELISpot PBb	PBMC IL-17 NK CD16+ Wk4	-0.872	0.0000	16
	ELISpot PBb	PBMC IL-17 NK CD16+ Wk9	-0.526	0.0365	16
	ELISpot Wk4	PBMC IL-17 NK CD16+ Wk9	0.529	0.0350	16
	ELISpot Wk4	PBMC IL-17 NK CD16+ Wk12	0.711	0.0020	16
	ELISpot PBb	PBMC IL-17 NK CD16+ Wk16	-0.905	0.0020	8
	ELISpot PBb	PBMC IL-17 NK CD16+CD56+ Wk4	-0.875	0.0000	16
	ELISpot PBb	PBMC IL-17 NK CD16+CD56+ Wk9	-0.609	0.0122	16
	ELISpot PBb	PBMC IL-17 NK CD16+CD56+ Wk16	-0.738	0.0366	8
	ELISpot Wk9	PBMC IL-17 nonL CD14+CD16- Wk16	0.805	0.0159	8
	ELISpot Wk12	PBMC IL-17 nonL CD14+CD16- Wk16	0.903	0.0021	8
	ELISpot PBb	PBMC IL-17 NK CD56+ Wk4	-0.655	0.0059	16
	ELISpot PBb	PBMC IL-17 NK CD56+ Wk9	-0.600	0.0140	16

Table 4.12 Correlations between the frequency of PPD-specific IFNγ SFU measured by ELISpot and cytokine-positive cells (peripheral blood mononuclear cells - PBMC)

Spearman's rank correlation coefficient ('r(s)') was calculated to compare the frequency of PPD-specific IFNγ spot forming units and frequencies of cytokine-positive (IFNγ, IL-2 or IL-17) cells among PBMC cell subsets. Negative correlations are highlighted in blue and positive correlations are highlighted in yellow. The number of data points compared ('n=') and significance of each correlation ('significance') are also shown.

	IFNg ELISpot correlations with cytokine+ BAL cells				
	Readout 1	**Readout 2**	**r(s)**	**Significance**	**n=**
IFNg	ELISpot PBa	BAL IFNg MAIT 7.2+ Wk4	-0.499	0.0491	16
	ELISpot Wk2	BAL IFNg MAIT 7.2+ Wk4	-0.592	0.0158	16

	Readout 1	**Readout 2**	**r(s)**	**Significance**	**n=**
IL-2	ELISpot PBb	BAL IL-2 CD4 PBa	-0.611	0.0156	15
	ELISpot PBb	BAL IL-2 CD4 Wk2	-0.502	0.0476	16
	ELISpot Wk9	BAL IL-2 CD4 Wk2	-0.685	0.0034	16
	ELISpot PBb	BAL IL-2 CD4 Wk9	0.709	0.0021	16
	ELISpot PBb	BAL IL-2 gd Wk9	0.664	0.0051	16
	ELISpot Wk2	BAL IL-2 gd Wk9	-0.519	0.0393	16
	ELISpot Wk4	BAL IL-2 gd Wk9	-0.547	0.0282	16
	ELISpot Wk9	BAL IL-2 NK CD16+CD56- Wk4	0.549	0.0276	16
	ELISpot Wk9	BAL IL-2 NK CD16+CD56- Wk12	0.522	0.0383	16

	Readout 1	**Readout 2**	**r(s)**	**Significance**	**n=**
IL-17	ELISpot Wk2	BAL IL-17 CD4 Wk4	0.717	0.0026	15
	ELISpot Wk4	BAL IL-17 CD4 Wk4	0.607	0.0164	15
	ELISpot Wk16	BAL IL-17 NKT-L CD16+CD56+ Wk2	-0.644	0.0096	15
	ELISpot Wk16	BAL IL-17 NKT-L CD16+CD56+ Wk9	-0.629	0.0120	15
	ELISpot Wk2	BAL IL-17 nonL CD14+CD16+ PBa	0.657	0.0077	15
	ELISpot Wk9	BAL IL-17 nonL CD14+CD16+ PBa	0.600	0.0180	15
	ELISpot Wk9	BAL IL-17 nonL CD14+CD16+ Wk2	0.550	0.0338	15
	ELISpot Wk12	BAL IL-17 nonL CD14+CD16+ Wk2	0.690	0.0044	15

Table 4.13 Correlations between the frequency of PPD-specific IFNγ SFU measured by ELISpot and cytokine-positive broncho-alveolar lavage (BAL) cells

Spearman's rank correlation coefficient ('r(s)') was calculated to compare the frequency of PPD-specific IFNγ spot forming units and frequencies of cytokine-positive (IFNγ, IL-2 or IL-17) cells among BAL cell subsets. Negative correlations are highlighted in blue and positive correlations are highlighted in yellow. The number of data points compared ('n=') and significance of each correlation ('significance') are also shown.

A) IFNg ELISpot vs IgG				
Readout 1	**Readout 2**	**r(s)**	**Significance**	**n=**
ELISpot Wk2	neat BALf IgM PBa	-0.508	0.0446	16
ELISpot PBb	neat BALf IgM Wk4	0.499	0.0494	16
ELISpot Wk2	neat BALf IgM Wk16	-0.676	0.0041	16
ELISpot Wk4	neat BALf IgM Wk16	-0.615	0.0112	16
ELISpot PBa	conc. BALf IgM Wk9	-0.568	0.0216	16
ELISpot PBa	conc. BALf IgM Wk12	-0.555	0.0257	16
ELISpot Wk4	conc. BALf IgM Wk16	-0.516	0.0410	16

B) IFNg ELISpot vs IgM				
Readout 1	**Readout 2**	**r(s)**	**Significance**	**n=**
ELISpot Wk2	serum IgM PBa	0.580	0.0186	16
ELISpot Wk2	serum IgM Wk2	0.667	0.0048	16
ELISpot Wk2	serum IgM Wk4	0.572	0.0205	16
ELISpot Wk2	serum IgM Wk16	0.510	0.0438	16
ELISpot Wk9	neat BALf IgM Wk9	0.761	0.0006	16
ELISpot Wk9	neat BALf IgM Wk12	0.628	0.0092	16
ELISpot PBb	neat BALf IgM Wk16	0.578	0.0190	16
ELISpot PBa	conc. BALf IgM Wk4	0.557	0.0250	16
ELISpot Wk2	conc. BALf IgM Wk9	0.583	0.0177	16
ELISpot Wk9	conc. BALf IgM Wk12	0.585	0.0174	16
ELISpot Wk9	conc. BALf IgM Wk16	0.542	0.0299	16

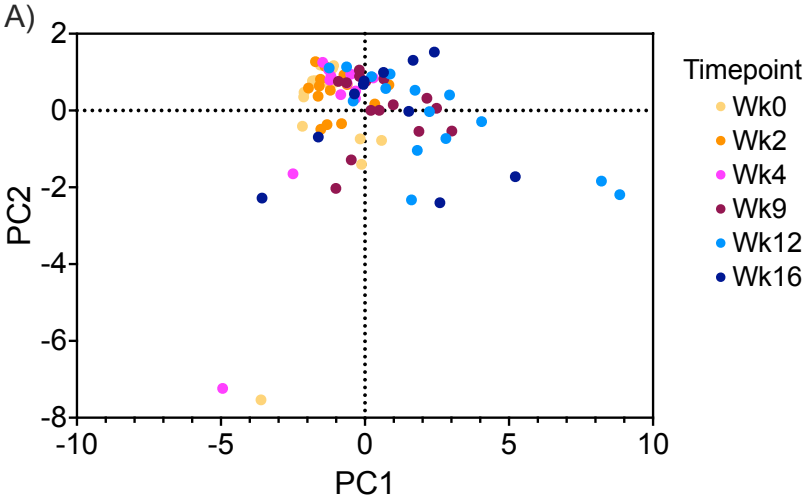
Table 4.14 Correlations between the frequency of PPD-specific IFNγ SFU measured by ELISpot and antibody titre

*Spearman's rank correlation coefficient ('r(s)') was calculated to compare the frequency of PPD-specific IFNγ spot forming units and PPD-specific IgG (**A**) or IgM (**B**) antibody titre. Negative correlations are highlighted in blue and positive correlations are highlighted in yellow. Comparisons to antibody titre in serum (yellow), neat broncho-alveolar lavage fluid (neat BALf) and concentrated BAL fluid (conc. BALf) are shown. The number of data points compared ('n=') and significance of each correlation ('significance') are also shown.*

4.4.13 Principal component analysis of BAL cell populations

PCA was performed on one subset of data to explore this method and visualise a larger dataset at once. The selected dataset examined cytokine expression among different cell subsets in the BAL (CD4+/CD8+/MAIT/γδ, CD16+/CD56+ NK/NKT-L cells, CD14+/-CD16+/- non-lymphocytes). Eight principal components were identified as having Eigenvalues above the cut-off threshold of 1, four of which had values above 1.5. PCA analysis showed that cytokine clusters differ by time point after aeBCG, with the largest amount of variance accounted for by Principal component 1 (PC1, Figure 4.27). PC1 accounted for 21.92% of the variance, with an Eigenvalue of 4.822 (T-cell IFNγ+ expression), and PC2 accounted for 10.58% of the variance, with an Eigenvalue of 2.329 (CD4+, NK and NKT-L cell IL-2 and CD8+ IL-17 expression). In total 72.18% of the variance was accounted for by the eight selected PCs.

A)



B)

	PC1	PC2	PC3	PC4	PC5	PC6	PC7	PC8
IFNg CD4+	0.329	-0.042	0.002	-0.165	0.051	-0.030	0.209	-0.228
IFNg CD8+	0.362	-0.145	-0.091	0.178	-0.044	-0.174	-0.049	0.040
IFNg MAIT	0.172	-0.043	-0.077	0.075	-0.196	0.027	-0.264	-0.436
IFNg gd	0.357	-0.087	-0.025	-0.076	0.163	0.055	-0.050	-0.021
IFNg NKT CD16+	0.216	-0.083	-0.040	-0.156	0.478	0.044	0.323	-0.106
IFNg NKT CD56+	0.358	-0.180	-0.115	0.151	0.007	-0.024	-0.196	0.123
IFNg NK CD16+	0.139	0.054	-0.108	-0.503	-0.291	-0.194	-0.040	0.312
IFNg NK CD56+	0.075	-0.023	-0.372	-0.047	0.088	0.217	-0.219	0.418
IFNg nonL CD14+CD16+	0.062	0.092	0.438	-0.006	-0.254	0.161	0.236	0.119
IFNg nonL CD14+CD16-	0.037	-0.165	0.224	-0.255	0.541	0.097	-0.016	0.024
IFNg nonL CD14-CD16+	0.110	0.058	-0.240	-0.534	-0.160	-0.198	0.152	0.021
IL-2 CD4+	-0.211	-0.365	0.130	0.065	0.036	-0.368	-0.120	0.170
IL-2 CD8+	0.268	-0.050	-0.022	0.217	-0.119	-0.212	0.206	-0.259
IL-2 MAIT	0.029	0.003	-0.107	0.322	0.193	-0.238	0.376	0.463
IL-2 gd	0.306	-0.218	-0.095	0.218	-0.083	0.060	-0.189	0.113
IL-2 NKT CD16+	-0.130	-0.529	-0.108	-0.062	-0.195	0.233	0.225	-0.046
IL-2 NKT CD56+	0.205	-0.052	0.345	-0.189	-0.105	0.001	-0.270	0.130
IL-2 NK CD16+	-0.158	-0.354	0.219	-0.049	0.005	-0.398	-0.179	0.034
IL-2 NK CD56+	-0.039	-0.090	0.096	-0.142	0.234	-0.265	-0.218	-0.225
IL-17 CD4+	0.225	0.033	0.357	0.054	-0.183	-0.209	0.310	0.087
IL-17 CD8+	-0.123	-0.530	-0.104	-0.096	-0.173	0.241	0.249	-0.059
IL-17 MAIT	0.161	-0.073	0.396	-0.008	0.006	0.423	-0.127	0.192

Figure 4.27 Principal component analysis (PCA) of bronchoalveolar lavage (BAL) cytokine expression among cell populations

*PCA divulges patterns in cytokine expression and was performed to graphically exhibit the dissemination of data from time points after aerosol BCG (time point indicated by colour). Principal components of variation with Eigenvalues over 1 were selected. Principal component 1 (PC1) is shown graphically in comparison to PC2 (**A**). Eigenvectors are summarised to illustrate how cytokine expression from each cell subset influences each component (B).*

4.5 Discussion

4.5.1 Late response to aeBCG

In terms of antigen-specific cytokine production, up-regulation of immune cell subsets, and antibody production, the peak immune response to 1x10^7 CFU aeBCG in RM occurred between Wk9 and Wk16. aeBCG was well tolerated at this dose, with the only clinical signs of note being a transient and clinically insignificant drop in haemoglobin levels at Wk2/Wk4, and weight loss in one animal. After temporary removal from the group, the animal regained weight, and was returned to the group.

Haemoglobin levels can drop after repeated blood samples[279] or could be a result of the aeBCG itself. The volumes of blood taken, and the frequency of blood collections were within the NC3Rs guidelines. Throughout the study, animals were asymptomatic, and haemoglobin remained within the range considered normal. *M.tb* can use haem from haemoglobin 324 to sequester iron[280], but a drop in haemoglobin caused by this would be expected later after aeBCG, alongside clinical signs. Haemoglobin had returned to baseline levels by Wk9, at which point the immune response was beginning to peak. The Wk2/Wk4 drop in haemoglobin may indicate mycobacterial expansion before aeBCG is controlled. However, Tullius *et al.,* recently showed that BCG lacks a family of proteins (PPE37) that are important for haem-iron acquisition in *M.tb*, which makes BCG less able to sequester iron[281].

The overall kinetic of the immune response to aeBCG was explored using a PPD-specific IFNγ ELISpot assay. IFNγ SFU frequency increased from Wk4 to Wk16, with no discernible peak. White *et al*., have previously published two aeBCG studies in RM (2-8x10^6 CFU dose), that showed a more defined ELISpot peak at Wk10[3, 7]. The animals in

this project are from the same breeding colony, and the same experimental setup was used. It is interesting that the $1x10^7$ CFU aeBCG (this project) resulted in a slower kinetic than $2\text{-}8x10^6$ CFU (previously published). Verreck *et al.*, also showed that the RM response to mucosal BCG peaks at about Wk10, using $2\text{-}8x10^6$ CFU of EB BCG, which is likely similar to 'delivered' dose of aeBCG in Study 6181. After EB installation of BCG, PPD-specific IFNγ SFU frequency peaked at Wk9, after a transient drop at Wk6 compared to Wk3[10]. The delivered dose after aerosolisation is estimated to be at least one log lower than the dose added to the nebuliser[3], but this loss would also have affected previous studies and does not explain the difference in kinetic.

In Study 6181, half of the animals in each delivery group were male and half were female (due to NHP availability). Previous NHP TB vaccine studies have not seen any difference between male and female animals[91]. In humans, there is evidence suggesting that males are more susceptible to TB, perhaps due to a less strong inflammatory response in the initial stages of *M.tb* infection, or to other factors including social interactions[282]. In Study 6181, differences between male and female RM were hard to determine when animals were also split by delivery group (n=4). There were no significant differences between male and female IFNγ SFU frequencies after aeBCG when data from both delivery methods were pooled (n=8 per gender). There was a trend for lower IFNγ SFU frequency for male animals at Wk2/Wk4, but this was not significant and there was little difference between sexes from Wk9-Wk16. There was few detectable differences between sexes in other readouts, particularly when factoring in baseline responses.

4.5.2 aeBCG and mucosal BCG studies so far

aeBCG was evaluated to the immune response to mycobacteria, with methods that could be run in parallel in humans. aeBCG was first tested in the 1970s[105], and the immune response to aeBCG has also been explored in three recent published studies to our knowledge[3, 5, 7]. Further studies looking at other mucosal delivery methods of BCG in the NHP model have also been published[2, 8, 10]. Methodology and dosing used in published studies so far is variable.

In humans, aeBCG was first explored as a possible improvement on ID vaccination, and as a treatment for bladder cancer in the 1960/70s[283, 284, 285]. More recently, EB BCG and PPD installation have been explored within the human lung, with a focus on the locality of the immune response induced[104, 286]. As previously mentioned, and discussed in more detail in Chapter 5, experimental medicine studies using $1x10^7$ CFU aeBCG are underway in Oxford (ClinicalTrials.gov ID: NCT03912207 and NCT02709278).

4.5.3 mask vs mouthpiece delivery of aeBCG

The second objective of Study 6181 was to compare the immune responses of animals exposed to aeBCG by mask or mouthpiece delivery. aeBCG is delivered by mouthpiece in ongoing human experimental medicine studies in Oxford, whereas aeBCG has previously been delivered by modified paediatric mask to NHPs. Relevant mucosal BCG studies are summarised in Table 4.15**.** The effect of aerosolisation device has been compared[106, 107], but to our knowledge the effect of delivery attachment has not been explored.

In Study 6181, there were very few significant differences between immune readouts for animals in different delivery groups, despite pilot data showing that delivery attachment alters the deposition of aerosolised particles in the lung (White *et al.*, unpublished). The IFNγ SFU measured after aeBCG significantly increased at an earlier

time point after mask (Wk4) than mouthpiece delivery (Wk9), perhaps indicating a subtle difference, but did not differ by AUC or at any particular time point. Often, differences between mask and mouthpiece group animals were already identifiable at baseline, which suggests a difference caused the group of animals, rather than by delivery method.

Mucosal BCG studies									
Year	**Paper title**	**Authors**	**Species**	**Study aim**	**Details**	**Target dose (CFU)**	**Delivery**	**Number (n=)**	**Time points**
1973	Protection of Monkeys against Airborne Tuberculosis by Aerosol Vaccination with BCG	Barclay *et al.* (Wolinsky)	NHP (RM)	*M.tb* challenge: IV vs intracutaneous vs aeBCG	IV and aeBCG gave better protection than intracutaneous, no side effects	8x10^5 viable	Aerosol cloud	6	PB + week 2-8
1968	Aerogenic BCG Vaccination Against Tuberculosis in Animal and Human Subjects	Rosenthal *et al.* (Raisys)	humans + guinea pigs	aeBCG methods paper	testing aeBCG setups, e.g. does higher = more consistent TST conversion	6x10^5 viable	Darby vs DeVilbiss	10 guinea + 100+ people	2 months - 4 years
1975	2x phase I trials of aeBCG against lung cancer	Waldman *et al.*, + Lipton *et al.*	humans	aeBCG to treat bronch cancer	local and systemic side effects	multiple doses given	N/A	N/A	N/A
2005	Resident Th1-Like Effector Memory Cells in Pulmonary Recall Responses to *M.tb*	Walrath *et al.* (Silver)	humans	immunology of EB PPD 'challenge'	showed resident T cell responses	0.5 TU of PPD	EB	4	PB + day 2
2015	Evaluation of the Immunogenicity of *M.b* BCG Delivered by Aerosol to the Lungs of Macaques	White *et al.* (Sharpe)	NHP (RM)	immune response to aeBCG	aeBCG Delivered byB:K Aerosol to the Lungs of Macaques	2-8x10^6, 1/10th dose	mask	4/group	PB + week 2-12
2016	Alternative BCG delivery strategies improve protection against *M.tb* in NHPs...	Sharpe *et al.*	NHP (RM)	*M.tb* challenge: ID vs IV vs ID+IT	BCG delivery methods (ID + IT group)	2-8x10^6	ID, IV or ID+IT	6/group	PB + week 12-20
2017	...Pulmonary BCG provides protection where standard ID vaccination fails	Verreck *et al.*	NHP (RM)	*M.tb* challenge: ID vs EB BCG	EB gave better protection than ID	2-8x10^6	ID or EB	6/group	PB + week 3-15
2019	M.tb–Induced BAL Gene Expression Sig. in LTBI Is Dominated by Pleiotropic Effects of CD4 + T cells	Jarvel *et al.* (Silver)	humans	BAL genetics LTBI	dominated by IFNg+ CD4+ T cells in BAL	N/A	N/A	11	N/A
2019	Prevention of tuberculosis infection and disease by local BCG in repeatedly exposed rhesus macaques	Dijkman *et al.* (Verreck)	NHP (RM)	*M.tb* challenge (repeat low dose): EB immunology	protection against repeated low dose, Th17 correlate with protection	1.5–6.0×10^5	EB	8	PB + week 8-12
2019	A Human Lung Challenge Model to Evaluate the Safety and Immunogenicity of PPD and Live BCG	Davids *et al.* (Dheda)	humans	EB PPD or BCG 'challenge'	EB PPD or BCG in different lobes was localised, challenge feasible and safe	1x10^3-1x10^4 BCG (0.5 TU PPD)	EB	65	PB + day 3
2020	Protective Efficacy of Inhaled BCG Vaccination vs Ultra-Low Dose Aerosol *M.tb* Challenge in RM	White *et al.* (Sharpe)	NHP (RM)	*M.tb* challenge (repeat low dose): ID vs aeBCG	aeBCG reduced extrapulmonary path. + delayed response compared to ID	2-8x10^6	aeBCG (mask)	6/group	PB + week 2-20
2020	Prevention of tuberculosis in macaques after intravenous BCG immunization	Darrah *et al.* (Seder)	NHP (RM)	*M.tb* challenge: IV vs ID (high/low/+ae) vs aeBCG	IV gave better protection than other methods, aeBCG did not	5x10^7 (aeBCG)	aeBCG (mask)	1-9/group	PB + week 4-24
2021	Robust IgM responses following vaccination are associated with prevention of *M.tb* infection...	Darrah *et al.* (Seder)	NHP (RM)	antibody after BCG by different delivery methods	IV BCG lead to more IgM (IgG) than other BCG delivery	N/A	N/A	N/A	N/A
2021	T Cells Specific for a Mycobacterial Glycolipid Expand after Intravenous BCG-vaccination	Layton *et al.* (Seder)	NHP (RM)	CD1-restricted lipid-specific T cells after IV BCG	mycobacterial lipid specific Ts expanded at Wk4 after IV BCG	N/A	N/A	N/A	N/A
2018-2021	This project: parallel human work - dose escalation in Study TB041 (Chapter 5)	Marshall, Satti *et al.* (unpublished)	humans	dose escalation of aeBCG in humans	aeBCG safe and feasible in humans at 1x10^7	1x10^5-1x10^7	aeBCG (mouthpiece)	4	PB + week 1-24
2018-2021	This project: parallel human work - immunology study TB043 (Chapter 5)	Marshall, Satti et al. (unpublished)	humans	immunology of aeBCG in humans	peak immune response to aeBCG in humans is at day 7	1x10^7	aeBCG (mouthpiece)	10/group	PB + day 2 - week 56
2018-2021	This project: NHP study 6165 - CM immune response early after aeBCG (Chapter 3)	Hoogkamer *et al.* (unpublished)	NHP (CM)	early immunology of aeBCG in CM NHPs	immune response in NHP is minimal up to week 2 after aeBCG	1x10^7	aeBCG (mouthpiece)	9	PB + day 2 - 14
2018-2021	This project: NHP studies 6114/6143/6266/6282 - RM immune response early after aeBCG (Chapter 3)	Hoogkamer *et al.* (unpublished)	NHP (RM)	early immunology of aeBCG in RM NHPs	immune response in NHP is minimal up to week 2 after aeBCG	1x10^7	aeBCG (mouthpiece)	3-12/group	PB + day 2 - 14
2018-2021	This project: NHP study 6181 - RM immune response later after aeBCG (Chapter 4)	Hoogkamer *et al.* (unpublished)	NHP (RM)	later immunology of aeBCG in RM NHPs	peak immune response to aeBCG in RM is at Wk12-Wk16	1x10^7	aeBCG (mask vs mouthpiece)	8/group	PB + week 2-16

Table 4.15 Mucosal BCG studies

Published studies of mucosal BCG are summarised alongside the human (yellow) and non-human primate (blue) studies discussed in this project. First authors are listed for each paper, with final authors listed in brackets. Abbreviations used in this table: Mycobacterium tuberculosis (M.tb), Mycobacterium bovis (M.b), non-human primate (NHP), rhesus macaques (RM), cynomolgus macaques (CM), T-helper 1 (Th1), broncho-alveolar lavage (BAL) pre-BCG (PB), tuberculosis disease (TB), latent TB infection (LTBI), intradermal (ID), aerosol BCG (aeBCG), intravenous (IV), intratracheal (IT) and endobronchial (EB).

Robust differences attributable to delivery method were not identified between PBMC/BAL cell populations. AUC did not detect a difference in IgG/IgM antibody titre between delivery groups, and the three differences detected between groups for IgM titre were attributed to the lack of change in IgM titre in a proportion of animals. Following confirmation that the outcome was similar between delivery groups, data from animals in both delivery groups were included for analysis of the immune response to aeBCG. This increased the group size to 16.

4.5.4 Lymphocyte response to aeBCG

At Wk2, CD3+ T-cell frequency in PBMC samples was lower than at baseline (measured by flow), and fewer lymphocytes were detected by haematology analyser in WB. However CD3+ T-cell frequency was not decreased at Wk2 in WB or BAL. Peripheral T-cell reduction could be caused by migrating of cells to the lungs, but there was no increase in T-cell frequency in the BAL at Wk2 to support this hypothesis, and this hypothesis would not explain the difference between PBMC and WB samples. It is possible that T-cells migrate from the blood into the lung parenchyma, which would mean increased T-cell frequency in lung tissue, rather than

BALf. Intravascular staining can be used to discriminate between tissue resident cells and those in the vasculature, in mice. Bull *et al.*, showed that intranasal BCG vaccination in mice induced a particular subset of tissue resident CD4+ T-cells (PD-1+ KLRG1-) with enhanced proliferative capacity, that were not induced by ID BCG[233]. The decrease in peripheral lymphocytes detected in this study may represent homing to a similar lung-resident population.

After aeBCG the CD4+:CD8+ T-cell ratio increased in the BAL and decreased in PBMCs, following the time course identified by other measures. The increased ratio in the BAL fits with a strong local immune response, while a decreased ratio in the periphery could be caused by CD4+ T-cell migration out of the blood. Compared to the PBMCs, there was a larger CD8+ T-cell population in the BAL at all time points.

A proportion of the T-cells detected expressed CD4 and CD8. Published literature presents conflicting opinions on the relevance of these double positive cells; CD4+CD8+ T-cells may be characterised as an artefact or intermediate cell type[261]. In this study CD4+CD8+ and CD4+CD8++ cell populations were analysed separately because a proportion of animals had very clear and distinct CD8++ cell population. CD4+CD8+ T-cell frequency showed the same trends as CD8+ T-cell frequency, whereas CD4+CD8++ T-cell frequency was more similar to CD4+ T-cell frequency.

In line with the results reported in Chapter 3, CD161+ expression was increased at Wk2 in several lymphocyte populations in Study 6181. Overlap between the markers used to identify different cell populations could also explain why this increase was identified in more than one subset. For example, a proportion of the cells identified as $\gamma\delta$ and NKT-L cells also

co-express CD4+ and CD8, which means that up-regulation of CD161+ cells within one subset (e.g. γδ T-cells) may also be detectable within another subset (e.g. CD4+ T-cells).

CD161 expression was also increased at later time points for a proportion of lymphocyte cell subsets. This biphasic pattern could represent distinct stages of the immune response. The exact function of CD161 is unknown, especially with regard to mycobacterial infection. CD161+ T-cells may represent a 'fast-acting' population, capable of cytokine and enzyme production in response to mycobacteria[265, 266]. Fergussen *et al.*, used CyTOF and mRNA microarray analysis to show that T lymphocytes expressing CD161 share a conserved transcription signature and show an innate-like response to IL-12/IL-18[277]. Later in the immune response, CD161 may represent the induction of immune memory.

At Wk2, CD56+ CD4+ BAL T-cell frequency was increased in the early time point dataset (Chapter 3), but this result was not repeated in Study 6181. Instead, CD4+ CD56+ T-cell frequency in BAL decreased at Wk9/Wk2/Wk16 compared to baseline. The CD4+CD56+ may be subpopulation of NKT-L cells – T-cells expressing NK cell markers, but not necessarily expressing the semi-invariant TCR Vα24[162]. Decreased frequency of pro-inflammatory NKT-L cells at the peak immune response could indicate regulation of the immune response, to limit unnecessary pathology.

CD16+ NKT-L cell frequency increased at Wk4/Wk9 after aeBCG in PBMCs, as did CD16+CD56- NK cells frequency. This CD16+ cell frequency increase was not seen in non-lymphocyte cells, or in the BAL. CD16 binds to the conserved Fc region of antibodies, and can trigger inflammatory cytokine production. Increased CD16 NK and NKT-L frequency around the peak of the immune response to aeBCG may contribute to the increase in IFNγ production at this time[164].

Antibody panel 2 was a version of panel 1, modified to include additional markers: CD95, CD20, MerTK and CD163. Despite successful test runs showing comparable staining patterns to panel 1, the CD161 and γδ antibodies failed to clearly identify CD161+ and γδ+ cells when applied to thawed WBICS. The changes in lymphocyte cell population frequency detected in PBMC were not detected in WB. This could be due to failed CD161/γδ staining and subsequent alterations in the antibody balance, or the fact that WB includes more cell types than isolated PBMCs, or the fact that WB samples were stimulated and then frozen (PBMCs were used immediately after isolation).

4.5.5 Non-lymphocyte response to aeBCG

There was little change in non-lymphocyte subset frequency in PBMCs. In BAL, at Wk2: total CD14+ and total CD16+, CD14+CD16+ and CD14+CD16- non-lymphocyte frequency were all increased. Total CD14+ and CD14+CD16+ non-lymphocyte frequency remained increased compared to baseline at later time points. CD14+CD16- classical monocytes are the most abundant monocyte subset in normal human circulation, and are phagocytic, but are not necessarily pro-inflammatory or proficient at antigen presentation[147]. CD16+(+) co-expression can distinguish between non-classical and intermediate monocyte subsets[147], but in this dataset, no distinct CD16++ subset could be identified.

A biphasic pattern was identified for CD14+ and CD16+ non-lymphocyte frequency in BAL, which increased at Wk2 compared to baseline, reduced again at Wk4/Wk9, before increasing again at Wk12. Monocytes and macrophages are the major reservoir for mycobacterial infection in the lungs and are readily available during initial infection[144]. The Wk2 increase in monocyte markers may reflect the initial response to infection, and the gradual increase weeks later may reflect induction of the adaptive immune by primed T-cells. The Wk2

increase in monocyte marker frequency identified in Study 6181 was not observed at Wk2 time point in Chapter 3 (n=3).

4.5.6 Activation markers

HLA-DR is as a marker of cell activation and Fletcher *et al.*, showed that HLA-DR+ CD4+ T-cell frequency is associated with increased risk of developing TB[80]. PPD-specific cytokine production peaked at Wk12 at which point HLA-DR+ γδ T-cell frequency was increased (PBMCs), and HLA-DR+ CD16+/CD16+CD56+ NKT-L cell frequency was increased (BAL), both compared to baseline. Increased HLA-DR expression at Wk12 may represent the peak of activation of these cell types. In WB, HLA-DR frequency decreased at Wk16 compared to baseline at for CD4+ and CD8+ T-cells, and for B-cells, which could represent peripheral down-regulation of the immune response.

MerTK+/CD163+ non-lymphocyte decreased at Wk4 in all subsets. Dijkman *et al.*, showed that CD16+ MerTK+CD163+ monocyte frequency was higher in RM than CM[4]. RM are more susceptible to TB than CM, and increased CD163/MerTK expression may indicate a more anti-inflammatory phenotype that inhibits the early immune response to *M.tb*[4]. In this study, decreased CD163+/MerTK+ non-lymphocyte frequency coincided with production of pro-inflammatory IFNγ cytokine production. This supports the hypothesis that more CD163/MerTK expression is associated with more inflammation.

CD95 (or Fas) is up-regulated on mature lymphocytes, and can trigger apoptosis in these cells[287]. CD8+ T-cells expressing Fas can induce apoptosis of other cells by binding to Fas-ligand[288], and activated T-cells can induce activation and Fas expression on B-cells[287]. CD95+ CD8+ T-cell frequency increased at D2/D7 (Chapter 3), but was reduced at Wk4, before increasing at Wk12 compared to baseline (this chapter). CD95+ B-cell frequency was

increased at Wk16, perhaps indicating B-cell activation by already activated T-cells. This pattern may demonstrate initial CD8+ cytotoxicity, followed by a second wave of activation, culminating in B-cell activation.

4.5.7 Antigen-specific cytokine response to aeBCG

Darrah *et al.*, showed a trend for increased cytokine-positive CD4+ T-cell frequency in PBMC at Wk4 after aeBCG, but this was not significant (IFNγ/IL-2/IL-17/TNFα)[5]. Most CD4+ T-cells (90%) produced Th1 cytokines, and very few (<10%) produced IL-17[5]. White *et al.*, showed increased cytokine-positive CD4+ PBMC T-cells at Wk13 after aeBCG (and CD8+ to a lesser extent)[3]. In Study 6181, IFNγ+ cells were more frequent than IL-2+ or IL-17+ cells, and cytokine-positive cell frequency peaked was at Wk12 after $1x10^7$ CFU aeBCG. Given the wealth of data supporting the essential role of CD4+ T-cells and IFNγ in the immune response against TB[67, 192, 208], it is unsurprising that IFNγ+ CD4+ T-cell frequency was the main change detected among PBMCs in this study.

There was a higher frequency of cytokine-positive cells in the BAL than PBMCs, and frequency peaked between Wk9 and Wk16. Darrah *et al.*, also showed that higher cytokine-positive cell frequency in BAL than PBMCs, but peaking at Wk8 after aeBCG[5]. Verreck *et al.*, showed increased cytokine-positive T-cell frequency in BAL at Wk13 after EB BCG, mirroring the results shown here[2]. In combination with these previously published results, this study shows that aeBCG induces conventional T-cell cytokine production (stronger for CD4+ T-cells than CD8+ T-cells), that is stronger in the BAL than PBMCs. The timing of the peak response may be dependent on dose, with a higher dose inducing an earlier peak. For example, Darrah *et al.* showed peak cytokine production by CD4+ T-cells at Wk8 ($5x10^7$ CFU), where Study 6181 showed peak cytokine production at Wk12 ($1x10^7$ CFU).

Smith *et al.*, showed that polyfunctional cytokine-positive CD4+ T-cells are induced by BCG vaccination in infants, and that the capacity of PBMCs to inhibit *in vitro* mycobacterial growth correlates with polyfunctional T-cells[289]. In Study 6181, polyfunctional cytokine-positive cells were detected in BAL and PBMCs, peaking at Wk12. In both PBMCs and BAL, the most common cytokine combinations among these T-cell subsets were IFNγ+IL-17+ and IL-2+IL-17+.

Cytokine-positive NKT-L cell frequency also increased at the peak immune response to aeBCG: IFNγ+ at Wk9/Wk12, IL-2 at Wk12, IL-17 at Wk9. CD16+CD3+ NKT-L cells could also express CD4, and therefore contribute to the cytokine-positive CD4+ T response discussed above. NKT-L are defined by co-expression of NK cell markers (CD16 and CD56 in this study) and CD3. In this study, presence/absence of the semi-invariant TCR (Vα24), which defines NKT (or iNKTs) cells cannot be confirmed so it is unclear exactly what other functions this subset of cytokine-positive cells might have[162].

4.5.8 Antibody to aeBCG

There are several classes of antibody, all of which are relatively under-explored in the context of mycobacterial infection[219]. IgA is dimeric in structure and is found in mucus, saliva, tears and breast milk, and functions to protect against pathogens. After *M.tb* challenge of RM and CM, IgA increased at Wk12 in serum and BALf, but this increase was not significant[4]. IgA was not explored in Study 6181 because it was not possible to identify a commercial source for IgA secondary antibody.

IgG can opsonise pathogens for phagocytosis and killing, activate complement, and assist with antibody-dependent cell-mediated cytotoxicity, and is the majority antibody type in serum[219]. IgG antibodies have been identified after BCG vaccination[276], and can enhance

mycobacterial killing in vitro[290], but their exact function in TB is unclear. In Study 6181, IgG titre increased from Wk4-Wk16. One animal had high levels of PPD-specific IgG from baseline, and this animal also had higher baseline frequency of Vα7.2+ CD8+ T-cells in both PBMC and BAL. IgG titre also increased at Wk9 and Wk12 in BALf samples for a proportion of animals. Although the induction of an antibody response was not universal across animals, this study provides further evidence that an antibody response is induced BCG.

IgM is pentameric and can be attached to the surface of B-cells, or be secreted in the blood. IgM roles in infection include: T-cell regulation, stimulating phagocytosis, agglutination, and activation of complement. Alter *et al*., showed that a strong IgM antibody response was induced at Wk8 after IV BCG and that this response was stronger than the antibody response to aeBCG[226]. IgM titre was the only plasma antibody feature to inversely correlate with *M.tb* burden after challenge, although IgM, IgG and IgA were all expanded in plasma and BALf[226]. In Study 6181, IgM titre was increased at Wk9 for three animals, but this response was less clear than the IgG response. Antibody titre in BALf can be compared to antibody in the serum to understand the local immune response and how this compares to the overall response in the periphery. After aeBCG, serum and BALf IgG/IgM titre positively correlated at a proportion of time points. The strongest correlations occurred between compartments at the same time point.

Given the localisation of the immune response (measured by flow cytometry), a stronger antibody response might be expected in BALf than in serum. In Study 6181, IgG and IgM antibody titre were substantially higher in serum than in BALf (neat and concentrated). Therefore, higher levels of T-cell activity in the BAL (compared to PBMC) did not coincide with

increased local antibody production. It is possible that activated T-cells migrate from the lungs to the draining LNs, before stimulating B-cells and antibody production in the periphery.

4.5.9 Other measures of the immune response to aeBCG

The experiments discussed here were designed to be performed in parallel with human studies of aeBCG, and to allow bridging between these aeBCG studies and studies of *M.tb* challenge in NHPs. After 40-60 CFU of *M.tb* (standard challenge dose), PPD-specific IFNγ SFU substantially was increased compared to baseline from Wk8 until Wk46 in RM[9]. More recently, single or repeated low dose(s) of *M.tb* have been used to more accurately mimic natural exposure to mycobacteria, instead of the relatively large single dose of *M.tb* favoured for challenge studies (where the aim is to infect all animals). After repeated low dose EB *M.tb*, IFNγ SFU increased from Wk4 until the end of the study at Wk11[2].

Where *M.tb* challenge is not possible, *in vitro* methods to measure protection against *M.tb* have been developed to act as a surrogate. Throughout the duration of this project, the MGIA was developed and tested on NHP samples; in the MGIA, *in vitro* control of BCG is measure to determine control of mycobacterial growth[238]. Unfortunately, an attempt to evaluate samples from Study 6181 using this assay was disrupted by problems with the BCG used as the *in vitro* challenge agent. Control samples used to determine the success of the experiment were outside of the expected range, and the results could not be interpreted (data not shown).

4.5.10 Correlations between measures of the immune response to aeBCG

It was hypothesised that measures of IFNγ by ELISpot and by cell population specific flow cytometry would correlate. This was not the case. Although there were specific time points that correlated between these two measures of IFNγ, these were sporadic and did not reflect

the similar kinetic detected by these two assays. The ELISpot assay used in this project is a measure of ex-vivo production of IFNγ by PBMCs. The frequency of IFNγ+ cells in any one population (e.g. when measured by flow cytometry) may not reflect the overall IFNγ production from PBMCs, because different cell types may contribute more or less IFNγ to the response, depending on the individual and local environment[65, 159].

Antibody titre is related to the number of activated B-cells, which can be activated with the help of T-cells. B-cells can also help to activate T-cells by forming bacterial-antibody complexes that increase antigen presentation to T-cells[219]. Therefore, it is possible that T-cell activation (measured by IFNγ ELISpot) would lead to increased B-cell responses (measured by ELISA). In this project, IFNγ SFU did not positively correlate with serum IgG titre, and only Wk2 IFNγ SFU correlated with serum IgM titre (PBa/Wk2/Wk4/Wk12). It is possible that animals with a higher serum IgM titre have a stronger initial T-cell response. Negative correlations between BALf IgG titre and IFNγ SFU do not support the hypothesis that T-cell and B-cell activity would increase with the same kinetic. Further PCA could be used to visualise different combinations of this data, as demonstrated by the example of BAL cytokine data, where cytokine clusters differed according to time point after aeBCG.

4.6 Summary and conclusions

4.6.1 Summary

- aeBCG delivered by mask or mouthpiece attachment is safe and immunogenic from Wk2-Wk16 weeks.

In response to aeBCG:

- PPD-specific IFNγ SFU frequency increased from Wk4-Wk16 after aeBCG, supporting hypothesis b). A Wk16 peak response is later than other published mucosal BCG/ID BCG studies[3, 10].
- The immune response to aeBCG was not different when delivered by mask compared to mouthpiece attachment, in contrary to hypothesis a) and despite differences in AE deposition in the lung (White *et al.*, unpublished). Data were combined to explore the response to aeBCG with a larger and more robust dataset.
- Antigen-specific cytokine producing cells increased compared to baseline as postulated in hypothesis b) (peaking between Wk9-Wk12), but did not correlate with IFNγ SFU frequency (ELISpot).
- Antigen-specific cytokine production was strongest in BAL, particularly from CD4+ T-cells, in line with published data[274] and as postulated in hypothesis e). CD8+ T-cells and NKT-L cells were among the other subsets that showed increased cytokine production.
- The kinetic of the cytokine response to aeBCG is similar to previously published mucosal BCG studies (a single peak at Wk4-Wk13). Increased mucosal BCG dose may reduce the time between mycobacterial exposure and cytokine response[3, 5, 10].
- The CD4+:CD8+ T-cell ratio decreased in the PBMCs, and increased in BAL, which may reflect migration of activated CD4+ T-cells into the lung.
- MAIT-cell markers CD161 and Vα7.2 were up-regulated in both PBMC (strongest at Wk2) and BAL (from Wk2, stronger at Wk4/Wk9)
- CD161 expression increased among lymphocyte subsets (PBMCs and BAL), particularly at Wk2 as predicted in hypothesis d) and Wk9. This biphasic expression could

represent CD161+ cells with an innate-like phenotype early on[277], and a memory phenotype at later time points. Early expression of CD161 and other cell populations which showed a biphasic response supports the hypothesis that an early innate response pre-ceeds the adaptive immune response to aeBCG as outlined in hypothesis c).

- In BAL, CD14+ and CD16+ non-lymphocyte frequency increased at Wk2/Wk12. This biphasic pattern may represent phases of the immune response.
- MerTK/CD163+ non-lymphocyte frequency decreased at Wk4 (anti-inflammatory monocyte phenotype[4]), which coincided with the induction IFNγ production.
- PPD-specific IgG and IgM titre (less clear) increased in a proportion of animals, peaking at Wk9. This increase in antibodies supports hypothesis f). The function of these antibodies is unknown[219].
- BALf concentration successfully increased the measurable PPD-specific IgG titre, but could not be reliably quantified using a phospholipid quantification assay.

4.6.2 Conclusions

- The immune response to aeBCG in RM peaked at Wk9-Wk16, which is similar to published studies of mucosal BCG[3, 10], and delayed compared to ID BCG[7].
- Despite differences in AE deposition in the lungs (White *et al.*, unpublished), aeBCG delivery method did not alter the immune response induced.
- CD161 expression increased across lymphocyte subsets in a biphasic pattern which may indicate two stages of the immune response and requires further exploration to determine the functional implications of increased CD161 expression.

- Increased cytokine-positive cell frequency was pronounced in BAL than PBMCs, which suggests a local antigen-specific response.
- Increased PPD-specific IgG and IgM titre requires further exploration to understand the function of these antibodies.

Chapter 5: NHP vs human responses to aeBCG

Chapter 5: NHP vs human responses to aeBCG

5.1 Statement of authorship

Authorship surrounding NHP samples is described in previous chapters. Human samples were obtained by the McShane clinical trial team (University of Oxford), and processed by the McShane lab group. ELISpot analysis was led by Stephanie Harris, and flow cytometry data acquisition and analysis was led by Julia Marshall and Iman Satti. Where included, unpublished data from this work is identified and referenced. Comparison of proliferation in baseline NHP and human samples was performed by the author.

5.2 Background

NHPs are considered to be the most relevant animal model for human TB disease because they are naturally susceptible to *M.tb* infection, exhibit a human-like spectrum of disease[115], and respond to BCG vaccination. The quality and kinetic of the immune response to aeBCG were explored in parallel NHP and human studies. Parallel experiments across species are logistically complicated, but important to provide directly relevant comparisons. To our knowledge, the human aeBCG studies described here are the first to describe the immune response to aeBCG in *M.tb* naïve humans.

5.3 Objectives & hypotheses

The analysis and experiments in this chapter were designed to:

1. Compare the immune response to aeBCG infection in NHPs and humans, measured by:

- PPD-specific IFNγ ELISpot
- flow cytometry (PBMC and BAL)
- PPD-specific ELISA

2. Explore any difference in the kinetic identified between NHPs and humans
3. Explore the following hypotheses:
    a) The immune response to $1x10^7$ CFU aeBCG will follow the same kinetic in humans and macaques.
    b) Antigen-specific antibody will be induced by aeBCG in both humans and macaques.

5.4 Results

5.4.1 Human aeBCG studies in parallel with NHP studies

The NHP studies in this project were designed in parallel with an experimental medicine study TB043 in humans, which examined the immune response to $1x10^7$ CFU aeBCG delivered by Omron nebuliser with mouthpiece attachment (ClinicalTrials.gov ID: NCT03912207 – Figure 5.1). Before TB043, dose escalation study TB041 was completed (ClinicalTrials.gov ID: NCT02709278) to confirm the safety of this dose in humans ($1x10^4$ – $1x10^7$ CFU of BCG Bulgaria). TB041 also included a group of matched controls who received ID BCG at a target dose of $1x10^6$ CFU (to mimic the estimated dose delivered by aeBCG at a target dose of $1x10^7$ CFU). Delivery of aeBCG was safe in humans at $1x10^7$ CFU, with no serious adverse events related to the challenge agent (Marshall, Satti *et al,* unpublished). NHP early and late time point studies were designed in parallel with the time points in TB043 (D2/D7 with BAL, Wk2/Wk4/Wk8/Wk12). In humans, baseline samples were taken on the day of aeBCG exposure, and are referred at as PBa. For logistical reasons, there was no Wk16 time point in TB043, and Wk24 (included in TB043) was not included for NHPs, because animals were euthanised at Wk16.

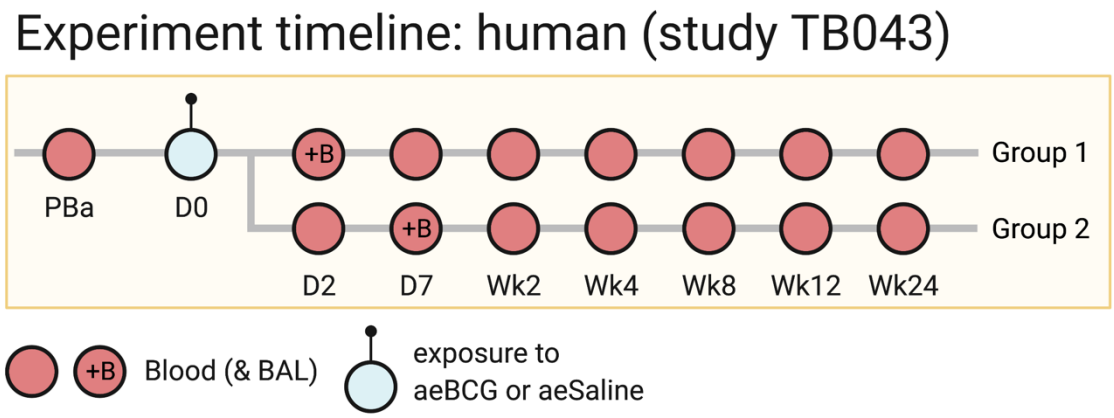


Figure 5.1 Study design (human study TB043)

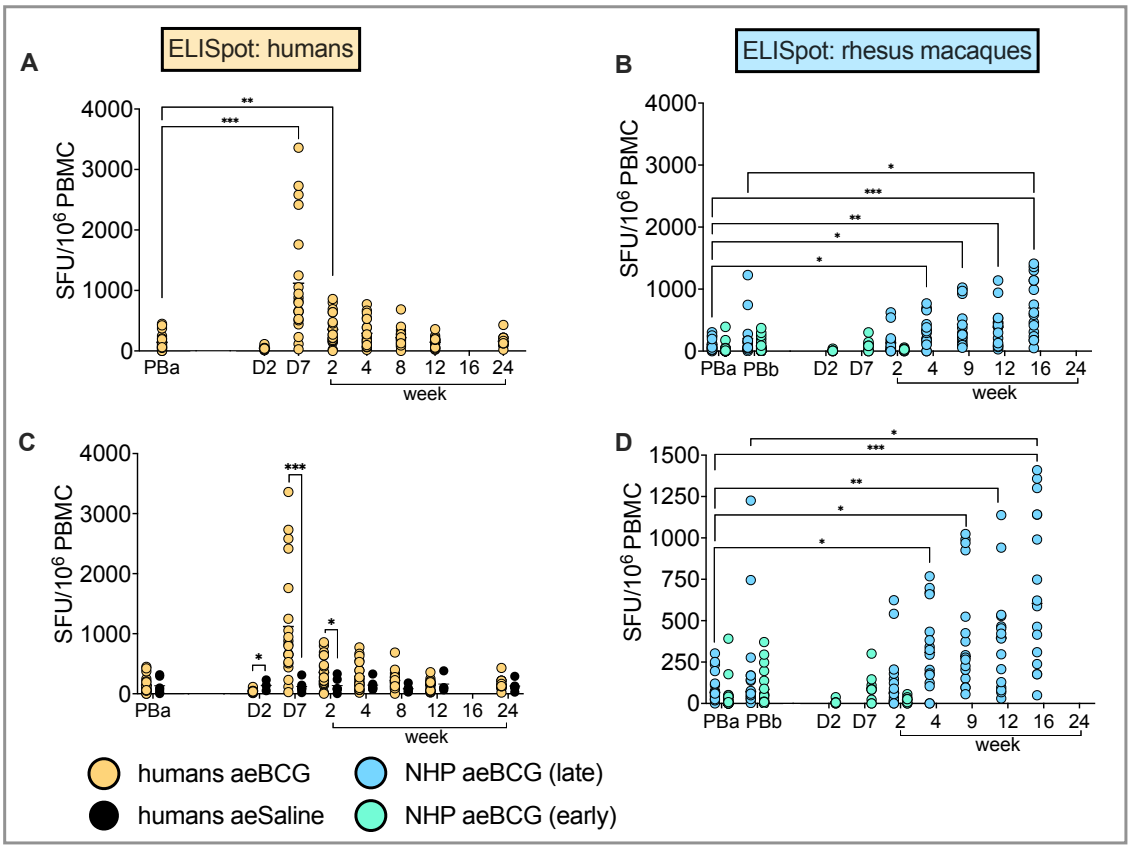
Experimental design for the study of the immune response to aerosol BCG (aeBCG) in humans. $1x10^7$ CFU of aeBCG (target dose) or aeSaline was delivered via Omron nebuliser at Day 0. Clinical data, and blood samples were taken at pre-BCG A (PBa), and at different time points after aeBCG (day 2 – week 24, D2-Wk24). In addition to clinical data and blood samples, broncho-alveolar lavage (BAL) samples were collected at one early time point (D2/D7/Wk2), depending on which group each individual was allocated to. For each group, ten individuals were exposed to aeBCG, and a further three individuals were exposed to aeSaline only. Image created with Biorender.com.

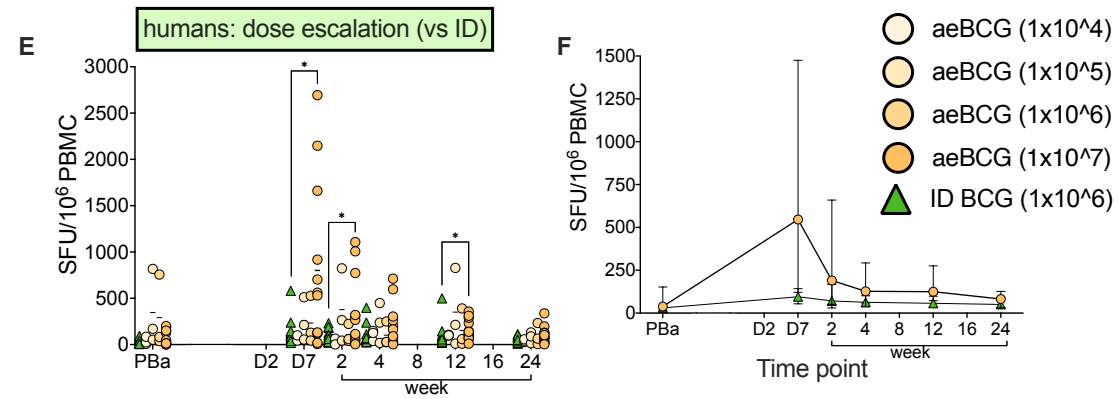
5.4.2 PPD-specific IFNγ SFU frequency in humans and NHPs

The frequency of PPD-specific IFNγ SFU was measured in humans (yellow) and NHPs (blue) using an *ex vivo* ELISpot after aeBCG (Marshall, Satti *et al.,* unpublished – Figure 5.2). PPD-specific SFU frequency in humans peaked at D7 after aeBCG. From Wk2-Wk9, the frequency remained increased. IFNγ SFU frequency in humans was significantly higher at D2/D7/Wk2 after aeBCG than after aeSaline. The peak SFU frequency measured in RM was at Wk16, and there was no change at D2/D7/Wk2. The median peak SFU frequency higher in humans than NHPs (807 in humans at D7, 695 in NHPs at Wk16). There was no difference in AUC between species, but fold change was significantly different between species at D7/Wk2/WK12, compared to baseline. There was no difference between fold change in IgG titre at the peak time point for humans and NHPs (D7 and Wk16, respectively).

In TB041 (Marshall, Satti *et al.,* unpublished), a proportion of individuals had increased IFNγ SFU frequency at D7 compared to baseline. This was not significant when

all time points were compared to baseline by ANOVA (with Dunnett's corrections for multiple comparisons). SFU frequency was higher after $1x10^7$ CFU aeBCG than after ID BCG (black) at D7/Wk2/Wk12 (p=0.0449/0.0455/0.0500 - Mann-Whitney U-testing).





G

ELISpot fold change: human vs NHP							
analysis	**Mann-Whitney U-test**						
human time point	Day 2	Day 7	Wk2	Wk4	Wk8	Wk12	D7
NHP time point	Day 2	Day 7	Wk2	Wk4	Wk9	Wk12	Wk16
Significance	ns	**	****	ns	ns	*	ns
	0.3500	0.0031	0.0009	0.3856	0.1135	0.0204	0.7080

Figure 5.2 PPD-specific IFNg SFU in humans and NHPs

*Systemic PPD-specific IFNγ spot forming units (SFU) are shown per million peripheral blood mononuclear cells (PBMCs), at baseline (PBa), Day 2 and Day 7 (D2 and D7), and 2-24 weeks. Humans exposed to aerosol BCG/Saline (aeBCG/aeSaline) are shown in yellow/black (**A** & **C**) Rhesus macaques from early/late time point studies in blue/turquoise (**B** & **D**). **A** & **B** have matched axes, where **D** shows NHP data with a smaller x-axis. Individual humans/animals and group medians are shown. Baseline values are shown at pre-BCG A and B (PBa and PBb) before aeBCG or aeSaline. Paired data were compared using a Mixed Effects model with Dunnett's corrections for multiple comparisons, and unpaired using Mann-Whitney U-testing (**C**). Significant comparisons are marked as P < 0.05 (*), P < 0.005 (**) or P < 0.001 (***). At each time point with comparable data, Mann-Whitney U-testing was used to compare fold change compared to baseline between NHP and human data (**G**).*

*Humans from a separate dose escalation study (Study TB041) are shown in **E** & **F**, with four groups exposed to aeBCG in yellow ($1x10^4$-$1x10^7$) and one group exposed to intradermal (ID) BCG in green ($1x10^6$). There were no significant changes compared to baseline for any delivery method. Significant differences between aeBCG at $1x10^7$ and ID BCG are shown. **F** shows the group medians and interquartile range for the group exposed to $1x10^7$ aeBCG and the ID group.*

5.4.3 Peak immune response in NHPs vs humans comparison

In NHPs, the peak immune response measured by flow cytometry occurred at Wk12 after aeBCG. At Wk12, CD4+ T-cell frequency increased (CD8+ T-cell decreased, Figure 5.3) and CD56+CD4+ T-cell frequency decreased. In NHP BAL, non-lymphocyte population frequencies increased at Wk12 and Wk2. In humans, the peak immune response measured by flow cytometry was at D7 (Marshall, Satti *et al.,* unpublished). Human BAL samples were only collected at one time point for any individual; the focus on early time points in the study design limited these to D2/D7. CD4+/CD8+ T-cell frequency increased in BAL at D7 in humans and increased CD4+:CD8+ T-cell ratio was detected at D7 in human PBMCs, mirroring the increased CD4+:CD8+ T-cell ratio at the peak of response in NHPs. There was a trend for increased MAIT cells at D7 in human BAL (not significant).

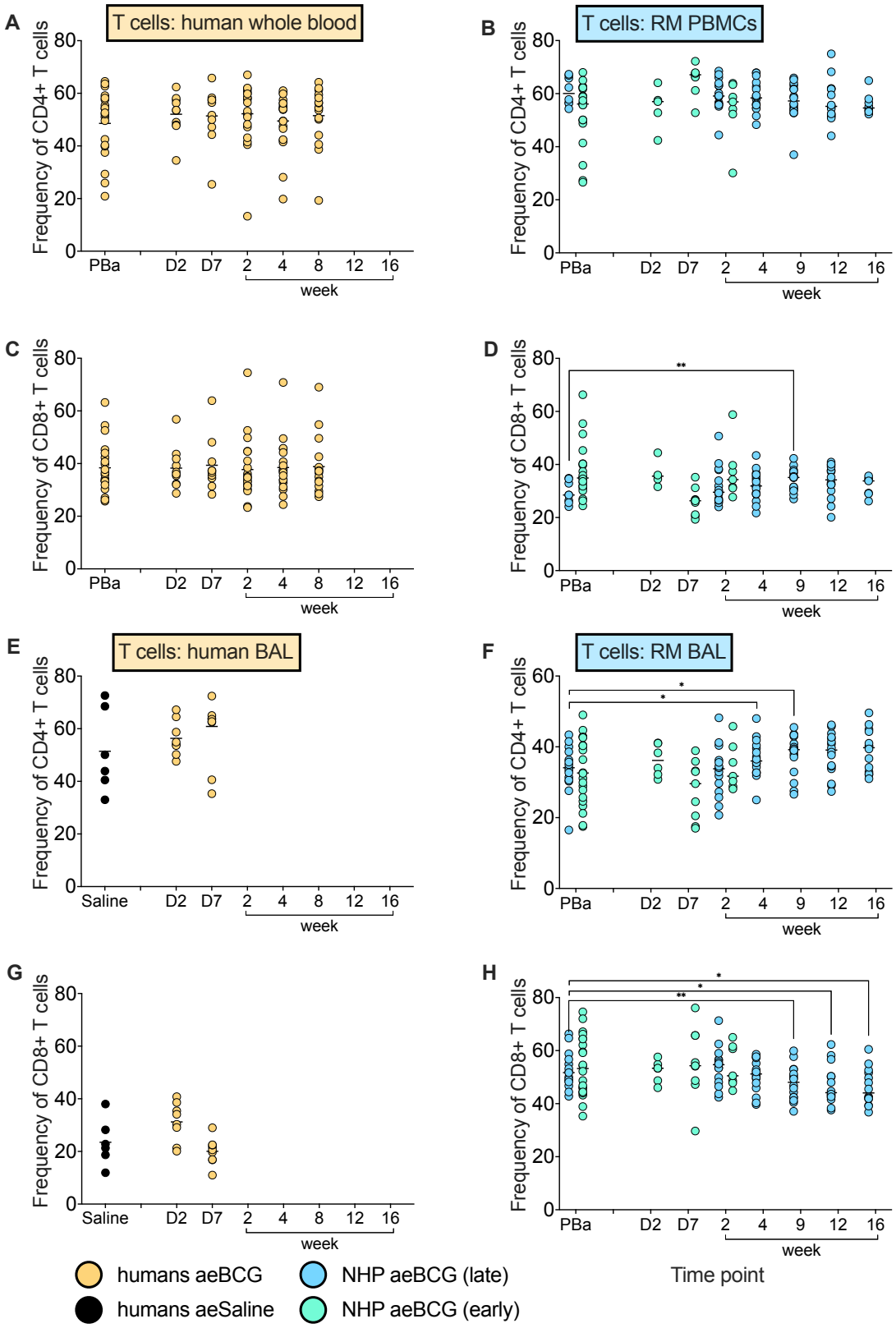

A
T cells: human whole blood
Frequency of CD4+ T cells
PBa
D2
D7
2
4
8
12
16
week
B
T cells: RM PBMCs
Frequency of CD4+ T cells
PBa
D2
D7
2
4
9
12
16
week
C
Frequency of CD8+ T cells
D
Frequency of CD8+ T cells
**
E
T cells: human BAL
Frequency of CD4+ T cells
Saline
F
T cells: RM BAL
Frequency of CD4+ T cells
*
G
Frequency of CD8+ T cells
H
Frequency of CD8+ T cells
humans aeBCG
humans aeSaline
NHP aeBCG (late)
NHP aeBCG (early)
Time point

Figure 5.3 CD4+/CD8+ T-cell frequency in humans and non-human primates

*The frequency of CD4+/CD8+ T-cells among CD3+ lymphocytes are shown at baseline (PBa), Day 2 and Day 7 (D2 and D7), and at 2-16 weeks. Human CD4+ (**A** & **E**) and CD8+ (**C** & **G**) T-cell frequency is shown in yellow for whole blood (**A** & **C**) and broncho-alveolar lavage (BAL) cells (**E** & **G**). Saline control BAL samples are shown where no baseline samples were available (black - **E** & **G**). Rhesus macaque CD4+ (**B** & **F**) and CD8+ (**D** & **H**) T-cell frequency from early/late time point studies are shown in blue/turquoise for PBMCs (**B** & **D**) and BAL (**F** & **H**). Individual humans or animals and group medians are shown. Paired data were compared using a Mixed Effects model with Dunnett's corrections for multiple comparisons, and unpaired using Mann-Whitney U-testing (**C**). Significant comparisons are marked as P < 0.05 (*), P < 0.005 (**).*

In NHPs, cytokine positive CD4+ T-cell frequency peaked at Wk12 (PBMC and BAL, Figure 5.4). IFNγ+/IL-2+ CD16+ and CD16+CD56+ T-cell frequency also increased at Wk12, as did IL-2+/IL-17+ γδ T-cell frequency (BAL only). Increased IFNγ+ CD4+ T-cell frequency at Wk12 was the only significant change in cytokine producing cell frequency among NHP PBMCs. Among human BAL cells, BCG-specific IFNγ+ CD4+ T-cell frequency increased at D7, compared to either D2 samples (different individuals), or to individuals exposed to aeSaline. PPD-specific IFNγ+ CD4+ T-cell frequency increased at the peak time point in NHPs, with a significantly higher frequency from Wk4-Wk16. There was no change in antigen-specific IFNγ+ CD8+ T-cell frequency in human or NHP BAL cells.

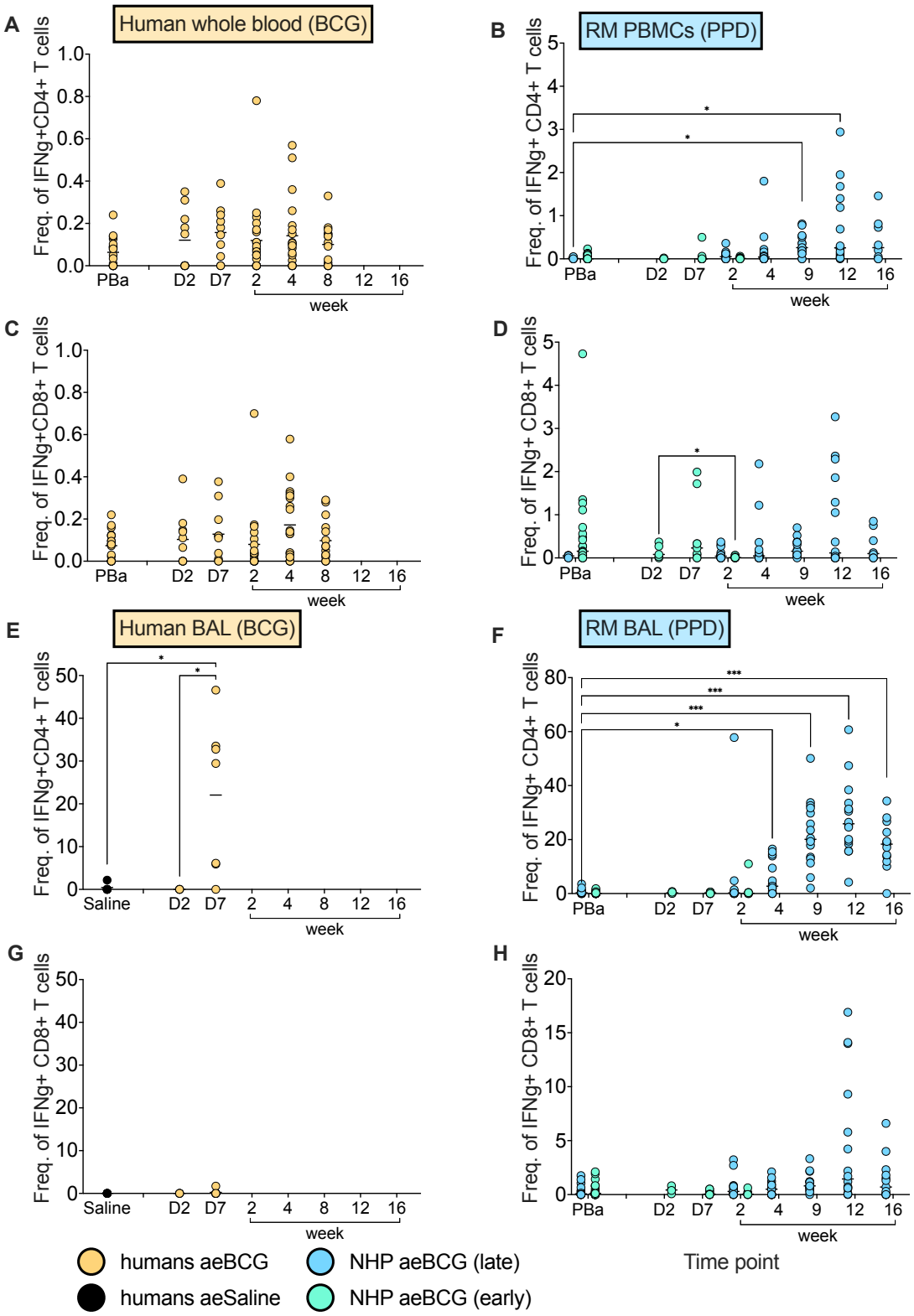
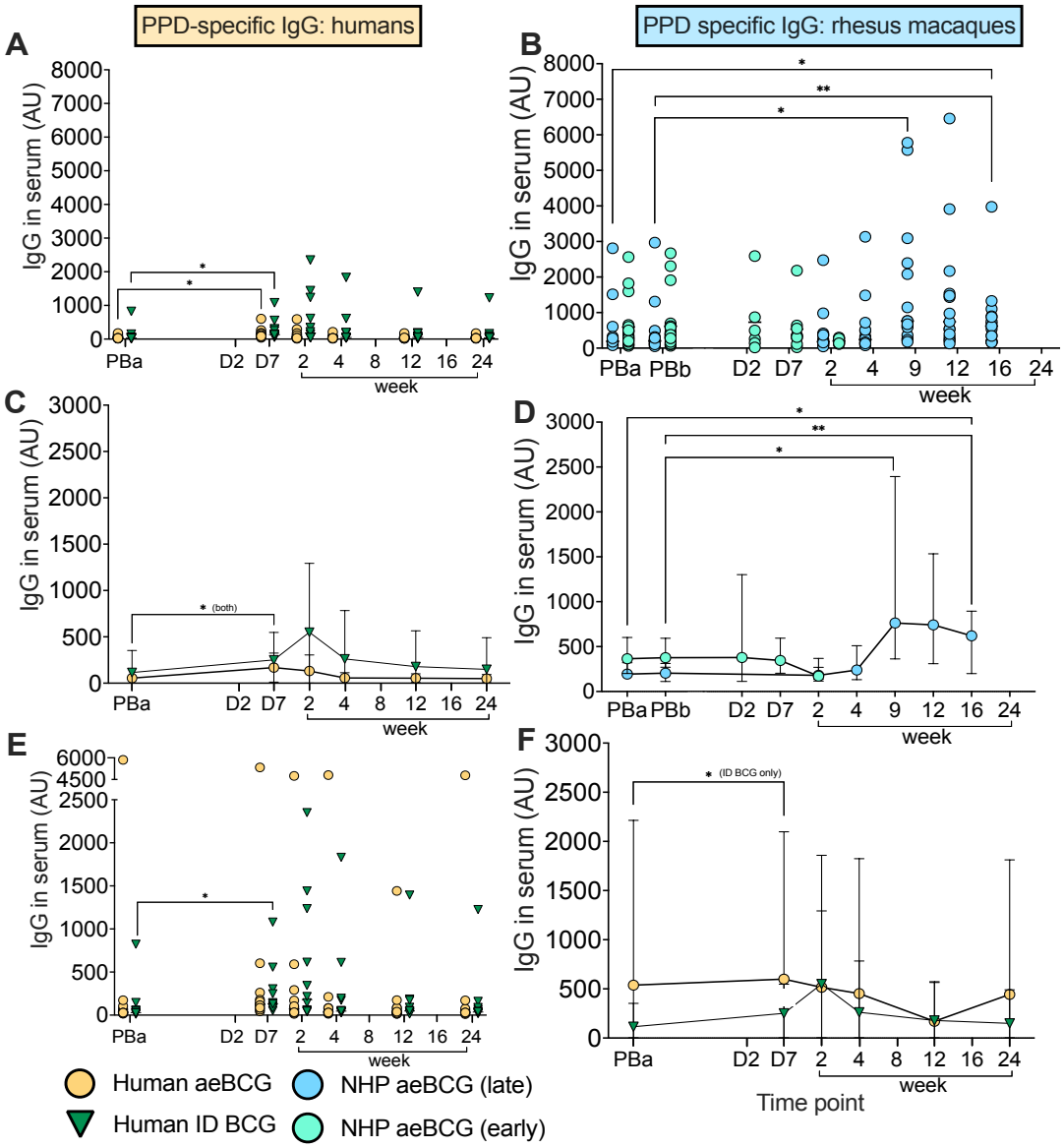

A
Human whole blood (BCG)
Freq. of IFNg+CD4+ T cells
B
RM PBMCs (PPD)
Freq. of IFNg+ CD4+ T cells
C
Freq. of IFNg+CD8+ T cells
D
Freq. of IFNg+ CD8+ T cells
E
Human BAL (BCG)
Freq. of IFNg+CD4+ T cells
F
RM BAL (PPD)
Freq. of IFNg+ CD4+ T cells
G
Freq. of IFNg+ CD8+ T cells
H
Freq. of IFNg+ CD8+ T cells
PBa
Saline
D2
D7
2
4
8
9
12
16
week
humans aeBCG
humans aeSaline
NHP aeBCG (late)
NHP aeBCG (early)
Time point

Figure 5.4 Antigen-specific IFNγ production after aerosol BCG (aeBCG)

*The frequency of antigen-specific IFNγ+ CD4+/CD8+ T-cells are shown at baseline (PBa), Day 2 and Day 7 (D2 and D7), and at 2 to 16 weeks. Human IFNγ+ CD4+ (**A** & **E**) and CD8+ (**C** & **G**) T-cell frequency is shown in yellow for whole blood (**A** & **C**) and broncho-alveolar lavage (BAL) cells (**E** & **G**). Saline control BAL samples are shown in black for human BAL graphs where no baseline samples were available (**E** & **G**). Rhesus macaque IFNγ+ CD4+ (**B** & **F**) and CD8+ (**D** & **H**) T-cell frequency from early/late time point studies are shown in blue/turquoise for peripheral blood mononuclear cells – PBMCs (**B** & **D**) and BAL cells **F** & **H**). Individual humans or animals and group medians are shown. Paired data were compared using a Mixed Effects model with Dunnett's corrections for multiple comparisons, and unpaired using Mann-Whitney U-testing (**C**). Significant comparisons are marked as P < 0.05 (*), P < 0.005 (**) or P < 0.001 (***).*

5.4.4 Antibody response in NHPs vs humans

In human serum samples from TB041 (dose escalation using BCG Bulgaria), aeBCG PPD-specific IgG antibody titre was increased at D7 compared to baseline (adjusted *p*=0.0292, Figure 5.5 - Peralta-Alverez, Harris *et al.,* unpublished). One volunteer in the aeBCG group had a high baseline response and was identified as an outlier by Grubb's test (alpha=0.05). This volunteer was excluded from statistical analysis, but is included in Figure 5.5E/F for reference (D7 was not significantly different from baseline when this volunteer was included). There was also an ID BCG group in TB041. IgG antibody titre was also increased at D7 after ID BCG (adjusted *p*=0.0111). There was no difference between IgG antibody titre after aeBCG compared to ID BCG at D7 (*p*=0.6505).



G

ELISA - IgG antibody fold change (AU): human vs NHP					
analysis	**Mann-Whitney U-test**				
human time point	D7	Wk2	Wk4	Wk12	D7
NHP time point	D7	Wk2	Wk4	Wk12	Wk9
Significance	****	***	ns	***	ns
	<0.0001	0.0008	0.4982	0.0004	0.5744

Figure 5.5 IgG titre in humans and non-human primate serum

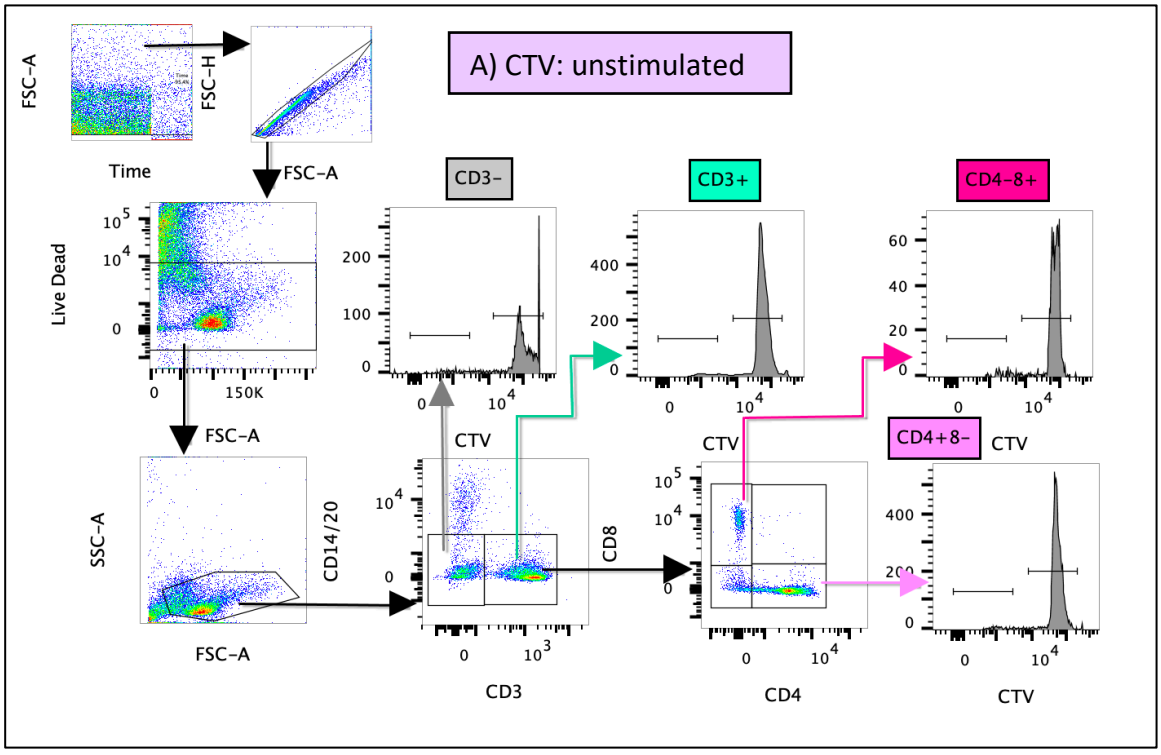
*PPD-specific IgG titre in serum are shown at baseline (PBa), Day 2 and Day 7 (D2 and D7), and at 2 to 16 weeks. Humans exposed to aerosol BCG (aeBCG) are shown in yellow (**A** & **C**) and rhesus macaques are shown in blue/turquoise (**B** & **D**). Humans exposed to intradermal (ID) are shown in yellow (**A** & **C**). Individual humans or animals and group medians are shown (**A** & **B**) alongside group medians with interquartile range (**C** & **D**). One individual was excluded from human analysis due to high baseline (Grubb's, alpha=0.05). For reference, graphs including this individual are below (**E** & **F**). Paired data were compared using an ANOVA or Mixed Effects model (missing data) with Dunnett's corrections for multiple comparisons. Significant comparisons are marked as P < 0.05 (*) or P < 0.005 (**).*

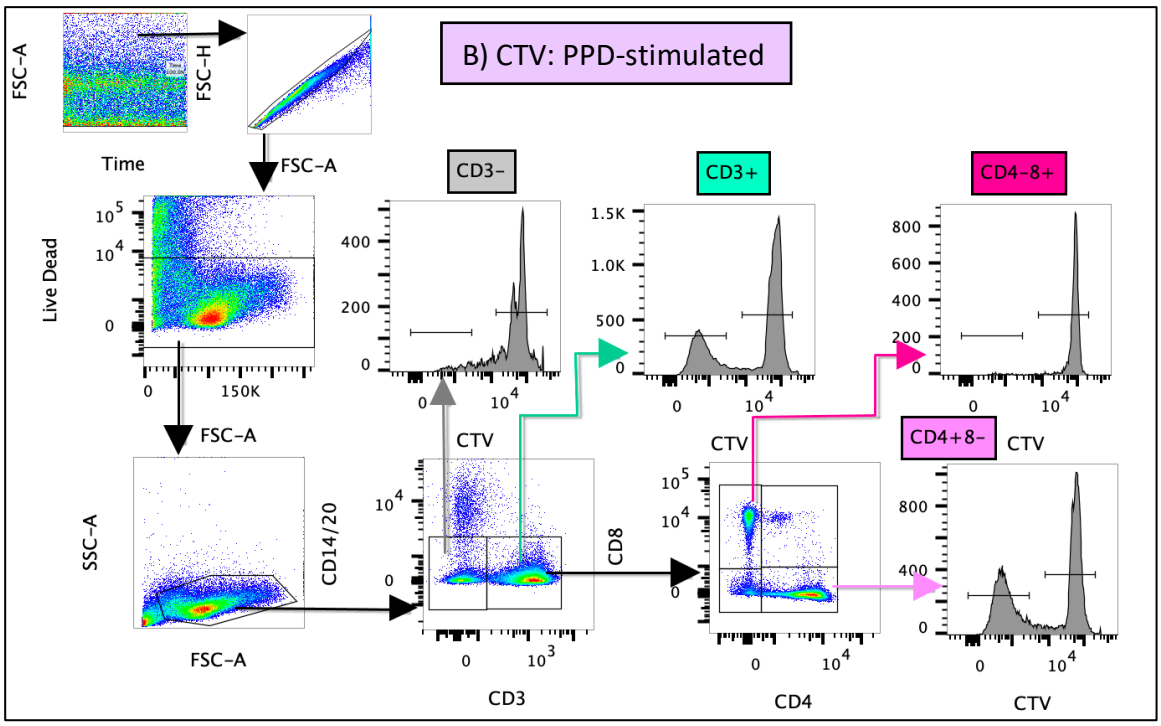
*At each time point with comparable data, Mann-Whitney U-testing was used to compare fold change values (compared to baseline) for NHPs and humans (**G**).*

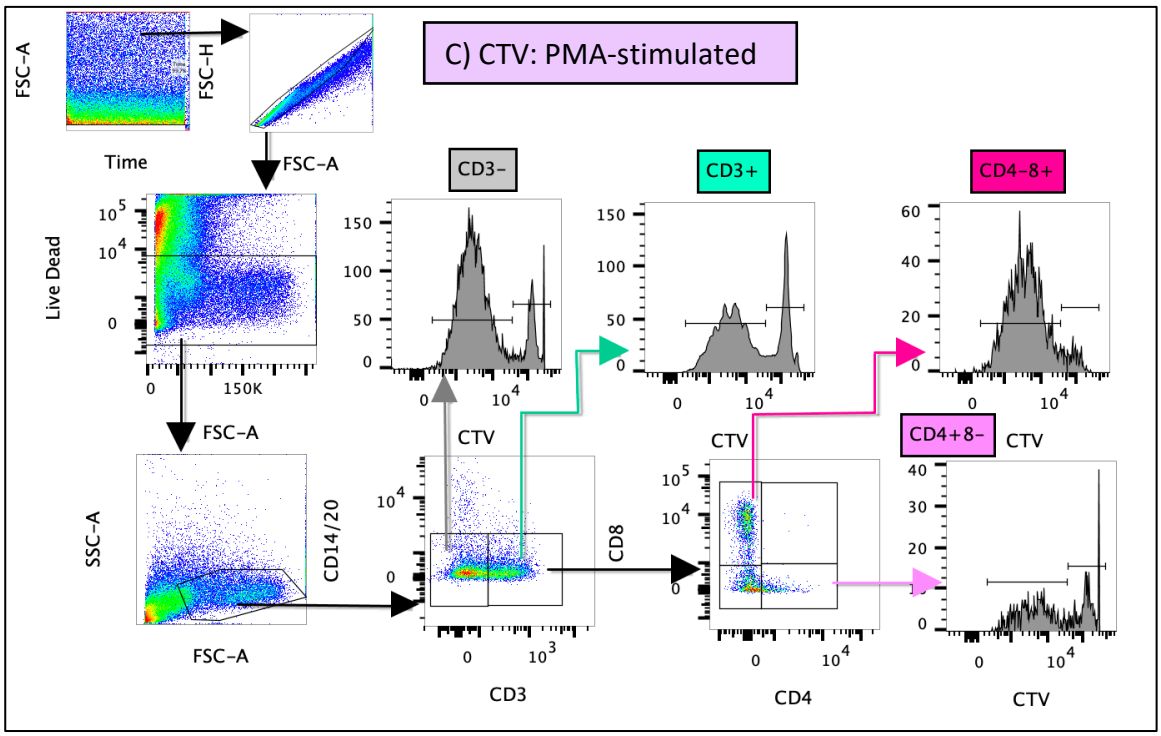
PPD-specific IgG titre in NHP sera significantly increased after aeBCG, peaking at Wk9. One animal was excluded from the ELISA graphs shown in this chapter, because this animal had a high baseline response and was identified as an outlier by Grubb's test (see Chapter 4). A similar trend for increased antibody production was detected in NHP BALf from a proportion of animals, and for IgM titre in serum samples. After excluding outliers, fold change in PPD-specific IgG titre compared to baseline was significantly different at D7/Wk2/Wk12 between human and NHP samples. There was no difference between fold change in IgG titre at the peak time point for humans and NHPs (D7 and Wk9, respectively).

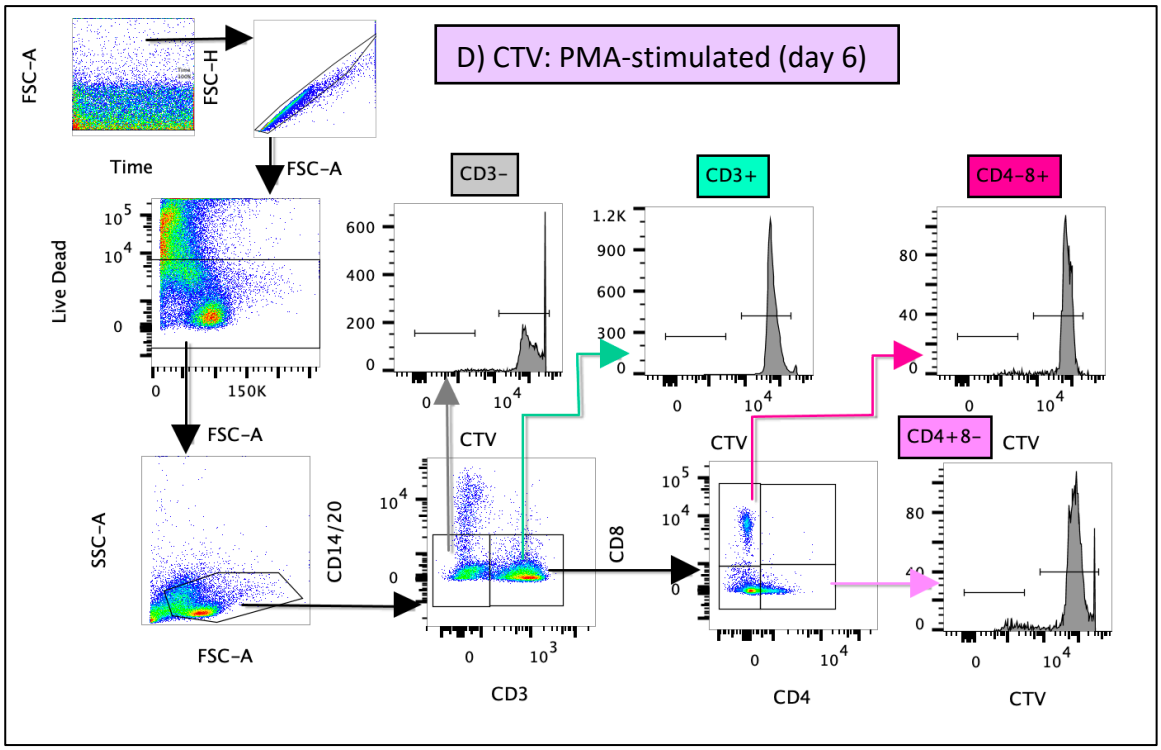
5.4.5 Optimisation of an antigen-specific proliferation assay

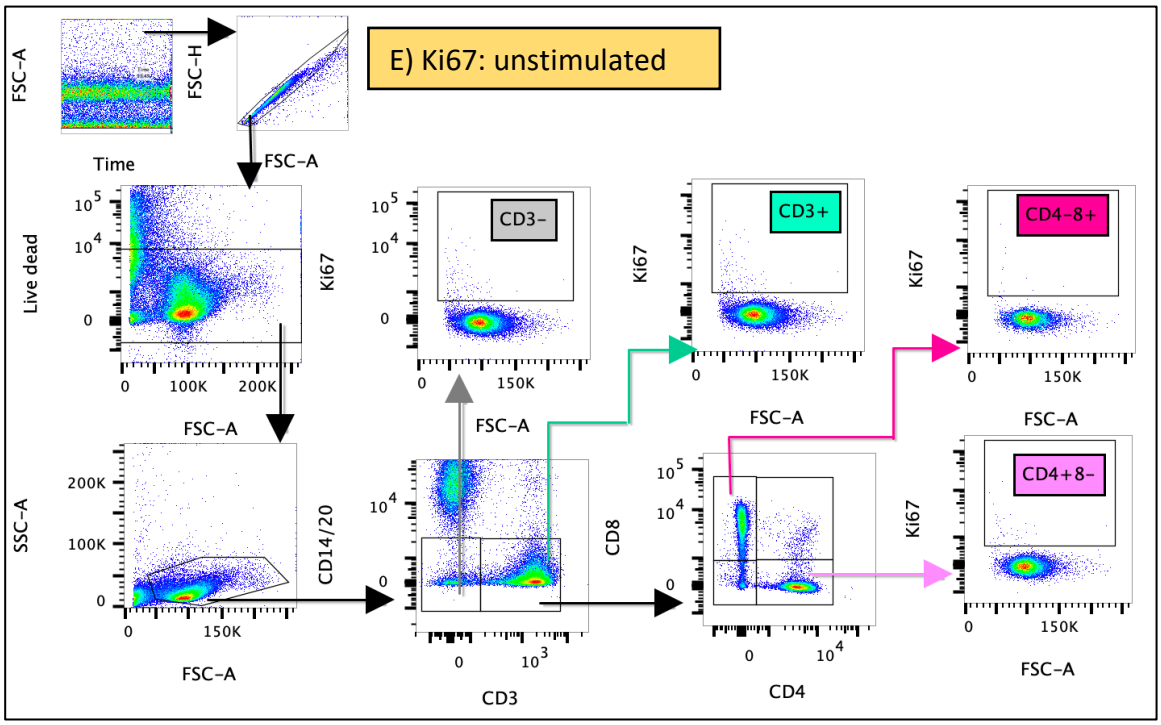
Humans and NHPs studied in this project were BCG naïve at enrolment, but may have different levels of pre-exposure to mycobacterial antigens (e.g. through NTM exposure). A proliferation assay was developed to explore antigen-specific proliferation at baseline. Two proliferation markers were tested (Ki67 and Cell Trace Violet - CTV) using PBMC samples from known PPD-responsive humans and from NHP at Wk16 after aeBCG. Antigen-specific proliferation among CD3-/CD3+ lymphocytes and CD4+/CD8+ T-cells was determined by subtracting the percentage of proliferating cells after culture with media only from the percentage of proliferating cells after culture in media with PPD (added D0), or with PMA (added at D0 or D6). PMA added at D0 was chosen as the better positive control, because PMA addition at D6 had no effect on proliferation compared to unstimulated samples. Ki67+ cells were identified using a gate based on FMOs, and CTV- samples were based on gating of the negative peak shown by histogram (Figure 5.6).

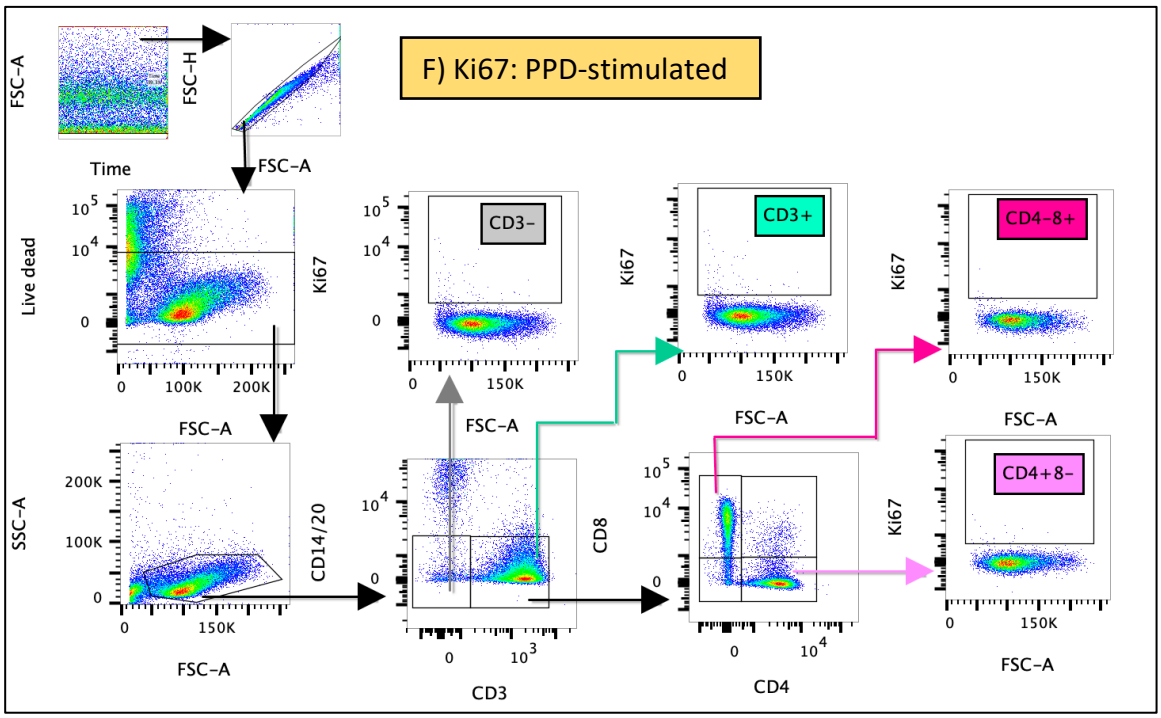

A) CTV: unstimulated
FSC-A
FSC-H
Time
FSC-A
Live Dead
150K
FSC-A
SSC-A
FSC-A
CD14/20
CD3-
CD3+
CD4-8+
CTV
CD8
CD3
CD4
CD4+8-
CTV
CTV


B) CTV: PPD-stimulated
FSC-A
FSC-H
Time
FSC-A
Live Dead
150K
FSC-A
SSC-A
FSC-A
CD14/20
CD3-
CD3+
CD4-8+
CTV
CD8
CD3
CD4
CD4+8-
CTV
CTV


C) CTV: PMA-stimulated
FSC-A
FSC-H
Time
FSC-A
Live Dead
150K
CD3-
CD3+
CD4-8+
CTV
CD4+8-
FSC-A
SSC-A
CD14/20
CD8
FSC-A
CD3
CD4
CTV


D) CTV: PMA-stimulated (day 6)
FSC-A
FSC-H
Time
FSC-A
Live Dead
150K
CD3-
CD3+
CD4-8+
CTV
CD4+8-
FSC-A
SSC-A
CD14/20
CD8
FSC-A
CD3
CD4
CTV


E) Ki67: unstimulated
FSC-A
FSC-H
Time
FSC-A
Live dead
Ki67
CD3-
CD3+
CD4-8+
CD4+8-
SSC-A
CD14/20
CD8
CD3
CD4


F) Ki67: PPD-stimulated
FSC-A
FSC-H
Time
FSC-A
Live dead
Ki67
CD3-
CD3+
CD4-8+
CD4+8-
SSC-A
CD14/20
CD8
CD3
CD4

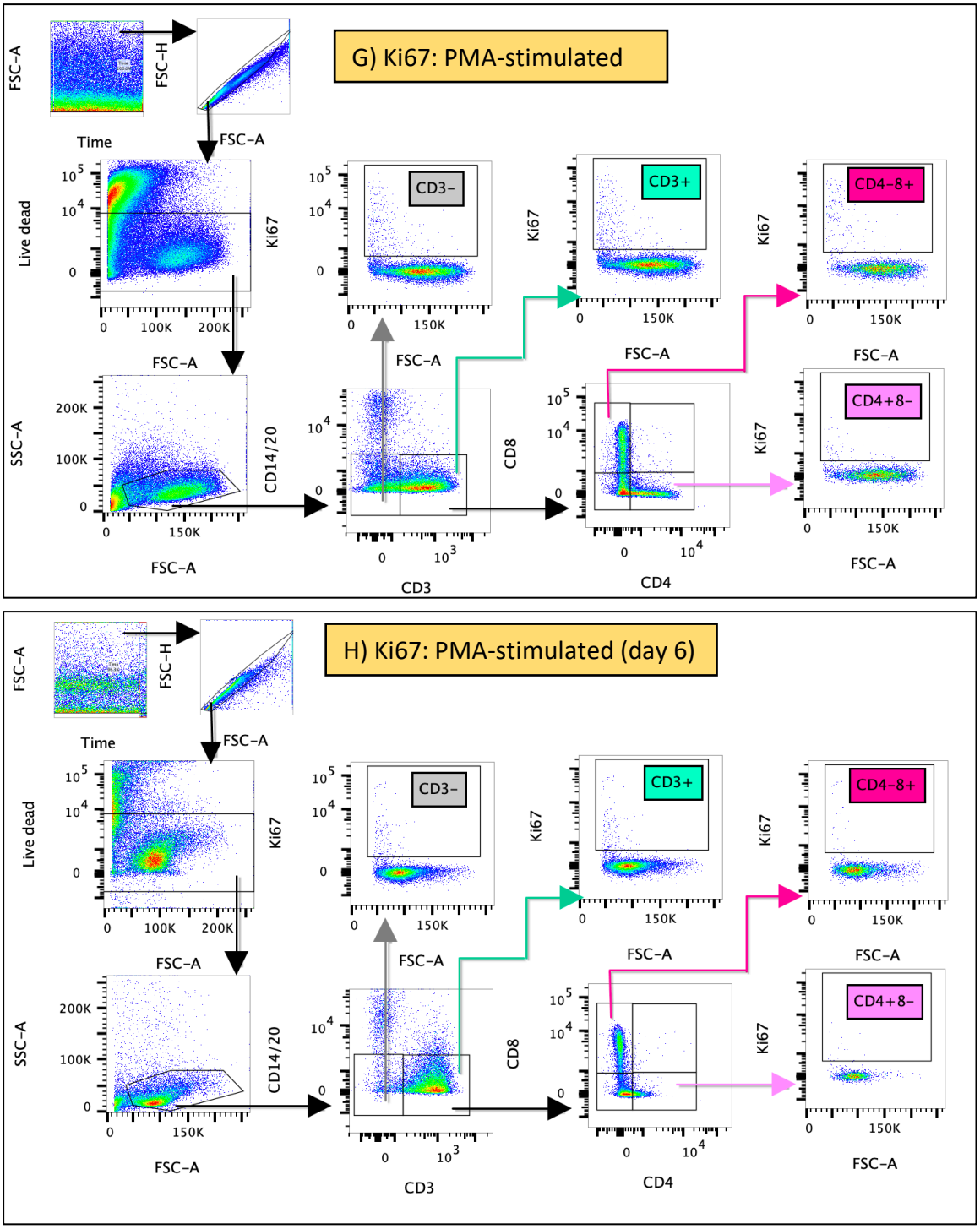


Figure 5.6 Example gating to identify proliferating cells

*Representative gating is shown to identify proliferating cells using Ki67 (**A**-**D**) or cell trace violet (CTV, **E** & **H**). Samples were cultured for six days with media only (Nil, **A** & **E**), or plus PPD (**B** & **F**), plus PMA (**C** & **G**), or plus PMA at day 6 (D6, **D** & **H**). Gates were positioned according to fluorescence minus one controls.*

Antigen-specific proliferating cells were identified using both markers (Figure 5.7). Statistical comparison of human and NHP samples showed that there was no difference in PPD-specific proliferation between species. PMA-specific proliferation was higher than PPD-specific proliferation for all lymphocyte subsets. There were no unstimulated NHP CTV samples in the pilot proliferation experiment (technical error), so it was not possible to determine NHP antigen-specific proliferation using CTV. CTV was chosen as the proliferation marker for further experiments because proliferating cells were more clearly distinguishable using this method. At the end of the six-day culture, a clear lymphocyte population was visible, but there was no clear monocyte population.

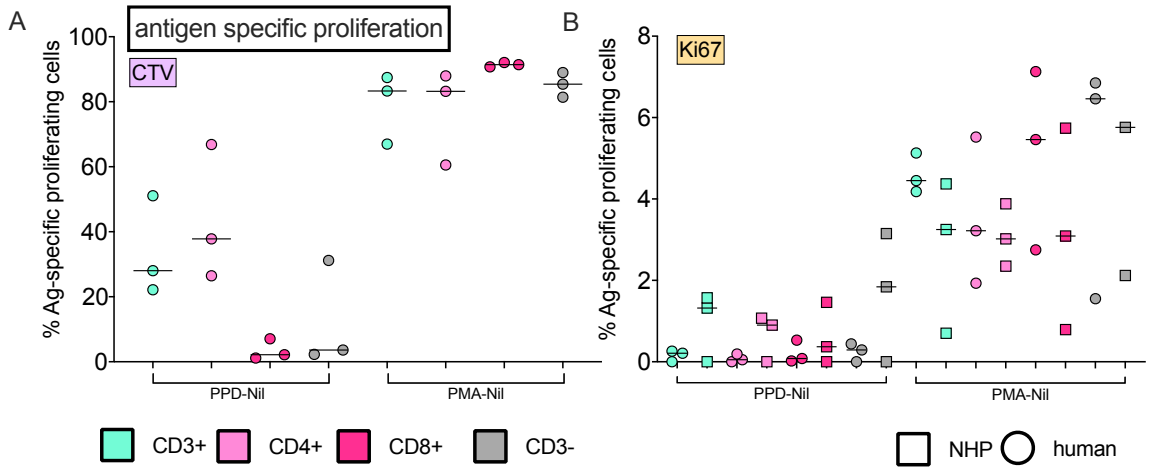


Figure 5.7 Comparison of proliferation detected by Ki67 vs cell trace violet (CTV).

*Antigen-specific proliferation was measured by the frequency of Ki67+ (**B**) or CTV- (**A**) among lymphocyte subsets, after six days of culture in media with antigen (PPD – left, PMA – right), with media only values subtracted. Human samples are marked by circles, and non-human samples by squares. There were no significant differences between antigen-specific proliferation in human and NHP samples.*

5.4.6 Antigen-specific proliferation assay

The CTV proliferation assay was applied to baseline samples from humans and NHPs to determine antigen-specific proliferation pre-aeBCG (Figure 5.8). PMA-specific proliferating cell frequency was significantly higher for all cell types (both species, data not shown). There was no difference between human and NHP baseline proliferation, for: CD3+, CD3-, CD3+CD4+CD8- or CD3+CD4-CD8+ lymphocytes. Compared to known PPD-responders (pilot), the frequency of PPD-specific proliferating cells was lower in these baseline samples. For example, the median frequency of PPD-specific CD3+ lymphocytes was 28.01 in the PPD-responder human PBMCs, compared to median 0.235 in baseline samples from TB043.

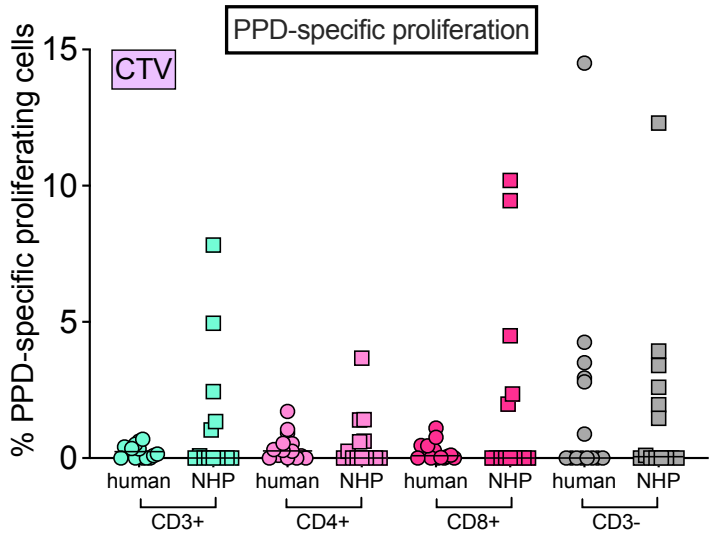


Figure 5.8 PPD-specific proliferation in baseline human and NHP samples.

*Proliferation among human (left) and NHP baseline (right) was measured by the frequency of CTV- cells after six days of culture in media alone (unstimulated, green), or with PPD (pink) or PMA (yellow). The frequency of proliferating CD3- (**A** & **E**) and Cd3+ (**B** & **F**) lymphocytes, CD4+ (**C** & **G**) and CD8+ (**D** & **H**) T-cells are shown for individuals with group medians (**A**-**D**), and with individuals tracked between conditions (**E**-**H**). P-values generated by Wilcoxon-Rank testing between paired samples is marked where significant as: P < 0.05 (*).*

5.5 Discussion

The peak immune response to aeBCG was at D7 in humans, whereas the peak immune response to aeBCG was at Wk12 in NHPs. The peak immune response in NHPs was broader, spanning Wk4-Wk16, depending on the immune response in question. The methods, time points and samples used in this project and the parallel human work were designed to be aligned wherever possible. The difference detected in the parallel studies described here are important for the field, and warrant further investigation.

5.5.1 PPD-specific IFNγ SFU measured by ELISpot

McShane *et al*., previously showed that although the frequency of PPD-specific IFNγ SFU is increased at D7 after ID BCG than at baseline in humans, the peak of this response is at Wk4[291]. The human work discussed here showed that after aeBCG, the peak frequency of IFNγ SFU was at D7, and that there was no detectable difference at Wk4. In NHPs, a more gradual response was observed from Wk4 to the final study time point of Wk16.

Previously published NHP studies exploring the immune response to mucosal BCG also showed a broad peak in PPD-specific IFNγ SFU frequency. White *et al.*, found the peak response to standard (2-8x10^6 CFU) to be at Wk10 in two independent studies[3, 7], and the kinetic was the same for a 1/10^{th} dose (2-8x10^5 CFU)[4]. After EB instillation of 2-8x10^6 CFU of BCG, Verreck *et al*., showed that the peak PPD-specific IFNγ SFU frequency was at Wk9, also with a broad peak (e.g. increased frequency at other consecutive time points)[10]. The kinetic detected within this project is in-keeping with this previously published data in that the response increases over a number of weeks.

5.5.2 Peak response to aeBCG

Although the peak responses were weeks apart in humans and NHPs, it is interesting to consider which cell types were up-regulated or down-regulated at these time points, and whether their functional capacity was changed in the same way. Comparison of cell populations and their ability to produce cytokines was limited in humans, because BAL samples could only be taken at one time point (for logistical and ethical reasons).

Cell populations in the periphery were explored in unstimulated/BCG-stimulated whole blood samples from humans, and unstimulated/PPD-stimulated PBMCs from NHPs. Despite parallel study design, PPD was used for NHPs to align with previously published work. PPD is a culture filtrate from virulent *M.tb*, containing secreted antigens, whereas BCG is a live bacteria. Whole blood and PBMCs both represent the peripheral response, but whole blood samples include granulocytes, serum, and other blood components, which may influence responses *in vitro*. It is unlikely that the overall kinetic of the immune differs between whole blood and PBMCs. Human PBMCs were cryopreserved for future work.

The peak immune response to aeBCG in NHPs is delayed compared to the immune response to ID BCG and *M.tb*, both of which peak earlier (Wk6-Wk8)[3, 9]. After ID BCG or *M.tb*, a small peak in response is sometimes detected at around Wk4 in humans[9]. The magnitude and speed of the human response to aeBCG is unexpectedly early given the kinetic shown in published mucosal BCG studies in NHPs, and the timing of the human response to ID BCG. One possible theory is that AE delivery allows direct contact with alveolar macrophages, faster antigen presentation and recruitment of immune cells. Increased antigen presentation would not explain why a faster immune response would occur in humans, but not in NHPs.

It is possible that more BCG is delivered using $1x10^7$ CFU of aeBCG, compared to the standard $1x10^6$ CFU ID dose. $1x10^7$ CFU was selected as the target dose for this project, because of previously published estimates that at least 1 log CFU is lost in nebulisation[3]. If more than $1x10^6$ CFU aeBCG are delivered using $1x10^7$ CFU of aeBCG, it is possible that antigen exposure in the lungs is increased by dose itself. In theory, increased dose could shorten the time for an immune response to develop, by increasing antigen exposure. This would also be the case for NHPs, and does not explain the species difference, unless more of the $1x10^7$ CFU of aeBCG is successfully delivered in humans than NHPs.

A biological difference between humans and NHPs could also alter the kinetic of the immune response to aeBCG. A recent genetic study of total blood leukocytes by Hawash *et al.*, compared the immune response of humans/chimpanzees (apes) and African/Asian monkeys (AAMs – including RM) to see if there was a difference in responses to bacterial and viral pathogens[292]. Hawash *et al*., found that apes mounted a faster, stronger, and less specific response four hours after exposure to antigen (smaller different 24 hours after exposure). It is possible that faster transcriptional changes increase the speed of the human response to BCG compared to NHPs, and that this difference is exacerbated in aeBCG studies because of the increased antigen availability throughout the lungs (compared to ID BCG).

The differing immune response kinetic detected in this project is likely to be mycobacteria specific, and may also be specific to AE delivery. For example, previously published studies in humans and NHPs showed that after vaccination with MVA85A, both species showed a peak antigen-specific response at D7[97, 293]. This presents evidence that in other contexts, these two species respond in a comparable manner.

5.5.3 Baseline antigen-specific proliferation

After optimising the method used to thaw cells to ensure maximum cell yield, and testing two protocols[294, 295], PPD-specific proliferation at baseline was evaluated for human and NHP PBMCs (both n=16). Both Ki67 and CTV were able to detect PPD-specific proliferation, but CTV was selected because the staining was clearer. The pilot experiment showed that addition of PMA at D6 was not sufficient to stimulate proliferation compared to unstimulated samples. For this reason, D0 addition of PMA was used as a positive control in the follow-on experiments. It was not possible to include NTM antigens to in this comparison, in part due to a lack of suitable antigen availability.

Although the same number of cells were added to each well, NHP samples had fewer live cells upon acquisition than human samples. Samples with fewer than 12000 live cells on acquisition were excluded, leaving: n=15 PPD, n=7 PMA for human samples, n=14 PPD, n=5 PMA for NHP. PMA samples were not included for every individual, to allow samples to be run across two plates only, thus avoiding additional batch effect. The frequency of PPD-specific proliferating cells in baseline samples from this project was lower than the frequency detected in PPD-responsive humans/NHPs in the pilot experiment. No difference was detected between NHP and human PPD-specific proliferation at baseline. This could mean that NHPs and humans do not have different levels of baseline exposure to mycobacterial antigens, or it could mean that this assay cannot detect the difference. It is possible that an NTM-specific antigen used in this assay would show a difference in species.

5.5.4 Humoral response to aeBCG

PPD-specific IgG titre increased at the peak response to aeBCG in humans and NHPs. There was also a significant increase in IgA titre in humans at D7 (TB041, data not shown). Data from

TB041 also showed significantly increased PPD-specific IgG and IgA at D7 after ID BCG, despite no increase in frequency of PPD-specific IFNγ SFU at D7 after ID BCG. This indicates that the increased D7 antibody titre was not specific to AE delivery. The increased PPD-specific antibody titre at D7 after aeBCG/ID BCG was transient and could not be detected at any other time point. The antibody titre detected in humans was consistently lower than the antibody titre detected in NHPs. The two species were most similar at D7 and Wk2, at which time points the human antibody response was at its peak, and the NHP antibody response had not begun.

Published data exploring the humoral response to mycobacteria is historically conflicting, with more recent experiments pointing to a positive role for some types of antibodies in some circumstances, possibly through unexpected mechanisms such as Fc-activity and antibody-mediated enhancement of cellular immunity[219, 220]. The NHP antibody response detected in this study further confirms that an antibody response is induced after BCG, and is in line with the increase towards Wk10 identified by White *et al.*, after aeBCG (2-8x10^6 CFU, not significant)[3]. The increase in antibody detected at D7 after BCG in humans (both ID and aeBCG) is yet to be confirmed using TB043 samples (this was the main human aeBCG study). More work is required to determine whether any protection is conferred by these antibodies, and by what mechanisms they might interact with other components of the immune response.

5.5.5 Possible reasons for a species difference

There was no difference between species in PPD-specific proliferation at baseline. If there is a difference in previous exposure to mycobacterial antigens at baseline, this could be caused by different levels of exposure to NTM and not be detectable using PPD. Other possible factors include: respiration patterns, lung size, average body temperature of macaques being

higher than humans, the possibility of aeBCG ending up in the stomach and technical differences between experiments.

The average rectal temperature of macaques measured in this project was from 38-41°C, which is higher than the average human body temperature of 36-37.5°C. It is also possible that temperature readings for macaques are artificially high, as animals must be caught before a reading can be taken. BCG grows optimally at 37°C, and higher body temperature in macaques could decrease the amount of/slow the mycobacterial growth after infection, thus altering the kinetic of the immune response. Although *in vitro* study of the effect of temperature on BCG growth is possible, it would be difficult to study this *in vivo* or extrapolate results to the *in vivo* setting, given the number of other factors involved. If the growth rate of BCG or other live TB vaccines differs between humans and macaques because of this temperature difference, this should be considered for vaccine safety and efficacy studies. However, BCG is immunogenic in both species, and provides a similar level of protection, which suggests that a temperature difference may not explain the differences observed in this study. In addition, the magnitude of the immune response induced by BCG vaccination (measured by ELISpot) is higher in RM than CM, despite RM having a slightly higher average temperature (Sharpe *et al.,* personal communication), which does not support the hypothesis that increased temperature would inhibit BCG growth and therefore limit the immune response induced.

Sedation of the NHPs might cause respiratory differences, such as shallower breathing and reduced breathing rate. However, preliminary AE deposition data using aerosolised gold nanoparticles showed that there was AE particle distribution throughout the lungs, despite sedation (White *et al.*, unpublished). In the preliminary AE deposition data using aerosolised

gold, substantially more gold settled in the digestive tract and stomach than in the airways (White *et al.*, unpublished). It is possible that more of the $1x10^7$ CFU of aeBCG was swallowed by NHPs compared to humans, because animals were sedated. After swallowing a fraction of the BCG, a lower dose would be available for antigen presentation in the lungs, as it would likely be destroyed by the stomach acid. Other technical differences were minimised by the parallel design of the experiments described in this project.

5.5.6 Possible implications for TB research

Further work is needed to explore the difference in immune response to aeBCG identified in this project. It might be possible to adapt the NHP aeBCG model to give a faster immune response kinetic (like in humans), perhaps by extending studies to other NHP species, or by altering the aeBCG dose. The difference detected here should be treated as mycobacteria specific (given that the immune response to MVA85A is comparable across species), and may also only be apparent after exposure to mycobacteria via aerosol. More detailed and sensitive description of baseline immunity would help to determine whether baseline mycobacterial exposure differs between these species. If this were the case, prior NTM exposure in humans could be replicated in the NHP model using exposure to *M.avium* or similar. However, this would increase the variability of the model.

5.6 Summary and conclusions

5.6.1 Summary

- aeBCG ($1x10^7$ CFU) delivered to the lungs is safe and immunogenic in both humans and NHPs. The peak immune response to aeBCG was at D7 in humans, compared to Wk12 in NHPs, contrary to hypothesis a).
- PPD-specific cytokine producing cell frequency increased at the time of the peak PPD-specific IFNγ SFU frequency in both species, particularly in the BAL.
- There was no difference in the amount of PPD-specific proliferation in human PBMCs compared to NHP PBMCs at baseline. The frequency of proliferating cells at baseline was over 100 times less than in known PPD-responsive cells.
- Possible explanations for the difference in kinetic include: evolutionary differences between immune systems (exacerbated by AE delivery), NHP sedation, possible swallowing of aeBCG by NHPs and species size difference.
- PPD-specific antibody production in serum increased compared to baseline in both humans and NHPs at the peak of the immune response as postulated in hypothesis c), at D7 and Wk9, respectively). The function of these antibodies is yet to be determined.

5.6.2 Conclusions

- The kinetic of the immune response to aeBCG is different between humans and NHPs, but is dominated by local cytokine production in both species, particularly IFNγ-production by CD4+ T-cells.
- Further exploration of this difference may shed light on the mechanisms of local immune responses in the lung.

Chapter 6: Conclusions and future directions

Chapter 6: Conclusions and future directions

6.1 Summary

TB is a major threat to global health and a financial burden. As increased mobility allows more communities to mix, and antibiotic resistance continues to emerge as a worldwide problem, reducing the threat posed by *M.tb* remains imperative. In light of the COVID-19 pandemic, continued research to enhance our preventative and treatment strategies to combat TB is more urgent than ever; the World Health Organisation 'end TB' strategy continues to fall behind targets[11, 296].

Effective vaccination is the best form of protection against an infectious disease, but BCG remains the only licensed vaccine to prevent TB disease, and provides only limited protection against disseminated forms of disease. BCG is insufficient in providing protection against pulmonary TB disease, but candidate vaccines in phase II-III clinical trials provide hope for improvement on the protection provided by BCG. Clinical trials to test new vaccines are lengthy and costly, but cannot be improved upon without a valid correlate of protection. IFNγ is used as a primary readout in many vaccine studies, but IFNγ alone does not correlate with protection.

Mucosal vaccine delivery mimics the natural route of infection with *M.tb*. Methods developed for mucosal vaccination against other pathogens, and to provide AE *M.tb* in animal challenge model, can be used to explore the immune response to airborne mycobacteria. The aeBCG challenge model can be used safely to mimic *M.tb* infection in both humans and animals, and allows exploration of early time points after mycobacterial exposure. Experiments conducted in RM and CM showed very little detectable response to aeBCG at

D2/D7, among the immune parameters measured. At D14, CD161+ cell frequency increased among multiple lymphocyte subsets, perhaps identifying a subset of transcriptionally similar cells[277], capable of responding to mycobacterial infection quickly[278]. Further experiments showed that from Wk4, an immune response to aeBCG was detectable: cytokine and antibody production, increased cellular activation. There was no difference between the immune response induced by aeBCG with a mask or mouthpiece attachment.

The experiments in this project were designed to run in parallel with a human CHIM model (McShane group, Oxford – ClinicalTrials.gov ID: NCT03912207 TB043 and NCT02709278 TB041), allowing direct comparison between the NHP aeBCG model and the target species. Unlike the NHP immune response to aeBCG, the human immune response was unexpectedly different in kinetic to the responses previously observed after ID BCG. The fast peak response at D7 after aeBCG measured in humans raises a number of questions. Why is the immune response to aeBCG not similar in NHPs and humans, despite parallel experiments with the same setup, and previously demonstrated similarities between the immune response to ID BCG in both species? Why is the human systemic immune response to aeBCG so much faster than to ID BCG? Do the differences in immune responses detected reflect a basic difference in immune response between the two species or something mycobacteria specific, and why is this only detectable when exploring the immune response to BCG delivered by AE?

6.2 Key findings

6.2.1 aeBCG at early time points

Up to 2 weeks after aeBCG, there was little change in the immune parameters measured in this project. D2/D7/D14 were explored across a range of tissue: PBMCs, BAL cells and MCs from lung and LNs. There was no detectable immune response measured by PPD-specific IFNγ ELISpot in PBMCs or in PPD-specific antibody titre in serum. There was a transient increase in the CD4+:CD8+ T-cell ratio at D7, and an increase in CD56+CD4+ T-cell frequency (RM and CM). CD4+:CD8+ T-cell ratio was higher in RM than CM from baseline. γδ T-cell and cytokine producing cell frequency did not substantially change at these early time points after aeBCG.

CD161+ cell frequency increased among a number of lymphocyte populations across tissues, to some extent at D7 (CM), and more markedly at D14 (RM). The increase in CD161+ cell frequency was more pronounced in RM. MerTK+/CD163+ non-lymphocyte frequency was lower in RM, but MerTK+/CD163+ frequency did not change after aeBCG. Differences detected between RM and CM were therefore largely restricted to baseline differences between the species, rather than a difference in immune response to aeBCG. These results suggest that the early immune response to aeBCG is limited, regardless of macaque species. Previously published data demonstrated that it takes upwards of two weeks for an immune response to be detected after ID BCG or *M.tb* challenge[8].

6.2.2 aeBCG at late time points

The second part of this project explored Wk2-Wk16 after aeBCG. Serial blood and BAL samples were evaluated, giving an overall kinetic for the immune response of each individual. Half the animals were exposed to aeBCG with a mouthpiece delivery attachment to match the early time point studies, and the ongoing human CHIM work. The other half were exposed

using a modified paediatric mask, as used in previous NHP studies of AE delivered vaccines[7, 293]. This was a valuable opportunity to directly compare these methods, particularly given the increasing interest in aeBCG as a deployable vaccine delivery method. Although preliminary data suggested a difference in the deposition of aerosolised particles delivery with each method (White *et al.,* unpublished), no difference in the response to aeBCG were detected in this study. For this reason, results from all animals were examined together.

The peak immune response detected was from Wk9-Wk16. By maximum PPD-specific IFNγ SFU frequency was measured at Wk16 (ELISpot), increasing gradually from Wk4. This is similar to previous data published by White *et al*[3]. The CD4+:CD8+ T-cell ratio increased in BAL cells, peaking at Wk12, alongside increased cytokine-positive cell frequency. The CD4+:CD8+ T-cell ratio decreased at Wk12 in PBMCs. More cells produced IFNγ than IL-2, and more produced IL-2 than IL-17. Polyfunctional T-cell populations increased, particularly among CD4+ BAL cells. CD161+ cell frequency increased transiently at Wk2, and more gradually up to Wk12. It is possible that the early (Wk2) increase in CD161+ cells represents a faster acting subset of cells with a shared transcriptional phenotype[277, 278], while the more gradual increase up to Wk12 represents an increase alongside the adaptive immune response. Increased PPD-specific IgG was detected in a proportion of animals, peaking at Wk9. The function of antigen-specific antibody production in response to BCG is not well defined.

The kinetic of the immune response to aeBCG measured here is similar to previously published work on mucosal BCG in NHPs. A gradual increase in the immune response, peaking weeks after aeBCG suggests a primarily adaptive immune response. The innate immune response to aeBCG appears to be minimal, with the exception of increased CD161+ cell

frequency. Unlike previous reports[177, 183], the γδ T-cell population did not expand after aeBCG, but there was an increase in cytokine producing γδ T-cell frequency, which suggests activation. As expected, the immune response to aeBCG was stronger locally.

6.2.3 aeBCG in humans vs NHPs

The third part of this project was to compare the immune response to aeBCG in NHPs to a parallel human CHIM study. In the absence of parallel experiments, differences in the immune response between species may take longer to determine, which means that work on mechanisms using models (in the intervening time) may have less relevance to humans.

The immune response to aeBCG in humans was less gradual and peaked at D7, rather than weeks after aeBCG (NHPs). In this project, the dose of aeBCG and methods used to quantify the immune response in NHPs were aligned as closely as possible. In humans, the frequency of PPD-specific IFNγ SFUs (ELISpot) peaked at D7, and was no longer significantly different to baseline at Wk4. In contrast, there was no difference in IFNγ SFU frequency at D2/D7/Wk2 in NHPs, but frequency was significantly higher from Wk4, peaking at Wk16 (all compared to baseline). Changes in cell population and cytokine producing cell frequency also increased from Wk4, and peaked at Wk12. In humans, cytokine producing cell frequency peaked at D2/D7 in PBMC. In BAL, differences could be detected at D7 compared to D2, including increased IFNγ+ CD4+ T-cell frequency.

It is unclear why the kinetic of the immune response to aeBCG is different between NHPs and humans. To explore this, a proliferation assay was developed to quantify baseline antigen-specific proliferation. In theory, higher baseline antigen-specific proliferation in humans, would show pre-sensitisation to mycobacteria. Pre-sensitisation could speed up the immune response, as a form of immunological memory may exist. No difference in antigen-

specific proliferation at baseline was detected between species. Further investigation into this species difference is required.

6.3 Future directions

6.3.1 parallel human NHP work

One of the key aims of this project was to closely align experiments in NHPs and humans. This is logistically difficult, and requires collaboration across organisations. Humans and NHPs are heterogenous. Human behaviours are difficult to control, and travel increases the chance of exposure to other pathogens. The NHP animal model can be controlled, but social hierarchy and genetics inevitably create differences. Despite the challenges of parallel work, it remains an important goal for transferrable research. By running this project, a clear difference in the kinetic of the immune response to aeBCG has been detected; this highlights the need for exploration into the reason for this difference.

6.3.2 aeBCG in NHPs

This project has shown that aeBCG can be safely used as model of mycobacterial infection in both species. The NHP immune response to aeBCG can be compared to other NHP studies of mycobacterial infection. Sibley *et al.,* showed that after ID BCG, a proportion of CM have an adaptive immune response (measured by ELISpot) as early as two weeks after *M.tb* challenge[253], whereas RM typically respond to ID BCG from Wk4 onwards[7, 8]. Dijkman *et al.,* showed that CM have early increases in pro-inflammatory monocytes compared to RM[4]. Additional studies to determine how the CM immune response to aeBCG develops after D7 may further differentiate between macaque species. For example, earlier onset of the immune response in CM (e.g. before Wk9-Wk12) would support the idea that CM mount a more aggressive response to mycobacteria, perhaps helping CM to resist pathology.

In this project, macaque group sizes were largely determined by animal availability and husbandry requirements of the colonies from which animals were obtained. The number

of animals available for each study was determined by availability, but allocation to each test group was determined by the project team, allowing for a balance between the group number required for a robust result and the number of conditions that could be investigated. Sample sizes were sufficient for this type of descriptive work, and the sample size (n=8 of animals in the late time point dataset was comparable to group sizes in the parallel human study (n=10).Given the ethical considerations for animal work and the principles of 3Rs, work should be designed to account for biological variation in a way that results in meaningful data. Where possible, future experiments should be powered to allow for diverse responses between different animals. Expanding this work to include the use of an *in vitro* assay to determine possible correlates of protection against TB disease would increase the utility of this dataset, and further attempts to use human datasets to explore the immune response to TB.

6.3.3 aeBCG in humans vs NHPs

The difference in kinetic between the immune response to aeBCG in NHPs compared to humans is striking. PPD-specific proliferation at baseline could not distinguish between species. To further explore the hypothesis that humans have higher mycobacterial exposure than NHPs, baseline proliferation in response to NTM antigens or BCG could be explored. Lipid (and other non-peptide) antigens expressed by BCG are absent for PPD, and may engage different receptors on innate cells in particular. Antigenic overlap with other microorganisms could also contribute to priming of the immune system, and merits further exploration.

As previously published, AE delivery of MVA85A resulted in a fast immune response kinetic in both NHPs and humans (peak response at D7)[97, 293]. It is possible that in the MVA85A studies, both NHPs and humans exposed to MVA85A by AE had a more secondary response. In the studies discussed in this project, only the human response to aeBCG seems like a

secondary immune response. Coupled with the observation that the peak immune response to ID BCG is more similar between humans and NHPs, this suggests that the difference in kinetic identified here is not only specific to AE delivery, but also specific to mycobacteria.

Although aeBCG dose and delivery equipment were the same in these studies, it was necessary to sedate NHPs before exposure to aeBCG. Sedation could affect AE deposition within the lungs, and therefore antigen exposure to the immune system. NHPs are smaller than humans, but this is unlikely to provide an explanation for a faster immune response in humans, because smaller size would mean that using the same dose in both species gave the NHPs a larger amount of antigen exposure.

After ID BCG vaccination in humans, the frequency of PPD-specific IFNγ SFU increases at D7, and increases further to Wk4-Wk8[291,297]. In NHPs, ID BCG induces an increase in SFU from Wk4 until approximately Wk16 (peaking around Wk6)[8, 9, 10] – to our knowledge the earliest published time point is Wk2 and showed no change in SFU[7]. These results suggest that the increased frequency of IFNγ producing cells after ID BCG is similar in NHPs and humans. A direct comparison of the immune response to ID BCG in these species at early time points would help to clarify if there is any difference in this kinetic. A subtle species difference may be clearer after aeBCG than ID BCG, because of increased antigen exposure to the lung.

Humans and NHPs are genetically distinct. Hawash *et al.* showed that apes (humans/chimpanzees) respond to both bacterial and viral stimulation more quickly than African/Asian monkeys (RM/baboons)[292]. The most divergent genes were involved in IFN production and inflammation regulation, and the ape response was less specific[292]. Faster bacterial recognition and a more inflammatory initial response could contribute to the faster

kinetic noted in humans in this project. To explore this, it would be interesting to compare antigen-specific transcriptional changes at early time points after aeBCG.

6.3.4 correlates of protection

Animal studies of mycobacterial infection often include a challenge phase, in which animals are exposed to *M.tb*. Protection against *M.tb* can be compared to immune parameters measured on an individual basis, to see which, if any, influence protection. *In vitro* substitutes have been developed to try to determine levels of protection in humans, in the absence of challenge. The mycobacterial growth inhibition assay has been developed in humans and NHPs. In this project, the mycobacterial growth inhibition assay was applied to NHP samples, but not successfully. A problem with BCG standardisation meant that the assay results were not within an acceptable range, and could not be interpreted. Further work optimising the BCG stock in question and re-testing of samples could provide another dataset to compare.

To combine the novel dataset examined in this project, correlations between multiple immunological readouts and different aspects of the same response were used. A combinatorial approach to reduce the number of parameters and pairwise comparisons could be used to further explore this data. This type of analysis might identify correlation between assays that would otherwise be missed by the more conservative approach applied here, and may help to understand the impact of the difference in kinetic identified between macaques and humans here. Possible approaches for this analysis include both unsupervised and supervised approaches. The principal component analysis described for BAL flow cytometry data at late time points in Chapter 4 is an example of an unsupervised approach which does not make use of labels in the computation. Supervised approaches that have not yet been

explored for this dataset include least absolute shrinkage and selection operator (LASSO) and partial least squares discriminant analysis (PLSDA). Supervised approaches have the advantage of 'learning' from the dataset, but require additional initial input compared to approaches such as PCA.

6.3.5 role of CD161+ cells

CD161+ cells were upregulated at Wk2 after aeBCG in NHPs. Although CD161+CD8+ T-cells can be defined as MAIT cells when Vα7.2 is co-expressed, CD161+ frequency also increased independently of Vα7.2. Without a MAIT-specific tetramer, the possibility that the identified CD161+ cells are MAIT cells cannot be ruled out, but CD161 expression on non-CD8+ lymphocytes increases the likelihood that this marker does not only distinguish MAIT cells. CD161+CD4+ T-cells have the capacity to act before conventional T-cell responses are expected[278], and lymphocytes expressing CD161 share a transcriptional phenotype[277]. CD161 up-regulation at Wk2 may demonstrate innate-like cell activation, and warrants further investigation, perhaps through transcriptional analysis of the samples in this project.

6.3.6 role of antibodies

A PPD-specific antibody response was detected at the peak immune response in both species. The role of antibodies in the immune response to TB disease continues to be unclear. Recently, Alter *et al.,* showed that antibody titre distinguishes between animals given BCG IV, compared to aeBCG or ID BCG[226]. IV BCG provides superior protection to ID BCG[5, 8], and Alter *et al.,* showed that lipoarabinomannan-specific IgM monoclonal antibody could restrict *M.tb* growth *in vitro*[226]. A similar *in vitro* method could be applied to serum samples from this project, to determine whether antibody produced after aeBCG can control *M.tb* growth. It would also be possible to explore further antibody classes, antibody glycosylation and

binding, to better determine the quality of the antibody response to aeBCG. In this project, PPD-specific IgG titre was determined for all samples, and IgM for late time point samples (after observing no change in IgG titre at early time points). A supply problem with commercially available secondary NHP IgA antibody during this project, prevented exploration of this subtype.

6.3.7 aeBCG as a vaccine

There is continued interest in improving upon protection provided by ID BCG using BCG itself: either with BCG re-vaccination[98], or using a mucosal delivery route. The most practical method of mucosal vaccination is aeBCG. Recently, Darrah *et al.,* showed that aeBCG did not provide significantly superior protection to ID BCG[5]. White *et al.,* showed that although aeBCG did not have increased capacity to control disease compared to animals given ID BCG, animals vaccinated with aeBCG had lower extra-pulmonary pathology scores[7]. Further studies of aeBCG at different doses, in comparison with ID BCG, are necessary to determine the merits of aeBCG as a vaccine in terms of protection.

6.4 Concluding remarks

Despite use as a vaccine for 100 years, the critical protective elements of the immune response to BCG have remained difficult to determine. Efforts to improve upon the protection provided by BCG are ongoing, and include alternative BCG delivery strategies, as well as novel vaccine boosters or alternatives. To further these efforts and build upon treatment strategies in a rational manner, searching for a valid correlate of protection against TB disease continues to be a priority.

Using aeBCG as a model of mycobacterial infection provides a safe way to explore mycobacterial infection in humans and animals. By designing work in parallel, like in this project, models can be complimentary, and models differences are highlighted. Heterogeneity increases the complexity of studying mycobacterial infections in humans or large animal models, and some bias is inevitably introduced in the planning phase of experiments like the ones described here. Continued investigation into other possible elements of the immune response to TB disease, including relatively un-biased techniques and conditions wherever possible may further our existing knowledge.

The species difference highlighted by this project warrants further investigation, and shows that route of BCG vaccination alters the kinetic of the immune response, particularly in humans. Further work to determine the reason behind these differences may shed light on which components of the immune system act in the lungs, and how increased/alternative antigen exposure can bias the immune response.

Appendices

Appendices

7.1 Additional tables

7.1.1 Wordcount

Wordcount in this thesis	
section	wordcount
Abstract	291
Chapter 1	11807
Chapter 2	4082
Chapter 3	12812
Chapter 4	12272
Chapter 5	4915
Chapter 6	3287
Overall	49466

Supplementary Table 1 Wordcount

Summary of wordcounts for each section of this thesis.

7.1.2 Study details

BCG dosing across studies in this project													
Species	**non-human primates**											**humans**	
Study ID	**6114**		**6143**	**6282**		**6165**			**6181**			**TB041**	**TB043**
Date	2019.1.28	2019.1.29	2019.2.25	2020.9.22	2020.9.24	2019.3.21	2019.3.23	2019.3.28	2019.7.3	2019.7.3	2019.7.3	study median	study median
CFU (x10^6)	3.15	1.52	0.67	7.60	5.40	5.30	12.45	6.95	18.95	13.60	18.50	1.10	2.64

Supplementary Table 2 BCG dosing across studies

BCG dose was back-calculated from colony counts of plate cultures of left-over BCG on 7H11 Agar plates. CFU/mL and CFU/vial were calculated and are shown for different studies (x10^6). The target dose was 1x10^7 CFU/mL, and the stated dose on each vial was

7.1.3 Acronyms and abbreviations

Abbreviations and acronyms used in this thesis			
acronym	**meaning**	**acronym**	**meaning (continued)**
aeBCG	aerosol BCG	LTBI	latent TB infection
AE	aerosol	M:L	monocyte:lymphocyte
AIDS	acquired immunodeficiency syndrome	*M.tb*	*Mycobacterium tuberculosis*
ANOVA	analysis of variance	MAIT	mucosal associated invariant T cell
AUC	area under the curve	MC	mononuclear cells
BAL	broncho-alveolar lavage	MGIA	mycobacterial growth inhibition assay
BCG	Bacille Calmette-Guérin	MVA	modified vaccinia virus ankara
CD(4)	cluster of differntiation (4)	N:L	neutrophil:lymphocyte
CFU	colony forming unit	NHP	non human primate
CMV	cytomegalovirus	NK	natural killer cells
CV	coefficient of variation	NKT	T cell expressing CD16/CD56
D(2)	day (2)	NTM	non-tuberculous mycobcteria
EB	endobronchial	PBMC	peripheral blood mononuclear cell
ELISA	enzyme-linked immunosorbent assay	PBS	phosphate-buffered saline
ELISpot	enzyme-linked ImmunoSpot	PMA	phorbol 12-myristate 13-acetate
ESAT	early secretory antigen target	PPD	purified protein derivative
FSC-A	forward scatter-area	R(10)	media (see solutions)
g	graviational force	SIV	simian immunodeficiency virus
HIV	human immunodeficiency virus	SSC-A	side scatter-area
HLA-DR	human leukocyte antigen-DR	T-reg	regulatory T cell
ID	intradermal	TB	tuberculosis
IFNg	interferon-gamma	Th(17)	T-helper (17) cell
IgA/G/M	Immunoglobulin A/G/M	UK-HSA	United Kingdom Health Security Agency
IGRA	interferon gamma release assay	Va7.2	V-alpha 7.2 invariant TCR chain
IL(-17)	interleukin (-17)	WB	whole blood
IT	intra-tracheal	WBICS	whole blood intracellular cytokine staining
IV	intravenous	WBICS	WB intracellular staining (WBICS)
LN	lymph node	Wk(2)	week (2)

Supplementary Table 3 Abbreviations & acronyms

Explanations of abbreviations and acronyms used throughout – in alphabetic order.

7.1.4 Additional data tables

Cell counts (medians)										
Tissue	**PBMC**		**BAL**		**Hi LN**		**Ax LN**		**lung**	
Stimulation	**Nil**	**PPD**	**Nil**	**PPD**	**Nil**	**PPD**	**Nil**	**PPD**	**Nil**	**PPD**
NKT 16+	1974	2019	107	113.5	259	216	207.5	221.5	1776	1939
NKT 56+	2749	2685	3137	3780.5	4917	4732	4944.5	4775.5	1848	1560
NKT 16+56+	99	130	69	77.5	148	59	106	83.5	113	108.5
CD4+	43231	39845	7110	8277	113661	107597	123419	110224	5053	3975.5
CD4+56+	516	671	334	379	1055	1592	1488	1482.5	315	245.5
CD4+8+	1309	1437.5	1044	1081.5	1868	1480	2999	2257.5	605	436
CD4+8++	613	756.5	426	448	312	255	621.5	578.5	185	91
CD4-8-	3770	3180.5	733	1029	5820	6036	3819	4549	766	954.5
CD8+	19596	22901	10298	12339	48927	45705	52244	47254	16738	14471
MAIT 7.2+	255	268	187	285.5	626	698	638	463	128	105
gd	3087	3165.5	730	816.5	3325	4062	4036	3230.5	1857	1744
NK 16+56+	147	154.5	46	59	8	8	19.5	12	264	214.5
Nk 16-56+	186	221.5	379	457.5	294	292	338	306.5	112	74
NK 16+56-	2598	3240	37	35	20	12	26.5	42	2430	1804
nonL CD14+	8645	17482	3779.5	6525	50.5	50	418.5	234	2665	2361.5
nonL CD16+	1857	1821	675	963	32	28	90	70	429	377
nonL CD14+CD16+	1551.5	879	509.5	804	11	8	50	33	296	107
nonL CD14+CD16-	6214.5	15695	2870.5	4920	61	58	347	198.5	2254	2207
nonL CD14-CD16+	235.5	547	98	84	20	15	36.5	37	181	222.5

Supplementary Table 4 Median cell population counts, characterised by flow cytometry

Median cell counts from cell populations within different tissue compartments are shown in the table. Medians were taken from rhesus macaque samples collected as part of the early time point studies. Median counts under 100 cells are highlighted in yellow.

A

ELISpot vs PBMC CD3

PBMC CD3		ELISpot Wk0B	ELISpot Wk0A	ELISpot Wk2	ELISpot Wk4	ELISpot Wk9	ELISpot Wk12	ELISpot Wk16
Wk0	CC	0.278	-0.129	0.033	0.155	-0.666	-0.043	0.082
	Sig.	0.505	0.761	0.938	0.715	0.071	0.920	0.847
	N	8	8	8	8	8	8	8
Wk2	CC	-0.266	0.389	0.649	0.382	0.149	0.228	0.018
	Sig.	0.319	0.136	0.007	0.144	0.581	0.395	0.947
	N	16	16	16	16	16	16	16
Wk4	CC	-0.194	0.567	0.435	0.231	0.129	0.565	0.333
	Sig.	0.472	0.022	0.092	0.390	0.635	0.023	0.208
	N	16	16	16	16	16	16	16
Wk9	CC	-0.328	0.439	0.154	0.015	-0.013	0.197	0.332
	Sig.	0.215	0.089	0.570	0.955	0.961	0.464	0.209
	N	16	16	16	16	16	16	16
Wk12	CC	-0.071	-0.010	0.348	0.439	0.172	-0.165	0.086
	Sig.	0.793	0.972	0.187	0.089	0.525	0.541	0.753
	N	16	16	16	16	16	16	16
Wk16	CC	-0.037	-0.369	0.036	-0.638	0.410	0.084	-0.423
	Sig.	0.931	0.369	0.933	0.088	0.313	0.844	0.296
	N	8	8	8	8	8	8	8

B

ELISpot vs PBMC gd

PBMC gd		ELISpot Wk0B	ELISpot Wk0A	ELISpot Wk2	ELISpot Wk4	ELISpot Wk9	ELISpot Wk12	ELISpot Wk16
Wk0	CC	-0.452	-0.286	-0.452	-0.262	0.119	-0.095	-0.381
	Sig.	0.260	0.493	0.260	0.531	0.779	0.823	0.352
	N	8	8	8	8	8	8	8
Wk2	CC	-0.221	-0.118	0.172	-0.091	0.194	0.118	0.000
	Sig.	0.412	0.664	0.524	0.737	0.471	0.664	1.000
	N	16	16	16	16	16	16	16
Wk4	CC	-0.026	-0.065	0.121	-0.197	0.309	0.212	-0.009
	Sig.	0.922	0.812	0.656	0.464	0.244	0.431	0.974
	N	16	16	16	16	16	16	16
Wk9	CC	0.000	-0.184	0.071	-0.229	0.282	0.015	0.012
	Sig.	1.000	0.495	0.795	0.393	0.289	0.957	0.966
	N	16	16	16	16	16	16	16
Wk12	CC	-0.124	-0.122	0.155	0.012	0.250	-0.026	0.088
	Sig.	0.649	0.652	0.568	0.966	0.350	0.922	0.745
	N	16	16	16	16	16	16	16
Wk16	CC	0.405	-0.143	-0.024	-0.214	0.524	0.762	0.286
	Sig.	0.320	0.736	0.955	0.610	0.183	0.028	0.493
	N	8	8	8	8	8	8	8

C

ELISpot vs PBMC CD4

PBMC CD4		ELISpot Wk0B	ELISpot Wk0A	ELISpot Wk2	ELISpot Wk4	ELISpot Wk9	ELISpot Wk12	ELISpot Wk16
Wk0	CC	0.286	0.190	0.071	-0.048	-0.167	0.024	-0.024
	Sig.	0.493	0.651	0.867	0.911	0.693	0.955	0.955
	N	8	8	8	8	8	8	8
Wk2	CC	0.344	-0.115	-0.063	-0.147	0.079	-0.329	-0.262
	Sig.	0.192	0.672	0.816	0.587	0.770	0.213	0.327
	N	16	16	16	16	16	16	16
Wk4	CC	0.018	-0.175	0.284	0.329	0.271	-0.365	0.118
	Sig.	0.948	0.517	0.286	0.213	0.311	0.165	0.664
	N	16	16	16	16	16	16	16
Wk9	CC	0.200	0.205	0.260	0.200	-0.021	-0.241	0.279
	Sig.	0.458	0.447	0.330	0.458	0.940	0.368	0.295
	N	16	16	16	16	16	16	16
Wk12	CC	-0.046	0.022	0.105	-0.041	-0.346	-0.090	-0.228
	Sig.	0.867	0.935	0.700	0.880	0.189	0.741	0.395
	N	16	16	16	16	16	16	16
Wk16	CC	-0.310	0.286	0.643	0.238	0.119	-0.048	-0.214
	Sig.	0.456	0.493	0.086	0.570	0.779	0.911	0.610
	N	8	8	8	8	8	8	8

D

ELISpot vs PBMC CD8

PBMC CD8		ELISpot Wk0B	ELISpot Wk0A	ELISpot Wk2	ELISpot Wk4	ELISpot Wk9	ELISpot Wk12	ELISpot Wk16
Wk0	CC	-0.479	-0.719	-0.192	0.132	0.084	0.180	-0.275
	Sig.	0.230	0.045	0.649	0.756	0.844	0.670	0.509
	N	8	8	8	8	8	8	8
Wk2	CC	-0.535	0.077	0.277	0.276	0.062	0.218	-0.082
	Sig.	0.033	0.778	0.300	0.300	0.820	0.418	0.762
	N	16	16	16	16	16	16	16
Wk4	CC	-0.188	0.007	-0.421	-0.488	-0.315	0.441	-0.053
	Sig.	0.485	0.978	0.104	0.055	0.235	0.087	0.846
	N	16	16	16	16	16	16	16
Wk9	CC	-0.184	-0.230	-0.477	-0.439	-0.037	0.356	-0.057
	Sig.	0.495	0.392	0.062	0.089	0.892	0.176	0.833
	N	16	16	16	16	16	16	16
Wk12	CC	-0.113	-0.121	-0.143	-0.128	0.131	0.018	0.109
	Sig.	0.676	0.656	0.598	0.637	0.629	0.948	0.688
	N	16	16	16	16	16	16	16
Wk16	CC	-0.429	0.214	-0.286	-0.607	-0.143	-0.071	0.000
	Sig.	0.337	0.645	0.535	0.148	0.760	0.879	1.000
	N	7	7	7	7	7	7	7

E

ELISpot vs PBMC CD4+8+

PBMC CD4+8+		ELISpot Wk0B	ELISpot Wk0A	ELISpot Wk2	ELISpot Wk4	ELISpot Wk9	ELISpot Wk12	ELISpot Wk16
Wk0	CC	0.143	0.286	0.405	0.238	0.381	0.238	0.690
	Sig.	0.736	0.493	0.320	0.570	0.352	0.570	0.058
	N	8	8	8	8	8	8	8
Wk2	CC	0.232	-0.026	0.088	0.271	0.129	0.056	0.012
	Sig.	0.387	0.922	0.745	0.311	0.633	0.837	0.966
	N	16	16	16	16	16	16	16
Wk4	CC	0.094	0.286	0.278	0.271	0.056	0.156	0.079
	Sig.	0.729	0.284	0.297	0.311	0.837	0.564	0.770
	N	16	16	16	16	16	16	16
Wk9	CC	-0.032	0.128	0.163	0.356	-0.035	-0.244	-0.056
	Sig.	0.905	0.637	0.546	0.176	0.897	0.362	0.837
	N	16	16	16	16	16	16	16
Wk12	CC	0.112	0.032	0.049	0.324	0.156	-0.165	0.121
	Sig.	0.680	0.905	0.858	0.222	0.564	0.542	0.656
	N	16	16	16	16	16	16	16
Wk16	CC	-0.048	0.048	0.143	0.714	-0.762	-0.881	-0.310
	Sig.	0.911	0.911	0.736	0.047	0.028	0.004	0.456
	N	8	8	8	8	8	8	8

F

ELISpot vs PBMC CD4+8++

PBMC CD4+8++		ELISpot Wk0B	ELISpot Wk0A	ELISpot Wk2	ELISpot Wk4	ELISpot Wk9	ELISpot Wk12	ELISpot Wk16
Wk0	CC	0.071	0.524	-0.119	-0.214	-0.214	-0.262	0.262
	Sig.	0.867	0.183	0.779	0.610	0.610	0.531	0.531
	N	8	8	8	8	8	8	8
Wk2	CC	0.518	-0.087	-0.235	-0.141	-0.135	-0.162	0.000
	Sig.	0.040	0.749	0.380	0.602	0.617	0.549	1.000
	N	16	16	16	16	16	16	16
Wk4	CC	0.322	0.135	-0.094	-0.074	-0.153	-0.075	0.052
	Sig.	0.223	0.619	0.730	0.787	0.571	0.782	0.850
	N	16	16	16	16	16	16	16
Wk9	CC	0.224	0.009	-0.015	0.024	-0.229	-0.124	0.032
	Sig.	0.405	0.974	0.957	0.931	0.393	0.649	0.905
	N	16	16	16	16	16	16	16
Wk12	CC	0.272	-0.202	-0.097	-0.132	-0.097	-0.184	-0.059
	Sig.	0.308	0.454	0.720	0.625	0.720	0.495	0.829
	N	16	16	16	16	16	16	16
Wk16	CC	0.357	-0.071	0.119	0.952	-0.452	-0.548	-0.143
	Sig.	0.385	0.867	0.779	0.000	0.260	0.160	0.736
	N	8	8	8	8	8	8	8

G

ELISpot vs PBMC CD4-8-

PBMC CD4-8-		ELISpot Wk0B	ELISpot Wk0A	ELISpot Wk2	ELISpot Wk4	ELISpot Wk9	ELISpot Wk12	ELISpot Wk16
Wk0	CC	-0.024	0.238	-0.143	-0.143	-0.286	-0.571	-0.071
	Sig.	0.955	0.570	0.736	0.736	0.493	0.139	0.867
	N	8	8	8	8	8	8	8
Wk2	CC	0.588	-0.393	-0.695	-0.526	-0.062	0.109	0.279
	Sig.	0.017	0.132	0.003	0.036	0.820	0.688	0.295
	N	16	16	16	16	16	16	16
Wk4	CC	-0.071	0.047	-0.205	-0.250	-0.129	-0.124	0.188
	Sig.	0.795	0.863	0.447	0.350	0.633	0.649	0.485
	N	16	16	16	16	16	16	16
Wk9	CC	-0.088	-0.334	-0.077	-0.006	0.285	0.044	0.200
	Sig.	0.745	0.206	0.778	0.983	0.284	0.871	0.458
	N	16	16	16	16	16	16	16
Wk12	CC	-0.171	-0.013	-0.053	0.076	-0.047	0.109	0.347
	Sig.	0.528	0.961	0.845	0.778	0.863	0.688	0.188
	N	16	16	16	16	16	16	16
Wk16	CC	0.214	-0.548	-0.667	-0.738	0.619	0.500	0.190
	Sig.	0.610	0.160	0.071	0.037	0.102	0.207	0.651
	N	8	8	8	8	8	8	8

H

ELISpot vs PBMC CD4+56+

PBMC CD4+56+		ELISpot Wk0B	ELISpot Wk0A	ELISpot Wk2	ELISpot Wk4	ELISpot Wk9	ELISpot Wk12	ELISpot Wk16
Wk0	CC	-0.238	0.643	-0.190	-0.500	0.262	0.619	0.500
	Sig.	0.570	0.086	0.651	0.207	0.531	0.102	0.207
	N	8	8	8	8	8	8	8
Wk2	CC	0.271	0.383	-0.125	-0.391	0.016	0.206	-0.074
	Sig.	0.310	0.143	0.646	0.135	0.952	0.443	0.786
	N	16	16	16	16	16	16	16
Wk4	CC	0.075	0.254	-0.035	-0.146	-0.228	0.022	-0.171
	Sig.	0.782	0.342	0.896	0.590	0.395	0.935	0.527
	N	16	16	16	16	16	16	16
Wk9	CC	0.146	0.129	0.308	-0.116	0.522	0.361	-0.175
	Sig.	0.590	0.634	0.246	0.668	0.038	0.170	0.517
	N	16	16	16	16	16	16	16
Wk12	CC	-0.294	0.393	0.172	-0.259	0.044	0.429	-0.191
	Sig.	0.269	0.132	0.524	0.333	0.871	0.097	0.478
	N	16	16	16	16	16	16	16
Wk16	CC	0.095	0.071	0.048	0.571	-0.476	-0.238	-0.381
	Sig.	0.823	0.867	0.911	0.139	0.233	0.570	0.352
	N	8	8	8	8	8	8	8

I

ELISpot vs MAIT Va7.2+

PBMC MAIT 7.2+		ELISpot Wk0B	ELISpot Wk0A	ELISpot Wk2	ELISpot Wk4	ELISpot Wk9	ELISpot Wk12	ELISpot Wk16
Wk0	CC	-0.143	0.905	-0.476	-0.714	-0.429	-0.310	0.310
	Sig.	0.736	0.002	0.233	0.047	0.289	0.456	0.456
	N	8	8	8	8	8	8	8
Wk2	CC	0.124	-0.200	-0.184	0.196	-0.159	-0.305	0.336
	Sig.	0.648	0.457	0.495	0.468	0.557	0.251	0.204
	N	16	16	16	16	16	16	16
Wk4	CC	0.291	-0.032	0.127	0.400	-0.135	-0.421	0.276
	Sig.	0.274	0.905	0.640	0.125	0.617	0.105	0.300
	N	16	16	16	16	16	16	16
Wk9	CC	0.191	-0.130	-0.084	0.271	-0.188	-0.421	0.382
	Sig.	0.478	0.633	0.757	0.311	0.485	0.105	0.144
	N	16	16	16	16	16	16	16
Wk12	CC	0.000	0.050	0.132	0.379	-0.144	-0.471	0.265
	Sig.	1.000	0.854	0.625	0.147	0.594	0.066	0.322
	N	16	16	16	16	16	16	16
Wk16	CC	0.167	-0.286	-0.214	0.714	-0.405	-0.381	0.310
	Sig.	0.693	0.493	0.610	0.047	0.320	0.352	0.456
	N	8	8	8	8	8	8	8

J

ELISpot vs MAIT CD161+Va7.2+

PBMC MAIT ++		ELISpot Wk0B	ELISpot Wk0A	ELISpot Wk2	ELISpot Wk4	ELISpot Wk9	ELISpot Wk12	ELISpot Wk16
Wk0	CC	0.366	0.561	0.024	-0.220	0.073	-0.317	0.146
	Sig.	0.373	0.148	0.954	0.601	0.863	0.444	0.729
	N	8	8	8	8	8	8	8
Wk2	CC	0.479	-0.156	-0.271	-0.103	-0.203	-0.212	0.126
	Sig.	0.060	0.564	0.310	0.704	0.451	0.431	0.641
	N	16	16	16	16	16	16	16
Wk4	CC	0.165	0.260	0.163	0.329	-0.176	-0.294	0.309
	Sig.	0.542	0.330	0.546	0.213	0.513	0.269	0.244
	N	16	16	16	16	16	16	16
Wk9	CC	0.244	0.146	0.032	0.157	-0.210	-0.237	0.268
	Sig.	0.362	0.590	0.905	0.560	0.434	0.377	0.316
	N	16	16	16	16	16	16	16
Wk12	CC	-0.168	0.155	0.374	0.453	-0.035	-0.338	0.052
	Sig.	0.535	0.567	0.153	0.078	0.897	0.200	0.850
	N	16	16	16	16	16	16	16
Wk16	CC	-0.049	0.317	0.244	0.830	-0.732	-0.415	0.171
	Sig.	0.909	0.444	0.560	0.011	0.039	0.307	0.686
	N	8	8	8	8	8	8	8

K

ELISpot vs MAIT CD161+Va7.2-

PBMC MAIT +		ELISpot Wk0B	ELISpot Wk0A	ELISpot Wk2	ELISpot Wk4	ELISpot Wk9	ELISpot Wk12	ELISpot Wk16
Wk0	CC	-0.357	0.048	-0.095	-0.048	-0.119	-0.071	0.548
	Sig.	0.385	0.911	0.823	0.911	0.779	0.867	0.160
	N	8	8	8	8	8	8	8
Wk2	CC	0.677	-0.172	-0.570	-0.508	0.003	0.074	0.159
	Sig.	0.004	0.523	0.021	0.045	0.991	0.787	0.557
	N	16	16	16	16	16	16	16
Wk4	CC	0.001	0.458	-0.110	-0.021	-0.066	0.143	0.213
	Sig.	0.996	0.074	0.684	0.940	0.807	0.598	0.427
	N	4	16	16	16	16	16	16
Wk9	CC	0.362	0.096	-0.233	-0.196	0.134	0.249	0.436
	Sig.	0.168	0.724	0.384	0.468	0.621	0.353	0.092
	N	16	16	16	16	16	16	16
Wk12	CC	-0.623	0.029	0.423	0.274	0.168	0.041	-0.175
	Sig.	0.010	0.916	0.103	0.305	0.535	0.880	0.517
	N	16	16	16	16	16	16	16
Wk16	CC	0.095	0.786	0.381	0.024	0.190	0.524	0.452
	Sig.	0.823	0.021	0.352	0.955	0.651	0.183	0.260
	N	8	8	8	8	8	8	8

L

ELISpot vs MAIT CD161-Va7.2+

PBMC MAIT - +		ELISpot Wk0B	ELISpot Wk0A	ELISpot Wk2	ELISpot Wk4	ELISpot Wk9	ELISpot Wk12	ELISpot Wk16
Wk0	CC	-0.263	0.455	-0.707	-0.539	-0.599	-0.467	0.252
	Sig.	0.528	0.257	0.050	0.168	0.117	0.243	0.548
	N	8	8	8	8	8	8	8
Wk2	CC	-0.346	-0.119	-0.138	0.116	-0.269	-0.380	0.163
	Sig.	0.189	0.662	0.609	0.668	0.313	0.147	0.546
	N	16	16	16	16	16	16	16
Wk4	CC	0.259	-0.405	-0.007	0.476	-0.159	-0.600	0.303
	Sig.	0.333	0.120	0.978	0.062	0.557	0.014	0.254
	N	16	16	16	16	16	16	16
Wk9	CC	0.163	-0.354	-0.317	0.049	-0.124	-0.414	0.377
	Sig.	0.546	0.178	0.232	0.858	0.648	0.111	0.150
	N	16	16	16	16	16	16	16
Wk12	CC	0.282	-0.305	-0.284	-0.003	-0.029	-0.441	0.326
	Sig.	0.289	0.251	0.286	0.991	0.914	0.087	0.217
	N	16	16	16	16	16	16	16
Wk16	CC	0.263	-0.539	-0.611	0.383	-0.216	-0.527	0.347
	Sig.	0.528	0.168	0.108	0.349	0.608	0.180	0.399
	N	8	8	8	8	8	8	8

M

ELISpot vs NKT 16+

PBMC NKT 16+		ELISpot Wk0B	ELISpot Wk0A	ELISpot Wk2	ELISpot Wk4	ELISpot Wk9	ELISpot Wk12	ELISpot Wk16
Wk0	CC	-0.619	-0.476	-0.310	-0.143	-0.357	0.548	-0.310
	Sig.	0.102	0.233	0.456	0.736	0.385	0.160	0.456
	N	8	8	8	8	8	8	8
Wk2	CC	-0.182	0.113	0.070	0.014	0.196	0.536	-0.207
	Sig.	0.516	0.689	0.805	0.960	0.483	0.040	0.459
	N	15	15	15	15	15	15	15
Wk4	CC	-0.010	0.122	-0.227	-0.305	-0.235	0.486	-0.138
	Sig.	0.970	0.652	0.398	0.251	0.380	0.057	0.609
	N	16	16	16	16	16	16	16
Wk9	CC	0.194	-0.185	-0.293	-0.129	-0.038	0.418	-0.126
	Sig.	0.471	0.492	0.271	0.633	0.888	0.107	0.641
	N	16	16	16	16	16	16	16
Wk12	CC	-0.057	0.010	-0.119	0.000	-0.184	0.288	-0.022
	Sig.	0.833	0.970	0.660	1.000	0.495	0.279	0.935
	N	16	16	16	16	16	16	16
Wk16	CC	0.286	0.714	0.333	0.024	0.190	0.310	0.000
	Sig.	0.493	0.047	0.420	0.955	0.651	0.456	1.000
	N	8	8	8	8	8	8	8

N

ELISpot vs NKT 56+

PBMC NKT 56+		ELISpot Wk0B	ELISpot Wk0A	ELISpot Wk2	ELISpot Wk4	ELISpot Wk9	ELISpot Wk12	ELISpot Wk16
Wk0	CC	-0.357	0.762	-0.071	-0.452	-0.119	0.476	0.714
	Sig.	0.385	0.028	0.867	0.260	0.779	0.233	0.047
	N	8	8	8	8	8	8	8
Wk2	CC	0.129	0.137	-0.099	-0.382	-0.179	0.297	-0.094
	Sig.	0.633	0.613	0.716	0.144	0.506	0.264	0.729
	N	16	16	16	16	16	16	16
Wk4	CC	0.206	0.143	-0.104	-0.341	-0.106	0.041	-0.106
	Sig.	0.444	0.598	0.700	0.196	0.696	0.880	0.696
	N	16	16	16	16	16	16	16
Wk9	CC	-0.119	0.033	0.224	-0.250	0.330	0.386	-0.152
	Sig.	0.660	0.903	0.405	0.350	0.212	0.140	0.575
	N	16	16	16	16	16	16	16
Wk12	CC	-0.188	0.115	0.252	-0.197	0.106	0.285	-0.221
	Sig.	0.485	0.672	0.347	0.464	0.696	0.284	0.412
	N	16	16	16	16	16	16	16
Wk16	CC	0.333	-0.667	-0.238	0.214	0.024	-0.310	-0.667
	Sig.	0.420	0.071	0.570	0.610	0.955	0.456	0.071
	N	8	8	8	8	8	8	8

O

ELISpot vs NKT ++

PBMC NKT ++		ELISpot Wk0B	ELISpot Wk0A	ELISpot Wk2	ELISpot Wk4	ELISpot Wk9	ELISpot Wk12	ELISpot Wk16
Wk0	CC	-0.910	0.132	-0.850	-0.778	-0.635	0.263	-0.120
	Sig.	0.002	0.756	0.007	0.023	0.091	0.528	0.778
	N	8	8	8	8	8	8	8
Wk2	CC	0.082	0.455	0.174	-0.165	0.259	0.562	0.318
	Sig.	0.762	0.077	0.520	0.542	0.333	0.024	0.231
	N	16	16	16	16	16	16	16
Wk4	CC	0.047	0.474	-0.082	-0.356	0.118	0.541	0.132
	Sig.	0.863	0.064	0.762	0.176	0.664	0.030	0.625
	N	16	16	16	16	16	16	16
Wk9	CC	0.157	0.162	0.127	-0.227	0.436	0.391	0.076
	Sig.	0.561	0.550	0.640	0.398	0.091	0.134	0.781
	N	16	16	16	16	16	16	16
Wk12	CC	-0.361	0.194	0.217	-0.090	0.315	0.476	0.085
	Sig.	0.169	0.472	0.420	0.741	0.234	0.062	0.753
	N	16	16	16	16	16	16	16
Wk16	CC	0.738	0.357	0.190	0.071	0.714	0.429	0.262
	Sig.	0.037	0.385	0.651	0.867	0.047	0.289	0.531
	N	8	8	8	8	8	8	8

P

ELISpot vs NK 16+56+

PBMC NK 16+56+		ELISpot Wk0B	ELISpot Wk0A	ELISpot Wk2	ELISpot Wk4	ELISpot Wk9	ELISpot Wk12	ELISpot Wk16
Wk0	CC	-0.263	0.455	-0.707	-0.539	-0.599	-0.467	0.252
	Sig.	0.528	0.257	0.050	0.168	0.117	0.243	0.548
	N	8	8	8	8	8	8	8
Wk2	CC	0.163	-0.354	-0.317	0.049	-0.124	-0.414	0.377
	Sig.	0.546	0.178	0.232	0.858	0.648	0.111	0.150
	N	16	16	16	16	16	16	16
Wk4	CC	0.282	-0.305	-0.284	-0.003	-0.029	-0.441	0.326
	Sig.	0.289	0.251	0.286	0.991	0.914	0.087	0.217
	N	16	16	16	16	16	16	16
Wk9	CC	0.263	-0.539	-0.611	0.383	-0.216	-0.527	0.347
	Sig.	0.528	0.168	0.108	0.349	0.608	0.180	0.399
	N	8	8	8	8	8	8	8
Wk12	CC	-0.619	-0.476	-0.310	-0.143	-0.357	0.548	-0.310
	Sig.	0.102	0.233	0.456	0.736	0.385	0.160	0.456
	N	8	8	8	8	8	8	8
Wk16	CC	-0.182	0.113	0.070	0.014	0.196	0.536	-0.207
	Sig.	0.516	0.689	0.805	0.960	0.483	0.040	0.459
	N	15	15	15	15	15	15	15

Q

ELISpot vs NK 16+56-

PBMC NK 16+56-		ELISpot Wk0B	ELISpot Wk0A	ELISpot Wk2	ELISpot Wk4	ELISpot Wk9	ELISpot Wk12	ELISpot Wk16
Wk0	CC	-0.619	-0.476	-0.310	-0.143	-0.357	0.548	-0.310
	Sig.	0.102	0.233	0.456	0.736	0.385	0.160	0.456
	N	8	8	8	8	8	8	8
Wk2	CC	0.194	-0.185	-0.293	-0.129	-0.038	0.418	-0.126
	Sig.	0.471	0.492	0.271	0.633	0.888	0.107	0.641
	N	16	16	16	16	16	16	16
Wk4	CC	-0.057	0.010	-0.119	0.000	-0.184	0.288	-0.022
	Sig.	0.833	0.970	0.660	1.000	0.495	0.279	0.935
	N	16	16	16	16	16	16	16
Wk9	CC	0.286	0.714	0.333	0.024	0.190	0.310	0.000
	Sig.	0.493	0.047	0.420	0.955	0.651	0.456	1.000
	N	8	8	8	8	8	8	8
Wk12	CC	-0.357	0.762	-0.071	-0.452	-0.119	0.476	0.714
	Sig.	0.385	0.028	0.867	0.260	0.779	0.233	0.047
	N	8	8	8	8	8	8	8
Wk16	CC	0.129	0.137	-0.099	-0.382	-0.179	0.297	-0.094
	Sig.	0.633	0.613	0.716	0.144	0.506	0.264	0.729
	N	16	16	16	16	16	16	16

R

ELISpot vs NK 16-56+

PBMC NK -+		ELISpot Wk0B	ELISpot Wk0A	ELISpot Wk2	ELISpot Wk4	ELISpot Wk9	ELISpot Wk12	ELISpot Wk16
Wk0	CC	0.405	-0.095	0.262	0.238	-0.190	-0.333	-0.476
	Sig.	0.320	0.823	0.531	0.570	0.651	0.420	0.233
	N	8	8	8	8	8	8	8
Wk2	CC	-0.324	-0.102	0.228	0.182	-0.118	-0.009	-0.150
	Sig.	0.222	0.708	0.395	0.499	0.664	0.974	0.579
	N	16	16	16	16	16	16	16
Wk4	CC	-0.050	-0.194	0.098	0.082	-0.231	-0.218	-0.218
	Sig.	0.854	0.471	0.718	0.762	0.389	0.418	0.418
	N	16	16	16	16	16	16	16
Wk9	CC	0.102	-0.559	-0.122	0.155	-0.187	-0.527	-0.166
	Sig.	0.708	0.024	0.652	0.568	0.488	0.036	0.538
	N	16	16	16	16	16	16	16
Wk12	CC	0.208	-0.292	0.019	0.528	-0.155	-0.575	0.311
	Sig.	0.441	0.273	0.944	0.035	0.568	0.020	0.242
	N	16	16	16	16	16	16	16
Wk16	CC	-0.419	-0.695	-0.024	-0.299	0.072	-0.144	-0.826
	Sig.	0.301	0.056	0.955	0.471	0.866	0.734	0.011
	N	8	8	8	8	8	8	8

S

ELISpot vs nonL 14+

PBMC nonL 14+		ELISpot Wk0B	ELISpot Wk0A	ELISpot Wk2	ELISpot Wk4	ELISpot Wk9	ELISpot Wk12	ELISpot Wk16
Wk0	CC	-0.190	-0.333	-0.333	-0.071	0.262	-0.048	-0.286
	Sig.	0.651	0.420	0.420	0.867	0.531	0.911	0.493
	N	8	8	8	8	8	8	8
Wk2	CC	-0.515	0.187	-0.112	-0.271	-0.382	-0.094	-0.056
	Sig.	0.041	0.488	0.680	0.311	0.144	0.729	0.837
	N	16	16	16	16	16	16	16
Wk4	CC	-0.024	0.472	0.135	-0.171	-0.176	0.041	-0.197
	Sig.	0.931	0.065	0.617	0.528	0.513	0.880	0.464
	N	16	16	16	16	16	16	16
Wk9	CC	0.088	-0.110	-0.266	-0.279	-0.221	-0.068	-0.329
	Sig.	0.745	0.684	0.319	0.295	0.412	0.803	0.213
	N	16	16	16	16	16	16	16
Wk12	CC	-0.300	-0.364	0.037	-0.006	-0.009	0.121	-0.465
	Sig.	0.259	0.166	0.892	0.983	0.974	0.656	0.070
	N	16	16	16	16	16	16	16
Wk16	CC	-0.095	0.333	-0.262	-0.571	0.286	0.381	0.405
	Sig.	0.823	0.420	0.531	0.139	0.493	0.352	0.320
	N	8	8	8	8	8	8	8

T

ELISpot vs nonL 16+

PBMC nonL 16+		ELISpot Wk0B	ELISpot Wk0A	ELISpot Wk2	ELISpot Wk4	ELISpot Wk9	ELISpot Wk12	ELISpot Wk16
Wk0	CC	0.024	-0.524	0.262	0.381	0.143	-0.095	-0.476
	Sig.	0.955	0.183	0.531	0.352	0.736	0.823	0.233
	N	8	8	8	8	8	8	8
Wk2	CC	-0.409	-0.127	0.081	0.259	-0.256	-0.129	-0.285
	Sig.	0.116	0.640	0.766	0.333	0.339	0.633	0.284
	N	16	16	16	16	16	16	16
Wk4	CC	-0.368	0.434	0.162	-0.029	-0.259	0.106	-0.324
	Sig.	0.161	0.093	0.549	0.914	0.333	0.696	0.222
	N	16	16	16	16	16	16	16
Wk9	CC	-0.032	-0.250	-0.231	-0.138	-0.041	-0.103	-0.450
	Sig.	0.905	0.350	0.389	0.610	0.880	0.704	0.080
	N	16	16	16	16	16	16	16
Wk12	CC	-0.565	-0.181	0.278	0.324	-0.021	-0.050	-0.406
	Sig.	0.023	0.502	0.297	0.222	0.940	0.854	0.119
	N	16	16	16	16	16	16	16
Wk16	CC	0.000	-0.156	-0.407	-0.096	0.036	0.443	0.491
	Sig.	1.000	0.713	0.317	0.821	0.933	0.272	0.217
	N	8	8	8	8	8	8	8

U

ELISpot vs nonL ++

PBMC nonL ++		ELISpot Wk0B	ELISpot Wk0A	ELISpot Wk2	ELISpot Wk4	ELISpot Wk9	ELISpot Wk12	ELISpot Wk16
Wk0	CC	-0.383	-0.455	-0.407	-0.072	-0.084	-0.072	-0.347
	Sig.	0.349	0.257	0.317	0.866	0.844	0.866	0.399
	N	8	8	8	8	8	8	8
Wk2	CC	-0.591	0.024	0.082	0.009	-0.244	-0.309	-0.612
	Sig.	0.016	0.931	0.762	0.974	0.362	0.244	0.012
	N	16	16	16	16	16	16	16
Wk4	CC	-0.344	0.447	0.187	-0.056	-0.200	0.088	-0.382
	Sig.	0.192	0.082	0.488	0.837	0.458	0.745	0.144
	N	16	16	16	16	16	16	16
Wk9	CC	-0.191	-0.085	-0.135	-0.206	-0.147	-0.115	-0.476
	Sig.	0.478	0.753	0.617	0.444	0.587	0.672	0.062
	N	16	16	16	16	16	16	16
Wk12	CC	-0.529	-0.184	0.328	0.362	-0.053	-0.065	-0.456
	Sig.	0.035	0.495	0.215	0.169	0.846	0.812	0.076
	N	16	16	16	16	16	16	16
Wk16	CC	-0.024	-0.310	-0.571	-0.048	-0.143	0.238	0.429
	Sig.	0.955	0.456	0.139	0.911	0.736	0.570	0.289
	N	8	8	8	8	8	8	8

V

ELISpot vs nonL 14+16-

PBMC nonL +-		ELISpot Wk0B	ELISpot Wk0A	ELISpot Wk2	ELISpot Wk4	ELISpot Wk9	ELISpot Wk12	ELISpot Wk16
Wk0	CC	-0.190	-0.333	-0.333	-0.071	0.262	-0.048	-0.286
	Sig.	0.651	0.420	0.420	0.867	0.531	0.911	0.493
	N	8	8	8	8	8	8	8
Wk2	CC	-0.492	0.247	-0.109	-0.225	-0.443	-0.131	0.022
	Sig.	0.053	0.356	0.688	0.402	0.086	0.629	0.935
	N	16	16	16	16	16	16	16
Wk4	CC	0.115	0.377	0.031	-0.265	-0.141	0.018	-0.097
	Sig.	0.672	0.150	0.910	0.322	0.602	0.948	0.721
	N	16	16	16	16	16	16	16
Wk9	CC	0.121	-0.025	-0.268	-0.294	-0.282	-0.009	-0.224
	Sig.	0.656	0.927	0.316	0.269	0.289	0.974	0.405
	N	16	16	16	16	16	16	16
Wk12	CC	-0.279	-0.333	-0.041	-0.147	0.012	0.188	-0.406
	Sig.	0.295	0.208	0.880	0.587	0.966	0.485	0.119
	N	16	16	16	16	16	16	16
Wk16	CC	-0.190	0.500	-0.071	-0.595	0.238	0.333	0.429
	Sig.	0.651	0.207	0.867	0.120	0.570	0.420	0.289
	N	8	8	8	8	8	8	8

W

ELISpot vs nonL 14-16+

PBMC nonL 14-16+		ELISpot Wk0B	ELISpot Wk0A	ELISpot Wk2	ELISpot Wk4	ELISpot Wk9	ELISpot Wk12	ELISpot Wk16
Wk0	CC	0.120	0.012	0.228	0.156	-0.539	-0.216	-0.120
	Sig.	0.778	0.978	0.588	0.713	0.168	0.608	0.778
	N	8	8	8	8	8	8	8
Wk2	CC	-0.288	0.054	0.288	0.397	0.103	0.276	-0.035
	Sig.	0.279	0.841	0.279	0.128	0.704	0.300	0.897
	N	16	16	16	16	16	16	16
Wk4	CC	-0.018	-0.094	-0.230	0.078	-0.193	0.278	0.032
	Sig.	0.948	0.730	0.392	0.774	0.474	0.297	0.905
	N	16	16	16	16	16	16	16
Wk9	CC	0.297	-0.109	-0.084	0.200	0.500	0.159	0.141
	Sig.	0.264	0.688	0.757	0.458	0.049	0.557	0.602
	N	16	16	16	16	16	16	16
Wk12	CC	-0.303	-0.311	0.205	0.085	0.432	0.426	-0.224
	Sig.	0.254	0.242	0.447	0.753	0.094	0.099	0.405
	N	16	16	16	16	16	16	16
Wk16	CC	-0.071	0.048	0.500	0.048	0.310	0.571	0.167
	Sig.	0.867	0.911	0.207	0.911	0.456	0.139	0.693
	N	8	8	8	8	8	8	8

Supplementary Table 5 Correlations between IFNγ SFU+ and PBMC cell populations

*Spearman's rank correlations were calculated between the frequency of cell populations characterised among PBMCs, and PPD-specific IFNγ+ SFU (ELISpot). Correlation co-efficient ('CC'), significance ('Sig.') and number of values included in each comparison ('N') are shown at each combination of time points. PB1B is shown as the first column (blue text), as this time point was only analysed by ELISpot. PB1 for flow cytometry data (row title) is the same time point as PB1A for ELISpot (column title). Results are shown for CD3+ lymphocytes (**A**, grey), $\gamma\delta$ T cells (**B**, blue), conventional T markers CD4+/CD8+ (**C-G**, pink), CD56+CD4+ T cells (**H**, pink), MAIT cell markers (**I-L**, purple), CD16/56 combinations of CD3+ (NKT-L) cells (**M-O**, yellow), CD16/56 combinations of CD3-CD8+ (NK) cells (**P-R**, green), CD14+/CD16+ combinations of HLA-DR+ non-lymphocyte cells (**S-W**, red).*

A **ELISpot vs BAL CD3**

BAL CD3		ELISpot Wk0B	ELISpot Wk0A	ELISpot Wk2	ELISpot Wk4	ELISpot Wk9	ELISpot Wk12	ELISpot Wk16
Wk0	CC	0.568	0.186	-0.503	-0.290	-0.077	-0.018	0.366
	Sig.	0.027	0.507	0.056	0.295	0.785	0.950	0.179
	N	15	15	15	15	15	15	15
Wk2	CC	-0.594	0.450	0.203	0.279	-0.315	0.171	0.226
	Sig.	0.015	0.080	0.451	0.295	0.235	0.528	0.399
	N	16	16	16	16	16	16	16
Wk4	CC	-0.100	0.442	-0.134	0.050	-0.509	0.246	0.280
	Sig.	0.712	0.087	0.621	0.854	0.044	0.359	0.294
	N	16	16	16	16	16	16	16
Wk9	CC	-0.253	0.315	0.069	0.241	-0.406	-0.047	0.285
	Sig.	0.345	0.235	0.799	0.368	0.119	0.863	0.284
	N	16	16	16	16	16	16	16
Wk12	CC	-0.026	0.057	0.492	0.518	-0.071	-0.141	0.115
	Sig.	0.922	0.833	0.053	0.040	0.795	0.602	0.672
	N	16	16	16	16	16	16	16
Wk16	CC	-0.011	0.086	-0.029	-0.011	0.037	0.051	0.305
	Sig.	0.970	0.771	0.923	0.970	0.899	0.864	0.288
	N	14	14	14	14	14	14	14

B **ELISpot vs BAL gd**

BAL gd		ELISpot Wk0B	ELISpot Wk0A	ELISpot Wk2	ELISpot Wk4	ELISpot Wk9	ELISpot Wk12	ELISpot Wk16
Wk0	CC	0.179	0.266	0.424	-0.057	0.368	0.182	0.057
	Sig.	0.524	0.337	0.116	0.840	0.177	0.516	0.840
	N	15	15	15	15	15	15	15
Wk2	CC	-0.224	0.057	0.299	-0.009	0.229	0.044	-0.041
	Sig.	0.405	0.833	0.261	0.974	0.393	0.871	0.880
	N	16	16	16	16	16	16	16
Wk4	CC	-0.241	0.094	0.636	0.244	0.185	0.021	-0.135
	Sig.	0.368	0.729	0.008	0.362	0.492	0.940	0.617
	N	16	16	16	16	16	16	16
Wk9	CC	-0.159	0.000	0.558	0.356	0.212	-0.082	0.041
	Sig.	0.557	1.000	0.025	0.176	0.431	0.762	0.880
	N	16	16	16	16	16	16	16
Wk12	CC	-0.376	0.032	0.518	0.288	0.238	0.003	-0.009
	Sig.	0.151	0.905	0.040	0.279	0.374	0.991	0.974
	N	16	16	16	16	16	16	16
Wk16	CC	-0.363	0.187	0.393	0.064	0.174	0.138	-0.090
	Sig.	0.203	0.523	0.164	0.829	0.553	0.637	0.759
	N	14	14	14	14	14	14	14

C **ELISpot vs BAL CD8**

BAL CD8		ELISpot Wk0B	ELISpot Wk0A	ELISpot Wk2	ELISpot Wk4	ELISpot Wk9	ELISpot Wk12	ELISpot Wk16
Wk0	CC	0.504	-0.261	-0.395	-0.546	0.296	0.179	-0.046
	Sig.	0.056	0.348	0.145	0.035	0.283	0.524	0.869
	N	15	15	15	15	15	15	15
Wk2	CC	0.121	0.085	-0.113	-0.388	0.132	0.297	-0.179
	Sig.	0.656	0.753	0.676	0.137	0.625	0.264	0.506
	N	16	16	16	16	16	16	16
Wk4	CC	0.475	-0.094	-0.447	-0.664	0.110	0.137	-0.112
	Sig.	0.063	0.730	0.083	0.005	0.684	0.613	0.680
	N	16	16	16	16	16	16	16
Wk9	CC	0.358	-0.053	-0.455	-0.680	0.109	0.052	0.079
	Sig.	0.174	0.845	0.077	0.004	0.688	0.850	0.770
	N	16	16	16	16	16	16	16
Wk12	CC	0.100	-0.081	-0.244	-0.416	0.090	-0.175	0.052
	Sig.	0.712	0.766	0.361	0.109	0.741	0.517	0.850
	N	16	16	16	16	16	16	16
Wk16	CC	-0.095	-0.160	0.108	0.055	0.020	-0.530	-0.341
	Sig.	0.748	0.584	0.714	0.852	0.946	0.051	0.233
	N	14	14	14	14	14	14	14

D **ELISpot vs BAL CD4**

PBMC CD4		ELISpot Wk0B	ELISpot Wk0A	ELISpot Wk2	ELISpot Wk4	ELISpot Wk9	ELISpot Wk12	ELISpot Wk16
Wk0	CC	-0.532	0.029	-0.113	0.214	-0.379	-0.171	-0.018
	Sig.	0.041	0.919	0.689	0.443	0.164	0.541	0.950
	N	15	15	15	15	15	15	15
Wk2	CC	0.118	-0.368	-0.194	0.218	-0.126	-0.379	0.135
	Sig.	0.664	0.161	0.471	0.418	0.641	0.147	0.617
	N	16	16	16	16	16	16	16
Wk4	CC	-0.344	-0.157	0.182	0.397	0.012	-0.171	0.076
	Sig.	0.192	0.560	0.499	0.128	0.966	0.528	0.778
	N	16	16	16	16	16	16	16
Wk9	CC	-0.333	-0.149	0.190	0.480	-0.049	-0.066	-0.077
	Sig.	0.208	0.582	0.481	0.060	0.858	0.807	0.778
	N	16	16	16	16	16	16	16
Wk12	CC	-0.206	-0.174	-0.162	0.218	-0.288	0.035	-0.094
	Sig.	0.444	0.520	0.549	0.418	0.279	0.897	0.729
	N	16	16	16	16	16	16	16
Wk16	CC	0.059	0.086	-0.358	-0.165	-0.218	0.332	0.437
	Sig.	0.840	0.771	0.208	0.573	0.455	0.246	0.118
	N	14	14	14	14	14	14	14

E **ELISpot vs BAL CD4+8+**

BAL CD4+8+		ELISpot Wk0B	ELISpot Wk0A	ELISpot Wk2	ELISpot Wk4	ELISpot Wk9	ELISpot Wk12	ELISpot Wk16
Wk0	CC	-0.275	0.198	0.416	0.400	0.014	0.221	-0.011
	Sig.	0.321	0.478	0.123	0.140	0.960	0.428	0.970
	N	15	15	15	15	15	15	15
Wk2	CC	-0.450	0.266	0.437	0.391	-0.053	0.124	0.074
	Sig.	0.080	0.319	0.090	0.134	0.846	0.649	0.787
	N	16	16	16	16	16	16	16
Wk4	CC	-0.332	0.175	0.352	0.376	0.009	0.244	0.115
	Sig.	0.208	0.517	0.182	0.151	0.974	0.362	0.672
	N	16	16	16	16	16	16	16
Wk9	CC	0.006	0.075	0.427	0.582	0.074	-0.047	0.053
	Sig.	0.983	0.782	0.099	0.018	0.787	0.863	0.846
	N	16	16	16	16	16	16	16
Wk12	CC	0.057	0.027	0.285	0.397	0.057	0.074	0.024
	Sig.	0.833	0.922	0.285	0.128	0.833	0.787	0.931
	N	16	16	16	16	16	16	16
Wk16	CC	-0.174	0.077	0.446	0.490	0.068	0.024	-0.024
	Sig.	0.553	0.794	0.110	0.075	0.817	0.935	0.935
	N	14	14	14	14	14	14	14

F **ELISpot vs BAL CD4+8++**

BAL CD4+8++		ELISpot Wk0B	ELISpot Wk0A	ELISpot Wk2	ELISpot Wk4	ELISpot Wk9	ELISpot Wk12	ELISpot Wk16
Wk0	CC	0.563	0.211	0.072	0.046	-0.120	0.007	0.245
	Sig.	0.029	0.450	0.800	0.869	0.671	0.980	0.379
	N	15	15	15	15	15	15	15
Wk2	CC	0.415	0.141	-0.228	-0.209	-0.115	0.174	-0.053
	Sig.	0.110	0.602	0.395	0.438	0.672	0.520	0.846
	N	16	16	16	16	16	16	16
Wk4	CC	0.471	0.118	0.021	0.000	-0.009	-0.162	-0.056
	Sig.	0.066	0.664	0.940	1.000	0.974	0.549	0.837
	N	16	16	16	16	16	16	16
Wk9	CC	0.350	0.319	-0.041	-0.194	-0.162	0.009	0.182
	Sig.	0.184	0.228	0.880	0.471	0.549	0.974	0.499
	N	16	16	16	16	16	16	16
Wk12	CC	0.432	0.044	-0.043	-0.076	-0.112	-0.103	0.150
	Sig.	0.094	0.871	0.875	0.778	0.680	0.704	0.579
	N	16	16	16	16	16	16	16
Wk16	CC	0.516	-0.112	-0.029	0.156	-0.033	-0.327	0.226
	Sig.	0.059	0.703	0.923	0.594	0.911	0.253	0.436
	N	14	14	14	14	14	14	14

G **ELISpot vs BAL CD4-8-**

BAL CD4-8-		ELISpot Wk0B	ELISpot Wk0A	ELISpot Wk2	ELISpot Wk4	ELISpot Wk9	ELISpot Wk12	ELISpot Wk16
Wk0	CC	0.502	0.261	0.083	0.063	0.098	-0.181	0.239
	Sig.	0.056	0.347	0.768	0.825	0.727	0.520	0.390
	N	15	15	15	15	15	15	15
Wk2	CC	0.221	0.353	0.347	0.185	0.138	-0.115	0.144
	Sig.	0.412	0.180	0.187	0.492	0.610	0.672	0.594
	N	16	16	16	16	16	16	16
Wk4	CC	-0.147	0.268	0.446	0.388	0.038	-0.206	0.024
	Sig.	0.587	0.316	0.083	0.137	0.888	0.444	0.931
	N	16	16	16	16	16	16	16
Wk9	CC	0.032	0.146	0.411	0.447	0.062	-0.271	0.003
	Sig.	0.905	0.590	0.114	0.083	0.820	0.311	0.991
	N	16	16	16	16	16	16	16
Wk12	CC	-0.079	0.311	0.384	0.518	0.038	-0.200	0.241
	Sig.	0.770	0.242	0.142	0.040	0.888	0.458	0.368
	N	16	16	16	16	16	16	16
Wk16	CC	-0.134	0.569	0.187	0.116	-0.007	0.253	-0.024
	Sig.	0.648	0.034	0.523	0.692	0.982	0.383	0.935
	N	14	14	14	14	14	14	14

H **ELISpot vs BAL CD4+56+**

BAL CD4+56+		ELISpot Wk0B	ELISpot Wk0A	ELISpot Wk2	ELISpot Wk4	ELISpot Wk9	ELISpot Wk12	ELISpot Wk16
Wk0	CC	0.295	-0.032	-0.018	-0.100	-0.034	0.243	0.223
	Sig.	0.286	0.909	0.950	0.723	0.904	0.383	0.423
	N	15	15	15	15	15	15	15
Wk2	CC	0.229	-0.174	-0.222	-0.291	0.006	0.197	-0.056
	Sig.	0.393	0.520	0.408	0.274	0.983	0.464	0.837
	N	16	16	16	16	16	16	16
Wk4	CC	0.138	-0.271	-0.138	-0.356	0.074	0.256	-0.165
	Sig.	0.610	0.310	0.609	0.176	0.787	0.339	0.542
	N	16	16	16	16	16	16	16
Wk9	CC	-0.091	-0.088	0.199	0.115	-0.082	0.203	-0.232
	Sig.	0.737	0.745	0.461	0.672	0.762	0.451	0.387
	N	16	16	16	16	16	16	16
Wk12	CC	0.068	-0.153	-0.169	-0.246	-0.141	0.037	-0.165
	Sig.	0.803	0.571	0.531	0.359	0.602	0.892	0.542
	N	16	16	16	16	16	16	16
Wk16	CC	0.112	-0.033	-0.235	-0.152	-0.459	-0.235	-0.121
	Sig.	0.703	0.911	0.418	0.605	0.098	0.418	0.681
	N	14	14	14	14	14	14	14

I **ELISpot vs BAL Va7.2+**

BAL MAIT 7.2+		ELISpot Wk0B	ELISpot Wk0A	ELISpot Wk2	ELISpot Wk4	ELISpot Wk9	ELISpot Wk12	ELISpot Wk16
Wk0	CC	-0.064	-0.114	0.129	0.282	-0.539	-0.382	0.157
	Sig.	0.820	0.685	0.648	0.308	0.038	0.160	0.576
	N	15	15	15	15	15	15	15
Wk2	CC	0.260	-0.054	-0.060	0.199	-0.374	-0.125	0.121
	Sig.	0.330	0.843	0.824	0.461	0.154	0.644	0.656
	N	16	16	16	16	16	16	16
Wk4	CC	-0.053	-0.015	0.372	0.585	-0.326	-0.538	0.021
	Sig.	0.846	0.957	0.156	0.017	0.217	0.031	0.940
	N	16	16	16	16	16	16	16
Wk9	CC	0.044	-0.155	0.190	0.426	-0.447	-0.429	-0.059
	Sig.	0.871	0.568	0.481	0.099	0.083	0.097	0.829
	N	16	16	16	16	16	16	16
Wk12	CC	-0.079	-0.001	0.294	0.497	-0.482	-0.450	0.012
	Sig.	0.770	0.996	0.268	0.050	0.058	0.080	0.966
	N	16	16	16	16	16	16	16
Wk16	CC	0.178	-0.134	0.033	0.284	-0.516	-0.336	-0.064
	Sig.	0.543	0.648	0.911	0.326	0.059	0.240	0.829
	N	14	14	14	14	14	14	14

J **ELISpot vs BAL MAIT CD161+Va7.2+**

BAL MAIT ++		ELISpot Wk0B	ELISpot Wk0A	ELISpot Wk2	ELISpot Wk4	ELISpot Wk9	ELISpot Wk12	ELISpot Wk16
Wk0	CC	0.065	-0.028	0.069	0.101	-0.361	-0.095	0.009
	Sig.	0.819	0.922	0.806	0.721	0.186	0.736	0.975
	N	15	15	15	15	15	15	15
Wk2	CC	0.359	-0.066	-0.206	0.026	-0.300	-0.053	0.059
	Sig.	0.172	0.807	0.444	0.922	0.259	0.846	0.829
	N	16	16	16	16	16	16	16
Wk4	CC	-0.193	0.212	0.382	0.608	-0.238	-0.296	0.116
	Sig.	0.474	0.430	0.144	0.013	0.374	0.266	0.668
	N	16	16	16	16	16	16	16
Wk9	CC	0.110	-0.113	0.029	0.222	-0.369	-0.224	-0.137
	Sig.	0.684	0.676	0.914	0.408	0.159	0.405	0.613
	N	16	16	16	16	16	16	16
Wk12	CC	-0.553	0.380	0.347	0.194	-0.388	0.024	-0.124
	Sig.	0.026	0.147	0.187	0.471	0.137	0.931	0.649
	N	16	16	16	16	16	16	16
Wk16	CC	0.231	-0.024	0.103	0.323	-0.437	-0.402	-0.086
	Sig.	0.427	0.935	0.725	0.260	0.118	0.154	0.771
	N	14	14	14	14	14	14	14

K **ELISpot vs BAL MAIT CD161+Va7.2-**

BAL MAIT +		ELISpot Wk0B	ELISpot Wk0A	ELISpot Wk2	ELISpot Wk4	ELISpot Wk9	ELISpot Wk12	ELISpot Wk16
Wk0	CC	-0.039	0.000	0.200	-0.168	0.318	0.521	-0.250
	Sig.	0.889	0.292	0.474	0.550	0.248	0.046	0.369
	N	15	15	15	15	15	15	15
Wk2	CC	0.624	0.024	-0.355	-0.482	0.159	0.294	-0.041
	Sig.	0.010	0.931	0.178	0.058	0.557	0.269	0.880
	N	16	16	16	16	16	16	16
Wk4	CC	-0.409	0.393	0.280	-0.024	0.224	0.244	-0.509
	Sig.	0.116	0.132	0.294	0.931	0.405	0.362	0.044
	N	16	16	16	16	16	16	16
Wk9	CC	0.382	0.141	-0.110	-0.188	0.076	0.141	-0.168
	Sig.	0.144	0.602	0.684	0.485	0.778	0.602	0.535
	N	16	16	16	16	16	16	16
Wk12	CC	-0.529	0.308	0.358	0.038	0.132	0.309	-0.491
	Sig.	0.035	0.247	0.174	0.888	0.625	0.244	0.053
	N	16	16	16	16	16	16	16
Wk16	CC	0.125	-0.112	-0.112	0.024	-0.108	0.024	-0.393
	Sig.	0.670	0.703	0.703	0.935	0.714	0.935	0.164
	N	14	14	14	14	14	14	14

L **ELISpot vs BAL MAIT CD161-Va7.2+**

BAL MAIT - +		ELISpot Wk0B	ELISpot Wk0A	ELISpot Wk2	ELISpot Wk4	ELISpot Wk9	ELISpot Wk12	ELISpot Wk16
Wk0	CC	-0.050	-0.200	0.063	0.275	-0.543	-0.486	0.125
	Sig.	0.860	0.474	0.825	0.321	0.037	0.066	0.657
	N	15	15	15	15	15	15	15
Wk2	CC	0.043	-0.116	0.006	0.263	-0.442	-0.296	0.088
	Sig.	0.875	0.670	0.983	0.324	0.087	0.266	0.745
	N	16	16	16	16	16	16	16
Wk4	CC	0.163	-0.185	0.192	0.403	-0.271	-0.517	0.078
	Sig.	0.546	0.493	0.476	0.121	0.310	0.040	0.774
	N	16	16	16	16	16	16	16
Wk9	CC	0.024	-0.132	0.171	0.435	-0.441	-0.453	0.091
	Sig.	0.931	0.625	0.527	0.092	0.087	0.078	0.737
	N	16	16	16	16	16	16	16
Wk12	CC	0.180	0.028	0.088	0.368	-0.431	-0.406	0.294
	Sig.	0.506	0.918	0.747	0.161	0.095	0.118	0.268
	N	16	16	16	16	16	16	16
Wk16	CC	0.112	-0.147	-0.068	0.213	-0.569	-0.363	0.011
	Sig.	0.703	0.615	0.817	0.464	0.034	0.203	0.970
	N	14	14	14	14	14	14	14

M ELISpot vs BAL NKT 16+

BAL NKT 16+		ELISpot Wk0B	ELISpot Wk0A	ELISpot Wk2	ELISpot Wk4	ELISpot Wk9	ELISpot Wk12	ELISpot Wk16
Wk0	CC	-0.098	-0.189	0.336	0.057	0.034	0.238	0.052
	Sig.	0.727	0.501	0.220	0.840	0.904	0.394	0.854
	N	15	15	15	15	15	15	15
Wk2	CC	0.087	-0.539	-0.009	0.068	0.021	0.143	0.238
	Sig.	0.749	0.031	0.974	0.803	0.940	0.598	0.374
	N	16	16	16	16	16	16	16
Wk4	CC	-0.147	-0.434	0.059	0.056	0.024	0.435	-0.059
	Sig.	0.587	0.093	0.829	0.837	0.931	0.092	0.829
	N	16	16	16	16	16	16	16
Wk9	CC	-0.400	-0.313	0.249	0.162	-0.041	0.344	-0.026
	Sig.	0.125	0.237	0.353	0.549	0.880	0.192	0.922
	N	16	16	16	16	16	16	16
Wk12	CC	-0.150	-0.571	0.216	0.199	-0.013	0.037	-0.050
	Sig.	0.579	0.021	0.421	0.461	0.961	0.892	0.854
	N	16	16	16	16	16	16	16
Wk16	CC	0.302	-0.214	-0.172	-0.152	0.104	0.291	0.150
	Sig.	0.294	0.463	0.557	0.604	0.725	0.313	0.609
	N	14	14	14	14	14	14	14

N ELISpot vs BAL NKT 56+

BAL NKT 56+		ELISpot Wk0B	ELISpot Wk0A	ELISpot Wk2	ELISpot Wk4	ELISpot Wk9	ELISpot Wk12	ELISpot Wk16
Wk0	CC	-0.189	0.045	0.181	-0.371	0.004	0.004	-0.054
	Sig.	0.499	0.874	0.520	0.173	0.990	0.990	0.850
	N	15	15	15	15	15	15	15
Wk2	CC	-0.468	0.190	0.291	-0.085	-0.259	0.141	-0.132
	Sig.	0.068	0.481	0.274	0.753	0.333	0.602	0.625
	N	16	16	16	16	16	16	16
Wk4	CC	-0.512	0.169	0.369	-0.026	-0.265	0.068	-0.165
	Sig.	0.043	0.531	0.159	0.922	0.322	0.803	0.542
	N	16	16	16	16	16	16	16
Wk9	CC	-0.318	-0.135	0.271	0.103	-0.283	-0.047	-0.180
	Sig.	0.230	0.619	0.310	0.704	0.289	0.862	0.506
	N	16	16	16	16	16	16	16
Wk12	CC	-0.541	0.010	0.430	0.171	-0.047	0.188	-0.065
	Sig.	0.030	0.970	0.097	0.528	0.863	0.485	0.812
	N	16	16	16	16	16	16	16
Wk16	CC	-0.562	0.055	0.324	-0.035	-0.289	-0.051	-0.233
	Sig.	0.037	0.852	0.259	0.905	0.317	0.863	0.422
	N	14	14	14	14	14	14	14

O ELISpot vs BAL NKT ++

BAL NKT ++		ELISpot Wk0B	ELISpot Wk0A	ELISpot Wk2	ELISpot Wk4	ELISpot Wk9	ELISpot Wk12	ELISpot Wk16
Wk0	CC	-0.359	-0.055	0.308	-0.032	-0.173	0.080	-0.105
	Sig.	0.188	0.847	0.265	0.909	0.537	0.776	0.708
	N	15	15	15	15	15	15	15
Wk2	CC	-0.404	-0.249	0.083	-0.009	-0.124	0.127	0.044
	Sig.	0.121	0.351	0.761	0.974	0.648	0.640	0.871
	N	16	16	16	16	16	16	16
Wk4	CC	-0.333	-0.072	0.313	0.029	-0.074	0.230	-0.071
	Sig.	0.207	0.790	0.238	0.914	0.786	0.391	0.794
	N	16	16	16	16	16	16	16
Wk9	CC	-0.520	-0.199	0.260	0.103	-0.185	0.227	-0.128
	Sig.	0.039	0.459	0.331	0.703	0.494	0.397	0.636
	N	16	16	16	16	16	16	16
Wk12	CC	-0.265	-0.406	0.244	0.189	-0.021	0.035	-0.012
	Sig.	0.320	0.119	0.363	0.484	0.939	0.896	0.965
	N	16	16	16	16	16	16	16
Wk16	CC	0.363	-0.145	-0.205	-0.211	0.152	0.273	0.335
	Sig.	0.201	0.620	0.482	0.468	0.604	0.345	0.242
	N	14	14	14	14	14	14	14

P ELISpot vs BAL NK 16+56+

BAL NK 16+56+		ELISpot Wk0B	ELISpot Wk0A	ELISpot Wk2	ELISpot Wk4	ELISpot Wk9	ELISpot Wk12	ELISpot Wk16
Wk0	CC	-0.050	-0.200	0.063	0.275	-0.543	-0.486	0.125
	Sig.	0.860	0.474	0.825	0.321	0.037	0.066	0.657
	N	15	15	15	15	15	15	15
Wk2	CC	0.024	-0.132	0.171	0.435	-0.441	-0.453	0.091
	Sig.	0.931	0.625	0.527	0.092	0.087	0.078	0.737
	N	16	16	16	16	16	16	16
Wk4	CC	0.180	0.028	0.088	0.368	-0.431	-0.406	0.294
	Sig.	0.506	0.918	0.747	0.161	0.095	0.118	0.268
	N	16	16	16	16	16	16	16
Wk9	CC	0.112	-0.147	-0.068	0.213	-0.569	-0.363	0.011
	Sig.	0.703	0.615	0.817	0.464	0.034	0.203	0.970
	N	14	14	14	14	14	14	14
Wk12	CC	-0.098	-0.189	0.336	0.057	0.034	0.238	0.052
	Sig.	0.727	0.501	0.220	0.840	0.904	0.394	0.854
	N	15	15	15	15	15	15	15
Wk16	CC	0.087	-0.539	-0.009	0.068	0.021	0.143	0.238
	Sig.	0.749	0.031	0.974	0.803	0.940	0.598	0.374
	N	16	16	16	16	16	16	16

Q ELISpot vs BAL NK 16+56-

BAL NK 16+56-		ELISpot Wk0B	ELISpot Wk0A	ELISpot Wk2	ELISpot Wk4	ELISpot Wk9	ELISpot Wk12	ELISpot Wk16
Wk0	CC	-0.098	-0.189	0.336	0.057	0.034	0.238	0.052
	Sig.	0.727	0.501	0.220	0.840	0.904	0.394	0.854
	N	15	15	15	15	15	15	15
Wk2	CC	-0.400	-0.313	0.249	0.162	-0.041	0.344	-0.026
	Sig.	0.125	0.237	0.353	0.549	0.880	0.192	0.922
	N	16	16	16	16	16	16	16
Wk4	CC	-0.150	-0.571	0.216	0.199	-0.013	0.037	-0.050
	Sig.	0.579	0.021	0.421	0.461	0.961	0.892	0.854
	N	16	16	16	16	16	16	16
Wk9	CC	0.302	-0.214	-0.172	-0.152	0.104	0.291	0.150
	Sig.	0.294	0.463	0.557	0.604	0.725	0.313	0.609
	N	14	14	14	14	14	14	14
Wk12	CC	-0.189	0.045	0.181	-0.371	0.004	0.004	-0.054
	Sig.	0.499	0.874	0.520	0.173	0.990	0.990	0.850
	N	15	15	15	15	15	15	15
Wk16	CC	-0.468	0.190	0.291	-0.085	-0.259	0.141	-0.132
	Sig.	0.068	0.481	0.274	0.753	0.333	0.602	0.625
	N	16	16	16	16	16	16	16

R ELISpot vs BAL NK 16-56+

BAL NK -+		ELISpot Wk0B	ELISpot Wk0A	ELISpot Wk2	ELISpot Wk4	ELISpot Wk9	ELISpot Wk12	ELISpot Wk16
Wk0	CC	0.039	-0.295	0.199	0.352	0.013	-0.381	-0.207
	Sig.	0.889	0.286	0.476	0.198	0.965	0.162	0.458
	N	15	15	15	15	15	15	15
Wk2	CC	0.209	-0.436	0.099	-0.053	0.029	-0.118	-0.268
	Sig.	0.438	0.092	0.716	0.846	0.914	0.664	0.316
	N	16	16	16	16	16	16	16
Wk4	CC	0.259	-0.522	-0.202	-0.132	-0.021	-0.268	-0.391
	Sig.	0.333	0.038	0.454	0.625	0.940	0.316	0.134
	N	16	16	16	16	16	16	16
Wk9	CC	-0.121	-0.442	0.227	0.174	0.091	-0.279	-0.271
	Sig.	0.656	0.087	0.399	0.520	0.737	0.295	0.311
	N	16	16	16	16	16	16	16
Wk12	CC	-0.026	-0.649	-0.025	0.056	-0.068	-0.421	-0.332
	Sig.	0.922	0.007	0.927	0.837	0.803	0.105	0.208
	N	16	16	16	16	16	16	16
Wk16	CC	-0.385	-0.059	-0.108	-0.370	-0.304	0.051	-0.077
	Sig.	0.174	0.840	0.714	0.193	0.291	0.864	0.794
	N	14	14	14	14	14	14	14

S **ELISpot vs BAL nonL 14+**

BAL nonL 14+		ELISpot Wk0B	ELISpot Wk0A	ELISpot Wk2	ELISpot Wk4	ELISpot Wk9	ELISpot Wk12	ELISpot Wk16
Wk0	CC	-0.214	0.298	0.705	0.270	0.184	-0.098	-0.061
	Sig.	0.443	0.281	0.003	0.331	0.511	0.727	0.830
	N	15	15	15	15	15	15	15
Wk2	CC	-0.279	-0.331	-0.396	-0.253	-0.385	0.068	-0.112
	Sig.	0.295	0.210	0.129	0.345	0.141	0.803	0.680
	N	16	16	16	16	16	16	16
Wk4	CC	0.456	-0.415	-0.244	0.068	-0.247	-0.303	0.029
	Sig.	0.076	0.110	0.362	0.803	0.356	0.254	0.914
	N	16	16	16	16	16	16	16
Wk9	CC	-0.109	-0.547	-0.181	-0.088	-0.259	-0.212	-0.324
	Sig.	0.688	0.028	0.502	0.745	0.333	0.431	0.222
	N	16	16	16	16	16	16	16
Wk12	CC	0.024	-0.490	-0.085	-0.106	-0.053	-0.006	0.009
	Sig.	0.931	0.054	0.753	0.696	0.846	0.983	0.974
	N	16	16	16	16	16	16	16
Wk16	CC	0.064	-0.248	-0.389	-0.468	0.033	0.103	0.121
	Sig.	0.829	0.392	0.169	0.091	0.911	0.725	0.681
	N	14	14	14	14	14	14	14

T **ELISpot vs BAL nonL 16+**

BAL nonL 16+		ELISpot Wk0B	ELISpot Wk0A	ELISpot Wk2	ELISpot Wk4	ELISpot Wk9	ELISpot Wk12	ELISpot Wk16
Wk0	CC	-0.793	0.098	0.531	0.257	-0.032	0.146	-0.332
	Sig.	0.000	0.727	0.042	0.355	0.909	0.603	0.226
	N	15	15	15	15	15	15	15
Wk2	CC	-0.244	0.049	-0.202	0.035	-0.482	0.097	0.088
	Sig.	0.362	0.858	0.454	0.897	0.058	0.721	0.745
	N	16	16	16	16	16	16	16
Wk4	CC	0.450	-0.377	-0.028	0.182	-0.150	-0.482	-0.032
	Sig.	0.080	0.150	0.918	0.499	0.579	0.058	0.905
	N	16	16	16	16	16	16	16
Wk9	CC	0.379	-0.609	-0.224	-0.103	0.000	-0.179	-0.268
	Sig.	0.147	0.012	0.405	0.704	1.000	0.506	0.316
	N	16	16	16	16	16	16	16
Wk12	CC	-0.318	-0.572	0.134	0.224	-0.015	-0.206	-0.182
	Sig.	0.231	0.020	0.621	0.405	0.957	0.444	0.499
	N	16	16	16	16	16	16	16
Wk16	CC	0.257	-0.618	-0.209	0.095	-0.064	-0.020	0.191
	Sig.	0.375	0.019	0.474	0.748	0.829	0.946	0.513
	N	14	14	14	14	14	14	14

U **ELISpot vs BAL nonL ++**

BAL nonL ++		ELISpot Wk0B	ELISpot Wk0A	ELISpot Wk2	ELISpot Wk4	ELISpot Wk9	ELISpot Wk12	ELISpot Wk16
Wk0	CC	-0.782	0.182	0.595	0.271	0.032	0.186	-0.182
	Sig.	0.001	0.516	0.019	0.328	0.909	0.508	0.516
	N	15	15	15	15	15	15	15
Wk2	CC	-0.153	-0.028	-0.303	0.068	-0.529	-0.021	0.041
	Sig.	0.572	0.918	0.254	0.803	0.035	0.940	0.880
	N	16	16	16	16	16	16	16
Wk4	CC	0.468	-0.412	-0.071	0.156	-0.135	-0.459	-0.079
	Sig.	0.068	0.113	0.795	0.564	0.617	0.074	0.770
	N	16	16	16	16	16	16	16
Wk9	CC	0.418	-0.614	-0.265	-0.112	-0.021	-0.176	-0.235
	Sig.	0.107	0.011	0.321	0.680	0.940	0.513	0.380
	N	16	16	16	16	16	16	16
Wk12	CC	-0.276	-0.609	0.091	0.244	-0.044	-0.162	-0.147
	Sig.	0.300	0.012	0.737	0.362	0.871	0.549	0.587
	N	16	16	16	16	16	16	16
Wk16	CC	0.284	-0.578	-0.226	0.090	-0.077	-0.011	0.222
	Sig.	0.326	0.030	0.436	0.759	0.794	0.970	0.446
	N	14	14	14	14	14	14	14

V **ELISpot vs BAL nonL 14+16-**

BAL nonL +-		ELISpot Wk0B	ELISpot Wk0A	ELISpot Wk2	ELISpot Wk4	ELISpot Wk9	ELISpot Wk12	ELISpot Wk16
Wk0	CC	-0.025	0.279	0.558	0.048	0.265	-0.043	-0.109
	Sig.	0.929	0.314	0.031	0.864	0.341	0.879	0.699
	N	15	15	15	15	15	15	15
Wk2	CC	-0.317	-0.349	-0.281	-0.420	-0.057	0.184	-0.169
	Sig.	0.232	0.185	0.292	0.106	0.833	0.495	0.531
	N	16	16	16	16	16	16	16
Wk4	CC	0.564	-0.162	-0.494	-0.187	-0.305	-0.206	0.244
	Sig.	0.023	0.549	0.052	0.488	0.251	0.444	0.362
	N	16	16	16	16	16	16	16
Wk9	CC	-0.278	-0.300	-0.156	-0.157	-0.060	-0.019	-0.191
	Sig.	0.297	0.259	0.564	0.560	0.824	0.944	0.478
	N	16	16	16	16	16	16	16
Wk12	CC	0.374	-0.155	-0.391	-0.515	-0.097	0.126	0.259
	Sig.	0.154	0.568	0.134	0.041	0.721	0.641	0.333
	N	16	16	16	16	16	16	16
Wk16	CC	-0.077	-0.158	-0.431	-0.427	-0.191	0.057	0.191
	Sig.	0.794	0.589	0.124	0.128	0.512	0.846	0.512
	N	14	14	14	14	14	14	14

W **ELISpot vs BAL nonL 14-16+**

BAL nonL 14-16+		ELISpot Wk0B	ELISpot Wk0A	ELISpot Wk2	ELISpot Wk4	ELISpot Wk9	ELISpot Wk12	ELISpot Wk16
Wk0	CC	-0.574	0.097	0.213	-0.095	-0.127	0.241	-0.329
	Sig.	0.025	0.730	0.446	0.737	0.652	0.386	0.231
	N	15	15	15	15	15	15	15
Wk2	CC	-0.303	0.275	-0.016	-0.097	-0.235	0.300	0.265
	Sig.	0.254	0.302	0.953	0.721	0.380	0.259	0.322
	N	16	16	16	16	16	16	16
Wk4	CC	0.250	-0.299	0.102	0.059	-0.121	-0.297	-0.038
	Sig.	0.350	0.261	0.708	0.829	0.656	0.264	0.888
	N	16	16	16	16	16	16	16
Wk9	CC	0.271	-0.517	0.007	0.159	0.059	-0.321	-0.291
	Sig.	0.311	0.040	0.978	0.557	0.829	0.226	0.274
	N	16	16	16	16	16	16	16
Wk12	CC	-0.007	-0.186	0.099	0.422	-0.131	-0.352	0.313
	Sig.	0.978	0.491	0.716	0.103	0.629	0.182	0.237
	N	16	16	16	16	16	16	16
Wk16	CC	0.204	-0.631	0.152	0.402	0.143	-0.108	0.015
	Sig.	0.483	0.016	0.605	0.154	0.626	0.714	0.958
	N	14	14	14	14	14	14	14

Supplementary Table 6 Correlations between IFNγ+ SFU and BAL cell populations

*Spearman's rank correlations were calculated between the frequency of cell populations characterised BAL cells, and PPD-specific IFNγ+ SFU (ELISpot). Correlation co-efficient ('CC'), significance ('Sig.') and number of values included in each comparison ('N') are shown at each combination of time points. PB1B is shown as the first column (blue text), as this time point was only analysed by ELISpot data. PB1 for flow cytometry data (row title) is the same time point as PB1A for ELISpot (column title). Results are shown for CD3+ lymphocytes (**A**, grey), $\gamma\delta$ T cells (**B**, blue), conventional T markers CD4+/CD8+ (**C-G**, pink), CD56+CD4+ T cells (**H**, pink), MAIT cell markers (**I-L**, purple), CD16/56 combinations of CD3+ (NKT-L) cells (**M-O**, yellow), CD16/56 combinations of CD3-CD8+ (NK) cells (**P-R**, green), CD14+/CD16+ combinations of HLA-DR+ non-lymphocyte cells (**S-W**, red).*

A **ELISpot vs PBMC IFNg CD4**

PBMC IFNg CD4		ELISpot PB2	ELISpot PB1	ELISpot Wk2	ELISpot Wk4	ELISpot Wk9	ELISpot Wk12	ELISpot Wk16
PB1	CC	-0.659	-0.268	-0.293	-0.049	-0.561	-0.220	0.195
	Sig.	0.076	0.520	0.482	0.909	0.148	0.601	0.643
	N	8	8	8	8	8	8	8
Wk2	CC	-0.123	0.110	0.252	-0.236	0.065	0.068	-0.173
	Sig.	0.650	0.686	0.346	0.379	0.810	0.802	0.521
	N	16	16	16	16	16	16	16
Wk4	CC	-0.657	0.356	0.207	-0.055	-0.310	0.436	0.221
	Sig.	0.006	0.175	0.441	0.839	0.242	0.091	0.411
	N	16	16	16	16	16	16	16
Wk9	CC	-0.220	-0.251	-0.092	-0.186	0.162	-0.080	0.141
	Sig.	0.414	0.347	0.734	0.491	0.549	0.770	0.601
	N	16	16	16	16	16	16	16
Wk12	CC	-0.389	-0.046	0.255	-0.147	0.241	0.118	-0.228
	Sig.	0.137	0.867	0.341	0.587	0.368	0.664	0.395
	N	16	16	16	16	16	16	16
Wk16	CC	-0.048	-0.108	-0.132	-0.695	0.575	0.287	0.275
	Sig.	0.910	0.799	0.756	0.056	0.136	0.490	0.509
	N	8	8	8	8	8	8	8

B **ELISpot vs PBMC IFNg CD8**

PBMC IFNg CD8		ELISpot PB2	ELISpot PB1	ELISpot Wk2	ELISpot Wk4	ELISpot Wk9	ELISpot Wk12	ELISpot Wk16
PB1	CC	-0.778	-0.168	-0.216	-0.275	-0.503	0.299	-0.204
	Sig.	0.023	0.691	0.608	0.509	0.204	0.471	0.629
	N	8	8	8	8	8	8	8
Wk2	CC	0.027	-0.169	0.105	-0.260	0.379	0.445	-0.269
	Sig.	0.921	0.532	0.700	0.331	0.148	0.084	0.314
	N	16	16	16	16	16	16	16
Wk4	CC	-0.290	0.429	0.181	-0.110	-0.099	0.498	0.284
	Sig.	0.275	0.097	0.503	0.686	0.715	0.050	0.286
	N	16	16	16	16	16	16	16
Wk9	CC	-0.316	0.091	0.029	0.007	-0.044	-0.069	0.253
	Sig.	0.232	0.737	0.914	0.978	0.871	0.799	0.344
	N	16	16	16	16	16	16	16
Wk12	CC	-0.453	-0.074	0.429	0.148	0.197	0.157	-0.197
	Sig.	0.078	0.785	0.097	0.584	0.465	0.561	0.465
	N	16	16	16	16	16	16	16
Wk16	CC	-0.342	0.268	0.146	0.586	-0.878	-0.464	0.268
	Sig.	0.408	0.520	0.729	0.127	0.004	0.247	0.520
	N	8	8	8	8	8	8	8

C **ELISpot vs PBMC IFNg gd**

PBMC IFNg gd		ELISpot PB2	ELISpot PB1	ELISpot Wk2	ELISpot Wk4	ELISpot Wk9	ELISpot Wk12	ELISpot Wk16
PB1	CC	-0.464	0.082	-0.109	-0.436	0.164	0.300	-0.518
	Sig.	0.247	0.847	0.797	0.280	0.699	0.470	0.188
	N	8	8	8	8	8	8	8
Wk2	CC	-0.075	0.260	0.006	-0.367	0.551	0.339	0.109
	Sig.	0.784	0.331	0.983	0.163	0.027	0.199	0.689
	N	16	16	16	16	16	16	16
Wk4	CC	-0.513	0.470	0.244	0.111	-0.107	0.353	0.286
	Sig.	0.042	0.066	0.362	0.684	0.692	0.180	0.284
	N	16	16	16	16	16	16	16
Wk9	CC	-0.559	0.152	0.200	-0.069	-0.088	0.090	0.127
	Sig.	0.024	0.575	0.457	0.800	0.745	0.741	0.639
	N	16	16	16	16	16	16	16
Wk12	CC	-0.108	0.080	-0.168	-0.500	0.311	0.385	-0.094
	Sig.	0.691	0.769	0.533	0.048	0.240	0.141	0.728
	N	16	16	16	16	16	16	16
Wk16	CC	0.469	0.279	0.025	-0.241	0.583	0.647	0.710
	Sig.	0.241	0.503	0.952	0.565	0.129	0.083	0.048
	N	8	8	8	8	8	8	8

D **ELISpot vs PBMC IFNg Va7.2+**

PBMC IFNg MAIT 7.2+		ELISpot PB2	ELISpot PB1	ELISpot Wk2	ELISpot Wk4	ELISpot Wk9	ELISpot Wk12	ELISpot Wk16
PB1	CC	0.577	-0.577	0.412	0.577	0.247	0.082	-0.412
	Sig.	0.134	0.134	0.310	0.134	0.555	0.846	0.310
	N	8	8	8	8	8	8	8
Wk2	CC	0.068	-0.310	-0.344	-0.293	-0.251	-0.102	-0.070
	Sig.	0.810	0.261	0.209	0.289	0.367	0.717	0.804
	N	15	15	15	15	15	15	15
Wk4	CC	-0.343	0.575	0.304	0.139	-0.406	-0.167	-0.105
	Sig.	0.193	0.020	0.252	0.609	0.119	0.536	0.699
	N	16	16	16	16	16	16	16
Wk9	CC	0.089	-0.602	-0.313	-0.061	0.028	0.077	-0.335
	Sig.	0.743	0.014	0.237	0.821	0.919	0.778	0.205
	N	16	16	16	16	16	16	16
Wk12	CC	-0.615	0.018	0.569	0.125	0.254	0.100	-0.404
	Sig.	0.011	0.948	0.021	0.644	0.343	0.712	0.121
	N	16	16	16	16	16	16	16
Wk16	CC							
	Sig.							
	N							

E **ELISpot vs PBMC IFNg NK 16+56-**

PBMC IFNg NK 16+56-		ELISpot PB2	ELISpot PB1	ELISpot Wk2	ELISpot Wk4	ELISpot Wk9	ELISpot Wk12	ELISpot Wk16
PB1	CC	-0.528	0.356	-0.687	-0.565	-0.393	0.331	0.479
	Sig.	0.179	0.387	0.060	0.145	0.336	0.423	0.230
	N	8	8	8	8	8	8	8
Wk2	CC	-0.611	0.116	0.551	0.061	0.172	0.175	-0.386
	Sig.	0.012	0.668	0.027	0.823	0.525	0.516	0.140
	N	16	16	16	16	16	16	16
Wk4	CC	-0.086	-0.006	-0.090	0.405	-0.203	-0.390	-0.088
	Sig.	0.750	0.982	0.741	0.119	0.452	0.136	0.746
	N	16	16	16	16	16	16	16
Wk9	CC	-0.485	0.207	0.627	0.203	0.232	0.315	-0.076
	Sig.	0.057	0.442	0.009	0.451	0.387	0.235	0.779
	N	16	16	16	16	16	16	16
Wk12	CC	-0.408	0.025	0.277	0.442	-0.553	-0.332	-0.454
	Sig.	0.116	0.928	0.300	0.086	0.026	0.210	0.077
	N	16	16	16	16	16	16	16
Wk16	CC	-0.275	0.515	0.012	0.371	-0.826	-0.575	0.383
	Sig.	0.509	0.192	0.978	0.365	0.011	0.136	0.349
	N	8	8	8	8	8	8	8

F **ELISpot vs PBMC IFNg NK 16-56+**

PBMC IFNg NK 16-56+		ELISpot PB2	ELISpot PB1	ELISpot Wk2	ELISpot Wk4	ELISpot Wk9	ELISpot Wk12	ELISpot Wk16
PB1	CC	0.342	0.586	0.024	-0.098	-0.146	-0.464	0.293
	Sig.	0.408	0.127	0.954	0.818	0.729	0.247	0.482
	N	8	8	8	8	8	8	8
Wk2	CC	-0.240	0.057	0.211	0.170	-0.344	0.269	-0.046
	Sig.	0.370	0.835	0.432	0.530	0.192	0.314	0.867
	N	16	16	16	16	16	16	16
Wk4	CC	-0.558	-0.097	-0.252	-0.084	-0.451	0.125	-0.119
	Sig.	0.025	0.721	0.346	0.758	0.080	0.644	0.660
	N	16	16	16	16	16	16	16
Wk9	CC	-0.133	-0.066	0.214	0.386	0.295	-0.062	-0.091
	Sig.	0.624	0.807	0.426	0.139	0.267	0.820	0.736
	N	16	16	16	16	16	16	16
Wk12	CC	-0.280	0.197	0.277	0.267	-0.117	0.277	-0.268
	Sig.	0.293	0.466	0.299	0.318	0.666	0.299	0.315
	N	16	16	16	16	16	16	16
Wk16	CC	-0.355	-0.381	-0.101	0.089	-0.152	0.127	-0.140
	Sig.	0.388	0.352	0.811	0.834	0.719	0.765	0.742
	N	8	8	8	8	8	8	8

G **ELISpot vs PBMC IFNg NKT 16+**

PBMC IFNg NKT 16+		ELISpot PB2	ELISpot PB1	ELISpot Wk2	ELISpot Wk4	ELISpot Wk9	ELISpot Wk12	ELISpot Wk16
PB1	CC	0.327	0.164	0.218	-0.027	0.518	0.627	-0.191
	Sig.	0.429	0.699	0.604	0.949	0.188	0.096	0.651
	N	8	8	8	8	8	8	8
Wk2	CC	0.041	0.460	-0.224	-0.454	0.187	0.291	0.220
	Sig.	0.881	0.073	0.405	0.077	0.487	0.273	0.412
	N	16	16	16	16	16	16	16
Wk4	CC	-0.211	-0.211	0.295	-0.043	0.206	-0.042	-0.160
	Sig.	0.434	0.433	0.268	0.874	0.444	0.879	0.554
	N	16	16	16	16	16	16	16
Wk9	CC	-0.678	0.326	0.481	0.457	-0.139	0.059	-0.077
	Sig.	0.004	0.218	0.059	0.075	0.609	0.828	0.778
	N	16	16	16	16	16	16	16
Wk12	CC	-0.224	-0.013	0.255	0.069	0.340	0.266	-0.227
	Sig.	0.404	0.961	0.340	0.801	0.197	0.320	0.398
	N	16	16	16	16	16	16	16
Wk16	CC	-0.156	-0.072	0.479	0.144	0.012	-0.084	0.012
	Sig.	0.713	0.866	0.230	0.734	0.978	0.844	0.978
	N	8	8	8	8	8	8	8

H **ELISpot vs PBMC IFNg NKT 56+**

PBMC IFNg NKT 56+		ELISpot PB2	ELISpot PB1	ELISpot Wk2	ELISpot Wk4	ELISpot Wk9	ELISpot Wk12	ELISpot Wk16
PB1	CC	0.024	-0.145	0.241	0.313	0.313	-0.157	0.205
	Sig.	0.955	0.733	0.565	0.450	0.450	0.711	0.627
	N	8	8	8	8	8	8	8
Wk2	CC	0.294	-0.006	-0.777	-0.707	0.121	0.339	0.287
	Sig.	0.269	0.984	0.000	0.002	0.655	0.199	0.280
	N	16	16	16	16	16	16	16
Wk4	CC	-0.394	-0.070	-0.090	-0.449	-0.191	0.441	-0.265
	Sig.	0.131	0.796	0.739	0.081	0.479	0.087	0.321
	N	16	16	16	16	16	16	16
Wk9	CC	-0.419	-0.024	0.050	0.160	-0.099	0.123	0.264
	Sig.	0.106	0.928	0.853	0.554	0.715	0.650	0.324
	N	16	16	16	16	16	16	16
Wk12	CC	-0.260	-0.255	-0.181	-0.293	-0.072	0.194	-0.182
	Sig.	0.331	0.340	0.503	0.271	0.792	0.471	0.500
	N	16	16	16	16	16	16	16
Wk16	CC	-0.082	0.577	0.577	-0.412	0.577	0.577	0.247
	Sig.	0.846	0.134	0.134	0.310	0.134	0.134	0.555
	N	8	8	8	8	8	8	8

I **ELISpot vs PBMC IFNg NKT ++**

PBMC IFNg NKT ++		ELISpot PB2	ELISpot PB1	ELISpot Wk2	ELISpot Wk4	ELISpot Wk9	ELISpot Wk12	ELISpot Wk16
PB1	CC	0.546	-0.218	-0.031	0.218	0.047	-0.312	-0.187
	Sig.	0.162	0.604	0.942	0.604	0.912	0.452	0.657
	N	8	8	8	8	8	8	8
Wk2	CC	0.388	0.322	-0.494	-0.656	0.069	0.135	0.102
	Sig.	0.153	0.242	0.061	0.008	0.807	0.631	0.717
	N	15	15	15	15	15	15	15
Wk4	CC	-0.172	-0.299	0.161	0.053	0.005	0.184	-0.687
	Sig.	0.524	0.260	0.552	0.846	0.987	0.495	0.003
	N	16	16	16	16	16	16	16
Wk9	CC	-0.521	0.059	0.431	0.549	-0.052	-0.003	-0.056
	Sig.	0.038	0.828	0.095	0.028	0.849	0.991	0.837
	N	16	16	16	16	16	16	16
Wk12	CC	-0.221	0.120	0.006	-0.039	0.039	0.272	-0.242
	Sig.	0.411	0.659	0.982	0.887	0.887	0.309	0.367
	N	16	16	16	16	16	16	16
Wk16	CC	0.238	-0.405	-0.429	0.214	-0.048	-0.286	0.548
	Sig.	0.570	0.320	0.289	0.610	0.911	0.493	0.160
	N	8	8	8	8	8	8	8

J **ELISpot vs PBMC IFNg nonL ++**

PBMC IFNg nonL ++		ELISpot PB2	ELISpot PB1	ELISpot Wk2	ELISpot Wk4	ELISpot Wk9	ELISpot Wk12	ELISpot Wk16
PB1	CC							
	Sig.							
	N							
Wk2	CC							
	Sig.							
	N							
Wk4	CC	-0.420	0.196	0.140	0.028	-0.420	-0.308	-0.140
	Sig.	0.105	0.466	0.605	0.918	0.105	0.246	0.605
	N	16	16	16	16	16	16	16
Wk9	CC	-0.252	0.420	0.420	-0.028	0.420	0.364	0.028
	Sig.	0.346	0.105	0.105	0.918	0.105	0.166	0.918
	N	16	16	16	16	16	16	16
Wk12	CC	0.281	0.297	-0.320	-0.499	0.128	0.038	0.199
	Sig.	0.291	0.264	0.227	0.049	0.637	0.888	0.459
	N	16	16	16	16	16	16	16
Wk16	CC	-0.577	0.082	-0.082	-0.247	-0.577	-0.577	-0.082
	Sig.	0.134	0.846	0.846	0.555	0.134	0.134	0.846
	N	8	8	8	8	8	8	8

K **ELISpot vs PBMC IFNg nonL 14+16-**

PBMC IFNg nonL +-		ELISpot PB2	ELISpot PB1	ELISpot Wk2	ELISpot Wk4	ELISpot Wk9	ELISpot Wk12	ELISpot Wk16
PB1	CC							
	Sig.							
	N							
Wk2	CC	0.150	-0.013	-0.199	-0.093	-0.132	-0.123	-0.382
	Sig.	0.578	0.963	0.461	0.732	0.627	0.649	0.144
	N	16	16	16	16	16	16	16
Wk4	CC	-0.189	0.059	0.217	-0.398	0.684	0.620	-0.228
	Sig.	0.483	0.828	0.421	0.127	0.003	0.010	0.396
	N	16	16	16	16	16	16	16
Wk9	CC	0.044	-0.409	-0.279	-0.041	0.464	0.168	0.143
	Sig.	0.870	0.116	0.295	0.881	0.070	0.534	0.597
	N	16	16	16	16	16	16	16
Wk12	CC	-0.472	-0.283	0.172	0.088	0.115	0.095	-0.214
	Sig.	0.065	0.288	0.524	0.747	0.671	0.726	0.427
	N	16	16	16	16	16	16	16
Wk16	CC	-0.013	0.165	0.583	-0.013	0.381	0.457	0.241
	Sig.	0.976	0.696	0.129	0.976	0.352	0.255	0.565
	N	8	8	8	8	8	8	8

L **ELISpot vs PBMC IFNg nonL 14-16+**

PBMC IFNg nonL 14-16+		ELISpot PB2	ELISpot PB1	ELISpot Wk2	ELISpot Wk4	ELISpot Wk9	ELISpot Wk12	ELISpot Wk16
PB1	CC							
	Sig.							
	N							
Wk2	CC							
	Sig.							
	N							
Wk4	CC							
	Sig.							
	N							
Wk9	CC	-0.455	0.179	0.571	0.263	0.179	0.141	-0.220
	Sig.	0.077	0.507	0.021	0.324	0.507	0.603	0.413
	N	16	16	16	16	16	16	16
Wk12	CC	-0.509	0.354	0.635	0.393	-0.095	0.151	0.026
	Sig.	0.044	0.178	0.008	0.133	0.727	0.577	0.924
	N	16	16	16	16	16	16	16
Wk16	CC							
	Sig.							
	N							

Supplementary Table 7 Correlations between IFNγ+ SFU and IFNγ-positive cells among PBMCs

*Spearman's rank correlations were calculated between IFNγ+ SFU frequency and the frequency of IFNγ+ cells among different cell populations, measured among PBMCs by flow cytometry. IFNγ+ frequency was explored among: CD4, CD8+ and γδ T cells (**A, B** and **C**), Va7.2+ CD8+ T cells (**D**), CD16+/CD56+ CD3-CD8+ lymphocytes (NK cells, **E** and **F**), CD16+/CD56+ CD3+ T cells (NKT-L, **G**-**I**), CD14+/CD16+ non-lymphocyte cells (**J**-**L**). Correlation co-efficient ('CC'), significance ('Sig.') and number of values included in each comparison ('N') are shown at each combination of time points. PB2 is shown in blue, as this time point was only analysed by ELISpot.*

A **ELISpot vs PBMC IL-2 CD4**

PBMC IL-2 CD4		ELISpot PB2	ELISpot PB1	ELISpot Wk2	ELISpot Wk4	ELISpot Wk9	ELISpot Wk12	ELISpot Wk16
PB1	CC	-0.262	-0.310	-0.190	0.024	-0.238	-0.667	-0.214
	Sig.	0.531	0.456	0.651	0.955	0.570	0.071	0.610
	N	8	8	8	8	8	8	8
Wk2	CC	0.233	-0.049	-0.441	-0.480	-0.152	0.131	-0.016
	Sig.	0.386	0.858	0.088	0.060	0.575	0.628	0.953
	N	16	16	16	16	16	16	16
Wk4	CC	-0.230	0.422	0.230	0.006	-0.226	0.376	0.372
	Sig.	0.391	0.103	0.391	0.983	0.401	0.151	0.156
	N	16	16	16	16	16	16	16
Wk9	CC	-0.287	-0.150	0.066	-0.119	0.032	-0.163	0.178
	Sig.	0.281	0.579	0.807	0.660	0.905	0.546	0.509
	N	16	16	16	16	16	16	16
Wk12	CC	-0.469	-0.091	0.235	-0.009	0.164	0.046	-0.248
	Sig.	0.067	0.738	0.382	0.974	0.545	0.867	0.355
	N	16	16	16	16	16	16	16
Wk16	CC	-0.095	-0.119	0.333	-0.262	0.286	0.238	0.024
	Sig.	0.823	0.779	0.420	0.531	0.493	0.570	0.955
	N	8	8	8	8	8	8	8

B **ELISpot vs PBMC IL-2 CD8**

PBMC IL-2 CD8		ELISpot PB2	ELISpot PB1	ELISpot Wk2	ELISpot Wk4	ELISpot Wk9	ELISpot Wk12	ELISpot Wk16
PB1	CC	0.013	0.342	-0.013	-0.228	0.330	-0.317	0.076
	Sig.	0.976	0.406	0.976	0.587	0.425	0.444	0.858
	N	8	8	8	8	8	8	8
Wk2	CC	-0.228	0.408	0.014	-0.165	-0.455	0.109	-0.324
	Sig.	0.395	0.117	0.958	0.541	0.077	0.689	0.221
	N	16	16	16	16	16	16	16
Wk4	CC	0.098	-0.092	-0.160	-0.356	0.117	0.442	-0.144
	Sig.	0.717	0.734	0.554	0.175	0.667	0.086	0.594
	N	16	16	16	16	16	16	16
Wk9	CC	-0.300	-0.147	0.279	0.231	0.124	-0.223	-0.210
	Sig.	0.258	0.586	0.296	0.389	0.648	0.405	0.435
	N	16	16	16	16	16	16	16
Wk12	CC	-0.300	-0.148	0.455	0.087	0.058	-0.102	-0.368
	Sig.	0.260	0.585	0.077	0.748	0.832	0.707	0.161
	N	16	16	16	16	16	16	16
Wk16	CC	0.455	0.587	0.611	0.671	0.012	0.072	0.132
	Sig.	0.257	0.126	0.108	0.069	0.978	0.866	0.756
	N	8	8	8	8	8	8	8

C **ELISpot vs PBMC IL-2 gd**

PBMC IL-2 gd		ELISpot PB2	ELISpot PB1	ELISpot Wk2	ELISpot Wk4	ELISpot Wk9	ELISpot Wk12	ELISpot Wk16
PB1	CC	-0.156	0.443	-0.144	-0.467	-0.299	-0.228	-0.323
	Sig.	0.713	0.272	0.734	0.243	0.471	0.588	0.435
	N	8	8	8	8	8	8	8
Wk2	CC	-0.397	0.259	0.341	0.086	0.304	0.112	-0.085
	Sig.	0.128	0.334	0.196	0.751	0.252	0.679	0.756
	N	16	16	16	16	16	16	16
Wk4	CC	-0.297	-0.100	0.064	-0.164	-0.081	0.324	-0.548
	Sig.	0.264	0.712	0.813	0.543	0.766	0.221	0.028
	N	16	16	16	16	16	16	16
Wk9	CC	-0.013	0.384	0.324	0.401	-0.147	0.022	0.047
	Sig.	0.962	0.142	0.221	0.123	0.588	0.937	0.861
	N	16	16	16	16	16	16	16
Wk12	CC	-0.599	0.085	0.496	0.552	-0.125	-0.419	-0.253
	Sig.	0.014	0.755	0.051	0.027	0.644	0.106	0.344
	N	16	16	16	16	16	16	16
Wk16	CC	0.881	0.214	0.119	0.524	0.310	0.119	0.190
	Sig.	0.004	0.610	0.779	0.183	0.456	0.779	0.651
	N	8	8	8	8	8	8	8

D **ELISpot vs PBMC IL-2 Va7.2+**

PBMC IL-2 MAIT 7.2+		ELISpot PB2	ELISpot PB1	ELISpot Wk2	ELISpot Wk4	ELISpot Wk9	ELISpot Wk12	ELISpot Wk16
PB1	CC	-0.220	-0.220	-0.220	-0.122	-0.366	0.439	-0.171
	Sig.	0.601	0.601	0.601	0.774	0.373	0.276	0.686
	N	8	8	8	8	8	8	8
Wk2	CC	0.035	0.345	-0.018	-0.364	0.178	0.305	-0.278
	Sig.	0.899	0.191	0.947	0.165	0.511	0.251	0.297
	N	16	16	16	16	16	16	16
Wk4	CC	0.137	-0.264	-0.107	0.046	-0.306	-0.363	0.147
	Sig.	0.614	0.322	0.694	0.865	0.249	0.168	0.586
	N	16	16	16	16	16	16	16
Wk9	CC	-0.265	0.041	-0.318	-0.243	-0.336	0.372	0.215
	Sig.	0.322	0.880	0.229	0.364	0.203	0.156	0.425
	N	16	16	16	16	16	16	16
Wk12	CC	0.194	-0.301	0.046	-0.045	0.221	-0.097	-0.525
	Sig.	0.473	0.257	0.865	0.870	0.410	0.721	0.037
	N	16	16	16	16	16	16	16
Wk16	CC	0.368	0.241	-0.089	0.381	-0.190	0.013	-0.152
	Sig.	0.370	0.565	0.834	0.352	0.652	0.976	0.719
	N	8	8	8	8	8	8	8

E **ELISpot vs PBMC IL-2 NK 16+56-**

PBMC IL-2 NK 16+56-		ELISpot PB2	ELISpot PB1	ELISpot Wk2	ELISpot Wk4	ELISpot Wk9	ELISpot Wk12	ELISpot Wk16
PB1	CC	-0.457	-0.190	0.063	0.178	-0.495	-0.101	0.368
	Sig.	0.255	0.652	0.881	0.674	0.213	0.811	0.370
	N	8	8	8	8	8	8	8
Wk2	CC	-0.230	-0.115	-0.067	-0.469	0.116	0.597	-0.472
	Sig.	0.392	0.671	0.805	0.067	0.668	0.015	0.065
	N	16	16	16	16	16	16	16
Wk4	CC	0.089	-0.535	-0.318	-0.375	0.004	0.025	-0.136
	Sig.	0.742	0.033	0.229	0.152	0.990	0.927	0.616
	N	16	16	16	16	16	16	16
Wk9	CC	0.230	-0.309	0.008	0.029	0.176	-0.035	-0.164
	Sig.	0.392	0.245	0.975	0.916	0.515	0.896	0.544
	N	16	16	16	16	16	16	16
Wk12	CC	0.216	-0.156	-0.415	-0.334	-0.398	-0.054	0.035
	Sig.	0.421	0.565	0.110	0.206	0.127	0.842	0.898
	N	16	16	16	16	16	16	16
Wk16	CC	0.685	0.406	0.266	0.457	0.089	0.089	0.076
	Sig.	0.061	0.318	0.524	0.255	0.834	0.834	0.858
	N	8	8	8	8	8	8	8

F **ELISpot vs PBMC IL-2 NK 16-56+**

PBMC IL-2 NK 16-56+		ELISpot PB2	ELISpot PB1	ELISpot Wk2	ELISpot Wk4	ELISpot Wk9	ELISpot Wk12	ELISpot Wk16
PB1	CC	-0.234	0.031	0.156	-0.171	0.546	0.312	-0.265
	Sig.	0.577	0.942	0.712	0.685	0.162	0.452	0.526
	N	8	8	8	8	8	8	8
Wk2	CC	-0.255	-0.119	0.048	0.002	0.105	0.030	0.000
	Sig.	0.340	0.660	0.859	0.995	0.699	0.911	1.000
	N	16	16	16	16	16	16	16
Wk4	CC	-0.350	0.037	-0.084	0.207	-0.425	-0.457	0.175
	Sig.	0.184	0.891	0.756	0.441	0.101	0.075	0.517
	N	16	16	16	16	16	16	16
Wk9	CC	0.118	0.390	0.247	0.039	0.050	-0.104	0.558
	Sig.	0.663	0.135	0.357	0.885	0.854	0.702	0.025
	N	16	16	16	16	16	16	16
Wk12	CC	0.130	-0.232	-0.192	-0.267	0.381	0.483	0.353
	Sig.	0.632	0.387	0.476	0.317	0.146	0.058	0.179
	N	16	16	16	16	16	16	16
Wk16	CC	-0.013	-0.051	0.292	0.406	-0.190	-0.101	-0.723
	Sig.	0.976	0.905	0.483	0.318	0.652	0.811	0.043
	N	8	8	8	8	8	8	8

G **ELISpot vs PBMC IL-2 NKT 16+**

PBMC IL-2 NKT 16+		ELISpot PB2	ELISpot PB1	ELISpot Wk2	ELISpot Wk4	ELISpot Wk9	ELISpot Wk12	ELISpot Wk16
PB1	CC	0.171	0.109	0.203	-0.109	0.234	0.546	-0.343
	Sig.	0.685	0.797	0.630	0.797	0.577	0.162	0.406
	N	8	8	8	8	8	8	8
Wk2	CC	0.075	0.036	0.003	-0.012	-0.254	-0.591	-0.313
	Sig.	0.784	0.895	0.991	0.965	0.343	0.016	0.237
	N	16	16	16	16	16	16	16
Wk4	CC	0.187	0.108	-0.071	-0.110	0.622	0.274	0.151
	Sig.	0.487	0.691	0.794	0.685	0.010	0.305	0.577
	N	16	16	16	16	16	16	16
Wk9	CC	-0.290	-0.035	0.296	0.482	-0.335	-0.509	-0.306
	Sig.	0.275	0.897	0.266	0.058	0.205	0.044	0.249
	N	16	16	16	16	16	16	16
Wk12	CC	0.199	-0.193	0.017	-0.020	-0.121	-0.136	-0.092
	Sig.	0.459	0.475	0.949	0.942	0.656	0.616	0.734
	N	16	16	16	16	16	16	16
Wk16	CC	0.098	0.317	0.805	0.634	0.000	-0.049	-0.171
	Sig.	0.818	0.444	0.016	0.091	1.000	0.909	0.686
	N	8	8	8	8	8	8	8

H **ELISpot vs PBMC IL-2 NKT 56+**

PBMC IL-2 NKT 56+		ELISpot PB2	ELISpot PB1	ELISpot Wk2	ELISpot Wk4	ELISpot Wk9	ELISpot Wk12	ELISpot Wk16
PB1	CC	-0.732	-0.244	-0.171	-0.122	-0.488	0.024	-0.073
	Sig.	0.039	0.560	0.686	0.774	0.220	0.954	0.863
	N	8	8	8	8	8	8	8
Wk2	CC	0.422	0.466	-0.218	-0.238	0.269	0.132	0.231
	Sig.	0.104	0.069	0.417	0.376	0.314	0.626	0.389
	N	16	16	16	16	16	16	16
Wk4	CC	-0.162	0.093	0.116	0.039	-0.193	0.251	-0.071
	Sig.	0.548	0.732	0.669	0.887	0.473	0.348	0.792
	N	16	16	16	16	16	16	16
Wk9	CC	-0.227	0.392	0.269	0.269	-0.415	-0.240	0.159
	Sig.	0.398	0.133	0.313	0.314	0.110	0.371	0.557
	N	16	16	16	16	16	16	16
Wk12	CC	-0.541	-0.038	-0.036	-0.065	-0.151	-0.151	-0.269
	Sig.	0.037	0.894	0.899	0.819	0.592	0.592	0.333
	N	15	15	15	15	15	15	15
Wk16	CC	0.286	0.619	0.738	0.238	0.214	0.238	0.024
	Sig.	0.493	0.102	0.037	0.570	0.610	0.570	0.955
	N	8	8	8	8	8	8	8

I **ELISpot vs PBMC IL-2 NKT ++**

PBMC IL-2 NKT ++		ELISpot PB2	ELISpot PB1	ELISpot Wk2	ELISpot Wk4	ELISpot Wk9	ELISpot Wk12	ELISpot Wk16
PB1	CC	-0.171	0.016	-0.094	0.016	0.078	0.483	0.452
	Sig.	0.685	0.971	0.826	0.971	0.854	0.225	0.261
	N	8	8	8	8	8	8	8
Wk2	CC	0.087	-0.078	0.073	-0.229	0.623	0.005	0.005
	Sig.	0.758	0.782	0.795	0.411	0.013	0.987	0.987
	N	15	15	15	15	15	15	15
Wk4	CC	-0.128	0.067	-0.155	-0.036	-0.008	0.263	0.402
	Sig.	0.636	0.807	0.566	0.896	0.976	0.326	0.122
	N	16	16	16	16	16	16	16
Wk9	CC	-0.107	0.354	0.555	0.661	-0.055	-0.191	0.253
	Sig.	0.693	0.179	0.026	0.005	0.839	0.478	0.345
	N	16	16	16	16	16	16	16
Wk12	CC	0.368	-0.131	0.368	0.548	0.396	0.069	0.118
	Sig.	0.160	0.627	0.161	0.028	0.129	0.798	0.664
	N	16	16	16	16	16	16	16
Wk16	CC	-0.695	0.084	0.323	-0.204	-0.407	-0.347	-0.755
	Sig.	0.056	0.844	0.435	0.629	0.317	0.399	0.031
	N	8	8	8	8	8	8	8

J **ELISpot vs PBMC IL-2 nonL ++**

PBMC IL-2 nonL ++		ELISpot PB2	ELISpot PB1	ELISpot Wk2	ELISpot Wk4	ELISpot Wk9	ELISpot Wk12	ELISpot Wk16
PB1	CC	-0.082	-0.412	0.247	0.247	0.577	-0.082	-0.247
	Sig.	0.846	0.310	0.555	0.555	0.134	0.846	0.555
	N	8	8	8	8	8	8	8
Wk2	CC	0.028	-0.280	-0.252	-0.196	-0.308	-0.252	-0.252
	Sig.	0.918	0.293	0.346	0.467	0.246	0.346	0.346
	N	16	16	16	16	16	16	16
Wk4	CC	-0.022	0.069	0.426	0.342	0.050	-0.454	0.121
	Sig.	0.936	0.799	0.100	0.194	0.853	0.077	0.655
	N	16	16	16	16	16	16	16
Wk9	CC	0.181	0.147	0.264	0.028	0.605	0.144	-0.181
	Sig.	0.502	0.586	0.323	0.919	0.013	0.594	0.502
	N	16	16	16	16	16	16	16
Wk12	CC	0.346	0.350	0.243	0.072	0.588	0.146	0.069
	Sig.	0.189	0.184	0.363	0.792	0.017	0.589	0.801
	N	16	16	16	16	16	16	16
Wk16	CC	0.109	0.518	0.218	0.518	-0.627	-0.464	-0.109
	Sig.	0.797	0.188	0.604	0.188	0.096	0.247	0.797
	N	8	8	8	8	8	8	8

K **ELISpot vs PBMC IL-2 nonL 14+16-**

PBMC IL-2 nonL +-		ELISpot PB2	ELISpot PB1	ELISpot Wk2	ELISpot Wk4	ELISpot Wk9	ELISpot Wk12	ELISpot Wk16
PB1	CC	0.000	-0.300	0.382	0.355	0.136	-0.464	-0.218
	Sig.	1.000	0.470	0.351	0.389	0.747	0.247	0.604
	N	8	8	8	8	8	8	8
Wk2	CC	0.258	-0.214	-0.238	-0.199	-0.015	-0.020	-0.064
	Sig.	0.334	0.427	0.375	0.459	0.955	0.940	0.814
	N	16	16	16	16	16	16	16
Wk4	CC	-0.176	0.134	0.154	-0.156	0.115	0.110	-0.151
	Sig.	0.513	0.620	0.570	0.564	0.671	0.685	0.577
	N	16	16	16	16	16	16	16
Wk9	CC	0.252	0.084	-0.308	-0.252	0.028	-0.420	0.196
	Sig.	0.346	0.757	0.245	0.346	0.918	0.105	0.467
	N	16	16	16	16	16	16	16
Wk12	CC	-0.090	-0.201	-0.198	-0.232	-0.233	-0.113	-0.433
	Sig.	0.741	0.456	0.462	0.388	0.384	0.676	0.094
	N	16	16	16	16	16	16	16
Wk16	CC	0.026	0.038	0.383	0.306	-0.064	0.268	0.268
	Sig.	0.952	0.928	0.349	0.460	0.881	0.521	0.521
	N	8	8	8	8	8	8	8

L **ELISpot vs PBMC IL-2 nonL 14-16+**

PBMC IL-2 nonL 14-16+		ELISpot PB2	ELISpot PB1	ELISpot Wk2	ELISpot Wk4	ELISpot Wk9	ELISpot Wk12	ELISpot Wk16
PB1	CC	-0.082	-0.412	0.247	0.247	0.577	-0.082	-0.247
	Sig.	0.846	0.310	0.555	0.555	0.134	0.846	0.555
	N	8	8	8	8	8	8	8
Wk2	CC	-0.196	0.364	0.252	0.252	-0.364	0.084	0.364
	Sig.	0.467	0.165	0.346	0.346	0.166	0.757	0.166
	N	16	16	16	16	16	16	16
Wk4	CC	0.322	-0.165	0.265	0.193	0.404	0.104	0.290
	Sig.	0.224	0.542	0.322	0.474	0.121	0.702	0.277
	N	16	16	16	16	16	16	16
Wk9	CC	-0.348	-0.080	-0.005	0.270	-0.500	-0.226	0.077
	Sig.	0.187	0.768	0.986	0.311	0.048	0.400	0.776
	N	16	16	16	16	16	16	16
Wk12	CC	0.241	-0.045	-0.299	-0.168	-0.093	-0.199	0.214
	Sig.	0.368	0.867	0.261	0.534	0.733	0.460	0.425
	N	16	16	16	16	16	16	16
Wk16	CC	-0.262	0.690	0.500	0.190	-0.500	-0.310	-0.286
	Sig.	0.531	0.058	0.207	0.651	0.207	0.456	0.493
	N	8	8	8	8	8	8	8

Supplementary Table 8 Correlations between IFNγ+ SFU and IL-2-positive cells among PBMCs

*Spearman's rank correlations were calculated between IFNγ+ SFU frequency and the frequency of IL-2+ cells among different cell populations, measured among PBMCs by flow cytometry. IL-2 frequency was explored among: CD4, CD8+ and $\gamma\delta$ T cells (**A, B** and **C**), Va7.2+ CD8+ T cells (**D**), CD16+/CD56+ CD3-CD8+ lymphocytes (NK cells, **E** and **F**), CD16+/CD56+ CD3+ T cells (NKT-L, **G**-**I**), CD14+/CD16+ non-lymphocyte cells (**J**-**L**). Correlation co-efficient ('CC'), significance ('Sig.') and number of values included in each comparison ('N') are shown at each combination of time points. PB2 is shown in blue, as this time point was only analysed by ELISpot.*

A **ELISpot vs PBMC IL-17 CD4**

PBMC IL-17 CD4		ELISpot PB2	ELISpot PB1	ELISpot Wk2	ELISpot Wk4	ELISpot Wk9	ELISpot Wk12	ELISpot Wk16
PB1	CC	-0.507	0.317	-0.101	-0.406	0.228	0.875	0.279
	Sig.	0.199	0.444	0.811	0.318	0.587	0.004	0.503
	N	8	8	8	8	8	8	8
Wk2	CC	-0.359	0.225	0.189	0.218	-0.655	-0.410	-0.272
	Sig.	0.172	0.402	0.482	0.417	0.006	0.115	0.307
	N	16	16	16	16	16	16	16
Wk4	CC	0.504	-0.289	0.071	0.138	0.316	-0.086	0.344
	Sig.	0.047	0.278	0.795	0.610	0.233	0.752	0.192
	N	16	16	16	16	16	16	16
Wk9	CC							
	Sig.							
	N							
Wk12	CC	0.124	0.271	0.514	0.335	0.136	-0.437	-0.089
	Sig.	0.646	0.309	0.041	0.205	0.615	0.091	0.743
	N	16	16	16	16	16	16	16
Wk16	CC	0.546	0.355	-0.136	0.655	-0.218	-0.273	0.245
	Sig.	0.162	0.389	0.747	0.078	0.604	0.513	0.558
	N	8	8	8	8	8	8	8

B **ELISpot vs PBMC IL-17 CD8**

PBMC IL-17 CD8		ELISpot PB2	ELISpot PB1	ELISpot Wk2	ELISpot Wk4	ELISpot Wk9	ELISpot Wk12	ELISpot Wk16
PB1	CC	-0.913	-0.114	-0.469	-0.482	-0.507	0.355	-0.228
	Sig.	0.002	0.788	0.241	0.226	0.199	0.388	0.587
	N	8	8	8	8	8	8	8
Wk2	CC	-0.422	0.184	0.299	-0.015	0.184	-0.085	-0.314
	Sig.	0.104	0.494	0.261	0.956	0.494	0.755	0.236
	N	16	16	16	16	16	16	16
Wk4	CC	0.435	0.096	-0.238	-0.016	-0.216	-0.413	0.361
	Sig.	0.092	0.723	0.375	0.952	0.421	0.112	0.169
	N	16	16	16	16	16	16	16
Wk9	CC	-0.199	0.445	0.412	0.499	-0.314	-0.095	-0.033
	Sig.	0.459	0.084	0.113	0.049	0.236	0.727	0.903
	N	16	16	16	16	16	16	16
Wk12	CC	0.201	0.077	0.447	0.581	0.201	-0.419	0.177
	Sig.	0.456	0.778	0.082	0.018	0.456	0.106	0.512
	N	16	16	16	16	16	16	16
Wk16	CC	0.095	-0.381	-0.524	-0.690	0.238	0.333	-0.024
	Sig.	0.823	0.352	0.183	0.058	0.570	0.420	0.955
	N	8	8	8	8	8	8	8

C **ELISpot vs PBMC IL-17 gd**

PBMC IL-17 gd		ELISpot PB2	ELISpot PB1	ELISpot Wk2	ELISpot Wk4	ELISpot Wk9	ELISpot Wk12	ELISpot Wk16
PB1	CC	-0.082	0.327	0.109	-0.300	0.627	0.600	-0.136
	Sig.	0.847	0.429	0.797	0.470	0.096	0.116	0.747
	N	8	8	8	8	8	8	8
Wk2	CC	-0.290	0.236	0.150	0.039	0.151	-0.134	-0.148
	Sig.	0.276	0.378	0.578	0.885	0.577	0.620	0.584
	N	16	16	16	16	16	16	16
Wk4	CC	-0.065	0.388	0.606	0.523	0.061	-0.141	0.059
	Sig.	0.810	0.138	0.013	0.038	0.823	0.603	0.827
	N	16	16	16	16	16	16	16
Wk9	CC	0.195	0.336	0.079	0.174	-0.033	-0.166	0.143
	Sig.	0.469	0.203	0.770	0.520	0.904	0.539	0.597
	N	16	16	16	16	16	16	16
Wk12	CC	0.086	0.186	0.404	0.552	-0.130	-0.347	0.270
	Sig.	0.753	0.490	0.121	0.027	0.632	0.188	0.312
	N	16	16	16	16	16	16	16
Wk16	CC	0.026	0.404	-0.065	-0.287	0.143	0.717	0.496
	Sig.	0.951	0.321	0.878	0.491	0.735	0.045	0.212
	N	8	8	8	8	8	8	8

D **ELISpot vs PBMC IL-17 Va7.2+**

PBMC IL-17 MAIT 7.2+		ELISpot PB2	ELISpot PB1	ELISpot Wk2	ELISpot Wk4	ELISpot Wk9	ELISpot Wk12	ELISpot Wk16
PB1	CC	-0.109	-0.300	-0.082	0.027	0.245	0.000	-0.436
	Sig.	0.797	0.470	0.847	0.949	0.558	1.000	0.280
	N	8	8	8	8	8	8	8
Wk2	CC	-0.097	-0.169	-0.139	-0.084	0.230	0.055	0.181
	Sig.	0.720	0.532	0.606	0.756	0.391	0.839	0.501
	N	16	16	16	16	16	16	16
Wk4	CC	-0.055	0.006	0.130	0.191	-0.120	0.055	0.065
	Sig.	0.839	0.981	0.632	0.478	0.658	0.839	0.811
	N	16	16	16	16	16	16	16
Wk9	CC	-0.284	0.192	0.098	-0.085	-0.120	0.220	-0.415
	Sig.	0.286	0.475	0.719	0.754	0.659	0.412	0.110
	N	16	16	16	16	16	16	16
Wk12	CC	-0.051	0.264	-0.082	-0.108	-0.150	-0.367	0.193
	Sig.	0.852	0.324	0.763	0.690	0.578	0.162	0.475
	N	16	16	16	16	16	16	16
Wk16	CC	-0.048	0.048	0.571	-0.238	0.643	0.619	-0.429
	Sig.	0.911	0.911	0.139	0.570	0.086	0.102	0.289
	N	8	8	8	8	8	8	8

E **ELISpot vs PBMC IL-17 NK 16+56-**

PBMC IL-17 NK 16+56-		ELISpot PB2	ELISpot PB1	ELISpot Wk2	ELISpot Wk4	ELISpot Wk9	ELISpot Wk12	ELISpot Wk16
PB1	CC	-0.873	0.055	-0.518	-0.518	-0.682	0.464	0.055
	Sig.	0.005	0.898	0.188	0.188	0.062	0.247	0.898
	N	8	8	8	8	8	8	8
Wk2	CC	-0.226	-0.085	0.053	-0.115	-0.057	-0.319	-0.360
	Sig.	0.400	0.755	0.844	0.672	0.835	0.229	0.171
	N	16	16	16	16	16	16	16
Wk4	CC	0.246	-0.014	-0.033	0.011	0.287	-0.361	0.175
	Sig.	0.358	0.960	0.905	0.969	0.281	0.169	0.516
	N	16	16	16	16	16	16	16
Wk9	CC	-0.084	0.252	0.308	0.420	-0.084	-0.196	-0.364
	Sig.	0.757	0.346	0.245	0.105	0.757	0.467	0.166
	N	16	16	16	16	16	16	16
Wk12	CC	0.168	0.062	0.362	0.481	0.103	-0.516	0.168
	Sig.	0.534	0.820	0.169	0.059	0.704	0.041	0.534
	N	16	16	16	16	16	16	16
Wk16	CC	0.132	-0.419	0.132	-0.407	0.695	0.611	-0.503
	Sig.	0.756	0.301	0.756	0.317	0.056	0.108	0.204
	N	8	8	8	8	8	8	8

F **ELISpot vs PBMC IL-17 NK 16-56+**

PBMC IL-17 NK 16-56+		ELISpot PB2	ELISpot PB1	ELISpot Wk2	ELISpot Wk4	ELISpot Wk9	ELISpot Wk12	ELISpot Wk16
PB1	CC	0.393	-0.685	0.469	0.634	-0.013	-0.355	-0.621
	Sig.	0.335	0.061	0.241	0.091	0.976	0.388	0.100
	N	8	8	8	8	8	8	8
Wk2	CC	0.262	-0.488	-0.027	-0.093	0.405	0.423	-0.085
	Sig.	0.326	0.055	0.922	0.733	0.119	0.103	0.755
	N	16	16	16	16	16	16	16
Wk4	CC	0.105	-0.583	0.037	0.082	0.306	0.093	-0.608
	Sig.	0.698	0.018	0.892	0.764	0.249	0.733	0.012
	N	16	16	16	16	16	16	16
Wk9	CC	-0.151	-0.052	-0.212	0.216	-0.237	0.017	0.276
	Sig.	0.577	0.849	0.432	0.422	0.376	0.949	0.301
	N	16	16	16	16	16	16	16
Wk12	CC	0.500	-0.045	0.453	0.427	0.515	0.080	0.121
	Sig.	0.049	0.870	0.078	0.099	0.041	0.768	0.656
	N	16	16	16	16	16	16	16
Wk16	CC	0.073	-0.512	-0.756	-0.317	-0.073	-0.439	-0.049
	Sig.	0.863	0.194	0.030	0.444	0.863	0.276	0.909
	N	8	8	8	8	8	8	8

G **ELISpot vs PBMC IL-17 NKT 16+**

PBMC IL-17 NKT 16+		ELISpot PB2	ELISpot PB1	ELISpot Wk2	ELISpot Wk4	ELISpot Wk9	ELISpot Wk12	ELISpot Wk16
PB1	CC	0.049	0.488	0.073	-0.024	-0.415	-0.122	0.781
	Sig.	0.909	0.220	0.863	0.954	0.307	0.774	0.022
	N	8	8	8	8	8	8	8
Wk2	CC	-0.242	0.027	-0.230	-0.370	0.203	0.012	-0.036
	Sig.	0.367	0.921	0.391	0.158	0.451	0.965	0.895
	N	16	16	16	16	16	16	16
Wk4	CC	-0.872	0.200	0.479	0.358	-0.326	0.027	-0.378
	Sig.	0.000	0.459	0.061	0.173	0.217	0.920	0.149
	N	16	16	16	16	16	16	16
Wk9	CC	-0.526	0.097	0.302	0.529	-0.186	-0.089	-0.147
	Sig.	0.037	0.722	0.255	0.035	0.490	0.742	0.588
	N	16	16	16	16	16	16	16
Wk12	CC	0.171	-0.274	0.388	0.711	0.325	-0.508	0.071
	Sig.	0.527	0.304	0.137	0.002	0.219	0.044	0.795
	N	16	16	16	16	16	16	16
Wk16	CC	-0.905	-0.143	0.333	-0.357	-0.286	0.000	-0.310
	Sig.	0.002	0.736	0.420	0.385	0.493	1.000	0.456
	N	8	8	8	8	8	8	8

H **ELISpot vs PBMC IL-17 NKT 56+**

PBMC IL-17 NKT 56+		ELISpot PB2	ELISpot PB1	ELISpot Wk2	ELISpot Wk4	ELISpot Wk9	ELISpot Wk12	ELISpot Wk16
PB1	CC	0.228	0.063	0.545	0.266	0.761	0.101	0.038
	Sig.	0.587	0.881	0.162	0.524	0.028	0.811	0.929
	N	8	8	8	8	8	8	8
Wk2	CC	0.307	0.063	-0.017	-0.237	0.254	-0.205	0.151
	Sig.	0.248	0.818	0.951	0.377	0.343	0.445	0.577
	N	16	16	16	16	16	16	16
Wk4	CC	-0.655	0.328	0.692	0.115	0.000	0.221	-0.360
	Sig.	0.006	0.215	0.003	0.671	1.000	0.410	0.171
	N	16	16	16	16	16	16	16
Wk9	CC	-0.600	0.319	0.398	0.436	-0.005	0.133	0.034
	Sig.	0.014	0.229	0.127	0.091	0.985	0.622	0.901
	N	16	16	16	16	16	16	16
Wk12	CC	0.094	-0.138	0.153	0.580	0.068	-0.497	0.209
	Sig.	0.729	0.611	0.571	0.019	0.803	0.050	0.437
	N	16	16	16	16	16	16	16
Wk16	CC	-0.279	-0.304	-0.101	0.051	-0.495	-0.469	0.013
	Sig.	0.503	0.464	0.811	0.905	0.213	0.241	0.976
	N	8	8	8	8	8	8	8

I **ELISpot vs PBMC IL-17 NKT ++**

PBMC IL-17 NKT ++		ELISpot PB2	ELISpot PB1	ELISpot Wk2	ELISpot Wk4	ELISpot Wk9	ELISpot Wk12	ELISpot Wk16
PB1	CC	-0.293	0.586	-0.073	-0.366	-0.610	-0.073	0.293
	Sig.	0.482	0.127	0.863	0.373	0.108	0.863	0.482
	N	8	8	8	8	8	8	8
Wk2	CC	0.327	-0.138	-0.431	-0.456	0.050	-0.207	-0.019
	Sig.	0.217	0.610	0.095	0.076	0.853	0.442	0.943
	N	16	16	16	16	16	16	16
Wk4	CC	-0.875	0.237	0.519	0.313	-0.307	-0.018	-0.461
	Sig.	0.000	0.378	0.039	0.238	0.247	0.946	0.073
	N	16	16	16	16	16	16	16
Wk9	CC	-0.609	0.358	0.424	0.394	-0.104	0.261	0.031
	Sig.	0.012	0.174	0.102	0.131	0.702	0.329	0.908
	N	16	16	16	16	16	16	16
Wk12	CC	0.127	-0.471	-0.163	0.225	-0.066	-0.356	-0.169
	Sig.	0.640	0.065	0.545	0.402	0.807	0.176	0.531
	N	16	16	16	16	16	16	16
Wk16	CC	-0.738	-0.429	-0.024	-0.357	-0.381	-0.190	-0.333
	Sig.	0.037	0.289	0.955	0.385	0.352	0.651	0.420
	N	8	8	8	8	8	8	8

J **ELISpot vs PBMC IL-17 nonL ++**

PBMC IL-17 nonL ++		ELISpot PB2	ELISpot PB1	ELISpot Wk2	ELISpot Wk4	ELISpot Wk9	ELISpot Wk12	ELISpot Wk16
PB1	CC	-0.109	-0.245	0.164	0.191	-0.245	-0.518	-0.327
	Sig.	0.797	0.558	0.699	0.651	0.558	0.188	0.429
	N	8	8	8	8	8	8	8
Wk2	CC	-0.275	0.293	0.268	0.182	-0.343	0.175	0.136
	Sig.	0.302	0.270	0.315	0.499	0.193	0.516	0.616
	N	16	16	16	16	16	16	16
Wk4	CC	0.005	0.135	0.375	0.176	0.412	0.189	-0.193
	Sig.	0.985	0.617	0.152	0.515	0.113	0.483	0.475
	N	16	16	16	16	16	16	16
Wk9	CC	-0.196	0.364	0.252	0.252	-0.364	0.084	0.364
	Sig.	0.467	0.165	0.346	0.346	0.166	0.757	0.166
	N	16	16	16	16	16	16	16
Wk12	CC	0.176	0.066	0.433	0.472	0.113	-0.466	-0.078
	Sig.	0.514	0.809	0.094	0.065	0.676	0.069	0.775
	N	16	16	16	16	16	16	16
Wk16	CC	0.082	0.412	0.082	0.247	-0.412	0.247	0.412
	Sig.	0.846	0.310	0.846	0.555	0.310	0.555	0.310
	N	8	8	8	8	8	8	8

K **ELISpot vs PBMC IL-17 nonL 14+16-**

PBMC IL-17 nonL +-		ELISpot PB2	ELISpot PB1	ELISpot Wk2	ELISpot Wk4	ELISpot Wk9	ELISpot Wk12	ELISpot Wk16
PB1	CC	-0.245	-0.109	0.300	0.327	-0.109	0.027	0.627
	Sig.	0.558	0.797	0.470	0.429	0.797	0.949	0.096
	N	8	8	8	8	8	8	8
Wk2	CC	0.519	-0.040	-0.001	0.461	-0.125	-0.504	0.374
	Sig.	0.039	0.883	0.998	0.073	0.644	0.046	0.153
	N	16	16	16	16	16	16	16
Wk4	CC	-0.594	0.414	0.572	0.355	0.137	0.239	-0.233
	Sig.	0.015	0.111	0.021	0.177	0.612	0.373	0.385
	N	16	16	16	16	16	16	16
Wk9	CC	-0.337	0.392	0.328	0.541	-0.045	-0.113	0.136
	Sig.	0.202	0.133	0.216	0.030	0.867	0.676	0.615
	N	16	16	16	16	16	16	16
Wk12	CC	0.188	-0.104	-0.065	0.053	0.135	-0.141	0.068
	Sig.	0.485	0.700	0.812	0.846	0.617	0.602	0.803
	N	16	16	16	16	16	16	16
Wk16	CC	0.317	0.000	-0.073	-0.634	0.805	0.903	0.293
	Sig.	0.444	1.000	0.863	0.091	0.016	0.002	0.482
	N	8	8	8	8	8	8	8

L **ELISpot vs PBMC IL-17 nonL 14-16+**

PBMC IL-17 nonL 14-16+		ELISpot PB2	ELISpot PB1	ELISpot Wk2	ELISpot Wk4	ELISpot Wk9	ELISpot Wk12	ELISpot Wk16
PB1	CC	-0.082	-0.412	0.247	0.247	0.577	-0.082	-0.247
	Sig.	0.846	0.310	0.555	0.555	0.134	0.846	0.555
	N	8	8	8	8	8	8	8
Wk2	CC	0.337	0.115	-0.227	0.055	-0.165	-0.480	0.386
	Sig.	0.202	0.671	0.398	0.839	0.541	0.060	0.140
	N	16	16	16	16	16	16	16
Wk4	CC	0.009	0.112	0.211	0.062	0.112	-0.086	0.065
	Sig.	0.974	0.679	0.433	0.820	0.679	0.753	0.811
	N	16	16	16	16	16	16	16
Wk9	CC	-0.196	0.364	0.252	0.252	-0.364	0.084	0.364
	Sig.	0.467	0.165	0.346	0.346	0.166	0.757	0.166
	N	16	16	16	16	16	16	16
Wk12	CC	0.252	0.084	-0.308	-0.252	0.028	-0.420	0.196
	Sig.	0.346	0.757	0.245	0.346	0.918	0.105	0.467
	N	16	16	16	16	16	16	16
Wk16	CC	-0.279	-0.304	-0.101	0.051	-0.495	-0.469	0.013
	Sig.	0.503	0.464	0.811	0.905	0.213	0.241	0.976
	N	8	8	8	8	8	8	8

Supplementary Table 9 Correlations between IFNγ+ SFU and IL-17-positive cells among PBMCs

*Spearman's rank correlations were calculated between the IFNγ+ SFU frequency and the frequency of IL-17+ cells among different cell populations, measured among PBMCs by flow cytometry. IL-17 frequency was explored among: CD4, CD8+ and $\gamma\delta$ T cells (**A, B** and **C**), Va7.2+ CD8+ T cells (**D**), CD16+/CD56+ CD3-CD8+ lymphocytes (NK cells, **E** and **F**), CD16+/CD56+ CD3+ T cells (NKT-L, **G**-**I**), CD14+/CD16+ non-lymphocyte cells (**J**-**L**). Correlation co-efficient ('CC'), significance ('Sig.') and number of values included in each comparison ('N') are shown at each combination of time points. PB2 is shown in blue, as this time point was only analysed by ELISpot.*

A **ELISpot vs BAL IFNg CD4**

BAL IFNg CD4		ELISpot PB2	ELISpot PB1	ELISpot Wk2	ELISpot Wk4	ELISpot Wk9	ELISpot Wk12	ELISpot Wk16
PB1	CC	-0.319	-0.139	-0.160	-0.060	-0.451	0.113	0.063
	Sig.	0.228	0.608	0.554	0.826	0.080	0.676	0.818
	N	16	16	16	16	16	16	16
Wk2	CC	-0.253	-0.130	0.098	0.145	-0.447	-0.293	0.191
	Sig.	0.344	0.630	0.718	0.592	0.082	0.270	0.478
	N	16	16	16	16	16	16	16
Wk4	CC	-0.162	0.055	0.509	0.322	0.083	-0.280	-0.360
	Sig.	0.548	0.841	0.044	0.225	0.761	0.293	0.171
	N	16	16	16	16	16	16	16
Wk9	CC	0.068	-0.249	0.331	0.374	0.026	-0.265	-0.106
	Sig.	0.803	0.353	0.210	0.154	0.922	0.322	0.696
	N	16	16	16	16	16	16	16
Wk12	CC	-0.084	-0.140	0.137	-0.038	-0.110	-0.156	-0.116
	Sig.	0.757	0.605	0.613	0.888	0.684	0.564	0.668
	N	16	16	16	16	16	16	16
Wk16	CC	-0.153	-0.124	0.263	0.156	0.459	0.500	0.265
	Sig.	0.572	0.648	0.324	0.564	0.074	0.049	0.322
	N	16	16	16	16	16	16	16

B **ELISpot vs BAL IFNg CD8**

BAL IFNg CD8		ELISpot PB2	ELISpot PB1	ELISpot Wk2	ELISpot Wk4	ELISpot Wk9	ELISpot Wk12	ELISpot Wk16
PB1	CC	-0.141	0.022	-0.251	-0.218	-0.104	-0.059	-0.052
	Sig.	0.603	0.935	0.349	0.418	0.702	0.827	0.849
	N	16	16	16	16	16	16	16
Wk2	CC	-0.190	-0.150	0.188	0.047	-0.176	0.093	0.022
	Sig.	0.482	0.578	0.487	0.862	0.514	0.731	0.935
	N	16	16	16	16	16	16	16
Wk4	CC	0.302	-0.156	0.047	-0.139	0.328	0.033	-0.002
	Sig.	0.256	0.565	0.863	0.608	0.215	0.903	0.996
	N	16	16	16	16	16	16	16
Wk9	CC	0.427	-0.250	-0.080	0.155	-0.209	-0.425	-0.233
	Sig.	0.099	0.350	0.770	0.568	0.437	0.101	0.386
	N	16	16	16	16	16	16	16
Wk12	CC	-0.341	-0.049	0.028	-0.035	-0.018	-0.153	0.103
	Sig.	0.196	0.858	0.918	0.897	0.948	0.572	0.704
	N	16	16	16	16	16	16	16
Wk16	CC	-0.197	-0.218	0.049	-0.197	0.036	0.525	0.048
	Sig.	0.465	0.417	0.856	0.465	0.895	0.037	0.861
	N	16	16	16	16	16	16	16

C **ELISpot vs BAL IFNg gd**

BAL IFNg gd		ELISpot PB2	ELISpot PB1	ELISpot Wk2	ELISpot Wk4	ELISpot Wk9	ELISpot Wk12	ELISpot Wk16
PB1	CC	0.138	-0.052	-0.180	-0.528	0.012	-0.138	-0.243
	Sig.	0.610	0.848	0.505	0.035	0.964	0.610	0.365
	N	16	16	16	16	16	16	16
Wk2	CC	0.161	0.085	-0.342	-0.066	-0.248	-0.012	0.439
	Sig.	0.551	0.754	0.195	0.809	0.355	0.965	0.089
	N	16	16	16	16	16	16	16
Wk4	CC	0.254	-0.021	-0.294	-0.039	-0.254	-0.531	-0.075
	Sig.	0.343	0.939	0.269	0.887	0.343	0.034	0.784
	N	16	16	16	16	16	16	16
Wk9	CC	0.021	0.274	0.208	0.037	0.184	-0.092	-0.421
	Sig.	0.939	0.305	0.439	0.892	0.496	0.735	0.105
	N	16	16	16	16	16	16	16
Wk12	CC	-0.126	-0.077	-0.231	-0.147	-0.253	-0.232	-0.112
	Sig.	0.641	0.778	0.389	0.587	0.345	0.387	0.680
	N	16	16	16	16	16	16	16
Wk16	CC	-0.144	-0.204	-0.245	-0.259	-0.061	0.362	0.095
	Sig.	0.608	0.466	0.379	0.350	0.828	0.185	0.735
	N	15	15	15	15	15	15	15

D **ELISpot vs BAL IFNg Va7.2+**

BAL IFNg MAIT 7.2+		ELISpot PB2	ELISpot PB1	ELISpot Wk2	ELISpot Wk4	ELISpot Wk9	ELISpot Wk12	ELISpot Wk16
PB1	CC	-0.181	0.341	0.134	0.173	-0.302	-0.552	-0.233
	Sig.	0.502	0.196	0.621	0.523	0.256	0.027	0.385
	N	16	16	16	16	16	16	16
Wk2	CC	0.164	-0.390	-0.009	0.511	-0.236	-0.475	0.436
	Sig.	0.543	0.135	0.974	0.043	0.379	0.063	0.091
	N	16	16	16	16	16	16	16
Wk4	CC	0.161	-0.499	-0.592	-0.451	0.125	0.033	-0.069
	Sig.	0.551	0.049	0.016	0.080	0.644	0.904	0.801
	N	16	16	16	16	16	16	16
Wk9	CC	0.310	0.376	-0.158	-0.466	0.021	0.203	0.113
	Sig.	0.242	0.151	0.558	0.069	0.939	0.451	0.676
	N	16	16	16	16	16	16	16
Wk12	CC	-0.542	0.337	0.240	-0.164	-0.070	0.098	0.058
	Sig.	0.030	0.202	0.370	0.543	0.798	0.719	0.832
	N	16	16	16	16	16	16	16
Wk16	CC	0.418	-0.259	0.091	0.270	-0.118	-0.203	0.357
	Sig.	0.107	0.334	0.737	0.312	0.664	0.452	0.175
	N	16	16	16	16	16	16	16

E **ELISpot vs BAL IFNg NK 16+56-**

BAL IFNg NK 16+56-		ELISpot PB2	ELISpot PB1	ELISpot Wk2	ELISpot Wk4	ELISpot Wk9	ELISpot Wk12	ELISpot Wk16
PB1	CC	0.422	-0.115	-0.074	-0.049	0.248	0.309	-0.008
	Sig.	0.104	0.671	0.785	0.858	0.354	0.244	0.978
	N	16	16	16	16	16	16	16
Wk2	CC	-0.077	0.171	0.243	0.156	-0.268	-0.488	0.064
	Sig.	0.778	0.526	0.364	0.564	0.315	0.055	0.814
	N	16	16	16	16	16	16	16
Wk4	CC	-0.473	0.377	0.225	-0.077	-0.162	0.083	-0.323
	Sig.	0.064	0.150	0.402	0.776	0.548	0.760	0.223
	N	16	16	16	16	16	16	16
Wk9	CC	-0.253	0.155	0.139	-0.167	-0.033	0.068	-0.628
	Sig.	0.345	0.567	0.607	0.538	0.903	0.804	0.009
	N	16	16	16	16	16	16	16
Wk12	CC	-0.229	-0.093	0.415	-0.029	0.647	0.429	-0.265
	Sig.	0.394	0.732	0.110	0.916	0.007	0.097	0.322
	N	16	16	16	16	16	16	16
Wk16	CC	-0.110	0.114	0.258	0.169	-0.042	0.091	-0.006
	Sig.	0.685	0.676	0.335	0.533	0.877	0.738	0.981
	N	16	16	16	16	16	16	16

F **ELISpot vs BAL IFNg NK 16-56+**

BAL IFNg NK 16-56+		ELISpot PB2	ELISpot PB1	ELISpot Wk2	ELISpot Wk4	ELISpot Wk9	ELISpot Wk12	ELISpot Wk16
PB1	CC	-0.207	0.203	-0.010	-0.480	0.156	0.321	0.081
	Sig.	0.441	0.451	0.971	0.060	0.565	0.226	0.765
	N	16	16	16	16	16	16	16
Wk2	CC	-0.215	-0.332	0.022	0.030	-0.564	-0.093	-0.212
	Sig.	0.424	0.210	0.934	0.913	0.023	0.733	0.431
	N	16	16	16	16	16	16	16
Wk4	CC	0.142	-0.199	-0.515	-0.134	-0.296	-0.343	0.199
	Sig.	0.600	0.461	0.041	0.620	0.266	0.194	0.459
	N	16	16	16	16	16	16	16
Wk9	CC	-0.124	-0.240	0.036	0.494	-0.284	-0.310	0.518
	Sig.	0.648	0.370	0.896	0.052	0.287	0.243	0.040
	N	16	16	16	16	16	16	16
Wk12	CC	0.021	0.046	-0.236	-0.283	0.176	0.618	0.132
	Sig.	0.939	0.866	0.379	0.288	0.514	0.011	0.626
	N	16	16	16	16	16	16	16
Wk16	CC	0.011	-0.011	0.019	0.201	-0.041	0.451	0.456
	Sig.	0.968	0.968	0.945	0.455	0.881	0.080	0.076
	N	16	16	16	16	16	16	16

G **ELISpot vs BAL IFNg NKT 16+**

BAL IFNg NKT 16+		ELISpot PB2	ELISpot PB1	ELISpot Wk2	ELISpot Wk4	ELISpot Wk9	ELISpot Wk12	ELISpot Wk16
PB1	CC	0.051	0.412	0.102	-0.038	0.051	0.192	-0.184
	Sig.	0.851	0.113	0.706	0.888	0.851	0.477	0.495
	N	16	16	16	16	16	16	16
Wk2	CC	-0.207	0.154	0.244	0.088	-0.370	-0.077	-0.097
	Sig.	0.441	0.570	0.362	0.747	0.158	0.777	0.721
	N	16	16	16	16	16	16	16
Wk4	CC	-0.193	0.281	0.498	0.270	-0.055	-0.310	-0.295
	Sig.	0.473	0.292	0.050	0.312	0.839	0.242	0.268
	N	16	16	16	16	16	16	16
Wk9	CC	-0.115	0.564	0.309	0.162	0.047	-0.471	0.001
	Sig.	0.672	0.023	0.244	0.549	0.863	0.066	0.996
	N	16	16	16	16	16	16	16
Wk12	CC	-0.234	0.395	0.297	0.302	-0.295	-0.267	-0.139
	Sig.	0.383	0.130	0.265	0.255	0.268	0.318	0.607
	N	16	16	16	16	16	16	16
Wk16	CC	-0.060	0.243	-0.069	-0.227	-0.021	0.006	0.075
	Sig.	0.826	0.363	0.800	0.398	0.939	0.982	0.784
	N	16	16	16	16	16	16	16

H **ELISpot vs BAL IFNg NKT 56+**

BAL IFNg NKT 56+		ELISpot PB2	ELISpot PB1	ELISpot Wk2	ELISpot Wk4	ELISpot Wk9	ELISpot Wk12	ELISpot Wk16
PB1	CC	-0.162	-0.033	-0.264	-0.057	-0.263	-0.362	0.239
	Sig.	0.550	0.903	0.322	0.833	0.326	0.168	0.374
	N	16	16	16	16	16	16	16
Wk2	CC	0.043	-0.176	0.231	0.099	-0.064	-0.240	0.243
	Sig.	0.874	0.513	0.389	0.715	0.815	0.371	0.365
	N	16	16	16	16	16	16	16
Wk4	CC	0.263	-0.079	-0.112	-0.364	0.305	0.290	-0.143
	Sig.	0.326	0.771	0.680	0.165	0.251	0.277	0.596
	N	16	16	16	16	16	16	16
Wk9	CC	-0.018	0.047	0.122	-0.034	-0.082	-0.259	-0.286
	Sig.	0.948	0.862	0.652	0.901	0.762	0.333	0.284
	N	16	16	16	16	16	16	16
Wk12	CC	-0.159	-0.035	-0.153	-0.265	-0.206	-0.124	-0.091
	Sig.	0.557	0.897	0.571	0.322	0.444	0.649	0.737
	N	16	16	16	16	16	16	16
Wk16	CC	-0.156	-0.079	-0.347	-0.447	-0.249	0.520	0.104
	Sig.	0.565	0.772	0.188	0.082	0.353	0.039	0.702
	N	16	16	16	16	16	16	16

I **ELISpot vs BAL IFNg NKT ++**

BAL IFNg NKT ++		ELISpot PB2	ELISpot PB1	ELISpot Wk2	ELISpot Wk4	ELISpot Wk9	ELISpot Wk12	ELISpot Wk16
PB1	CC	0.000	0.000	0.000	0.000	0.000	0.000	0.000
	Sig.	0.000	0.000	0.000	0.000	0.000	0.000	0.000
	N	16	16	16	16	16	16	16
Wk2	CC	-0.049	-0.011	0.115	0.052	-0.185	-0.143	-0.369
	Sig.	0.858	0.967	0.671	0.849	0.493	0.598	0.159
	N	16	16	16	16	16	16	16
Wk4	CC	0.142	0.276	-0.188	-0.168	-0.177	0.263	0.147
	Sig.	0.599	0.300	0.486	0.533	0.512	0.325	0.588
	N	16	16	16	16	16	16	16
Wk9	CC	0.327	0.493	0.126	-0.145	0.207	-0.044	-0.109
	Sig.	0.234	0.062	0.656	0.605	0.458	0.877	0.699
	N	15	15	15	15	15	15	15
Wk12	CC	-0.411	0.208	0.083	0.260	-0.462	-0.119	-0.143
	Sig.	0.114	0.440	0.760	0.331	0.072	0.660	0.596
	N	16	16	16	16	16	16	16
Wk16	CC	-0.253	0.238	0.101	0.005	0.113	0.221	0.100
	Sig.	0.344	0.374	0.711	0.985	0.676	0.410	0.713
	N	16	16	16	16	16	16	16

J **ELISpot vs BAL IFNg nonL ++**

BAL IFNg nonL ++		ELISpot PB2	ELISpot PB1	ELISpot Wk2	ELISpot Wk4	ELISpot Wk9	ELISpot Wk12	ELISpot Wk16
PB1	CC	-0.420	0.196	0.140	0.028	-0.420	-0.308	-0.140
	Sig.	0.105	0.466	0.605	0.918	0.105	0.246	0.605
	N	16	16	16	16	16	16	16
Wk2	CC	0.081	-0.196	0.037	0.407	-0.176	-0.395	0.024
	Sig.	0.765	0.467	0.891	0.117	0.515	0.130	0.931
	N	16	16	16	16	16	16	16
Wk4	CC	0.220	-0.003	-0.472	-0.042	-0.146	-0.412	0.285
	Sig.	0.412	0.990	0.065	0.877	0.590	0.113	0.284
	N	16	16	16	16	16	16	16
Wk9	CC	0.168	0.315	0.035	-0.214	0.014	0.033	0.158
	Sig.	0.534	0.234	0.898	0.425	0.960	0.904	0.558
	N	16	16	16	16	16	16	16
Wk12	CC	-0.084	-0.323	0.442	0.345	0.054	-0.270	-0.311
	Sig.	0.757	0.222	0.086	0.190	0.843	0.311	0.240
	N	16	16	16	16	16	16	16
Wk16	CC	0.196	-0.364	-0.028	0.084	0.364	-0.028	-0.028
	Sig.	0.467	0.165	0.918	0.757	0.166	0.918	0.918
	N	16	16	16	16	16	16	16

K **ELISpot vs BAL IFNg nonL 14+16-**

BAL IFNg nonL +-		ELISpot PB2	ELISpot PB1	ELISpot Wk2	ELISpot Wk4	ELISpot Wk9	ELISpot Wk12	ELISpot Wk16
PB1	CC	-0.444	-0.073	0.462	0.298	0.056	-0.022	-0.677
	Sig.	0.085	0.787	0.072	0.263	0.837	0.937	0.004
	N	16	16	16	16	16	16	16
Wk2	CC	0.398	-0.229	-0.395	-0.290	-0.091	0.131	-0.267
	Sig.	0.127	0.393	0.130	0.276	0.738	0.628	0.318
	N	16	16	16	16	16	16	16
Wk4	CC	0.050	0.147	0.100	0.079	-0.361	-0.232	0.204
	Sig.	0.854	0.588	0.712	0.772	0.169	0.386	0.449
	N	16	16	16	16	16	16	16
Wk9	CC	0.163	0.249	-0.121	0.033	0.006	-0.346	0.017
	Sig.	0.546	0.353	0.656	0.903	0.982	0.190	0.951
	N	16	16	16	16	16	16	16
Wk12	CC	-0.078	0.295	-0.239	-0.375	-0.274	-0.127	0.020
	Sig.	0.775	0.267	0.372	0.152	0.305	0.640	0.941
	N	16	16	16	16	16	16	16
Wk16	CC	-0.262	0.332	-0.149	-0.376	-0.314	0.009	-0.131
	Sig.	0.387	0.268	0.628	0.206	0.295	0.977	0.670
	N	13	13	13	13	13	13	13

L **ELISpot vs BAL IFNg nonL 14-16+**

BAL IFNg nonL 14-16+		ELISpot PB2	ELISpot PB1	ELISpot Wk2	ELISpot Wk4	ELISpot Wk9	ELISpot Wk12	ELISpot Wk16
PB1	CC	0.000	0.000	0.000	0.000	0.000	0.000	0.000
	Sig.	0.000	0.000	0.000	0.000	0.000	0.000	0.000
	N	15	15	15	15	15	15	15
Wk2	CC	-0.186	0.371	0.248	0.247	-0.371	0.062	0.371
	Sig.	0.508	0.173	0.373	0.374	0.173	0.827	0.173
	N	15	15	15	15	15	15	15
Wk4	CC	-0.062	0.248	0.310	0.433	-0.062	-0.186	-0.371
	Sig.	0.827	0.373	0.262	0.107	0.827	0.508	0.173
	N	15	15	15	15	15	15	15
Wk9	CC	-0.581	0.105	0.578	0.126	0.110	0.239	-0.203
	Sig.	0.018	0.698	0.019	0.643	0.685	0.373	0.452
	N	16	16	16	16	16	16	16
Wk12	CC	-0.406	0.178	-0.006	-0.230	-0.269	0.406	0.075
	Sig.	0.119	0.510	0.982	0.392	0.314	0.119	0.784
	N	16	16	16	16	16	16	16
Wk16	CC	-0.288	0.629	0.524	0.035	0.105	0.358	0.262
	Sig.	0.339	0.021	0.066	0.910	0.733	0.230	0.387
	N	13	13	13	13	13	13	13

Supplementary Table 10 Correlations between IFNγ+ SFU and IFNγ-positive cells among BAL

*Spearman's rank correlations were calculated between IFNγ SFU frequency and the frequency of IFNγ+ cells among different cell populations, measured among BAL by flow cytometry. IFNγ frequency was explored among: CD4, CD8+ and $\gamma\delta$ T cells (**A, B** and **C**), Va7.2+ CD8+ T cells (**D**), CD16+/CD56+ CD3-CD8+ lymphocytes (NK cells, **E** and **F**), CD16+/CD56+ CD3+ T cells (NKT-L, **G-I**), CD14+/CD16+ non-lymphocyte cells (**J-L**). Correlation co-efficient ('CC'), significance ('Sig.') and number of values included in each comparison ('N') are shown at each combination of time points. PB2 is shown in blue, as this time point was only analysed by ELISpot.*

A **ELISpot vs BAL IL-2 CD4**

BAL IL-2 CD4		ELISpot PB2	ELISpot PB1	ELISpot Wk2	ELISpot Wk4	ELISpot Wk9	ELISpot Wk12	ELISpot Wk16
PB1	CC	-0.611	-0.143	0.114	0.257	-0.418	0.043	-0.189
	Sig.	0.016	0.611	0.685	0.355	0.121	0.879	0.499
	N	15	15	15	15	15	15	15
Wk2	CC	-0.502	0.242	0.295	0.378	-0.685	-0.180	-0.180
	Sig.	0.048	0.366	0.267	0.149	0.003	0.505	0.505
	N	16	16	16	16	16	16	16
Wk4	CC	-0.268	0.047	0.521	0.372	-0.029	-0.324	-0.425
	Sig.	0.315	0.862	0.038	0.156	0.914	0.220	0.101
	N	16	16	16	16	16	16	16
Wk9	CC	0.709	-0.284	-0.358	-0.221	-0.026	-0.109	0.165
	Sig.	0.002	0.286	0.174	0.412	0.922	0.688	0.542
	N	16	16	16	16	16	16	16
Wk12	CC	-0.235	-0.029	0.177	-0.071	-0.132	-0.100	-0.291
	Sig.	0.380	0.914	0.513	0.795	0.625	0.713	0.274
	N	16	16	16	16	16	16	16
Wk16	CC	0.000	-0.148	0.110	-0.137	0.538	0.379	0.115
	Sig.	1.000	0.629	0.721	0.655	0.058	0.201	0.707
	N	13	13	13	13	13	13	13

B **ELISpot vs BAL IL-2 CD8**

BAL IL-2 CD8		ELISpot PB2	ELISpot PB1	ELISpot Wk2	ELISpot Wk4	ELISpot Wk9	ELISpot Wk12	ELISpot Wk16
PB1	CC	-0.290	-0.184	-0.055	0.037	0.273	0.188	-0.009
	Sig.	0.295	0.512	0.845	0.896	0.325	0.502	0.974
	N	15	15	15	15	15	15	15
Wk2	CC	0.035	0.394	-0.154	-0.381	-0.030	0.618	0.329
	Sig.	0.896	0.131	0.568	0.146	0.914	0.011	0.213
	N	16	16	16	16	16	16	16
Wk4	CC	0.438	0.011	-0.120	-0.166	0.151	-0.059	0.280
	Sig.	0.090	0.969	0.657	0.538	0.576	0.828	0.294
	N	16	16	16	16	16	16	16
Wk9	CC	0.714	-0.381	-0.555	-0.230	-0.127	-0.038	0.044
	Sig.	0.002	0.146	0.026	0.391	0.640	0.888	0.871
	N	16	16	16	16	16	16	16
Wk12	CC	-0.332	0.037	-0.043	-0.179	0.006	0.006	0.176
	Sig.	0.208	0.892	0.875	0.506	0.983	0.983	0.513
	N	16	16	16	16	16	16	16
Wk16	CC	0.158	-0.220	-0.209	-0.390	-0.085	0.249	-0.073
	Sig.	0.606	0.469	0.493	0.188	0.783	0.413	0.811
	N	13	13	13	13	13	13	13

C **ELISpot vs BAL IL-2 gd**

BAL IL-2 gd		ELISpot PB2	ELISpot PB1	ELISpot Wk2	ELISpot Wk4	ELISpot Wk9	ELISpot Wk12	ELISpot Wk16
PB1	CC	-0.724	-0.122	0.244	0.194	-0.323	0.025	-0.086
	Sig.	0.002	0.665	0.381	0.489	0.241	0.929	0.761
	N	15	15	15	15	15	15	15
Wk2	CC	-0.170	0.199	-0.084	-0.400	-0.197	0.591	0.116
	Sig.	0.529	0.461	0.758	0.125	0.465	0.016	0.668
	N	16	16	16	16	16	16	16
Wk4	CC	0.045	0.191	0.185	0.084	0.024	-0.161	-0.278
	Sig.	0.869	0.478	0.492	0.758	0.930	0.551	0.298
	N	16	16	16	16	16	16	16
Wk9	CC	0.664	-0.082	-0.519	-0.547	0.035	0.025	0.087
	Sig.	0.005	0.761	0.039	0.028	0.897	0.927	0.749
	N	16	16	16	16	16	16	16
Wk12	CC	-0.100	0.118	-0.060	0.009	-0.147	-0.329	-0.306
	Sig.	0.713	0.664	0.824	0.974	0.587	0.213	0.249
	N	16	16	16	16	16	16	16
Wk16	CC	0.039	0.290	0.227	-0.160	0.241	-0.022	0.077
	Sig.	0.900	0.336	0.456	0.601	0.428	0.943	0.801
	N	13	13	13	13	13	13	13

D **ELISpot vs BAL IL-2 Va7.2+**

BAL IL-2 MAIT 7.2+		ELISpot PB2	ELISpot PB1	ELISpot Wk2	ELISpot Wk4	ELISpot Wk9	ELISpot Wk12	ELISpot Wk16
PB1	CC	-0.650	0.283	0.501	0.209	-0.174	0.053	-0.172
	Sig.	0.009	0.308	0.057	0.455	0.534	0.852	0.540
	N	15	15	15	15	15	15	15
Wk2	CC	0.110	0.116	-0.494	-0.175	-0.311	0.024	0.447
	Sig.	0.684	0.670	0.052	0.516	0.241	0.929	0.083
	N	16	16	16	16	16	16	16
Wk4	CC	0.009	0.152	-0.331	-0.650	-0.303	0.025	-0.064
	Sig.	0.972	0.573	0.211	0.006	0.254	0.926	0.813
	N	16	16	16	16	16	16	16
Wk9	CC	0.194	0.045	-0.120	-0.350	0.198	0.421	0.019
	Sig.	0.470	0.867	0.658	0.184	0.463	0.104	0.943
	N	16	16	16	16	16	16	16
Wk12	CC	-0.388	0.283	0.222	-0.094	0.088	0.098	0.086
	Sig.	0.137	0.288	0.408	0.730	0.747	0.718	0.751
	N	16	16	16	16	16	16	16
Wk16	CC	0.217	0.040	-0.147	-0.410	-0.078	0.101	0.107
	Sig.	0.477	0.896	0.631	0.164	0.800	0.742	0.728
	N	13	13	13	13	13	13	13

E **ELISpot vs BAL IL-2 NK 16+56-**

BAL IL-2 NK 16+56-		ELISpot PB2	ELISpot PB1	ELISpot Wk2	ELISpot Wk4	ELISpot Wk9	ELISpot Wk12	ELISpot Wk16
PB1	CC	0.000	0.000	0.000	0.000	0.000	0.000	0.000
	Sig.	0.000	0.000	0.000	0.000	0.000	0.000	0.000
	N	15	15	15	15	15	15	15
Wk2	CC	-0.141	0.143	0.141	-0.077	0.013	0.230	-0.146
	Sig.	0.603	0.597	0.603	0.778	0.963	0.391	0.590
	N	16	16	16	16	16	16	16
Wk4	CC	-0.184	0.224	0.208	-0.399	0.549	0.392	-0.159
	Sig.	0.495	0.404	0.440	0.126	0.028	0.133	0.557
	N	16	16	16	16	16	16	16
Wk9	CC	-0.068	-0.047	0.099	-0.058	0.107	0.233	-0.389
	Sig.	0.802	0.863	0.715	0.830	0.693	0.384	0.137
	N	16	16	16	16	16	16	16
Wk12	CC	0.082	-0.146	0.193	-0.204	0.522	0.028	-0.162
	Sig.	0.764	0.589	0.473	0.448	0.038	0.917	0.549
	N	16	16	16	16	16	16	16
Wk16	CC	0.322	-0.322	-0.282	-0.087	0.201	0.020	-0.208
	Sig.	0.283	0.283	0.351	0.777	0.510	0.948	0.495
	N	13	13	13	13	13	13	13

F **ELISpot vs BAL IL-2 NK 16-56+**

BAL IL-2 NK 16-56+		ELISpot PB2	ELISpot PB1	ELISpot Wk2	ELISpot Wk4	ELISpot Wk9	ELISpot Wk12	ELISpot Wk16
PB1	CC	-0.188	0.353	0.220	-0.188	0.211	0.238	-0.101
	Sig.	0.502	0.197	0.430	0.502	0.451	0.392	0.721
	N	15	15	15	15	15	15	15
Wk2	CC	-0.097	-0.367	-0.029	0.100	-0.100	0.081	-0.081
	Sig.	0.720	0.163	0.915	0.711	0.711	0.765	0.765
	N	16	16	16	16	16	16	16
Wk4	CC	-0.166	-0.234	0.498	0.212	0.356	0.098	-0.239
	Sig.	0.539	0.384	0.050	0.431	0.176	0.717	0.372
	N	16	16	16	16	16	16	16
Wk9	CC	0.448	-0.273	-0.018	0.147	0.080	0.255	0.255
	Sig.	0.082	0.305	0.946	0.586	0.769	0.341	0.341
	N	16	16	16	16	16	16	16
Wk12	CC	-0.308	0.182	0.216	0.156	0.089	0.032	-0.377
	Sig.	0.246	0.500	0.422	0.565	0.743	0.907	0.149
	N	16	16	16	16	16	16	16
Wk16	CC	0.030	0.340	-0.113	-0.113	0.072	0.370	0.251
	Sig.	0.923	0.255	0.712	0.712	0.816	0.213	0.408
	N	13	13	13	13	13	13	13

G **ELISpot vs BAL IL-2 NKT 16+**

BAL IL-2 NKT 16+		ELISpot PB2	ELISpot PB1	ELISpot Wk2	ELISpot Wk4	ELISpot Wk9	ELISpot Wk12	ELISpot Wk16
PB1	CC	0.000	0.000	0.000	0.000	0.000	0.000	0.000
	Sig.	0.000	0.000	0.000	0.000	0.000	0.000	0.000
	N	15	15	15	15	15	15	15
Wk2	CC	-0.305	0.307	-0.132	-0.155	-0.676	0.068	0.116
	Sig.	0.250	0.247	0.625	0.568	0.004	0.804	0.669
	N	16	16	16	16	16	16	16
Wk4	CC	0.043	-0.017	0.378	0.461	-0.114	-0.513	-0.439
	Sig.	0.874	0.950	0.149	0.073	0.675	0.042	0.089
	N	16	16	16	16	16	16	16
Wk9	CC	0.591	0.253	-0.244	-0.282	0.109	-0.303	0.015
	Sig.	0.016	0.344	0.362	0.289	0.688	0.254	0.957
	N	16	16	16	16	16	16	16
Wk12	CC	-0.121	0.645	0.249	-0.026	-0.029	0.068	-0.115
	Sig.	0.656	0.007	0.353	0.922	0.914	0.803	0.672
	N	16	16	16	16	16	16	16
Wk16	CC	-0.096	-0.082	-0.149	-0.356	0.064	-0.004	0.178
	Sig.	0.766	0.800	0.643	0.256	0.843	0.991	0.580
	N	12	12	12	12	12	12	12

H **ELISpot vs BAL IL-2 NKT 56+**

BAL IL-2 NKT 56+		ELISpot PB2	ELISpot PB1	ELISpot Wk2	ELISpot Wk4	ELISpot Wk9	ELISpot Wk12	ELISpot Wk16
PB1	CC	0.006	-0.097	-0.369	0.006	0.013	-0.218	0.072
	Sig.	0.984	0.731	0.176	0.984	0.964	0.436	0.799
	N	15	15	15	15	15	15	15
Wk2	CC	0.124	0.464	-0.031	-0.297	0.071	0.206	0.632
	Sig.	0.649	0.071	0.910	0.264	0.795	0.444	0.009
	N	16	16	16	16	16	16	16
Wk4	CC	0.054	-0.027	-0.421	-0.502	0.299	0.397	0.164
	Sig.	0.843	0.921	0.104	0.048	0.261	0.128	0.543
	N	16	16	16	16	16	16	16
Wk9	CC	0.626	-0.175	-0.511	-0.444	-0.118	-0.153	0.179
	Sig.	0.009	0.517	0.043	0.085	0.664	0.572	0.506
	N	16	16	16	16	16	16	16
Wk12	CC	-0.206	0.119	-0.171	-0.335	-0.141	-0.082	-0.026
	Sig.	0.444	0.660	0.527	0.204	0.602	0.762	0.922
	N	16	16	16	16	16	16	16
Wk16	CC	0.131	0.044	-0.312	-0.529	-0.138	0.218	0.210
	Sig.	0.686	0.893	0.324	0.077	0.669	0.497	0.512
	N	12	12	12	12	12	12	12

I **ELISpot vs BAL IL-2 NKT ++**

BAL IL-2 NKT ++		ELISpot PB2	ELISpot PB1	ELISpot Wk2	ELISpot Wk4	ELISpot Wk9	ELISpot Wk12	ELISpot Wk16
PB1	CC	0.000	0.000	0.000	0.000	0.000	0.000	0.000
	Sig.	0.000	0.000	0.000	0.000	0.000	0.000	0.000
	N	15	15	15	15	15	15	15
Wk2	CC	-0.420	0.196	0.140	0.028	-0.420	-0.308	-0.140
	Sig.	0.105	0.466	0.605	0.918	0.105	0.246	0.605
	N	16	16	16	16	16	16	16
Wk4	CC	-0.178	0.182	-0.076	-0.066	-0.350	-0.066	-0.062
	Sig.	0.510	0.501	0.779	0.809	0.184	0.809	0.820
	N	16	16	16	16	16	16	16
Wk9	CC	0.575	0.066	-0.221	-0.135	0.156	-0.342	-0.070
	Sig.	0.020	0.808	0.411	0.619	0.565	0.194	0.798
	N	16	16	16	16	16	16	16
Wk12	CC	-0.319	0.270	0.111	0.206	-0.233	-0.316	-0.107
	Sig.	0.228	0.311	0.684	0.444	0.385	0.232	0.692
	N	16	16	16	16	16	16	16
Wk16	CC	0.114	0.160	-0.039	-0.374	0.093	0.288	0.153
	Sig.	0.724	0.619	0.904	0.231	0.775	0.363	0.635
	N	12	12	12	12	12	12	12

J **ELISpot vs BAL IL-2 nonL ++**

BAL IL-2 nonL ++		ELISpot PB2	ELISpot PB1	ELISpot Wk2	ELISpot Wk4	ELISpot Wk9	ELISpot Wk12	ELISpot Wk16
PB1	CC	-0.371	-0.124	0.371	0.433	-0.124	-0.186	-0.371
	Sig.	0.173	0.660	0.173	0.107	0.660	0.508	0.173
	N	15	15	15	15	15	15	15
Wk2	CC	0.379	-0.555	-0.304	-0.136	0.011	0.197	0.039
	Sig.	0.148	0.026	0.252	0.616	0.969	0.465	0.885
	N	16	16	16	16	16	16	16
Wk4	CC	0.020	0.024	-0.028	0.135	-0.591	-0.371	-0.093
	Sig.	0.940	0.929	0.919	0.618	0.016	0.158	0.733
	N	16	16	16	16	16	16	16
Wk9	CC	-0.126	-0.125	-0.240	-0.198	-0.220	0.143	-0.146
	Sig.	0.641	0.645	0.371	0.463	0.412	0.598	0.590
	N	16	16	16	16	16	16	16
Wk12	CC	0.076	0.195	0.126	0.052	0.081	-0.103	-0.370
	Sig.	0.780	0.468	0.642	0.847	0.765	0.704	0.158
	N	16	16	16	16	16	16	16
Wk16	CC	0.367	-0.210	0.149	0.559	0.017	-0.210	-0.384
	Sig.	0.218	0.492	0.628	0.047	0.955	0.492	0.195
	N	13	13	13	13	13	13	13

K **ELISpot vs BAL IL-2 nonL 14+16-**

BAL IL-2 nonL +-		ELISpot PB2	ELISpot PB1	ELISpot Wk2	ELISpot Wk4	ELISpot Wk9	ELISpot Wk12	ELISpot Wk16
PB1	CC	-0.433	-0.121	0.501	0.444	0.305	0.102	-0.169
	Sig.	0.107	0.669	0.057	0.097	0.269	0.719	0.546
	N	15	15	15	15	15	15	15
Wk2	CC	0.677	-0.454	-0.182	-0.042	0.123	0.029	0.256
	Sig.	0.004	0.077	0.501	0.877	0.650	0.915	0.338
	N	16	16	16	16	16	16	16
Wk4	CC	0.154	-0.180	0.257	0.301	-0.092	0.107	0.071
	Sig.	0.570	0.505	0.337	0.257	0.734	0.692	0.795
	N	16	16	16	16	16	16	16
Wk9	CC	-0.462	0.119	0.031	0.090	-0.401	-0.019	-0.388
	Sig.	0.072	0.659	0.908	0.742	0.124	0.945	0.138
	N	16	16	16	16	16	16	16
Wk12	CC	-0.125	-0.064	0.103	0.298	-0.069	-0.472	-0.117
	Sig.	0.643	0.815	0.703	0.262	0.798	0.065	0.667
	N	16	16	16	16	16	16	16
Wk16	CC	0.185	-0.144	0.092	-0.069	0.465	0.225	-0.136
	Sig.	0.545	0.638	0.764	0.822	0.109	0.459	0.658
	N	13	13	13	13	13	13	13

L **ELISpot vs BAL IL-2 nonL 14-16+**

BAL IL-2 nonL 14-16+		ELISpot PB2	ELISpot PB1	ELISpot Wk2	ELISpot Wk4	ELISpot Wk9	ELISpot Wk12	ELISpot Wk16
PB1	CC	-0.237	0.092	0.281	0.291	-0.207	-0.202	0.041
	Sig.	0.394	0.744	0.310	0.293	0.460	0.471	0.885
	N	15	15	15	15	15	15	15
Wk2	CC	0.541	-0.281	-0.171	0.033	-0.070	-0.263	-0.099
	Sig.	0.030	0.291	0.526	0.904	0.798	0.326	0.717
	N	16	16	16	16	16	16	16
Wk4	CC	0.214	0.331	0.344	0.410	-0.035	-0.106	0.180
	Sig.	0.425	0.211	0.192	0.115	0.898	0.695	0.506
	N	16	16	16	16	16	16	16
Wk9	CC	0.079	0.104	0.383	0.259	0.058	0.058	-0.104
	Sig.	0.773	0.702	0.143	0.332	0.832	0.832	0.702
	N	16	16	16	16	16	16	16
Wk12	CC	0.057	0.072	0.132	0.039	0.079	0.164	0.182
	Sig.	0.833	0.792	0.625	0.885	0.772	0.543	0.499
	N	16	16	16	16	16	16	16
Wk16	CC	0.027	0.517	0.268	-0.074	0.195	0.557	0.208
	Sig.	0.931	0.071	0.375	0.811	0.524	0.048	0.495
	N	13	13	13	13	13	13	13

Supplementary Table 11 Correlations between IFNγ+ SFU and IL-2-positive cells among BAL

Spearman's rank correlations were calculated between IFNγ SFU and the frequency of IL-2+ cells among different cell populations, measured among PBMCs by flow cytometry. IL-2 frequency was explored among: CD4, CD8+ and $\gamma\delta$ T cells (A, B and C), Va7.2+ CD8+ T cells (D), CD16+/CD56+ CD3-CD8+ lymphocytes (NK cells, E and F), CD16+/CD56+ CD3+ T cells (NKT-L, G-I), CD14+/CD16+ non-lymphocyte cells (J-L). Correlation co-efficient ('CC'), significance ('Sig.') and number of values included in each comparison ('N') are shown at each combination of time points. PB2 is shown in blue, as this time point was only analysed by ELISpot.

A **ELISpot vs BAL IL-17 CD4**

BAL IL-17 CD4		ELISpot PB2	ELISpot PB1	ELISpot Wk2	ELISpot Wk4	ELISpot Wk9	ELISpot Wk12	ELISpot Wk16
PB1	CC	-0.110	-0.023	0.147	-0.031	-0.326	-0.303	-0.123
	Sig.	0.696	0.934	0.601	0.914	0.235	0.272	0.663
	N	15	15	15	15	15	15	15
Wk2	CC	-0.178	-0.097	0.399	0.178	0.389	0.357	-0.016
	Sig.	0.527	0.731	0.140	0.527	0.152	0.192	0.954
	N	15	15	15	15	15	15	15
Wk4	CC	-0.307	0.295	0.717	0.607	-0.018	-0.350	-0.161
	Sig.	0.265	0.286	0.003	0.016	0.950	0.201	0.567
	N	15	15	15	15	15	15	15
Wk9	CC	0.094	-0.233	0.252	0.262	-0.009	-0.359	-0.268
	Sig.	0.729	0.386	0.347	0.327	0.974	0.172	0.316
	N	16	16	16	16	16	16	16
Wk12	CC	-0.262	-0.087	0.250	-0.021	-0.174	-0.491	-0.462
	Sig.	0.327	0.749	0.350	0.940	0.520	0.053	0.072
	N	16	16	16	16	16	16	16
Wk16	CC	-0.297	-0.297	0.297	0.060	0.209	-0.187	-0.346
	Sig.	0.325	0.325	0.325	0.845	0.494	0.541	0.247
	N	13	13	13	13	13	13	13

B **ELISpot vs BAL IL-17 CD8**

BAL IL-17 CD8		ELISpot PB2	ELISpot PB1	ELISpot Wk2	ELISpot Wk4	ELISpot Wk9	ELISpot Wk12	ELISpot Wk16
PB1	CC	0.047	-0.314	-0.371	-0.093	-0.090	0.029	0.301
	Sig.	0.869	0.255	0.173	0.741	0.751	0.919	0.276
	N	15	15	15	15	15	15	15
Wk2	CC	0.058	0.047	0.073	-0.524	0.520	0.735	-0.265
	Sig.	0.837	0.867	0.797	0.045	0.047	0.002	0.339
	N	15	15	15	15	15	15	15
Wk4	CC	-0.081	0.050	0.294	-0.234	0.395	0.522	-0.258
	Sig.	0.774	0.860	0.288	0.401	0.145	0.046	0.353
	N	15	15	15	15	15	15	15
Wk9	CC	0.135	-0.277	-0.121	0.007	-0.132	-0.101	-0.294
	Sig.	0.618	0.299	0.656	0.978	0.626	0.710	0.270
	N	16	16	16	16	16	16	16
Wk12	CC	-0.419	0.319	0.037	-0.183	-0.106	-0.038	-0.032
	Sig.	0.106	0.229	0.892	0.498	0.695	0.888	0.905
	N	16	16	16	16	16	16	16
Wk16	CC	-0.780	0.211	0.332	0.182	-0.341	-0.217	-0.014
	Sig.	0.002	0.489	0.267	0.552	0.254	0.477	0.963
	N	13	13	13	13	13	13	13

C **ELISpot vs BAL IL-17 gd**

BAL IL-17 gd		ELISpot PB2	ELISpot PB1	ELISpot Wk2	ELISpot Wk4	ELISpot Wk9	ELISpot Wk12	ELISpot Wk16
PB1	CC	-0.240	0.335	-0.025	-0.254	0.004	0.509	0.333
	Sig.	0.389	0.222	0.929	0.360	0.990	0.053	0.225
	N	15	15	15	15	15	15	15
Wk2	CC	0.487	-0.175	-0.098	-0.371	0.506	0.455	-0.229
	Sig.	0.065	0.533	0.727	0.173	0.055	0.089	0.411
	N	15	15	15	15	15	15	15
Wk4	CC	-0.061	-0.445	0.030	0.115	0.079	-0.240	-0.789
	Sig.	0.829	0.097	0.914	0.684	0.780	0.389	0.000
	N	15	15	15	15	15	15	15
Wk9	CC	-0.030	0.063	0.131	0.124	0.065	-0.208	-0.445
	Sig.	0.912	0.818	0.629	0.648	0.811	0.439	0.084
	N	16	16	16	16	16	16	16
Wk12	CC	-0.535	0.147	0.264	0.177	0.095	0.094	-0.248
	Sig.	0.033	0.586	0.322	0.513	0.726	0.730	0.355
	N	16	16	16	16	16	16	16
Wk16	CC	-0.404	-0.066	0.066	0.276	-0.351	-0.407	0.041
	Sig.	0.171	0.831	0.831	0.362	0.240	0.167	0.895
	N	13	13	13	13	13	13	13

D **ELISpot vs BAL IL-17 Va7.2+**

BAL IL-17 MAIT 7.2+		ELISpot PB2	ELISpot PB1	ELISpot Wk2	ELISpot Wk4	ELISpot Wk9	ELISpot Wk12	ELISpot Wk16
PB1	CC	0.117	0.264	0.185	0.169	-0.410	-0.034	0.410
	Sig.	0.679	0.342	0.510	0.546	0.129	0.905	0.129
	N	15	15	15	15	15	15	15
Wk2	CC	-0.238	-0.111	0.079	0.010	0.151	0.329	-0.014
	Sig.	0.393	0.694	0.780	0.972	0.590	0.232	0.960
	N	15	15	15	15	15	15	15
Wk4	CC	-0.361	-0.158	-0.206	-0.350	-0.168	-0.047	-0.063
	Sig.	0.205	0.588	0.479	0.220	0.566	0.874	0.830
	N	14	14	14	14	14	14	14
Wk9	CC	-0.012	-0.280	-0.118	-0.341	0.233	0.267	-0.298
	Sig.	0.964	0.294	0.663	0.196	0.384	0.317	0.263
	N	16	16	16	16	16	16	16
Wk12	CC	0.012	0.348	0.024	-0.143	0.412	0.245	0.251
	Sig.	0.965	0.187	0.929	0.596	0.113	0.361	0.349
	N	16	16	16	16	16	16	16
Wk16	CC	0.108	-0.239	0.090	0.352	0.358	0.042	0.119
	Sig.	0.727	0.432	0.771	0.238	0.229	0.892	0.697
	N	13	13	13	13	13	13	13

E **ELISpot vs BAL IL-17 NK 16+56-**

BAL IL-17 NK 16+56-		ELISpot PB2	ELISpot PB1	ELISpot Wk2	ELISpot Wk4	ELISpot Wk9	ELISpot Wk12	ELISpot Wk16
PB1	CC	0.371	0.062	0.248	0.247	0.062	-0.371	0.247
	Sig.	0.173	0.826	0.373	0.374	0.827	0.173	0.374
	N	15	15	15	15	15	15	15
Wk2	CC	0.000	0.000	0.000	0.000	0.000	0.000	0.000
	Sig.	0.000	0.000	0.000	0.000	0.000	0.000	0.000
	N	15	15	15	15	15	15	15
Wk4	CC	0.174	0.197	-0.119	-0.339	0.399	0.165	0.014
	Sig.	0.535	0.481	0.672	0.216	0.141	0.557	0.961
	N	15	15	15	15	15	15	15
Wk9	CC	-0.225	0.201	0.202	0.211	-0.421	-0.213	-0.003
	Sig.	0.403	0.455	0.453	0.432	0.105	0.429	0.990
	N	16	16	16	16	16	16	16
Wk12	CC	0.102	0.230	0.172	-0.198	0.534	0.476	0.083
	Sig.	0.717	0.410	0.539	0.480	0.040	0.073	0.769
	N	15	15	15	15	15	15	15
Wk16	CC	0.138	-0.435	-0.060	0.157	0.103	-0.110	-0.360
	Sig.	0.653	0.137	0.847	0.609	0.737	0.721	0.227
	N	13	13	13	13	13	13	13

F **ELISpot vs BAL IL-17 NK 16-56+**

BAL IL-17 NK 16-56+		ELISpot PB2	ELISpot PB1	ELISpot Wk2	ELISpot Wk4	ELISpot Wk9	ELISpot Wk12	ELISpot Wk16
PB1	CC	-0.418	0.536	0.312	-0.099	-0.300	0.310	0.163
	Sig.	0.121	0.039	0.257	0.726	0.277	0.261	0.562
	N	15	15	15	15	15	15	15
Wk2	CC	0.612	-0.165	-0.137	0.020	0.218	-0.064	0.121
	Sig.	0.015	0.556	0.626	0.943	0.436	0.819	0.668
	N	15	15	15	15	15	15	15
Wk4	CC	-0.352	0.093	0.375	-0.069	0.144	0.283	-0.105
	Sig.	0.199	0.742	0.169	0.808	0.608	0.306	0.711
	N	15	15	15	15	15	15	15
Wk9	CC	0.234	-0.138	-0.253	-0.223	0.094	-0.006	-0.050
	Sig.	0.383	0.612	0.344	0.405	0.730	0.982	0.855
	N	16	16	16	16	16	16	16
Wk12	CC	-0.283	-0.039	-0.022	-0.218	-0.128	-0.226	-0.316
	Sig.	0.287	0.885	0.935	0.417	0.638	0.401	0.233
	N	16	16	16	16	16	16	16
Wk16	CC	-0.435	-0.182	0.401	-0.047	0.392	0.244	-0.388
	Sig.	0.137	0.552	0.175	0.879	0.186	0.421	0.190
	N	13	13	13	13	13	13	13

G **ELISpot vs BAL IL-17 NKT 16+**

BAL IL-17 NKT 16+		ELISpot PB2	ELISpot PB1	ELISpot Wk2	ELISpot Wk4	ELISpot Wk9	ELISpot Wk12	ELISpot Wk16
PB1	CC	0.101	-0.133	0.257	0.325	-0.014	-0.096	0.092
	Sig.	0.721	0.636	0.355	0.237	0.961	0.733	0.745
	N	15	15	15	15	15	15	15
Wk2	CC	0.040	-0.224	-0.036	-0.338	0.359	0.294	-0.443
	Sig.	0.887	0.423	0.898	0.217	0.189	0.287	0.098
	N	15	15	15	15	15	15	15
Wk4	CC	-0.591	0.477	0.396	0.564	-0.402	-0.362	-0.083
	Sig.	0.026	0.085	0.161	0.036	0.154	0.204	0.777
	N	14	14	14	14	14	14	14
Wk9	CC	-0.393	-0.096	0.493	0.575	0.033	-0.319	-0.347
	Sig.	0.184	0.754	0.087	0.040	0.915	0.288	0.246
	N	13	13	13	13	13	13	13
Wk12	CC	-0.408	0.408	0.398	0.226	-0.145	-0.121	-0.313
	Sig.	0.117	0.117	0.127	0.399	0.592	0.656	0.239
	N	16	16	16	16	16	16	16
Wk16	CC	-0.523	-0.205	0.317	0.321	-0.138	-0.414	-0.336
	Sig.	0.081	0.522	0.315	0.309	0.669	0.181	0.286
	N	12	12	12	12	12	12	12

H **ELISpot vs BAL IL-17 NKT 56+**

BAL IL-17 NKT 56+		ELISpot PB2	ELISpot PB1	ELISpot Wk2	ELISpot Wk4	ELISpot Wk9	ELISpot Wk12	ELISpot Wk16
PB1	CC	0.144	0.042	-0.164	0.184	0.054	-0.014	0.510
	Sig.	0.608	0.881	0.559	0.512	0.848	0.959	0.052
	N	15	15	15	15	15	15	15
Wk2	CC	0.066	-0.112	0.206	0.085	0.620	0.397	0.074
	Sig.	0.814	0.692	0.462	0.764	0.014	0.143	0.794
	N	15	15	15	15	15	15	15
Wk4	CC	-0.387	-0.408	0.139	0.271	-0.083	-0.163	-0.499
	Sig.	0.154	0.132	0.621	0.329	0.770	0.561	0.058
	N	15	15	15	15	15	15	15
Wk9	CC	-0.004	-0.032	0.158	0.127	0.037	-0.079	-0.332
	Sig.	0.987	0.907	0.559	0.638	0.892	0.773	0.209
	N	16	16	16	16	16	16	16
Wk12	CC	-0.504	0.469	0.128	0.021	0.012	0.022	0.218
	Sig.	0.047	0.067	0.638	0.939	0.965	0.935	0.418
	N	16	16	16	16	16	16	16
Wk16	CC	-0.315	0.081	0.188	0.075	0.017	-0.136	0.003
	Sig.	0.294	0.792	0.538	0.807	0.955	0.658	0.993
	N	13	13	13	13	13	13	13

I **ELISpot vs BAL IL-17 NKT ++**

BAL IL-17 NKT ++		ELISpot PB2	ELISpot PB1	ELISpot Wk2	ELISpot Wk4	ELISpot Wk9	ELISpot Wk12	ELISpot Wk16
PB1	CC	0.000	-0.232	-0.155	-0.077	-0.231	0.231	0.309
	Sig.	1.000	0.446	0.614	0.802	0.447	0.447	0.305
	N	13	13	13	13	13	13	13
Wk2	CC	-0.120	-0.179	0.335	0.045	0.425	0.241	-0.644
	Sig.	0.669	0.523	0.222	0.873	0.114	0.387	0.010
	N	15	15	15	15	15	15	15
Wk4	CC	-0.452	0.493	0.406	0.385	-0.567	-0.240	-0.056
	Sig.	0.091	0.062	0.133	0.156	0.028	0.389	0.842
	N	15	15	15	15	15	15	15
Wk9	CC	-0.360	-0.102	0.630	0.433	0.131	-0.102	-0.629
	Sig.	0.187	0.718	0.012	0.107	0.642	0.718	0.012
	N	15	15	15	15	15	15	15
Wk12	CC	-0.311	0.390	0.243	0.093	-0.089	-0.086	-0.397
	Sig.	0.241	0.135	0.364	0.732	0.742	0.752	0.128
	N	16	16	16	16	16	16	16
Wk16	CC	-0.098	-0.052	0.249	0.133	0.092	-0.046	-0.341
	Sig.	0.774	0.879	0.461	0.697	0.787	0.893	0.305
	N	11	11	11	11	11	11	11

J **ELISpot vs BAL IL-17 nonL ++**

BAL IL-17 nonL ++		ELISpot PB2	ELISpot PB1	ELISpot Wk2	ELISpot Wk4	ELISpot Wk9	ELISpot Wk12	ELISpot Wk16
PB1	CC	-0.126	0.077	0.657	0.168	0.600	0.225	-0.238
	Sig.	0.654	0.786	0.008	0.551	0.018	0.420	0.393
	N	15	15	15	15	15	15	15
Wk2	CC	0.210	-0.144	0.118	-0.360	0.550	0.690	0.022
	Sig.	0.452	0.609	0.675	0.188	0.034	0.004	0.938
	N	15	15	15	15	15	15	15
Wk4	CC	0.035	0.242	0.386	0.215	-0.020	0.446	0.036
	Sig.	0.903	0.384	0.155	0.442	0.944	0.096	0.898
	N	15	15	15	15	15	15	15
Wk9	CC	0.319	-0.251	-0.230	0.009	-0.143	-0.212	-0.248
	Sig.	0.228	0.348	0.391	0.974	0.596	0.431	0.355
	N	16	16	16	16	16	16	16
Wk12	CC	-0.442	-0.255	0.235	0.236	0.009	-0.147	-0.295
	Sig.	0.086	0.340	0.381	0.378	0.973	0.586	0.268
	N	16	16	16	16	16	16	16
Wk16	CC	0.428	-0.092	-0.237	-0.087	0.220	0.104	0.399
	Sig.	0.189	0.787	0.483	0.800	0.516	0.761	0.224
	N	11	11	11	11	11	11	11

K **ELISpot vs BAL IL-17 nonL 14+16-**

BAL IL-17 nonL +-		ELISpot PB2	ELISpot PB1	ELISpot Wk2	ELISpot Wk4	ELISpot Wk9	ELISpot Wk12	ELISpot Wk16
PB1	CC	-0.202	-0.226	0.253	0.026	0.248	0.212	-0.143
	Sig.	0.471	0.418	0.363	0.928	0.374	0.448	0.611
	N	15	15	15	15	15	15	15
Wk2	CC	-0.393	-0.252	0.366	0.243	0.047	0.101	-0.276
	Sig.	0.147	0.365	0.180	0.382	0.868	0.720	0.319
	N	15	15	15	15	15	15	15
Wk4	CC	-0.418	-0.179	0.036	-0.281	-0.155	0.327	-0.409
	Sig.	0.121	0.523	0.899	0.311	0.581	0.234	0.130
	N	15	15	15	15	15	15	15
Wk9	CC	0.091	-0.329	-0.312	-0.188	-0.281	-0.035	-0.254
	Sig.	0.737	0.213	0.239	0.484	0.291	0.899	0.342
	N	16	16	16	16	16	16	16
Wk12	CC	-0.551	0.291	0.548	0.275	-0.132	0.137	0.123
	Sig.	0.027	0.274	0.028	0.302	0.627	0.613	0.649
	N	16	16	16	16	16	16	16
Wk16	CC	0.356	-0.517	-0.087	0.174	0.342	-0.060	-0.168
	Sig.	0.233	0.071	0.777	0.569	0.252	0.845	0.584
	N	13	13	13	13	13	13	13

L **ELISpot vs BAL IL-17 nonL 14-16+**

BAL IL-17 nonL 14-16+		ELISpot PB2	ELISpot PB1	ELISpot Wk2	ELISpot Wk4	ELISpot Wk9	ELISpot Wk12	ELISpot Wk16
PB1	CC	0.199	-0.007	-0.183	0.188	-0.014	-0.046	0.496
	Sig.	0.476	0.981	0.513	0.503	0.962	0.869	0.060
	N	15	15	15	15	15	15	15
Wk2	CC	-0.219	0.226	0.540	0.434	-0.097	-0.011	-0.133
	Sig.	0.434	0.418	0.038	0.106	0.732	0.970	0.638
	N	15	15	15	15	15	15	15
Wk4	CC	-0.290	0.387	-0.048	-0.634	-0.165	0.477	-0.075
	Sig.	0.294	0.154	0.864	0.011	0.557	0.072	0.790
	N	15	15	15	15	15	15	15
Wk9	CC	0.230	0.405	-0.037	-0.204	0.162	-0.143	-0.097
	Sig.	0.391	0.119	0.891	0.448	0.549	0.598	0.720
	N	16	16	16	16	16	16	16
Wk12	CC	-0.377	0.384	0.315	0.199	-0.385	0.046	-0.074
	Sig.	0.150	0.142	0.234	0.459	0.141	0.867	0.786
	N	16	16	16	16	16	16	16
Wk16	CC	0.269	-0.007	0.280	0.157	0.463	0.090	0.123
	Sig.	0.398	0.982	0.378	0.627	0.130	0.782	0.703
	N	12	12	12	12	12	12	12

Supplementary Table 12 Correlations between IFNγ+ SFU and IL-17-positive cells among BAL

Spearman's rank correlations were calculated between IFNγ SFU and the frequency of IL-17+ cells among different cell populations, measured among PBMCs by flow cytometry. IL-17 frequency was explored among: CD4, CD8+ and $\gamma\delta$ T cells (A, B and C), Va7.2+ CD8+ T cells (D), CD16+/CD56+ CD3-CD8+ lymphocytes (NK cells, E and F), CD16+/CD56+ CD3+ T cells (NKT-L, G-I), CD14+/CD16+ non-lymphocyte cells (J-L). Correlation co-efficient ('CC'), significance ('Sig.') and number of values included in each comparison ('N') are shown at each combination of time points. PB2 is shown in blue, as this time point was only analysed by ELISpot.

A

		ELISpot PB2	ELISpot PB1	ELISpot Wk2	ELISpot Wk4	ELISpot Wk9	ELISpot Wk12	ELISpot Wk16
Serum IgG PB2	CC	0.203	0.422	0.022	-0.085	0.176	-0.006	-0.091
	Sig.	0.451	0.103	0.935	0.753	0.513	0.983	0.737
	N	16	16	16	16	16	16	16
Serum IgG PB1	CC	0.235	0.434	0.040	0.059	0.150	-0.109	0.018
	Sig.	0.380	0.093	0.884	0.829	0.579	0.688	0.948
	N	16	16	16	16	16	16	16
Serum IgG Wk2	CC	0.174	0.418	0.065	0.000	0.059	-0.126	-0.094
	Sig.	0.520	0.107	0.812	1.000	0.829	0.641	0.729
	N	16	16	16	16	16	16	16
Serum IgG Wk4	CC	0.174	0.399	0.060	0.115	0.065	-0.200	0.076
	Sig.	0.520	0.126	0.824	0.672	0.812	0.458	0.778
	N	16	16	16	16	16	16	16
Serum IgG Wk9	CC	0.444	0.097	-0.312	-0.418	0.103	-0.071	-0.109
	Sig.	0.085	0.720	0.239	0.107	0.704	0.795	0.688
	N	16	16	16	16	16	16	16
Serum IgG Wk12	CC	0.429	-0.046	-0.419	-0.491	0.079	-0.032	-0.112
	Sig.	0.097	0.867	0.106	0.053	0.770	0.905	0.680
	N	16	16	16	16	16	16	16
Serum IgG Wk16	CC	0.350	0.197	-0.116	-0.291	0.194	0.124	-0.038
	Sig.	0.184	0.464	0.668	0.274	0.471	0.649	0.888
	N	16	16	16	16	16	16	16
Serum IgG Wk17	CC	0.147	0.340	-0.132	-0.374	0.156	0.265	0.041
	Sig.	0.587	0.198	0.625	0.154	0.564	0.322	0.880
	N	16	16	16	16	16	16	16

ELISpot vs IgG

B

		ELISpot PB2	ELISpot PB1	ELISpot Wk2	ELISpot Wk4	ELISpot Wk9	ELISpot Wk12	ELISpot Wk16
BALn IgG PB1	CC	-0.389	-0.051	-0.200	-0.185	-0.151	-0.187	-0.102
	Sig.	0.136	0.851	0.458	0.493	0.577	0.489	0.706
	N	16	16	16	16	16	16	16
BALn IgG Wk2	CC	0.020	0.340	-0.015	0.023	-0.263	-0.222	0.417
	Sig.	0.940	0.197	0.955	0.933	0.324	0.408	0.108
	N	16	16	16	16	16	16	16
BALn IgG Wk4	CC	0.135	-0.005	0.215	0.406	-0.148	0.084	0.225
	Sig.	0.617	0.985	0.424	0.118	0.584	0.756	0.402
	N	16	16	16	16	16	16	16
BALn IgG Wk9	CC	-0.071	-0.096	0.265	-0.166	0.761	0.469	-0.153
	Sig.	0.792	0.724	0.321	0.539	0.001	0.067	0.573
	N	16	16	16	16	16	16	16
BALn IgG Wk12	CC	0.054	-0.049	0.398	0.017	0.628	0.099	-0.021
	Sig.	0.842	0.856	0.127	0.949	0.009	0.717	0.938
	N	16	16	16	16	16	16	16
BALn IgG Wk16	CC	0.578	0.047	-0.082	-0.052	0.229	-0.358	0.367
	Sig.	0.019	0.861	0.763	0.849	0.394	0.173	0.162
	N	16	16	16	16	16	16	16

C

		ELISpot PB2	ELISpot PB1	ELISpot Wk2	ELISpot Wk4	ELISpot Wk9	ELISpot Wk12	ELISpot Wk16
BALc IgG PB1	CC	0.252	0.084	-0.308	-0.252	0.028	-0.420	0.196
	Sig.	0.346	0.757	0.245	0.346	0.918	0.105	0.467
	N	16	16	16	16	16	16	16
BALc IgG Wk2	CC	0.020	0.340	-0.015	0.023	-0.263	-0.222	0.417
	Sig.	0.940	0.197	0.955	0.933	0.324	0.408	0.108
	N	16	16	16	16	16	16	16
BALc IgG Wk4	CC	-0.155	0.557	0.268	0.022	0.022	0.056	0.375
	Sig.	0.566	0.025	0.316	0.937	0.937	0.837	0.152
	N	16	16	16	16	16	16	16
BALc IgG Wk9	CC	-0.443	0.018	0.583	0.264	0.237	0.047	-0.206
	Sig.	0.086	0.947	0.018	0.323	0.376	0.862	0.445
	N	16	16	16	16	16	16	16
BALc IgG Wk12	CC	-0.047	-0.029	0.029	-0.478	0.585	0.324	-0.210
	Sig.	0.862	0.916	0.916	0.061	0.017	0.220	0.436
	N	16	16	16	16	16	16	16
BALc IgG Wk16	CC	-0.005	0.004	-0.010	-0.422	0.542	0.373	0.105
	Sig.	0.985	0.988	0.970	0.103	0.030	0.154	0.699
	N	16	16	16	16	16	16	16

Supplementary Table 13 Correlations between IFNγ SFU frequency and IgG antibody titre

*Spearman's rank correlations were calculated between IFNγ+ SFU frequency and IgG antibody titre, measured in serum (**A**), neat BALf(**B**) and concentrated BAL (**C**). Correlation co-efficient ('CC'), significance ('Sig.') and number of values included in each comparison ('N') are shown at each combination of time points. PB1B and Wk17 are shown in blue, as these time points were not available for all sample sets.*

A

		ELISpot PB2	ELISpot PB1	ELISpot Wk2	ELISpot Wk4	ELISpot Wk9	ELISpot Wk12	ELISpot Wk16
Serum	CC	-0.368	0.478	0.580	0.244	0.147	0.003	-0.159
IgM	Sig.	0.161	0.061	0.019	0.362	0.587	0.991	0.557
PB1	N	16	16	16	16	16	16	16
Serum	CC	-0.215	0.419	0.667	0.374	0.144	-0.026	-0.129
IgM	Sig.	0.425	0.106	0.005	0.154	0.594	0.922	0.633
Wk2	N	16	16	16	16	16	16	16
Serum	CC	-0.253	0.369	0.572	0.291	0.068	-0.003	-0.162
IgM	Sig.	0.345	0.159	0.020	0.274	0.803	0.991	0.549
Wk4	N	16	16	16	16	16	16	16
Serum	CC	-0.350	0.281	0.333	0.015	-0.056	0.012	-0.047
IgM	Sig.	0.184	0.292	0.208	0.957	0.837	0.966	0.863
Wk9	N	16	16	16	16	16	16	16
Serum	CC	-0.250	0.271	0.383	0.147	-0.029	-0.006	0.012
IgM	Sig.	0.350	0.310	0.144	0.587	0.914	0.983	0.966
Wk12	N	16	16	16	16	16	16	16
Serum	CC	-0.157	0.383	0.510	0.099	0.155	0.185	0.169
IgM	Sig.	0.560	0.143	0.044	0.716	0.568	0.492	0.531
Wk16	N	16	16	16	16	16	16	16

ELISpot vs IgM

B

		ELISpot PB2	ELISpot PB1	ELISpot Wk2	ELISpot Wk4	ELISpot Wk9	ELISpot Wk12	ELISpot Wk16
BALn	CC	-0.389	-0.051	-0.200	-0.185	-0.151	-0.187	-0.102
IgM	Sig.	0.136	0.851	0.458	0.493	0.577	0.489	0.706
PB1	N	16	16	16	16	16	16	16
BALn	CC	0.020	0.340	-0.015	0.023	-0.263	-0.222	0.417
IgM	Sig.	0.940	0.197	0.955	0.933	0.324	0.408	0.108
Wk2	N	16	16	16	16	16	16	16
BALn	CC	0.135	-0.005	0.215	0.406	-0.148	0.084	0.225
IgM	Sig.	0.617	0.985	0.424	0.118	0.584	0.756	0.402
Wk4	N	16	16	16	16	16	16	16
BALn	CC	-0.071	-0.096	0.265	-0.166	0.761	0.469	-0.153
IgM	Sig.	0.792	0.724	0.321	0.539	0.001	0.067	0.573
Wk9	N	16	16	16	16	16	16	16
BALn	CC	0.054	-0.049	0.398	0.017	0.628	0.099	-0.021
IgM	Sig.	0.842	0.856	0.127	0.949	0.009	0.717	0.938
Wk12	N	16	16	16	16	16	16	16
BALn	CC	0.578	0.047	-0.082	-0.052	0.229	-0.358	0.367
IgM	Sig.	0.019	0.861	0.763	0.849	0.394	0.173	0.162
Wk16	N	16	16	16	16	16	16	16

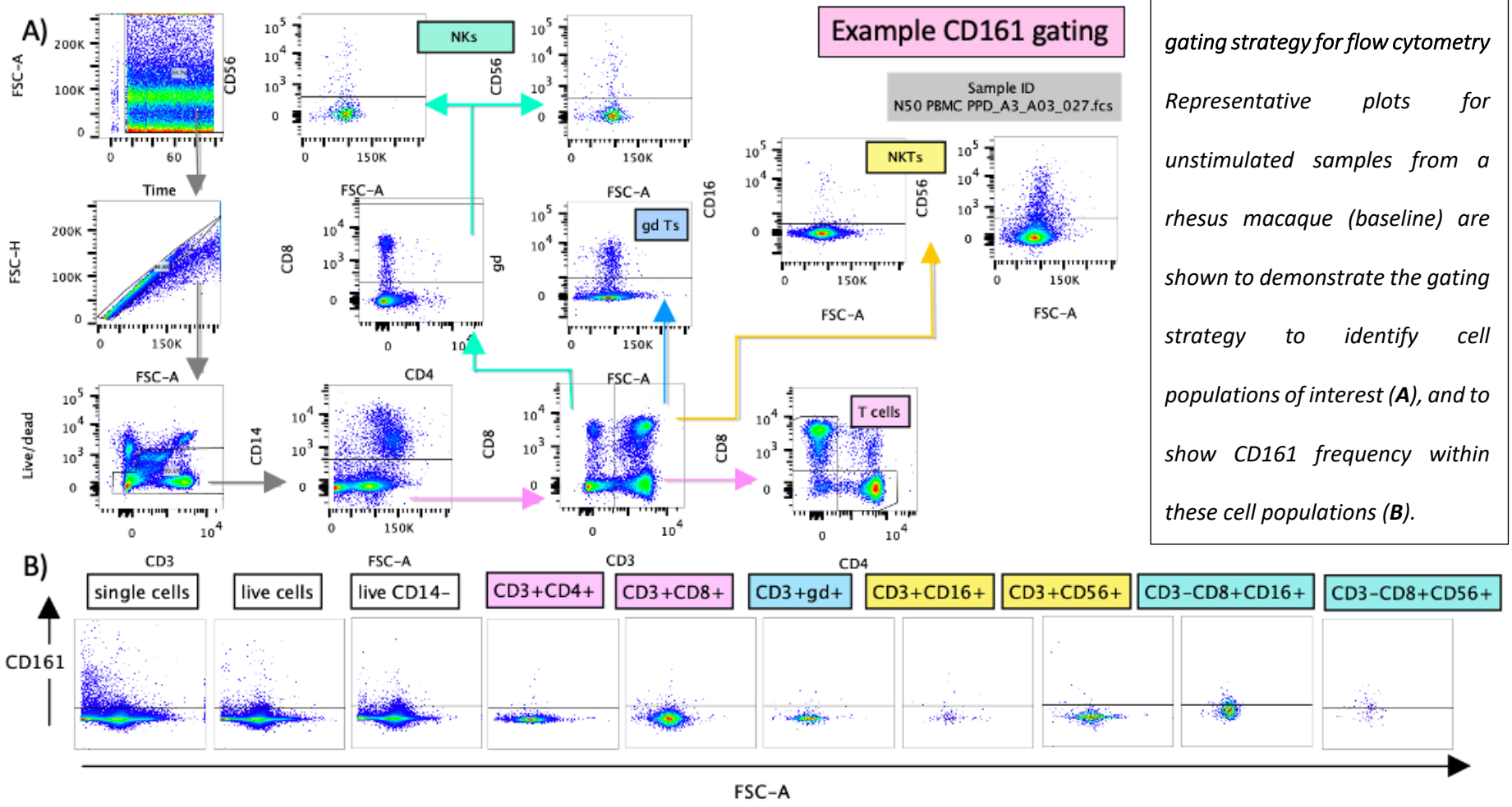
C

		ELISpot PB2	ELISpot PB1	ELISpot Wk2	ELISpot Wk4	ELISpot Wk9	ELISpot Wk12	ELISpot Wk16
BALc	CC	0.252	0.084	-0.308	-0.252	0.028	-0.420	0.196
IgM	Sig.	0.346	0.757	0.245	0.346	0.918	0.105	0.467
PB1	N	16	16	16	16	16	16	16
BALc	CC	0.020	0.340	-0.015	0.023	-0.263	-0.222	0.417
IgM	Sig.	0.940	0.197	0.955	0.933	0.324	0.408	0.108
Wk2	N	16	16	16	16	16	16	16
BALc	CC	-0.155	0.557	0.268	0.022	0.022	0.056	0.375
IgM	Sig.	0.566	0.025	0.316	0.937	0.937	0.837	0.152
Wk4	N	16	16	16	16	16	16	16
BALc	CC	-0.443	0.018	0.583	0.264	0.237	0.047	-0.206
IgM	Sig.	0.086	0.947	0.018	0.323	0.376	0.862	0.445
Wk9	N	16	16	16	16	16	16	16
BALc	CC	-0.047	-0.029	0.029	-0.478	0.585	0.324	-0.210
IgM	Sig.	0.862	0.916	0.916	0.061	0.017	0.220	0.436
Wk12	N	16	16	16	16	16	16	16
BALc	CC	-0.005	0.004	-0.010	-0.422	0.542	0.373	0.105
IgM	Sig.	0.985	0.988	0.970	0.103	0.030	0.154	0.699
Wk16	N	16	16	16	16	16	16	16

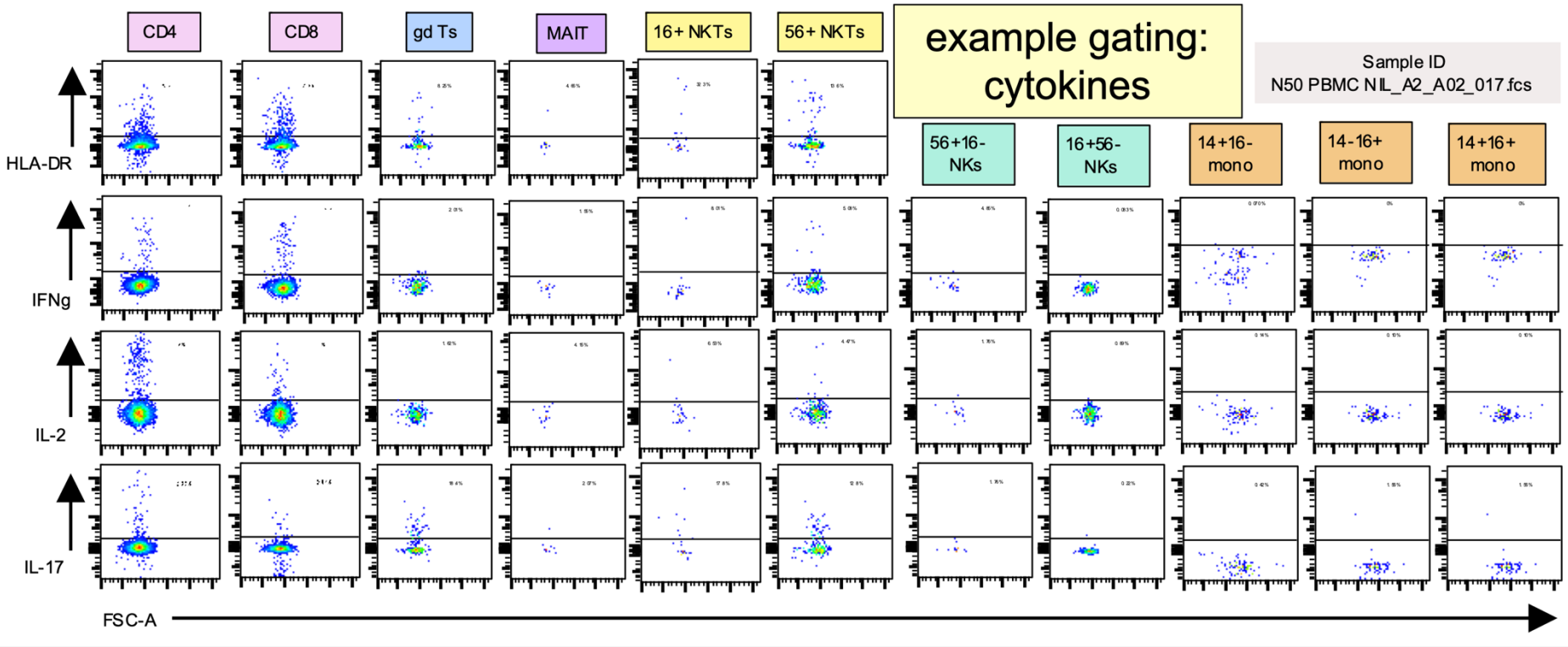
Supplementary Table 14 Correlations between IFNγ+ SFU frequency and IgM antibody titre

*Spearman's rank correlations were calculated between IFNγ+ SFU frequency and IgM antibody titre, measured in serum (**A**), neat BALf(**B**) and concentrated BAL (**C**). Correlation co-efficient ('CC'), significance ('Sig.') and number of values included in each comparison ('N') are shown at each combination of time points. PB1B is shown in blue, as this time point not available for all sample sets.*

7.2 Supplementary figures



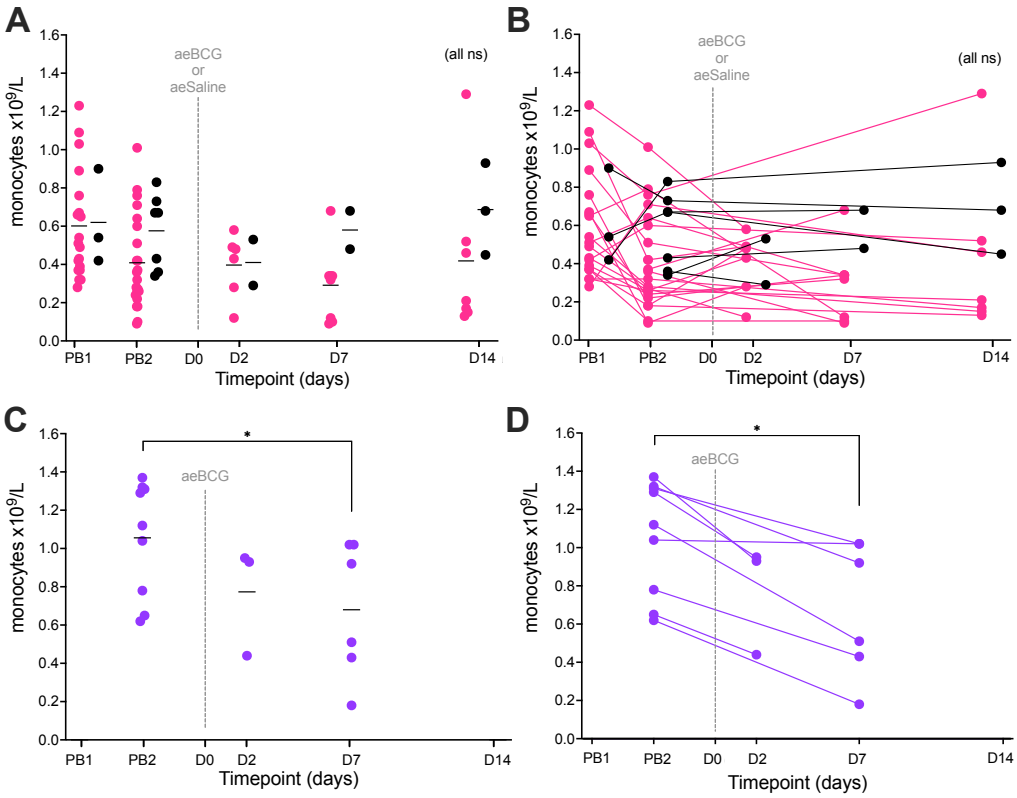
*Supplementary Figure 1 CD161 gating strategy for flow cytometry Representative plots for unstimulated samples from a rhesus macaque (baseline) are shown to demonstrate the gating strategy to identify cell populations of interest (**A**), and to show CD161 frequency within these cell populations (**B**).*



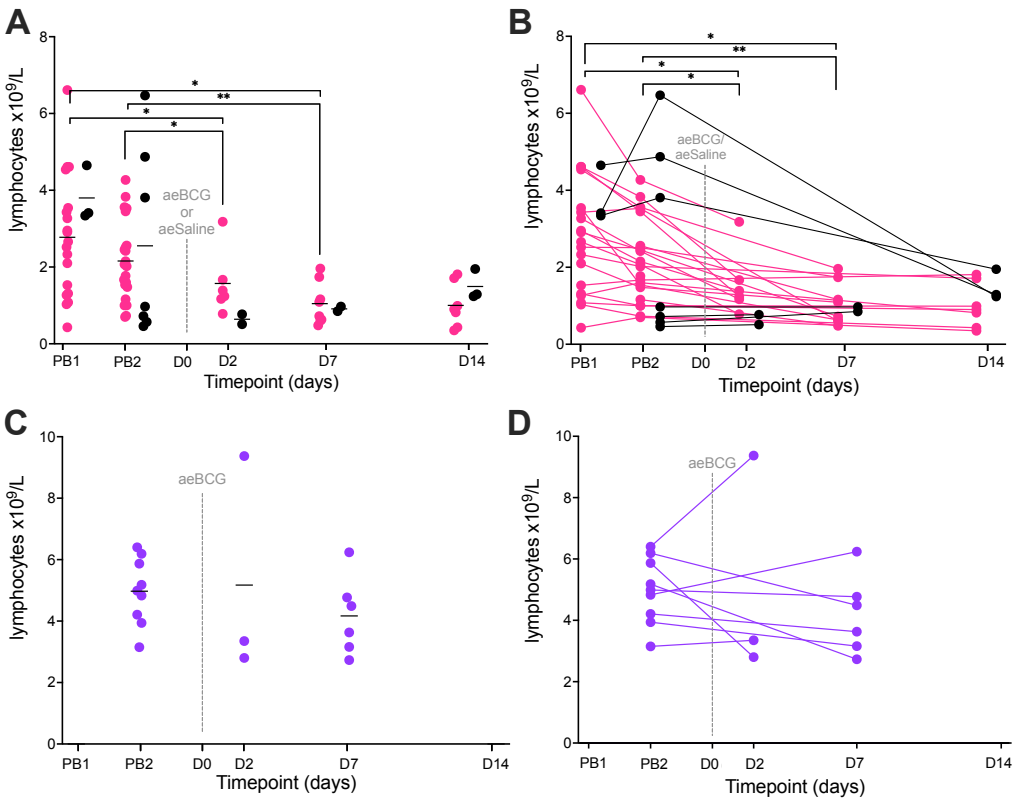
Supplementary Figure 2 Example gating for cytokine and HLA-DR frequency

Representative plots for unstimulated samples from a rhesus macaque (baseline) are shown to demonstrate the gating strategy to determine the frequency of cytokine-positive (IFNγ, IL-2 and IL-17) or HLA-DR-positive cells.

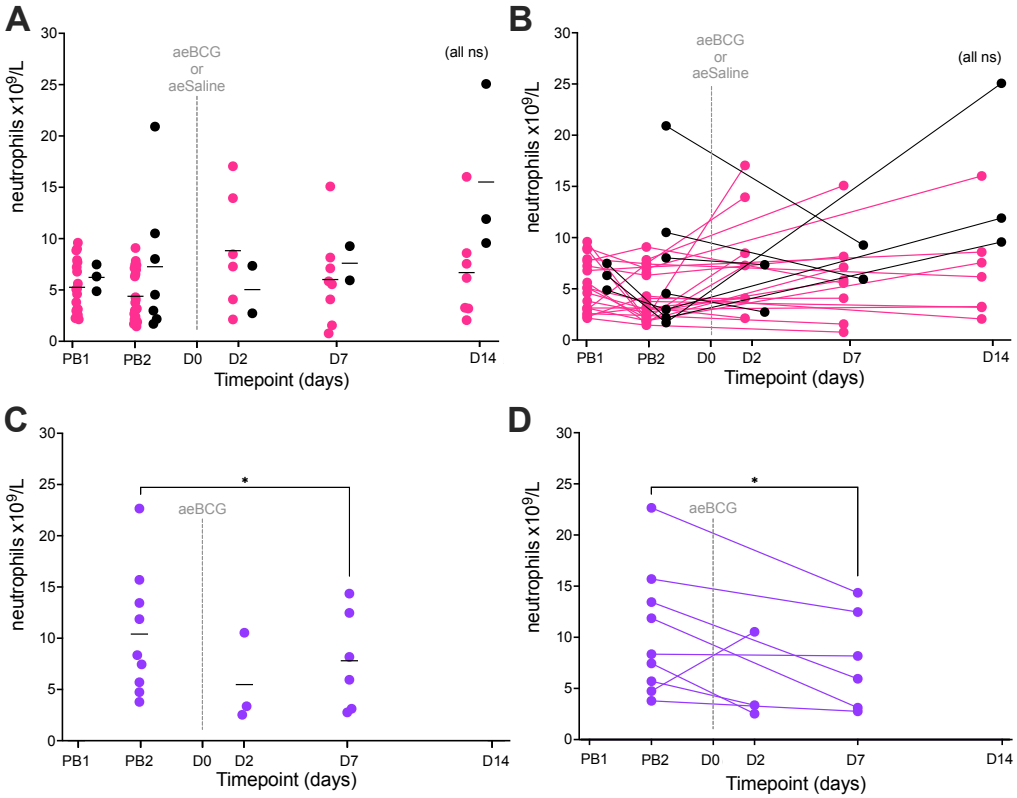
i) Monocytes



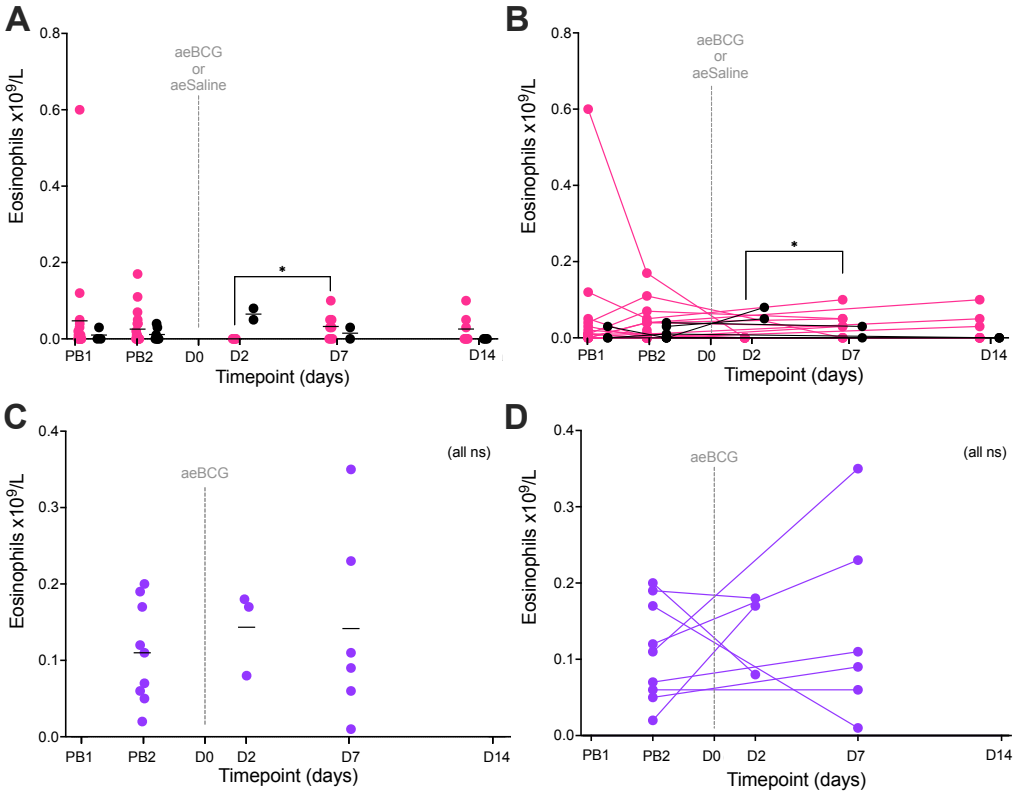
ii) Lymphocytes



iii) Neutrophils



iv) Eosinophils



Supplementary Figure 3 *(i-iv) Cell population ratios, measured by IDEXX Lasercyte Haematology analyser.*

*The cell populations of monocytes (**i**), lymphocytes (**ii**), neutrophils (**iii**), eosinophils (**iv**) and basophils (data not shown) were measured in anti-coagulated blood samples from individual animals, as per manufacturer instructions, and plotted for BCG-exposed RM in pink (**A, B**) and CM in green (**C, D**). Control RM animals exposed to aeSaline are shown in blue (**A, B**). Individual animals and group medians are shown (**A, C**) in comparison to animals tracked over time (**B, D**). Pre-infection population ratios are shown at PBs (PB1/2), before aerosol BCG (aeBCG), as marked by a grey dashed line. Paired data (e.g. from one animal at baseline vs D2/7/14) is compared using a Wilcoxon-Rank Test, and unpaired comparisons (e.g. between the animals at D2 vs. D7 or vs.D14) were performed using the Mann-Whitney U-test.*

7.3 Publications

1. Rachel Tanner, Andrew D. White, Charelle Boot, Claudia C. Sombroek, Matthew K. O'Shea, Daniel Wright, Emily Hoogkamer, Julia Bitencourt, Stephanie A. Harris, Charlotte Sarfas, Rachel Wittenberg, Iman Satti, Helen A. Fletcher, Frank A. W. Verreck, Sally A. Sharpe & Helen McShane. A non-human primate in vitro functional assay for the early evaluation of TB vaccine candidates. *npj Vaccines* **6**, 1-11 (2021). [238]

2. Rachel Tanner, Emily Hoogkamer, Julia Bitencourt, Andrew White, Charelle Boot, Claudia C. Sombroek, Stephanie A. Harris et al. "The in vitro direct mycobacterial growth inhibition assay (MGIA) for the early evaluation of TB vaccine candidates and assessment of protective immunity: a protocol for non-human primate cells." *F1000Research* **10** (2021). [302]

7.4 References

1. Cervantes, J. & Hong, B.-y. The gut–lung axis in tuberculosis. *Pathogens and Disease* **75**, ftx097 (2017).

2. Dijkman, K. *et al.* Prevention of tuberculosis infection and disease by local BCG in repeatedly exposed rhesus macaques. *Nature medicine* **25**, 255 (2019).

3. White, A. *et al.* Evaluation of the immunogenicity of Mycobacterium bovis BCG delivered by aerosol to the lungs of macaques. *Clinical and Vaccine Immunology* **22**, 992-1003 (2015).

4. Dijkman, K. *et al.* Disparate tuberculosis disease development in macaque species is associated with innate immunity. *Frontiers in immunology* **10**, 2479 (2019).

5. Darrah, P.A. *et al.* Prevention of tuberculosis in macaques after intravenous BCG immunization. *Nature* **577**, 95-102 (2020).

6. Osei Sekyere, J., Maningi, N.E. & Fourie, P.B. Mycobacterium tuberculosis, antimicrobials, immunity, and lung–gut microbiota crosstalk: Current updates and emerging advances. *Annals of the New York Academy of Sciences* **1467**, 21-47 (2020).

7. White, A.D. *et al.* Protective efficacy of inhaled BCG vaccination against ultra-low dose aerosol M. tuberculosis challenge in Rhesus Macaques. *Pharmaceutics* **12**, 394 (2020).

8. Sharpe, S. *et al.* Alternative BCG delivery strategies improve protection against Mycobacterium tuberculosis in non-human primates: protection associated with mycobacterial antigen-specific CD4 effector memory T-cell populations. *Tuberculosis* **101**, 174-190 (2016).

9. Sharpe, S. *et al.* Establishment of an aerosol challenge model of tuberculosis in rhesus macaques and an evaluation of endpoints for vaccine testing. *Clin. Vaccine Immunol.* **17**, 1170-1182 (2010).

10. Verreck, F.A. *et al.* Variable BCG efficacy in rhesus populations: pulmonary BCG provides protection where standard intra-dermal vaccination fails. *Tuberculosis* **104**, 46-57 (2017).

11. Organisation, W.H. Global tuberculosis report 2021. *Geneva: World Health Organisation; 2021* (2021).

12. Comstock, G.W., Livesay, V.T. & WOOLPERT, S.F. The prognosis of a positive tuberculin reaction in childhood and adolescence. *American journal of epidemiology* **99**, 131-138 (1974).

13. Törün, T. *et al.* Side effects associated with the treatment of multidrug-resistant tuberculosis. *The International Journal of Tuberculosis and Lung Disease* **9**, 1373-1377 (2005).

14. Knight, G.M., McQuaid, C.F., Dodd, P.J. & Houben, R.M. Global burden of latent multidrug-resistant tuberculosis: trends and estimates based on mathematical modelling. *The Lancet Infectious Diseases* **19**, 903-912 (2019).

15. Manjelievskaia, J., Erck, D., Piracha, S. & Schrager, L. Drug-resistant TB: deadly, costly and in need of a vaccine. *Transactions of the Royal Society of Tropical Medicine and Hygiene* **110**, 186-191 (2016).

16. Trunz, B.B., Fine, P. & Dye, C. Effect of BCG vaccination on childhood tuberculous meningitis and miliary tuberculosis worldwide: a meta-analysis and assessment of cost-effectiveness. *The Lancet* **367**, 1173-1180 (2006).

17. Simmons, J.D. *et al.* Immunological mechanisms of human resistance to persistent Mycobacterium tuberculosis infection. *Nature Reviews Immunology* **18**, 575 (2018).

18. Cruz-Knight, W. & Blake-Gumbs, L. Tuberculosis: an overview. *Primary Care: Clinics in Office Practice* **40**, 743-756 (2013).

19. Singh, P., Kant, S., Gaur, P., Tripathi, A. & Pandey, S. Extra pulmonary Tuberculosis: An overview and review of literature. *Int. J. Life. Sci. Scienti. Res* **4**, 1539-1541 (2018).

20. Sharma, S.K., Mohan, A. & Sharma, A. Miliary tuberculosis: A new look at an old foe. *Journal of Clinical Tuberculosis and other mycobacterial diseases* **3**, 13-27 (2016).

21. Cohen, A., Mathiasen, V.D., Schön, T. & Wejse, C. The global prevalence of latent tuberculosis: a systematic review and meta-analysis. *European Respiratory Journal* **54** (2019).

22. Ahmad, S. Pathogenesis, immunology, and diagnosis of latent Mycobacterium tuberculosis infection. *Clinical and Developmental Immunology* **2011** (2011).

23. Ai, J.-W., Ruan, Q.-L., Liu, Q.-H. & Zhang, W.-H. Updates on the risk factors for latent tuberculosis reactivation and their managements. *Emerging microbes & infections* **5**, 1-8 (2016).

24. Reichler, M.R. *et al.* Predictive value of TNF-α, IFN-γ, and IL-10 for tuberculosis among recently exposed contacts in the United States and Canada. *BMC infectious diseases* **20**, 1-14 (2020).

25. Drain, P.K. *et al.* Incipient and subclinical tuberculosis: a clinical review of early stages and progression of infection. *Clinical microbiology reviews* **31** (2018).

26. Zhang, H. *et al.* Reversion of QuantiFERON-TB Gold In-Tube test in individuals with and without prophylactic treatment for latent tuberculosis infection: A systematic review and meta-analysis. *Journal of Infection* **77**, 276-282 (2018).

27. Morrison, J., Pai, M. & Hopewell, P.C. Tuberculosis and latent tuberculosis infection in close contacts of people with pulmonary tuberculosis in low-income and middle-income countries: a systematic review and meta-analysis. *The Lancet infectious diseases* **8**, 359-368 (2008).

28. Thapa, J. *et al.* Wildlife Tuberculosis: An Emerging Threat for Conservation in South Asia. Global Exposition of Wildlife Management; 2017: InTech; 2017.

29. Godfray, H.C.J., Donnelly, C., Hewinson, G., Winter, M. & Wood, J. Bovine TB strategy review. (2018).

30. Cosivi, O. *et al.* Zoonotic tuberculosis due to Mycobacterium bovis in developing countries. *Emerging infectious diseases* **4**, 59 (1998).

31. Waters, W.R., Palmer, M.V., Buddle, B.M. & Vordermeier, H.M. Bovine tuberculosis vaccine research: historical perspectives and recent advances. *Vaccine* **30**, 2611-2622 (2012).

32. Vordermeier, H.M. *et al.* Viral booster vaccines improve Mycobacterium bovis BCG-induced protection against bovine tuberculosis. *Infection and immunity* **77**, 3364-3373 (2009).

33. Mangtani, P. *et al.* Protection by BCG vaccine against tuberculosis: a systematic review of randomized controlled trials. *Clinical infectious diseases* **58**, 470-480 (2013).

34. Luca, S. & Mihaescu, T. History of BCG Vaccine. *Maedica* **8**, 53-58 (2013).

35. Romanus, V. *et al.* Atypical mycobacteria in extrapulmonary disease among children. Incidence in Sweden from 1969 to 1990, related to changing BCG-vaccination coverage. *Tubercle and Lung Disease* **76**, 300-310 (1995).

36. Wilson, M.E., Fineberg, H.V. & Colditz, G.A. Geographic latitude and the efficacy of bacillus Calmette-Guerin vaccine. *Clinical Infectious Diseases* **20**, 982-991 (1995).

37. Nnoaham, K.E. & Clarke, A. Low serum vitamin D levels and tuberculosis: a systematic review and meta-analysis. *International journal of epidemiology* **37**, 113-119 (2008).

38. Aibana, O. *et al.* Vitamin D status and risk of incident tuberculosis disease: A nested case-control study, systematic review, and individual-participant data meta-analysis. *PLoS medicine* **16**, e1002907 (2019).

39. Shah, J.A., Lindestam Arlehamn, C.S., Horne, D.J., Sette, A. & Hawn, T.R. Nontuberculous mycobacteria and heterologous immunity to tuberculosis. *The Journal of infectious diseases* **220**, 1091-1098 (2019).

40. Hayward, S.E. *et al.* A systematic review of the impact of psychosocial factors on immunity: Implications for enhancing BCG response against tuberculosis. *SSM-Population Health* **10**, 100522 (2020).

41. Kagina, B.M. *et al.* Delaying BCG vaccination from birth to 10 weeks of age may result in an enhanced memory CD4 T cell response. *Vaccine* **27**, 5488-5495 (2009).

42. de Bree, L.C.J. *et al.* Circadian rhythm influences induction of trained immunity by BCG vaccination. *The Journal of Clinical Investigation* (2020).

43. Abdallah, A.M. & Behr, M.A. Evolution and strain variation in BCG. *Strain Variation in the Mycobacterium tuberculosis Complex: Its Role in Biology, Epidemiology and Control*. Springer, 2017, pp 155-169.

44. Nikas, C.V. & Smith, A.B. Goldilocks and the BCG: Bacillus Calmette-Guérin Dose Reduction in the Age of Shortage. *European Urology* (2020).

45. Qureshi, S. *et al.* Outcome of inadvertent high dose BCG administration in newborns at a tertiary care hospital, Karachi-Case series. *PloS one* **14**, e0219324 (2019).

46. Manjaly Thomas, Z.-R. & McShane, H. Aerosol immunisation for TB: matching route of vaccination to route of infection. *Transactions of The Royal Society of Tropical Medicine and Hygiene* **109**, 175-181 (2015).

47. Roy, P. *et al.* Potential effect of age of BCG vaccination on global paediatric tuberculosis mortality: a modelling study. *The Lancet Global Health* **7**, e1655-e1663 (2019).

48. Katelaris, A.L. *et al.* Effectiveness of BCG vaccination against Mycobacterium tuberculosis infection in adults: a cross-sectional analysis of a UK-based cohort. *The Journal of Infectious Diseases* **221**, 146-155 (2020).

49. Zhang, L. *et al.* Variable virulence and efficacy of BCG vaccine strains in mice and correlation with genome polymorphisms. *Molecular Therapy* **24**, 398-405 (2016).

50. Warren, R.M. *et al.* Patients with active tuberculosis often have different strains in the same sputum specimen. *American journal of respiratory and critical care medicine* **169**, 610-614 (2004).

51. Zodpey, S.P. & Shrikhande, S.N. The geographic location (latitude) of studies evaluating protective effect of BCG vaccine and it's efficacy/effectiveness against tuberculosis. *Indian journal of public health* **51**, 205 (2007).

52. Hoe, E. *et al.* Anti-inflammatory effects of vitamin D on human immune cells in the context of bacterial infection. *Nutrients* **8**, 806 (2016).

53. Martineau, A.R. *et al.* A single dose of vitamin D enhances immunity to mycobacteria. *American journal of respiratory and critical care medicine* **176**, 208-213 (2007).

54. Ganmaa, D. *et al.* Vitamin D Supplements for Prevention of Tuberculosis Infection and Disease. *New England Journal of Medicine* **383**, 359-368 (2020).

55. Sinha, P. *et al.* Undernutrition and tuberculosis: public health implications. *The Journal of infectious diseases* **219**, 1356-1363 (2019).

56. Organization, W.H. Global tuberculosis report 2018. 2018. *Geneva: World Health* (2019).

57. Honda, J.R., Virdi, R. & Chan, E.D. Global environmental nontuberculous mycobacteria and their contemporaneous man-made and natural niches. *Frontiers in Microbiology* **9**, 2029 (2018).

58. Poyntz, H.C. *et al.* Non-tuberculous mycobacteria have diverse effects on BCG efficacy against Mycobacterium tuberculosis. *Tuberculosis* **94**, 226-237 (2014).

59. Arregui, S., Sanz, J., Marinova, D., Martín, C. & Moreno, Y. On the impact of masking and blocking hypotheses for measuring the efficacy of new tuberculosis vaccines. *PeerJ* **4**, e1513 (2016).

60. Palmer, C.E. & Long, M.W. Effects of infection with atypical mycobacteria on BCG vaccination and tuberculosis. *American review of respiratory disease* **94**, 553-568 (1966).

61. Barreto, M.L. *et al.* Causes of variation in BCG vaccine efficacy: examining evidence from the BCG REVAC cluster randomized trial to explore the masking and the blocking hypotheses. *Vaccine* **32**, 3759-3764 (2014).

62. Pawlowski, A., Jansson, M., Sköld, M., Rottenberg, M.E. & Källenius, G. Tuberculosis and HIV co-infection. *Plos pathog* **8**, e1002464 (2012).

63. Corbett, E.L. *et al.* The growing burden of tuberculosis: global trends and interactions with the HIV epidemic. *Archives of internal medicine* **163**, 1009-1021 (2003).

64. Lawn, S.D. *et al.* Antiretrovirals and isoniazid preventive therapy in the prevention of HIV-associated tuberculosis in settings with limited health-care resources. *The Lancet infectious diseases* **10**, 489-498 (2010).

65. Caruso, A.M. *et al.* Mice deficient in CD4 T cells have only transiently diminished levels of IFN-γ, yet succumb to tuberculosis. *The Journal of Immunology* **162**, 5407-5416 (1999).

66. Scanga, C.A. *et al.* Depletion of CD4+ T cells causes reactivation of murine persistent tuberculosis despite continued expression of interferon γ and nitric oxide synthase 2. *The Journal of experimental medicine* **192**, 347-358 (2000).

67. Lin, P.L. *et al.* CD4 T cell depletion exacerbates acute Mycobacterium tuberculosis while reactivation of latent infection is dependent on severity of tissue depletion in cynomolgus macaques. *AIDS research and human retroviruses* **28**, 1693-1702 (2012).

68. Corleis, B. *et al.* HIV-1 and SIV infection are associated with early loss of lung interstitial CD4+ T cells and dissemination of pulmonary tuberculosis. *Cell reports* **26**, 1409-1418. e1405 (2019).

69. La Rosa, C. & Diamond, D.J. The immune response to human CMV. *Future virology* **7**, 279-293 (2012).

70. Stockdale, L. *et al.* Human cytomegalovirus epidemiology and relationship to tuberculosis and cardiovascular disease risk factors in a rural Ugandan cohort. *PloS one* **13**, e0192086 (2018).

71. Stockdale, L. *et al.* Cytomegalovirus Antibody Responses Associated With Increased Risk of Tuberculosis Disease in Ugandan Adults. *The Journal of Infectious Diseases* **221**, 1127-1134 (2020).

72. Müller, J. *et al.* Cytomegalovirus infection is a risk factor for tuberculosis disease in infants. *JCI insight* **4** (2019).

73. Stockdale, L. *et al.* HIV, HCMV and mycobacterial antibody levels: a cross-sectional study in a rural Ugandan cohort. *Tropical Medicine & International Health* **24**, 247-257 (2019).

74. Group, B.D.W. *et al.* Biomarkers and surrogate endpoints: preferred definitions and conceptual framework. *Clinical pharmacology & therapeutics* **69**, 89-95 (2001).

75. Kaufmann, S.H., Weiner 3rd, J. & Maertzdorf, J. Accelerating tuberculosis vaccine trials with diagnostic and prognostic biomarkers. *Expert review of vaccines* **16**, 845-853 (2017).

76. Srivastava, B.S. *et al.* Commentary: Bettering BCG: a tough task for a TB vaccine? *Frontiers in immunology* **10** (2019).

77. Control, C.f.D. & Prevention. Licensure of a 13-valent pneumococcal conjugate vaccine (PCV13) and recommendations for use among children-Advisory Committee on Immunization Practices (ACIP), 2010. *MMWR. Morbidity and mortality weekly report* **59**, 258-261 (2010).

78. Andrews, N.J. *et al.* Serotype-specific effectiveness and correlates of protection for the 13-valent pneumococcal conjugate vaccine: a postlicensure indirect cohort study. *The Lancet infectious diseases* **14**, 839-846 (2014).

79. Morrison, H. & McShane, H. Local Pulmonary Immunological Biomarkers in Tuberculosis. *Frontiers in Immunology* **12**, 533 (2021).

80. Fletcher, H.A. *et al.* T-cell activation is an immune correlate of risk in BCG vaccinated infants. *Nature communications* **7**, 11290 (2016).

81. Zeng, G., Zhang, G. & Chen, X. Th1 cytokines, true functional signatures for protective immunity against TB? *Cellular & Molecular Immunology* **15**, 206-215 (2018).

82. Mittrücker, H.-W. *et al.* Poor correlation between BCG vaccination-induced T cell responses and protection against tuberculosis. *Proceedings of the National Academy of Sciences* **104**, 12434-12439 (2007).

83. Bhatt, K., Verma, S., Ellner, J.J. & Salgame, P. Quest for correlates of protection against tuberculosis. *Clinical and Vaccine Immunology* **22**, 258-266 (2015).

84. Zak, D.E. *et al.* A blood RNA signature for tuberculosis disease risk: a prospective cohort study. *The Lancet* **387**, 2312-2322 (2016).

85. Angelidou, A. *et al.* BCG as a Case Study for Precision Vaccine Development: Lessons From Vaccine Heterogeneity, Trained Immunity, and Immune Ontogeny. *Frontiers in Microbiology* **11**, 332 (2020).

86. Brazier, B. & McShane, H. Towards new TB vaccines. Seminars in Immunopathology; 2020: Springer; 2020. p. 1-17.

87. Nieuwenhuizen, N.E. *et al.* The recombinant Bacille Calmette–Guérin vaccine VPM1002: ready for clinical efficacy testing. *Frontiers in immunology* **8**, 1147 (2017).

88. Tameris, M. *et al.* Live-attenuated Mycobacterium tuberculosis vaccine MTBVAC versus BCG in adults and neonates: a randomised controlled, double-blind dose-escalation trial. *The Lancet Respiratory Medicine* **7**, 757-770 (2019).

89. Dijkman, K. *et al.* Pulmonary MTBVAC vaccination induces immune signatures previously correlated with prevention of tuberculosis infection. *Cell Reports Medicine* **2**, 100187 (2021).

90. Vierboom, M.P. *et al.* Stronger induction of trained immunity by mucosal BCG or MTBVAC vaccination compared to standard intradermal vaccination. *Cell Reports Medicine* **2**, 100185 (2021).

91. White, A.D. *et al.* MTBVAC vaccination protects rhesus macaques against aerosol challenge with M. tuberculosis and induces immune signatures analogous to those observed in clinical studies. *NPJ vaccines* **6**, 1-10 (2021).

92. Ji, Z. *et al.* Immunogenicity and Safety of the M72/AS01E Candidate Vaccine Against Tuberculosis: A Meta-Analysis. *Available at SSRN 3346517* (2019).

93. Van Der Meeren, O. *et al.* Phase 2b controlled trial of M72/AS01E vaccine to prevent tuberculosis. *New England Journal of Medicine* **379**, 1621-1634 (2018).

94. Woodworth, J.S. *et al.* Mucosal boosting of H56: CAF01 immunization promotes lung-localized T cells and an accelerated pulmonary response to Mycobacterium tuberculosis infection without enhancing vaccine protection. *Mucosal immunology* **12**, 816 (2019).

95. McShane, H. Insights and challenges in tuberculosis vaccine development. *The Lancet Respiratory Medicine* (2019).

96. Baldwin, S.L. *et al.* Prophylactic efficacy against Mycobacterium tuberculosis using ID93 and lipid-based adjuvant formulations in the mouse model. *Plos one* **16**, e0247990 (2021).

97. Tameris, M.D. *et al.* Safety and efficacy of MVA85A, a new tuberculosis vaccine, in infants previously vaccinated with BCG: a randomised, placebo-controlled phase 2b trial. *The Lancet* **381**, 1021-1028 (2013).

98. Nemes, E. *et al.* Prevention of M. tuberculosis infection with H4: IC31 vaccine or BCG revaccination. *New England Journal of Medicine* **379**, 138-149 (2018).

99. Rodrigues, L.C. *et al.* Effect of BCG revaccination on incidence of tuberculosis in school-aged children in Brazil: the BCG-REVAC cluster-randomised trial. *The Lancet* **366**, 1290-1295 (2005).

100. Zasheva, S., Gugleva, V. & Andonova, V. Aerosol vaccines–perspectives and therapeutic impact. *Scripta Scientifica Pharmaceutica* **6** (2020).

101. Mutsch, M. *et al.* Use of the inactivated intranasal influenza vaccine and the risk of Bell's palsy in Switzerland. *New England journal of medicine* **350**, 896-903 (2004).

102. Stowe, J., Andrews, N., Wise, L. & Miller, E. Bell's palsy and parenteral inactivated influenza vaccine. *Human vaccines* **2**, 110-112 (2006).

103. Kamath, A., Maity, N. & Nayak, M.A. Facial Paralysis Following Influenza Vaccination: A Disproportionality Analysis Using the Vaccine Adverse Event Reporting System Database. *Clinical Drug Investigation*, 1-7 (2020).

104. Davids, M. *et al.* A human lung challenge model to evaluate the safety and immunogenicity of PPD and live bacillus Calmette-Guérin. *American journal of respiratory and critical care medicine* **201**, 1277-1291 (2020).

105. Barclay, W.R. *et al.* Protection of monkeys against airborne tuberculosis by aerosol vaccination with bacillus Calmette-Guerin. *American review of respiratory disease* **107**, 351-358 (1973).

106. Ari, A. Effect of nebulizer type, delivery interface, and flow rate on aerosol drug delivery to spontaneously breathing pediatric an
d infant lung models. *Pediatric pulmonology* (2019).

107. Sagalla, R.B. & Smaldone, G.C. Capturing the efficiency of vibrating mesh nebulizers: minimizing upper airway deposition. *Journal of aerosol medicine and pulmonary drug delivery* **27**, 341-348 (2014).

108. Orme, I.M. & Ordway, D.J. Mouse and guinea pig models of tuberculosis. *Tuberculosis and the Tubercle Bacillus*, 143-162 (2017).

109. Williams, A. *et al.* Evaluation of vaccines in the EU TB Vaccine Cluster using a guinea pig aerosol infection model of tuberculosis. *Tuberculosis* **85**, 29-38 (2005).

110. Cardona, P.-J. & Williams, A. Experimental animal modelling for TB vaccine development. *International Journal of Infectious Diseases* **56**, 268-273 (2017).

111. Kurtz, S.L. *et al.* The Diversity Outbred Mouse Population Is an Improved Animal Model of Vaccination against Tuberculosis That Reflects Heterogeneity of Protection. *Msphere* **5** (2020).

112. Arrey, F. *et al.* Humanized mouse model mimicking pathology of human tuberculosis for in vivo evaluation of drug regimens. *Frontiers in immunology* **10**, 89 (2019).

113. Gupta, U. & Katoch, V. Animal models of tuberculosis. *Tuberculosis* **85**, 277-293 (2005).

114. Orme, I.M. & Basaraba, R.J. The formation of the granuloma in tuberculosis infection. Seminars in immunology; 2014: Elsevier; 2014. p. 601-609.

115. Kaushal, D., Mehra, S., Didier, P. & Lackner, A. The non-human primate model of tuberculosis. *Journal of medical primatology* **41**, 191-201 (2012).

116. Langermans, J.A. *et al.* Divergent effect of bacillus Calmette–Guerin (BCG) vaccination on Mycobacterium tuberculosis infection in highly related macaque species: Implications for primate models in tuberculosis vaccine research. *Proceedings of the National Academy of Sciences* **98**, 11497-11502 (2001).

117. Sibley, L. *et al.* Differences in monocyte: lymphocyte ratio and Tuberculosis disease progression in genetically distinct populations of macaques. *Scientific reports* **9**, 3340 (2019).

118. Sharpe, S. *et al.* Determination of lesion volume by MRI and stereology in a macaque model of tuberculosis. *Tuberculosis* **89**, 405-416 (2009).

119. Maiello, P. *et al.* Rhesus macaques are more susceptible to progressive tuberculosis than cynomolgus macaques: a quantitative comparison. *Infection and immunity* **86**, e00505-00517 (2018).

120. Sibley, L. *et al.* Differences in host immune populations between rhesus macaques and cynomolgus macaque subspecies in relation to susceptibility to Mycobacterium tuberculosis infection. *Scientific reports* **11**, 1-9 (2021).

121. Sharpe, S. *et al.* Ultra low dose aerosol challenge with Mycobacterium tuberculosis leads to divergent outcomes in rhesus and cynomolgus macaques. *Tuberculosis* **96**, 1-12 (2016).

122. Peña, J.C. & Ho, W.-Z. Monkey models of tuberculosis: lessons learned. *Infection and immunity* **83**, 852-862 (2015).

123. Sarfas, C. *et al.* Characterization of the Infant Immune System and the Influence and Immunogenicity of BCG Vaccination in Infant and Adult Rhesus Macaques. *Frontiers in immunology*, 4268 (2021).

124. Silver, R.F. *et al.* Diversity of human and macaque airway immune cells at baseline and during tuberculosis infection. *American journal of respiratory cell and molecular biology* **55**, 899-908 (2016).

125. McShane, H. & Williams, A. A review of preclinical animal models utilised for TB vaccine evaluation in the context of recent human efficacy data. *Tuberculosis* **94**, 105-110 (2014).

126. Scriba, T.J., Coussens, A.K. & Fletcher, H.A. Human Immunology of Tuberculosis. *Microbiology spectrum* **5** (2016).

127. Ehrt, S., Rhee, K. & Schnappinger, D. Mycobacterial genes essential for the pathogen's survival in the host. *Immunological reviews* **264**, 319-326 (2015).

128. Clemens, D.L. & Horwitz, M.A. Characterization of the Mycobacterium tuberculosis phagosome and evidence that phagosomal maturation is inhibited. *The Journal of experimental medicine* **181**, 257-270 (1995).

129. Chackerian, A.A., Alt, J.M., Perera, T.V., Dascher, C.C. & Behar, S.M. Dissemination of Mycobacterium tuberculosis is influenced by host factors and precedes the initiation of T-cell immunity. *Infection and immunity* **70**, 4501-4509 (2002).

130. Wolf, A.J. *et al.* Initiation of the adaptive immune response to Mycobacterium tuberculosis depends on antigen production in the local lymph node, not the lungs. *The Journal of experimental medicine* **205**, 105-115 (2008).

131. Marino, S. *et al.* Dendritic cell trafficking and antigen presentation in the human immune response to Mycobacterium tuberculosis. *The Journal of Immunology* **173**, 494-506 (2004).

132. Jasenosky, L.D., Scriba, T.J., Hanekom, W.A. & Goldfeld, A.E. T cells and adaptive immunity to Mycobacterium tuberculosis in humans. *Immunological reviews* **264**, 74-87 (2015).

133. Ramakrishnan, L. Revisiting the role of the granuloma in tuberculosis. *Nature Reviews Immunology* **12**, 352-366 (2012).

134. Guirado, E. & Schlesinger, L. Modeling the Mycobacterium tuberculosis granuloma–the critical battlefield in host immunity and disease. *Frontiers in immunology* **4**, 98 (2013).

135. Netea, M.G., Latz, E., Mills, K.H. & O'neill, L.A. Innate immune memory: a paradigm shift in understanding host defense. *Nature immunology* **16**, 675-679 (2015).

136. Sia, J.K., Georgieva, M. & Rengarajan, J. Innate immune defenses in human tuberculosis: an overview of the interactions between Mycobacterium tuberculosis and innate immune cells. *Journal of immunology research* **2015** (2015).

137. Kleinnijenhuis, J., Oosting, M., Joosten, L.A., Netea, M.G. & Van Crevel, R. Innate immune recognition of Mycobacterium tuberculosis. *Clinical and Developmental Immunology* **2011** (2011).

138. Gupta, N., Kumar, R. & Agrawal, B. New players in immunity to tuberculosis: the host microbiome, lung epithelium, and innate immune cells. *Frontiers in immunology* **9**, 709 (2018).

139. Lowe, D.M., Redford, P.S., Wilkinson, R.J., O'Garra, A. & Martineau, A.R. Neutrophils in tuberculosis: friend or foe? *Trends in immunology* **33**, 14-25 (2012).

140. Esin, S. & Batoni, G. Natural killer cells: a coherent model for their functional role in Mycobacterium tuberculosis infection. *Journal of innate immunity* **7**, 11-24 (2015).

141. Joosten, S.A. *et al.* Harnessing donor unrestricted T-cells for new vaccines against tuberculosis. *Vaccine* (2019).

142. Kleinnijenhuis, J. *et al.* Bacille Calmette-Guerin induces NOD2-dependent nonspecific protection from reinfection via epigenetic reprogramming of monocytes. *Proceedings of the National Academy of Sciences* **109**, 17537-17542 (2012).

143. Rajaram, M.V., Ni, B., Dodd, C.E. & Schlesinger, L.S. Macrophage immunoregulatory pathways in tuberculosis. Seminars in immunology; 2014: Elsevier; 2014. p. 471-485.

144. Cohen, S.B. *et al.* Alveolar macrophages provide an early Mycobacterium tuberculosis niche and initiate dissemination. *Cell host & microbe* **24**, 439-446. e434 (2018).

145. Rothchild, A.C. *et al.* Alveolar macrophages generate a noncanonical NRF2-driven transcriptional response to Mycobacterium tuberculosis in vivo. *Science immunology* **4** (2019).

146. Leemans, J.C. *et al.* Depletion of alveolar macrophages exerts protective effects in pulmonary tuberculosis in mice. *The journal of immunology* **166**, 4604-4611 (2001).

147. Sampath, P., Moideen, K., Ranganathan, U.D. & Bethunaickan, R. Monocyte subsets: phenotypes and function in tuberculosis infection. *Frontiers in immunology* **9**, 1726 (2018).

148. Lastrucci, C. *et al.* Tuberculosis is associated with expansion of a motile, permissive and immunomodulatory CD16+ monocyte population via the IL-10/STAT3 axis. *Cell research* **25**, 1333-1351 (2015).

149. Naranbhai, V. *et al.* Ratio of monocytes to lymphocytes in peripheral blood identifies adults at risk of incident tuberculosis among HIV-infected adults initiating antiretroviral therapy. *The Journal of infectious diseases* **209**, 500-509 (2014).

150. Iqbal, S. Monocyte lymphocyte ratio as a possible prognostic marker in antituberculous therapy. *Journal of Rawalpindi Medical College* **18**, 178-181 (2014).

151. Mazza, M.G., Tringali, A.G.M., Rossetti, A., Botti, R.E. & Clerici, M. Cross-sectional study of neutrophil-lymphocyte, platelet-lymphocyte and monocyte-lymphocyte ratios in mood disorders. *General hospital psychiatry* **58**, 7-12 (2019).

152. Chen, H. *et al.* Monocyte/lymphocyte ratio is related to the severity of coronary artery disease and clinical outcome in patients with non-ST-elevation myocardial infarction. *Medicine* **98** (2019).

153. Wang, X., Su, S. & Guo, Y. The clinical use of the platelet to lymphocyte ratio and lymphocyte to monocyte ratio as prognostic factors in renal cell carcinoma: a systematic review and meta-analysis. *Oncotarget* **8**, 84506 (2017).

154. Bodnar, K.A., Serbina, N.V. & Flynn, J.L. Fate of Mycobacterium tuberculosis within murine dendritic cells. *Infection and immunity* **69**, 800-809 (2001).

155. Tian, T., Woodworth, J., Sköld, M. & Behar, S.M. In vivo depletion of CD11c+ cells delays the CD4+ T cell response to Mycobacterium tuberculosis and exacerbates the outcome of infection. *The Journal of Immunology* **175**, 3268-3272 (2005).

156. Kumar, K.P., Nicholls, A.J. & Wong, C.H. Partners in crime: neutrophils and monocytes/macrophages in inflammation and disease. *Cell and tissue research* **371**, 551-565 (2018).

157. Gideon, H.P., Phuah, J., Junecko, B.A. & Mattila, J.T. Neutrophils express pro-and anti-inflammatory cytokines in granulomas from Mycobacterium tuberculosis-infected cynomolgus macaques. *Mucosal immunology* **12**, 1370-1381 (2019).

158. Junqueira-Kipnis, A.P. *et al.* NK cells respond to pulmonary infection with Mycobacterium tuberculosis, but play a minimal role in protection. *The Journal of Immunology* **171**, 6039-6045 (2003).

159. Feng, C.G. *et al.* NK cell-derived IFN-γ differentially regulates innate resistance and neutrophil response in T cell-deficient hosts infected with Mycobacterium tuberculosis. *The Journal of Immunology* **177**, 7086-7093 (2006).

160. Harris, L.D. *et al.* Distinct human NK cell phenotypes and functional responses to Mycobacterium tuberculosis in adults from TB endemic and non-endemic regions. *Frontiers in cellular and infection microbiology* **10**, 120 (2020).

161. Godfrey, D.I., Uldrich, A.P., McCluskey, J., Rossjohn, J. & Moody, D.B. The burgeoning family of unconventional T cells. *Nature immunology* **16**, 1114 (2015).

162. Godfrey, D.I., MacDonald, H.R., Kronenberg, M., Smyth, M.J. & Van Kaer, L. NKT cells: what's in a name? *Nature Reviews Immunology* **4**, 231-237 (2004).

163. Krovi, S.H. & Gapin, L. Invariant natural killer T cell subsets—more than just developmental intermediates. *Frontiers in immunology* **9**, 1393 (2018).

164. Sada-Ovalle, I., Chiba, A., Gonzales, A., Brenner, M.B. & Behar, S.M. Innate invariant NKT cells recognize Mycobacterium tuberculosis–infected macrophages, produce interferon-γ, and kill intracellular bacteria. *PLoS pathogens* **4**, e1000239 (2008).

165. Rothchild, A.C., Jayaraman, P., Nunes-Alves, C. & Behar, S.M. iNKT cell production of GM-CSF controls Mycobacterium tuberculosis. *PLoS Pathog* **10**, e1003805 (2014).

166. Paquin-Proulx, D. *et al.* Latent Mycobacterium tuberculosis infection is associated with a higher frequency of mucosal-associated invariant T and invariant natural killer T cells. *Frontiers in immunology* **9**, 1394 (2018).

167. Provine, N.M. & Klenerman, P. MAIT cells in health and disease. *Annual review of immunology* **38**, 203-228 (2020).

168. Gold, M.C., Napier, R.J. & Lewinsohn, D.M. MR 1-restricted mucosal associated invariant T (MAIT) cells in the immune response to M ycobacterium tuberculosis. *Immunological reviews* **264**, 154-166 (2015).

169. Suliman, S. *et al.* MR1-independent activation of human mucosal-associated invariant T cells by mycobacteria. *The Journal of Immunology* **203**, 2917-2927 (2019).

170. Gherardin, N.A. *et al.* Human blood MAIT cell subsets defined using MR1 tetramers. *Immunology and cell biology* **96**, 507-525 (2018).

171. Kauffman, K.D. *et al.* Limited pulmonary mucosal-associated invariant T cell accumulation and activation during Mycobacterium tuberculosis infection in rhesus macaques. *Infection & Immunity* **10**, 10 (2018).

172. Ellis-Connell, A.L. *et al.* MAIT cells are minimally responsive to Mycobacterium tuberculosis within granulomas, but are functionally impaired by SIV in a macaque model of SIV and Mtb co-infection. *bioRxiv* (2020).

173. Sakala, I.G. *et al.* Functional heterogeneity and antimycobacterial effects of mouse mucosal-associated invariant T cells specific for riboflavin metabolites. *The Journal of Immunology* **195**, 587-601 (2015).

174. Chua, W.-J. *et al.* Polyclonal mucosa-associated invariant T cells have unique innate functions in bacterial infection. *Infection and immunity* **80**, 3256-3267 (2012).

175. Sakai, S. *et al.* MAIT cell-directed therapy of Mycobacterium tuberculosis infection. *Mucosal Immunology*, 1-10 (2020).

176. Lawand, M., Déchanet-Merville, J. & Dieu-Nosjean, M.-C. Key features of gamma-delta T-cell subsets in human diseases and their immunotherapeutic implications. *Frontiers in immunology* **8**, 761 (2017).

177. Janis, E.M., Kaufmann, S., Schwartz, R.H. & Pardoll, D.M. Activation of gamma delta T cells in the primary immune response to Mycobacterium tuberculosis. *Science* **244**, 713-716 (1989).

178. Tsukaguchi, K., Balaji, K.N. & Boom, W.H. CD4+ alpha beta T cell and gamma delta T cell responses to Mycobacterium tuberculosis. Similarities and differences in Ag recognition, cytotoxic effector function, and cytokine production. *The Journal of Immunology* **154**, 1786-1796 (1995).

179. Dieli, F. *et al.* Granulysin-dependent killing of intracellular and extracellular Mycobacterium tuberculosis by Vγ9/Vδ2 T lymphocytes. *The Journal of infectious diseases* **184**, 1082-1085 (2001).

180. Peng, M. *et al.* Interleukin 17-producing γ δ T cells increased in patients with active pulmonary tuberculosis. *Cellular & molecular immunology* **5**, 203-208 (2008).

181. Tanaka, Y. *et al.* Nonpeptide ligands for human gamma delta T cells. *Proceedings of the National Academy of Sciences* **91**, 8175-8179 (1994).

182. Zufferey, C., Germano, S., Dutta, B., Ritz, N. & Curtis, N. The contribution of non-conventional T cells and NK cells in the mycobacterial-specific IFNγ response in Bacille Calmette-Guérin (BCG)-immunized infants. *PloS one* **8**, e77334 (2013).

183. Shen, Y. *et al.* Adaptive immune response of Vγ2Vδ2+ T cells during mycobacterial infections. *Science* **295**, 2255-2258 (2002).

184. Ogongo, P. *et al.* Differential skewing of donor-unrestricted and γδ T cell repertoires in tuberculosis-infected human lungs. *The Journal of clinical investigation* **130** (2019).

185. Borger, J.G., Le Gros, G. & Kirman, J.R. The Role of Innate Lymphoid Cells in Mucosal Immunity. *Frontiers in Immunology* **11** (2020).

186. Murphy, K.M. & Stockinger, B. Effector T cell plasticity: flexibility in the face of changing circumstances. *Nature immunology* **11**, 674-680 (2010).

187. Spellberg, B. & Edwards Jr, J.E. Type 1/Type 2 immunity in infectious diseases. *Clinical Infectious Diseases* **32**, 76-102 (2001).

188. Kidd, P. Th1/Th2 balance: the hypothesis, its limitations, and implications for health and disease. *Alternative medicine review* **8**, 223-246 (2003).

189. Lienhardt, C. *et al.* Active tuberculosis in Africa is associated with reduced Th1 and increased Th2 activity in vivo. *European journal of immunology* **32**, 1605-1613 (2002).

190. Jung, Y.-J., Ryan, L., LaCourse, R. & North, R.J. Properties and protective value of the secondary versus primary T helper type 1 response to airborne Mycobacterium tuberculosis infection in mice. *The Journal of experimental medicine* **201**, 1915-1924 (2005).

191. Abel, L. *et al.* Genetics of human susceptibility to active and latent tuberculosis: present knowledge and future perspectives. *The Lancet Infectious diseases* **18**, e64-e75 (2018).

192. Hasan, Z. *et al.* Relationship between Circulating Levels of IFN-γ, IL-10, CXCL9 and CCL2 in Pulmonary and Extrapulmonary Tuberculosis is Dependent on Disease Severity. *Scandinavian journal of immunology* **69**, 259-267 (2009).

193. Elias, D., Akuffo, H. & Britton, S. PPD induced in vitro interferon gamma production is not a reliable correlate of protection against Mycobacterium tuberculosis. *Transactions of the Royal Society of Tropical Medicine and Hygiene* **99**, 363-368 (2005).

194. Harris, J. & Keane, J. How tumour necrosis factor blockers interfere with tuberculosis immunity. *Clinical & Experimental Immunology* **161**, 1-9 (2010).

195. Zhang, Z. *et al.* Risk of tuberculosis in patients treated with TNF-α antagonists: a systematic review and meta-analysis of randomised controlled trials. *BMJ open* **7**, e012567 (2017).

196. Evangelatos, G., Koulouri, V., Iliopoulos, A. & Fragoulis, G.E. Tuberculosis and targeted synthetic or biologic DMARDs, beyond tumor necrosis factor inhibitors. *Therapeutic Advances in Musculoskeletal Disease* **12**, 1759720X20930116 (2020).

197. Bruns, H. *et al.* Anti-TNF immunotherapy reduces CD8+ T cell–mediated antimicrobial activity against Mycobacterium tuberculosis in humans. *The Journal of clinical investigation* **119**, 1167-1177 (2009).

198. Davignon, J.-L. *et al.* Modulation of T-cell responses by anti-tumor necrosis factor treatments in rheumatoid arthritis: a review. *Arthritis research & therapy* **20**, 229 (2018).

199. Pipkin, M.E. *et al.* Interleukin-2 and inflammation induce distinct transcriptional programs that promote the differentiation of effector cytolytic T cells. *Immunity* **32**, 79-90 (2010).

200. Liu, X. *et al.* IL-2 restores T-cell dysfunction induced by persistent Mycobacterium tuberculosis antigen stimulation. *Frontiers in immunology* **10**, 2350 (2019).

201. Johnson, B. *et al.* Clinical and immune responses of tuberculosis patients treated with low-dose IL-2 and multidrug therapy. *Cytokines and molecular therapy* **1**, 185 (1995).

202. Zhang, R. *et al.* Therapeutic effects of recombinant human interleukin 2 as adjunctive immunotherapy against tuberculosis: a systematic review and meta-analysis. *PloS one* **13**, e0201025 (2018).

203. Gopal, R. *et al.* Unexpected role for IL-17 in protective immunity against hypervirulent Mycobacterium tuberculosis HN878 infection. *PLoS Pathog* **10**, e1004099 (2014).

204. Torrado, E. & Cooper, A.M. IL-17 and Th17 cells in tuberculosis. *Cytokine & growth factor reviews* **21**, 455-462 (2010).

205. Blanco, F.C. *et al.* Increased IL-17 expression is associated with pathology in a bovine model of tuberculosis. *Tuberculosis* **91**, 57-63 (2011).

206. Cruz, A. *et al.* Pathological role of interleukin 17 in mice subjected to repeated BCG vaccination after infection with Mycobacterium tuberculosis. *Journal of Experimental Medicine* **207**, 1609-1616 (2010).

207. Darrah, P.A. *et al.* Multifunctional TH 1 cells define a correlate of vaccine-mediated protection against Leishmania major. *Nature medicine* **13**, 843-850 (2007).

208. Lewinsohn, D.A., Lewinsohn, D.M. & Scriba, T.J. Polyfunctional CD4+ T cells as targets for tuberculosis vaccination. *Frontiers in immunology* **8**, 1262 (2017).

209. Jarvela, J. *et al.* Mycobacterium tuberculosis–Induced Bronchoalveolar Lavage Gene Expression Signature in Latent Tuberculosis Infection Is Dominated by Pleiotropic Effects of CD4+ T Cell–Dependent IFN-γ Production despite the Presence of Polyfunctional T Cells within the Airways. *The Journal of Immunology* **203**, 2194-2209 (2019).

210. Elias, D. *et al.* Effect of deworming on human T cell responses to mycobacterial antigens in helminth-exposed individuals before and after bacille calmette–guérin (BCG) vaccination. *Clinical & Experimental Immunology* **123**, 219-225 (2001).

211. Howard, A. & Zwilling, B. Reactivation of tuberculosis is associated with a shift from type 1 to type 2 cytokines. *Clinical and experimental immunology* **115**, 428 (1999).

212. Rook, W. & Graham, A. Th2 cytokines in susceptibility to tuberculosis. *Current molecular medicine* **7**, 327-337 (2007).

213. Ahmed, A. & Vyakarnam, A. Emerging patterns of regulatory T cell function in tuberculosis. *Clinical & Experimental Immunology* (2020).

214. Guyot-Revol, V., Innes, J.A., Hackforth, S., Hinks, T. & Lalvani, A. Regulatory T cells are expanded in blood and disease sites in patients with tuberculosis. *American journal of respiratory and critical care medicine* **173**, 803-810 (2006).

215. Schaible, U.E. *et al.* Apoptosis facilitates antigen presentation to T lymphocytes through MHC-I and CD1 in tuberculosis. *Nature medicine* **9**, 1039-1046 (2003).

216. Chen, C.Y. *et al.* A critical role for CD8 T cells in a nonhuman primate model of tuberculosis. *PLoS Pathog* **5**, e1000392 (2009).

217. Orme, I.M. & Henao-Tamayo, M.I. Trying to see the forest through the trees: deciphering the nature of memory immunity to mycobacterium tuberculosis. *Frontiers in Immunology* **9**, 461 (2018).

218. Sallusto, F., Geginat, J. & Lanzavecchia, A. Central memory and effector memory T cell subsets: function, generation, and maintenance. *Annu. Rev. Immunol.* **22**, 745-763 (2004).

219. Tanner, R., Villarreal-Ramos, B., Vordermeier, M. & McShane, H. The Humoral Immune Response to BCG Vaccination. *Frontiers in Immunology* **10**, 1317 (2019).

220. Kawahara, J.Y., Irvine, E.B. & Alter, G. A case for antibodies as mechanistic correlates of immunity in tuberculosis. *Frontiers in immunology* **10**, 996 (2019).

221. Hamasur, B. *et al.* A mycobacterial lipoarabinomannan specific monoclonal antibody and its F (ab') 2 fragment prolong survival of mice infected with Mycobacterium tuberculosis. *Clinical & Experimental Immunology* **138**, 30-38 (2004).

222. Li, H. *et al.* Latently and uninfected healthcare workers exposed to TB make protective antibodies against Mycobacterium tuberculosis. *Proceedings of the National Academy of Sciences* **114**, 5023-5028 (2017).

223. Johnson, C. *et al.* Mycobacterium tuberculosis aerogenic rechallenge infections in B cell-deficient mice. *Tubercle and Lung Disease* **78**, 257-261 (1997).

224. Maglione, P.J., Xu, J. & Chan, J. B cells moderate inflammatory progression and enhance bacterial containment upon pulmonary challenge with Mycobacterium tuberculosis. *The Journal of Immunology* **178**, 7222-7234 (2007).

225. Joosten, S.A. *et al.* Patients with tuberculosis have a dysfunctional circulating B-cell compartment, which normalizes following successful treatment. *PLoS pathogens* **12**, e1005687 (2016).

226. Alter, G. *et al.* Robust IgM responses following vaccination are associated with prevention of Mycobacterium tuberculosis infection in macaques. (2021).

227. Netea, M.G. & van der Meer, J.W. Trained immunity: an ancient way of remembering. *Cell host & microbe* **21**, 297-300 (2017).

228. Redelman-Sidi, G., Glickman, M.S. & Bochner, B.H. The mechanism of action of BCG therapy for bladder cancer—a current perspective. *Nature Reviews Urology* **11**, 153 (2014).

229. Rodrigues, T.S., Conti, B.J., Fraga-Silva, T.F.d.C., Almeida, F. & Bonato, V.L.D. Interplay between alveolar epithelial and dendritic cells and Mycobacterium tuberculosis. *Journal of Leukocyte Biology* (2020).

230. Krishna, P., Jain, A. & Bisen, P. Microbiome diversity in the sputum of patients with pulmonary tuberculosis. *European Journal of Clinical Microbiology & Infectious Diseases* **35**, 1205-1210 (2016).

231. Khan, N. *et al.* Alteration in the gut microbiota provokes susceptibility to tuberculosis. *Frontiers in immunology* **7**, 529 (2016).

232. Winglee, K. *et al.* Aerosol Mycobacterium tuberculosis infection causes rapid loss of diversity in gut microbiota. *PloS one* **9**, e97048 (2014).

233. Bull, N. *et al.* Enhanced protection conferred by mucosal BCG vaccination associates with presence of antigen-specific lung tissue-resident PD-1+ KLRG1− CD4+ T cells. *Mucosal immunology* **12**, 555 (2019).

234. Garcia, B.J. *et al.* Sputum is a surrogate for bronchoalveolar lavage for monitoring Mycobacterium tuberculosis transcriptional profiles in TB patients. *Tuberculosis* **100**, 89-94 (2016).

235. Davids, M. *et al.* Utility of Endobronchial Ultrasound-Guided Transbronchial Needle Aspiration as a Research Tool for Investigating the Cellular Immune Response in Lymph Nodes. *D32. IMMUNOLOGY: BASIC MECHANISMS*. American Thoracic Society, 2020, pp A6495-A6495.

236. Marsay, L. *et al.* Mycobacterial growth inhibition in murine splenocytes as a surrogate for protection against Mycobacterium tuberculosis (M. tb). *Tuberculosis (Edinburgh, Scotland)* **93**, 551-557 (2013).

237. Brennan, M.J. *et al.* The Cross-Species Mycobacterial Growth Inhibition Assay (MGIA) Project, 2010-2014. *Clinical and vaccine immunology : CVI* **24** (2017).

238. Tanner, R. *et al.* A non-human primate in vitro functional assay for the early evaluation of TB vaccine candidates. *npj Vaccines* **6**, 1-11 (2021).

239. O'Shea, M.K. *et al.* Immunological correlates of mycobacterial growth inhibition describe a spectrum of tuberculosis infection. *Scientific reports* **8**, 14480 (2018).

240. Tanner, R. *et al.* The in vitro direct mycobacterial growth inhibition assay (MGIA) for the early evaluation of TB vaccine candidates and assessment of protective immunity: a protocol for non-human primate cells. *F1000Research* **10** (2021).

241. Pepponi, I. *et al.* A mycobacterial growth inhibition assay (MGIA) for bovine TB vaccine development. *Tuberculosis* **106**, 118-122 (2017).

242. Sauerwein, R.W., Roestenberg, M. & Moorthy, V.S. Experimental human challenge infections can accelerate clinical malaria vaccine development. *Nature Reviews Immunology* **11**, 57-64 (2011).

243. Durbin, A.P. & Whitehead, S.S. The dengue human challenge model: has the time come to accept this challenge? : Oxford University Press; 2013.

244. Carrat, F. *et al.* Time lines of infection and disease in human influenza: a review of volunteer challenge studies. *American journal of epidemiology* **167**, 775-785 (2008).

245. Feasey, N.A. & Levine, M.M. Typhoid vaccine development with a human challenge model. *The Lancet* **390**, 2419-2421 (2017).

246. Minassian, A.M. *et al.* A Human Challenge Model for Mycobacterium tuberculosis Using M ycobacterium bovis Bacille Calmette-Guérin. *Journal of Infectious Diseases* **205**, 1035-1042 (2012).

247. Harris, S.A. *et al.* Evaluation of a human BCG challenge model to assess antimycobacterial immunity induced by BCG and a candidate tuberculosis vaccine, MVA85A, alone and in combination. *The Journal of infectious diseases* **209**, 1259-1268 (2013).

248. Guo, S. *et al.* The CFP10/ESAT6 complex of Mycobacterium tuberculosis may function as a regulator of macrophage cell death at different stages of tuberculosis infection. *Medical hypotheses* **78**, 389-392 (2012).

249. Hesseling, A. *et al.* Bacille Calmette-Guérin vaccine—induced disease in HIV-infected and HIV-uninfected children. *Clinical infectious diseases* **42**, 548-558 (2006).

250. Elhmouzi-Younes, J. *et al.* In depth comparative phenotyping of blood innate myeloid leukocytes from healthy humans and macaques using mass cytometry. *Cytometry Part A* **91**, 969-982 (2017).

251. Hanekom, W.A. *et al.* Novel application of a whole blood intracellular cytokine detection assay to quantitate specific T-cell frequency in field studies. *Journal of immunological methods* **291**, 185-195 (2004).

252. Sibley, L.S. *et al.* ELISPOT refinement using spot morphology for assessing host responses to tuberculosis. *Cells* **1**, 5-14 (2012).

253. Sibley, L. *et al.* High dose aerosol challenge with Mycobacterium tuberculosis fails to overcome BCG vaccination-induced protection in cynomolgus macaques of Chinese origin: implications of natural resistance for TB vaccine evaluation. (2021).

254. Reeves, R.K. *et al.* Antigen-specific NK cell memory in rhesus macaques. *Nature immunology* **16**, 927-932 (2015).

255. Kagina, B.M. *et al.* Qualification of a whole blood intracellular cytokine staining assay to measure mycobacteria-specific CD4 and CD8 T cell immunity by flow cytometry. *Journal of immunological methods* **417**, 22-33 (2015).

256. Satti, I. *et al.* Safety and immunogenicity of a candidate tuberculosis vaccine MVA85A delivered by aerosol in BCG-vaccinated healthy adults: a phase 1, double-blind, randomised controlled trial. *The Lancet Infectious diseases* **14**, 939-946 (2014).

257. Soares, A.P. *et al.* Longitudinal changes in CD4+ T-cell memory responses induced by BCG vaccination of newborns. *The Journal of infectious diseases* **207**, 1084-1094 (2013).

258. Lin, P.L. & Flynn, J.L. CD8 T cells and Mycobacterium tuberculosis infection. Seminars in immunopathology; 2015: Springer; 2015. p. 239-249.

259. Wolday, D. *et al.* Role of CD4/CD8 ratio on the incidence of tuberculosis in HIV-infected patients on antiretroviral therapy followed up for more than a decade. *PloS one* **15**, e0233049 (2020).

260. Lee, W.W., Nam, K.H., Terao, K., Akari, H. & Yoshikawa, Y. Age-related increase of peripheral CD4+ CD8+ double-positive T lymphocytes in cynomolgus monkeys: longitudinal study in relation to thymic involution. *Immunology* **109**, 217-225 (2003).

261. Parel, Y. & Chizzolini, C. CD4+ CD8+ double positive (DP) T cells in health and disease. *Autoimmunity reviews* **3**, 215-220 (2004).

262. Webster, R.L. & Johnson, R.P. Delineation of multiple subpopulations of natural killer cells in rhesus macaques. *Immunology* **115**, 206-214 (2005).

263. Carter, D. *et al.* CD56 identifies monocytes and not natural killer cells in rhesus macaques. *Cytometry: The Journal of the International Society for Analytical Cytology* **37**, 41-50 (1999).

264. Morrison, A., Sharpe, S., White, A. & Bodman-Smith, M. Cheap and Commonplace: Making the Case for BCG and gd T Cells in COVID-19. *Front. Immunol. 12: 743924. doi: 10.3389/fimmu* (2021).

265. Yang, Q. *et al.* Discriminating active tuberculosis from latent tuberculosis infection by flow cytometric measurement of CD161-expressing T cells. *Scientific reports* **5**, 1-8 (2015).

266. Yao, S. *et al.* CD4+ T cells contain early extrapulmonary tuberculosis (TB) dissemination and rapid TB progression and sustain multieffector functions of CD8+ T and CD3− lymphocytes: mechanisms of CD4+ T cell immunity. *The Journal of Immunology* **192**, 2120-2132 (2014).

267. Kang, Y.-H. *et al.* CD161+ CD4+ T cells are enriched in the liver during chronic hepatitis and associated with co-secretion of IL-22 and Interferon-gamma. *Frontiers in immunology* **3**, 346 (2012).

268. McGary, C.S. *et al.* The loss of CCR6+ and CD161+ CD4+ T-cell homeostasis contributes to disease progression in SIV-infected rhesus macaques. *Mucosal immunology* **10**, 1082-1096 (2017).

269. Billerbeck, E. *et al.* Analysis of CD161 expression on human CD8+ T cells defines a distinct functional subset with tissue-homing properties. *Proceedings of the National Academy of Sciences* **107**, 3006-3011 (2010).

270. Castaño, D., García, L.F. & Rojas, M. Increased frequency and cell death of CD16+ monocytes with Mycobacterium tuberculosis infection. *Tuberculosis* **91**, 348-360 (2011).

271. Mpande, C.A. *et al.* Antigen-specific T-cell activation distinguishes between recent and remote tuberculosis infection. *American Journal of Respiratory and Critical Care Medicine* **203**, 1556-1565 (2021).

272. Ravesloot-Chavez, M.M., Van Dis, E. & Stanley, S.A. The Innate Immune Response to Mycobacterium tuberculosis Infection. *Annual review of immunology* **39** (2021).

273. Chowdhury, I.H. *et al.* Alteration of serum inflammatory cytokines in active pulmonary tuberculosis following anti-tuberculosis drug therapy. *Molecular immunology* **62**, 159-168 (2014).

274. Domingo-Gonzalez, R., Prince, O., Cooper, A. & Khader, S. Cytokines and chemokines in Mycobacterium tuberculosis infection. *Microbiology spectrum* **4** (2016).

275. Iliaz, S. *et al.* Value of neutrophil/lymphocyte ratio in the differential diagnosis of sarcoidosis and tuberculosis. *Annals of thoracic medicine* **9**, 232 (2014).

276. Bitencourt, J. *et al.* Induction of specific antibodies, IgG-secreting plasmablasts and memory B cells following BCG vaccination. *bioRxiv* (2021).

277. Fergusson, J.R. *et al.* CD161 defines a transcriptional and functional phenotype across distinct human T cell lineages. *Cell reports* **9**, 1075-1088 (2014).

278. Shen, H. *et al.* A CD4+ CD161+ T-cell subset present in unexposed humans, not TB patients, are fast acting cells that inhibit the growth of intracellular mycobacteria involving CD161 pathway, perforin and IFN-γ/autophagy. *Frontiers in immunology* **12**, 88 (2021).

279. Tanner, R. *et al.* The influence of haemoglobin and iron on in vitro mycobacterial growth inhibition assays. *Scientific reports* **7**, 1-13 (2017).

280. Jones, C.M. & Niederweis, M. Mycobacterium tuberculosis can utilize heme as an iron source. *Journal of bacteriology* **193**, 1767-1770 (2011).

281. Tullius, M.V., Nava, S. & Horwitz, M.A. PPE37 is essential for Mycobacterium tuberculosis heme-iron acquisition (HIA), and a defective PPE37 in Mycobacterium bovis BCG prevents HIA. *Infection and immunity* **87**, e00540-00518 (2019).

282. Hertz, D. & Schneider, B. Sex differences in tuberculosis. Seminars in immunopathology; 2019: Springer; 2019. p. 225-237.

283. Rosenthal, S.R., McEnery, J.T. & Raisys, N. Aerogenic BCG vaccination against tuberculosis in animal and human subjects. *Journal of Asthma Research* **5**, 309-323 (1968).

284. Cusumano, C., Jernigan, J. & Waldman, R. Aerosolized BCG (Tice strain) treatment of bronchogenic carcinoma: phase I study. *Journal of the National Cancer Institute* **55**, 275-279 (1975).

285. Garner, F.B., Meyer, C.A., White, D.S. & Lipton, A. Aerosol BCG treatment of carcinoma metastatic to the lung: a phase I study. *Cancer* **35**, 1088-1094 (1975).

286. Walrath, J., Zukowski, L., Krywiak, A. & Silver, R.F. Resident Th1-like effector memory cells in pulmonary recall responses to Mycobacterium tuberculosis. *American Journal of Respiratory Cell and Molecular Biology* **33**, 48-55 (2005).

287. Nagata, S. Fas ligand-induced apoptosis. *Annual review of genetics* **33**, 29-55 (1999).

288. Ju, S.-T., Cui, H., Panka, D.J., Ettinger, R. & Marshak-Rothstein, A. Participation of target Fas protein in apoptosis pathway induced by CD4+ Th1 and CD8+ cytotoxic T cells. *Proceedings of the National Academy of Sciences* **91**, 4185-4189 (1994).

289. Smith, S.G., Zelmer, A., Blitz, R., Fletcher, H.A. & Dockrell, H.M. Polyfunctional CD4 T-cells correlate with in vitro mycobacterial growth inhibition following Mycobacterium bovis BCG-vaccination of infants. *Vaccine* **34**, 5298-5305 (2016).

290. Chen, T. *et al.* Association of human antibodies to arabinomannan with enhanced mycobacterial opsonophagocytosis and intracellular growth reduction. *The Journal of infectious diseases* **214**, 300-310 (2016).

291. McShane, H. *et al.* Recombinant modified vaccinia virus Ankara expressing antigen 85A boosts BCG-primed and naturally acquired antimycobacterial immunity in humans. *Nature medicine* **10**, 1240-1244 (2004).

292. Hawash, M.B. *et al.* Primate innate immune responses to bacterial and viral pathogens reveals an evolutionary trade-off between strength and specificity. *Proceedings of the National Academy of Sciences* **118** (2021).

293. White, A. *et al.* Evaluation of the safety and immunogenicity of a candidate tuberculosis vaccine, MVA85A, delivered by aerosol to the lungs of macaques. *Clin. Vaccine Immunol.* **20**, 663-672 (2013).

294. Soares, A. *et al.* Novel application of Ki67 to quantify antigen-specific in vitro lymphoproliferation. *Journal of immunological methods* **362**, 43-50 (2010).

295. Ogbe, A. *et al.* T cell assays differentiate clinical and subclinical SARS-CoV-2 infections from cross-reactive antiviral responses. *Nature communications* **12**, 1-14 (2021).

296. Pedrazzoli, D. & Wingfield, T. Biosocial strategies to address the socioeconomic determinants and consequences of the TB and COVID-19 pandemics. *The American journal of tropical medicine and hygiene* **104**, 407 (2021).

297. Fletcher, H.A. *et al.* Inhibition of mycobacterial growth in vitro following primary but not secondary vaccination with Mycobacterium bovis BCG. *Clinical and Vaccine Immunology* **20**, 1683-1689 (2013).

298. Lai, Hsin-Chih, *et al*. NK Cell–Derived IFN-γ Protects against Nontuberculous Mycobacterial Lung Infection. *The Journal of Immunology* **201,** 1478-1490 (2018).

299. Mochan, Ericka, et al. Compartmental model suggests importance of innate immune response to covid-19 infection in rhesus macaques. *Bulletin of mathematical biology* **83,** 1-26 (2021).

300. Loewendorf, A., and C. A. Benedict. Modulation of host innate and adaptive immune defenses by cytomegalovirus: timing is everything. *Journal of internal medicine* **267**, 483-501 (2010).

301. Medlar, E. M., and K. T. Sasano. A study of the pathology of experimental pulmonary tuberculosis in the rabbit. *American Review of Tuberculosis* **34,** 456-476 (1936).
302. Tanner, Rachel, et al. The in vitro direct mycobacterial growth inhibition assay (MGIA) for the early evaluation of TB vaccine candidates and assessment of protective immunity: a protocol for non-human primate cells. *F1000Research* **10**, (2021).